Déterminants moléculaires et spécificité du priming immunitaire chez le mollusque d'eau douce Biomphalaria glabrata

Julien Portela

Collège Doctoral du Languedoc-Roussillon

THÈSE

Pour obtenir le grade de

Docteur

Délivré par

UNIVERSITE DE PERPIGNAN VIA DOMITIA

Préparée au sein de l'école doctorale
ED305 Energie et Environnement
Et de l'unité de recherche
UMR5244 Ecologie et Evolution des Interactions

Spécialité : **Biologie**

Présentée par **Julien Portela**

Déterminants moléculaires et spécificité du Priming immunitaire chez le mollusque d'eau douce *Biomphalaria glabrata.*

Soutenue le 02/12/2013 devant le jury composé de

M. Mathieu SICARD, PR, UM2	Rapporteur
M. Jean-Marc REICHHART, PR, Université de Strasbourg	Rapporteur
Mme Delphine DESTOUMIEUX-GARZON, CR, UM2	Examinateur
M. Yannick MORET, CR, Université de Bourgogne	Examinateur
M. Guillaume MITTA, PR, UPVD	Examinateur
M. Benjamin GOURBAL, MC, UPVD	Co-Directeur
M. André THERON, DR, UPVD	Co-Directeur

UPVD Université de Perpignan Via Domitia

ACADEMIE DE MONTPELLIER

Université Via Domitia

THESE DE DOCTORAT

En vue de l'obtention du grade de

DOCTEUR DE L'UNIVERSITE DE PERPIGNAN VIA DOMITIA

BIOLOGIE ECOLOGIE EVOLUTION

Ecole doctorale : Energie et Environnement

Présentée par

Julien Portela

Déterminants moléculaires et spécificité du Priming immunitaire chez le mollusque d'eau douce *Biomphalaria glabrata.*

Thèse Co-dirigée par : André Théron et Benjamin Gourbal

Soutenue le 02/12/2013 devant un jury composé de :

Mathieu Sicard	PR, Université de Montpellier II	Rapporteur
Jean-Marc Reichhart	PR, Université de Strasbourg	Rapporteur
Yannick Moret	CR CNRS, Université de Bourgogne	Examinateur
Delphine Destoumieux-Garzón	CR CNRS, Université de Montpellier II	Examinateur
Guillaume Mitta	PR, Université de Perpignan	Examinateur
André Théron	DR CNRS, Université de Perpignan	Co-directeur
Benjamin Gourbal	MC, Université de Perpignan	Co-directeur

« Quand une lecture vous élève l'esprit, et qu'elle vous inspire des sentiments nobles et courageux ne cherchez pas une autre règle pour juger l'ouvrage ; il est bon et fait de main d'ouvrier »

Les Caractères, La Bruyère

Remerciements

On dirait bien que l'heure est venue de remercier tous les gens qui ont contribué à ma réussite au cours de ces quelques années (oui je sais chef je suis pas assez précis… alors je dirais 7 ans) passées au Centre de Biologie et Ecologie Tropicale et Méditerranéenne (c'est à peu près le seul truc qui n'a pas changé de nom).

Tout d'abord je vais commencer par Guillaume Mitta, directeur du labo, qui m'a permis de réaliser ce que je n'aurais jamais cru possible. Je n'oublierais jamais lorsque nous avons discuté du sujet de thèse et de l'éventualité que je pourrais en être le candidat. Je n'oublierais pas non plus les repas au labo et les fous rires.

J'adresse également un merci à Claude Combes qui, au travers des cours d'écologie des populations et de ses diverses conférences, m'a montré qu'on pouvait prendre du plaisir et en donner en enseignant ou plus simplement en communiquant.

Merci également à Delphine Destoumieux-Garzón et Yannick Moret pour leurs conseils très avisés lors des discussions au cours de mes comités de suivi de thèse et, bien sûr, merci à mes deux rapporteurs Jean-Marc Reichhart et Mathieu Sicard pour les discussions qui vont venir et seront, j'en suis sûr, très intéressantes et passionnantes.

Je poursuivrais en remerciant mon premier co-directeur de thèse, André Théron. Merci pour tout !! Ce fût un privilège et un honneur de travailler avec vous, d'échanger et surtout d'apprendre. J'aurais toujours mes yeux d'enfant en vous écoutant parler de science ou autre. Comment oublier mon Master I et cette séance d'anatomie du mollusque alors que je cherchais désespérément les sporocystes dans mes coupes histologiques.

Un grand merci à mon second co-directeur de thèse, Benjamin Gourbal. Tu étais sans doute prédestiné à travailler sur le modèle Biomphalaria glabrata puisque vous avez les mêmes initiales !!! Quoi qu'il en soit j'ai passé des moments superbes au cours de ma thèse. Tu es l'encadrant dont tous les doctorants devraient rêver. Tu m'as toujours soutenu et supporté. Tu m'as offert ma première expérience en laboratoire avec ce stage de M1. Tu es devenu bien plus pour moi qu'un « encadrant ».

Un grand merci à Jérôme (alias « le Docteur House du labo »). D'abord tu m'as offert un super stage de M2 pendant lequel on s'est marré en développant l'industrie pornographique du Schisto. Interracial, Plan à trois, Gang bang, on a tout testé. Ca t'avait pas suffit alors t'as remis ça avec l'ANR Schisto-Med. Encore une fois on s'est bien marré, surtout lors des premières réunions, quand on ne comprenait rien (« Une fluo-quoi ??!!!?? », « C'est quoi ça, le (RS)-2-(cyclohexylcarbonyl)-1,2,3,6,7,11b-hexahydro-

4H-pyrazino(2,1-alpha)isoquinoléin-4-one ? Beh le Praziquantel. Et vous pouvez pas dire Praziquantel ? »). Tester des molécules anti-schisto, quelle belle aventure !!! (surtout quand on testait l'aspirine ou l'huile de cacahuètes, des fois que le Schisto y soit allergique !!???!!). Et je n'oublie pas toutes les fois où j'ai eu besoin de parler, besoin d'avoir un avis extérieur et où tu as toujours répondu présent, mais ça je le garde pour moi. Même si ça va être difficile de faire des réplicas biologiques saches que tu as statistiquement beaucoup compté dans ma vie ($p<0.0001$).

Mon prochain « merci » est pour mes comparses : David (dit Dudu), Jean-François (dit Jeff) et Richard (lui il a trop de surnoms !!!). Sans parler des remontages de moral, je vous remercie surtout pour les délires divers et discussions épiques qu'on a pu avoir. Dudu, le beau gosse avec ses pubs « cougar » et ses bons vins. Jeff, le sportif et sa Jeff-mobile que j'ai connue plus souvent en panne que fonctionnant. Et Richard, avec tes mollets de Berger Allemand et ton humour un peu limite… Naaaaan j'déconne. Il y a tellement de souvenirs que je pourrais évoquer !!! Les pauses, toutes ces machines qu'on a déplacées, les journées confocal, la formation robot, Immuninv à Nice (Euh…)…

Je reviens un peu en arrière pour remercier à nouveau Benjamin, Jérôme, David, Jeff, et Richard ainsi que vos familles pour les moments hors labo qui furent également très important pour moi et ma santé mentale. J'en profite pour remercier les Roumains et leur Palinca…

Un grand merci à tous les gens du labo !!! (Je n'ai pas intérêt à en oublier !!). Merci donc à Sébastien Gourbière qui a formé à lui tout seul un axe de recherche, merci à Céline Cosseau et ses CHIPs (au bacon) et Christoph Grunau ([remerciement] merci beaucoup [/remerciement]), faites attention à ne pas trop vous hypermethyler… Merci à Juliette Langand qui a été ma colloc de bureau pendant presque deux ans et m'a fait décacheter les exams et témoigner de leurs notes. Merci à Hélène Moné et Gabriel Mouahid avec qui j'ai eu de grands fous rires. Merci à Eve Toulza, la dernière arrivée, qui occupe mon ancien bureau, et merci à ceux que j'ai côtoyé et qui sont parti du labo (Betty Faliex et Olivier Verneau)… Merci au personnel technique qui m'a formé ou supporté (c'est déjà pas mal) : Anne Rognon, Bernard Dejean, Irma Fagette, Rémy Emans, Diane Merceron. Un grand merci à ma coupine de salade, Nathalie (Nathouuuu) « C'est ça ton taf ? » ahahah et à ma 'tite Déborah. Un merci particulier à ma documentaliste préférée, Anne !! Un merci à mes petits bébés d'étudiants Raphaël, Fanny, et surtout Anaïs et Silvain, bonne continuation, je vous laisse mon sujet, prenez en soin et faites le grandir.

Je ne peux pas oublier les doctorants/post-doc du labo, passés et présents, Manu, Mathieu, Sophie, Nico, Rodrigue, Pauline, Yves, Jérémie, Guilhem, Julie L, Julie C, Sara, Marion, David… ça en fait mais en 7/8 ans j'en ai croisé pas mal. Je ne vous oublierais pas au travers des délires, pétages de boulon, soirée VnB, des amitiés fortes liées avec vous…

Je remercie les gens formidables avec qui j'ai pu travailler au cours des années Schisto-Med. Frédéric Coslédan avec qui nous avons beaucoup ri et qui nous a pas mal aidés à comprendre la chimie (enfin… comprendre est un bien grand mot). Merci à Vincent Pradines qui a mené quelques manips de chimie à Toulouse pendant que je testais les effets Biologiques à Perpignan. Merci à Anne Robert avec qui le contact facile fût très agréable et ses idées très enrichissantes. Et bien sûr un grand merci à Bernard Meunier. C'est pour moi un honneur de vous connaître et d'avoir partagé cette expérience génialissime, j'en suis sorti grandi.

On va maintenant passer à des remerciements plus personnels, et je commencerai par remercier ma prof de Biologie au lycée (Mme Luz) qui m'a fortement déconseillé de faire de la Biologie à la fac car j'étais trop nul et que je n'y arriverais jamais. Aujourd'hui je vais être Docteur et je vous répondrais : « Ah aaaahhh !!! On fait moins la maline !! ». Mais bon, sans elle je ne me serais pas orienté vers la Physique, et je n'aurais pas rencontré Pierre. Un vrai ami comme on n'en fait pas beaucoup qui m'a soutenu quand j'avais « envie de tirer une balle entre les yeux de chaque panda pas foutu de baiser pour sauver leur espèce, envie d'ouvrir les vannes de dégazage de tous les pétroliers et de polluer toutes ces plages françaises que je ne verrais jamais, envie de tout polluer d'une fumée bien noire ». Merci mec, je te dois beaucoup, toi-même tu sais !!! Merci également à Jean-Loup avec qui j'ai redécouvert les fléchettes… Merci aux potos, des plus anciens aux plus récents Romain (Rom-1), Laurent (alias Viejo), je resterais toujours Julilou les gars, Mathieu et sa bande de potes qui sont devenus les miens, et Marco, sans oublier Lolo (c'est qui le Papa ?)!!! Un méga merci à Damien, sans qui je serais devenu fou, encore un ami comme on n'en fait plus.

Et de manière plus subjective, un grand merci à tout ce qui a été près de moi pendant cette thèse, merci à tous les mollusques, souris, hamsters sacrifiés au nom de ma réussite, merci à la réunion Schisto-Med ou j'ai appris qu'on pouvait faire une présentation avec un fichier Word qu'on fait dérouler avec la molette de la souris, au « O'Shannon », à tous ces films que j'ai vus et revus pendant ces trois ans, à la baignoire et au rosé, au petit chat plein de tendresse, au CRUNCH et au sanglier sur la route, à

toutes les soirées intelligentes. Merci à Horatio pour ses répliques et ses cheveux roux, aux films de Steven Seagal. Merci à ma playstation (èh !!), à Sam Fisher (Tjjjuuuuiiiiiiiiii), à tous ces Cht'ao et Chicanos qu'on à flingués… Un grand merci à toutes mes répliques cultes devant les Licences qui resteront gravées dans ma mémoire et la leur, à toutes ces phrases qu'elles me disent toutes, au TABASCOOOOO de 1h30, au 6 juin, au tour du monde, à tous ces moments que j'avais cru partager… Un grand merci à Joker Mourillas pour ces deux saisons magnifiques (n'oublies pas, pars du principe que je suis jamais hors jeu tu gagneras du temps), à chacun des Superbowl qui m'ont empêché de dormir, à Baine qui s'est demandé qui de mon corps ou de mon esprit se briserait en premier, merci au gros lapin/lièvre qui a failli nous tuer à Opoul, merci au Jorki ball, à mon hématome Adidas (photo à l'appuis), au « OCCCRRR », à l'affaire Virginie, au choix entre les portes A, B ou C. Merci à Orelsan (moi aussi j'en ai marre d'escalader la pyramide de Maslow), merci à toutes ces soirées étoilées pendant lesquelles j'ai pu reposer mon esprit, merci au thé grenade (la science infuse…). Une petite pensée pour la Toledo et la 309, désolé mais fallait faire place à la jeunesse les filles. Un grand merci à ma guitare sans qui je n'aurais pas eu d'aussi beaux souvenirs et pas autant de filles non plus… A tous ces paris que j'aurais pas du faire. A tous ces matchs de XIII que j'ai vus, à tous ces matchs de XV que j'ai vus, à ce fameux match opposant les Lievremont aux Cantona. Merci au renard mais un jour je trouverais ce que tu dis. Merci à Steve Jobs pour cette formidable invention qu'est l'i-Phone…

Bien sûr je ne vais pas oublier mes parents, sans qui je ne serais pas là. Etant un enfant de Septembre j'ai probablement été conçu après une belle cuite de fin d'année mais ça ne m'aura pas trop mal réussi. Je n'oublie pas non plus mon frérot que j'aime plus que tout, t'as vu Berloul, c'est qui l'patron !!! J'espère que le buffet d'après thèse sera bon.

A ceux qui liront ceci, j'espère que vous aurez pris autant de plaisir à le lire que moi à l'écrire. J'ai essayé de ne pas donner dans le mélodramatique mais d'y laisser un peu d'humour et un peu de moi… Place à la science.

TABLE DES MATIERES

Prologue

PROLOGUE

Avant d'appréhender ce qui va suivre au cours de cette thèse concernant l'immunité du mollusque d'eau douce *Biomphalaria glabrata*, il est important de poser les bases de ce que signifie « immunité ». L'immunité est définie comme l'ensemble des mécanismes de défenses d'un organisme face à tout élément étranger à cet organisme et plus particulièrement les pathogènes (bactéries, virus et parasites). Pour comprendre mieux comment peut se définir l'immunité de nos jours prenons le temps d'un petit retour dans le passé au travers des différentes avancées majeures de ce domaine scientifique.

La première description d'un phénomène immunitaire :

Nous sommes en 430 avant Jésus Christ en Grèce. Sous l'impulsion de la puissance grandissante d'Athènes, Sparte se voit obligée de rentrer en guerre afin de protéger le Péloponnèse et surtout d'en rester maître. La guerre fait rage et cette année là un mal étrange frappe Athènes. C'est l'historien Thucydide qui décrit alors ce mal mystérieux qui décime peu à peu tous les Athéniens (Thucydide -400). Sans même avoir aucune connaissance de ce que peut être l'immunité il décrit en ces termes ses différentes observations :

« C'étaient ceux qui avaient échappé à la maladie qui se montraient les plus compatissants pour les mourants et les malades, car connaissant déjà le mal, ils étaient en sécurité. En effet les rechutes n'étaient pas mortelles. Enviés par tes autres, dans l'excès de leur bonne fortune présente, ils se laissaient bercer par l'espoir d'échapper à l'avenir à toute maladie. »

Thucydide « Histoire de la guerre du Péloponnèse » Livre II chapitre LI.

Le mal en question était la fièvre typhoïde et sans le savoir Thucydide venait d'observer le résultat de l'immunité adaptative.

La vaccination :

Avançons quelques peu dans l'histoire pour nous retrouver au XI^{ème} siècle en Asie où sévit la variole. L'Ayurveda, reconnue par l'OMS comme médecine traditionnelle d'Inde, décrit ce qui s'apparente à une vaccination. Il s'agit en effet d'inoculer à un patient de la

« matière varioleuse » vieille d'un an. Peu de temps après (XI^{ème} siècle toujours) en Chine, le procédé appelé « variolisation » est appliqué, cette fois-ci il s'agit d'injecter du pus de patients malades à des patients sains afin de les protéger, tout ceci en espérant que l'injection ne soit pas trop virulente et ne les tue pas. Cette méthode importée par la suite en Europe au XVIII^{ème} siècle fait alors l'objet de nombreuses revues et publications et ouvre même la porte à de nouvelles professions (inoculateur en grand) (Peter 1979). Au XVIII^{ème} siècle toujours, certaines personnes ont testés de manière indépendante d'inoculer la variole de la vache appelées « vaccine » et c'est le médecin anglais Edward Jenner qui demande la validation de son expérience ainsi que toutes celles qu'il a récoltées et retranscrites depuis 1770. En 1796, Jenner inocule la vaccine au jeune James Phipps, qui a alors huit ans. Six semaines plus tard il lui inocule la variole et note que l'enfant est immunisé (Stern and Markel 2005). C'est dès lors que le vaccin fût administré en masse.

Ce n'est qu'en 1885 que Louis Pasteur expose à l'Académie des Sciences ses données concernant la vaccination (Pasteur 1885). Il décrit alors le fonctionnement d'un vaccin, la préparation de celui-ci et présente ses résultats concernant la vaccination d'un cheptel de moutons contre la maladie du charbon, ainsi que la vaccination du jeune Joseph Meister contre la rage suite à sa morsure par un chien.

Les mécanismes et la mise en place des premières théories :

C'est au début du XX^{ème} siècle que les choses commencent à se préciser. Paul Ehrlich, immunochimiste, s'appuyant en partie sur les travaux d'Emil Adolph von Behring, propose que l'immunité repose sur des éléments contenus dans le sérum, ce qui représente le premier énoncé des interactions antigènes/anticorps. En effet il explique que les toxines se lient aux cellules et organes grâce à des chaines latérales à la surface de ces cellules et organes. Plus précisément c'est une partie de la toxine, qui n'a pas d'activité toxique, qu'il appelle « haptophore » qui se lierait à ces chaînes latérales nommées « récepteurs », la partie active de la toxine, appelée « toxophore » ne serait fonctionnelle qu'après cette liaison. Les récepteurs situés à la surface des cellules servent, d'après Ehrlich, à la nutrition cellulaire en liant les éléments nutritifs. Dès lors qu'ils seraient liés à une toxine, ils seraient rendus inactifs et pour compenser la perte de fonction nutritive il y aurait une régénération de ces récepteurs. Les cellules produiraient alors des récepteurs en grand nombre. Cette « superproduction » conduirait à un phénomène particulier. La concentration des récepteurs devenue trop

importante, les amènerait à être décrochés des cellules et se retrouver à l'état libre dans la circulation sanguine où ils auraient la même capacité à lier les toxines. Ce faisant, après une immunisation par la toxine, ces récepteurs libres dans le plasma viendraient se lier aux toxines, les rendant inactives. Ce sont les anticorps (Ehrlich 1900). Il définira par la même occasion des composants de toxines ayant une toxicité nulle, qu'il appelle « toxoïdes », obtenus à la suite de différents traitements chimiques de la toxine. Il propose donc de les utiliser afin d'engendrer la production d'anticorps spécifiques de la toxine et d'obtenir une immunisation.

Parallèlement, l'immunologiste Ilya Illitch Metchnikov découvre la phagocytose. C'est en travaillant sur l'anémone de mer puis l'étoile de mer que Metchnikov s'aperçoit qu'il existe des cellules se déplaçant vers les sites infectieux avant de s'organiser afin de phagocyter les corps étrangers. Cette découverte lui vaut le prix Nobel de médecine en 1908 conjointement à Ehrlich. (voir : "The Nobel Prize in Physiology or Medicine 1908". *Nobelprize.org.* Nobel Media AB 2013. Web. 12 Aug 2013. http://www.nobelprize.org/nobel_prizes/medicine/laureates/1908/)

Malgré ce prix, l'immunité cellulaire n'est pas réellement prise au sérieux et l'immunité humorale est, selon les chercheurs de l'époque, le moyen principal de défense. Cette idée prédominera pendant plusieurs dizaines d'années.

Immunité cellulaire et Immunité humorale :

Dans les années soixante Rodney Porter et Gerald Edelman élucident la structure des anticorps. C'est Porter qui commence en utilisant la papaïne pour cliver des anticorps de lapin. Il propose ainsi que les anticorps se décomposent en trois parties dont une qui cristallise. Par la suite, Edelman apporte de nouvelles idées à Porter en démontrant que les anticorps sont formés non pas d'une mais de plusieurs chaines peptidiques liées entre elles par des ponts disulfures (Edelman 1959). Edelman continua à travailler sur ces différences structurelles et sur leur spécificité (Edelman et al. 1961). Porter quand à lui se sert des résultats de son confrère pour montrer que les anticorps se décomposent en quatre parties, deux chaînes lourdes et deux chaines légères (Porter 1973).

En parallèle, Jean Dausset, Baruj Benacerraf et George Davis Snell, partageant tous trois le prix Nobel de Physiologie ou Médecine en 1980, font des découvertes fondamentales au niveau de l'immunité cellulaire puisqu'ils sont à l'origine de la découverte du CMH

(Complexe Majeur d'Histocompatibilité). Jean Dausset travaillait, de son côté, sur les greffes de peau lorsqu'il découvrit que l'histocompatibilité était dépendante d'un complexe qu'il nomma Hu-1, qui deviendra par la suite HLA (Human Leucocyte Antigens) (Dausset et al. 1970). Benacerraf quand à lui découvrit un gène qu'il nomma Ir gene (Immune response gene) responsable de la résistance à certains antigènes dans des lignées hybrides de Cochons d'Inde (Benacerraf 1980). Enfin les travaux de Snell sur la souris lui ont permis de mettre en évidence le complexe H-2, analogue chez la souris du HLA, et fit avancer grandement la recherche concernant la transplantation d'organes (Snell 1980).

Jacques Miller, dans les mêmes années, est le premier à décrire le rôle du thymus (Miller 1963). En effet il se rend compte que des animaux nés sans thymus sont sensibles à de nombreux pathogènes et sont réceptifs à la transplantation, il démontre ainsi le rôle que joue cet organe dans l'immunité. Par la suite il découvre que les lymphocytes sont divisés en deux catégories : les « thymus-derived cells » qui sont les lymphocytes T et les « non thymus-derived antibody-forming cell precursors » qui sont les lymphocytes B. Il décrit par la même occasion le rôle de chacun de ces types cellulaires dans l'immunité adaptative (Miller and Sprent 1971).

C'est à partir de ces découvertes que l'immunité cellulaire et l'immunité humorale ne furent plus mises en compétition. Les deux furent étudiées comme deux composantes de l'immunité.

Les théories de l'Immunité moderne :

Les théories sur l'immunité sont alors gouvernées par la reconnaissance du soi et du non-soi, mais cela ne suffit pas pour expliquer l'étendue des capacités du système immunitaire. En 1989, Charles Janeway propose alors une théorie nouvelle (Janeway 1989). Il pense que le déclanchement de l'immunité adaptative se fait via l'immunité innée. Ainsi un nombre limité de récepteurs, les PRR (Pattern Recognition Receptors) seraient en mesure de reconnaitre des motifs microbiens, les PAMP (Pathogen-Associated Molecular Patterns). D'après lui, cette voie de reconnaissance de l'immunité innée serait dérivée des invertébrés qui, eux, n'ont pas d'immunité adaptative. Cette hypothèse d'abord mise à l'écart, a connu un essor dès lors que les différentes voies de reconnaissances de l'immunité innées furent découvertes notamment les voies des Toll-like Receptors correspondant ainsi à la première famille de PRR.

La théorie de Janeway servira par la suite de base à Polly Matzinger pour établir sa nouvelle hypothèse, la « Danger Theory » (Matzinger 1994). Elle part de l'idée que l'immunité innée ne reconnait pas les pathogènes mais des signaux de danger émis par les organes lésés. Ainsi ce ne sont pas les pathogènes mais leur capacité à créer des lésions qui sont au cœur de la reconnaissance. Ces mêmes lésions peuvent d'ailleurs être d'origine pathogénique ou d'origine chirurgicale, ce qui explique le rejet de greffes.

Cette théorie, alors très à la mode, souffre de beaucoup de confusions dans les différentes observations faites par la suite et la conclusion logique est que les théories de Matzinger et de Janeway s'entrecroisent probablement et viennent expliquer une grande partie des observations faites sur l'immunité (Janeway and Medzhitov 1998), mais il reste encore des zones d'ombre et de nombreuses années de recherches afin de comprendre l'intégralité de ces mécanismes extrêmement complexes. Ainsi, comme le souligne justement Ruslan Medzhitov dans son papier de 2009 (Medzhitov 2009), c'est la compréhension de tous ces mécanismes qui nous propulsera vers l'élaboration de vaccins permettant de lutter contre tous types de pathogènes, à moins que les pathogènes n'aient un autre point de vue…

Les travaux présentés dans ce prologue visent principalement l'étude de l'immunité chez les vertébrés, et plus particulièrement l'immunité adaptative puisque l'immunité innée a longtemps été délaissée. La raison de cet engouement pour l'immunité adaptative est très compréhensible. En effet, la base des recherches engagées dans le domaine de l'immunité avait un but appliqué. Il s'agissait de comprendre le fonctionnement de l'immunisation afin de lutter contre les maladies de bétails et les maladies Humaines. Ces derniers étaient donc les modèles privilégiés dans l'étude des mécanismes immunitaires adaptatifs. De plus la définition de l'immunité repose sur des paradigmes repris par Janeway dans sa théorie qui stipule que : « l'immunité innée serait peu spécifique, pauvrement régulée et ancestrale. Elle serait la base chez les invertébrés servant de fondation à l'immunité adaptative que seuls les vertébrés ont pu développer ».

Pourquoi les vertébrés auraient seuls pu être en mesure de développer cette immunité adaptative ?

Pourquoi les invertébrés en sont ils dépourvu ?

La première partie de mon introduction sera consacrée à vous présenter et à discuter ces arguments afin d'aboutir à une nouvelle vision de l'immunité innée et de remettre en cause ce paradigme.

Introduction

INTRODUCTION

L'immunité se divise en deux composantes essentielles : une composante appelée immunité innée. Elle intervient dans une première réponse et repose sur une reconnaissance rapide est peu spécifique basée sur des motifs de reconnaissances (PRR). La seconde composante est l'immunité adaptative, qui intervient après l'immunité innée, est extrêmement spécifique et présente un phénomène de mémoire. Cette immunité adaptative repose sur des mécanismes particuliers qui sont la diversification des récepteurs immunitaires, la multiplication clonale des populations lymphocytaires capable de répondre spécifiquement à l'antigène et par extension au pathogène et la mise en mémoire de l'information par des cellules dédiées. Tous ces mécanismes sont portés par des cellules particulières, les lymphocytes B et T. Les lymphocytes B sont des cellules qui vont, suite à la reconnaissance d'un antigène, produire et sécréter des immunoglobulines et également mettre l'information en mémoire afin de garantir une action plus rapide lors d'une seconde rencontre avec le même pathogène (Mauri and Bosma 2012). Les lymphocytes T, quand à eux, sont chargés de reconnaitre et détruire les cellules de l'hôte infectées par un pathogène (Bloom 1976)

Chez les Invertébrés, l'absence des différents mécanismes régissant l'immunité adaptative ainsi que l'absence des cellules sur lesquelles elle repose fût la base sur laquelle reposa l'affirmation que l'immunité chez les invertébrés était dépourvue de spécificité et de mémoire. De plus de nombreuses hypothèses ont été émises pour expliquer cette absence de système adaptatif.

Rang taxonomique, complexité, durée de vie

Parmi ces hypothèses émises pour expliquer l'absence de phénomènes adaptatifs chez les invertébrés, il ne peut en être une plus fausse que la classification en terme de rang taxonomique. En effet, certainement par un abus de langage ou par une simplification erronée certains chercheurs continuent à définir les groupes du règne animal suivant une graduation des « moins évolués » vers les « plus évolués » (Kiss 2010). Cette graduation ferait donc des invertébrés le groupe le moins évolué tandis que les mammifères seraient au sommet de l'évolution. On ne peut pas considérer l'évolution comme une ligne droite avec différents groupes disposés tout du long. L'évolution est complexe, et peut être représentée par un arbre d'où jaillissent des branches et chaque groupe, chaque espèce, aujourd'hui présente est à

l'extrémité de ces branches avec le même niveau d'évolution, chacune reliée par un ancêtre commun situé au pied de cet arbre. Pour aller plus loin, la notion même de groupe pour les invertébrés a été abandonnée puisqu'il ne représente pas un groupe monophylétique (Goloboff et al. 2009) mais que les différents taxa d'invertébrés sont largement répartis autour des vertébrés. Le terme d'invertébré ne sert aujourd'hui qu'à définir un animal dépourvu de chorde ou notochorde associée aux somites métamérisés.

Une autre théorie avancée est celle de la complexité des organismes. Ainsi les organismes vertébrés seraient plus complexes que les invertébrés. Cette complexité à la fois morpho-anatomique et physiologique serait à la base de la complexité du système immunitaire. Encore un argument litigieux dans le sens où on trouve un panel d'animaux extrêmement variés chez les invertébrés. Qu'il s'agisse des cnidaires, des décapodes ou des mollusques, comment évaluer leur complexité ? Comment se risquer à dire qu'un poulpe est moins complexe qu'un poisson, qu'un homard est moins complexe qu'une grenouille ? Concernant leurs systèmes immunitaires les mêmes interrogations peuvent se poser. La grande diversité des réponses immunitaires mises en place au sein des différents taxa d'invertébrés reflète parfaitement la diversité morpho-anatomique de ces organismes (Loker et al. 2004).

Enfin l'argument principal mis en avant pour expliquer l'absence de système immunitaire adaptatif chez les invertébrés est la durée de vie des individus. En effet, les vertébrés et invertébrés ont longtemps été différentiés par les stratégies sélectives adoptées à savoir stratégie r ou stratégie K (Pianka 1970). Ainsi, les vertébrés ont été considérés comme des animaux adoptant une stratégie K caractérisée principalement par :

- une longue durée de vie
- une grande taille
- un développement lent
- une reproduction tardive
- un faible nombre de descendants

Alors que les invertébrés ont plutôt été considérés comme ayant adopté une stratégie r caractérisée à l'opposé par :

- une courte durée de vie
- une petite taille
- un développement très rapide

- une reproduction précoce
- un grand nombre de descendants

Cette définition étendue à l'immunité donne naissance à l'idée que les espèces adoptant une stratégie r (les invertébrés) n'auraient aucun besoin de posséder une immunité extrêmement développée, complexe, spécifique et principalement qu'ils ne devraient pas posséder une immunité adaptative alors que cette dernière deviendrait nécessaire chez les espèces adoptant une stratégie K (les vertébrés) (Medzhitov and Janeway 1997). Une fois de plus il est difficile de classer aussi strictement les invertébrés et les vertébrés dans ces catégories. On connait aujourd'hui des vertébrés ayant une courte durée de vie et une fécondité forte, le record étant détenu par un poisson de récif *Eviota sigillata* qui a une durée de vie de 8 semaines (Depczynski and Bellwood 2005). A l'opposé, des organismes invertébrés peuvent vivre très longtemps, comme le homard (31 ans pour le mâle et 54 ans pour la femelle en moyenne) (Sheehy et al. 1999), de nombreux mollusques vivent au-delà de 100 ans (Bodnar 2009) et le record de longévité pour un animal est détenu par un bivalve d'Islande, la cyprine (*Arctica islandica*) ayant 374 ans (Schone et al. 2005), ce qui le place loin devant les tortues géantes des Galápagos, *Chelonoidis spp* (150 à 200 ans) et la baleine boréale, *Balanea mysticetus* (115 à 130 ans). De plus, des travaux récents ont revu ces concepts pour les mettre à jour en montrant que même pour des individus possédant une stratégie r il y aurait des avantages sélectif à mettre en place une reconnaissance immunitaire spécifique (Rolff and Siva-Jothy 2003; Schulenburg et al. 2007).

Une nouvelle vision

En considérant tout ceci on est en droit de revoir un peu notre point de vue et de reconsidérer tous ces paradigmes établis depuis de nombreuses années sur l'immunité. Ainsi depuis maintenant 30 ans de nombreux chercheurs remettent en cause cette vision simpliste de l'immunité chez les invertébrés.

L'immunité adaptative des Gnathostomes repose sur une spécificité de reconnaissance et un phénomène de mise en mémoire. Concernant la spécificité de reconnaissance, elle est liée à différents mécanismes de diversification des récepteurs immuns. Tout d'abord il s'agit du Complexe Majeur d'Histocompatibilité (CMH). Ce sont des glycoprotéines portées par différents types cellulaires qui ont la capacité de lier divers peptides. Ce complexe ainsi formé sera présenté aux lymphocytes T (CD4 ou CD8) qui vont alors prendre en charge ces cellules

infectées présentant des peptides de non-soi en les lysant directement (CD4) ou en s'associant avec les lymphocytes B afin de produire des anticorps spécifiques du peptide (CD8) (Bernatchez and Landry 2003). La diversité des molécules du CMH est liée au nombre impressionnant de gènes qui les codent mais également au nombre de versions alléliques existant pour chacun de ces gènes (Bernatchez and Landry 2003). Dans cette spécificité de reconnaissance intervient également les Immunoglobulines (Ig) et les T-Cell Receptors (TCR), également très diversifiés. La diversification des Ig et TCR passe par un mécanisme différent de celui du CMH. En effet les *loci* des Ig et TCR sont organisés de la même manière. Il s'agit d'une succession de trois segments géniques nommés Variable (V), Diverse (D) et Joining (J), codant le domaine variable des Ig ou des TCR. Lors de la différentiation et maturation des lymphocytes dans la moelle osseuse les segments géniques V (D) J sont réarrangés par recombinaisons somatiques pour former les gènes fonctionnels codant pour les Ig ou les TCR. Cette recombinaison ce fait grâce à la présence de RAG1 et RAG2 (Recombination Activating Gene), deux enzymes de recombinaison (Du Pasquier 2001).

Ce sont ces deux mécanismes qui définissent la première composante de l'immunité adaptative. Cependant il existe une exception. Cette exception est retrouvée chez les Agnathes (Lamproies et Myxines). En effet ces « vertébrés sans mâchoire » sont dépourvus des mécanismes de diversifications des récepteurs de Gnathostomes (système V(D)J, enzymes RAG, gènes CMH). Pourtant il ne faisait aucun doute que ces animaux pouvaient être immunisés suite à une première exposition à un pathogène (Hagen et al. 1985) et avaient également la capacité de rejeter des allogreffes (Finstad and Good 1964). Les mécanismes de cette immunité ont été résolus très récemment et reposent sur l'existence de cellules immunitaires proches des lymphocytes (Pancer et al. 2004). De nouveaux récepteurs, contenant des zones répétées riches en Leucines (Leucin-Rich Repeats ou LRR), ont été découverts et nommés VLR (Variable Lymphocytes Receptors). En effet ces récepteurs sont produits principalement dans les lymphocytes et sont très diversifiés. Il existe chez la Lamproie deux gènes VLR-A et VLR-B codant les VLR. Les lymphocytes ne vont produire qu'un seul type de VLR. Les VLR-A seront produits et exprimés uniquement à la surface des lymphocytes alors que les VLR-B vont être produits et secrétés à la suite d'une stimulation par un pathogène (Pancer et al. 2004). Il existe donc deux types de lymphocytes chez les Lamproies, ceux qui expriment les VLR-A en surface (similaires aux lymphocytes T des Gnathostomes) et ceux qui produisent et sécrètent les VLR-B (similaires aux lymphocytes B des Gnathostomes) (Guo et al. 2009).

Ce système de diversification est suffisamment proche de celui des Gnathostomes pour avoir été classé dans la composante adaptative de l'immunité. Il représente donc une exception à la première définition de cette composante.

Qu'en est-il alors de l'immunité chez les invertébrés ?

L'immunité chez les Invertébrés

Si il est désormais clair que les pathogènes représentent la force sélective majeure de l'évolution de leurs hôtes (Howard 1991), il est également clair que les invertébrés sont confrontés à un panel aussi important de pathogènes que les vertébrés (Loker et al. 2004). La vision archaïque de l'immunité simple reposant sur une reconnaissance très peu spécifique par les PRR (Pattern Recognition Receptors) reconnaissant des PAMP (Pathogen-Associated Molecular Patterns) (Medzhitov and Janeway 1997) doit être réétudiée. Une reconnaissance si peu spécifique ne permet pas d'expliquer la capacité qu'ont les invertébrés à reconnaitre le large éventail de pathogènes auxquels ils sont confrontés (Hauton and Smith 2007). Il existe aujourd'hui de nombreuses études ayant pu mettre en évidence des molécules très diversifiées avec des rôles potentiellement immunitaires chez différentes espèces d'invertébrés.

C'est notamment le cas des VCBP (Variable Chitin-Binding Protein) de l'amphioxus. Ce Céphalocordé possède des molécules appartenant à la superfamille des immunoglobulines (IgSF) constituées de deux domaines de type immunoglobuline apparenté au domaine V (IgV-like) disposés en tandem et d'un domaine de liaison à la chitine (Chitin-Binding Domain ou CBD). Ces molécules sont réparties dans 5 familles (VCBP1 à 5), codées par une famille multigénique et secrétées (Cannon et al. 2002). Il a également été mis en évidence une forte variabilité de ces molécules liées au nombre de gènes et à des insertions/délétions au sein de chaque gène. La région génique codant les VCBP est riche en régions répétées inversées favorisant les évènements de recombinaison, de duplication de gènes et de délétion. Ceci explique le fort taux de polymorphisme retrouvé pour ces molécules (Dishaw et al. 2008). Bien qu'il n'existe aucune preuve que ces molécules soient impliquées dans l'immunité, la présence des deux domaines pourraient jouer un rôle dans des interactions avec des pathogènes. Le domaine IgV-like se lierait de manière spécifique au pathogène tandis que le CBD se lierait à la N-acétylglucosamine présente dans la chitine des bactéries et des champignons (Litman et al. 2005).

Chez les Echinodermes et plus particulièrement l'oursin *Strongylocentrotus purpuratus*, ce sont deux familles de molécules polymorphes et diversifiées qui ont été

découvertes. Les premières, bien connues dans différents groupes (Spongiaires, Nématodes, Echinodermes, Agnathes, Mammifères) sont les « Scavenger Receptor Cystein-Rich » (SRCR). Cette superfamille de molécules, connue pour son rôle immunitaire (reconnaissance ou régulation de la réponse), se caractérise par la présence de plusieurs domaines SRCR, domaine de 110 acides aminés contenant 6 ou 8 cystéines à des positions conservées (6 cystéines chez l'oursin) (Pancer et al. 1999). Chez l'oursin il existe 7 types de SRCR différents par le nombre de domaines SRCR et la présence d'autres domaines protéiques. Ces SRCR sont codés par une famille multigénique d'au moins 150 membres (Pancer 2000). Là encore, leur fonction n'a pas été élucidée même si la nature des domaines protéiques, leur fonction chez d'autres espèces et le fait qu'elles soient secrétées par les cœlomocytes (cellules immunitaires) chez l'oursin, laisse fortement présager de leur rôle dans la défense immunitaire de l'oursin (Pancer et al. 1999; Pancer 2000). La seconde famille découverte chez l'oursin a été appelée Sp185/333. Cette famille multigénique est composée de 50 à 60 membres, et la diversité des protéines produites vient de deux phénomènes. Tout d'abord, ces protéines sont constituées de 25 blocks de séquences nommés « éléments » (Nair et al. 2005). La présence/absence de certains de ces éléments constitue un premier niveau de diversification. Le second niveau de diversification est lié à la variation nucléotidique générée par des mutations ponctuelles ou des évènements d'insertion/délétion (Terwilliger et al. 2006). Cette fois encore la fonction n'a pas été démontrée mais les protéines Sp185/333 ne sont exprimées que dans les cœlomocytes, et il a été observé une augmentation de leur niveau d'expression ainsi qu'une augmentation de certains variants protéiques particuliers suite à l'injection de Lipopolysaccharides (LPS) (Nair et al. 2005; Terwilliger et al. 2006), indiquant probablement un rôle dans l'immunité.

Chez les Arthropodes, les Down Syndrom Cell Adhesion Molecules (Dscam) appartiennent à la superfamille des immunoglobulines et leur rôle dans l'immunité n'a que récemment été démontré suite à des travaux sur la drosophile, *Drosophila melanogaster* (Watson et al. 2005), et le moustique, *Anopheles gambiae* (Dong et al. 2006). Ces molécules ne sont codées que par un seul gène (*Dscam*) possédant 24 exons. Par des évènements de duplication les exons 4, 6, 9 et 17 sont présents en de nombreuses copies et la diversité des Dscam est liée à un épissage alternatif de ces différents exons. Il a également été montré que seuls les hémocytes (cellules immunitaires) exprimaient une telle diversité de Dscam et que la réduction de l'expression de ce gène par de l'ARN interférant entraînait une baisse de l'activité de phagocytose chez la drosophile et le moustique (Watson et al. 2005; Dong et al. 2006). Par la même occasion il a été démontré (Dong et al. 2006) que les répertoires de

Dscam exprimés par *Anopheles gambiae* étaient différents en réponse à deux espèces de *Plasmodium* (*P. falciparum* et *P. berghei*).

Chez les Mollusques et dans notre modèle d'intérêt en particulier, *Biomphalaria glabrata*, de telles molécules existent également. Ce sont les Fibrinogen Related Proteins (FREP). Elles ont été décrites comme étant des protéines solubles, secrétées dans l'hémolymphe du mollusque, produites par les hémocytes et pouvant précipiter des antigènes solubles de trématode (Adema et al. 1997). Ces FREP sont constituées de un ou deux domaines de type immunoglobuline (IgSF) et d'un domaine fibrinogène (FBG) contenant un site potentiel de liaison aux résidus glucidiques (Carbohydrate Recognition Domain ou CRD) (Zhang et al. 2001). Elles sont codées par une famille multigénique d'au moins 14 membres (Hanington and Zhang 2011) et la diversité de ces molécules est considérable. En effet l'étude du seul domaine IgSF1 de FREP3 a révélé une très grande diversité engendrée par des phénomènes de recombinaisons et de mutations ponctuelles (Zhang et al. 2004). De plus ces molécules sont induites lors d'interactions avec des pathogènes (bactéries, Trématodes) (Adema et al. 2010; Hanington et al. 2010a). En parallèle au sein du laboratoire il a pu être mis en évidence une famille de molécules extrêmement polymorphe et diversifiée chez un parasite naturel de *B. glabrata*, *Schistosoma mansoni*. Ces molécules ont été nommées *Sm*PoMuc (*Schistosoma mansoni* Polymorphic Mucins). Elles sont constituées d'une partie contenant des unités répétées portant des glycosylations et d'une partie conservée, et ne sont exprimées que dans les stades interagissant avec le mollusque. Elles possèdent un peptide signal indiquant une possible secrétion (Roger et al. 2008a; Roger et al. 2008b). De plus il a été démontré que ces molécules était polymorphes/diversifiées au niveau génomique et transcriptomique (famille multigénique, recombinaison ectopique, épissage alternatif/aberrant ou trans-épissage) mais également au niveau protéique par la quantité et la qualité des glycosylations associées à ces molécules (Roger et al. 2008c). Par la suite, différentes approches d'interactome entre de l'hémolymphe de mollusque et des extraits protéiques de parasite ont pu mener à l'observation que les FREP de *B. glabrata* interagissent avec les *Sm*PoMuc de *S. mansoni* (Mone et al. 2010). Ceci constitue la première mise en évidence chez un invertébré de l'interaction entre un récepteur immun diversifié (FREP) et un déterminant antigénique parasitaire (SmPoMuc)

Etant donné la masse de résultats accumulés concernant des molécules diversifiées ayant des potentiels immunitaires, provenant d'invertébrés, on est en droit de se demander si la vision actuelle de l'immunité adaptative ne doit pas être repensée. Ainsi, de nombreux chercheurs commencent à se dire que la terminologie employée n'est peut être pas la bonne et

qu'il y a plusieurs façon possible d'avoir une immunité adaptative en terme de mécanismes de diversification (Du Pasquier 2004). Peut être devons nous voir cette diversification de ces molécules de reconnaissance à potentiel immunitaire comme étant un moyen différent, sélectionné de manière indépendante par les invertébrés sous les pressions de sélection représentées par les pathogènes, afin de se défendre et de neutraliser ces derniers. D'autres auteurs vont encore plus loin en affirmant que la vision mécanistique de l'immunité adaptative a retardé de manière conséquente la recherche concernant l'immunité chez les invertébrés (Little et al. 2005). Pourquoi ne pas reconsidérer la question de l'immunité adaptative avec un œil nouveau, en oubliant les mécanismes connus chez les vertébrés et en partant simplement d'observations de descriptions phénotypiques des processus chez les invertébrés (Little et al. 2005; Vinkler and Albrecht 2011)

Qu'en est-il de la mémoire immunitaire ?

Il est, je pense, clair maintenant que les invertébrés font face à un éventail de pathogènes au moins aussi étendu que les vertébrés et que sous cette pression sélective ils ont développé des moyens leur permettant de diversifier des molécules de reconnaissance afin de lutter de manière spécifique contre ces pathogènes.

Si les invertébrés sont donc capables de hauts niveaux de spécificité dans la reconnaissance, pourquoi n'existerait-il pas également chez ces derniers la possibilité d'observer des processus de mémoire immunitaire ?

De nombreux travaux au cours des 15 dernières années ont pu mettre en évidence que la réponse à cette question n'est pas si évidente.

C'est en remarquant que plusieurs allogreffes successives sur du corail étaient rejetées de plus en plus rapidement que Hildemann fût le premier à suggérer l'existence d'une mémoire immunitaire chez un organisme invertébré (Hildemann et al. 1977). Plus tard il a pu être démontré chez la blatte américaine (*Periplaneta americana*) qu'une réponse comprenant deux phases se mettait en place suite à une première infestation par des bactéries (Faulhaber and Karp 1992). La première phase correspond à une réponse immunitaire forte mais non-spécifique qui dure 3-4 jours et la seconde phase constitue une réponse spécifique de la première immunisation et dure plus de 14 jours. Cette réponse présente, selon Faulhaber des caractéristiques claires de l'immunité adaptative. Par la suite les exemples se multiplient dans différents modèles apportant des observations plus précises laissant supposer l'existence d'une mémoire immunitaire chez les invertébrés (Kurtz and Franz 2003; Kurtz 2004, 2005;

Sadd and Schmid-Hempel 2006; Vazquez et al. 2009; Rodrigues 2010). Ces travaux mettent toutefois en avant deux hypothèses principales quant à la mise en place de ces phénomènes de mémoire ou priming immunitaire :

- Une réponse maintenue se met en place suite à la première rencontre et perdure sous la forme d'une réponse plus ou moins spécifique de longue durée et qui persiste même si le pathogène de la première rencontre est éliminé (Little and Kraaijeveld 2004).
- Une réelle mémoire se met en place avec un stockage de l'information et une réponse plus rapide et plus forte lors de la seconde rencontre avec le même pathogène (Kurtz 2005).

Quoi qu'il en soit cette immunité de type mémoire ne faisant pas appel aux mécanismes connus chez les vertébrés a été nommée priming immunitaire chez les invertébrés. En effet, en matière de terminologie le problème est épineux. Les termes attribués aux définitions de l'immunité manquent de flexibilité. Ainsi l'immunité adaptative fait référence à l'immunité des vertébrés et aux mécanismes associés. Pourtant, de manière intrinsèque l'immunité des invertébrés semble présenter certains caractères adaptatifs, dans le sens où ils s'adaptent à un pathogène afin de mieux répondre lors d'une seconde rencontre. De la même façon, ce terme de mémoire immunitaire est attribué à la mémoire immunitaire des vertébrés et aux mécanismes qui lui sont propres. C'est pour contourner ce problème que le terme de priming immunitaire a été donné au phénomène de réponse accrue lors d'une seconde rencontre, sans tenir compte de la manière dont cette réponse se manifeste (réponse maintenue ou réponse de type mémoire). Là encore un problème se pose puisque le terme de priming désigne avant tout la première rencontre avec un pathogène, le fait d'être exposé, sans tenir compte d'ailleurs du fait que l'hôte soit vertébré ou invertébré. Le but de ma thèse n'étant pas de résoudre ces questions étymologiques, le terme de priming immunitaire sera ici employé afin de définir l'ensemble du phénomène de première rencontre, d'adaptation et de réponse immunitaire améliorée lors d'une seconde rencontre.

Le priming immunitaire chez les invertébrés :

Kurtz fut l'un des premiers à présenter un phénomène immunitaire mémoire chez un invertébré (Kurtz and Franz 2003). Toutefois dans cette expérience, le temps séparant la primo-infection et le challenge n'était que de 4 jours et il est donc possible que la protection

observée ne soit simplement qu'une réponse à la première infection qui perdurerait quelques jours. Kurtz considère être en présence d'un réel processus immunitaire mémoire, bien que ne reposant pas sur des mécanismes similaires à ceux des vertébrés (Kurtz 2004, 2005). Un phénomène de priming immunitaire a été démontré chez le ver de farine *Tenebrio molitor* (Moret and Siva-Jothy 2003). En effet, en injectant des LPS à des larves de *Tenebrio* il en résulte une réponse immunitaire maintenue qui protège la larve face à un champignon pathogène *Metarhizium anisopliae*. En 2006 il fut démontré que le bourdon *Bombus terrestris* présentait, au même titre que la blatte américaine, un priming immunitaire spécifique. En injectant au bourdon un pathogène précis puis en challengeant ce dernier à l'aide de pathogènes différents il a pu être observé une protection non spécifique lorsque les injections ne sont espacées que de 8 jours, puis une protection spécifique (seule l'injection du pathogène homologue induit une protection) lorsque la primo-infection et le challenge sont espacés de 22 jours (Sadd and Schmid-Hempel 2006). Une réponse de priming immunitaire spécifique a également été démontrée chez la drosophile suite à une infestation par un streptocoque (Pham et al. 2007). Chez la crevette *Penaeus monodon* il a été démontré une réponse de mémoire immunitaire suite à une infection virale (Whitespot Syndrom Baculovirus complex ou WSSV). L'utilisation de protéines de l'enveloppe virale de WSSV dans des approches de vaccination montre en effet l'acquisition d'une résistance accrue à la ré-infection par WSSV (Witteveldt et al. 2004). Toutefois, Johnson et collaborateurs (Johnson et al. 2008) supposent que cette protection n'est en rien immunitaire chez *Penaeus*, mais repose sur le fait que les protéines de l'enveloppe virale injectées bloqueraient les récepteurs cellulaires à la surface des cellules cibles et ainsi empêcherait la liaison virus/cellule et l'internalisation du virus par endocytose. Chez l'isopode *Porcelio scaber*, il a été démontré *in vitro* que les capacités de phagocytoses de ses cellules immunitaires étaient augmentées suite à l'injection de bactéries tuées (Roth and Kurtz 2009). Par la suite, le même auteur rapporte un priming immunitaire spécifique chez le coléoptère *Tribolium castaneum* (Roth et al. 2009).

En plus de toutes ces observations de priming immunitaire chez de nombreuses espèces d'invertébrés, il faut également considérer une autre composante de l'immunité liée au mode de vie de certains invertébrés et qui est appelée « l'immunité sociale ». En effet chez les insectes sociaux il est facilement compréhensible qu'une infection peut rapidement se propager et éliminer toute une colonie. Il a ainsi été démontré chez la termite *Zootermopsis angusticollis* qu'il existait un phénomène de priming social qui engendre une meilleure survie d'une colonie lorsqu'un individu ayant expérimenté et survécu à une infection par le

pathogène *Metarhizium anisopliae* (Champignon) est introduit dans la colonie (Traniello et al. 2002). Ce transfert d'immunité peut se faire de deux façons d'après les auteurs, soit les individus s'échangent des quantités sub-létales spores de champignon afin de s'immuniser les un les autres lorsqu'ils se nettoient ou alors ils s'échangeant des facteurs immunitaires ou activateurs de l'immunité lors de trophallaxie (régurgitation d'éléments nutritifs pour d'autres individus). Ce transfert d'immunité a également été démontré chez d'autres hymenoptères, les fourmis *Camponotus pennsylvanicus* (Hamilton et al. 2011) et *Lasius neglectus* (Konrad et al. 2012). Chez *Camponotus pennsylvanicus* suite à une infection bactérienne il a pu être mis en évidence que les contenus de régurgitation avaient une plus grande activité antibactérienne. Le transfert d'immunité se ferait donc par trophallaxie (Hamilton et al. 2011). Chez *Lasius neglectus* c'est la réponse face à un champignon qui est étudiée. Cette fois ci, aucune activité antifongique augmentée n'est observée dans les produits issues de régurgitation suite à l'immunisation, en revanche il pourrait s'agir ici de transfert prophylactique de spores dans des quantités sub-létales, au travers du toilettage collectif des individus (Konrad et al. 2012).

Enfin, le priming immunitaire semble parfois pouvoir être transmis à la descendance. Ce phénomène largement étudié a été nommé « transfert trans-générationnel d'immunité » ou TTGI(Little et al. 2003; Sadd et al. 2005; Moret 2006). Ce transfert, réalisé au travers des œufs, peut être maternel ou paternel en fonction des espèces et peut selon les espèces concerner tous les stades de développement de l'hôte (Sadd and Schmid-Hempel 2007; Roth et al. 2010; Zanchi et al. 2011; Moreau et al. 2012).

Sans remettre en cause l'existence d'un priming immunitaire chez de nombreuses espèces d'invertébrés, il existe quand même des espèces chez qui un tel phénomène n'a jamais pu être mis en évidence. Ainsi, il n'y aurait aucun priming immunitaire chez la libellule *Hetaerina americana* (Gonzalez-Tokman et al. 2010) ni chez la fourmi *Formica selysi* (Reber and Chapuisat 2012).

Tout ceci montre encore une fois que l'immunité n'est pas quelque chose de simple, hérité d'un ancêtre et qui se serait complexifié avec la divergence des espèces. Il semblerait au contraire que chaque espèce ait sélectionné différentes façons de se protéger face à la pression exercée par les pathogènes. Tandis que certains ont optés pour des stratégies individuelles, d'autres ont choisis des stratégies de groupe et d'autres encore ont mis en place un transfert héréditaire de la protection.

Pour aller plus loin il est maintenant nécessaire de comprendre les mécanismes régissant ces phénomènes. En effet, si l'on veut convaincre et être convaincu de l'existence d'un genre d'adaptation dans l'immunité il est nécessaire d'en connaître les mécanismes (Rowley and

Powell 2007). Il semble donc évident que la prochaine étape est d'avoir une meilleure compréhension des mécanismes moléculaires sous jacents au priming immunitaire chez les invertébrés.

Les mécanismes du priming immunitaire

Une chose bien établie concernant la mémoire immunitaire chez les invertébrés est qu'elle ne repose pas sur des mécanismes moléculaires similaires à ceux connus chez les vertébrés. Pourtant les chercheurs sont tous d'accord sur ce point : on ne pourra parler de mémoire immunitaire que lorsque les mécanismes seront identifiés. A ce jour, peu de travaux se sont intéressés à cette question. Ces travaux ont pu mettre en évidence quelques pistes sur la mise en place de ce priming immunitaire.

- Chez *Tenebrio molitor* une augmentation de l'activité antimicrobienne a été observé suite à une immunisation par des LPS (Moret and Siva-Jothy 2003).
- Chez *Porcelio scaber* une augmentation de l'activité de phagocytose a été démontrée suite à une immunisation (Roth and Kurtz 2009).
- Chez *Anopheles gambiae* une différentiation des hémocytes et une sur-expression de gènes immunitaires, Thioester-containing protein 1 (TEP1) et Leucin rich repeat immune protein 1 (LRIM1) ont été démontrées suite à une primo-infection bactérienne générant une meilleure protection à la ré-infestation par le *Plasmodium* (Rodrigues 2010).
- Chez *Chlamys farreri* une induction de l'expression de C-type lectines a été démontrée suite à une immunisation par un *Vibrio* (Wang et al. 2013).

Une fois de plus, la diversité de ces mécanismes montre la complexité et l'hétérogénéité des différentes réponses mises en place par les différents organismes au cours de l'évolution. Il reste encore énormément de chemin à parcourir avant de cerner l'étendu des phénomènes et des mécanismes régissant l'immunité des invertébrés. Ce qui est sûr c'est qu'il nous faut partir avec un œil neuf, démarrer des phénotypes, afin d'aiguiller les recherches vers l'identification des voies moléculaires impliquées et vers la compréhension de ces réponses de priming immunitaire chez les invertébrés.

Aux vues de ces questions, il est donc nécessaire afin d'aller plus loin de posséder un modèle biologique adapté permettant d'appréhender l'ensemble de ces aspects tant phénotypiques que moléculaires. Au cours de ma thèse, j'ai donc eu l'occasion de travailler avec un modèle

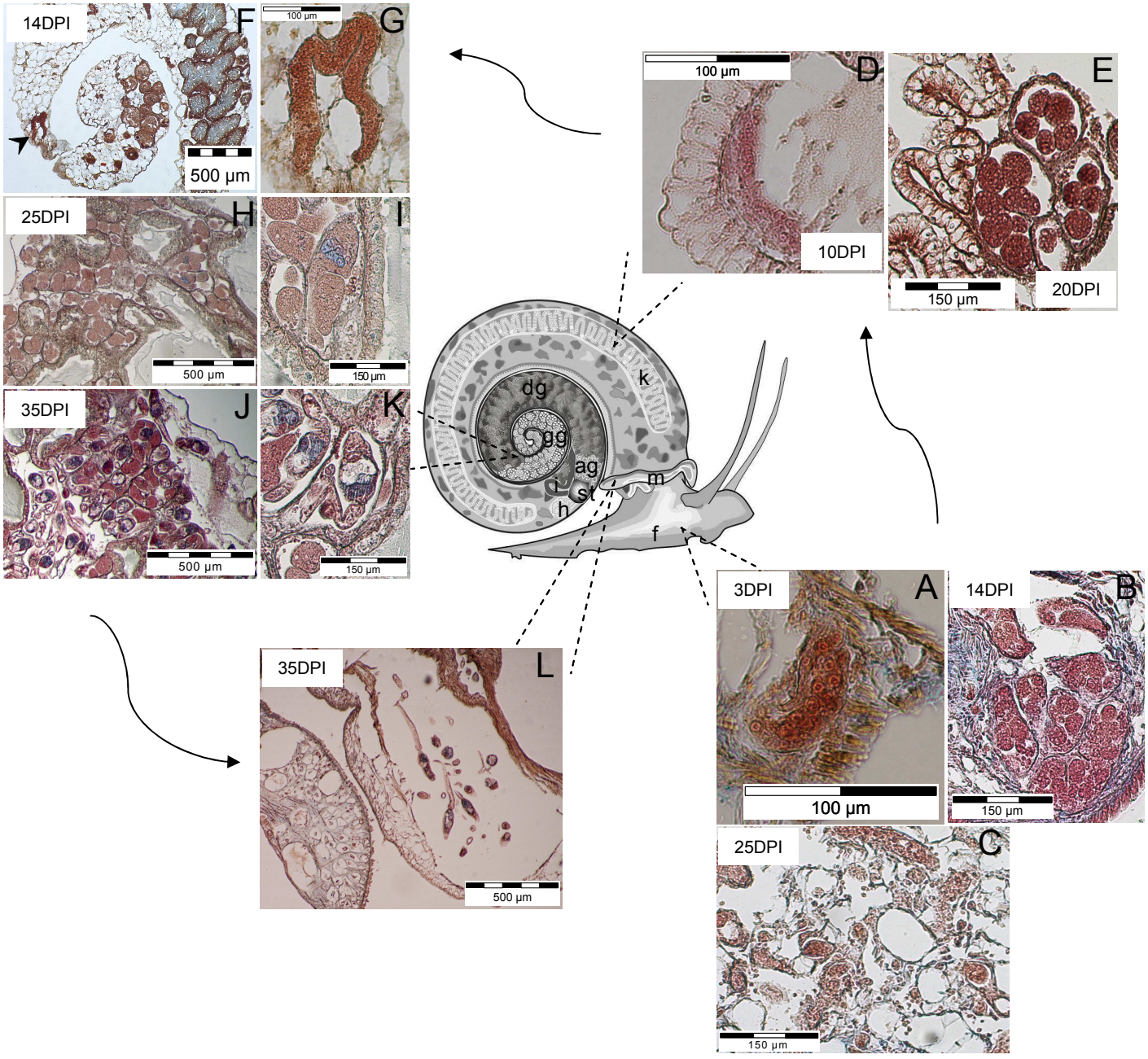

Figure 1 : Développement intramolluscal de *Schistosoma mansoni* dans les tissus de son hôte intermédiaire Biomphalaria glabrata.

A. SpI dans le pied du mollusque 3 jours après pénétration. B. SpI 14 jours après pénétration C. SpI dégradé 25 jours après pénétration. D. SpII en migration dans le rein 10 jours après pénétration du miracidium. E. Plusieurs SpII en migration dans le rein (20 jours). F. et G. SpII à l'interface gonade/glande digestive (14 jour). H. et I. Cercaires en formation dans les SpII (25 jours). J. et K. Cercaires prêtes à migrer (35 jours). L. Cercaires en migration dans le manteau (35 jours).

biologique impliquant l'interaction de deux Lophotrochozoaires le mollusque d'eau douce *Biomphalaria glabrata* et son parasite le trématode *Schistosoma mansoni*. En quoi ce modèle est particulièrement adapté à l'étude du priming immunitaire ? Comment nous permettrait-il de répondre aux questions essentielles qui se posent sur les mécanismes moléculaires du priming immunitaire ?

Le modèle : Biomphalaria glabrata (Say, 1818)/Schistosoma mansoni (Sambo, 1907)

Le mollusque d'eau douce *Biomphalaria glabrata* est un gastéropode pulmoné de la famille des planorbidés vivant dans les eaux douces des régions tropicales et subtropicales d'Amérique. De manière générale les mollusques du genre *Biomphalaria* sont les hôtes intermédiaires, en Amérique et en Afrique, du parasite trématode *Schistosoma mansoni* responsable de la bilharziose humaine (2nde maladie parasitaire mondiale en termes de mortalité et morbidité). Au sein du mollusque, le parasite va se métamorphoser, passant de l'état miracidium (Mi) qui est la larve nageante infestante du mollusque, à l'état de cercaire qui est la larve nageant infestante pour l'homme. Pour ce faire, différents stade de développement intra-molluscaux sont nécessaires : le sporocyste primaire (SpI) et le sporocyste secondaire (SpII). Après pénétration dans les tissus du mollusque, le miracidium va perdre immédiatement ses plaques ciliées (permettant la nage). Se faisant il va mettre en place un nouveau tégument de type syncytial et prendre une forme allongée présentant des repliements tégumentaires (Jourdane and Théron 1987) (Figure 1 A). Les cellules germinales qu'il contient vont alors grossir avant de se multiplier afin que le SpI se développe. Par la suite des clusters de cellules vont s'entourer d'un épithélium puis devenir des Sporocystes secondaires (SpII) contenu à l'intérieur du SpI (Figure 1 B). Lorsque ces SpIIs sont matures, ils sont libérés par le SpI dans les tissus du mollusque et vont alors réaliser une migration pour rejoindre la glande digestive (Figure 1 D, E, F et G). Arrivés à cette localisation, les SpIIs vont poursuivre leur développement, les cellules germinales qu'ils contiennent vont entrer en multiplication et se différentier pour former les cercaires (larves nageantes infestantes pour l'hôte définitif vertébrés) (Figure 1 H, I, J et K). Une fois à maturité les cercaires vont réalisées une migration inverse dans le mollusque afin de rejoindre le milieu extérieur aquatique afin de trouver un hôte définitif vertébré afin de poursuivre son cycle parasitaire (Jourdane and Théron 1987) (Figure 1 L). A partir d'un miracidium il est possible d'obtenir

Hôte définitif : Vertébré

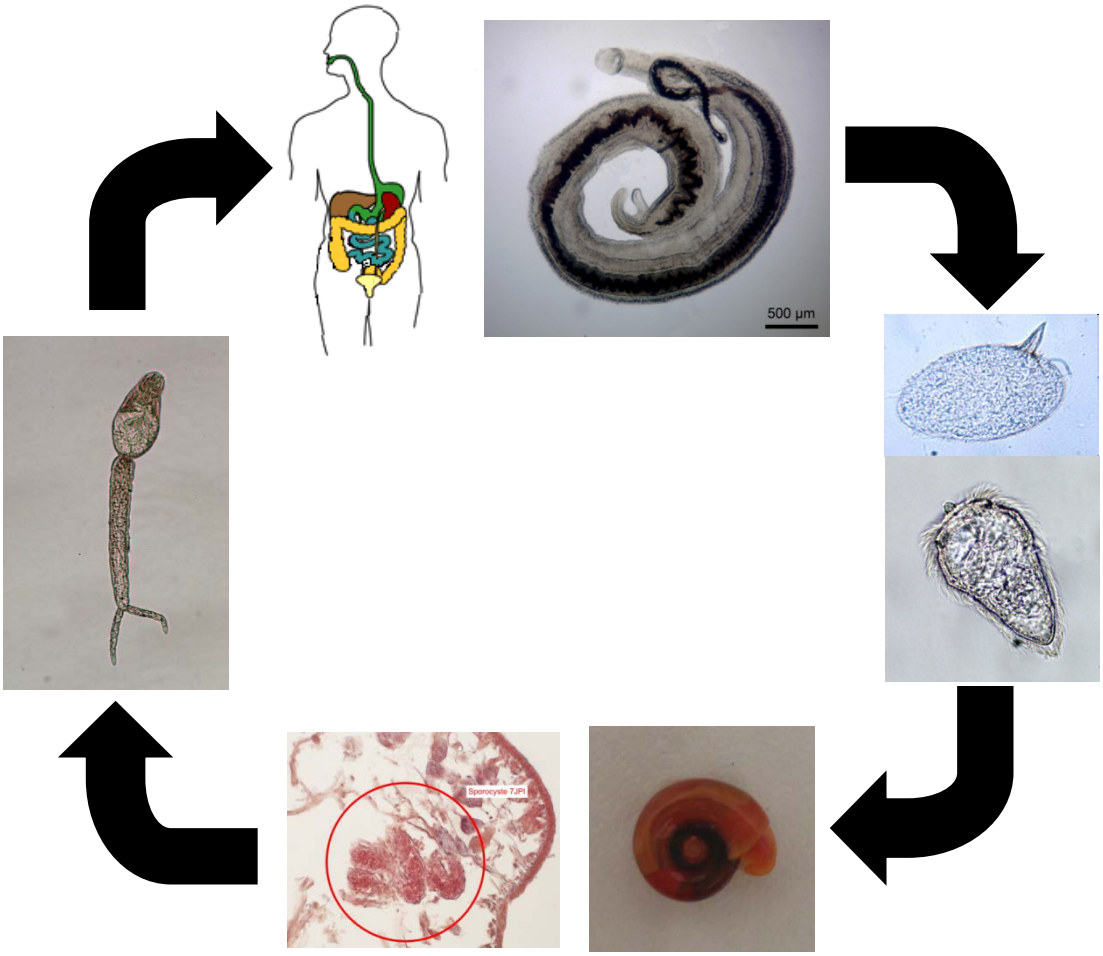

Hôte intermédiaire : *Biomphalaria glabrata*

Figure 2 : Cycle de vie de *Schistosoma mansoni*

des milliers de cercaires, le mollusque est donc le siège d'une importante multiplication clonale asexuée du parasite.

La suite du cycle se passe chez le vertébré. La tête de la cercaire se détache de la queue lors de la pénétration. Cette tête de cercaire appelée schistosomule va alors pénétrer dans la circulation sanguine pour effectuer une première étape de migration jusqu'aux poumons. Elles vont alors y maturer afin d'entamer la deuxième partie de leur migration jusqu'à leur point de « rendez-vous » au niveau du foie. C'est ici que les couples se forment. La femelle choisit son mâle et s'insère dans son canal gynécophore. Le couple va alors se diriger vers les capillaires mésentériques tout autour du tube digestif et les femelles vont se mettre à pondre. Les œufs passent alors vers la lumière du tube digestif à l'aide de l'éperon qu'ils possèdent et des mouvements péristaltiques. C'est lors de cette délicate étape qu'une partie des œufs (environs 50%) va échouer et se faire emporter par la circulation sanguine jusqu'à venir dans le foie et s'y retrouver enkysté. Le principal symptôme de la maladie est lié à ces œufs perdus qui vont engendrer des saignements, des ulcérations et une augmentation importante de la taille du foie. C'est aussi cette particularité que nous utilisons pour récupérer un grand nombre d'œufs par dissection du foie de souris malades lors de l'entretien de nos cycles parasitaires. Les œufs ayant réussi leur passage dans la lumière du tube digestif seront alors émis vers l'extérieur et au contact de l'eau douce et sous une stimulation lumineuse, le miracidium va éclore et pouvoir boucler le cycle en trouvant un nouveau mollusque à infester (Figure 2).

L'immunité chez Biomphalaria glabrata

L'immunité de notre mollusque d'intérêt est très étudiée. D'un point de vue cellulaire, il existe des études qui ont permis de décrire les hémocytes de *B. glabrata*. La plus récente (Cavalcanti et al. 2012) fait état de 5 types d'hémocytes :

- Les Blast-like cells, petites cellules rondes avec un fort ratio nucleo-cytoplasmique.
- Les Granulocytes, des cellules contenant un grand nombre de granulations.
- Les Hyalinocytes de type I, des cellules ayant un fort pouvoir d'adhésion.
- Les Hyalinocytes de type II, des cellules peu présentes, ovales avec un noyau excentré et un cytoplasme hétérogèn.
- Les Hyalinocytes de type III, des cellules faiblement représentées, avec un grand noyau ovale en position centrale et une structure fragile.

Ces cellules sont très bien décrites mais aucune étude n'a encore pu démontrer leurs différentes fonctions et leurs rôles précis joués dans la réponse cellulaire innée.
D'un point de vue moléculaire, une étude a pu montrer un transfert de résistance suite à l'injection, dans des mollusques susceptibles, de plasma provenant de mollusques résistants à *S. mansoni* (Granath and Yoshino 1984). De nombreuses études ont été menées afin de mesurer les variations d'expressions de gènes lors d'infestations par différents pathogènes (Adema et al. 1997; Zhang et al. 2001; Coustau et al. 2003; Guillou et al. 2004; Bouchut et al. 2007; Guillou et al. 2007; Lockyer et al. 2008; Adema et al. 2010; Hanington et al. 2010a; Hanington and Zhang 2011; Lockyer et al. 2012). Toutes ces études ont permis de mettre en évidence un grand nombre de molécules immunitaires produites par *B. glabrata* en réponse à un pathogène. Enfin les FREP, récepteurs immuns hyper variables dont nous avons déjà parlé, font partie des découvertes majeures nous conduisant à supposer l'existence d'un haut niveau de spécificité de la réponse immunitaire et également d'une immunité de type mémoire dans notre modèle.

Le priming immunitaire chez *Biomphalaria glabrata*

C'est en 1998 qu'une étude menée au sein de notre laboratoire a mis en évidence un phénomène de résistance acquise chez *Biomphalaria glabrata* (Sire et al. 1998). En effet suite à une première infection de *B. glabrata* par un miracidium de *S. mansoni* une réponse dépendante du temps se met en place progressivement jusqu'à rendre le mollusque totalement résistant à la ré-infestation à partir de 14 jours et ce jusqu'à la fin de sa vie. Cette protection semble de plus passer par l'activation de molécules cytotoxique/cytolytique faisant penser à un phénomène humoral (Sire et al. 1998). Toute fois à l'époque les auteurs ont interprété ces résultats comment étant la résultante d'un processus de compétition inter-parasitaire entre le parasite installé lors de la primo- infestation et le parasite issu du challenge (Sire et al. 1998).

L'interaction Biomphalaria / Schistosoma

Dans l'interaction entre *B. glabrata* et *S. mansoni* les mécanismes se mettant en place sont très certainement particuliers. En effet, dans toutes les interactions où un priming immunitaire a été montré les protagonistes étaient phylogénétiquement très éloignés, il s'agit même dans la plus part des cas d'interactions entre un hôte eucaryote métazoaire et un parasite procaryote. Dans notre cas nous avons face à face deux métazoaires eucaryotes, qui

de plus, sont deux Lophotrochozoaires. La proximité phylogénétique entre nos deux modèles engendre en toute vraisemblance des constitutions moléculaires antigéniques proches. Afin de reconnaître un pathogène qui lui ressemble et éviter les réponses auto-immunes, il est envisageable que l'organisme hôte doive posséder un panel de molécules de reconnaissance immunitaire complexe et un système immunitaire finement régulé. Il semble donc évident que le paradigme de Medzhitov et Janeway (Medzhitov and Janeway 1997) puisse connaître quelques failles dans notre modèle.

Ce sont exactement tous ces indices qui nous ont fait penser que l'étude de la réponse de priming immunitaire chez *Biomphalaria glabrata* en réponse à *Schistosoma mansoni* allait être un challenge passionnant et excitant. Nous avons donc décidé de nous plonger dans cette question du priming immunitaire chez *Biomphalaria glabrata*. Pour ce faire nous avons commencé par étudier d'un point de vue phénotypique la réponse de priming immunitaire et d'éliminer l'hypothèse de la compétition larvaire. Puis nous nous sommes penchés sur la question de la spécificité et avons cherché à savoir jusqu'où pouvait aller le niveau de reconnaissance du mollusque face au pathogène (espèce, génotype, stade de développement). Enfin, nous avons voulu aller plus loin en essayant de trouver les mécanismes régissant ces réponses de priming par l'intermédiaire d'une double approche protéomique et transcriptomique.

Methodologie générale

METHODOLOGIE GENERALE

Afin de pouvoir étudier les interactions immunobiologiques entre *Biomphalaria glabrata* et *Schistosoma mansoni* nous disposons au laboratoire de la plus formidable collection d'isolats géographiques concernant les mollusques et leurs parasites sympatriques. En effet depuis de nombreuses années le Centre de Biologie et d'Ecologie Tropicale et Méditerranéenne se distingue par sa capacité à entretenir et maintenir de grands élevages de mollusques provenant de localités très variées (Afrique, Péninsule Arabique, Amérique du Sud, Caraïbes). Chacun de ces isolats se caractérise par des différences de compatibilités entre les mollusques et leurs parasites sympatrique mais aussi au travers des différents croisements hôtes/parasites. Ces compatibilités ont été mesurées expérimentalement grâce à différents indices comme la prévalence et l'intensité suite à différentes infestations par 1, 2, 5, 10, 20 ou encore 50 miracidia. On a par exemple, sur le mollusque *B.glabrata* BRE infesté par 10 miracidia de *S. mansoni* BRE (son parasite sympatrique), une prévalence de 100% et une intensité de 3,6 alors qu'avec 10 miracidia de *S. rodhaini* sur ce même mollusque on a une prévalence de 75% et une intensité de 2.

Pour maintenir ces élevages nous disposons de cellules équipées en climatisations/chauffage afin de conserver une température ambiante de 26°C, température rencontrée en milieu naturel. De grands aquariums de 50 litres remplis d'eau douce provenant d'un forage nous permettent de recréer l'environnement adéquat pour la vie des mollusques. L'eau des grands aquariums est changée régulièrement (tous les mois) et les nouveaux nés sont triés et mis de côté pour l'entretien des cycles et les expérimentations. L'ensemble des mollusques est nourri tous les deux jours avec de la laitue fraiche.

Maintien des cycles

Les élevages ainsi que le maintien des cycles est assuré pas le personnel technique du laboratoire qui s'assure du matériel disponible pour l'ensemble des chercheurs en fonction de chaque isolat étudié et qui renouvelle régulièrement les lots d'hôtes disponibles (hôte intermédiaire et hôte définitif). Le maintien du cycle se décompose en deux phases : l'infestation de l'hôte intermédiaire, le mollusque, et l'infestation de l'hôte définitif, la souris.

Concernant l'hôte intermédiaire, à savoir le mollusque, tout commence par une sélection des individus par un critère de taille. En effet la taille du mollusque (donc son âge)

va avoir une incidence sur la prévalence et l'intensité lors de l'infestation (Théron et al. 1998). Des mollusques de 3-6 mm sont donc choisis pour l'infestation. Les parasites sont récupérés ensuite. Pour ce faire, le foie d'une souris infestée depuis deux mois est récupéré après dissection et placé dans une eau salée (8,5% NaCl). Il est ensuite broyé puis passé à travers des tamis de maille de taille différente (425, 180, 106 et 45 µm) et les œufs de schistosome sont récupérés dans le dernier tamis au travers duquel ils ne passent pas. Ils sont ensuite disposés dans un cristallisoir avec de l'eau provenant du forage et sous une source lumineuse. Le choc osmotique créé ajouté à la lumière va permettre l'éclosion des miracidia qui vont alors se mettre à nager. Les mollusques sont exposés individuellement aux parasites dans des piluliers contenant 5 mL d'eau douce provenant du forage pendant une heure. Le nombre de parasite mis au contact des mollusques a été déterminé pour chaque isolat en fonction de la prévalence, l'intensité et la virulence du parasite chez son mollusque sympatrique. Effectivement, expérimentalement, un nombre de parasite permettant d'avoir une prévalence optimale avec une survie des mollusques importante a été mesuré pour chaque isolat. Le nombre de parasites mis au contact des mollusques varie donc de 2 à 10 en fonction de la compatibilité dans leur interaction. Après une heure de contact, les mollusques sont récupérés et mis en bac de 10 litres, étiquetés avec les informations concernant l'isolat du mollusque, l'isolat du parasite, le nombre de mollusques soumis à l'infestation, le nombre de parasites présentés à chaque mollusque et la date de l'infestation.

Concernant l'hôte définitif, la souris, c'est très simple. Trente cinq jours après l'infestation des mollusques, ils vont commencer à émettre des cercaires. Les mollusques sont donc disposés dans un cristallisoir avec de l'eau douce du forage, sous une source lumineuse qui va stimuler l'émission des cercaires. De jeunes souris albinos de la souche Swiss sont individuellement exposées par pataugeage à un certain nombre de cercaires qui, comme pour le mollusque, est dépendant de la compatibilité du parasite et de l'hôte définitif. Ainsi un nombre de cercaires a été mesuré expérimentalement afin d'avoir une bonne intensité de parasite à l'intérieur de la souris mais en gardant une pathologie faible pour permettre aux souris de survivre suffisamment longtemps. Le nombre de cercaires présentés à la souris varie de 120 à 280 en fonction de l'isolat du parasite. Après une heure de pataugeage les souris sont mises en cage avec une étiquette comportant les informations concernant l'isolat du parasite, le nombre de cercaires mis au contact de chaque souris, le nombre de souris exposées au parasite et la date de l'infestation.

Figure 3 : Sporocystes primaires dans le pied d'un mollusque fixé au Raillet-Henry

Expériences de Priming

Dans le cadre de cette thèse, les effectifs importants dont nous avions besoins ont nécessité la création de nouveaux élevages. Pour la grande majorité des élevages nous avons utilisé des mollusques albinos provenant d'un isolat Brésilien (BgBRE) et différents parasites d'isolats variés. Le choix de ces mollusques à été guidé par les résultats des expériences visant à mesurer la prévalence et l'intensité de chaque isolat de parasites envers BgBRE. En effet, quel que soit l'isolat de parasites, les données de prévalence et d'intensité sont toujours très proches ce qui limite grandement dans nos expériences, un quelconque effet dose lors des différentes infestations.

Le protocole que nous avons suivit pour la majorité des expériences se définit de la façon suivante : nous avons tout d'abord mené une première infestation (primo infestation) au cours de laquelle des mollusques ont été exposés à 10 miracidia provenant d'un isolat particulier. Les mollusques infectés ont été maintenu suivant le protocole classique décrit ci-dessus pendant 25 jours, date à laquelle nous avons réalisés la seconde infestation (challenge). Cette infestation a consisté à exposer les mollusques primo infectés à 10 miracidia du même isolat dans le cas de ré-infestations homologues ou 10 miracidia provenant d'un isolat différent de la primo infestation dans le cas de ré-infestations hétérologues. Dans le même temps, des mollusques naïfs sont infestés suivant les conditions du challenge pour servir de contrôle de l'infestation. Quinze jours après ce challenge les mollusques sont fixés puis disséqués afin d'établir les prévalences et intensités suivant une méthode déjà établie (Théron and Gérard 1994; Sire et al. 1998). Cette méthode consiste à anesthésier les mollusques dans de l'eau contenant quelques cristaux de menthol pendant quelques heures (entre 6 et 8 heures) puis de disséquer leur coquille afin de plonger les corps des mollusques dans une solution de fixation de Raillet-Henry (6 g de NaCl, 20 mL d'acide acétique, 50 mL de formol 40%, dans 1 L d'eau). A cette date, c'est-à-dire 40 jours après la primo infestation (25 + 15) les sporocystes de la primo infestation ont disparu, donc par dissection on peut compter les sporocystes du challenge âgés de 15 jours. La méthode de fixation au Raillet Henry permet de faire apparaître en blanc ces sporocystes dans les tissus jaune/orangés du mollusque (dans le cas de BgBRE, un isolat de mollusques albinos) ce qui les rends très facile à distinguer (Figure 3). Pour chaque expérience nous avons essayé d'avoir des effectifs de mollusques compris entre 30 et 50 afin d'avoir des résultats robustes statistiquement.

Valeurs mesurées

Nous avons choisi de mesurer les prévalences et intensités dans chaque condition testée ainsi que dans les contrôles. En ce qui concerne les prévalences nous avons décidé de représenter un taux de protection calculé de la manière suivante :

$$\frac{Prévalence\ contrôle - Prévalence\ expérience}{Prévalence\ contrôle}$$

De cette façon si vous avez une prévalence de 100% dans le contrôle et de 40% dans le challenge vous aurez un taux de protection de 60% ([100-40]/100). Ce taux normalisé permet de rendre compte de la protection engendré par la primo infestation en tenant compte de la valeur contrôle de l'infestation au moment du challenge.

En ce qui concerne l'intensité nous avons choisi de normaliser l'intensité lors du challenge par l'intensité du contrôle ce qui donne une valeur correspondant aux taux de parasites implantés dans la condition de challenge par rapport au contrôle :

$$\frac{Intensité\ expérience}{Intensité\ contrôle}$$

Dans le cas où l'intensité serait de 10 dans le contrôle et de 6 dans l'expérience on aurait un taux de 60%, soit une intensité égale à 60% de la valeur lors d'une infestation sans priming.

Chapitre premier :

Le priming immunitaire chez *Biomphalaria glabrata*

CHAPITRE PREMIER :

LE PRIMING IMMUNITAIRE CHEZ *BIOMPHALARIA GLABRATA*

Evidence for specific genotype-dependent immune priming in the Lophotrochozoan *Biomphalaria glabrata* snail

Portela J, Duval D, Rognon A, Galinier R, Boissier J, Coustau C, Mitta G, Théron A and Gourbal B

Journal of Innate Immunity (2013) 5 :261-276

Des preuves de l'existence de processus de mémoire immunitaire chez les invertébrés, se multiplient depuis dix ans (Kurtz and Franz 2003; Schmid-Hempel 2005; Sadd and Schmid-Hempel 2006; Pham et al. 2007; Roth et al. 2009; Baruah et al. 2011; Pope et al. 2011; Tidbury et al. 2011; Konrad et al. 2012). Ce processus a été nommé priming immunitaire pour le différencier du terme de mémoire immunitaire connue chez les vertébrés. Le priming immunitaire est particulièrement controversé. En effet, toutes les espèces d'invertébrés semblent ne pas posséder cette potentialité (Gonzalez-Tokman et al. 2010; Reber and Chapuisat 2012), il semble que l'apparition du priming immunitaire se soit faite ponctuellement sous l'influence plus ou moins grande des pressions de sélection parasitaires et en fonction des traits d'histoire de vie des hôtes. Dans le cas de l'interaction entre *Biomphalaria glabrata* et *Schistosoma mansoni* des indices ont déjà été mis à jour permettant de supposer l'existence d'un processus de résistance acquise (Sire et al. 1998). Sire et al (1998) ont en effet démontré que suite à une infestation par *S. mansoni*, le mollusque *B. glabrata* devenait résistant à la ré-infestation par le même parasite. Dans ces travaux, cette résistance acquise a été mise en relation avec une compétition parasitaire intramolluscale puisque le premier parasite se développe normalement au sein de son hôte et reste présent dans les tissus du mollusque alors que les parasites des infestations successives ne peuvent s'implanter et meurent. De plus cette résistance se met progressivement en place au cours de l'infestation jusqu'à devenir totale après 14 jours d'infestation.

Nous avons donc étudié cette réponse sous plusieurs angles. Dans un premier temps nous avons pu mettre en évidence que le priming immunitaire dans notre modèle n'était pas dépendant d'une souche de parasite ou de mollusque particulière. Puis, nous avons tenté de savoir si cette réponse était liée à la présence du parasite et donc à une compétition intramolluscale ou non. Pour cela nous avons mené une expérience de vaccination avec des extraits totaux de parasite. Nous avons également étudié le développement intramolluscal du parasite par une approche histologique afin de comprendre la dynamique temporelle de mise en place de la résistance acquise du mollusque. Enfin nous avons mené une série d'expérience afin d'observer le niveau de spécificité de ce priming immunitaire en réalisant des séries d'infestations et ré-infestations homologues et hétérologues.

Research Article

Journal of Innate Immunity

J Innate Immun
DOI: 10.1159/000345909

Received: August 3, 2012
Accepted after revision: November 18, 2012
Published online: $ $ $

Evidence for Specific Genotype-Dependent Immune Priming in the Lophotrochozoan *Biomphalaria glabrata* Snail

Julien Portela[a, b] David Duval[a, b] Anne Rognon[a, b] Richard Galinier[a, b] Jérôme Boissier[a, b] Christine Coustau[c] Guillaume Mitta[a, b] André Théron[a, b] Benjamin Gourbal[a, b]

[a]CNRS, UMR 5244, Ecologie et Evolution des Interactions (2EI), and [b]Université de Perpignan Via Domitia, Perpignan, and [c]UMR 6243 Interactions Biotiques et Santé Végétale INRA, CNRS, Université de Nice Sophia-Antipolis, Nice, France

Key Words
Immune priming · Specificity · Genotype · lophotrochozoan · *Biomphalaria glabrata*

Abstract
Historically, the prevailing view in the field of invertebrate immunity was that invertebrates that do not possess acquired adaptive immunity rely on innate mechanisms with low specificity and no memory. Several recent studies have shaken this paradigm and suggested that the immune defenses of invertebrates are more complex and specific than previously thought. Mounting evidence has shown that at least some invertebrates (mainly Ecdysozoa) show high levels of specificity in their immune responses to different pathogens, and that subsequent reexposure may result in enhanced protection (recently called 'immune priming'). Here, we investigated immune priming in the Lophotrochozoan snail species *Biomphalaria glabrata,* following infection by the trematode pathogen *Schistosoma mansoni*. We confirmed that snails were protected against a secondary homologous infection whatever the host strain. We then investigated how immune priming occurs and the level of specificity of *B. glabrata* immune priming. In this report we confirmed that immune priming exists and we identified a genotype-dependent immune priming in the fresh-water snail *B. glabrata*.

Introduction

There is currently great debate as to whether immune memory is exclusive to vertebrate animals [1–4]. The prevailing opinion had been that only vertebrates possess the mechanisms of immune memory, which occur via their adaptive immune response and allow the immune system to specifically recognize antigens through somatically generated immune receptors [5, 6], and reuse these receptors and even amplify them through the use of memory cells [7]. Until recently, no diversified molecules or memory cells had been discovered in invertebrates, which thus were thought to lack acquired adaptive immunity and instead possess innate immune mechanisms with low specificity. The immune systems of invertebrates were believed to discriminate pathogen-associated molecular patterns using a limited repertoire of invariable germ line-encoded pattern recognition receptors that engaged effector pathways capable of acting on the recognized intruders [8, 9]. However, several lines of evidence countered this viewpoint, suggesting that invertebrate immunity could possess higher levels of specificity and acquired protection. The first hints of this came from experiments on graft rejection, which revealed the presence of allorecognition processes in diverse invertebrate phyla (i.e. Porifera, Cnidaria, Annelida, Echinodermata,

1662–811X/13/0000–0000$38.00/0

Accessible online at:
www.karger.com/jin

Fax +41 61 306 12 34
E-Mail karger@karger.com
www.karger.com

Dr. Benjamin Gourbal
Université de Perpignan Via Domitia
UMR 5244 CNRS Ecologie et Evolution des Interactions (2EI)
52 Avenue Paul Alduy, FR–66860 Perpignan Cedex (France)
E-Mail benjamin.gourbal@univ-perp.fr

etc.) [1, 10–13]. These studies showed that invertebrates were able to tolerate isografts, but rejected allografts (hallmark of specificity) and possessed the ability of faster graft rejection following a secondary allograft exposure (hallmark of memory). Although it was hypothesized that this could be explained by competition occurring between colonial organisms, the benefit of such recognition events was difficult to explain for noncolonial animals, such as earth worms [12]. Consequently, it was theorized that this specific recognition could be used for the identification of aberrant self-generated cells or pathogen-derived antigens [14]. In addition, several transcriptomic approaches recently developed in different invertebrate species have revealed large and individual repertoires of putative immune receptors that could represent the molecular mechanisms underlying immune specificity. These diversified molecules have been identified in echinoderms (SRCR or Sp185/333 of sea urchin [15]), insects (DsCAM of *Drosophila melanogaster* and *Anopheles gambiae* [16, 17]), and mollusks (fibrinogen-related proteins, FREPs, of *Biomphalaria glabrata* [18]). The arguments for the involvement of these molecules in antigen recognition have recently been strengthened, especially for FREPs, which were shown to be involved in immune complexes with various antigens of the *B. glabrata*-specific trematode pathogen, *Schistosoma mansoni* [19].

Thus, invertebrates seem to be able to specifically recognize antigens/pathogens and destroy them more efficiently upon a second exposure. In this context, two secondary immune response processes could be expected. Firstly, a process of acquired resistance or sustained response could be expected. This response is characterized by the induction of an immune response following a first stimulation that confers long-lasting protection against later challenge [20]. This immune response persists at high levels even if the pathogen is neutralized [20]. Secondly, an immune response, termed 'immune memory', reminiscent of vertebrate acquired immunity could also be expected in invertebrates. It is characterized by the induction of a primary immune response following first pathogen stimulation. The primary response returns to a basal level when the infection is cleared. This first immune stimulation provides the immune system with the ability to recognize and remember specific antigens/pathogens, and to mount a faster and more powerful response against a subsequent exposure to the same antigen/pathogen [1, 21]. Both of these secondary immune responses were called 'immune priming' in invertebrates.

Several studies have found evidence for (insects, crustaceans) [2, 14, 22–24] and others have failed to detect (insects) [3, 25, 26] immune priming in invertebrates. Thus it is difficult to conclude whether priming is universal, restricted to several invertebrate groups or species, or to specific host/parasite combinations. Immune priming was described mainly for arthropods (insects [2, 24, 27–29] or crustaceans [4, 21, 30, 31]) infected by bacteria, protozoa or virus. Immune priming might also occur in insects or crustaceans via trans-generational processes, where bacterial immune-challenged or infected parents produce protected offspring via a maternal and/or paternal transfer of immune protection [30, 32–35]. Finally, to our knowledge, only one paper has investigated immune priming against a metazoan parasite and this was also identified for a crustacean [23].

Immune priming specificity also appears to be controversial. In some models immune priming could be very specific at the species or even strain level [2, 23, 27, 28], while in others immune priming appeared to be nonspecific and cross-protection occurred. For example: (i) infection with bacteria or injection of lipopolysaccharides protect against fungal [36] or protozoan pathogens [24]; (ii) fungal -glucans protect against bacterial infections [37], and (iii) wounding was found to induce nonspecific immune responses that prevent bacterial or yeast opportunistic infections [38–40].

Most of our knowledge on immune priming comes from a few model species belonging to Ecdysozoa and much remains to be elucidated from Lophotrochozoa species. This is crucial for a better understanding of the evolutionary history of the invertebrate immune priming and is of central importance in understanding the diversity and evolution of innate memory processes from Ecdysozoa to Deuterostomia.

Here we used the *B. glabrata* snails and their natural trematode parasite *Schistosoma* spp. to investigate immune priming in a Lophotrochozoa species exposed to a metazoan parasite. Recent advances in understanding the *B. glabrata*/*Schistosoma* interaction at the phenotypic and molecular levels [18, 19, 41–46] and a previous study describing a time-dependent 'acquired resistance' in *B. glabrata* against *S. mansoni* challenges [47] make this model particularly well adapted to investigate the question of immune priming.

In this report we investigated how immune priming occurs and the level of specificity of *B. glabrata* immune priming using different approaches. First, we exposed two geographic isolates of *B. glabrata* snails to homologous challenges to test the effect of host strain on immune

priming. Second, we used a histological approach to investigate the putative role of parasite development and migration in the observed immune priming process. Third, we investigated the biological mechanisms involved in immune priming, using snails exposed to irradiated miracidia and tissue injuries. Finally, we investigated the specificity of immune priming in *B. glabrata* by comparing the infection success following homologous or heterologous challenges of four different genetic strains or species of *Schistosoma*.

Table 1. Prevalence and intensity of host/parasite combinations

Biomphalaria strain	*Schistosoma* strain	Miracidia n	Prevalence %	Intensity n
BgGUA	SmBRE	10	80	2.4
BgBRE	SmBRE	10	100	3.6
BgBRE	SmBRE-LE	10	100	5.1
BgBRE	SmVEN	10	100	3.2
BgBRE	Srod	10	75	2

Prevalence corresponds to the percentage of snails infected; intensity corresponds to the average number of SpIs for each infected snail.

Material and Methods

Ethics Statement

Our laboratory holds permit No. A66040 for experiments on animals from both the French Ministry of Agriculture and Fisheries, and the French Ministry of National Education, Research and Technology. The housing, breeding and animal care of the utilized animals followed the ethical requirements of our country. The experimenter also possesses an official certificate for animal experimentation from both French ministries (Decree No. 87-848, 19 October, 1987). Animal experimentation follows the guidelines of the French CNRS. The different protocols used in this study have been approved by the French veterinary agency from the DRAAF Languedoc-Roussillon (Direction Régionale de l'Alimentation, de l'Agriculture et de la Forêt), Montpellier, France (authorization No. 007083).

Snail and Parasite Strains

Two strains of *B. glabrata* [48] were used in this study. The Guadeloupean strain of pigmented *B. glabrata* (BgGUA) and the Brazilian strain of albino *B. glabrata* (BgBRE).

Three South American strains of *S. mansoni* originating from different geographic isolate were used, as well as two Brazilian strains (SmBRE and SmBRE-LE) and one Venezuelan strain (SmVEN). Finally, another species of *Schistosoma* was used, *Schistosoma rodhaini* (Srod), a murine species originating from Africa [49]. SmBRE and Srod had been maintained in the laboratory for thirty years and SmBRE-LE and SmVEN were recovered in 2011. All these *Schistosoma* strains or species were selected because of their similar prevalence and intensity for BgBRE snails (table 1). Here, susceptibility is estimated using snails exposed to 10 miracidia.

Each strain or species of *Schistosoma* was maintained in its homopatric strain of *B. glabrata*, and in hamsters *(Mesocricetus auratus)*, as described previously [48]. Miracidia from both strains were hatched from eggs axenically recovered from 50-day infected hamster livers according to the previously described procedures [50, 51]. Briefly, livers were collected and homogenized, and the eggs were filtered and washed to obtain miracidia.

Genotyping and Genetic Analyses of S. mansoni *Strains*

Genomic DNA was extracted from 20 adults (10 males and 10 females) of each *S. mansoni* strain according to the following protocol. Sixty microliters of TE (Tris 10 mM; EDTA 1 mM; pH 8) containing 1.67 mg/ml of proteinase K (Merck) was added to the parasite. The samples were incubated for 3 h at 55°C, with vortexes every 15 min. The samples were then heated for 10 min at 100°C for proteinase K inactivation. The genomic DNA was recovered in the supernatant and kept at –20°C until use.

S. mansoni strains were subjected to PCR-based genotyping using fourteen microsatellite markers: SmC1, SmDO11, SmDA28 [52], R95529, SmD57, SmD28, SmD25, SCMSMOXII, L46951 [53], SmBR16, SmBR10, SmBR13 [54], SmS7-1 [55] and SmBR1 [56]. PCR was performed in three multiplex reactions using a multiplex kit (Qiagen). Markers R95529, SmC1, SmDO11, SmBR16 and SmD57 were grouped in multiplex 1; SmDA28, SmBR1, SmS7-1, SmD28, SCMSMOXII were grouped in multiplex 2, and SmD25, L46951, SmBR10 and SmBR13 were grouped in multiplex 3. The multiplex reactions were carried out according to the manufacturer's standard microsatellite amplification protocol in a final volume of 10 l and with an annealing temperature of 57°C. The PCR products were diluted in sample loading solution (Beckman Coulter) containing a red-labeled size standard (CEQ™ DNA size standard kit, 400, Beckman Coulter), and electrophoresis was performed on an automatic sequencer (CEQ™ 8000, Beckman Coulter).

Genotyping of *S. rodhaini* was not realized because microsatellite markers were not available and no microsatellite cross-amplification occurred between *S. mansoni* and *S. rodhaini*.

Deviation from Hardy-Weinberg expectancies and linkage disequilibria were analyzed using the global test in FSTAT v.2.9.3.2 [57]. The level of significance was adjusted for multiple testing using a Bonferroni correction. Furthermore, polymorphism was estimated over all loci and for each strain using the number of alleles, allelic richness, expected heterozygosity (He) and inbreeding coefficient (FIS) computed with FSTAT v.2.9.3.2. Finally, observed He and Nei's genetic distances were calculated with GENETIX software v.4.05.2 [58].

Experimental Protocol of Immune Priming

For all experiments, primary infections were performed on juvenile *B. glabrata* (5–6 mm in diameter). Snails were individually exposed for 12 h to 10 miracidia in 5 ml of pond water. Individual snails were secondarily infected at 25 days after primary infection, using 10 miracidia per snail. As controls for each experiment, 50 unprimed snails with a size equivalent to that of the primary infected snails (8–9 mm in diameter) were exposed to 10

miracidia at the same time as the experimental snails underwent secondary infection (i.e. 25 days after primary infection).

Host Effect on Immune Priming

To test whether the *B. glabrata* host strain had an influence on the observed priming, we used BgGUA or BgBRE and we performed a homologous primary/secondary infection as follow BgGUA + SmBRE + SmBRE or BgBRE + SmBRE + SmBRE.

Specific Genotype-Dependent Immune Priming

To investigate the level of immune priming specificity in *B. glabrata*, we performed homologous and heterologous primary/secondary infections using the BgBRE strain, as follows: BgBRE was primary infected with SmBRE and then challenged with SmBRE (homologous combination) or SmBRE-LE (heterologous combination, same species, same country, different strain) or SmVEN (heterologous combination, same species, different country, different strain) or Srod (heterologous combination, different species). To confirm that the different infection rates upon secondary infection are a consequence of specific priming rather than a more general effect, the same experiment was done using the SmBRE-LE strain as the primo-infection and challenged with homologous or heterologous combinations as described above.

For each experiment, all snails (unprimed or primed) were fixed 15 days after the secondary infection, and the presence and number of primary sporocysts (SpIs) were determined following the previously described method [59] to estimate the prevalence and the intensity of the infection. Briefly, snails were relaxed for 6 h in pond water containing excess crystalline menthol and each snail body was then removed from the shell and fixed in modified Raillet-Henry's solution [59, 60]. After 24 h in fixative, a dissection of the head-foot, mantle and kidney was performed, and the presence and number of SpIs in each snail was determined [59]. The SpIs could be readily observed as translucent white bodies within an opaque yellow tissue background. SpIs arising from the primary infection (40 days old at fixation time) are small and opaque white corpuscle and could be easily distinguished from those of the secondary infection (15 days old at fixation time) that appeared as big translucent white corpuscle. For all the experiments, the success of the primary infection could be determined by the presence of secondary sporocysts (SpIIs) in the hepatopancreas, and only snails harboring SpIIs were subjected to secondary infections. The results were analyzed by calculating the protection level as a ratio between prevalence in primed snails and prevalence in unprimed snails [([prevalence in unprimed – prevalence in primed snails]/prevalence in unprimed snails) ! 100]. For intensity a ratio was calculated between primed and unprimed snails to estimate the effect of priming when snails were reinfected [intensity in primed snails/intensity in unprimed snails].

Histological Procedures

To investigate the intramollusk development of *S. mansoni* larvae, BgBRE snails (5–6 mm in diameter) were infected using 10 miracidia of SmBRE. Infected snails were collected at 3, 7, 10, 14, 20, 25 and 35 days postinfection (DPI; 10 snails per condition), and fixed in Halmi's fixative (mercuric chloride 4.5%, sodium chloride 0.5%, trichloroacetic acid 2%, formol 20%, acetic acid 4% and picric acid 10%). The fixed mollusks were then dehydrated and embedded in paraffin, as previously described [46, 61]. Transverse histological sections (10 m thick) were cut and stained using azocarmine G and Heidenhain's azan (Sigma). Briefly, sections were rehydrated (in successive baths of toluene, 95% ethanol, 70% ethanol, 30% ethanol and distilled water), stained (azocarmine G, 70% ethanol + 1% aniline, 1% acetic alcohol, distilled water, 5% phosphotungstic acid, distilled water, Heidenhain's azan) and dehydrated (in 95% ethanol, 100% ethanol and toluene). The preparations were then mounted with Entellan and observed under a microscope. Pictures were taken with a Nikon MICROPHOT-FX microscope and a Nikon digital sight DS-Fi1 camera.

Experimental Infection with Irradiated Miracidia

To investigate whether immune priming depends on the development and migration of *S. mansoni* in snail tissues, we used UV-irradiated SmBRE miracidia to infect BgBRE snails. The irradiated parasites penetrated the snails normally, but then failed to develop and died. Thus, SpI growth was abolished and there was no development and migration of SpIIs.

In this experiment, juvenile BgBRE (5–6 mm in diameter) were individually exposed for 12 h to 10 irradiated SmBRE miracidia (see below for irradiation procedure) in 5 ml of pond water. Twenty-five days later, secondary infections were performed on experimental irradiated miracidia primary infected snails using 10 nonirradiated SmBRE miracidia, while 25 additional BgBRE snails of comparable size (8–9 mm in diameter) were exposed to 10 nonirradiated SmBRE miracidia and used as a positive control. Fifteen days after the secondary infection, all snails were fixed and the presence of SpI prevalence (% of snail infected) was determined following exhaustive dissection. We performed a positive control of primary infection/secondary infection using the combination BgBRE + SmBRE + SmBRE and following the procedure described in the 'Experimental Protocol of Immune Priming' section.

For irradiation, SmBRE miracidia were exposed to UV emissions from the fluorescent lamp of a BLX 254 nm crosslinker (Bio-Link; radiant exposure = 0.05 J/cm^{-2}). This intensity of UV radiation was sufficient to induce apoptosis among the pluripotent stem cells of the miracidia (germinal cells), which are involved in the development, maturation and cellular differentiation of SpIs, leading to the release of SpIIs [62]. This level of irradiation did not, however, affect the penetration of miracidia (see the following section).

PCR Diagnostics

As irradiated miracidia developed into very small SpIs not detected even under histological staining and did not produce SpIIs, it was difficult to visually assess the success of primary infection. Thus, we developed a PCR-based diagnostic procedure to confirm the penetration of irradiated miracidia and calculate their prevalence following primary infection. Genomic DNA was extracted from BgBRE snails 15 days after individuals were exposed to 10 miracidia irradiated SmBRE. Each snail was relaxed with crystalline menthol, the shell was removed, the snail body was put in DNAzol reagent (Invitrogen), and genomic DNA was recovered according to the manufacturer's instructions. Specific PCR amplification of *S. mansoni* miracidium DNA was performed using the SmAlphaFem gene (GenBank accession No. U12442.1) with the Advantage 2 PCR Enzyme System (Clontech). To ascertain SmAlphaFem gene amplification, two fragments were amplified using specific primer pairs: SmAlphaFem1 (forward, GCTT-

TATCGAGGCAATACGC; reverse, GTTTCGTTCGATTTGCCACT; 270-bp product) and SmAlphaFem2 (forward, TGCACAAGTGAGTGGCTGTGGG; reverse, TGGATGTACCTGCATCCCGTGT; 120-bp product). The PCR cycling conditions consisted of 30 s at 95°C, 30 s at 60°C and 20 s at 72°C for 40 cycles.

Tissue Injury Experiments

Snails were subjected to tissue injuries using two different procedures: (i) 15 BgBRE were pricked six times in the head-foot using a needle (26 G ! 0.5 ; 0.45 ! 12 mm) and then infected with 10 miracidia SmBRE at 5 and 10 DPTI, and (ii) gold microparticles (0.6–1.6 m) were used with a biolistic gene transfer apparatus (PDS-1000/He system; BioRad) to provoke numerous microinjuries on the snails' tegumental cells. Briefly, snails were relaxed in pond water containing excess crystalline menthol for 12 h so the head-foot protruded outside the shell and would not be retracted during the biolistic procedure. The gene transfer system used a burst of high-pressure helium gas (1,350 psi) to accelerate 20 l of gold microparticles toward the snail head-foot target cells under a vacuum. Gold microparticle penetration in snail tissue was confirmed by microscopic observation. After 5 and 10 DPTI, 15 BgBRE were infected by 10 miracidia SmBRE. For each tissue injury procedure and each infection time, uninjured snails were infected under the same conditions and used as controls. For all these experimental devices, snails were assessed for their level of protection against secondary infection; the parasite prevalence was estimated following the procedure described in the 'Experimental Protocol of Immune Priming' section.

Vaccination Experiment

For vaccination a whole miracidium protein extract was prepared as follow: 1,000 miracidia from the *Sm*BRE strain were natively extracted in 0.05% TBS-Tween 20 (TBS-T) by sonication (3 pulses of 30 s at 40% of amplitude), centrifuged and the protein amount of supernatant was quantified and conserved at –80°C until used.

Three groups of snails were anesthetized in 500 ml of fresh water with menthol for 8 h. The first group (69 individuals) was injected with 1 g of parasite extracts in 20 l of TBS-T. The second group (25 individuals) was injected with 20 l of TBS-T alone and used as a control for the injection. The third group (48 individuals) constituted of naïve snails used as a control for the infection. Fifteen days after those treatments, snails of the three groups were exposed to 10 miracidia of *Sm*BRE. Fifteen DPI, the snails were fixed in Raillet-Henry's solution and dissected to evaluate the parasite prevalence.

Statistical Analysis

All results concerning prevalence were tested using Fisher's exact test which considers two binary variables: infected/noninfected and control/experimental groups. The presence of an association between immune priming prevalence (a two category-variable) and Nei genetic distances (a variable with *k* categories) was tested using ^{2} test for trend (also called Cochran-Armitage test for trend). This test incorporates a suspected ordering in the effects of the *k* categories of the second variable. All results concerning the intensities (a continuous variable) were compared using a Mann-Whitney U test. For all the experiments, differences were considered significant at p ! 0.05.

Table 2. Genetic information for *Schistosoma* strains

a Summary of genetic information for *Schistosoma* strains

	SmBRE	SmBRE-LE	SmVEN	Srod
Expected heterozygosity	0	10.15	5.73	ND
Observed heterozygosity	0	9.33	5.41	ND
Number of alleles	1	8.08	2.33	ND
Allelic richness	1	5.82	2.29	ND
Inbreeding coefficient	ND	0.082	0.056	ND

b Nei's genetic distances

	SmBRE-LE	SmVEN	Srod
SmBRE	0.644	0.735	ND
SmBRE-LE		0.546	ND
SmVEN			ND

ND = Not determined.

Results

Genotyping of S. mansoni *Strains*

The genetic diversities of each strain were determined using fourteen microsatellite markers (table 2). From the SmBRE strain, we obtained the following results: He = 0.0 8 0; allelic richness = 1.0 8 0, and FIS = not determined (table 2a). This indicates that SmBRE displays no genetic diversity based on the microsatellite markers tested herein. For the SmBRE-LE and the SmVEN stains, we observed some genetic differentiation with an expected He of 10.15 and 5.73 and an allelic richness of 5.82 and 2.29, respectively. The FIS were 0.082 and 0.056 for these two strains. Nei genetic distance between SmBRE and SmBRE-LE was equal to 0.644 and between SmBRE and SmVEN to 0.735 (table 2b). This result demonstrates that the SmBRE strain is genetically closer to SmBRE-LE than SmVEN.

Genotyping of *S. rodhaini* was not realized because microsatellite markers were not available for this species. We were not able to use the *S. mansoni* microsatellites because no cross-amplification occurred between *S. mansoni* and *S. rodhaini*. However, as *S. rodhaini* is a different species of the genus Schistosoma, we considered this strain as the more genetically distant from the SmBRE strain.

Immune Priming in Different Host/Parasite Combinations: Host Effect

To test whether the *B. glabrata* host strain had an influence on immune priming, we used two combinations

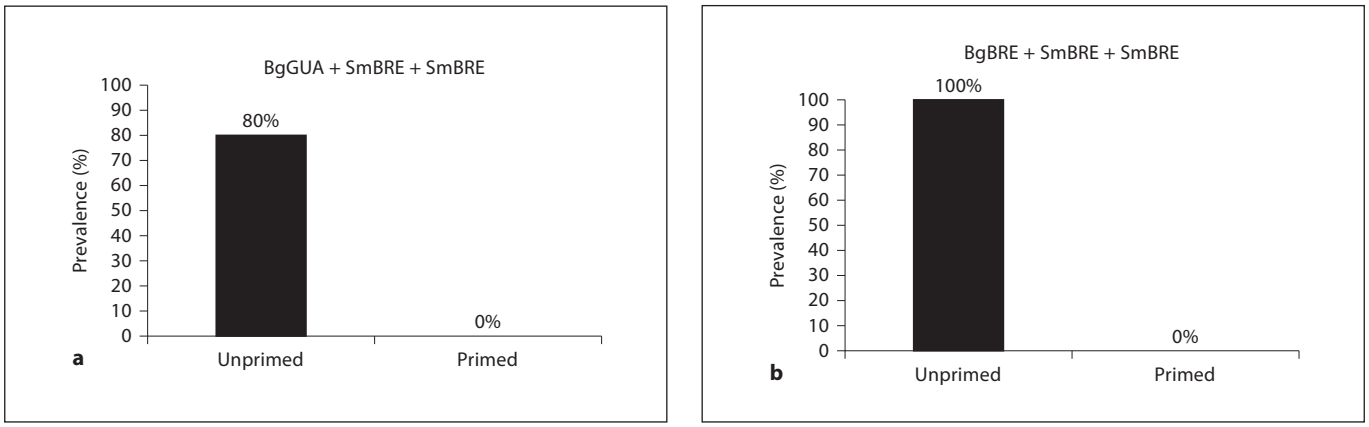

Fig. 1. Reinfection rates of BgGUA and BgBRE primary infected with 10 miracidia SmBRE (**a**) and reexposed to 10 miracidia of the homologous strain SmBRE (**b**). 'Unprimed' corresponds to snails that were not primary infected and exposed solely to the secondary infection.

involving BgGUA or BgBRE snails infected by homologous primary/secondary infection as follows: BgGUA + SmBRE + SmBRE or BgBRE + SmBRE + SmBRE (fig. 1).

For BgGUA snails, the prevalence decreased from 80% for unprimed snails to 0% for primed snails (Fisher's exact test: p ! 0.0001; fig. 1a). For BgBRE snails, the prevalence decreased from 100% for unprimed snails to 0% in primed snails (fig. 1b) (Fisher's exact test: p ! 0.0001). Primary infections with SmBRE fully and equally protected against homologous secondary infection by SmBRE whatever the host strain (fig. 1a, b). These results show that the immune priming response does not depend on the snail host strain.

Intramolluskal Development of S. mansoni

In order to investigate the putative role of parasite development and migration events in the protection against secondary infection observed in *B. glabrata*, we used a histological approach to follow the infection of *B. glabrata* by *S. mansoni*. After miracidial penetration, SpIs developed in the snail head/foot. At 3 DPI, we observed growing SpIs containing dividing germinal cells that differentiated, maturated and developed into SpIIs (fig. 2A). At 14 DPI, the SpIs were full of SpIIs, some of which had left the SpIs to migrate through the host tissues toward the genital glands (fig. 2B). SpIIs began migrating at approximately 10 DPI (fig. 2D), and the first SpIIs reached the interface between the digestive and genital glands at 14 DPI (fig. 2F, G). The migration of SpIIs was very abundant at 20 DPI (fig. 2E), but it was complete by 25 DPI. At this point, the SpIs were degenerating in the snail foot tissue (fig. 2C), and the digestive/genital glands were full of SpIIs, some of which contained developing cercariae (the vertebrate infecting stage of the parasite; fig. 2H, I). At 35 DPI, the SpIIs were full of cercariae (fig. 2J, K), which were ready to escape and migrate to the snail mantle and the water environment beyond (fig. 2L).

Priming in Snails Infected with Irradiated Miracidia

To evaluate whether priming requires the development and migration of *S. mansoni* in snail tissues, *B. glabrata* were primary infected by UV-irradiated miracidia and secondarily infected at 25 DPI with nonirradiated miracidia. UV-irradiated miracidia could penetrate into the snails, but SpIs did not grow, parasitic development was interrupted and the migration of SpIIs did not occur (data not shown). When we examined protection against secondary infection among snails subjected to primary infection with irradiated miracidia, we found that no protection occurred (fig. 3a). The prevalence is similar to unprimed snails (fig. 3a). Primary infection with nonirradiated miracidia provides total protection against secondary infection (Fisher's exact test: p ! 0.0001). The infectivity of irradiated miracidia was verified using a PCR-based diagnostic method that we developed using a specific marker of the *S. mansoni* genome (SmAlpha-Fem gene; GenBank accession No. U12442.1). This assay revealed that six of the seven individuals exposed to irradiated miracidia had been infected (fig. 3b). This represents a prevalence of 87.6%, which is similar to that observed for healthy miracidia (see controls in the present study).

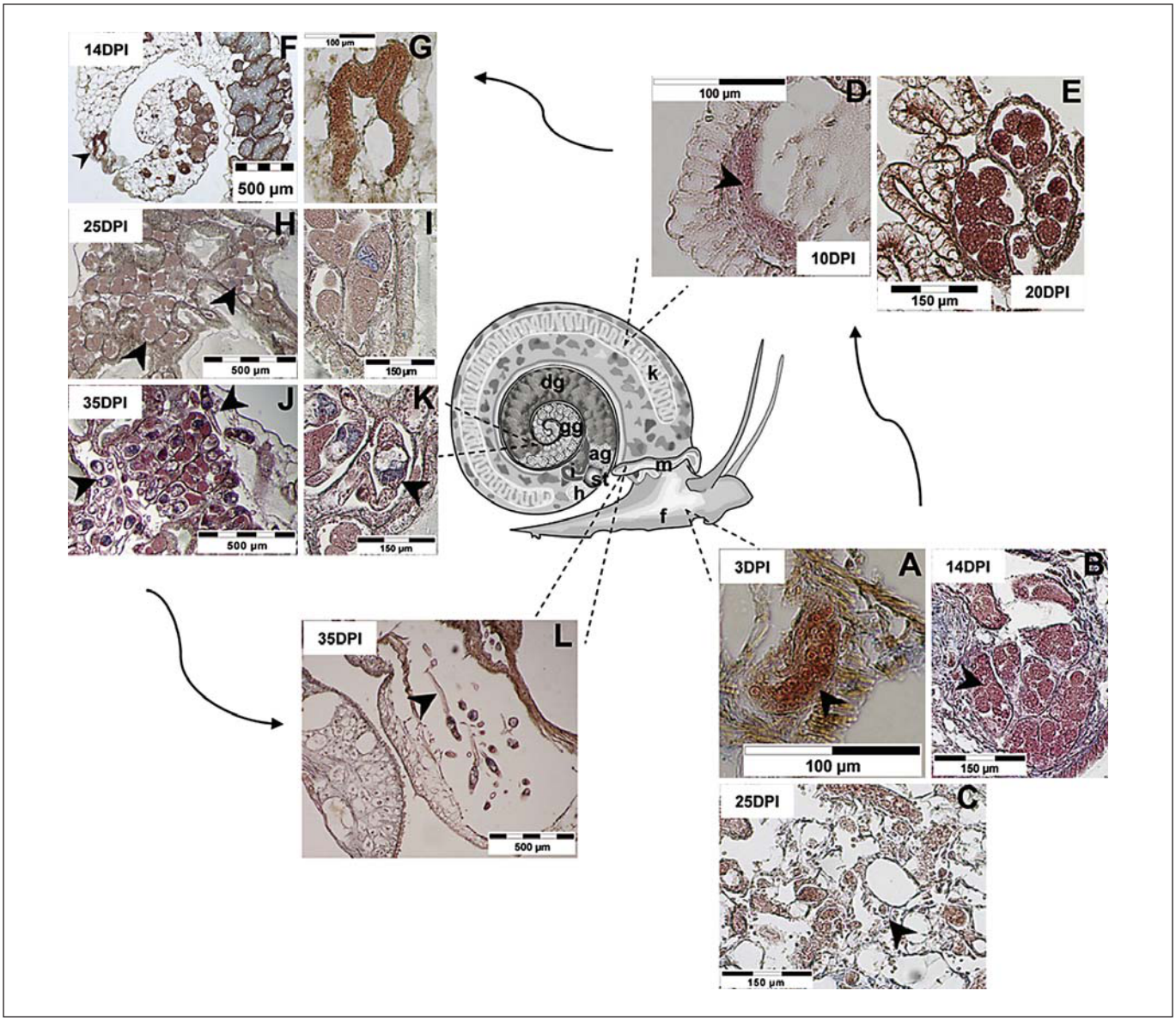

Fig. 2. *S. mansoni* intramolluskal-stage development in the intermediate snail host, *B. glabrata*. **A** SpIs at 3 DPI in the snail foot. **B** SpIs full of SpIIs at 14 DPI in the foot. **C** SpIs degenerating at 25 DPI in the foot. **D** One SpII migrating in the snail kidney at 10 DPI. **E** The kidney full of migrating SpIIs at 20 DPI. **F** The first SpII (black arrowhead) observed at the digestive/genital gland interface at 14 DPI. **G** Higher magnification of the adjacent image. **H** The digestive and genital gland full of SpIIs at 25 DPI, showing some developing cercariae. **I** Higher magnification of the adjacent image. **J** SpIIs full of cercariae in the digestive and genital glands at 35 DPI. **K** Higher magnification of the adjacent image. **L** Cercariae in the snail mantle at 35 DPI. All scale bars are indicated. f = Foot; m = mantle; k = kidney; h = heart; i = intestine; st = stomach; ag = albumen gland; dg = digestive gland; gg = genital gland.

Priming in Snails Subjected to Tissue Injuries

During miracidial penetration and the migration of SpIIs through the snail tissues, lesions and associated inflammatory processes may occur and could potentially be responsible for the observed priming. To test the putative involvement of tissue lesions in priming, we subjected snails to experimental tissue injuries at different times before infection. However, following needle-induced tissue injuries (fig. 4a) or biolistic particle-induced tissue injuries (fig. 4b), we failed to observe significant protection against infections by *S. mansoni* realized 5 or 10 days DPTI.

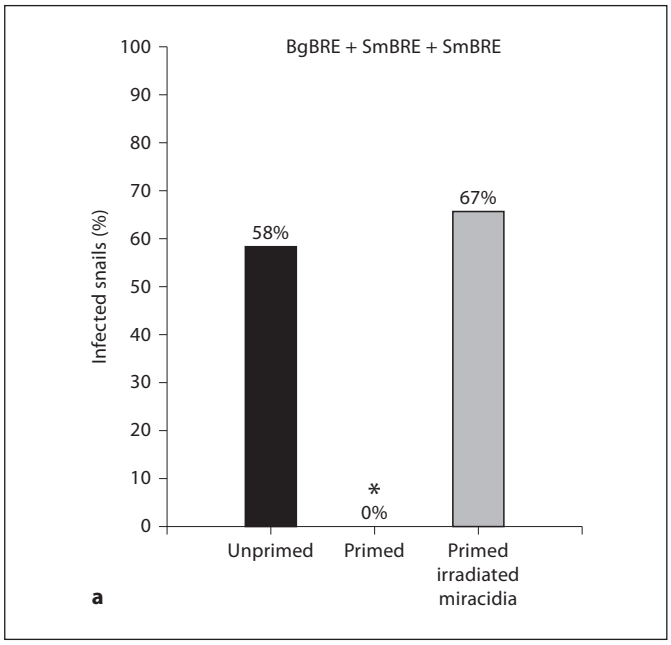

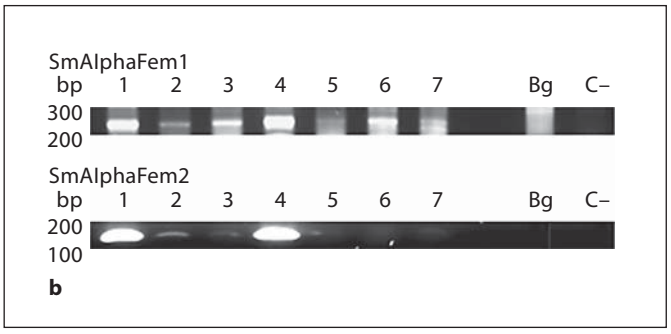

Fig. 3. a Infection rates of BgBRE snails subjected to primary infection with 10 irradiated or nonirradiated SmBRE miracidia, and then secondarily infected with 10 SmBRE miracidia. 'Unprimed' corresponds to snails that were not primarily infected and exposed solely to the secondary infection. **b** Detection of irradiate SmBRE miracidia in infected snails using diagnostic PCR amplification of the *S. mansoni*-specific SmAlphaFem gene (GenBank accession No. U12442.1) using primer pairs SmAlphaFem1 (270 bp) and SmAlphaFem2 (120 bp). * p ! 0.05.

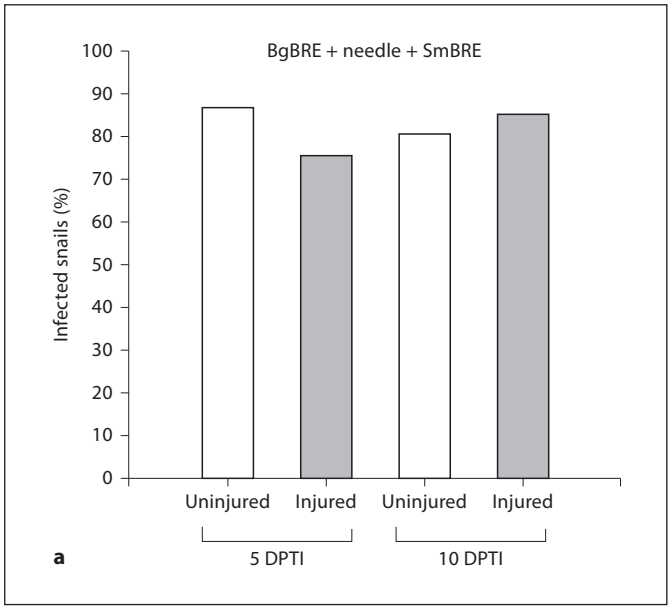

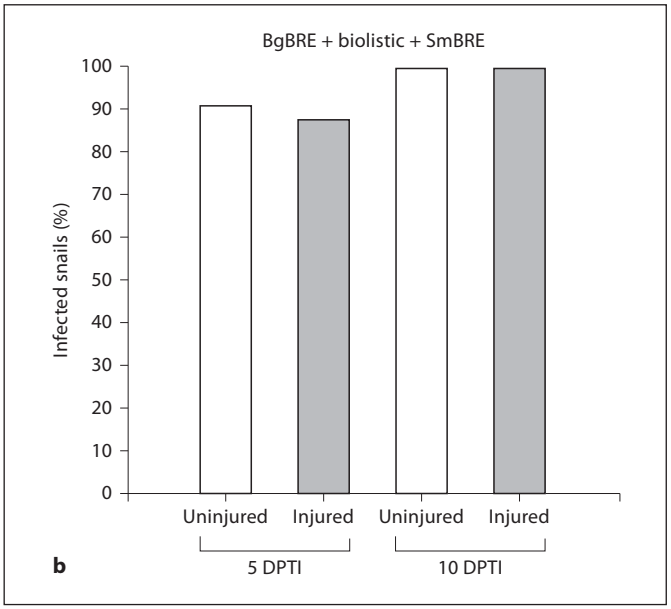

Fig. 4. Infection rates of BgBRE snails infected with 10 miracidia of SmBRE at 5 or 10 days DPTI. 'Uninjured' corresponds to healthy snails that did not receive tissue injuries. **a** Results from snails subjected to needle-induced tissue injuries. **b** Results from snails subjected to biolistic particle-induced tissue injuries.

Priming in Vaccinated Snails

Considering priming, two alternative hypotheses could be formulated to explain the observed phenomenon. Priming could be due to either an immune response of the host or an antagonistic interaction between parasites. The distinction between these alternatives would be a true challenge in this model. Thus, we developed an experimental vaccination approach as a tool to answer this question (fig. 5). One group of snails was injected with 1 g of whole miracidium extracts from SmBRE in

Table 3. Number of snails infected or not and prevalence values

a Following SmBRE primary infection

	SmBRE	SmBRE-LE	SmVEN	Srod
Unprimed				
Infected	45	28	18	26
Uninfected	0	0	2	9
Prevalence, %	100	100	90	74.3
Primed				
Infected	0	4	12	8
Uninfected	41	32	29	11
Prevalence, %	0	11.1	29.3	42.1
p value	<0.0001	<0.0001	<0.0001	0.037

b Following SmBRE-LE primary infection

	SmBRE	SmBRE-LE	SmVEN	Srod
Unprimed				
Infected	41	21	39	35
Uninfected	3	9	4	15
Prevalence, %	93.2	70	90.7	70
Primed				
Infected	10	9	15	25
Uninfected	20	25	13	3
Prevalence, %	33.3	26.5	53.6	89.3
p value	<0.0001	0.001	0.0005	0.09

p values: Fisher's exact tests were calculated for each condition comparing unprimed and primed values.

Table 4. Mean intensity values

a Following SmBRE primary infection

	SmBRE	SmBRE-LE	SmVEN	Srod
Unprimed	3.58	4.5	1.89	2
Primed	ND	1.25	1.17	1.62
Mann-Whitney				
n1	41	28	18	26
n2	0	4	12	8
U	ND	4	62	81.5
p value	ND	0.003	0.026	0.331

b Following SmBRE-LE primary infection

	SmBRE	SmBRE-LE	SmVEN	Srod
Unprimed	2.36	2.14	2.46	1.85
Primed	1	1.3	1.25	2.08
Mann Whitney				
n1	41	21	39	35
n2	10	9	15	25
U	55	130.5	173	397.5
p value	<0.001	0.07	0.016	0.519

ND = Not determined – for primed snails in SmBRE homologous challenge condition no infected snails could be observed thus intensity and Mann-Whitney U tests could not be calculated.

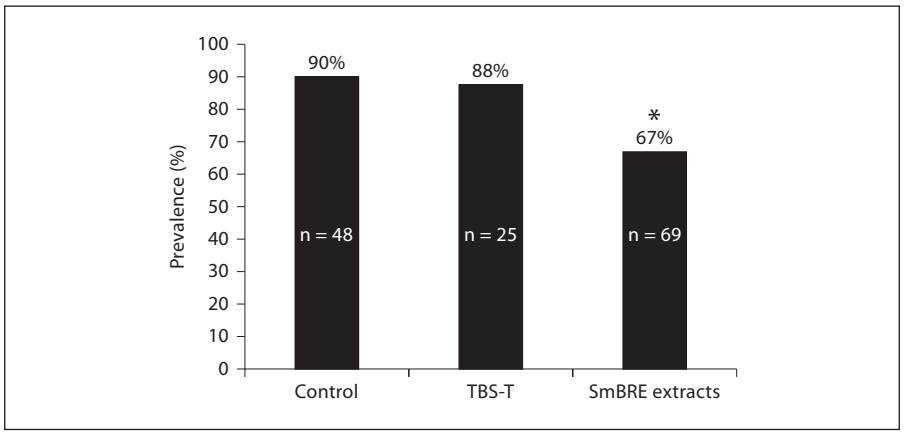

Fig. 5. Experimental vaccination of *B. glabrata* with *Sm*BRE miracidium extracts. Prevalence of naïve snails (control), snails injected with 20 l of TBS-T and snails vaccinated with 1 g of SmBRE miracidium extracts in 20 l of TBS-T. Snails were treated 15 days before the exposure to 10 miracidia of *Sm*BRE. n = Number of snails used in each group. * p ! 0.05.

TBS-T (SmBRE extracts). As controls, a second group received an injection of TBS-T alone (TBS-T) and a third group did not receive any treatment (control). The prevalence for the TBS-T group was 88% and did not differ significantly from the prevalence of the control group, which was 90% (fig. 5). In the SmBRE extracts group the prevalence decreased significantly to 67% compared to the control and TBS-T groups (Fisher's exact test: p ! 0.05). This experiment invalidated the parasite antagonistic interaction hypothesis. Indeed, when infections were made

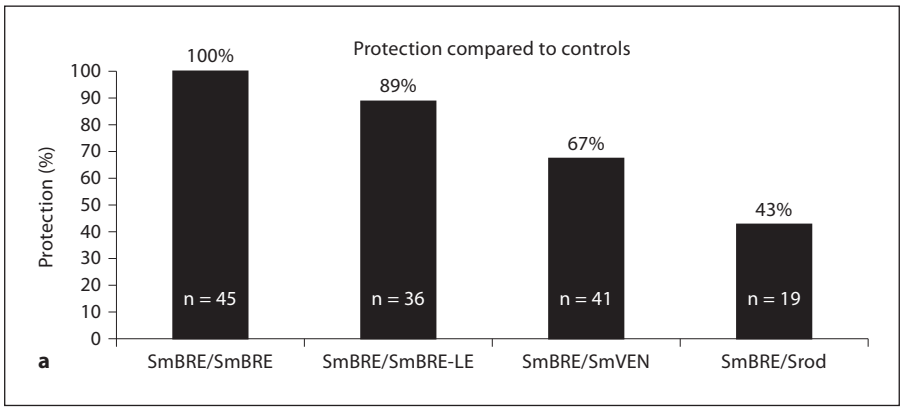

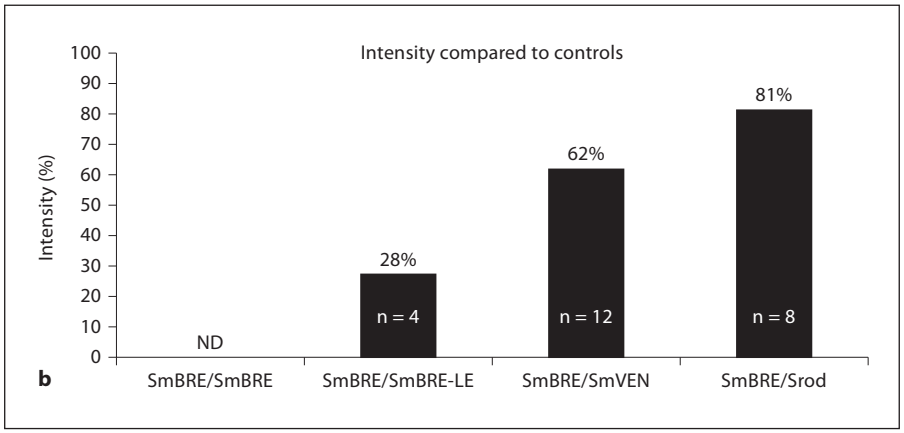

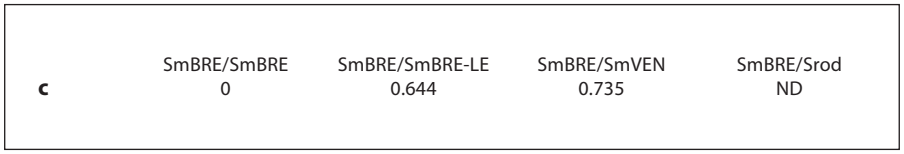

Fig. 6. Specific genotype-dependent immune priming in *B. glabrata* snails. Effect of a primary infection with SmBRE on prevalence (**a**) and intensity (**b**) after secondary infections with different *Schistosoma* strains. ND = Not determined – no intensity rate could be calculated because there was no snail infected. **c** Nei's genetic distances between the strain used for the primary infection and the strain used for the secondary infections (table 2b); Nei's distance could not be calculated because microsatellite markers for *S. rodhaini* were not available.

15 days after SmBre extract injection, we could suppose that all the parasite proteins injected had been ubiquitinated and addressed to the proteasome to be destroyed and recycled. Thus a direct parasite antagonism could not be considered and the host immune response hypothesis appeared to be more relevant.

Specific Genotype-Dependent Immune Priming

Primary infection of BgBRE snails was done with SmBRE (fig. 6a) or SmBRE-LE (fig. 6b) and snails were secondary infected with 4 different *Schistosomes*: SmBRE, SmBRE-LE, SmVEN and Srod.

For SmBRE primary infection (fig. 6a) the prevalence values for all the secondary infections tested decreased significantly compared to unprimed snails (table 3a). Thus, immune priming is efficient for each condition. When comparing the prevalence for all the secondary infections tested we could observe that prevalence in primed snails increased from 0% for SmBRE to 42.1% for Srod secondary infections. The link between this increase of prevalence and genetic distance was tested using a ^{2} for trends that are highly significant (^{2} for trend = 18.384; d.f. = 1; p ! 0.0001). Protection levels were calculated as a ratio between prevalence values of primed and controls snails (fig. 6a). In the case of homologous combinations (SmBRE/SmBRE) the protection level was 100%. In the case of heterologous combinations protection levels were 89% for SmBRE-LE (same species, same country, different strain), 67% for SmVEN (same species, different country, different strain), and 43% for Srod (different species). Concerning intensity values, for the homologous combination (SmBRE/SmBRE) no reinfection occurred

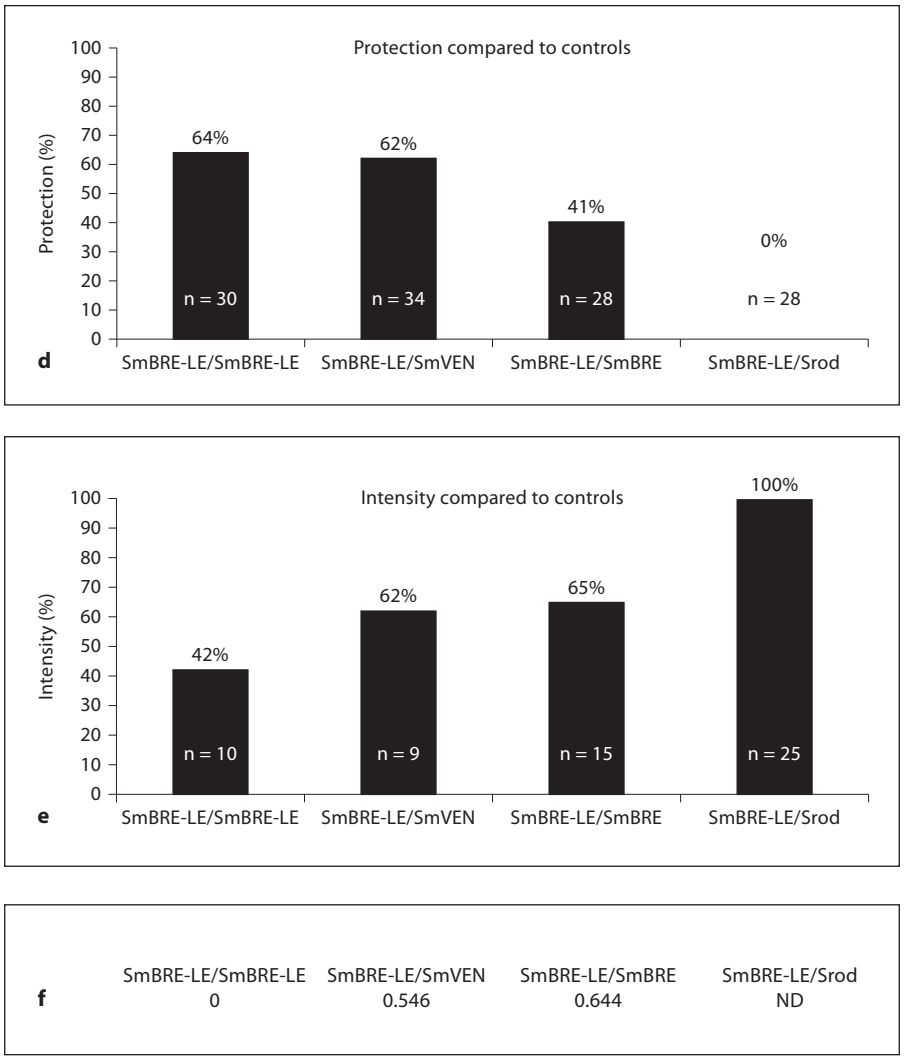

Fig. 6. Effect of a primary infection with SmBRE-LE on prevalence (**d**) and intensity (**e**) after secondary infections with different *Schistosoma* strains. **f** Nei's genetic distances between the strain used for the primary infection and the strain used for the secondary infections (table 2b); Nei's distance could not be calculated because microsatellite markers for *S. rodhaini* were not available.

(protection 100%; fig. 6a), hence intensity could not be calculated (table 4a). For heterologous combinations intensity levels were calculated as described in the Material and Methods section. We could observe that intensity deceased in primed snails compared to unprimed snails. This decrease was significant for secondary infection with SmBRE, SmBRE-LE and SmVEN (table 4a). Investigating the link between intensity and genetic distance, we observed that intensity levels increased regularly with the genetic distance (fig. 6b, c): 28% for SmBRE-LE secondary infection (same species, same country, different strain), 62% with SmVEN (same species, different country, different strain) and 81% with Srod (different species).

For SmBRE-LE primary infection (fig. 6d–f) the prevalence values for all the secondary infections tested decreased significantly compared to unprimed snails except for Srod secondary infection for which the prevalence was not affected by SmBRE-LE primary infection (table 3b). When comparing the prevalence for all the secondary infections tested we could observe that prevalence in primed snails increased from 26.5% for SmVEN to 89.3% for Srod. The link between this increase of prevalence and genetic distance was tested using a ^{2} for trends that are significant (^{2} for trend = 8.52; d.f. = 1; p = 0.0035). Protection levels were calculated as a ratio between prevalence values of primed and controls snails (fig. 6d). In the case of homologous combinations (SmBRE-LE/SmBRE-LE) the protection level was of 64%. In the case of heterologous combinations protection levels were 62% for SmVEN (same species, different country, different strain), 41% for SmBRE (same species, same country, different strain) and 0% with Srod (different spe-

cies). The intensity decreased in primed snails compared to unprimed snails except for the secondary infection with Srod for which the intensity was not affected by SmBRE-LE primary infection (table 4b). This decrease is significant for secondary infection with SmBRE-LE and SmBRE (table 4a). Investigating the link between intensity and genetic distance, we observed that intensity levels increased regularly with genetic distance (fig. 6e, f): 42% for SmBRE-LE secondary infection (homologous combination), 62% for SmVEN (same species, different country, different strain), 65% for SmBRE (same species, same country, different strain) and 100% with Srod (different species).

These results confirmed that immune priming affects prevalence and intensity, i.e. the number of SpIs that penetrated and developed in snail tissues decreased in primed snails compared to unprimed snails. However, whatever the strain used for the primary infection (SmBRE or SmBRE-LE), protection levels decreased and intensity levels increased with the increase of the Nei genetic distance between primary and secondary infections (fig. 6a, b). Immune priming appeared to be less efficient when genetic distance increased. These results concerning prevalence and intensity indicate that priming in *B. glabrata* is highly specific, and seems to be genotype-dependent.

Discussion

A better understanding of Lophotrochozoan innate immunity, which remains poorly investigated, appears to be crucial to bridge the gap between Deuterostoma and Ecdysozoa immunity and will help achieve a better understanding of the diversity and evolution of innate immune processes. In this study, we investigated the occurrence, the origin and the specificity of immune priming among fresh-water snails *B. glabrata* exposed to trematode pathogens of the genus *Schistosoma*. The existence of efficient immune priming was confirmed using homologous primo/secondary infections in different *B. glabrata* strains. When homologous primo/secondary infections were performed no secondary infections were observed, regardless of whether it was the host strain (fig. 1). After a primary infection of BgGUA or BgBRE snails, the mollusks were totally protected from secondary infection.

We were able to confirm the occurrence of immune priming in our model; however, the characterization of immune priming in an invertebrate animal model requires consideration regarding the timing of this process (i.e. when priming first appears after infection and how long it is maintained thereafter). The first study reporting the discovery of this process in *B. glabrata* showed that BgBRE snails developed a time-dependent 'acquired resistance' starting 3 DPI [47]. The success of secondary infection decreased from 3 to 7 DPI, the snails became totally protected against secondary infections between 7 and 14 days, and they remained protected until the end of the snail's life [47].

To further investigate the cause of this partial protection against secondary infection within the first 7 days following primary infection, and the total protection against secondary infections occurring between 7 and 14 DPI, we examined the intramolluskal development of the parasite (fig. 2). The histological approach conducted in the present paper showed that SpIs grew and developed in snail tissues to produce SpIIs during the first 14 DPI (fig. 2A, B); the migration of SpIIs through host tissues started at 10 DPI (fig. 2D) and the first SpIIs reached the digestive/genital gland interface at 14 DPI (fig. 2F, G). Furthermore, the growth of SpIs and the development of SpIIs, which occurred during the first 7 DPI, were correlated with the decreased success of secondary infection, while the start of SpII migration (10 DPI) was concomitant with the acquisition of complete protection against secondary infections. These observations suggest that the dynamics of parasitic development are linked to the acquisition of protection. In this context, we can hypothesize that the tissue damage induced by the parasite during miracidial penetration and SpII migration could activate the snail inflammatory and immune processes responsible for the observed immune priming. In order to test the impact of miracidial penetration on immune priming, we used UV-irradiated miracidia that were capable of infecting the host snails, but did not show subsequent development (no growth, no SpII differentiation or migration). Under these irradiated conditions, no resistance was observed (fig. 3a). This result is in agreement with a previous study showing that immune stimulation of *B. glabrata* with irradiated miracidia did not induce protection [63]. One hypothesis could be that tissue lesions resulting from the growth and development of SpIs/SpIIs and/or the migration of SpIIs could trigger a nonspecific acquired protection; this phenomenon was previously described for different invertebrate species where wounding was found to induce nonspecific immune responses that prevented opportunistic infections [38–40]. We tested this hypothesis by submitting snails to simple needle- or biolistic particle-induced tissue injuries (fig. 4) without

any specific antigenic stimulation prior to infection, as previously examined in insects [64]. No significant protection against parasitic infection was observed, showing that lesion-induced immune stimulation was not responsible for the observed protection against *S. mansoni*.

These results supported the view that SpI/SpII growth and development in snail tissues resulted in the stimulation of snail immunity that was probably the cause of the immune priming response developed against secondary infections. However, an alternative hypothesis has to be considered. The priming effect disappeared when irradiated parasites were used for primary infection (fig. 3). Based on this observation the acquired protection against secondary infections observed could be interpreted as kin-mediated competition among parasites [2, 47] rather than as the result of the host immune priming response. Indeed, after the primary infection, the parasite *S. mansoni* remained in the host's tissues throughout the snail's life. Sire et al. [47] have thus suggested that the failure of secondary infection could well be due to intraspecific larval antagonism. However, this is a subject of controversy, as some authors expected a higher competition between more closely related parasites that use similar resources [3], while others hypothesized that kin cooperation should facilitate rather than reduce secondary infection rates [23]. Moreover, it was recently shown that coinfections could enhance certain parasite life history traits (reproduction, growth, etc.) [65] or increase parasite prevalence [66] indicating no evidence for regulatory processes or larval antagonism [48]. Axenic cultivation studies performed on several trematode species, including *S. mansoni*, did not show any evidence for a direct antagonistic effect in vitro [67]. Finally, we developed recently a global bi-dimensional proteomic approach conducted on primed snail plasma following *S. mansoni* infection (data not shown). This approach did not identify any circulating parasite molecules in these plasmas, another clue for the absence of a direct larval antagonism in this model.

However, all these assumptions constituted indirect arguments. To be fully convinced of the existence of efficient immune priming in the *B. glabrata/Schistosoma* spp. model, we developed a vaccination experiment (fig. 5). We showed that vaccination with miracidium protein extracts significantly reduce prevalence (fig. 5), resulting in a partial protection against secondary infection. This partial protection could not be related to a direct larval antagonism but supports the view that SpI/SpII growth and development were important steps toward the acquisition of a total immune priming response.

The fact that immune stimulation along the parasite development from miracidium penetration to SpII migration appeared to be essential to the acquisition of a total immune priming response (a partial protection is obtained with miracidium proteins) asks the question of the specificity of immune priming response in *B. glabrata*. Most of the models used for studying immune priming in invertebrates were conducted for arthropods (insects [2, 24, 27–29] or crustaceans [4, 21, 30, 31]) infected by bacteria, yeast or virus. For eukaryote hosts, it could be easy with a limited set of pattern recognition receptors to discriminate or recognize lipopolysaccharides, peptidoglycans or -glucans, some very specific pathogen-associated molecular patterns of micro-organisms and respond to them efficiently. This was perfectly illustrated for Drosophila immune priming response for which response to fungal and bacterial infection occurred through two distinct signaling cascades, which are known as the Toll and immune deficiency pathways, respectively [9]. These activations resulted in separated intracellular signaling cascades inducing the synthesis of seven families of antimicrobial peptides that were directed against fungi, Gram-positive or Gram-negative bacteria and protect the fly against subsequent infections more or less specifically [9, 27].

In the *B. glabrata/Schistosoma* spp. model both partners are metazoan eukaryotes belonging to the Lophotrochozoan group and this phylogenetic proximity is particularly interesting when studying the mechanisms involved in the specificity of immune priming. Here a higher level of specificity is expected because of the potential molecular proximity between host and parasite antigens. The mechanisms involved in host immune recognition were expected to be sophisticated to discriminate between self- and nonself-eukaryote cells and avoid autoimmunity.

When studying immune priming specificity in invertebrate systems, care is needed to ensure that the specificity of the putative changes in immune reactivity is fully addressed by secondary challenge with a wide range of related and unrelated pathogens or parasites. The different geographic isolates or species of parasites maintained in our laboratory were used to show a high degree of specificity using homologous and heterologous challenges (fig. 6, table 2). The protection decreased from homologous to heterologous conditions alongside the genetic distance between parasites used for primary infections and challenges (different geographic isolates or different species of parasites were used; fig. 6). Parasite intensity also gives the same interesting results. Indeed,

figure 6 showed that intensity in primed snails increases together with the genetic distance. This indicates that prior exposure to genetically closer parasites resulted in fewer parasites that penetrated and developed in the host than occurred after exposure to genetically distant parasites.

This result is interesting because it shows that the first stimulation activated immune components that were able to discriminate more or less efficiently between the parasite strain used for the primary infection and for the challenge. In this context, it is important to note that the strains used are genetically distinct (table 2). Immune priming specificity appeared to be dependent on the genetic distance between the parasite used for the primary infection and for the challenge and illustrated that the specificity of the immune priming in *B. glabrata* is probably genotype dependent.

To date, to our knowledge, only one paper has investigated immune priming specificity in a host/parasite metazoan eukaryote interaction. In that paper, evidence for specific immune priming has been uncovered in the small crustacean copepod *Macrocyclops albidus* infected with different strains of its natural tapeworm parasite, *Schistocephalus solidus* [23]. The authors reported that prior exposure to related parasites resulted in less secondary infection than occurred after exposure to unrelated parasites. Here also the authors were able to demonstrate a genotype-dependent immune priming [23]. However, this effect was studied over only 3 days after primary infection and the specificity observed could result from the primary response and not from immune priming or memory.

Collectively, our observations demonstrate the specificity of the protection process. Better protection against a homologous (vs. heterologous) secondary infection in immune priming (fig. 1, 6) may arise via processes that involve specific immune receptors and/or effectors that are mobilized to target certain subsets of *S. mansoni* genotypes. Previous reports make the FREPs, some polymorphic and diversified putative immune receptor variants, promising candidates for involvement in the immune priming taking place in *B. glabrata* [18, 42, 68]. FREPs are diversified recognition and/or effector proteins involved in *B. glabrata* defense against parasitic infection that exhibit functional specialization with respect to the pathogen encountered [69–72]. These molecules are hemolymph lectins [73] that exhibited a remarkable degree of diversification [18]. Finally, their crucial role in the fate of infection was previously demonstrated using siRNA-mediated knockdown, which rendered approximately 30% of constitutively resistant adult snails susceptible to *Echinostoma paraensei* [68].

Interestingly, we recently showed that a specific set of these highly variable FREPs from *B. glabrata* forms immune complexes with mucin molecules from *S. mansoni* (*S. mansoni* polymorphic mucins; SmPoMucs), which are also highly polymorphic and individually variable [19]. This was the first evidence of an interaction between FREP, one of the putative diversified immune receptors and antigenic variants in an invertebrate host/pathogen model [19]. Each *S. mansoni* individual expresses a particular SmPoMuc profile [44, 45], which may be recognized by a specific set of FREPs produced by the mollusk. Consequently, the specific sets of FREPs produced in response to the parasitic strains or genotypes found in the primary infection may form the basis for the specific immune priming described herein. The snails would then be protected against secondary infection, with the degree of protection depending on the antigenic similarities between the strains used for the primary and secondary infections. Confirming the role played by FREPs in this priming process deserves further functional experiment using siRNA approaches.

Until now, priming observations in invertebrates were mainly phenomenological and based on ecological or phenotypic studies, and they lacked a clear understanding or description of the potential underlying molecular and/or cellular mechanisms. The exception to this was the enhanced phagocytosis described in two prior studies in *Porcellio scaber* (Crustacea, Isopoda) and *A. gambiae* (Insecta, Diptera) [24, 28]. The international community working on invertebrate innate immunity believes that observations cannot be used in isolation and should solely be used to construct hypotheses but such hypotheses must be exhaustively tested and backed by rigorous functional cellular, biochemical and molecular methods to eliminate all alternative explanations [3, 74].

Thus, future studies should use gene-discovery approaches (e.g. global comparative proteomic or transcriptomic studies) to identify all of the determinants involved in the specific immune priming of the Lophotrochozoan snail, *B. glabrata*, in response to *S. mansoni* infections. A better understanding of the immune priming response of the Lophotrochozoan snails could help us decipher the evolutionary history of innate immune memory or immune priming in organisms ranging from the Ecdysozoa to the Deuterostomia.

Acknowledgements

This work was funded by the ANR (grant No. 25402 BiomGenIm; ANR-07-BLAN-0214-03), the CNRS and the UPVD. The funders had no role in the study design, data collection, data analysis, decision to publish or preparation of the manuscript.

We thank Jean-Marc Reichhart and Louis Du Pasquier for advice and fruitful discussions. We thank Bernard Dejean and Nathalie Arancibia for technical assistance (2EI, Perpignan). We thank Cécile Antonelli (LGDP, Perpignan) for expert technical assistance with the biolistic particle delivery system. We thank Christoph Grunau and Céline Cosseau for their help with the PCR-based diagnostics. This paper is dedicated to my friend and exceptional researcher Didier Mouginot (1963–2012).

References

1 Kurtz J: Specific memory within innate immune systems. Trends Immunol 2005;26:186–192.
2 Sadd BM, Schmid-Hempel P: Insect immunity shows specificity in protection upon secondary pathogen exposure. Curr Biol 2006;16:1206–1210.
3 Hauton C, Smith VJ: Adaptive immunity in invertebrates: a straw house without a mechanistic foundation. Bioessays 2007;29:1138–1146.
4 Vazquez L, Alpuche J, Maldonado G, Agundis C, Pereyra-Morales A, Zenteno E: Review: immunity mechanisms in crustaceans. Innate immunity 2009;15:179–188.
5 Litman GW, Dishaw LJ, Cannon JP, Haire RN, Rast JP: Alternative mechanisms of immune receptor diversity. Curr Opin Immunol 2007;19:526–534.
6 Tonegawa S: Somatic generation of antibody diversity. Nature 1983;302:575–581.
7 Guo P, Hirano M, Herrin BR, Li J, Yu C, Sadlonova A, Cooper MD: Dual nature of the adaptive immune system in lampreys. Nature 2009;459:796–801.
8 Medzhitov R, Janeway CA Jr: Innate immunity: the virtues of a nonclonal system of recognition. Cell 1997;91:295–298.
9 Ferrandon D, Imler JL, Hetru C, Hoffmann JA: The *Drosophila* systemic immune response: sensing and signalling during bacterial and fungal infections. Nat Rev Immunol 2007;7:862–874.
10 Hildemann WH, Johnson IS, Jokiel PL: Immunocompetence in the lowest metazoan phylum: transplantation immunity in sponges. Science 1979;204:420–422.
11 Hildemann WH, Raison RL, Cheung G, Hull CJ, Akaka L, Okamoto J: Immunological specificity and memory in a scleractinian coral. Nature 1977;270:219–223.
12 Cooper EL: Transplantation immunity in annelids. I. Rejection of xenografts exchanged between lumbricus terrestris and eisenia foetida. Transplantation 1968;6:322–327.
13 Coffaro KA, Hinegardner RT: Immune response in the sea urchin lytechinus pictus. Science 1977;197:1389–1390.
14 Kurtz J: Memory in the innate and adaptive immune systems. Microbes Infect 2004;6:1410–1417.
15 Pancer Z: Dynamic expression of multiple scavenger receptor cysteine-rich genes in coelomocytes of the purple sea urchin. Proc Natl Acad Sci USA 2000;97:13156–13161.
16 Dong Y, Taylor HE, Dimopoulos G: Agdscam, a hypervariable immunoglobulin domain-containing receptor of the *Anopheles gambiae* innate immune system. PLoS biology 2006;4:e229.
17 Watson FL, Puttmann-Holgado R, Thomas F, Lamar DL, Hughes M, Kondo M, Rebel VI, Schmucker D: Extensive diversity of Ig-superfamily proteins in the immune system of insects. Science 2005;309:1874–1878.
18 Zhang SM, Adema CM, Kepler TB, Loker ES: Diversification of ig superfamily genes in an invertebrate. Science 2004;305:251–254.
19 Moné Y, Gourbal B, Duval D, Du Pasquier L, Kieffer-Jaquinod S, Mitta G: A large repertoire of parasite epitopes matched by a large repertoire of host immune receptors in an invertebrate host/parasite model. PLoS Negl Trop Dis 2010;4:e813.
20 Little TJ, Kraaijeveld AR: Ecological and evolutionary implications of immunological priming in invertebrates. Trends Ecol Evol 2004;19:58–60.
21 Witteveldt J, Cifuentes CC, Vlak JM, van Hulten MC: Protection of penaeus monodon against white spot syndrome virus by oral vaccination. J Virol 2004;78:2057–2061.
22 Cooper EL, Rinkevich B, Uhlenbruck G, Valembois P: Invertebrate immunity: another viewpoint. Scand J Immunol 1992;35:247–266.
23 Kurtz J, Franz K: Innate defence: evidence for memory in invertebrate immunity. Nature 2003;425:37–38.
24 Rodrigues J, Brayner FA, Alves LC, Dixit R, Barillas-Mury C: Hemocyte differentiation mediates innate immune memory in *Anopheles gambiae* mosquitoes. Science 2010;329:1353–1355.
25 Gonzalez-Tokman D, Gonzalez-Santoyo I, Lanz-Mendoza H, Aguilar A: Territorial damselflies do not show immunological priming in the wild. Physiol Entomol 2010;35:364–372.
26 Reber A, Chapuisat M: No evidence for immune priming in ants exposed to a fungal pathogen. PloS One 2012;7:e35372.
27 Pham LN, Dionne MS, Shirasu-Hiza M, Schneider DS: A specific primed immune response in *Drosophila* is dependent on phagocytes. PLoS Pathog 2007;3:e26.
28 Roth O, Kurtz J: Phagocytosis mediates specificity in the immune defence of an invertebrate, the woodlouse *Porcellio scaber* (Crustacea: Isopoda). Dev Comp Immunol 2009;33:1151–1155.
29 Tidbury HJ, Pedersen AB, Boots M: Within and transgenerational immune priming in an insect to a DNA virus. Proceedings 2011;278:871–876.
30 Little TJ, O'Connor B, Colegrave N, Watt K, Read AF: Maternal transfer of strain-specific immunity in an invertebrate. Curr Biol 2003;13:489–492.
31 Pope EC, Powell A, Roberts EC, Shields RJ, Wardle R, Rowley AF: Enhanced cellular immunity in shrimp *(Litopenaeus vannamei)* after 'vaccination'. PloS One 2011;6:e20960.
32 Sadd BM, Kleinlogel Y, Schmid-Hempel R, Schmid-Hempel P: Trans-generational immune priming in a social insect. Biol Lett 2005;1:386–388.
33 Sadd BM, Schmid-Hempel P: Facultative but persistent trans-generational immunity via the mother's eggs in bumblebees. Curr Biol 2007;17:R1046–R1047.
34 Moret Y: 'Trans-generational immune priming': specific enhancement of the antimicrobial immune response in the mealworm beetle, tenebrio molitor. Proc Biol Sci 2006;273:1399–1405.
35 Roth O, Joop G, Eggert H, Hilbert J, Daniel J, Schmid-Hempel P, Kurtz J: Paternally derived immune priming for offspring in the red flour beetle, *Tribolium castaneum*. J Anim Ecol 2010;79:403–413.
36 Moret Y, Siva-Jothy MT: Adaptive innate immunity? Responsive-mode prophylaxis in the mealworm beetle, *Tenebrio molitor*. Proc Biol Sci 2003;270:2475–2480.
37 Korner P, Schmid-Hempel P: In vivo dynamics of an immune response in the bumble bee *Bombus terrestris*. J Invertebr Pathol 2004;87:59–66.
38 Franchini A, Ottaviani E: Repair of molluscan tissue injury: role of PDGF and TGF- . Tissue Cell 2000;32:312–321.

39 Kubo T, Komano H, Okada M, Natori S: Identification of hemagglutinating protein and bactericidal activity in the hemolymph of adult *Sarcophaga peregrina* on injury of the body wall. Dev Comp Immunol 1984;8: 283–291.

40 Paterson HM, Murphy TJ, Purcell EJ, Shelley O, Kriynovich SJ, Lien E, Mannick JA, Lederer JA: Injury primes the innate immune system for enhanced Toll-like receptor reactivity. J Immunol 2003;171:1473–1483.

41 Baeza Garcia A, Pierce RJ, Gourbal B, Werkmeister E, Colinet D, Reichhart JM, Dissous C, Coustau C: Involvement of the cytokine mif in the snail host immune response to the parasite *Schistosoma mansoni*. PLoS Pathog 2010;6:e1001115.

42 Hanington PC, Lun CM, Adema CM, Loker ES: Time series analysis of the transcriptional responses of *Biomphalaria glabrata* throughout the course of intramolluscan development of *Schistosoma mansoni* and *Echinostoma paraensei*. Int J Parasitol 2010;40: 819–831.

43 Mone Y, Ribou AC, Cosseau C, Duval D, Theron A, Mitta G, Gourbal B: An example of molecular co-evolution: reactive oxygen species (ROS) and ROS scavenger levels in *Schistosoma mansoni*/*Biomphalaria glabrata* interactions. Int J Parasitol 2011;41:721–730.

44 Roger E, Gourbal B, Grunau C, Pierce RJ, Galinier R, Mitta G: Expression analysis of highly polymorphic mucin proteins (Sm PoMuc) from the parasite *Schistosoma mansoni*. Mol Biochem Parasitol 2008;157:217–227.

45 Roger E, Grunau C, Pierce RJ, Hirai H, Gourbal B, Galinier R, Emans R, Cesari IM, Cosseau C, Mitta G: Controlled chaos of polymorphic mucins in a metazoan parasite *(Schistosoma mansoni)* interacting with its invertebrate host *(Biomphalaria glabrata)*. PLoS Negl Trop Dis 2008;2:e330.

46 Roger E, Mitta G, Mone Y, Bouchut A, Rognon A, Grunau C, Boissier J, Theron A, Gourbal BE: Molecular determinants of compatibility polymorphism in the *Biomphalaria glabrata*/*Schistosoma mansoni* model: new candidates identified by a global comparative proteomics approach. Mol Biochem Parasitol 2008;157:205–216.

47 Sire C, Rognon A, Theron A: Failure of *Schistosoma mansoni* to reinfect *Biomphalaria glabrata* snails: acquired humoral resistance or intra-specific larval antagonism? Parasitology 1998;117:117–122.

48 Theron A, Pages JR, Rognon A: *Schistosoma mansoni*: distribution patterns of miracidia among *Biomphalaria glabrata* snail as related to host susceptibility and sporocyst regulatory processes. Exp Parasitol 1997;85:1–9.

49 Theron A, Touassem R: *Schistosoma rodhaini*: intramolluscan larval development, migration and replication processes of daughter sporocysts. Acta Trop 1989;46:39–45.

50 Mattos AC, Kusel JR, Pimenta PF, Coelho PM: Activity of praziquantel on in vitro transformed *Schistosoma mansoni* sporocysts. Mem Inst Oswaldo Cruz 2006;101 (suppl 1):283–287.

51 Guillou F, Roger E, Mone Y, Rognon A, Grunau C, Theron A, Mitta G, Coustau C, Gourbal BE: Excretory-secretory proteome of larval *Schistosoma mansoni* and *Echinostoma caproni*, two parasites of *Biomphalaria glabrata*. Mol Biochem Parasitol 2007; 155:45–56.

52 Curtis J, Sorensen RE, Page LK, Minchella DJ: Microsatellite loci in the human blood fluke *Schistosoma mansoni* and their utility for other schistosome species. Mol Ecol Notes 2001;1:143–145.

53 Durand P, Sire C, Theron A: Isolation of microsatellite markers in the digenetic trematode *Schistosoma mansoni* from Guadeloupe island. Mol Ecol 2000;9:997–998.

54 Rodrigues NB, Silvia MR, Pucci MM, Minchella DJ, Sorensen R, Loverde PT, Romanha AJ, Oliveira G: Microsatellite-enriched genomic libraries as a source of polymorphic loci for *Schistosoma mansoni*. Mol Ecol Notes 2007;7:263–265.

55 Blair L, Webster JP, Barker GC: Isolation and caracterization of polymorphic microsatellite markers in *Schistosoma mansoni* from Africa. Mol Ecol Notes 2001;1:93–95.

56 Rodrigues NB, Loverde PT, Romanha AJ, Oliveira G: Characterization of new *Schistosoma mansoni* microsatellite loci in sequences obtained from public DNA databases and microsatellite enriched genomic libraries. Mem Inst Oswaldo Cruz 2002;97(suppl 1):71–75.

57 Goudet J: FSTAT, a program to estimate and test gene diversities and fixation indices (version 2.9.3). 2001. http://www2unilch/popgen/softwares/ fstathtml.

58 Belkhir K, Borsa P, Chikhi L, Raufaste N, Bonhomme F: GENETIX 4.05, logiciel sous Windows TM pour la génétique des populations. Laboratoire Génome, Populations, Interactions, CNRS UMR 5000, Université de Montpellier II, Montpellier, 1996.

59 Allienne JF, Theron A, Gourbal B: Recovery of primary sporocysts in vivo in the *Schistosoma mansoni*/*Biomphalaria glabrata* model using a simple fixation method suitable for extraction of genomic DNA and RNA. Exp Parasitol 2011;129:11–16.

60 Mone Y, Mitta G, Duval D, Gourbal BE: Effect of amphotericin B on the infection success of *Schistosoma mansoni* in *Biomphalaria glabrata*. Exp Parasitol 2010;125:70–75.

61 Gourbal BE, Gabrion C: Histomorphological study of the preputial and clitoral glands in BALB/c mice with experimental taenia crassiceps infections. J Parasitol 2006;92: 189–192.

62 Ruelas DS, Karentz D, Sullivan JT: Sublethal effects of ultraviolet B radiation on miracidia and sporocysts of *Schistosoma mansoni*: intramolluscan development, infectivity, and photoreactivation. J Parasitol 2007;93: 1303–1310.

63 Azevedo CM, Borges CC, Andrade ZA: Changes induced in *Biomphalaria glabrata* (Say, 1818) following trials for artificial stimulation of its internal defense system. Mem Inst Oswaldo Cruz 2006;101(suppl 1):199–203.

64 Schmid-Hempel P: Natural insect host-parasite systems show immune priming and specificity: puzzles to be solved. Bioessays 2005;27:1026–1034.

65 Sandland GJ, Rodgers JK, Minchella DJ: Interspecific antagonism and virulence in hosts exposed to two parasite species. J Invertebr Pathol 2007;96:43–47.

66 Pereira CA, Martins-Souza RL, Coelho PM, Lima WS, Negrao-Correa D: Effect of *Angiostrongylus vasorum* infection on *Biomphalaria tenagophila* susceptibility to *Schistosoma mansoni*. Acta Tropica 2006;98:224–233.

67 Coustau C, Yoshino TP: Flukes without snails: advances in the in vitro cultivation of intramolluscan stages of trematodes. Exp Parasitol 2000;94:62–66.

68 Hanington PC, Forys MA, Dragoo JW, Zhang SM, Adema CM, Loker ES: Role for a somatically diversified lectin in resistance of an invertebrate to parasite infection. Proc Natl Acad Sci USA 2010;107:21087–21092.

69 Hertel LA, Adema CM, Loker ES: Differential expression of FREP genes in two strains of *Biomphalaria glabrata* following exposure to the digenetic trematodes *Schistosoma mansoni* and *Echinostoma paraensei*. Dev Comp Immunol 2005;29:295–303.

70 Loker ES, Adema CM, Zhang SM, Kepler TB: Invertebrate immune systems – not homogeneous, not simple, not well understood. Immunol Rev 2004;198:10–24.

71 Zhang SM, Loker ES: Representation of an immune responsive gene family encoding fibrinogen-related proteins in the freshwater mollusc *Biomphalaria glabrata*, an intermediate host for *Schistosoma mansoni*. Gene 2004;341:255–266.

72 Zhang SM, Zeng Y, Loker ES: Expression profiling and binding properties of fibrinogen-related proteins (FREPs), plasma proteins from the schistosome snail host *Biomphalaria glabrata*. Innate Immun 2008;14: 175–189.

73 Adema CM, Hertel LA, Miller RD, Loker ES: A family of fibrinogen-related proteins that precipitates parasite-derived molecules is produced by an invertebrate after infection. Proc Natl Acad Sci USA 1997;94:8691–8696.

74 Rowley AF, Powell A: Invertebrate immune systems specific, quasi-specific, or nonspecific? J Immunol 2007;179:7209–7214.

Chapitre deux :

La vaccination chez *Biomphalaria glabrata*

CHAPITRE 2 :
LA VACCINATION CHEZ *BIOMPHALARIA GLABRATA*

Vaccination of *Biomphalaria glabrata* with proteic exctracts from differents larval stages of its Trematode parasite *Schistosoma mansoni*

Portela J, Pinaud S, Théron A and Gourbal B

En préparation

L’étude de l’immunité chez les invertébrés a permis de mettre en évidence qu’une mémoire immunitaire existait chez ces organismes. De nombreux travaux visant à vacciner des organismes à l’aide de bactéries mortes ou de peptides bactériens ou viraux ont été menés et ont permis de mettre cette réponse en lumière (Faulhaber and Karp 1992; Johnson et al. 2008; Pope et al. 2011; Powell et al. 2011; Rowley and Pope 2012; Wang et al. 2013).

Nous avons été en mesure de mener ce type d’approche vaccinale chez *Biomphalaria glabrata* en utilisant des extraits parasitaires de miracidium de *Schistosoma mansoni* (voir Chapitre 1). Nous avons démontré qu’une vaccination du mollusque engendrait une protection partielle et nous avons donc décidé de mener des expériences plus complètes afin de mieux caractériser ce phénomène de vaccination chez notre mollusque. Ainsi nous avons vacciné des individus avec différentes quantités d’extraits protéiques parasitaires afin d’observer un effet dose. Nous avons également essayé de vacciner des individus avec des extraits protéiques provenant des différents stades parasitaires intramolluscaux se développant successivement dans le mollusque, à savoir les miracidia (Mi), les sporocystes primaires (SpI) et les sporocystes secondaires (SpII).

Introduction

Composante de l'immunité adaptative, la mémoire immunitaire a longtemps été attribuée aux vertébrés et uniquement à ces derniers. L'idée majeure était que l'immunité des invertébrés reposait sur une immunité innée simple et peu, voire non spécifique consistant en la reconnaissance de motifs pathogéniques (Pathogen associated molecular patterns : PAMP) communs à un grand nombre de parasites par des récepteurs (Pathogen recognition receptors : PRR) (Janeway 1989; Medzhitov and Janeway 1997). Cette vision simpliste est de plus en plus remise en question avec la découverte de nombreuses molécules diversifiées et polymorphes avec de potentielles fonctions immunitaires chez des invertébrés, les DsCam d'arthropodes (Dong et al. 2006; Chou et al. 2009), les SRCR et les protéines 185/333 d'échinodermes (Pancer 2000; Cannon et al. 2004; Nair et al. 2005; Terwilliger et al. 2006), et les FREPs de mollusques (Adema et al. 1997; Loker et al. 2004; Hanington et al. 2010b). Toutes ces découvertes mettent à mal le paradigme proposé par Janeway en 1989.

Les études sur l'immunité des invertébrés ont également permis de mettre en évidence un phénomène particulier de mémoire immunitaire nommé priming immunitaire. Ce priming immunitaire se manifeste par une meilleure réponse immunitaire après une immunisation de l'organisme (Faulhaber and Karp 1992; Schmid-Hempel 2005; Pham et al. 2007; Mowlds et al. 2008; Roth et al. 2009; Baruah et al. 2011; Tidbury et al. 2011). Ce priming se met en place suite à une exposition à un pathogène ou suite à une vaccination. Ces vaccinations chez les invertébrés se font la plus part du temps à l'aide de bactéries inactivées ou bien à partir d'extraits protéiques de bactéries (Faulhaber and Karp 1992; Johnson et al. 2008; Pope et al. 2011; Powell et al. 2011; Rowley and Pope 2012; Wang et al. 2013).

Dans notre modèle, le mollusque *Biomphalaria glabrata*, un phénomène de priming immunitaire a pu être observé (Sire et al. 1998). Dans ce processus, une résistance se met en place au cours du temps face au trématode parasite *Schistosoma mansoni*. Par la suite nous avons démontré que ce priming immunitaire était extrêmement spécifique et dépendant du génotype de la primo infestation (voir Chapitre 1 (Portela et al. 2013)). Dans cette étude nous avons mené une première expérience de vaccination afin de répondre à une question cruciale : le parasite de la primo infestation étant présent dans les tissus du mollusque, la réponse observée est-elle liée à une réponse immunitaire ou à une compétition entre le parasite présent et les nouveaux entrants ?

Nous avons donc injecté un extrait protéique de miracidium (Mi), le stade infestant du mollusque, puis soumis les mollusques à un challenge et mesuré la prévalence. Suite à ce

traitement nous avons observé une protection partielle avec une prévalence de 67% alors qu'elle était de 90% dans l'infestation contrôle (mollusque n'ayant pas subit d'injection) indiquant donc qu'il s'agissait bien d'une réponse immunitaire faisant suite à une immunisation. De plus, la stimulation du mollusque à l'aide de miracidium irradiés ou de lésions, n'a engendré aucune réponse immunitaire. Ces résultats laissent penser que c'est très certainement la succession des différents stades larvaires et le changement de couverture antigénique du parasite qui engendre la protection observée. En effet, après sa pénétration dans les tissus du mollusque, le miracidium va perdre ses plaques ciliées et mettre en place un nouveau tégument. De ce fait il va modifier sa couverture antigénique. Puis se développant il va produire des SpII qui vont à leur tour migrer, présentant une nouvelle couverture antigénique.

Afin de démontrer que notre hypothèse est correcte nous avons décidé de mener une approche de vaccination avec des extraits protéiques provenant des différents stades parasitaires rencontrés par le mollusque. Nous avons donc vacciné des mollusques avec des extraits de protéines venant de miracidium (Mi), de sporocystes primaires (SpI) ou de sporocystes secondaires (SpII). Avant cela nous avons tenu à nous assurer que la réponse observée était bien liée à un effet vaccinant en menant une approche de vaccination avec des doses croissantes d'extraits protéiques. Il est connu chez les vertébrés que la dose d'antigènes injectés lors de l'immunisation était positivement corrélée avec l'intensité de la réponse immunitaire (Asano et al. 1982; Frey et al. 2002; Disis et al. 2004; Ni et al. 2013). C'est pourquoi nous avons mené cette approche afin de valider l'effet vaccinant des protéines de parasite.

Matériel et méthode

Souches de parasites et de mollusques

Un isolat géographique Brésilien du mollusque *Biomphalaria glabrata* (BgBRE) est utilisé dans cette étude. La souche de parasite utilisée est S*chistosoma mansoni* isolat Brésil (SmBRE), son parasite sympatrique, responsable de la bilharziose intestinale. La souche de SmBRE est maintenue au laboratoire sur son mollusque sympatrique et sur souris (*Mus musculus*) comme décrit précédemment par Théron (Théron et al. 1997). En résumé, les miracidia sont récupérés de manière axénique à partir d'œufs accumulés dans le foie de souris infestées depuis 50 jours. Ces œufs sont récupérés sur des foies frais, ces derniers sont

homogénéisés dans une solution de NaCl 8,5%. Ensuite les foies broyés sont filtrés sur des tamis de maille de taille décroissante afin de récupérer les œufs dans le derniers tamis de 45 µm. Ces œufs sont alors récupérés dans de l'eau de forage et placés à la lumière à 26°C pendant 1-2 heures environ pour déclencher l'éclosion des miracidia.

Transformation in-vitro des miracidia en SpI

Pour la culture in vitro les œufs de miracidia fraichement récoltés sont placés pour l'éclosion dans de l'eau minérale naturelle contenant un mélange d'antibiotique et antimycotique à 1X (pénicilline 100 unités/ml, streptomycine 0,1 mg/ml et amphotéricine 0,025 µg/ml). Après éclosion, les miracidia sont récoltés à la pipette pasteur effilée puis concentrés sur glace par sédimentation dans un tube conique en verre de 10 ml. Les miracidia sont ensuite mis en culture dans un tube contenant du CBSS (NaCl 2,8 g/L + KCl 0,15 g/L + Na_2HPO_4 0,07g/L + $MgS0_4.7H_20$ 0,45 g/L + $CaCl_2.2H_2O$ 0,53 g/L + $NaHCO_3$ 0,05 g/L) additionné de la solution antibiotique/antimycotique à 2X. Le tube est placé en chambre de culture à 26°C pendant 24h afin que les miracidia se transforment en sporocystes primaires (Sp I). Les Sp I sont alors récupérés par centrifugation (2500 rpm, 15 min, température pièce) et stockés à -80°C avant utilisation (Guillou et al. 2007).

Récupération des Sporocystes secondaires et des échantillons contrôles

Parmi les différents stades intra-molluscaux du parasite, le stade sporocyste secondaire est celui qui est le plus difficile d'accès dans la glande digestive du mollusque mais également le plus abondant. La récupération de ce stade nécessite donc la dissection du mollusque. Lors d'infestations massives, la quasi intégralité de la glande digestive et de la gonade est saturée de parasites. Les animaux sont sélectionnés par observation à travers la coquille, celle-ci laissant entrevoir l'état d'infestation de l'animal par le niveau de saturation de la glande et de la gonade. Seuls les mollusques les plus infestés sont utilisés dans cette expérience. Ces animaux sont alors débarrassés de leur coquilles, et la glande digestive est prélevée et conservée à -80°C dans du Tris Buffer Saline – Tween 20 (Tween 20 : 0,05%) (TBS-Tween : TBS-T) jusqu'à l'extraction native. Pour le contrôle la glande digestive des mollusques est prélevée cette fois-ci sur des individus sains.

Extraction protéique native des miracidia, Sp1 et SpII

Les protéines sont extraites à partir de miracidia/SpI/SpII entier. Pour l'extraction miracidiale, environ 20 000 miracidia SmBRE sont récupérés d'un stock congelé à -80°C. S'en suit une extraction native dans du TBS-T (50 mM de Tris et 150 mM NaCl, le pH est ajusté avec HCl à 7,6Tween 20 à 0,05%). Dans un premier temps les échantillons sont fragmentés par 3 séries de congélation/décongélation successives, puis les échantillons sont soumis à une sonication (Amplitude 40%, 3 pulses de 30s avec dépôt sur glace entre chaque pulse). Les échantillons sont centrifugés et le surnageant contenant les protéines en solution est dosé au 2DQuantKit (Amersham) et conservé à -80°C avant utilisation.

Effet dose

Six groupes de mollusques BgBRE sexuellement matures (8-12 mm de diamètre) sont isolés et anesthésiés par balnéation de 4 heures dans de l'eau mentholée. Les différents groupes reçoivent des doses croissantes de protéines parasitaires. Les stades sporocystes secondaires et des glandes digestives saines (contrôle) sont prélevés par dissection. Trois groupes de 35 mollusques reçoivent des doses croissantes de protéine de sporocyste secondaire (1 µg, 10 µg, 50 µg). Deux autres groupes de 35 mollusques reçoivent respectivement 1 µg et 50 µg de protéine de glande digestive et permettront de contrôler l'effet d'injection d'une protéine exogène non parasitaire (protéine neutre). Enfin le dernier groupe (35 mollusques) est le contrôle de l'infestation, il ne subit aucune vaccination. Pour l'ensemble des groupes, quinze jours après les traitements, les animaux sont infestés individuellement avec 10 miracidia SmBRE. Quinze jours après l'infestation les mollusques sont fixés dans une solution de Raillet-Henry (NaCl 6 g/L, Acide acétique 20 mL/L, Formol 40% 50mL/L, Eau QSP 1L) et disséqués pour évaluer les prévalences et intensités.

Vaccination

La vaccination est réalisée sur des individus sexuellement matures de 8-12 mm de diamètre. Six groupes (de 35 individus) de BgBRE sont anesthésiés par une balnéation de 4h dans de l'eau mentholée. Le premier groupe reçoit une injection de 1 µg de protéines de miracidia (Mi) de SmBRE solubilisé dans 20 µl de PBS (phosphate buffer saline) mollusque. Le second groupe reçoit 1 µg de protéine de sporocyste I (SpI) de SmBRE. Le troisième groupe reçoit 1 µg de protéine de sporocyste II (SpII) de SmBRE. Un des groupes reçoit 50

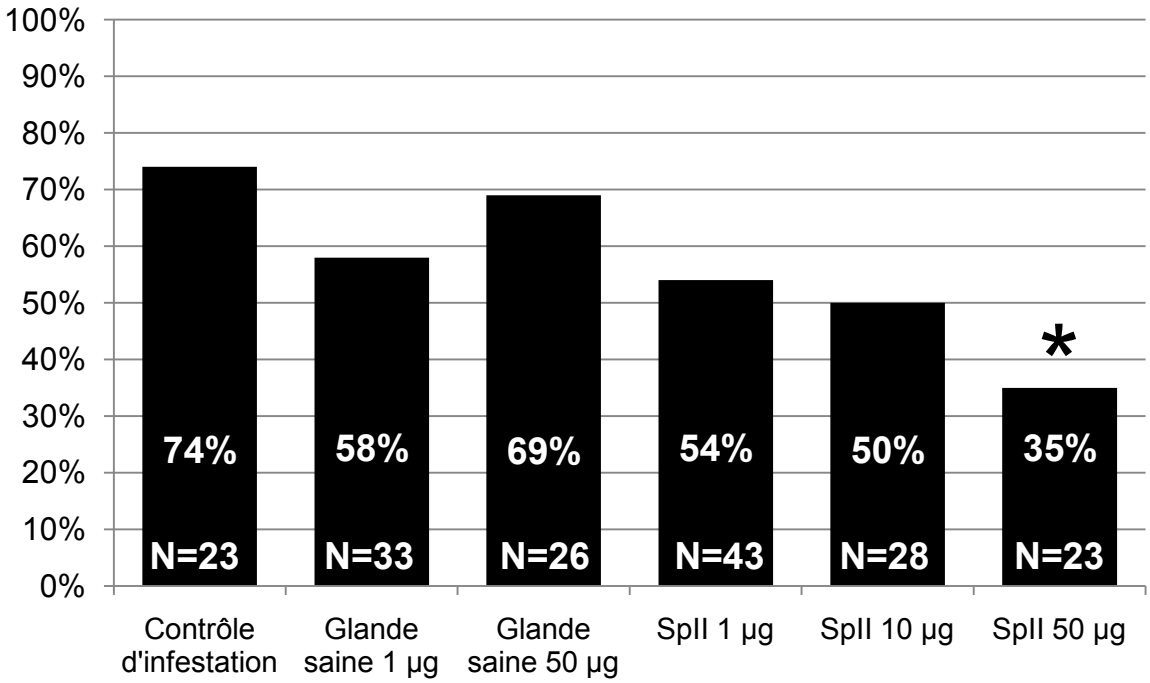

Figure 4 : Prévalences chez des mollusques vaccinés avec des doses croissantes d'extraits protéiques de SpII.
Contrôle d'infestation : mollusques naïfs infestés. Glande saine : mollusques vaccinés avec un extrait protéique de glande digestive de mollusque sain. SpII : mollusques vaccinés par un extrait protéique de sporocystes secondaires. N : effectifs disséqués par condition. * : différence significative en comparaison avec le contrôle d'infestation.

µg de protéine de glande digestive issue d'animaux sains, il sert de contrôle d'une injection de protéines non parasitaires. Un groupe recevra un mélange de protéine de miracidia et de sporocyste II, le tout dosé à 1 µg. Le manque de matériel ne nous a pas permis de rajouter les extraits protéiques de SpI. Le dernier groupe constituera le contrôle de l'infestation et aucune vaccination n'y sera réalisée. Quinze jours après les traitements, l'ensemble des groupes expérimentaux, sont infestés individuellement avec 10 miracidia SmBRE. Quinze jours après l'infestation, les mollusques sont fixés dans une solution de Raillet-Henry et disséqués afin d'évaluer les prévalences et intensités.

Analyses statistiques

Les résultats concernant les prévalences ont été testés en utilisant un Test exact de Fisher qui prend en compte deux variables binaires, les individus infestés d'une part et les sains d'autre part. Pour ce test, les différences significatives sont observées à $p<0,05$.

Résultats

Effet dose

Pour tester l'effet de l'augmentation de la quantité de protéines injectées sur la réponse immunitaire, une expérience d'effet dose à été mise en place. D'une part l'effet dose est testé sur de la protéine parasitaire et plus précisément sur le stade sporocyste secondaire (Figure 4)

Le groupe contrôle de l'infestation n'ayant subit aucune vaccination présente une prévalence de 74%. Les deux groupes ayant reçus des doses de 1 µg et 50 µg de protéines extraites de glande digestive provenant de mollusques sains présentent respectivement des prévalences de 58% et 69% (Figure 4). Ces deux valeurs ne sont pas statistiquement différentes du contrôle d'infestation et n'indiquent aucun effet dose suite à l'injection de protéines de mollusque.

Les groupes ayant eu des injections de doses croissantes d'extraits protéiques de SpII (1 µg, 10 µg, 50 µg) présentent des prévalences décroissantes (54%, 50%, 35% respectivement) et le groupe recevant 50 µg d'extrait protéique présente une prévalence statistiquement différente du contrôle ($p = 0,028$) (Figure 4).

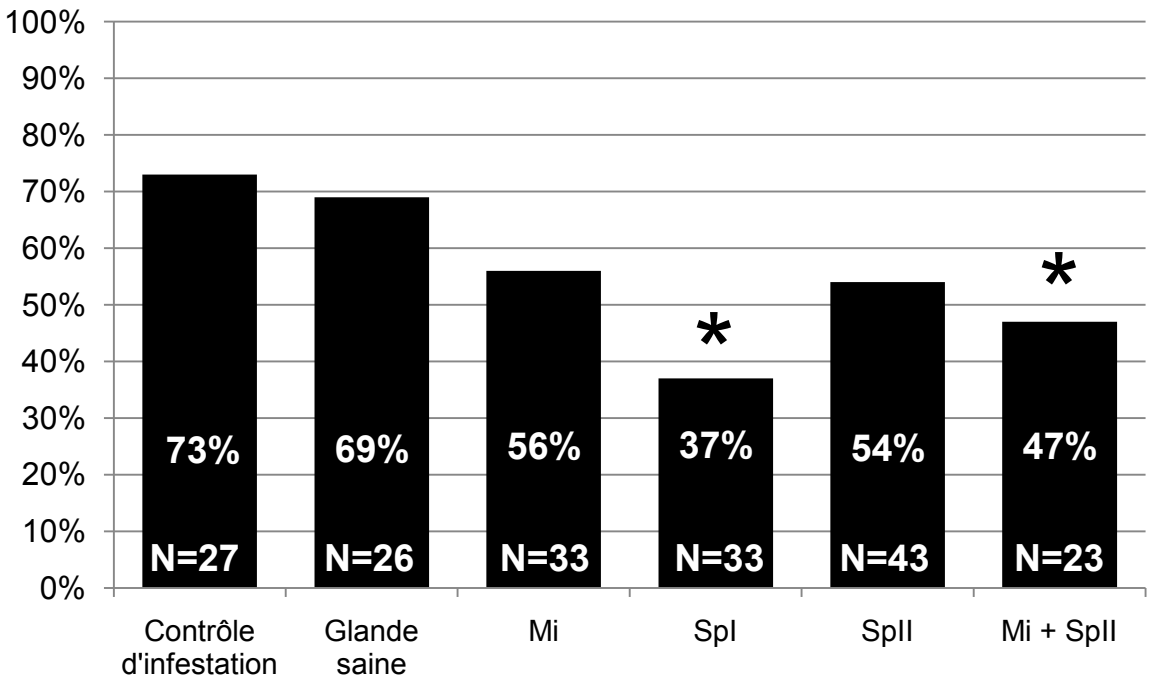

Figure 5 : Prévalences chez des mollusques vaccinés avec des extraits protéiques des différents stades larvaires parasitaires.
Contrôle d'infestation : mollusques naïfs infestés. Glande saine : mollusques vaccinés avec un extrait protéique de glande digestive de mollusque sain. Mi : mollusques vaccinés par un extrait protéique de miracidia. SpI : mollusques vaccinés par un extrait protéique de sporocystes primaires. SpII : mollusques vaccinés par un extrait protéique de sporocystes secondaires. N : effectifs disséqués par condition. * : différence significative en comparaison avec le contrôle d'infestation.

Vaccination

Cette expérience de vaccination par les différents stades de développement parasitaire intramolluscaux permet d'engendrer une protection sans faire intervenir le cycle classique du parasite comme dans le priming (Portela et al. 2013). Ainsi donc il sera possible de mimer la présence de chaque stade parasitaire de manière indépendante (Figure 5).

Dans le contrôle de l'infestation la prévalence est de 73%. Concernant le contrôle de l'injection d'un extrait protéique de mollusque la prévalence est de 69% ce qui ne diffère pas significativement du contrôle de l'infestation. On observe, en revanche, une baisse de la prévalence, 56% pour la vaccination avec un extrait de Mi, 37% pour la vaccination avec un extrait de SpI (baisse significative de la prévalence : $p = 0,031$) et 54% pour la vaccination avec un extrait de SpII (Figure 5). L'association entre des extraits de Mi et de SpII montre également une baisse significative de la prévalence. La prévalence est de 47%, et est significativement différente du contrôle ($p = 0,045$) ce qui laisse entrevoir un effet synergique de l'association de ces deux sources d'antigènes parasitaires (Figure 5).

Discussion

Le priming immunitaire a souvent été abordé par la vaccination, la plus part du temps il s'agissait d'injecter des bactéries tuées à des organismes avant de les soumettre à une vraie infestation (Faulhaber and Karp 1992; Wang et al. 2013). Dans d'autres cas, la vaccination se fait à l'aide de peptides bactériens ou viraux (Pope et al. 2011; Powell et al. 2011; Rowley and Pope 2012). Dans le modèle *Biomphalaria glabrata* il a été mis en évidences un phénomène de résistance acquise suite à une première infestation par *Schistosoma mansoni* (Sire et al. 1998). Lors de cette expérience il a également pu être mis en évidence que cette résistance se mettait en place au cours du temps. Cette particularité à tout d'abord été attribuée à une compétition que le parasite installé mettrait en place pour limiter l'installation d'autres parasites. Par la suite, nous avons démontré que ce phénomène était lié à une réponse immunitaire du mollusque par des approches indirectes mais également par une approche préliminaire de vaccination (Portela et al. 2013).

Chez les vertébrés la réponse immunitaire faisant suite à une stimulation est dépendante de la quantité d'antigènes injecté lors de l'immunisation (Asano et al. 1982; Frey et al. 2002; Disis et al. 2004; Ni et al. 2013). Afin de mieux décrire la réponse de *B. glabrata* suite à une vaccination nous avons mené une approche similaire visant à augmenter la

quantité de protéines injectées lors de l'immunisation et d'observer la prévalence suite à un challenge. Après avoir vacciné avec des doses croissantes d'extraits protéiques (1 µg, 10 µg et 50 µg) nous avons observé, suite au challenge, une diminution de la prévalence inversement proportionnelle à la dose de protéines injectées. De la dose injectées la plus faible à la plus élevée les prévalences ont été de 54%, 50% et 35% (Figure 4). Cette tendance de protection plus élevée suite à une immunisation par des doses croissantes d'extraits protéiques souligne à nouveau le caractère immunitaire de la réponse observée. Il pourrait être également intéressant de mener une expérience avec des injections de protéines à différents intervalles de temps puisque cette variable joue également un rôle dans l'immunisation au même titre que la dose (Asano et al. 1982).

Dans l'étude précédente (Portela et al. 2013), nous avons démontré que la mise en place au cours du temps du priming immunitaire n'était pas lié à une compétition larvaire entre les parasites primo-entrants et ceux entrés secondairement. Nous avons également démontré que ce priming immunitaire même si il se trouve être concomitant avec la migration massive des sporocystes secondaires n'était pas lié aux lésions cellulaires engendrées par cette migration. Nous avons donc supposé que le priming immunitaire pouvait être lié au développement du parasite au sein du mollusque. Ainsi, pour vérifier cet effet du développement du parasite ou plus précisément afin de déterminer si les différents antigènes exprimés par différents stades parasitaires intra-molluscaux au cours de leur développement et différentiation chez le mollusque pouvaient expliquer la mise en place progressive de la protection immunitaire observée, nous avons mené une approche de vaccination par des extraits protéiques provenant des différents stades parasitaires intra-molluscaux (miracidium, sporocyste primaire et sporocyste secondaire). Un effet vaccinant a pu être observé pour chacun des extraits protéiques issus des différents stades parasitaires, toute fois les seuls effets significatifs ont été observés avec l'extrait provenant des SpI (prévalence = 37%) et de l'extrait contenant un mélange de Mi et SpII (prévalence = 47%) alors que la vaccination était moins importante pour les Mi (56%) et les SpII (54%) seuls (Figure 5). Ceci pourrait s'expliquer par la période durant laquelle le SpI se développe et est en contact avec le mollusque. En effet, si le miracidium perd ses plaques cilliées extrêmement rapidement après sa pénétration, le SpI se développe durant plus de dix jours avant de commencer à émettre les SpII qui vont migrer jusqu'à la glande digestive (Jourdane and Théron 1987; Portela et al. 2013). Dans ce travail, nous avons vacciné un lot de mollusque avec un mélange de protéines de miracidia et de sporocystes secondaires. Ce mélange présente une efficacité supérieure pour vacciner en comparaison aux deux extraits qui les composent pris indépendamment (Mi

seuls : 56%, SpII seuls : 54%, Mi + SpII : 47%) (Figure 5). Cette différence peut s'expliquer par un effet additif du potentiel antigénique des deux extraits protéiques de Mi et de SpII. Ainsi des fonctions de reconnaissance différentes pourraient être engagées lors de l'injection de ces deux compartiments et le mélange aurait donc un meilleur effet protecteur. Il serait très intéressant, dans un premier temps, de refaire cette expérience avec un mélange contenant une association des trois extraits protéiques : Mi, SpI et SpII afin d'observer si le cumul des trois extraits protéiques permettrait d'obtenir une protection encore plus efficace se rapprochant de la protection observée *in vivo*. Toutefois, cette expérience permet de confirmer que le développement des différents stades intra-molluscaux du parasite et plus particulièrement la diversité des antigènes de surface exprimés par ces parasites pourrait être à l'origine de la mise en place progressive d'un priming immunitaire conférant au mollusque une résistance totale à partir de 14 jours après infestation.

Ce phénomène particulier n'est pas sans rappeler l'immunité concomitante existante chez de nombreuses espèces vertébrées. Cette immunité existe d'ailleurs dans la seconde partie du cycle de *Schistosoma mansoni* puisque chez la souris il s'avère que le premier parasite entrant se sert d'antigènes du stade schistosomule afin de vacciner l'hôte. L'immunité engendrée est alors efficace contre les parasites nouveaux entrant mais inefficace contre le parasite déjà en place (Smithers and Terry 1969). Il a également été démontré que cette immunité concomitante est nettement plus efficace contre les parasites dont le génotype est plus proche du parasite vaccinant (Dumont et al. 2007; Beltran et al. 2010). Dans notre cas, le parasite entrant vaccinerait l'hôte. L'immunité concomitante qui se mettrait alors en place serait efficace contre tout nouveau parasite entrant mais inefficace contre le parasite déjà présent qui continuerait à se développer. De plus, la démonstration que cette protection est plus efficace contre des génotypes proches (Portela et al. 2013) augmente encore la ressemblance avec l'immunité concomitante rencontré chez l'hôte vertébré vis-à-vis du parasite et nous pousse à mettre ces deux phénomènes en parallèle.

Enfin, pour aller plus loin et comprendre et valider toutes ces découvertes, il semble nécessaire d'élucider les mécanismes régissant la reconnaissance qui semble extrêmement spécifique puisque elle est non seulement dépendante du génotype du parasite primo entrant (Portela et al. 2013), mais également, comme nous venons de le montrer, du stade de développement du parasite au sein du mollusque. Différentes approches pourraient être envisagées dans ce sens afin de trouver des molécules candidates permettant une telle précision dans la reconnaissance du pathogène comme par exemple des approches de

protéomique comparative ou une approche de transcriptomique massive. Quoi qu'il en soit, l'immunité du mollusque *B. glabrata* est très complexe et met à mal les grands paradigmes immunitaires concernant les invertébrés établis par Medzhitov et Janeway (Medzhitov and Janeway 1997).

Chapitre trois :

Mécanismes moléculaires du priming immunitaire chez *Biomphalaria glabrata*

CHAPITRE TROIS :

MECANISMES MOLECULAIRES DU PRIMING IMMUNITAIRE CHEZ *BIOMPHALARIA GLABRATA*

A global comparative proteomic approach to investigate the first humoral factors responsible for immune priming in the Lophotrochozoan snail *Biomphalaria glabrata*.

Portela J, Duval D, Nowacki F, Allienne J-F, Galinier R, Dheilly N, Kieffer-Jacquinod S, Mitta G, Théron A and Gourbal B

Soumis à Molecular and Cellular Proteomics

Pour pouvoir étudier en détail le priming immunitaire il est clair que les phénotypes ne suffisent pas et que seuls les mécanismes moléculaires permettront d'élucider la question de la mémoire immunitaire chez les invertébrés (Hauton and Smith 2007). Pour ce faire, il semble essentiel de laisser de côté nos connaissances concernant les mécanismes régissant l'immunité des vertébrés. Il faut démarrer avec un œil neuf, partir des observations de phénotypes pour décortiquer les mécanismes sous-jacents (Little et al. 2005; Vinkler and Albrecht 2011; Criscitiello and de Figueiredo 2013). Malgré les avancées sur la mise en évidence de phénomènes de priming immunitaire chez de nombreuses espèces et le besoin évident de comprendre ce phénomène, l'étude des mécanismes moléculaires et des voies métaboliques impliquées dans cette réponse reste délaissée. Seules quelques études se sont penchées sur la question et ont apporté des éléments de réponse. La première démontre que le priming immunitaire chez *Porcellio scaber* est à mettre en relation avec une augmentation de l'activité de phagocytose des hémocytes suite à une stimulation immunitaire (Roth and Kurtz 2009). La suivante met en évidence une multiplication et une différentiation des hémocytes entraînant une surexpression de certains gènes immunitaires chez *Anopheles gambiae* en réponse à *Plasmodium* (Rodrigues 2010). Enfin, la plus récente présente l'implication de C-type lectines, celles-ci s'induisent chez *Chlamys farreri* lors d'un challenge suite à une primo stimulation par *Vibrio* (Wang et al. 2013).

Après avoir démontré l'existence du priming immunitaire chez *B. glabrata* nous nous sommes lancés dans l'étude des mécanismes régissant ce phénomène. Pour ce faire nous avons observé les phénotypes associés à la réponse de priming immunitaire chez le mollusque puis nous avons procédé à une approche globale d'analyse du protéome suite à une infestation et un challenge. Nous avons ensuite réalisé une étude de transcriptomique par PCR-quantitative visant à valider les différentiels d'expressions des transcrits au cours d'une cinétique d'infestation/ré-infestation très détaillée.

A global comparative proteomic approach to investigate the first humoral factors responsible for immune priming in the Lophotrochozoan snail *Biomphalaria glabrata*.

Julien Portela[1, 2], David Duval[1, 2], Fanny Nowacki[1, 2, 3], Jean-François Allienne[1, 2], Richard Galinier[1, 2], Nolwenn Dheilly[1, 2], Sylvie Kieffer-Jaquinod[4], Guillaume Mitta[1, 2], André Théron[1, 2], and Benjamin Gourbal[1, 2] *.

[1] CNRS, UMR 5244, Ecologie et Evolution des Interactions (2EI), Perpignan, F-66860, France.

[2] Université de Perpignan Via Domitia, Perpignan, F-66860, France.

[3] Institute of Biological, Environmental & Rural Sciences, Aberystwyth University, Aberystwyth Ceredigion SY23 3FG, United Kingdom.

[4] Plate-forme d'analyses protéomiques EDyP-Service, Laboratoire de Biologie à Grande Echelle UMR_S 1038 Inserm/CEA/UJF CEA ; 17, rue des Martyrs, Grenoble Cedex 9, F-38054, France.

*Corresponding author: Benjamin Gourbal

Université de Perpignan Via Domitia

UMR 5244 CNRS Ecologie et Evolution des Interactions (2EI)

52 Avenue Paul Alduy, 66860 Perpignan Cedex, France

Phone: 33 (0)4 30 19 23 12

Fax: 33 (0)4 68 66 22 81

e-mail: benjamin.gourbal@univ-perp.fr

ABSTRACT

Recently several interesting studies have provided evidences that the immune defence system of invertebrates is far more complex and specific than previously thought. Moreover some studies have suggested that the invertebrate antiparasitic response may be “primed” in a sustainable manner, leading to the failure of secondary parasitic infections. These immune responses have been described as acquired resistance or sustained responses and have been designated “immune priming” for invertebrates. However, as the molecular and cellular mechanisms of immune priming have not yet been described, the distinction between immune priming and immune memory is ambiguous and the existence of immune memory in invertebrates remains controversial. In the present paper we investigate this question studying the molecular processes of immune priming in a suitable model involving the Lophotrochozoan snail, *Biomphalaria glabrata*, and its metazoan parasite, the trematode *Schistosoma mansoni*. First we demonstrate that the specific resistance of *B. glabrata* to secondary exposure to *S. mansoni* relies on humoral mechanisms. Humoral factors were responsible for parasite killing in *B. glabrata* immune priming. Indeed a humoral immune pathway was activated in *B. glabrata* immune priming and this pathway differed from the innate immune cellular response classically observed in other models. Plasma transfer from primed snails to healthy ones provided protection, suggesting that plasmatic factors were responsible for the neutralization of the sporocysts from the challenge infection. Thus a comparative proteomic approach was conducted to identify the plasma proteins potentially involved in this humoral priming response. Immune recognition molecules were mainly identified (C-type lectins, Beta-1,3-glucan binding protein and Hemagglutinin/amebocyte aggregation factors). Some of these molecules were up-regulated after the primo-infection and remained expressed at high level assuming a pattern of sustained immune response; others were up-regulated after the primo-infection and were induced again following the challenges

assuming a memory immune response profile. This study provides the first evidence of a humoral immune priming response in a mollusc, identifies the first molecular candidates and have shaken the paradigm that invertebrate immune response do not benefit from immune memory.

1. INTRODUCTION

Invertebrates are confronted by an environment filled with complex changing populations of microorganisms and potential pathogens, engendering selective pressures comparable to those experienced by Gnathostomes (Loker et al. 2004). Therefore, it can be expected that invertebrates should also possess sophisticated recognition systems for dealing with these pathogens. It can be speculated that this specific recognition has evolved from the identification and control of pathogens, conferring the specificity of invertebrate immune systems (Kurtz 2005). The existence of polymorphic and/or diversified putative immune receptor variants that vary considerably between individuals, yielding an enlarged repertoire of putative recognition molecules was demonstrated in invertebrates. These receptors can be somatically diversified in a manner analogous to vertebrate immunoglobulins or T and B cell receptors. These diversified and somatically generated receptors have been identified in echinoderms (SRCR or Sp185/333 of sea urchin (Pancer 2000)), insects (Dscam of *Drosophila melanogaster* and *Anopheles gambiae* (Watson et al. 2005; Dong et al. 2006)), crustaceans (Brites et al. 2008), and molluscs (FREPs of *Biomphalaria glabrata* (Zhang et al. 2004)).

If invertebrates possess diversified immune receptors involved in the specific recognition of pathogens it is realistic to envisage that they also possess a kind of immune memory, especially for long-lived species that might encounter the same pathogens on multiple occasions. Indeed, recent studies have shown that the immune defence of invertebrates are more complex and specific than previously thought and suggest the existence of innate immune memory in invertebrates (Cooper et al. 1992; Kurtz and Franz 2003; Kurtz 2004, 2005; Sadd and Schmid-Hempel 2006; Hauton and Smith 2007; Vazquez et al. 2009; Rodrigues 2010). Two distinct mechanisms have been described including:

- (i), a process of acquired resistance or sustained response called priming (Little and Kraaijeveld 2004) that consists of a more or less specific and long-lasting protection against later challenge and persists even if the pathogen is neutralized.
- (ii) an immune memory that consists of the ability to store information and recall it later for a faster and more powerful response against subsequent exposure to the same pathogen (Kurtz 2005).

Until now, immune priming or memory observations in invertebrates were mainly phenomenological and based on ecological or phenotypic studies. As the molecular and cellular mechanisms underlying these different processes have not yet been fully described in invertebrates, the distinction between priming and immune memory remains ambiguous. Indeed, the existence of immune memory in invertebrates remains controversial and is doubted by many traditional immunologists (for the polemic see (Little et al. 2005; Hauton and Smith 2007)). The international community working on invertebrate innate immunity believes that the existing observations cannot be used in isolation, and should be used to construct hypotheses, which must be exhaustively tested with rigorous functional cellular, biochemical and molecular methods, to eliminate all alternative explanations (Hauton and Smith 2007).

To date, to our knowledge, just few studies have tried to investigate this question. (i), An enhanced phagocytosis after a first encounter with a pathogen was described in *Porcellio scaber* (Roth and Kurtz 2009). (ii), A differentiation of hemocytes associated with an increase of the mRNA levels of hemocyte-specific genes such as thioester-containing protein 1 (TEP1) and leucine rich repeat immune protein 1 (LRIM1) was reported when primed *Anopheles gambiae* mosquitoes were reinfected, indicating an enhanced response to rechallenge rather than a persistent long-lasting response after the initial exposure to Plasmodium and bacteria (Rodrigues et al. 2010). (iii), The expression of C-type lectin increased in scallop *Chlamys*

farreri after vaccination with heat-killed *Vibrio anguillarum* and successive challenges with *V. anguillarum* or *Micrococcus luteus* (Wang et al. 2013). However, these studies remained targeted approaches on a limited set of cellular or molecular candidates and thus the molecular mechanisms remain partially described.

It may not be possible to explain the observations on immune priming or memory in invertebrate systems in terms of what we know about non-self recognition and immune memory in vertebrates. If invertebrates do show specificity and memory in their immune response, it is probably a mistake to look to the vertebrate immune system for explanations (Little et al. 2005; Litman 2006; Vinkler and Albrecht 2011).

Thus to fully understand the capabilities of invertebrate immune systems, we must investigate the underlying mechanisms while being guided by observations, phenotype descriptions and using global molecular approaches at the whole-organism level. This is our ambition and our intention in the present paper.

We investigated immune priming in the Lophotrochozoan snail species, *Biomphalaria glabrata*, following infections and challenges by the trematode pathogen, *Schistosoma mansoni*. Recently, we demonstrated that *B. glabrata* snails were protected against *S. mansoni* re-infections. Following a primo-infection with 10 miracidia of *S. mansoni*, the parasites penetrated and developed normally in snail tissues. But, 10 days after the primo-infection the snails became totally resistant to a homologous challenge with 10 miracidia of *S. mansoni* (Portela et al. 2013). The establishment of the protection is progressive and seems to be associated with the transformation of miracidia into primary sporocysts (SpI), the asexual multiplication of secondary sporocysts (SpII) and their migration in snail tissues from the head-foot to the digestive/genital gland interface (Portela et al. 2013). After 10 days the protection was maintained for the rest of the snail's lifespan, indicating a time dependant

acquired immune priming in *B. glabrata* snails (Sire et al. 1998; Portela et al. 2013). Through homologous and heterologous challenges, we were able to identified a genotype-dependant immune priming in *Biomphalaria glabrata* (Portela et al. 2013). Following homologous challenges, the protection was of 100%, for heterologous challenges, the protection decreased with increasing neutral genetic distance between the parasites used for primo-infections and challenges (Portela et al. 2013).

The failure of snail reinfection by *Schistosoma mansoni* has been demonstrated few years ago by Sire et al. (1998). Using histological observations, these authors revealed that sporocysts from the challenge infection degenerated in snail tissue in the absence of hemocytic reaction of the host. They proposed that humoral factors could be responsible for the non-development of the sporocysts from the challenge infections. They concluded that an intraspecific larval antagonism process between primary sporocysts from the primo-infection and those from the challenge infection may be involved. In this context, the general scope of the present paper is to go further in the understanding of the molecular mechanisms of immune priming in the Lophotrochozoan snail, *Biomphalaria glabrata* in response to *S. mansoni* infections. A precise description of snail immune response phenotypes, a global comparative proteomic approach and real-time quantitative PCR were used to describe and characterize the molecular determinants involved in *B. glabrata* immune priming. We believe this work provides the first global identification of molecular processes supporting immune priming in a model involving the interaction between two eukaryotic metazoan organisms.

2. MATERIAL AND METHODS

2.1. Ethic statements

Our laboratory holds permit # A66040 for experiments on animals from both the French Ministry of Agriculture and Fisheries, and the French Ministry of National Education, Research, and Technology. The housing, breeding and animal care of the utilized animals followed the ethical requirements of our country. The experimenter also possesses an official certificate for animal experimentation from both French ministries (Decree # 87–848, October 19, 1987). Animal experimentation follows the guidelines of the French CNRS. The different protocols used in this study have been approved by the French veterinary agency from the DRAAF Languedoc-Roussillon (Direction Régionale de l'Alimentation, de l'Agriculture et de la Forêt), Montpellier, France (authorization # 007083).

2.2. Snail and parasite strains

A strain of *Biomphalaria glabrata* originated from Brazil and its homopatric strain of *Schistosoma mansoni* was used in this study (Théron et al. 1997). The Brazilian strain of albinos *B. glabrata* (BgBRE) is 100% susceptible (for ten miracidia and upwards) to its corresponding strain of *S. mansoni* (SmBRE). When infecting a snail with 10 miracidia of *S. mansoni* half of the parasites developed normally in snail's tissues while the others are recognized and destroyed by the snail cellular immune response.

S. mansoni was maintained (i) in their homopatric strain of *B. glabrata* and (ii) in hamsters (*Mesocricetus auratus*) as described previously (Théron et al. 1997). Briefly, miracidia were hatched from eggs axenically recovered from 50-day infected hamster livers according to previously described procedures (Mattos et al. 2006; Guillou et al. 2007). Livers were collected and homogenized and the eggs were filtered and washed to obtain miracidia.

2.3. Histological procedures

A histological approach was conducted to investigate and describe the fate of *S. mansoni* sporocysts in the mollusc host after primo-infection and challenge. Primo-infections were performed on juvenile *B. glabrata* (5-6 mm in diameter). Snails were individually exposed for 12 h to 10 miracidia (10Mi) in 5 ml of pond water. Ten snails were recovered 48 h after exposure and fixed in Halmi's fixative (see below). Individual challenge infections of the snails were done at 25 days after primo-infection using 10 Mi per snail. Ten snails were recovered 48 h after exposure and fixed in Halmi's fixative (mercuric chloride 4.5%, sodium chloride 0.5%, trichloracetic acid 2%, formol 20%, acetic acid 4% and 10% of picric acid saturated water's solution). Fixed molluscs were then dehydrated and embedded in paraffin as previously described (Gourbal and Gabrion 2006; Roger et al. 2008b). Transverse histological sections, 10 µm thick, were cut and stained using azocarmine G and Heidenhain's azan using procedures of re-hydration (toluene, 95°, 70°, 30° ethanol and distillate water) coloration (azocarmine G, 70° ethanol / 1% aniline, 1% acetic alcohol, distillate water, 5% Phosphotungstic acid, distillate water, Heidenhain's azan) and dehydration (95° ethanol, absolute ethanol, toluene). Preparations were then mounted with entellan prior to microscopic examination. Pictures were taken with a Nikon MICROPHOT-FX microscope and a Nikon digital sight DS-Fi1 camera.

2.4. Plasma transfer

To investigate the implication of plasmatic factors in immune priming, an experiment of plasma transfer was conducted. Hemolymph from 15 days infected snails was recovered and hemocytes were removed by centrifugation (5 min at 2500 rpm). Hemolymph from naïve snails was recovered following the same procedure and was used as control. Plasmas were frozen at -80°C until used. Twenty five naive snails were injected with 20 µL of plasma from

infected snails and twenty three with plasma from naïve snails. We also injected saline solution (TBS tween : 150 mM of Tris, 20 mM of NaCl and 0.05% Tween20) to 25 snails as a control of injection. Fifteen days after injections, all the experimental groups were infected with 10 Mi of SmBRE and 48 naïve snails were also exposed to 10 Mi and were used as control of the infection. Fifteen days after infections, snails were fixed and the primary sporocyst (SpI) numbers they harboured were determined following previously described methods (Mone et al. 2010; Allienne et al. 2011). Briefly, snails were relaxed in pond water containing excess crystaline menthol for 6 h. The snail body was removed from the shell and fixed in modified Raillet-Henry's solution (Pointier et al. 2002). Using this technique, SpI were readily observable as translucent white bodies within an opaque yellow tissue background. The number of SpI present in each snail was determined following exhaustive dissection to determine the prevalence of infection.

2.5. Proteomics

Snail plasma was recovered along a kinetic of immune priming. BgBRE snails were infected with 10 miracidia of SmBRE and 25 days after the primo infection the snails were challenged with 10 miracidia of SmBRE (Figure 1). For all the experiments the success of the primo-infection was attested by the presence of SpII in the hepatopancreas and only snails harbouring SpII were individually challenged. Fifteen days post challenge (15 DPC), snails were fixed (in Raillet-Henry's solution) to count the number of SpI from the challenge and to confirm the success of the immune priming. Because of the difference in the age (and size) between the SpI from the primo-infection (40 days old at fixation time) and those from the challenge (15 days old at fixation time), it was easy to distinguish them.

Along this kinetic of infection four plasma samples were collected: (i), a control sample recovered from naïve snails (before the primo-infection); (ii), a 15 Day Post Primo Infection

(DPPI) sample recovered after SpI development and spII asexual multiplication; (iii), a 25 DPPI sample recovered after the spII migration and before the challenge and (iv), a 15 days post challenge (DPC) sample (Figure 1). For each sample, the hemolymph was collected from the head-foot region of 50 BgBRE snails as previously described (Bouchut et al. 2007; Mone et al. 2010). Hemocytes were removed by centrifugation (2 500 rpm; 10 min; 4°C) and the plasma was recovered. Then, hemoglobin was removed from plasma using an ultra-centrifugation (55 000 rpm; 2.5 hours; 4°C) (Figure 1). Quantification of total protein concentration was performed with the 2D Quant Kit and plasmas were conserved at -80°C until used.

Proteomic comparative approach was conducted by 2D gel electrophoresis on the four plasma samples previously described. For each sample (Naïve, 15 DPPI, 25 DPPI and 15 DPC) 100 µg of plasma were lyophilised and resuspended in 2D lysis buffer (8 M urea, 40 mM Tris, 4% CHAPS, 65 mM DTT) to solubilise and denaturate the proteins. The first dimension of 2D gel was performed on 17 cm Ready IPG Strips, pH 3–10 non-linear gradient (Bio-Rad). Isoelectrofocusing (IEF) was performed as previously described with a gradual increasing voltage to 8000 V and running for 90,000 Vh at 20°C (Roger et al. 2008b; Beltran et al. 2011). Second dimension SDS-PAGE electrophoresis was performed in 12% acrylamide gels and proteins were visualized by silver staining. 2D gels were scanned using a densitometer (GS-800 Calibrated Densitometer, Bio-Rad). Although the silver stain is the most sensitive currently available, the protocol can generate staining differences within and between gels, notably in the case of background staining. Thus to avoid spurious differences, gels with similar spot intensities and background coloration were selected using an analytical approach (Roger et al. 2008b). Five gels for each experimental sample were selected to perform the comparative proteomic analysis. Replicate proteome images for each condition were aligned and matched to generate a composite map image. Comparative analysis of

digitized proteome maps was performed using the image analysis software PDQuest 7.4.0 (Bio-Rad). Significant differences in protein spot patterns and/or intensities (at least 2 fold) were identified by pair-wise comparisons of spots between gel images in naïve versus 15DPPI; 15DPPI versus 25DPPI and 25DPPI versus 15DPC proteomes.

Gel plugs containing the proteins of interest were excised from the gel that was silver-stained using a method compatible with mass spectrometry. Plugs were processed and characterized by nanoscale capillary liquid chromatography–tandem mass spectrometry (nanoLC–MS/MS) as described previously (Roger et al. 2008b). Digested proteins were analysed using a nanoscale capillary liquid chromatography Ultimate 3000 coupled to a LTQ-Orbitrap tandem mass spectrometer (nanoLC–MS/MS).

The resulting peptide MS/MS spectra were processed and converted into peak lists in dta format using the SEQUEST algorithm for interrogation of protein or nucleotide sequence databases (Swiss prot-trembl, *Schistosoma mansoni Express sequence tag* and *Biomphalaria glabrata* Brazil transcriptome (BgBRE1and2: available on 2EI website bioinformatics resources (http://2ei.univ-perp.fr/?page_id=89)) using Mascot (http://www.matrixscience.com/). No missed cleavages were allowed and some variable modifications were taken into account in the search such as Acetylation (Protein N-term), Oxidation and Dioxidation (M), Trioxidation (C), Searches were performed using an error on experimental peptide mass values of ± 15.0 ppm and an error for MS/MS fragment ion mass values of 1.0 Da.

Mascot results were validated using IRMa software (interpretation of Mascot results) developed by "EDyP Service" laboratory (Grenoble, France). IRMa avoids redundant proteins in the analysis and reduced false positive to less than 1%. A protein was considered to be correctly identified if at least two peptides were confidently matched with database sequences.

In addition an overall Mascot score was given for each peptide, a score greater than 50 was considered significant ($p < 0.05$) (Beltran et al. 2010).

2.6. Quantitative Real time PCR (qRT-PCR)

qRT-PCR analyses were conducted to analyze the expression of immune candidates following primo infection and challenge to investigate more precisely the expression of the proteomic based approach candidates. For this experiment 400 BgBRE snails were primo-infected with 10 Mi of SmBRE and 25 days post primo-infection (DPPI) they were individually challenged again with 10 Mi of SmBRE. Eighteen individuals were collected at 0, 3, 6, 9, 12 hours post primo infection (HPPI) and at 1, 2, 4, 7, 15, 25 days post primo infection (DPPI). After the challenge 18 individuals were collected at 3, 6, 9, 12 hours post challenge (HPC) and at 1, 2, 4, 7, 15 days post challenge (DPC). Snails were frozen in liquid nitrogen and stored in liquid nitrogen until RNA extraction. At 25DPPI concomitantly with the challenges infections of primo-infected snails, 30 naive snails were infected with 10 Mi of SmBRE and used as a control of challenge infection.

At the end of the experiment the remaining primed snails (N=36) and the 30 snails used as control were fixed and the primary sporocyst (SpI) numbers they harboured were determined following previous described methods (see 2.4 Plasma transfer).

For each experimental sample of 18 *B. glabrata* snails, total RNA was extracted using Trizol Reagent (Life Technologies) following the manufacturer's instruction. Reverse transcription was performed according to previously described procedures (Guillou et al. 2004). cDNA were kept at -80°C until used for qRT-PCR analysis. qRT-PCR analyses were performed using a LightCycler 2.0 system (Roche Applied Science) and a Light Cycler Fast start DNA Master SYBR Green I kit (Roche Applied Science). qRT-PCR reactions were set up according to the Light Cycler Manual (Rocher Molecular Biochemials, Germany) as

previously described (Coustau et al. 2003; Guillou et al. 2004). Briefly, qRT-PCR amplification was performed using 2.5 µl of cDNA in a final volume of 10 µl containing 3 mM $MgCl_2$, 0.5µM of each primer and 1 µl of master mix. Relevant candidate genes identified in the proteomic approach were selected and specific primers were designed using either the LightCycler probe design software version 1.0 (Roche) or the PerlPrimer software and are given in Table1. The following Light-Cycler run protocol was used: denaturation at 95°C for 10 min, followed by 40 cycles of amplification and quantification at 95°C for 10 s, 60°C for 5 s and 72°C for 16 s, a melting curve of 60-95°C with a heating rate of 0.1°C/s and continuous fluorescence measurement, and then a cooling step to 40°C. For each reaction, the cycle treshold (Ct) was determined using the "Fit Point Method" of the LightCycler Software, version 3.3 (Roche Diagnostics). The PCR reactions were performed in duplicates and the mean Ct values were calculated. For each sample, the expression level of the target gene was normalized with regard to the expression of the constitutively expressed ribosomal gene 19S (19S ribosomal protein; accession number CK988928). For each mRNA to be analysed, the absence of contaminating genomic DNA was verified by running a no-RT control using primers for the S19 RNA. The expression ratio (R) was calculated according to the formula: $R= 2^{(\Delta Ct)}$ where ΔCt represents Ct (target gene) – Ct (constitutively expressed gene).

2.7. Statistical analysis

To compare prevalences between all the conditions a Fischer's exact test was used. The difference was considered significant when the p value of the test was under 0.05.

For the proteomic approach statistical analysis associated with quantitative differences between spots was performed using a Mann-Whitney U test directly available in PDQuest 7.4.0 software (Bio-Rad).

3. RESULTS

3.1. Histology

To analyze the immuno-biological process of parasite elimination by *Biomphalaria glabrata* snails, a fine histological investigation of *S. mansoni* parasites in host snail tissue was performed. Sporocyst development and/or neutralization/elimination by the snail immune system were analysed after a primo-infection or after a challenge in primed snails. Following a primo-infection with 10 Mi, 2 scenarios could be observed. (i), Some of the miracidia were able to penetrate, transform into SpI and develop normally in snail tissues (Figure 2A). (ii), other miracidia were immediately recognized by the snail immune system after penetration, they were encapsulated and killed by the hemocytes, the snail immune cells (Figure 2B). A multicellular capsule surrounding the parasite could be observed that lead to a “killing” event involving cytotoxic or cytolytic processes that result in the elimination of the SpI (Figure 2B). For primed snails, all the SpIs from the challenge appeared to degenerate spontaneously in snail tissue without apparent encapsulation or hemocyte infiltrations near the parasite (Figure 2C). In primed snails encapsulation processes were never observed (Figure 2C). Thus, if after a primo-infection a cellular immune response is mainly induced, we observed exclusively a humoral defence response in primed snails (Figure 2).

3.2. Plasma transfer

To confirm that humoral factors played a key role in immune priming a transfer of plasma was conducted. Plasmas were recovered from healthy and infected snails and different experiments were conducted (Figure 3). Injection of saline solution has no significant effect on the parasite infectivity, the prevalence remained similar to the control, 88% and 90%

respectively (Figure 3). Naive snail plasma transfer has no effect on snail protection. A slight decrease in prevalence (77%) could be observed but which remained non significant (Figure 3). However a significant ($p = 0.04$) decrease of the prevalence (68%) was observed for infected snail plasma transfer. Thus interestingly the transfer of infected snail plasmas to healthy snails results in a partial protection against *S. mansoni*. This protection is even effective 15 days after the transfer that confirm the role played by humoral factors in activating the immune system and preparing the snail to answer to a subsequent encounter with the parasite.

3.3. Global comparative proteomic approach of primed snail plasma

To identify the plasmatic factors that could be involved in this induced protection, we performed a global comparative 2D gel electrophoresis approach of snail plasma. *B. glabrata* snails were primo-infected and challenge with SmBre miracidia. Four plasma samples were recovered and correspond to Naive snails, 15 DPPI (days post primo-infection), 25 DPPI and 15 DPC (days post challenge). Following quantitative and qualitative bioinformatics analysis, 27 differential spots were found comparing Naive versus 15DPPI; 15DPPI versus 25DPPI and 25DPPI versus 15DPC conditions (Figure 4, Tables 2 and 3). In this global comparison, 17 quantitative and 10 qualitative differences were identified (Figure 4, Tables 2 and 3).

The ratio of expression of these spots was investigated on the entire kinetic of infection to follow their regulation (Figure 5). Four patterns of expression could be distinguished: (1), pattern of immune memory response: the spots were up-regulated after primo-infection and up-regulated after the challenge (Figure 5A). (2), pattern of immune sustained response: the spots were up-regulated after the primo-infection or the challenge and remained at a high expression level until 15 DPC (Figure 5B). (3), pattern of down-regulated response: the spots were down-regulated after the primo-infection or after the challenge and remained at lower

level than naïve snails until 15 DPC (Figure 5C). (4), Mix expression response: main of the spots in this category were up-regulated after the primo-infection and then down-regulated (Figure 5D). All these spots were excised from the gels, digested with trypsin and analysed by tandem mass spectrometry. All the identifications based on Blast2GO annotations of the BgBRE transcriptome were indicated in the Table 2 (quantitative differences) and Table 3 (qualitative differences).

The proteins identified can be classified mainly into 5 functional groups taking into account their putative function and/or structural features: glycolysis; cell signalling, reactive oxygen species scavengers, gametogenesis, and innate immune response (receptors, effectors, and regulators) (Table 2 and 3). In our results, proteins belonging to the innate immune functional group were the main represented. Indeed, 22 molecules out of 46 (48%) (Table 2) and, 15 molecules out of 27 (56%) (Table 3) were related to this group. It is important to note that in the transcriptome of *Biomphalaria glabrata* (http://2ei.univ-perp.fr/?page_id=89), 1140 transcripts out of 119 848 were associated to immune processes representing solely 0.95% of the transcriptome.

Among molecules involved in immune recognition and opsonisation we identified a huge number of different isoforms belonging to different families of immune receptors (C-type lectins, Beta-1,3-glucan binding protein, Hemagglutinin/amebocyte aggregation factors).

C-type lectins 46213_1.7 and 2573_1.7 and mannose C type 2 receptor (spots 1803, 7307, 7101) (Figure 5A) were all involved in immune priming. They were up-regulated after the primo-infection and up-regulated after the challenge assuming a pattern of immune memory response (Figure 5A). Two isofoms of C-type lectins 357_1.1 (spots 5214 and 2206) were up-regulated after the primo-infection and remain increased until 15 DPC assuming a pattern of sustained immune response (Figure 5B). In the same time, 2 other isoforms of C-type 357_1.1 (spots 6214 and 5213) were up-regulated after the primo-infection and then down-regulated.

They seemed to be involved exclusively in the primo-infection response and not in immune priming as they were not positively regulated after the challenge (Figure 5D). Finally C-type lectin 2573-1.7 (spot 0012) and C-type lectin 357_1.1 (spot 3208) were down-regulated after the primo-infection (Figure 5C).

Concerning the Beta-1,3-glucan binding protein (BGBP) few isoforms were identified. The BGBP in spot 5214 was up-regulated after the primo-infection and remain increased until 15 DPC assuming a pattern of sustained immune response (Figure 5B). The BGBP in spot 5213 was up-regulated after the primo-infection and then down-regulated (Figure 5D). The BGBP in spot 3208 was down-regulated after the primo-infection (Figure 5C).

Hemagglutinin/amebocyte aggregation factors (H/AAF) were also involved in immune priming. H/AAF 35403_4.6 and 19302_1.23 (spots 7009 and 8006) followed a pattern of sustained immune response. They were up-regulated after the primo-infection and remained increase until 15 DPC (Figure 5B). H/AAF 821_4.13 in spot 1316, positively regulated solely after the challenge (Figure 5B), could be a new isoform of H/AAF involved in immune priming response. Finally, H/AAF 821_4.13 in spot 1314 was down-regulated after the primo-infection (Figure 5C).

Concerning immune effector molecules: Biomphalysine (spot 7315) was down-regulated after the primo-infection and the spot 7315 was even absent at 25 DPPI and 15 DPC (Figure 5C). Chitinase (spot 3002) was up-regulated after the primo-infection and remained increase until 15 DPC (sustained immune response) (Figure 5B). In *B. glabrata* we identified two Fatty Acid Binding Protein (FABP) one isoforms in spot 4004 that was induced after challenge (Figure 5D) and one isoform in spot 1001 that was down-regulated after the primo infection (Figure 5C).

Concerning regulators of the immune response, thymosin was identified in spot 3002, Serpin was identified in spot 1314, and two isoforms of β chain acetylcholine binding protein

(BCABP) were identified in spots 2206 and 3008. Thymosin (spot 3002) presented a sustained immune response pattern, as it was up-regulated after the primo-infection and remained increased until 15 DPC (Figure 5B). For β chain acetylcholine binding protein (BCABP) one isoform (spot 3008) was up-regulated after the primo-infection and up-regulated after the challenge assuming a pattern of immune memory response (Figure 5A) and the second isoform (spot 2206) was up-regulated after the primo-infection and remained increase until 15 DPC and thus presented a pattern of sustained immune response (Figure 5B). The serine protease inhibitor Serpin (spot 1314) was down-regulated after the primo-infection and was even absent at 25 DPPI (Figure 5C). Serpins were shown to be involved in the regulation of Toll signaling pathway that is mediated via an interplayed between serine proteases and serine protease inhibitors (serpins) in the beetle, *Tenebrio molitor* (Park et al. 2011). An important role of Serpins in innate immunity of the Shrimp *Penaeus monodon* was also demonstrated (Homvises et al. 2010).

Among proteins involved in host/parasite interaction, some anti-oxidant molecules were also identified. The Glutathione peroxidase 3 precursor (spot 1803) was up-regulated after the primo-infection and up-regulated after the challenge assuming a pattern of immune memory response (Figure 5A). For the Glutathione s-transferase mu 3-like, 2 isoforms were identified in spots 7009 and 8006 and both were up-regulated after the primo-infection and remained increase until 15 DPC (sustained immune response) (Figure 5B). For the thioredoxin peroxidase, 2 isoforms were also identified; one isoform (spot 4004) was down-regulated after primo-infection and up-regulated after the challenge (Figure 5D) and the second isoform (spot 2101) was down-regulated after the primo-infection (Figure 5C).

To conclude concerning the immune response, if important differential expression pattern could be observed it is important to note that all the proteins identified in the spots associated

with immune memory or immune sustained pattern of expression (Figures 5A and 5B) were immune related molecules (Tables 2 and 3).

Except immune related molecules one other group was particularly well represented in the proteins identified in this global proteomic approach: the gametogenesis. All the molecules identified belonging to this group were down-regulated following infection. Indeed, schistosomin (spot 1004) and pathogen related protein (spots 2002 and 1009) were down-regulated after the primo-infection (Figure 5C). Ovipostatin (spot 1106) was down-regulated between 25 DPPI and 15 DPC (Figures 5C). Schistosomin played a role in the regulation of gametogenesis in gastropods and was demonstrated as differentially regulated in *Lymnea stagnalis* but not in *B. glabrata* following infection (Zhang et al. 2009). Pathogen related proteins were part of the cysteine rich secretory protein family (CRISP). CRISPs are expressed in the male reproductive accessory glands of the Mediterranean Fruit Fly (*Ceratitis capitata*) (Davies and Chapman 2006) and were identified in the seminal proteins of *Drosophila* (Ram and Wolfner 2009). Ovipostatin was also produced in male accessory gland in *Lymnaea stagnalis* and was part of the seminal-fluid-producing prostate gland having effects on oviposition and hatching (Koene et al. 2010). After *B. glabrata* infection with *S. mansoni* a parasitic castration occurs, this castration is totally effective after 25 to 30 days after infection (Theron et al. 1992a; Theron et al. 1992b; Faro et al. 2013). As a result of this parasitic castration we could observed that main of the molecules or hormones involved in gametogenesis were down-regulated in the present study.

3.4. Quantitative Real Time PCR (qRT-PCR)

In order to correlate or confirm differential protein profiling, a qRT-PCR was performed on a detailed kinetic of infection. At the end of this kinetic, it was important to confirm the immune priming phenotype to be confident in the following qRT-PCR experiments. The

prevalence in control snails was 100% (N=30 individuals), the prevalence for experimental snails (challenged snails) was 0% (N=36 individuals), thus the immune priming was effective.

In this qRT-PCR experiment we focus our attention on candidates that were expected to participate in immune priming. We followed the transcript expression of all the proteins that were regulated as memory response (Figure 5A), sustained response (Figure 5B) or proteins that were specifically induced after challenge (spot 1316 and spot 4004 in Figures 5B and 5D).

For most of the C-type lectins the transcript expression profiles followed an immune memory pattern. The C-type lectin 2573_1.7 expression is variable but we could observed an up-regulation (5 times) at 25DPPI, then the level of expression turns to naïve level and it was up-regulated at 4DPC (3 times) (Figure 6). The C-type 357_1.1 was up-regulated 3 times at 7DPPI, 15DPPI and 3HPC then turned to basal level and was up-regulated 4 times at 4DPC (Figure 6). The C-type lectin 46213_1.1 was up-regulated (3 times) at 2DPPI and then turned to basal level (Figure 6). Finally, the mannose receptor c type 2 appeared to be constitutively expressed (Figure 6).

For the Beta-1,3-glucan-binding protein we observed also a immune memory pattern of expression. BGBP was up-regulated 2 times at 7DPPI and 15DPPI and reached 5 times up-regulation at 25DPPI (Figure 6). Then the transcript level turns to a level of expression similar to naïve snails and increases 7 times at 4DPC (Figure 6).

For the three Hemagglutinin/amebocyte aggregation factor we could not observe any variation after primo infection or challenge (Figure 6). Their expressions appeared to be constitutive.

For the ROS scavengers, the Glutathione s-transferase mu 3-like was up-regulated (2 times) between 6HPPI and 12HPPI, then turned to basal level and increases 2 times at 12HPC (Figure 6). The glutathione peroxidase 3 precursor and the thioredoxin peroxidase appeared to

be not differentially regulated along the infection. Finally the Chitinase 1 presented a slight up-regulation (2 times) at 9HPPI and at 15DPC (Figure 6).

For Fatty Acid Binding Protein (FABP) and β chain acetylcholine binding protein (BCABP) intriguingly, they did not followed a pattern similar to the one observed in the proteomic approach. Both were down-regulated after 15 DPPI (Figure 6).

Unfortunately we were not successful to amplified thymosin by qRT-PCR, and thus we were not able to conclude on the expression pattern of this molecule.

DISCUSSION

The innate immune system of invertebrates is divided into humoral and cellular defense responses (Lavine and Strand 2002; Zanker 2010). Cellular defenses refer to hemocyte responses (phagocytosis, encapsulation). Humoral defenses include antimicrobial peptides, coagulation, melanization, and the production of cytolytic molecules or reactive intermediates of oxygen and nitrogen (Lavine and Strand 2002; Zanker 2010). When a pathogen is recognized cellular and humoral defense responses are coordinated to neutralize the intruder. The existing studies that have addressed the molecular mechanisms of immune priming in invertebrates have mainly suggested an improvement of the cellular response or elevated hemocytes phagocytosis (Rowley and Powell 2007; Netea et al. 2011; Wang et al. 2013). For example in *Porcellio scaber* an enhanced phagocytosis activity was demonstrated after a first encounter with a pathogen (Roth and Kurtz 2009), and for *Anopheles gambiae* mosquitoes a differentiation of hemocytes was reported after an initial exposure to *Plasmodium* and bacteria (Rodrigues et al. 2010). In shrimp an enhanced cellular immunity characterised by a significant increase in the percentage of phagocytic cells was also reported after bacterial challenges (Pope et al. 2011).

In the *B. glabrata/S. mansoni* model, we demonstrated recently that the lophotrochozoan *B. glabrata* snail was protected against *S. mansoni* re-infection (Portela et al. 2013). Following a primo-infection with *S. mansoni*, the parasites penetrated and developed normally in snail tissues. Ten days after the primo-infection the snails became totally resistant to a homologous challenge (Portela et al. 2013). The establishment of the protection is progressive and is associated with the transformation of miracidia into primary sporocysts (SpI), and secondary sporocysts (SpII) (Portela et al. 2013) (Figure 1). Once established the protection was maintained for the snail lifespan, indicating a time dependant immune priming in *B. glabrata* snails (Portela et al. 2013). In the present study we demonstrated that immune priming in *B. glabrata* was not associated with an enhanced cellular response but with a humoral defence response. Indeed, for primed snails, histological observations revealed that sporocysts from the challenge infection were free of encapsulation, their development was stopped and they degenerated slowly in the absence of hemocytic reaction of the host (Figure 2C). This strongly suggests that one or several unidentified humoral factors were responsible for the neutralization of the sporocysts from the challenge infection.

To validate the role of these humoral factors in the immune priming, an experiment of plasma transfer was conducted. This type of experiment has been yet conducted in *Biomphalaria tenagophila* but in the context of resistance to infection (Pereira et al. 2008). Plasma transfer from *S. mansoni* resistant *B. tenagophila* to susceptible ones results in the transfer of resistance (Pereira et al. 2008). In the context of immune priming in the present study, transferring the plasma of primed snails to healthy snails reduced significantly the prevalence of *S. mansoni* infection by more than 25 % compared to controls (non injected snails) (Figure 3). Thus primed snail plasma should contained immune humoral factors which can activate and regulate the snail immune response and conferred to healthy snails a partial protection against subsequent encounters with the parasite. The same conclusion was proposed in

another invertebrate model involving the mosquito *Anopheles gambiae* and its bacterial pathogens. After a transfer of plasma from infected mosquitoes towards healthy mosquitoes, these transferred mosquitoes presented an increase of hemocyte populations (Rodrigues et al. 2010). So humoral factors could trigger a immune cellular response, that resulted in a better protection of mosquitoes against subsequent bacterial challenges (Rodrigues et al. 2010).

Based on these histological and plasma transfer results, we developed a global comparative proteomic approach (Figures 4 and 5) followed by a qRT-PCR validation (Figure 6) to identify the humoral factors involved in *B. glabrata* immune priming.

Most of the proteins differentially regulated in the plasma of primo-infected and challenged snails were immune related (Table 2 and 3). However, just some of them were of interest in the present context and we focus our attention on candidates that were expected to participate in immune priming. These candidates corresponded to the proteins that followed a profile of memory response (Figure 5A), of sustained response (Figure 5B) or to proteins that were specifically induced after challenge (Figures 5B and 5D). All these candidates belonged to immune receptor, effector or regulator families and were the first humoral factors identified as potentially involved in *B. glabrata* immune priming.

In the immune receptors families we identified different isoforms of C-type lectins, Beta-1,3-glucan binding protein (BGBP), and Hemagglutinin/amebocyte aggregation factors (H/AAF).

C-type lectins 46213_1.7 and 2573_1.7 and C type mannose receptor 2 (MRC2) assumed a pattern of immune memory response (Figure 5A). Two isofoms of C-type lectins 357_1.1 followed a pattern of sustained immune response (Figure 5B). The role of C-type lectins in priming response have already been described for mollusks (Wang et al. 2013). The expression of C-type lectin increased in scallop *Chlamys farreri* after vaccination with heat-killed *Vibrio anguillarum* and successive challenges with *V. anguillarum* or *Micrococcus*

luteus resulting in an enhanced protection (Wang et al. 2013). Interestingly in *B. glabrata* a similar mechanism occurred, some specific isoforms of C type lectins appeared to be involved in the humoral priming response. MRC2 is up-regulated at protein level (Figure 5) but not validated by qRT-PCR (Figure 6). MRC2 was well described in humans and was known to be a C-type lectin carbohydrate binding protein primarily present on the surface of immune cells. The function of this receptor is to recognize complex carbohydrates mainly mannose and fucose moieties and participate in neutralization of pathogens (Kim, Ruiz et al. 1992; Mishra, Morris et al. 2013). In Schistosomes, the carbohydrate moieties of glycosylated molecules are known to be mainly fucoses (Castillo and Yoshino 2002; Castillo, Wu et al. 2007) and thus MRC2 of *B. glabrata* could be involved in recognition and neutralization of *S. mansoni* sporocysts from the challenge. However in *B. glabrata* MRC2 was identified in plasma an unusual localization for such molecules and thus seemed to be secreted. Signal peptide prediction confirmed that *B. glabrata* MRC2 possessed a signal peptide of secretion and was predicted as secreted that could explained its plasmatic localization (SignalP-4.1 prediction: Signal Peptide of secretion ='YES' Cleavage site between position 30 and 31; D-value=0.778 D-cutoff=0.450, http://www.cbs.dtu.dk/services/SignalP/; SecretomeP prediction: NN-score=0.795 > threshold value=0.5, http://www.cbs.dtu.dk/services/SecretomeP/).

Concerning BGBP solely the isoform in spot 5214 assumed a pattern of sustained immune response (Figure 5B) and could be involved in immune priming. This was validated by the qRT-PCR (Figure 6), BGBP transcription was up-regulated (5 fold) after the primo infection and a higher and faster up-regulation was observed after the challenge displaying a memory-like immune response (Figure 6). To our knowledge BGBP function in innate immune response was described exclusively in crustaceans. BGBPs were know to react to β-1,3-glucan on fungal surfaces and the glucan–BGBP complex induces degranulation and mediate melanization via the activation of prophenoloxidase (PPO)-activating cascade (Thornqvist et

al. 1994; Zheng and Xia 2012; Wang and Wang 2013). Interestingly, in *B. glabrata* melanisation process and PPO did not exist and BGBP were differentially regulated in response to *S. mansoni* a metazoan parasite. In addition BGBPs were identified for the first time for an invertebrate in a context of immune priming. All these results made *B. glabrata* BGBP to deserve further investigations.

H/AAF was also involved in immune priming. H/AAF 35403_4.6 and 19302_1.23 followed a pattern of sustained immune response (Figure 5B) and H/AAF 821_4.13 in spot 1316 was up-regulated after the challenge (Figure 5B). The differential expression of H/AAF was not confirmed at the transcript level by qRT-PCR (Figure 6) and thus seemed constitutively expressed. H/AAF possesses the property of inducing both aggregation of amebocytes and agglutination of erythrocytes in *Limulus polyphemus* (Fujii et al. 1992). Moreover, it has been suggested (Hanington et al. 2012) that this kind of molecule could play an opsonin role in the Biomphalaria glabrata/Schistosoma mansoni interaction model, by participating in the recruitment of hemocytes and further in the structuration of the capsule around the sporocyste.

In the present work, immune recognition molecules were mainly represented. These molecules were differentially regulated at the proteomic and transcriptomic level and more interestingly many isoforms were identified suggesting translational and post-translational modifications. The function of these molecules in the humoral immune priming response of *B. glabrata* needed to be thoroughly investigated. In addition to their role in recognition of pathogens and opsonisation, how lectins could be involved in the degeneration of *S. mansoni* sporocysts observed after challenge (Figure 2C). Interestingly some lectins were shown to possess direct cytotoxic activities. In plants, the cytotoxic lectin Ricin from *Ricinus communis* beans (Endo et al. 1987); in fungi, the N-acetyl-D-galactosamine-specific lectin from *Schizophyllum commune* (Chumkhunthod et al. 2006); or in invertebrates, the hemolytic lectin CELIII from *Cucumaria echinata* (Oda et al. 1997) were described. Thus it is possible to

imagine that some of the lectins identified in this approach could have also such a role and thus participate in the humoral immune priming response not only as recognition immune receptors but also as cytotoxic/cytolytic molecules involved in the killing of challenge SpIs.

Concerning immune effector molecules, they participated in the sustain immune response in *B. glabrata* immune priming. Chitinase (Figure 5B) is involved in digestion of chitin, one of the main components of pathogen cell walls (fungi, arthropods or worms). Fatty acid binding proteins (FABP) (Figure 5D) were shown to be up-regulated in inflammatory response in vertebrates (Hui et al. 2010) and were known as humoral factors up-regulated in shrimp after pathogen infections (Ren et al. 2009).

Concerning regulators of the immune response, thymosin was involved in sustained immune response (Figure 5B) and the β chain acetylcholine binding protein (BCABP) followed a pattern of immune memory response (Figure 5A) or a pattern of sustained immune response (Figure 5B). Thymosin was known to regulate the immune response and differentiation of immune cells. Thymosin was yet identified in *B. glabrata* as involved in snail immune response to yeast and bacteria pathogen infections (Deleury et al. 2012). Recently it was demonstrated an up-regulation of thymosin in hemocytes of *Haliotis discus discus* following LPS, poly I:C and vibrio immune stimulations (Kasthuri et al. 2013) and thymosin was involved in hemocytes homeostasis in Crustaceans (Saelee et al. 2013). In invertebrates the role of BCABP was demonstrated in hemipteran innate defense to rhabdovirus infection (Whitfield et al. 2011).

Among the immune related molecules repertoire potentially involved in immune priming, we identified 2 proteins playing a crucial role in the cellular response to oxidative stress and reactive oxygen species (ROS) scavenging. The glutathione peroxidase 3 precursor (GPx) (pattern of immune memory response) (Figure 5A) and the glutathione s-transferase mu 3-like (GST) (pattern of sustained immune response or up-regulated after the challenge)

(Figure 5B and 5D) played an important role in maintaining redox homeostasis and in protecting organisms from the accumulation of toxic ROS. GPx detoxified mainly hydrogen peroxide with the concomitant oxidation of glutathione. GPx catalyzed the oxidation of reduced glutathione (GSH) into oxidized glutathione (GS-SG). GSH played the role of an electron donor to scavenge hydrogen peroxide into water (Wu and Chu 2010). GST has been known to reduce lipid hydroperoxides and this enzyme can also detoxify lipid peroxidation end products (Kinnula et al. 1998; Sharma et al. 2004). We have to take in consideration that one of the main immune effectors in *B. glabrata* are the reactive oxygen species (ROS) produced by hemocytes (Hahn et al. 2000, 2001; Mourao et al. 2009). Previous studies conducted by Hahn and co-workers demonstrated that hydrogen peroxide plays a crucial role in the killing of *S.mansoni* sporocysts (Hahn et al. 2001; Bender et al. 2005). Thus we could suppose that *B. glabrata* had to produce and release in plasma antioxidant molecules to protect its own cells against the oxidative stress occurring in immune response.

Mounting evidence indicates that at least some invertebrates show immune priming or memories in their immune response to different pathogens, such that subsequent re-exposure results in enhanced protection (Cooper et al. 1992; Kurtz and Franz 2003; Kurtz 2004; Sadd and Schmid-Hempel 2006; Rodrigues 2010). However the molecular mechanisms of immune priming remain poorly described and two distinct processes have been proposed. Immune priming can be potentially based on sustainable response, a long lasting protection that persist even if the pathogen is neutralized (Little and Kraaijeveld 2004) or a memory-like response that correspond to a faster and/or stronger response to subsequent exposure to the same pathogen (Kurtz 2005).

In the study conducted herein we have looked carefully at the proteomic profils and qRT-PCR validations of humoral candidates involved in immune priming response of *B. glabrata* snails to *S. mansoni* infection. Most of the molecules investigated presented a long-lasting up-

regulation corresponding to a pattern of sustained immune response. Maintaining an efficient sustained immune response for the snail's lifespan would result in a huge energetic loss, which is expected to result in trade-offs with other life-history traits (Hangartner et al. 2013; McNamara et al. 2013). Interestingly in the present study we identified a down-regulation of molecules involved in gametogenesis (Figure 5, Tables 2 and 3). Following infection a trade-off between gametogenesis/reproduction (down-regulated) and immunity (up-regulated) was observed. This trade-off was expected to help in maintaining the efficient sustained immune priming response observed in *B. glabrata* snails.

However immune priming response in *B. glabrata* was not so straightforward and the sustainable response does not seem to be the only pattern of immune response observed. Some candidates presented a pattern of memory immune response: a first increasing of expression was observed following the primo-infection, and then expression return to a basal level and expression increased again after the challenge. Moreover, for some of these candidates a faster and stronger immune response following the challenge was observed (Figure 5A and Figure 6). Most of these candidates belonged to the C-type lectin family, thus a specific subset of C-type lectins seemed to be specifically re-induced following the homologous challenge conducted herein.

This link between lectins and specificity of recognition is very interesting. As proposed by (Schulenburg et al. 2007) we could expect that the association and the diversity of immune receptors could confer to the invertebrates a higher capacity of pathogen recognition than expected by (Janeway and Medzhitov 2002)These authors hypothesis that the invertebrates possessed a limited set of Pattern Recognition Receptors (PRRs) permitting to discriminate or recognize a limited set of Pathogen-Associated Molecular Patterns (PAMPs) (Janeway and Medzhitov 2002). Using homologous and heterologous challenges, we were able to demonstrate recently that the immune priming in *Biomphalaria glabrata* was genotype-

dependant (Portela et al. 2013). Following homologous challenges, the protection was of 100%, and for heterologous challenges, the protection decreased with increasing neutral genetic distance between the parasites used for primo-infections and the parasites used for the challenges (Portela et al. 2013). Based on this result, we could hypothesis that a better protection against a homologous (vs. heterologous) secondary infection in immune priming may arise via processes that involve specific repertoires of *B. glabrata* immune receptors that would be mobilized to target certain subsets of *S. mansoni* genotypes. In *B. glabrata / S. mansoni* model both partners are metazoan eukaryotes belonging to the Lophotrochozoan group. This phylogenetic proximity is particularly interesting when studying the mechanisms involved in the specificity of immune priming. Until now most of the models used for studying immune priming in invertebrates were conducted for arthropods (insects (Sadd and Schmid-Hempel 2006; Pham et al. 2007; Roth and Kurtz 2009; Rodrigues 2010; Tidbury et al. 2011) or crustaceans (Little et al. 2003; Witteveldt et al. 2004; Vazquez et al. 2009; Pope et al. 2011)) infected by bacteria, yeast or virus. For metazoan eukaryote hosts, it might be easy with a limited set of Pattern Recognition Receptors (PRRs) to discriminate or recognize Lipopolysaccharides (LPS), peptidoglycans or beta-glucans, some very specific Pathogen-Associated Molecular Patterns (PAMPs) of micro-organisms and respond to them efficiently without a high level of specificity. For the interaction between two Lophotrochozoans investigated herein, a high level of specificity is expected because of the potential molecular proximity between host and parasite antigens. The mechanisms involved in host immune recognition were expected to be sophisticated in *B. glabrata* to discriminate between self and non-self (*S. mansoni* parasite) and even avoid auto-immunity. To our knowledge in immune priming, solely one other example of interaction between two invertebrate metazoans was investigated (Kurtz and Franz 2003). In this model involving a copepode and its parasitic tapeworm a high level of specificity was also demonstrated (Kurtz and Franz 2003).

To conclude, our model appears to be very appropriate for the identification of molecular mechanisms involved in invertebrate immune priming. The existing studies that have addressed the molecular mechanisms of immune priming in invertebrates have mainly suggested the involvement of elevated hemocyte phagocytosis (Rowley and Powell 2007; Netea et al. 2011). In our model, priming seems to be supported by snail humoral factors that lead to the degeneration and death of the parasite. This process differs from the classical innate cellular immune response of invertebrates and appears to be highly specific such that different strains of the same pathogen specie may be differentiated (Portela et al. 2013). If we have identified the first molecular candidates involved in the immune priming response in *Biomphalaria glabrata*, we need now to investigate how these molecules mediate and regulate the specificity of this immune priming defence.

Acknowledgements

We thank Marie Aude Olive and Raphaël Palisse for their participation in this project as Master student at the Perpignan University. We thank Bernard Dejean and Nathalie Arancibia for technical assistance (2EI, Perpignan).

Funding: This work was funded by the ANR (grant # 25402 BiomGenIm; ANR-07-BLAN-0214-03), the CNRS, and the UPVD. The funders had no role in the study design, data collection, data analysis, decision to publish, or preparation of the manuscript.

REFERENCES

Allienne, J. F., A. Theron, et al. (2011). "Recovery of primary sporocysts in vivo in the Schistosoma mansoni/Biomphalaria glabrata model using a simple fixation method suitable for extraction of genomic DNA and RNA." Exp Parasitol **129**(1): 11-6.

Beltran, S., B. Gourbal, et al. (2010). "Vertebrate host protective immunity drives genetic diversity and antigenic polymorphism in Schistosoma mansoni." Journal of Evolutionary Biology **24**(3): 554-572.

Beltran, S., B. Gourbal, et al. (2011). "Vertebrate host protective immunity drives genetic diversity and antigenic polymorphism in Schistosoma mansoni." J Evol Biol **24**(3): 554-72.

Bender, R. C., E. J. Broderick, et al. (2005). "Respiratory burst of *Biomphalaria glabrata* hemocytes: *Schistosoma mansoni*-resistant snails produce more extracellular H2O2 than susceptible snails." J Parasitol **91**(2): 275-9.

Bouchut, A., C. Coustau, et al. (2007). "Compatibility in the Biomphalaria glabrata/Echinostoma caproni model: new candidate genes evidenced by a suppressive subtractive hybridization approach." Parasitology **134**: 575-588.

Brites, D., S. McTaggart, et al. (2008). "The Dscam homologue of the crustacean *Daphnia* is diversified by alternative splicing like in insects." Mol Biol Evol **25**(7): 1429-39.

Chumkhunthod, P., S. Rodtong, et al. (2006). "Purification and characterization of an N-acetyl-D-galactosamine-specific lectin from the edible mushroom Schizophyllum commune." Biochim Biophys Acta **1760**(3): 326-32.

Cooper, E. L., B. Rinkevich, et al. (1992). "Invertebrate immunity: another viewpoint." Scand J Immunol **35**(3): 247-66.

Cooper, E. L. and P. Roch (1986). "Second-set allograft responses in the earthworm Lumbricus terrestris. Kinetics and characteristics." Transplantation **41**(4): 514-20.

Coustau, C., G. Mitta, et al. (2003). "Schistosoma mansoni and Echinostoma caproni excretory-secretory products differentially affect gene expression in Biomphalaria glabrata embryonic cells." Parasitology **127**: 533-542.

Davies, S. J. and T. Chapman (2006). "Identification of genes expressed in the accessory glands of male Mediterranean Fruit Flies (Ceratitis capitata)." Insect Biochem Mol Biol **36**(11): 846-56.

Deleury, E., G. Dubreuil, et al. (2012). "Specific versus non-specific immune responses in an invertebrate species evidenced by a comparative de novo sequencing study." PLoS One **7**(3): e32512.

Dong, Y., H. E. Taylor, et al. (2006). "AgDscam, a hypervariable immunoglobulin domain-containing receptor of the Anopheles gambiae innate immune system." PLoS Biol **4**(7): e229.

Endo, Y., K. Mitsui, et al. (1987). "The mechanism of action of ricin and related toxic lectins on eukaryotic ribosomes. The site and the characteristics of the modification in 28 S ribosomal RNA caused by the toxins." J Biol Chem **262**(12): 5908-12.

Faro, M. J., M. Perazzini, et al. (2013). "Biological, biochemical and histopathological features related to parasitic castration of Biomphalaria glabrata infected by Schistosoma mansoni." Exp Parasitol **134**(2): 228-34.

Fujii, N., C. A. Minetti, et al. (1992). "Isolation, cDNA cloning, and characterization of an 18-kDa hemagglutinin and amebocyte aggregation factor from Limulus polyphemus." J Biol Chem **267**(31): 22452-9.

Gourbal, B. E. F. and C. Gabrion (2006). "Histomorphological study of the preputial and clitoral glands in BALB/c mice with experimental Taenia crassiceps infections." Journal of Parasitology **92**(1): 189-192.

Guillou, F., G. Mitta, et al. (2004). "Use of individual polymorphism to validate potential functional markers: case of a candidate lectin (BgSel) differentially expressed in susceptible and resistant strains of Biomphalaria glabrata." Comparative Biochemistry and Physiology B-Biochemistry & Molecular Biology **138**(2): 175-181.

Guillou, F., E. Roger, et al. (2007). "Excretory-secretory proteome of larval Schistosoma mansoni and Echinostoma caproni, two parasites of Biomphalaria glabrata." Molecular and Biochemical Parasitology **155**(1): 45-56.

Hahn, U. K., R. C. Bender, et al. (2000). "Production of reactive oxygen species by hemocytes of Biomphalaria glabrata: carbohydrate-specific stimulation." Dev Comp Immunol **24**(6-7): 531-41.

Hahn, U. K., R. C. Bender, et al. (2001). "Killing of Schistosoma mansoni sporocysts by hemocytes from resistant Biomphalaria glabrata: role of reactive oxygen species." The Journal of parasitology **87**(2): 292-9.

Hangartner, S., S. H. Sbilordo, et al. (2013). "Are there genetic trade-offs between immune and reproductive investments in Tribolium castaneum?" Infect Genet Evol **19C**: 45-50.

Hauton, C. and V. J. Smith (2007). "Adaptive immunity in invertebrates: a straw house without a mechanistic foundation." Bioessays **29**(11): 1138-46.

Homvises, T., A. Tassanakajon, et al. (2010). "Penaeus monodon SERPIN, PmSERPIN6, is implicated in the shrimp innate immunity." Fish Shellfish Immunol **29**(5): 890-8.

Hui, X., H. Li, et al. (2010). "Adipocyte fatty acid-binding protein modulates inflammatory responses in macrophages through a positive feedback loop involving c-Jun NH2-terminal kinases and activator protein-1." J Biol Chem **285**(14): 10273-80.

Janeway, C. A. and R. Medzhitov (2002). "Innate immune recognition." Annual Review of Immunology **20**: 197-216.

Kasthuri, S. R., H. K. Premachandra, et al. (2013). "Structural characterization and expression analysis of a beta-thymosin homologue (Tbeta) in disk abalone, Haliotis discus discus." Gene **527**(1): 376-83.

Kinnula, K., K. Linnainmaa, et al. (1998). "Endogenous antioxidant enzymes and glutathione S-transferase in protection of mesothelioma cells against hydrogen peroxide and epirubicin toxicity." Br J Cancer **77**(7): 1097-102.

Koene, J. M., W. Sloot, et al. (2010). "Male accessory gland protein reduces egg laying in a simultaneous hermaphrodite." PLoS One **5**(4): e10117.

Kurtz, J. (2004). "Memory in the innate and adaptive immune systems." Microbes Infect **6**(15): 1410-7.

Kurtz, J. (2005). "Specific memory within innate immune systems." Trends Immunol **26**(4): 186-92.

Kurtz, J. and K. Franz (2003). "Evidence for memory in invertebrate immunity." Nature **425**(6953): 37-38.

Kurtz, J. and K. Franz (2003). "Innate defence: evidence for memory in invertebrate immunity." Nature **425**(6953): 37-8.

Lavine, M. D. and M. R. Strand (2002). "Insect hemocytes and their role in immunity." Insect Biochem Mol Biol **32**(10): 1295-309.

Litman, G. W. (2006). "How Botryllus chooses to fuse." Immunity **25**(1): 13-5.

Little, T. J., N. Colegrave, et al. (2008). "Studying immunity at the whole organism level." Bioessays **30**(4): 404-5; author reply 406.

Little, T. J., D. Hultmark, et al. (2005). "Invertebrate immunity and the limits of mechanistic immunology." Nat Immunol **6**(7): 651-4.

Little, T. J. and A. R. Kraaijeveld (2004). "Ecological and evolutionary implications of immunological priming in invertebrates." Trends Ecol Evol **19**(2): 58-60.

Little, T. J., B. O'Connor, et al. (2003). "Maternal transfer of strain-specific immunity in an invertebrate." Curr Biol **13**(6): 489-92.

Loker, E. S., C. M. Adema, et al. (2004). "Invertebrate immune systems--not homogeneous, not simple, not well understood." Immunol Rev **198**: 10-24.

Mattos, A. C. A., J. R. Kusel, et al. (2006). "Activity of praziquantel on in vitro transformed Schistosoma mansoni sporocysts." Memorias Do Instituto Oswaldo Cruz **101**: 283-287.

McNamara, K. B., N. Wedell, et al. (2013). "Experimental evolution reveals trade-offs between mating and immunity." Biol Lett **9**(4): 20130262.

Mone, Y., B. Gourbal, et al. (2010). "A Large Repertoire of Parasite Epitopes Matched by a Large Repertoire of Host Immune Receptors in an Invertebrate Host/Parasite Model." Plos Neglected Tropical Diseases **4**(9).

Moné, Y., B. Gourbal, et al. (2010). "A Large Repertoire of Parasite Epitopes Matched by a Large Repertoire of Host Immune Receptors in an Invertebrate Host/Parasite Model." PLoS Negl Trop Dis **4**(9): e813.

Mourao, M. d. M., N. Dinguirard, et al. (2009). "Role of the Endogenous Antioxidant System in the Protection of *Schistosoma mansoni* Primary Sporocysts against Exogenous Oxidative Stress." PLoS Negl Trop Dis **3**(11): e550.

Netea, M. G., J. Quintin, et al. (2011). "Trained immunity: a memory for innate host defense." Cell Host Microbe **9**(5): 355-61.

Oda, T., M. Tsuru, et al. (1997). "Temperature- and pH-dependent cytotoxic effect of the hemolytic lectin CEL-III from the marine invertebrate Cucumaria echinata on various cell lines." J Biochem **121**(3): 560-7.

Pancer, Z. (2000). "Dynamic expression of multiple scavenger receptor cysteine-rich genes in coelomocytes of the purple sea urchin." Proc Natl Acad Sci U S A **97**(24): 13156-61.

Park, S. H., R. Jiang, et al. (2011). "Structural and functional characterization of a highly specific serpin in the insect innate immunity." J Biol Chem **286**(2): 1567-75.

Pereira, C. A., R. L. Martins-Souza, et al. (2008). "Participation of cell-free haemolymph of Biomphalaria tenagophila in the defence mechanism against Schistosoma mansoni sporocysts." Parasite Immunol **30**(11-12): 610-9.

Pham, L. N., M. S. Dionne, et al. (2007). "A specific primed immune response in Drosophila is dependent on phagocytes." PLoS Pathog **3**(3): e26.

Pointier, J. P., W. L. Paraense, et al. (2002). "A potential snail host of schistosomiasis in Bolivia: Biomphalaria amazonica Paraense, 1966." Memorias Do Instituto Oswaldo Cruz **97**(6): 793-796.

Pope, E. C., A. Powell, et al. (2011). "Enhanced cellular immunity in shrimp (Litopenaeus vannamei) after 'vaccination'." PLoS One **6**(6): e20960.

Portela, J., D. Duval, et al. (2013). "Evidence for Specific Genotype-Dependent Immune Priming in the Lophotrochozoan Biomphalaria glabrata Snail." J Innate Immun **5**(3): 261-76.

Ram, K. R. and M. F. Wolfner (2009). "A network of interactions among seminal proteins underlies the long-term postmating response in Drosophila." Proc Natl Acad Sci U S A **106**(36): 15384-9.

Ren, Q., Z. Q. Du, et al. (2009). "An acyl-CoA-binding protein (FcACBP) and a fatty acid binding protein (FcFABP) respond to microbial infection in Chinese white shrimp, Fenneropenaeus chinensis." Fish Shellfish Immunol **27**(6): 739-47.

Rodrigues, J., F. A. Brayner, et al. (2010). "Hemocyte differentiation mediates innate immune memory in Anopheles gambiae mosquitoes." Science **329**(5997): 1353-5.

Roger, E., G. Mitta, et al. (2008). "Molecular determinants of compatibility polymorphism in the Biomphalaria glabrata/Schistosoma mansoni model: New candidates identified by a global comparative proteomics approach." Molecular and Biochemical Parasitology **157**(2): 205-216.

Roth, O. and J. Kurtz (2009). "Phagocytosis mediates specificity in the immune defence of an invertebrate, the woodlouse Porcellio scaber (Crustacea: Isopoda)." Dev Comp Immunol **33**(11): 1151-5.

Rowley, A. F. and A. Powell (2007). "Invertebrate immune systems specific, quasi-specific, or nonspecific?" J Immunol **179**(11): 7209-14.

Sadd, B. M. and P. Schmid-Hempel (2006). "Insect immunity shows specificity in protection upon secondary pathogen exposure." Curr Biol **16**(12): 1206-10.

Saelee, N., C. Noonin, et al. (2013). "beta-thymosins and hemocyte homeostasis in a crustacean." PLoS One **8**(4): e60974.

Schulenburg, H., C. Boehnisch, et al. (2007). "How do invertebrates generate a highly specific innate immune response?" Molecular Immunology **44**(13): 3338-3344.

Sharma, R., Y. Yang, et al. (2004). "Antioxidant role of glutathione S-transferases: protection against oxidant toxicity and regulation of stress-mediated apoptosis." Antioxid Redox Signal **6**(2): 289-300.

Sire, C., A. Rognon, et al. (1998). "Failure of *Schistosoma mansoni* to reinfect *Biomphalaria glabrata* snails : acquired humoral resistance or intra-specific larval antagonism ?" Parasitology **117**: 117-122.

Theron, A., C. Gerard, et al. (1992). "Early enhanced growth of the digestive gland of Biomphalaria glabrata infected with Schistosoma mansoni: side effect or parasite manipulation?" Parasitol Res **78**(5): 445-50.

Theron, A., H. Mone, et al. (1992). "Spatial and energy compromise between host and parasite: the Biomphalaria glabrata-Schistosoma mansoni system." Int J Parasitol **22**(1): 91-4.

Theron, A., J. R. Pages, et al. (1997). "Schistosoma mansoni: Distribution patterns of miracidia among Biomphalaria glabrata snail as related to host susceptibility and sporocyst regulatory processes." Experimental Parasitology **85**(1): 1-9.

Thornqvist, P. O., M. W. Johansson, et al. (1994). "Opsonic activity of cell adhesion proteins and beta-1,3-glucan binding proteins from two crustaceans." Dev Comp Immunol **18**(1): 3-12.

Tidbury, H. J., A. B. Pedersen, et al. (2011). "Within and transgenerational immune priming in an insect to a DNA virus." Proc Biol Sci **278**(1707): 871-6.

Vazquez, L., J. Alpuche, et al. (2009). "Review: Immunity mechanisms in crustaceans." Innate Immun **15**(3): 179-88.

Vinkler, M. and T. Albrecht (2011). "Phylogeny, longevity and evolution of adaptive immunity." Folia zoologica **60**(3): 277-282.

Wang, J., L. Wang, et al. (2013). "The response of mRNA expression upon secondary challenge with Vibrio anguillarum suggests the involvement of C-lectins in the immune priming of scallop Chlamys farreri." Dev Comp Immunol **40**(2): 142-7.

Wang, X. W. and J. X. Wang (2013). "Pattern recognition receptors acting in innate immune system of shrimp against pathogen infections." Fish Shellfish Immunol **34**(4): 981-9.

Watson, F. L., R. Puttmann-Holgado, et al. (2005). "Extensive diversity of Ig-superfamily proteins in the immune system of insects." Science **309**(5742): 1874-8.

Whitfield, A. E., D. Rotenberg, et al. (2011). "Analysis of expressed sequence tags from Maize mosaic rhabdovirus-infected gut tissues of Peregrinus maidis reveals the presence of key components of insect innate immunity." Insect Mol Biol **20**(2): 225-42.

Witteveldt, J., C. C. Cifuentes, et al. (2004). "Protection of Penaeus monodon against white spot syndrome virus by oral vaccination." J Virol **78**(4): 2057-61.

Wu, L. T. and K. H. Chu (2010). "Characterization of an ovary-specific glutathione peroxidase from the shrimp Metapenaeus ensis and its role in crustacean reproduction." Comp Biochem Physiol B Biochem Mol Biol **155**(1): 26-33.

Zanker, K. S. (2010). "Immunology of Invertebrates: Humoral." Encyclopedia of Life Sciences. John Wiley & Sons, Ltd: Chichester.(DOI: 10.1002/9780470015902.a0000522.pub2).

Zhang, S. M., C. M. Adema, et al. (2004). "Diversification of Ig superfamily genes in an invertebrate." Science **305**(5681): 251-4.

Zhang, S. M., H. Nian, et al. (2009). "Schistosomin from the snail Biomphalaria glabrata: expression studies suggest no involvement in trematode-mediated castration." Mol Biochem Parasitol **165**(1): 79-86.

Zheng, X. and Y. Xia (2012). "beta-1,3-Glucan recognition protein (betaGRP) is essential for resistance against fungal pathogen and opportunistic pathogenic gut bacteria in Locusta migratoria manilensis." Dev Comp Immunol **36**(3): 602-9.

Table 1 Primers table for the Q-RT-PCR experiments

Name	Locus	Forward	Reverse
Chitinase 1	Locus_4280_Transcript_2/8	GTTTGAACGTAGTTGTGTCG	GTTCATCAAGAGGAACGGTTA
Mannose receptor c type 2	Locus_46101_Transcript_4/7	TAGCGGTTCTCATAAAGCAG	CATCTTCGTCACATTTACAGTTTC
Glutathione peroxidase 3 precursor	Locus_37254_Transcript_2/5	ACATATTGATCTAAATATCAAGTTGCTAAG	GTTAGCTCCAGAATACATGGG
Glutathione s-transferase mu 3-like	Locus_3196_Transcript_12/15	AAAGATTCCAGTGCAGGT	CAATCTGTATGGAAGTACAGTAGTT
Hemagglutinin/amebocyte aggregation factor 35403_4.6	Locus_35403_Transcript_4/6	TTTGAATTGCAGGTCAAGGC	GCGAGACAGAACTTTCTACT
Hemagglutinin/amebocyte aggregation factor 19302_1.23	Locus_19302_Transcript_1/23	CCATGTTGGCAGTGAAGTC	GTAGGAACCATGGAAACTGGTA
Hemagglutinin/amebocyte aggregation factor 821_4.13	Locus_821_Transcript_4/13	TGTTTAAGTTCTACTGCTGTACC	CTGCAGTGCTGTCGTAT
Beta-1,3-glucan-binding protein	Locus_838_Transcript_2/23	GCACTGTTAGCAGTACACTTCA	GTTGGTCGTCTACATAGGTAATTAAA
C-type lectin 46213_1.1	Locus_46213_Transcript_1/1	ATCTGATTTCTGAACTCTTTGGA	GGTGAATGGGATATTGATGACT
C-type lectin 357_1.1	Locus_357_Transcript_1/1	CGGAGTTATCCTCAACACTG	CCCTTGATGGAATCGACA
C-type lectin 2573_1.7	Locus_2573_Transcript_1/7	CAGTTCTGCAATAATTTCGGTG	AGTGCGTTGATGAACCC
β chain acetylcholine binding protein	Locus_2607_Transcript_1/15	CACATTGAGGTCTACAACTCTATT	CAAACTTTAAGGTGCAAGCG
Fatty acid binding protein	Locus_688_Transcript_2/3	CGCTTTCTATGGAACCTGG	CACCGTAGTCAACAATACATCT

Experimental condition	Spot #	Expression ratio	Protein name	Accession #	Score	Number of peptides
Naïve vs 15DPPI	1803	5	C-type lectin 46213_1.1	Locus_46213_Transcript_1/1	266.87	7
			Chitinase 1	Locus_4280_Transcript_2/8	221.12	5
			Glutathione peroxidase 3 precursor	Locus_37254_Transcript_2/5	172.11	3
			---NA---	Locus_625_Transcript_1/1	161.03	3
			Glutathione peroxidase	Locus_79388_Transcript_1/3	97.90	2
	7101	2	Mannose receptor c type 2	Locus_46101_Transcript_4/7	342.50	8
			---NA---	Locus_56177_Transcript_16/21	353.90	6
			Glutamate--tRNA ligase	Locus_79395_Transcript_1/1	177.00	3
	3002	6.7	Thymosin isoform 1	Locus_2956_Transcript_61/73	270.20	6
			Chitinase 1	Locus_4280_Transcript_2/8	89.26	2
	3008	3.81	β chain acetylcholine binding protein	Locus_2607_Transcript_1/15	547.22	8
			Actin	Locus_25_Transcript_5711/10008	272.29	5
			Actin 1	Locus_68811_Transcript_1/1	93.46	2
	1004	-11.73	Schistosomin-like precursor	Locus_879_Transcript_2/10	157.12	3
			---NA---	Locus_5413_Transcript_4/8	138.65	2
			---NA---	Locus_37131_Transcript_1/1	78.45	2
	2002	-3.74	Pathogen-related protein 1	Locus_12722_Transcript_1/1	321.85	5
15DPPI vs 25DPPI	7009	54,71	Glutathione s-transferase mu 3-like	Locus_3196_Transcript_12/15	399.92	10
			Hemagglutinin/amebocyte aggregation factor 35403_4.6	Locus_35403_Transcript_4/6	82.66	2
			Hemagglutinin/amebocyte aggregation factor 19302_1.23	Locus_19302_Transcript_1/23	70.94	2
	8006	2,35	Glutathione s-transferase mu 3-like	Locus_3196_Transcript_12/15	699,01	13
			Hemagglutinin/amebocyte aggregation factor 35403_4.6	Locus_35403_Transcript_4/6	185,21	5
			Hemagglutinin/amebocyte aggregation factor 19302_1.23	Locus_19302_Transcript_1/23	98,53	2
	2206	-2,26	β chain acetylcholine binding protein	Locus_2607_Transcript_1/15	608.85	10
			C-type lectin 357_1.1	Locus_357_Transcript_1/1	96.19	2
	2311	-3,88	Actin	Locus_25_Transcript_5684/10008	387.51	8
			Actin	Locus_25_Transcript_5722/10008	364.01	8
			Actin 1	Locus_68811_Transcript_1/1	143.99	3
	0012	-3,36	C-type lectin 2573_1.7	Locus_2573_Transcript_1/7	223.52	4
	1008	-2,11	Heat-responsive protein 12	Locus_2334_Transcript_2/3	235.89	3
			C-type lectin 27203_22.30	Locus_27203_Transcript_22/30	119.07	2
			Schistosomin-like precursor	Locus_879_Transcript_2/10	90.27	2
			C-type lectin 27203_17.30	Locus_27203_Transcript_17/30	111.26	2
25DPPI vs 15DPC	0012	8,01	C-type lectin 2573_1.7	Locus_2573_Transcript_1/7	219.21	4
	7307	5,64	C-type lectin 2573_1.7	Locus_2573_Transcript_1/7	66.42	2
	2311	3,3	Alpha-amylase	Locus_32287_Transcript_13/29	326.10	6
			Hypotetical protein	Locus_56177_Transcript_16/21	263.96	5
	1001	-2,91	Fatty acid binding protein h8-isoform	Locus_688_Transcript_2/3	365.53	6
	1106	-2,43	---NA---	Locus_6367_Transcript_1/6	556.21	9
			Ovipostatin	Locus_36026_Transcript_2/4	75.66	2
	2101	-3,15	Thioredoxin peroxidase	Locus_315_Transcript_3/11	307.94	7
			Alpha-amylase	Locus_32287_Transcript_13/29	344.62	6
	0005	-2,12	Calcium binding protein 2	Locus_330_Transcript_15/25	206.99	5

Table 2 Quantitative differences of plasma proteome identified by 2D gel electrophoresis

Accession #: correspond to the accession number of the transcript in the transcriptomic database of *Biomphalaria glabrata* Brazil (assembly of Rnaseq illumina sequencing) deposited in 2EI website (http://2ei.univ-perp.fr/?page_id=89). NA: not annotated.

Experimental condition	On in	Spot #	Protein name	Accession #	Score	Number of peptides
Naïve vs 15DPPI	Naïve	0504	Collagen alpha-1 chain	Locus_1344_Transcript_1/1	331.62	7
		3208	Beta-1,3-glucan-binding protein	Locus_838_Transcript_2/23	694.24	13
			C-type lectin 357_1.1	Locus_357_Transcript_1/1	120.01	2
		4004	Thioredoxin peroxidase	Locus_315_Transcript_3/11	196.08	5
		1009	Pathogen-related protein 1	Locus_12722_Transcript_1/1	308.00	5
	15DPPI	5213	Beta-1,3-glucan-binding protein	Locus_838_Transcript_2/23	329.54	7
			C-type lectin 357_1.1	Locus_357_Transcript_1/1	125.75	2
		5214	Beta-1,3-glucan-binding protein	Locus_838_Transcript_2/23	294.76	6
			C-type lectin 357_1.1	Locus_357_Transcript_1/1	62.51	2
		6214	C-type lectin 357_1.1	Locus_357_Transcript_1/1	67,52	2
15DPPI vs 25DPPI	15DPPI	1314	Proteinase inhibitor i4 serpin	Locus_36336_Transcript_1/5	380.23	9
		7315	Aldolase	Locus_2214_Transcript_13/14	1214.45	20
			Astacin family metalloendopeptidase farm-1	Locus_36391_Transcript_1/3	271.86	7
			Biomphalysin/predicted protein [Nematostella vectensis]	Locus_982_Transcript_69/85	65,20	2
		3208	Beta-1,3-glucan-binding protein	Locus_838_Transcript_2/23	229.35	5
			C-type lectin 357_1.1	Locus_357_Transcript_1/1	129.34	2
25DPPI vs 15DPC	15DPC	1314	Proteinase inhibitor i4 serpin	Locus_36336_Transcript_1/5	738.99	12
			Hemagglutinin/amebocyte aggregation factor 821_4.13	Locus_821_Transcript_4/13	158.27	4
			Actin	Locus_25_Transcript_5711/10008	64.88	2
		1316	Actin 1	Locus_68811_Transcript_1/1	91.33	2
			Hemagglutinin/amebocyte aggregation factor 821_4.13	Locus_821_Transcript_4/13	72.85	2
			Glycogen synthase	Locus_37921_Transcript_2/3	61.26	2
		4004	Fatty acid binding protein h8-isoform	Locus_688_Transcript_2/3	468.52	8
			---NA---	Locus_37131_Transcript_1/1	213.67	4

Table 3 Qualitative differences of plasma proteome identified by 2D gel electrophoresis

Accession #: correspond to the accession number of the transcript in the transcriptomic database of *Biomphalaria glabrata* Brazil (assembly of Rnaseq illumina sequencing) deposited in 2EI website (http://2ei.univ-perp.fr/?page_id=89). NA: not annotated.

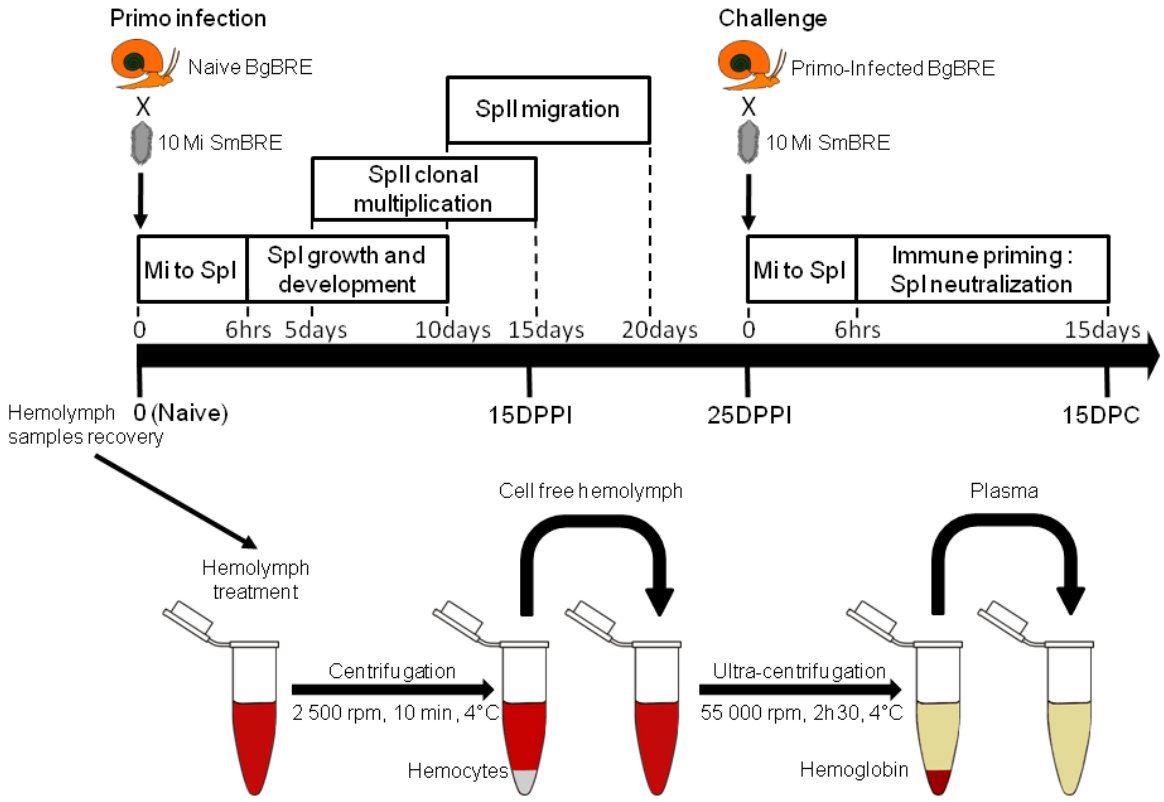

Figure 1: Schematic representation of intramolluscal development of *Schistosoma mansoni* and schematic procedure used to plasma recovery.

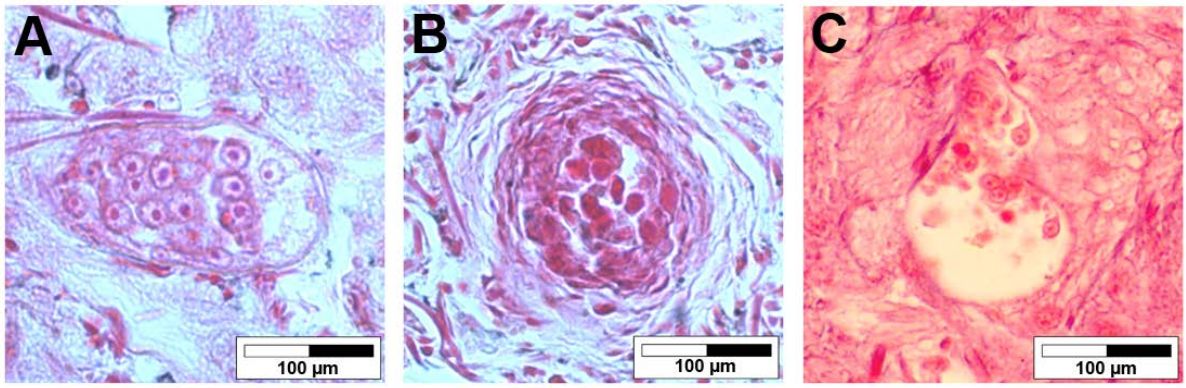

Figure 2: Histological sections of sporocysts in snail's tissues. A. Forty eight hours sporocyst in compatible interaction with snail, developing itself in the head-foot tissues. B. Forty eight hours encapsulated sporocyst in snail tissue. The capsule was formed by hemocytes. C. Forty eight hours sporocyst degenerating without any cellular reaction in a 25 days primed snail.

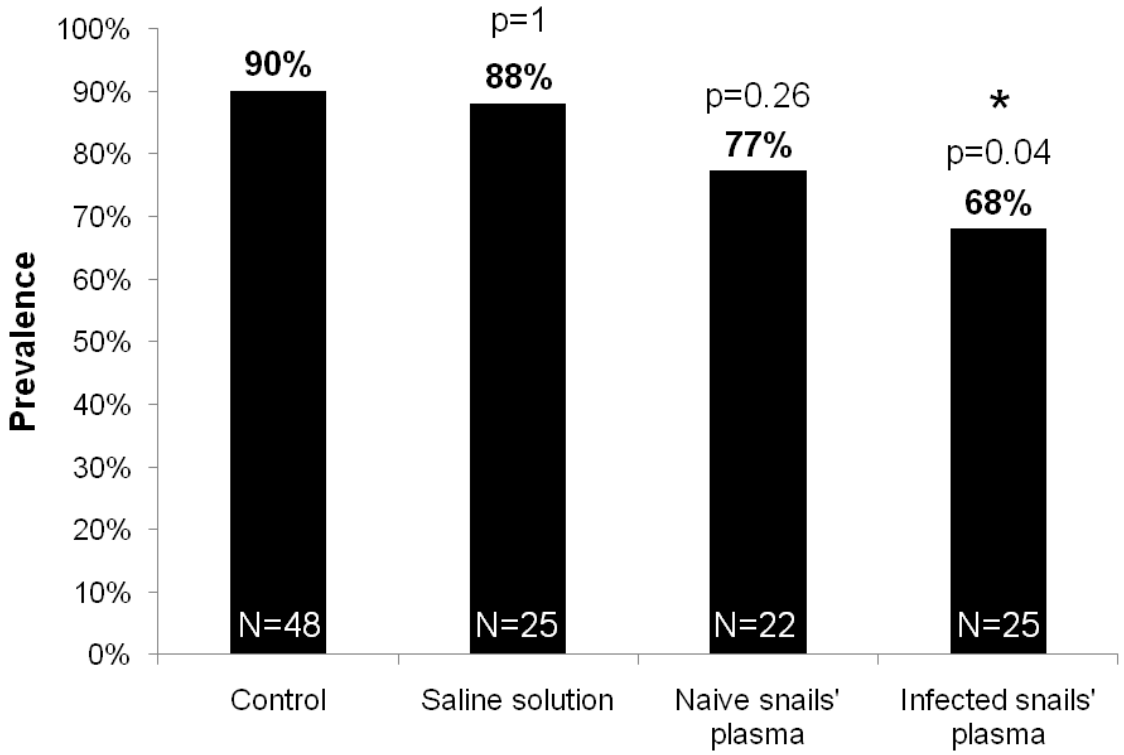

Figure 3: Prevalence after plasma transfert. Control represents 48 naive snails submitted to 10 miracidia of *S. mansoni*. The others conditions represents snails submitted to 10 miracidia of *S. mansoni* 15 days after an injection of, respectively Saline solution (PBS) (N=25), plasma coming from naive snails (N=22) and plasma coming from 15 days infected snails (N=25). All the p value was calculated using Fisher's exact test comparing each condition to the control.

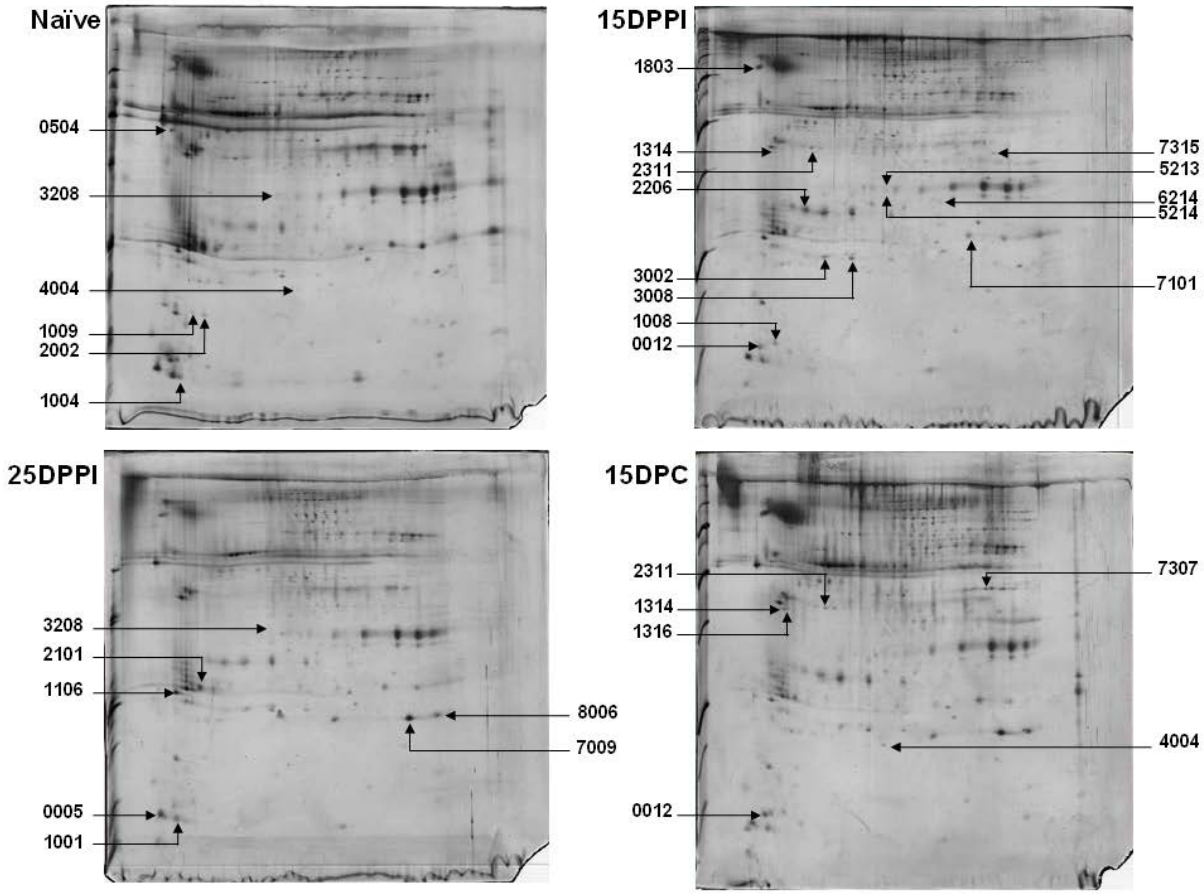

Figure 4: 2D electrophoresis gel separating proteins from plasma. Snails were exposed to 10 miracidia of *S. mansoni* and plasma was recovered from Naive snails (Naive), from 15 days post primary infection snails (15DPPI), from 25 days post primary infection snails (25DPPI). At this time point, the primed snails were challenged with 10 miracidia of *S. mansoni* and the last recovery of plasma was made 15 days after the challenge (15DPC) that means 40 days post primary infection.

A. Immune memory response

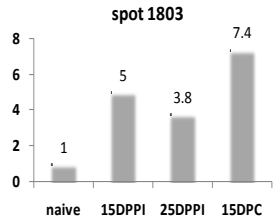

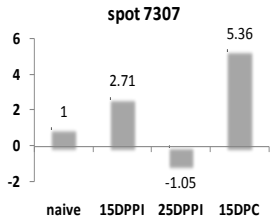

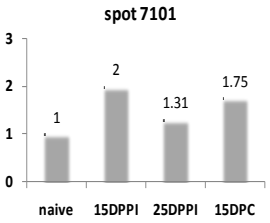

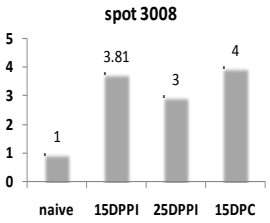

B. Immune sustained response

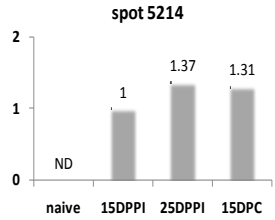

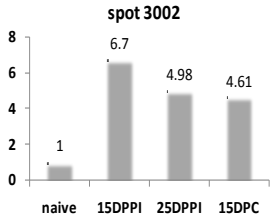

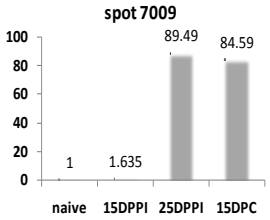

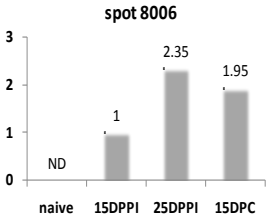

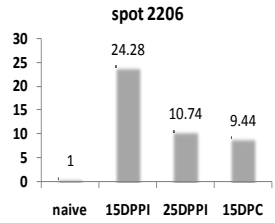

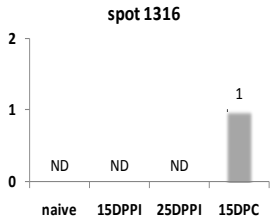

C. Down-regulated response

After primo-infection

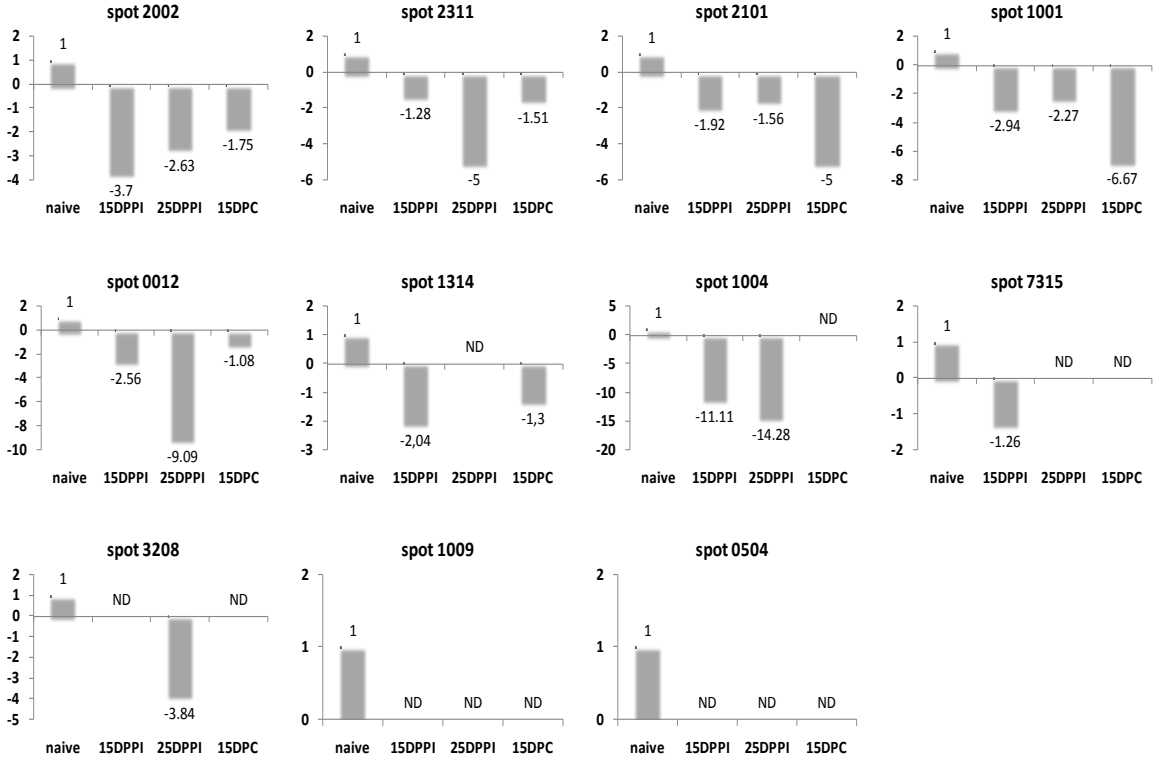

After challenge

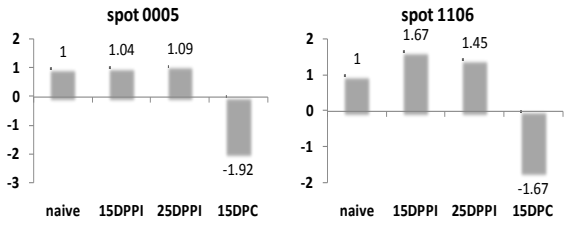

D. Mix expression response

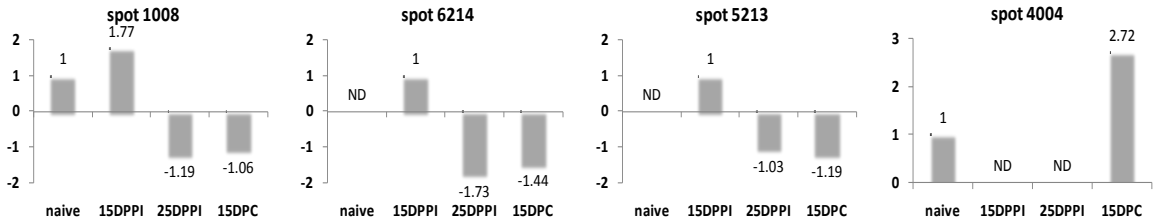

Figure 5: Histogramms representing spot's regulation in the course of the infection.

C-type lectin 2573_1.7

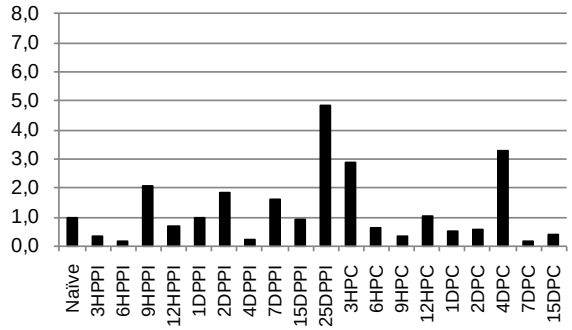

C-type lectin 46213_1.1

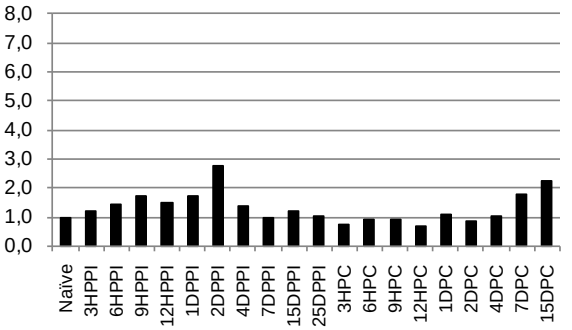

C-type lectin 357_1.1

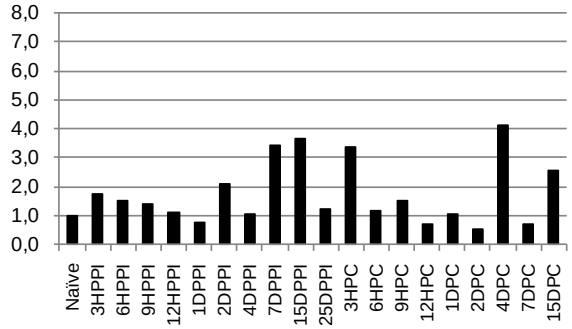

Mannose receptor c type 2

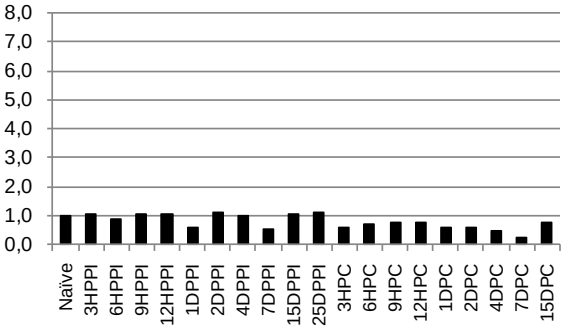

Beta-1,3-glucan-binding protein

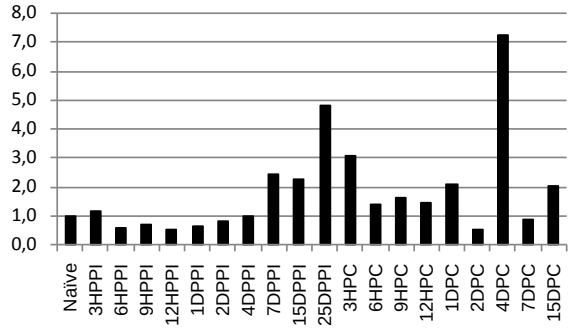

Hemagglutinin/amebocyte aggregation factor 35403_4.6

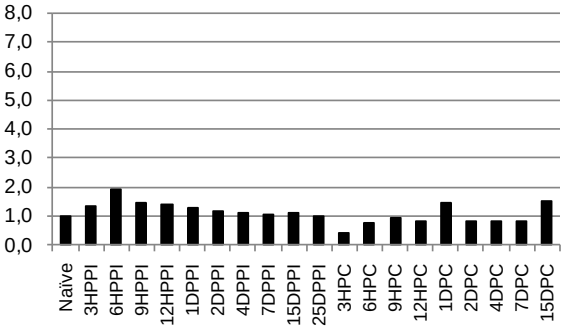

Hemagglutinin/amebocyte aggregation factor 19302_1.23

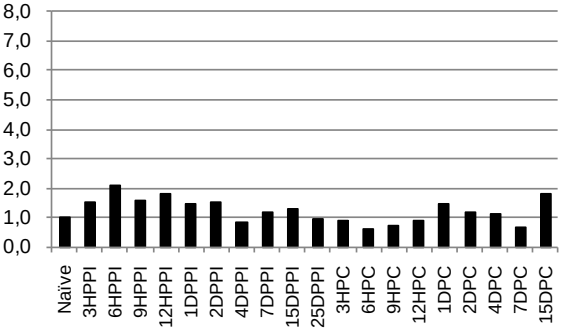

Hemagglutinin/amebocyte aggregation factor 821_4.13

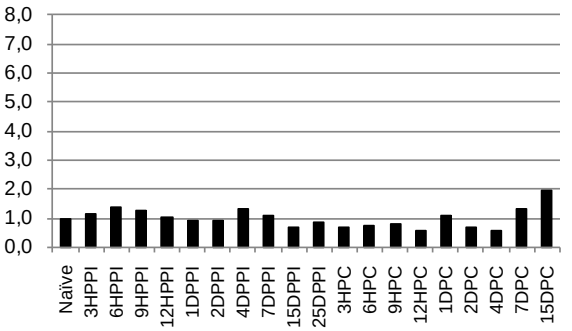

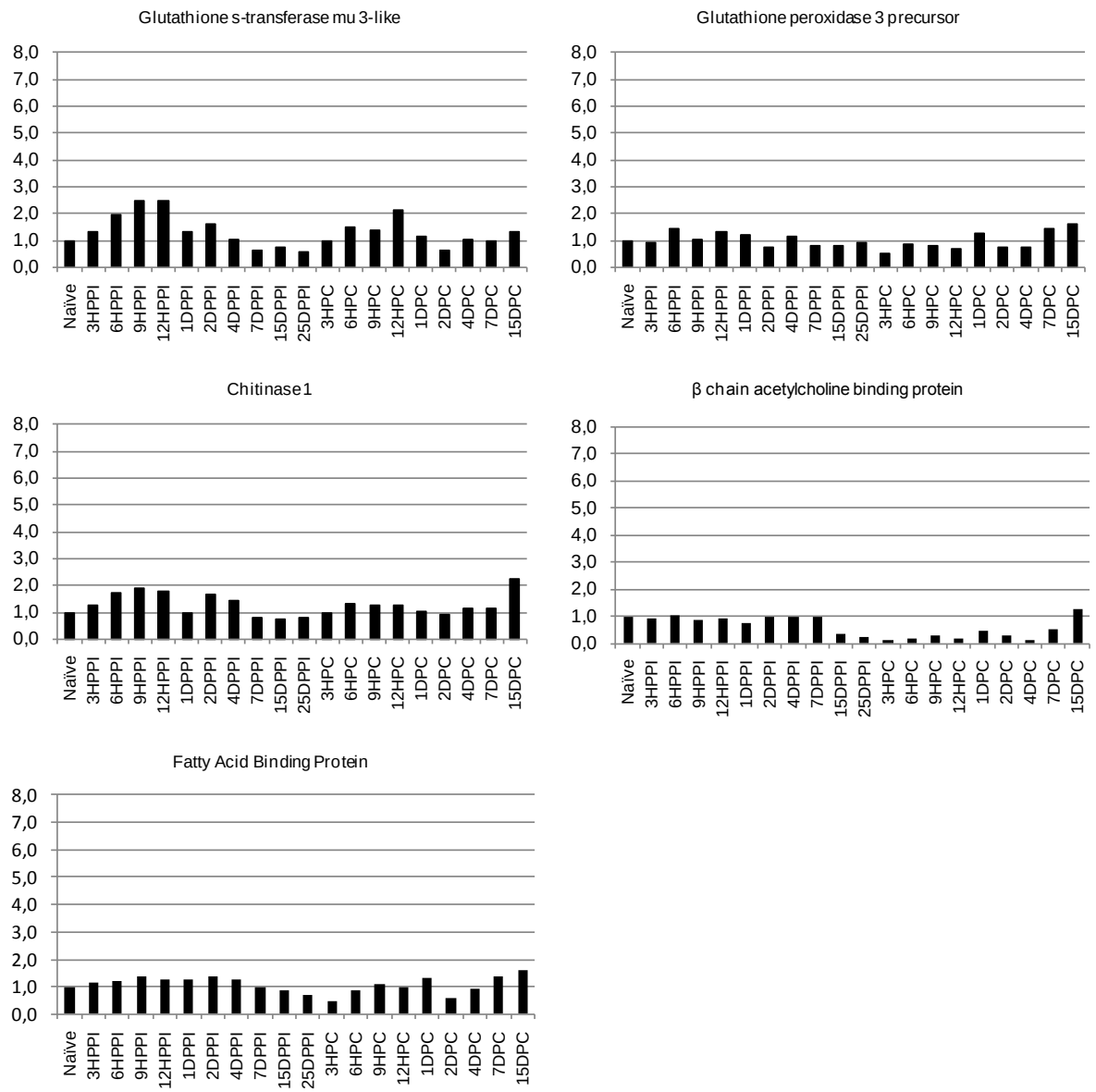

Figure 6: qRT-PCR ratio. All genes were normalized by the 19S ribosomal protein and by the Naïve condition. Each histogram presented the transcript level of a gene during an experiment of infection/re-infection. XHPPI represents the number of hours post primo-infection, XDPPI, the number of days post primo-infection, XHPC, the number of hours post challenge and XDPC, the number of days post challenge.

Chapitre quatre :

La Biomphalysine,

un effecteur de la réponse immunitaire

humorale de *Biomphalaria glabrata*

CHAPITRE QUATRE :

LA BIOMPHALYSINE, UN EFFECTEUR DE LA REPONSE IMMUNITAIRE HUMORALE DE *BIOMPHALARIA GLABRATA*

Biomphalysin, a new β pore-forming toxin involved in *Biomphalaria glabrata* immune defense against *Schistosoma mansoni*

Galinier R, Portela J, Moné Y, Allienne J-F, Henri H, Delbecq S, Mitta G, Gourbal B and Duval D

PLoS Pathogens (2013) 9 :3

La Biomphalysine est une « β-pore forming toxins » ou β-PFT. Ces molécules sont connues pour être des facteurs de virulences appartenant à la famille des Aérolysines essentiellement produites par des bactéries (Rossjohn et al. 1998; Knapp O 2010). La mise en évidence de cette molécule dans notre étude de protéomique chez *Biomphalaria glabrata* (Chapitre 3) ainsi que son potentiel mode d'action et son activité nous ont laissé imaginer qu'elle pouvait jouer un rôle dans le priming immunitaire. De plus, au cours des approches d'interactome menées dans le cadre de la thèse d'Yves Moné, qui visaient à identifier les molécules clés au cœur de l'interaction entre *Biomphalaria* et *Schistosoma*, la Biomphalysine avait déjà pu être mise en évidence (Mone et al. 2010).

La Biomphalysine constitue la première molécule identifiée chez *Biomphalaria glabrata* présentant une potentielle activité cytotoxique/cytolytique et pouvant jouer un rôle clé dans les interactions immunobiologiques mollusques/trématodes. Nous avons donc cherché à caractériser plus avant cette β-PFT chez *B. glabrata*. Dans le travail présenté dans le Chapitre 4, nous avons donc mené une étude approfondie concernant la structure de cette β-PFT que nous avons nommé Biomphalysine. Nous avons par la suite construit un arbre phylogénétique des différents domaines Aérolysine provenant des différents membres de cette superfamille afin de mieux comprendre comment cette molécule pouvait se retrouver chez un mollusque alors qu'elles sont principalement connues et décrites chez les procaryotes. Nous avons également étudié l'indicibilité de cette molécule suite à des stimulations immunitaires variées. Nous avons enfin poussé l'étude fonctionnelle en produisant une molécule recombinante afin de tester son activité hémolytique ainsi que son activité *in vitro* sur des sporocystes de *Schistosoma mansoni*. Enfin des approches d'immunolocalisation en microscopie confocale ont été réalisées afin de démontrer la liaison de la Biomphalysine à la surface des pathogènes.

OPEN ACCESS Freely available online

PLOS | PATHOGENS

Biomphalysin, a New β Pore-forming Toxin Involved in *Biomphalaria glabrata* Immune Defense against *Schistosoma mansoni*

Richard Galinier[1,2☯], Julien Portela[1,2☯], Yves Moné[1,2,3], Jean François Allienne[1,2], Hélène Henri[3], Stéphane Delbecq[4], Guillaume Mitta[1,2], Benjamin Gourbal[1,2], David Duval[1,2]*

1 CNRS, UMR 5244, Ecologie et Evolution des Interactions (2EI), Perpignan, France, **2** Université de Perpignan Via Domitia, Perpignan, France, **3** Université de Lyon, Lyon; Université Lyon 1; CNRS, UMR 5558, Laboratoire de Biométrie et Biologie Evolutive, Villeurbanne, France, **4** EA 4558, Vaccination Antiparasitaire, Laboratoire de Biologie Cellulaire et Moléculaire UFR Pharmacie, Montpellier, France

Abstract

Aerolysins are virulence factors belonging to the β pore-forming toxin (β-PFT) superfamily that are abundantly distributed in bacteria. More rarely, β-PFTs have been described in eukaryotic organisms. Recently, we identified a putative cytolytic protein in the snail, *Biomphalaria glabrata*, whose primary structural features suggest that it could belong to this β-PFT superfamily. In the present paper, we report the molecular cloning and functional characterization of this protein, which we call Biomphalysin, and demonstrate that it is indeed a new eukaryotic β-PFT. We show that, despite weak sequence similarities with aerolysins, Biomphalysin shares a common architecture with proteins belonging to this superfamily. A phylogenetic approach revealed that the gene encoding Biomphalysin could have resulted from horizontal transfer. Its expression is restricted to immune-competent cells and is not induced by parasite challenge. Recombinant Biomphalysin showed hemolytic activity that was greatly enhanced by the plasma compartment of *B. glabrata*. We further demonstrated that Biomphalysin with plasma is highly toxic toward *Schistosoma mansoni* sporocysts. Using *in vitro* binding assays in conjunction with Western blot and immunocytochemistry analyses, we also showed that Biomphalysin binds to parasite membranes. Finally, we showed that, in contrast to what has been reported for most other members of the family, lytic activity of Biomphalysin is not dependent on proteolytic processing. These results provide the first functional description of a mollusk immune effector protein involved in killing *S. mansoni*.

Citation: Galinier R, Portela J, Moné Y, Allienne JF, Henri H, et al. (2013) Biomphalysin, a New β Pore-forming Toxin Involved in *Biomphalaria glabrata* Immune Defense against *Schistosoma mansoni*. PLoS Pathog 9(3): e1003216. doi:10.1371/journal.ppat.1003216

Editor: Chris Bayne, Oregon State University, United States of America

Received November 1, 2012; **Accepted** January 9, 2013; **Published** March 21, 2013

Funding: This work was supported by funds from the Centre National de la Recherche (CNRS) and the Université de Perpignan Via Domitia (UPVD), and by a grant by the ANR (25390 Schistophepigen). The funders had no role in study design, data collection and analysis, decision to publish, or preparation of the manuscript.

Competing Interests: The authors have declared that no competing interests exist.

* E-mail: david.duval@univ-perp.fr

☯ These authors contributed equally to this work.

Introduction

Schistosomiasis, or bilharzia, is a tropical disease caused by worms of the genus *Schistosoma*. The main disease-causing species are *Schistosoma haematobium*, *Schistosoma japonicum*, and *Schistosoma mansoni*. An estimated 200 million people in 74 countries suffer from schistosomiasis [1,2]. The World Health Organization expert committee (WHO Technical Report Series 912: prevention and control of schistosomiasis and soil transmitted helminthiasis (WHO, Geneva, 2002)) concluded that yearly deaths could be as high as 200,000 making schistosomiasis the most severe tropical disease after malaria in terms of mortality [1]. No vaccines are yet available to fight *S. mansoni*, and current chemotherapy relies on a single drug, praziquantel, for which resistant cases have been reported [1,2].

The life cycle of the parasite requires contamination of surface water by excrement, specific freshwater snails as intermediate hosts, and human-to-water contact. Because of their medical and epidemiological importance as intermediate hosts for *Schistosoma* parasites, freshwater snails of the *Biomphalaria* genus have garnered considerable research attention. Given the limited options for treating *S. mansoni* infections, a better understanding of the immunobiological interactions between the invertebrate host *Biomphalaria glabrata* and its parasite *S. mansoni* could be invaluable in developing new strategies for preventing and/or controlling Schistosomiasis diseases.

A number of studies published over the last two decades have contributed greatly to our understanding of *B. glabrata* innate immune mechanisms involved in the defense against pathogens. The discovery of recognition molecules such as lectins contributed to a better understanding of the mechanisms involved in pathogen recognition. Among this family of recognition molecules, the discovery of the somatically diversified FREPs (fibrinogen-related proteins) was an important advance in elucidating the immune-recognition step [3,4]. Recently, FREPs were shown to play a crucial role in the fate of the interaction between *B. glabrata* and its trematode parasites [5]. A recent study described the putative involvement of the cytokine-like molecule, BgMIF (*B. glabrata*

Author Summary

Schistosomiasis is the second most widespread tropical parasitic disease after malaria. It is caused by flatworms of the genus *Schistosoma*. Its life cycle is complex and requires certain freshwater snail species as intermediate host. Given the limited options for treating *S. mansoni* infections, much research has focused on a better understanding of the immunobiological interactions between the invertebrate host *Biomphalaria glabrata* and its parasite *S. mansoni*. A number of studies published over the last two decades have contributed greatly to our understanding of *B. glabrata* innate immune mechanisms involved in the defense against parasite. However, most studies have focused on the identification of recognition molecules or immune receptors involved in the host/parasite interplay. In the present study, we report the first functional description of a mollusk immune effector protein involved in killing *S. mansoni*, a protein related to the β pore forming toxin that we named Biomphalysin.

macrophage migration inhibitory factor) in the anti-parasite response of *B. glabrata* [6]. A number of studies have analyzed the response of *B. glabrata* to different immune challenges, allowing the identification of numerous putative immune genes that could play a key role in *B. glabrata* immune processes [7,8,9,10,11,12]. Other studies based on comparisons of resistant and susceptible strains of *B. glabrata* to different trematode species from *Schistosoma* and *Echinostoma* genera [13,14,15,16,17] have also made a large contribution to the identification of factors putatively involved in the success or failure of parasite infection. Still other studies have explored mechanisms underlying compatibility polymorphism characteristics in certain *B. glabrata*/*S. mansoni* populations [18,19,20,21]. These latter studies allowed the identification of two repertoires of polymorphic and/or diversified molecules that were shown to interact: the parasite antigens SmPoMucs (*S. mansoni* polymorphic mucins) and *B. glabrata* FREP immune receptors. The interaction profile of these molecules defines the compatible/incompatible status of a specific snail/schistosome combination (for a recent review, see [22]). Studies specifically dedicated to immune effectors have clearly demonstrated that *B. glabrata* production of reactive oxygen species (ROS), particularly H_2O_2, plays a crucial role in anti-schistosome defense [23,24]. Moreover, hemocytes from *S. mansoni*-resistant snails have been shown to generate significantly more ROS than susceptible snails [25,26,27], and a reciprocal co-evolution has been demonstrated between ROS and ROS scavengers produced by sympatric populations of *B. glabrata* and *S. mansoni* [28]. Additional *B. glabrata* putative immune effectors have been identified, including LBP (lipopolysaccharide-binding protein) and BPI (bactericidal/permeability-increasing protein) [8,29], and antimicrobial peptides [29], but their functions remain to be determined.

Using an interactome approach employing *B. glabrata* plasma and *S. mansoni* primary sporocyst extracts, we recently identified a new, putative cytolytic protein from *B. glabrata* that displays similarities to members of the β-PFT superfamily known to form channels in targeted membranes [30]. The most studied members of this superfamily are the aerolysin toxins secreted by several *Aeromonas spp*. [31,32]. Other members of this β-PFT superfamily include the α-toxin produced by *Clostridium septicum* [33], the ε-toxin from *Clostridium perfringens* [34], the MTX (mosquito toxin)-type proteins secreted by *Bacillus sphaericus* [35], parasporin 2 and 4 from *Bacillus thuringiensis* [36,37], monalysin from *Pseudomonas entomophila* [38], and the vibrioaerolysin of *Vibrio splendidus* [39]. Most of these proteins are produced by bacteria, as confirmed by a recent bioinformatic analysis of protein database entries displaying an aerolysin signature, which revealed that 70% of the putative β-PFTs identified came from bacteria [40]. These β-PFTs are most often produced by pathogenic bacteria. Several functional studies have clearly documented their virulence and mode of action (for a review, see [41,42]). As an example, the entomopathogen *Pseudomonas entomophila* produces an aerolysin-like toxin that triggers the cytolysis and rupture of the drosophila intestinal epithelial barrier [38]. Other β-PFTs specifically target immune-competent cells, inducing their death [43,44].

Some β-PFTs have also been identified in eukaryotic multicellular organisms, both animals and plants, but few have been characterized functionally. *Hydra viridissima* secretes different hydralysins that may be involved in protecting against predators or killing prey [45]. The seeds of *Enterolobium contortisiliquum* produce enterolobin, a pro-inflammatory protein that may protect against herbivore grazing [46,47]. In cases in which the function of these eukaryotic β-PFTs was investigated, they were shown to share the same mode of action as their prokaryotic counterparts [48]. These β-PFTs, which are secreted as a soluble, inactive precursor called a protoxin, bind with high affinity to the glycosyl anchor of glycosylphosphatidyl inositol (GPI)-anchored proteins located on the surface membrane of target cells [49]. Some, including the aerolysins, show an affinity for carbohydrates, whereas others such as clostridium α-toxin lack this property [50,51,52]. This property of aerolysins is linked to their bilobal shape (for a review, see [42]): the large lobe common to all β-PFTs is involved in either oligomerization or binding to a GPI-anchored receptor, and the second smaller lobe contains a carbohydrate-binding domain. After binding to their ligand, all β-PFT protoxins oligomerize to form a ring-shaped heptameric channel [53,54,55]. Subsequent formation of a pore in the membrane requires an extracellular processing step that removes about forty amino acids of the aerolysin C-terminal region [56]. This last activation step can be achieved by pathogen proteases as well as by proteases from the host [38,49,57,58].

Here, we report the cloning and characterization of a new β-PFT, which we have named Biomphalysin because it is produced by the *Biomphalaria* species, *B. glabrata*. This protein is the first cytolytic β-PFT protein from a mollusk to be characterized.

Methods

Ethics statement

Our laboratory holds permit #A66040 for experiments on animals from both the French Ministry of Agriculture and Fisheries, and the French Ministry of National Education, Research, and Technology. The housing, breeding, and care of animals utilized here followed the ethical requirements of our country. The experimenter also possesses an official certificate for animal experimentation from both French ministries (Decree #87–848, October 19, 1987). Animal experimentation followed the guidelines of the CNRS (Centre National de la Recherche Scientifique). The protocols used in this study have been approved by the French veterinary agency from the DRAAF Languedoc-Roussillon (Direction Régionale de l'Alimentation, de l'Agriculture et de la Forêt), Montpellier, France (Authorization #007083).

Biological material and parasite challenge

B. glabrata and *S. mansoni* originated from Brazil and have been maintained in the laboratory for several years [59]. The parasite strain was maintained in hamsters (*Mesocricetus auratus*), as described previously [60]. Parasite recovery was conducted as follows:

Rodent livers were collected in sterile saline solution (150 mM NaCl) containing an antibiotic/antimycotic mixture (penicillin 100 units/ml, streptomycin 0.1 mg/ml, amphotericin B 0.25 μg/ml; Sigma). After grinding, parasite eggs were filtered and washed. Miracidia were hatched from eggs in sterile water and concentrated by sedimentation on ice for 1 h. Primary sporocysts for tests of Biomphalysin antischistosomal activity were obtained by transferring miracidia to Chernin's balanced salt solution (CBSS) and maintaining at 26°C under normoxic conditions for 24 h [61]. The Bge cell line (ATCC, CRL 1494), derived from *B. glabrata*, was grown at 26°C under normoxic conditions in complete Bge medium, as described previously [62].

For parasite challenge, infestation experiments were performed on juvenile *B. glabrata* (5–6 mm in diameter). Snails were individually exposed to 10 miracidia of *S. mansoni* in 5 ml of pond water. The infectivity of the miracidia was confirmed by exposing additional snails to parasites at the same time and dissecting them at 15 d post-exposure. All groups were treated in the same manner and at the same time. Seven snails were collected at each point in challenge and control kinetics experiments. All experiments reported in the present study were repeated at least two times.

5′ and 3′ rapid amplification of cDNA ends (RACE)

Total RNA was extracted from a pool of ten snails using TRIzol reagent according to the manufacturer's instructions (Invitrogen). Full-length Biomphalysin cDNA was obtained by performing 5′ and 3′ RACE polymerase chain reactions (PCRs) using the GeneRacer kit, as described by the manufacturer (Invitrogen). Briefly, 5 μg of total RNA were treated with calf intestinal phosphatase to remove the 5′ phosphates. After phenol extraction, dephosphorylated RNA was decapped with a tobacco acid pyrophosphatase treatment. The GeneRacer RNA oligo provided by the manufacturer was ligated to the 5′end of the mRNA using T4 RNA ligase. Reverse transcription was performed using SuperScript III reverse transcriptase and GeneRacer Oligo dT primer. Primers for 5′ (5′-GGC TGG CTT AGT GCA TCT TGC GCT CT-3′) and 3′ (5′-GCT GTC AAC GAT ACG CTA CGT AAC G-3′) RACE were designed from a contig obtained by the assembly of *B. glabrata* expressed sequence tags (ESTs) identified by MASCOT analysis [30]. The amplification cycling conditions for both consisted of an initial denaturation step at 95°C for 5 min followed by 35 cycles of 30 s denaturation at 95°C, 30 s annealing at 55°C and 5 min extension at 68°C, followed by a final extension at 68°C for 10 min. Advantage 2 PCR enzyme (Clontech) was used in PCR reactions. RACE PCR products were analyzed by agarose gel electrophoresis and cloned into the pCR4-TOPO vector according to the manufacturer's instructions (Invitrogen). Clones were then sequenced using GATC facilities (GATC Biotech, Germany).

Semi-quantitative RT-PCR

The tissue distribution of Biomphalysin mRNA was analyzed by preparing samples of albumen gland, head-foot, hepato-pancreas, and ovotestis, collected from ten snails under a binocular dissection microscope. Hemocytes from fifty snails were also collected from hemolymph after centrifugation at 10000×g for 10 min at 4°C. Total RNA from these different tissues, hemocytes, and Bge cells was extracted using TRIzol Reagent solution (Invitrogen) according to the manufacturer's protocol. Then, total RNA (10 μg) was treated with rDnase I (1 U/μg DNA; Ambion) to remove contaminating genomic DNA. cDNA was synthesized from DNA-free RNA (1 μg) by reverse transcription (RT) using random hexamer primers and Revertaid H minus M-MuLV reverse transcriptase (Fermentas). The absence of contaminating genomic DNA was confirmed using PCR primers (forward: 5′-CCC ATC TAT TGT TGG CAG ACC-3′, reverse: 5′-GTT TAG AGG TGC CTC TGT GAG-3′) for the actin gene (accession number U53348.1) designed to anneal to two different exons. Biomphalysin gene expression analyses were performed using primers allowing full-length cDNA amplification (forward: 5′-GGC TTA TAT TGC AGA AAA TGT TTT TA-3′, reverse: 5′-CTC TGA CAC AAT CAA GAC AAC AAG-3′). Semi-quantitative RT-PCR conditions were 94°C for 5 min followed by 32 cycles of 94°C for 30 s, 50°C for 30 s, 72°C for 1 min 30 s, and a final 5-min extension step at 72°C. PCR products were separated by electrophoresis on 2% agarose gels and cloned into pCR4-TOPO for subsequent sequencing.

Real-time quantitative PCR

Total RNA was extracted either from a pool of seven snails or from Bge cells using TRIzol reagent. Reverse transcription was performed as described previously [21]. Real-time quantitative PCR (Q-PCR) was performed on cDNAs (diluted 50-fold with nuclease-free water) using the Light Cycler System 480 (Roche, Idaho Technologies). Sequences of primers used for amplification of Biomphalysin (forward: 5′-CTG ATT ACA CCT GGG C-3′, reverse: 5′-ACC CTT TCG TCC CAT AC-3′) and ribosomal protein S19 (forward: 5′TTC TGT TGC TCG CCA C, reverse: 5′-CCT GTA TTT GCA TCC TGT T-3′) were designed using LightCycler Probe Design software version 1.0 (Roche Diagnostics). Q-PCR reactions were performed according to the Light Cycler procedure. Amplification conditions were as follows: 20 s denaturation at 95°C followed by 40 cycles of 5 s at 95°C, 7 s at 60°C, and 12 s at 72°C. After amplification, the specificity of PCR products was determined by analyzing melting curves, acquired by heating the product at 95°C, cooling at 70°C for 20 s, and then slowly remelting (0.31°C/s) up to 95°C. Each PCR product was verified by sequencing. The results of melting curve analyses were quantified by determining the crossing-point value (Cp) using the second derivative maximum method of the Light Cycler Software 3.3 (Roche Diagnostics). Expression data were normalized to ribosomal protein S19 (accession number CK988928) levels [29]. The Biomphalysin-to-S19 transcription ratio was calculated using the relative quantification analysis module of the LightCycler 480 software. All Q-PCR experiments reported in the present study were repeated at least three times.

Recombinant Biomphalysin production

A Biomphalysin cDNA lacking nucleotides encoding the signal peptide was amplified from the full-length gene by PCR using the primers, 5′-CGC TTA ATT AAA CAT ATG ACC CAA TGC ACC TAT TCC-3′ (forward) and 5′-TTA GTT AGT TAC CGG ATC CCT TAC TAG ACT TTC ACT TC-3′ (reverse), and subsequently cloned into the RTS pIVEX 1.4 Wheat Germ His_6-tag Vector (5 Prime) using the In-Fusion HD Cloning Kit (Clontech), as described by the manufacturer. The expression vector was transformed into Stellar competent cells (Clontech), amplified by bacterial culture, and then purified using the Qiagen Plasmid Plus kit. The Biomphalysin protein was expressed *in vitro* as an N-terminal His_6-tagged protein using the Rapid Translation System (RTS; 5 Prime), according the manufacturer's instructions. Briefly, 60 μg of expression vector were used per reaction of the RTS 500 Wheat Germ CECF Kit. The reaction was performed in the RTS ProteoMaster instrument by incubating at a temperature of 24°C for 2 h with shaking (900 rpm); the yield of N-terminal His_6-tagged Biomphalysin was approximately 100 μg/reaction. Recombinant protein production efficiency was evaluated by Western blot analysis. Total protein extract was separated by

sodium dodecyl sulfate-polyacrylamide gel electrophoresis (SDS-PAGE) on 12% gels and electrophoretically transferred onto a nitrocellulose membrane. The membrane was blocked by incubating for 3 h at room temperature in 4% non-fat dried milk in TBS (Tris-buffered saline)/0.05% Tween. The blot was subsequently incubated overnight at 4°C with anti-His antibody (Invitrogen) diluted 1:5000 in 4% non-fat dried milk in TBS/0.05% Tween-20. The blot was washed three times with TBS/0.05% Tween-20 and incubated at room temperature for 1.5 h with anti-mouse antibody (diluted 1:5000 in 1× phosphate-buffered saline [PBS], 4% milk, and 0.05% Tween-20), washed again with TBS/0.05% Tween-20, and then developed by incubating with an enhanced chemiluminescence (ECL) substrate (Pierce) followed by autoradiography. In order to determine rBiomphalysin concentration, several volumes (0.5 µl, 1 µl and 5 µl) of wheat germ extracts (WGE) containing or not rBiomphalysin were run on 12% SDS-PAGE, with a range of known amounts of bovine serum albumin (BSA, from 50 ng to 600 ng). The gel was subsequently stained with Coomassie blue using standard protocols [63]. rBiomphalysin concentration was assessed after separation and staining by densitometry analysis of the corresponding band. Briefly, the gel was scanned and digitized using a GS 800 calibrated densitometer (Bio Rad). rBiomphalysin and BSA colorations were estimated using the software Quantity One 1-D Analysis Software 4.6. As Coomassie blue only colors aromatic and basic amino acids which number vary between proteins, we verified the amount of basic and/or aromatic residues in both compared proteins. BSA and rBiomphalysin contain 598 and 607 amino acids and they display 157 and 154 basic and/or aromatic residues, respectively. Among them, BSA contains 17% of basic residues and 12% of aromatic residues and rBiomphalysin contains 13% of basic residues and 13% of aromatic residues. These close values allowed us to estimate the concentration of rBiomphalysin in WGE using the standard curve obtained with the different BSA amounts. This estimation is 90 ng of rBiomphalysin per µl of WGE.

Hemolytic assay

Hemolytic assays were performed according to a previously described procedure [64]. Briefly, different amounts of crude recombinant Biomphalysin (0.61–500 nM; total volume, 20 µl) were mixed with a 3% suspension of sheep erythrocytes (120 µl) and *B. glabrata* plasma or PBS (40 µl), and incubated overnight at 37°C with gentle agitation. After a 2-min centrifugation at 500×g, the supernatants were collected and their absorbance was measured at 405 nm (AD 340; Beckman Coulter). Percent hemolysis was calculated according to the equation, $100\times(A_{405}$ sample$-A_{405}$ negative control$)/(A_{405}$ positive control$-A_{405}$ negative control), where negative control corresponds to the same amount of RTS 500 reaction performed using empty pIVEX 1.4 vector (i.e. without the Biomphalysin gene) and positive control corresponds to total lysis caused by a nonionic surfactant (20 µl of 10% Triton X-100 in PBS in place of recombinant protein).

Cytotoxicity of Biomphalysin toward *S. mansoni* sporocysts

Primary sporocysts (Sp1) were obtained by *in vitro* transformation of 400 miracidia and then were exposed to rBiomphalysin (30 nM) with or without ultracentrifuged *B. glabrata* plasma (40 µl in a 200 µl reaction volume). Ultracentrifugation step (30,000 rpm, 3 h, 4°C) is used to remove free haemoglobin from plasma. Cytotoxicity was determined by direct light microscopic observations of (i) vacuolization, (ii) focal *lysis* of the *tegumental* matrix and/or underlying muscle fibers, and (iii) mortality. Primary sporocysts were considered dead if they failed to exhibit motility and/or beating of flame-cell flagella. Experiments were conducted in duplicate on 12-well plates using 25 sporocysts per well. Kaplan-Meier survival analyses followed by pairwise log-rank tests were used to compare survival data, as described previously [65].

Immunocytochemical detection of Biomphalysin on *S. mansoni* sporocysts

One hundred sporocysts were incubated with 40 µl of WGE with rBiomphalysin protein (~60 nM) or WGE for 1 h in the presence or absence of *B. glabrata* plasma. Then, sporocysts were rinsed and fixed by incubating with 4% paraformaldehyde in PBS for 1 h at room temperature. Afterwards, parasites were rinsed with PBS and centrifuged (1 min, 800×g) onto poly-D-Lysine–coated slides (CultureSlides; BD Falcon). Slides were blocked by incubating with PBS containing 3% bovine serum albumen (BSA) for 2 h at room temperature. Parasites were then incubated for 90 min with an anti-His antibody diluted 1:500 (Life Technologies). After being washed three times in PBS, parasites were incubated with an Alexa Flour 594-conjugated anti-mouse IgG (Life Technologies) diluted 1:1000 in PBS/1% BSA for 45 min at room temperature. After rinsing, slides were mounted in Dako fluorescent mounting medium (Dako) and examined using a fluorescence confocal laser-scanning microscope (Zeiss LSM 700, Tecnoviv platform). All images were acquired under the same conditions (63×, 1.40 oil DIC M27, pinhole 1.00 [arbitrary units], 8-bit sampling, average of 4 frames at 1400×1400 pixels). The resolution obtained was 13,778 pixels/µm. For presentation, images were imported into ImageJ software.

Detection of Biomphalysin on *S. mansoni* sporocysts by *in vitro* binding assay

Fifty sporocysts were recovered from cell culture plates after a 6-h incubation at 27°C in the presence or absence of *B. glabrata* plasma, with or without crude recombinant protein at the same concentration used for immunocytochemistry. Sporocysts were centrifuged for 5 min at 600×g and washed three times with CBSS medium. The recovered sporocyst pellets were subsequently denaturated by incubating for 10 min at 80°C in Laemmli buffer (Laemmli, 1970). The entire sample was resolved by SDS-PAGE on a 10% gel and treated as described previously.

Bioinformatic analysis

The presence of a signal peptide was determined by a primary structure analysis performed using SignalP 3.0. Potential glycosylation sites were predicted using NetNglyc 1.0 and NetOGlyc 3.1 (http://www.cbs.dtu.dk/services/). Protein domain searches were performed using SMART (http://smart.embl-heidelberg.de/) and Motif Scan (http://hits.isb-sib.ch/cgi-bin/PFSCAN) software. α-helical and β-sheet regions were identified by secondary structure prediction using Jpred3 and HHpred servers (http://toolkit.tuebingen.mpg.de/hhpred). Sequences were searched for putative transmembrane domains (TMDs) using the PRED-TMBB server [66,67].

Prediction of Biomphalysin three-dimensional (3D) structure and alignment with the crystal structure of proaerolysin were performed using I Tasser and TM-align servers [68,69]. The 3D structure was obtained by multiple threading using the I-Tasser server (available online), which combines two protein structure prediction methods: threading and *ab initio* prediction [70]. The quality of the computed model was estimated by the C-score (Confidence score). C-scores are typically in the range of −5 to 2, where a high C-score signifies a model with a high confidence;

Table 1. Sequences of Biomphalysin used to construct the phylogenetic tree.

Name	Organism	gi-Accession
Aerolysin	*Aeromonas hydrophila*	113485
Aerolysin precursor	*Aeromonas salmonicida*	2501303
hemolysin	*Aeromonas sobria*	148751473
Biomphalysin	*Biomphalaria glabrata*	KC012466
Hydralysin-2	*Bacillus thuringiensis* IBL 200	228911714
Hydralysin-2	*Bacillus thuringiensis serovar berliner*	228943424
Crystal protein	*Bacillus thuringiensis*	51090285
Alpha-toxin	*Clostridium botulinum*	253771270
Hypothetical protein CC1G_11805	*Coprinopsis cinerea*	299752492
Hypothetical protein CC1G_08369	*Coprinopsis cinerea*	299745505
Hypothetical protein CC1G_10318	*Coprinopsis cinerea*	299746325
Epsilon toxin precursor	*Clostridium perfringens*	315320199
Alpha-toxin	*Clostridium septicum*	27531080
Cytolytic protein enterolobin	*Enterolobium contortisiliquum*	2501305
hypothetical protein HCH_03563	*Hahella chejuensis*	83646295
hypothetical protein	*Hydra magnipapillata*	221130489
Predicted : similar to hydralysin	*Hydra magnipapillata*	221104132
Hydralysin-1	*Hydra viridissima*	39931521
Hydralysin-2	*Hydra viridissima*	74997549
Hydralysin	*Hydra vulgaris*	74996299
Secreted salivary gland peptide	*Ixodes scapularis*	241568118
Hypothetical protein IscW_ISCW013639	*Ixodes scapularis*	241838790
Pore-Forming Lectin	*Laetiporus sulphureus*	61680142
Hemolytic lectin LSLb	*Laetiporus sulphureus*	32261218
Hemolytic lectin LSLc	*Laetiporus sulphureus*	32261220
predicted protein	*Nematostella vectensis*	156373767
Predicted protein	*Nematostella vectensis*	156403083
Predicted protein	*Nematostella vectensis*	156403081
Cytotoxin	*Pseudomonas* phage phiCTX	17313218
Hypothetical protein PBPRB1941	*Photobacterium profundum*	54303595
Hypothetical protein Pecwa_1694	*Pectobacterium wasabiae*	261820982
Conserved hypothetical protein	*Ricinus communis*	255557038
Conserved hypothetical protein	*Ricinus communis*	255557040
Conserved hypothetical protein	*Ricinus communis*	255565071
Aerolysin/hemolysin/leukocidin toxin	*Shewanella baltica*	153000088
Pore-forming toxin-like protein Hfr-2	*Triticum aestivum*	57233444
hypothetical protein VIBC2010_03220	*Vibrio caribbenthicus*	312885265
Hypothetical protein VIBC2010_07664	*Vibrio caribbenthicus*	312883148
Hypothetical protein VIC_000420	*Vibrio coralliilyticus*	260775048
Pre-provibrioaerolysin	*Vibrio harveyi*	153831849
Hypothetical protein VINI7043_24062	*Vibrio nigripulchritudo*	343495132
hypothetical protein V12B01_24484	*Vibrio splendidus*	84387032
Hypothetical protein VITISV_020655	*Vitis vinifera*	147838248
Uncharacterized protein LOC100256767	*Vitis vinifera*	225465417
Uncharacterized protein LOC100251726	*Vitis vinifera*	225465423
Uncharacterized protein LOC100194135	*Zea mays*	212722702
Uncharacterized protein LOC100275466	*Zea mays*	226531001

doi:10.1371/journal.ppat.1003216.t001

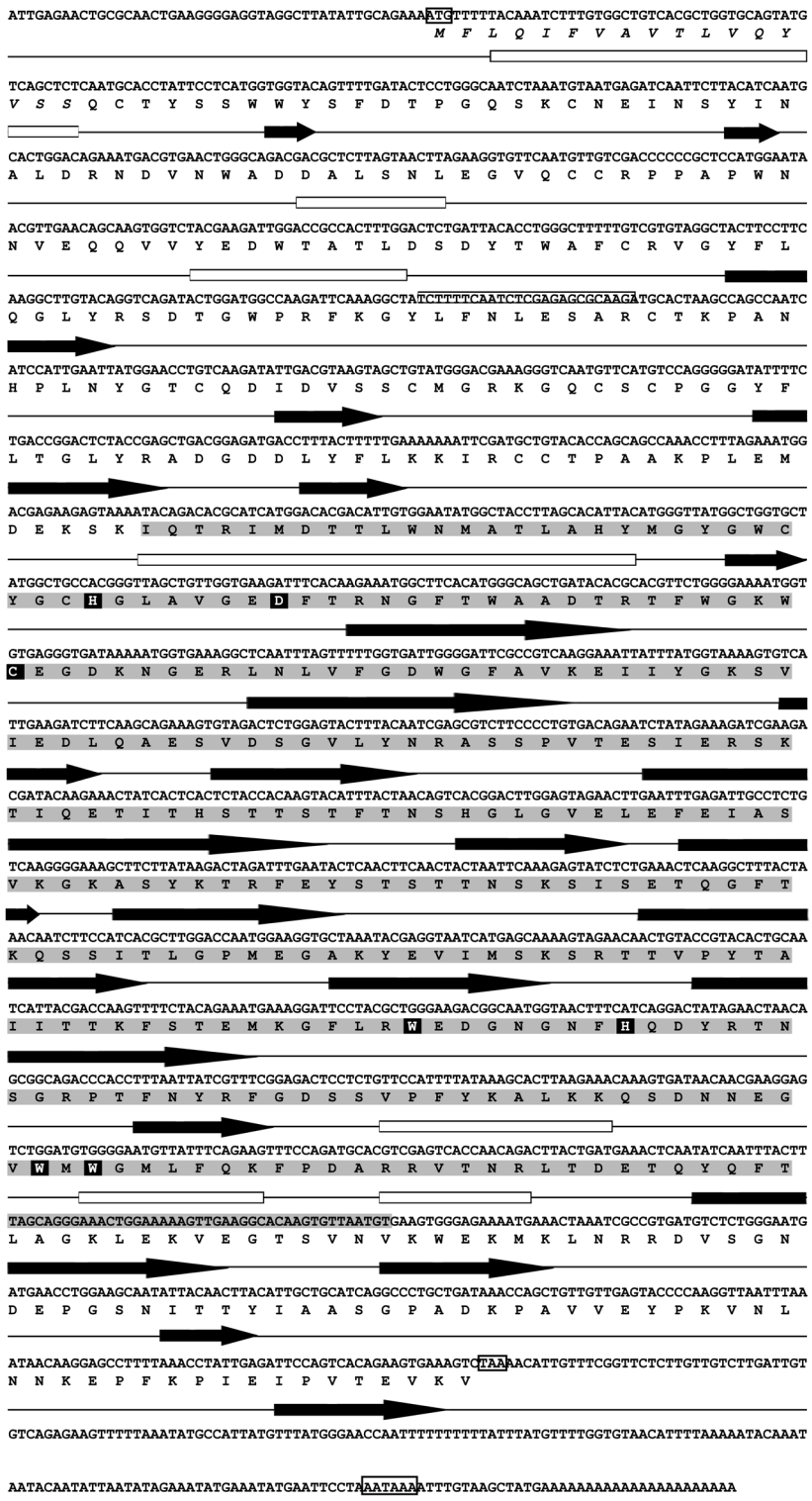

Figure 1. Full-length cDNA sequence and predicted amino acid sequence of Biomphalysin. The nucleotide sequence of Biomphalysin is shown with the initiation codon (ATG), terminator codon (TAA), and polyadenylation sites (AATAAA) boxed. For the protein sequence, italics are used to denote the putative signal peptide and the grey shadow region indicates the aerolysin domain signature. Amino acid residues crucial for oligomerization and those involved in cytolytic activity are in white on a black background. The positions of secondary structure elements were predicted using the Jpred3 server; α-helices are indicated by white rectangles and β-strands are depicted as black arrows.
doi:10.1371/journal.ppat.1003216.g001

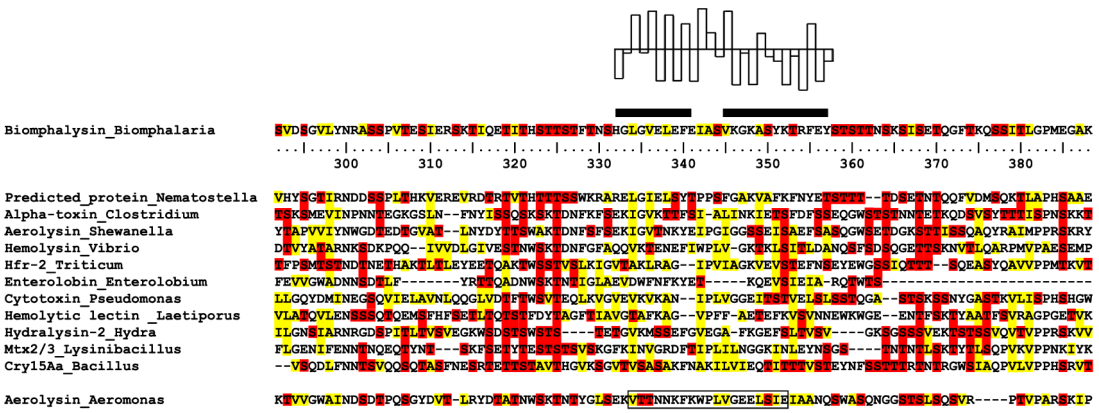

Figure 2. Identification of the Biomphalysin TMD, a conserved feature of the β-PFT family. Multiple alignments of aerolysin-like proteins were performed using the HHpred server. The UniProt accession numbers of the selected β-pore forming toxins are as follows: *N. vectensis*, A7RL10; *Clostridium botulinum*, C6DXY7; *Shewanella baltica*, A3D2W6; *Vibrio sp.*, A8T2E9; *A. hydrophila*, Q8RN77; *Triticum aestivum*, Q4JEV5; *E. contortisiliquum*, P81007; *Pseudomonas aeruginosa*, P14608; *Laetiporus sulphureus*, Q7Z8V0; *H. viridissima*, Q564A5; *Lysinibacillus sphaericus*, Q45471; *B. thuringiensis*, Q45729. The TMD, outlined in black, was predicted using the PRED-TMBB server (PREDiction of TransMembrane Beta Barrels proteins). The TMD is flanked by two hydrophilic regions; serine and threonine residues in these regions are shown in red. Hydrophobic residues (valine, leucine, isoleucine, and alanine) are shown in yellow. The putative TMD defined according to [40] is boxed. A hydropathy plot of the predicted TMD, according the hydrophobicity scale of Kyte and Doolittle [85], is indicated above the amino acid sequence.
doi:10.1371/journal.ppat.1003216.g002

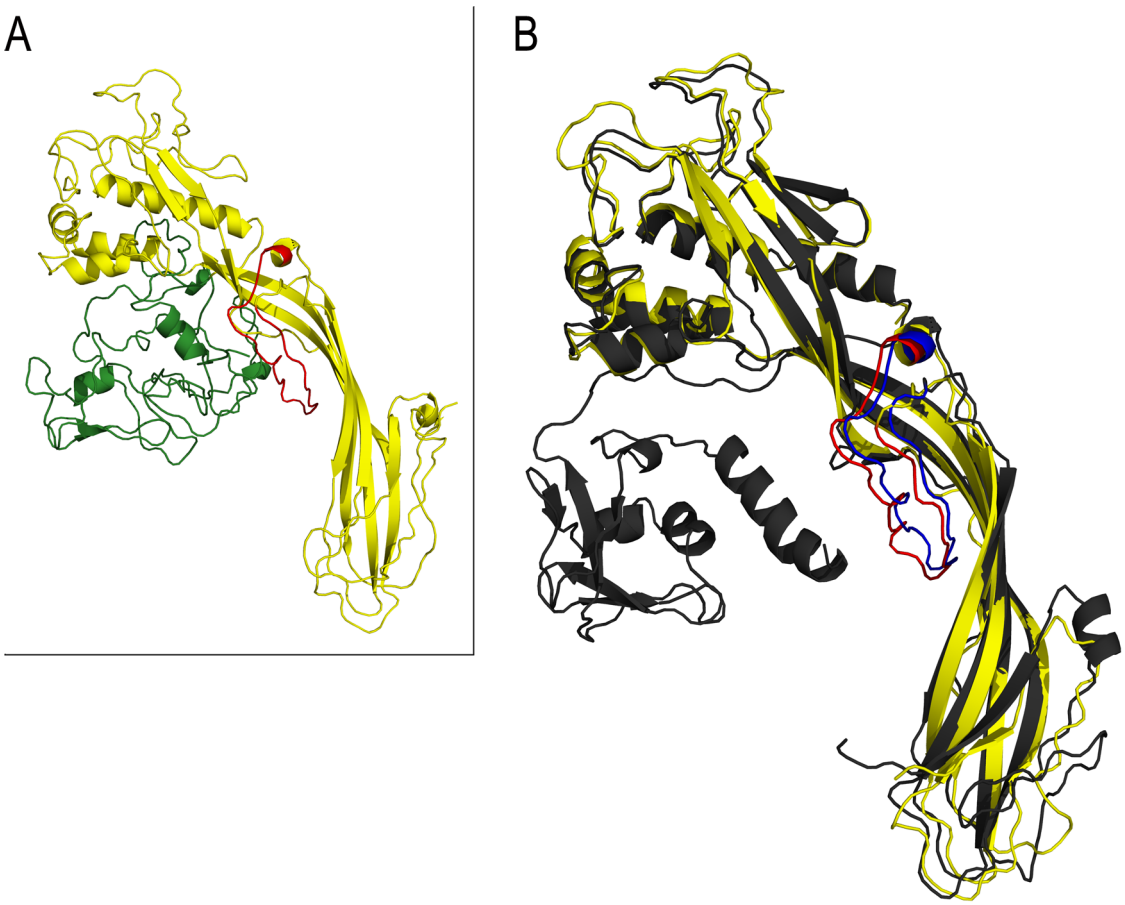

Figure 3. Structural alignment between the aerolysin domain of Biomphalysin and proaerolysin protein. A. Biomphalysin structure prediction. Biomphalysin and its aerolysin domain 3D structures were predicted by the I Tasser server. The quality of both predictions was estimated by calculating C-scores for the 3D structures of Biomphalysin (−0.5) and the aerolysin domain (1.5). The Biomphalysin protein is composed of two lobes: a small lobe (green) and a large lobe (yellow). The TMD predicted by PREDD TMBB software is shown in red. B. Structural comparison of the aerolysin domain of Biomphalysin (yellow) and the crystal structure of proaerolysin (PDB accession number 1Z52) template (grey). The proaerolysin TMD is shown in blue. The TMD predicted for the Biomphalysin is shown in red. A TM score of 0.92 was obtained over 372 aligned amino acids. All pictures were generated by PyMOLWin.
doi:10.1371/journal.ppat.1003216.g003

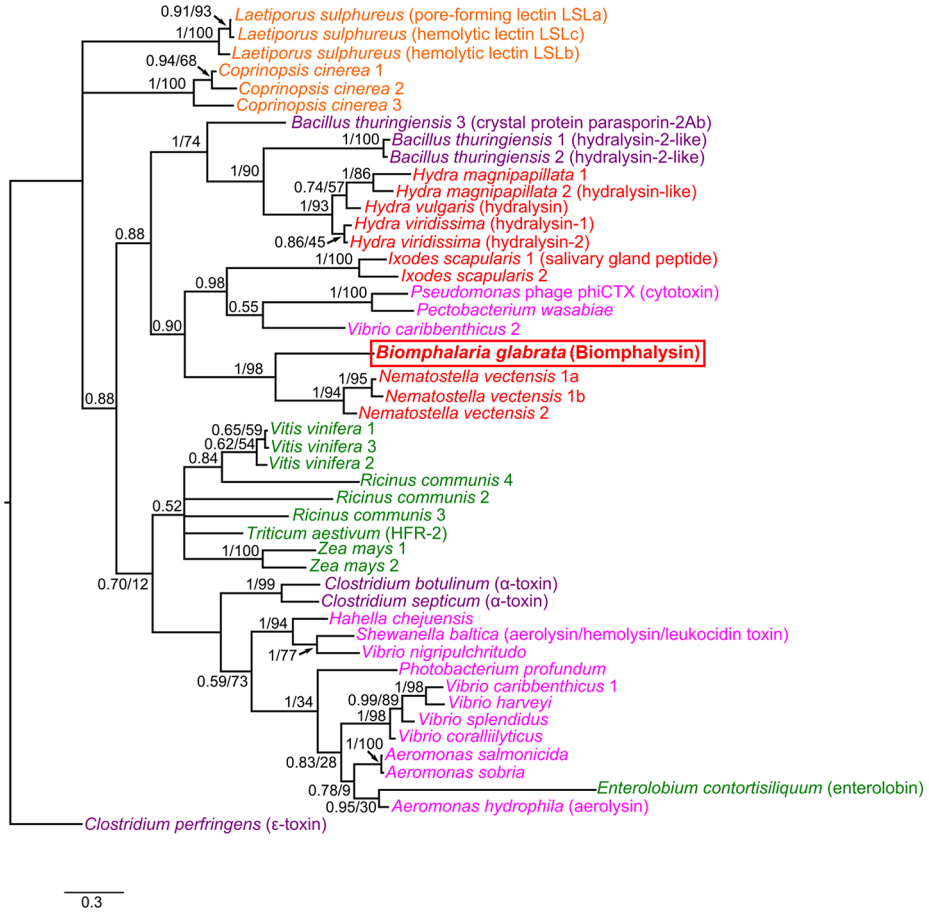

Figure 4. Phylogenetic tree of aerolysin-like molecules. The phylogenetic tree of aerolysin-like molecules is shown, with values of posterior probabilities and bootstraps for both Bayesian and ML analyses indicated at each node. Only the Bayesian tree is represented here, but both Bayesian and ML analyses produced trees with similar topologies. Aerolysin-like sequences from animals are represented in red, those from plant in green, those from fungi in dark red, those from Gammaproteobacteria in pink, and those from Firmicutes in purple. The sequence of ε-toxin from *C. perfringens* was used to root the tree. The scale bar corresponds to 0.3 estimated amino-acid substitutions per site.
doi:10.1371/journal.ppat.1003216.g004

models with a C-score greater than −1.5 are predictive of correct folding. We obtained a C-score of −0.5 for Biomphalysin protein and 1.5 for its aerolysin domain, values that satisfy this acceptability criterion. Structural similarities between the functional domain of aerolysin and Biomphalysin were determined by calculating a TM-score. A TM-score greater than 0.5 reveals significant alignment, whereas a TM-score less than 0.17 indicates random similarity.

Phylogenetic analysis

To investigate the phylogenetic position of Biomphalysin, we retrieved sequences of aerolysin homologues from a recent study [71]. Forty-seven sequences (Table 1) from organisms belonging to animal, plant, fungi, and bacterial kingdoms were used to construct a phylogenetic tree. Selected sequences were then aligned using the MUSCLE algorithm implemented in CLC Sequence DNA Workbench 6.6.2 software (CLC bio). Poorly aligned regions were trimmed using trimAl v1.4 with *automated1* option [72]. Phylogenetic analyses were performed using Bayesian and maximum-likelihood (ML) inferences. ProtTest v3.2 was used to select the model of protein evolution (amino acids substitution) that best fit the multiple sequence alignment [73]. The WAG+F model was selected. A Bayesian analysis was performed using MrBayes 3.2.1 [74] with 1,500,000 generations. We estimated that the analysis reached convergence when the average standard deviation of split frequencies between the two runs was less than 0.01 and the potential scale reduction factor reached 1.0 (burn-in = 3750). The robustness of the nodes was evaluated using the Bayesian posterior probabilities. A maximum likelihood analysis was also performed on the same alignment using PhyML 3.0 [75]. The reliability of the nodes was tested using a bootstrap test (100 replicates). Finally, the tree was edited using FigTree v1.3.1 (http://tree.bio.ed.ac.uk).

Accession number

Nucleotide sequence data reported in this paper are available in the GenBank database under the accession number KC012466

Results

Molecular characterization of Biomphalysin

In a previous study designed to characterize the interactome between *B. glabrata* plasma and *S. mansoni* primary sporocyst extracts, we identified a partial coding sequence corresponding to a new, putative cytolytic protein from *B. glabrata* [30]. Because of its similarities to proteins of the β-PFTs superfamily, the corresponding protein was named Biomphalysin. In the present work, we obtained a full-length cDNA clone of Biomphalysin using the RACE method

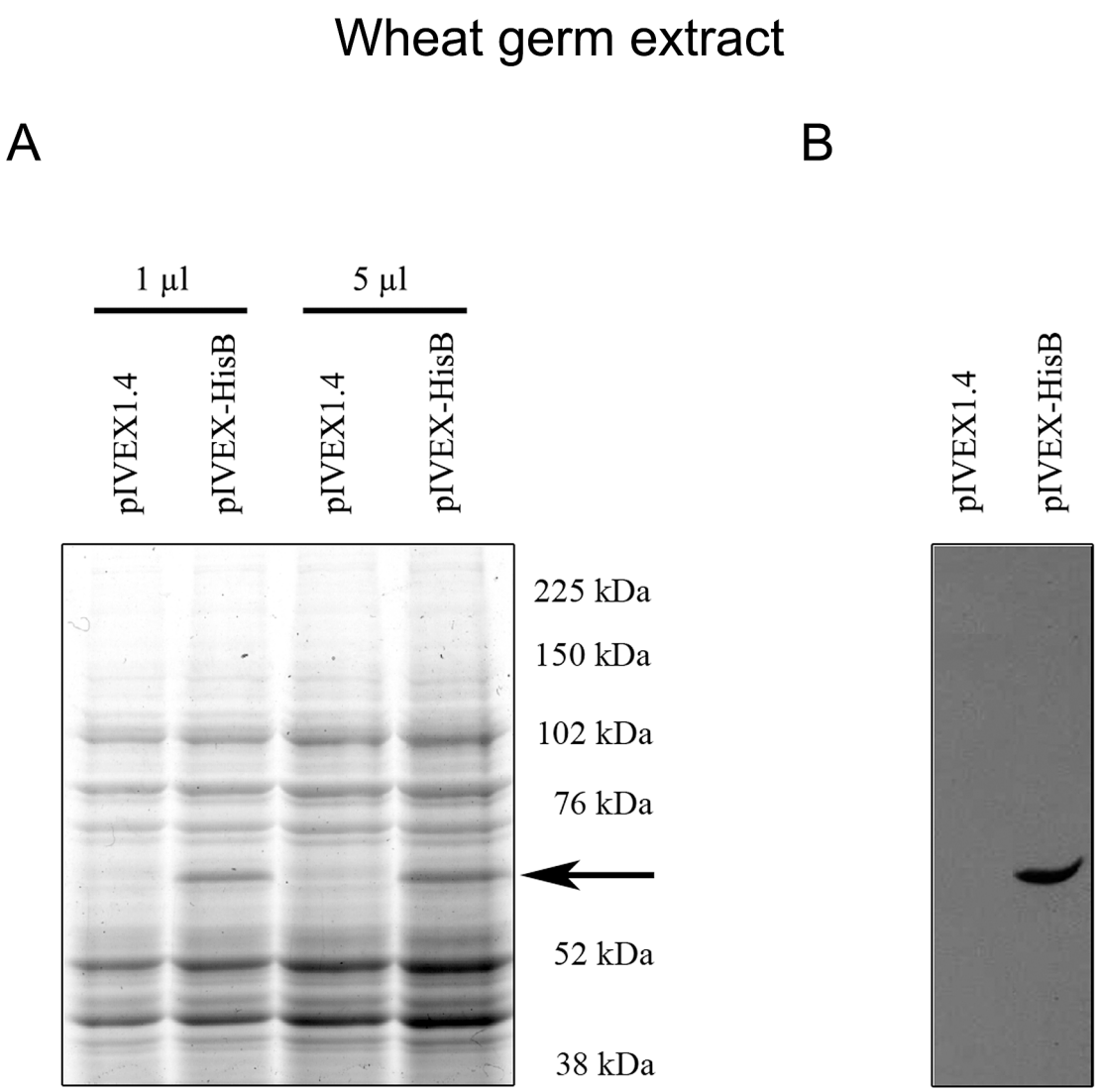

Figure 5. Analysis of rBiomphalysin expressed *in vitro* using wheat germ extracts (RTS 500). A. The amount of rBiomphalysin production was assessed by comparing the RTS 500 His-tagged Biomphalysin reaction (lanes 2 and 4) with 1 and 5 µl of RTS 500 control reactions (lanes 1 and 3) in Coomassie blue-stained, 12% SDS-PAGE gels. Values on the right indicate the masses of the molecular weight markers, whereas the arrow indicates the position of the His-tagged Biomphalysin band (lanes 2 and 4). B. Western blot analysis of RTS 500 control (lane 1) and Biomphalysin (lane 2) reactions. Five microliters of each reaction were separated by SDS-PAGE on a 12% gel and then electrotransferred onto a nitrocellulose membrane. The membrane was then incubated sequentially with a monoclonal anti-His_6 antibody and a goat anti-mouse IgG, and immunoreactive proteins were visualized by ECL.
doi:10.1371/journal.ppat.1003216.g005

(Figure 1). The complete sequence is 1972 base pairs (bp) in length and displays a 5′-untranslated region (UTR) of 47 bp, a 3′-UTR of 206 bp, and an open reading frame (ORF) of 1719 bp (GenBank accession number : KC012466). The ORF encodes a precursor protein of 572 amino acid residues, of which the first 17 amino acids correspond to a putative signal peptide, as predicted by the SignalP program. After signal peptide removal, Biomphalysin displayed a theoretical pI of 6.2 and predicted molecular weight of 62.8 kDa. An analysis of putative post-translational modifications using the NetOglyc and NetNglyc server suggested the absence of O-glycosylation and a putative N-glycosylation event at N_{530}. A BLASTP similarity analysis revealed significant similarities with members of the β-PFT superfamily, including aerolysin-like proteins. The most closely related sequence was a hypothetical protein from *Nematostella vectensis* (XP_001629482) with 55% similarity and 39% identity (E-value = 2×10^{-123}). An analysis with the SMART and MotifScan programs revealed an aerolysin signature (pfam 01117) at residues 178–525 of Biomphalysin (E-value = 1.3×10^{-43}). HHpred (homology detection and structure prediction by HMM-HMM comparison) software predicted a high structural homology with the pore-forming lobe of aerolysin (E-value = 1×10^{-89}) and a high proportion of β sheets (31%). Members of the aerolysin-like protein family are virulence factors belonging to the superfamily of β pore-forming toxins produced and secreted predominantly by Gram-positive and -negative bacteria [40,76]. They exert cytolytic activity triggered by channel formation in target cell membranes through insertion of β-hairpins, which form a β-barrel pore [48]. The formation of this pore requires a proteolytic cleavage event and the presence of the pore-forming transmembrane domain (TMD). Despite the poor level of similarity at the amino acid level, a putative TMD (from His_{332} to Tyr_{357}) corresponding to an amphipathic sequence involved in the

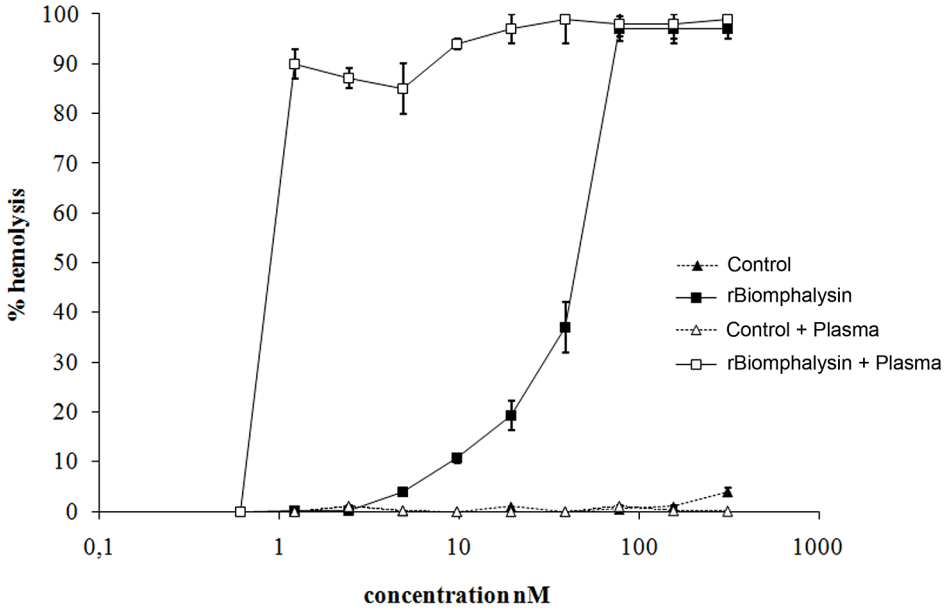

Figure 6. rBiomphalysin hemolytic activity. Different concentrations of rBiomphalysin, prepared by serial dilution of the Biomphalysin RTS 500 reaction, were tested for hemolytic activity towards sheep erythrocytes. The RTS 500 control reaction (WGE) was used as a negative control, and a 10% Triton-X100 solution was used as a positive control. The hemolytic activity of RTS 500 reactions was assessed in the presence or absence of *B. glabrata* plasma. The hemolytic activity of rBiomphalysin without and with plasma is shown by full and empty squares, respectively; full and empty triangles denote the corresponding activity for the negative control reaction without and with plasma. Hemolytic assay was performed with three replicates and error bars represent SD.
doi:10.1371/journal.ppat.1003216.g006

formation of membrane-inserted β barrels was clearly identified (Figure 2). This membrane-spanning domain was flanked by two hydrophilic regions, a feature shared by members of the aerolysin toxin family, like *cnidarian* hydralysins [45], *C. perfringens* α toxin [77], and *Aeromonas hydrophila* proaerolysin [55,78]. A number of studies have identified several key amino acids that are involved in pore formation through oligomerization of β-PFT or that contribute to cytolytic activity. These critical residues are conserved in the Biomphalysin amino acid sequence, and include His_{228}, Asp_{235} and $Cystein_{255}$, which play a crucial role in oligomerization of the heptameric ring [79,80,81]; $Tryp_{466}$ and $Tryp_{468}$, which are involved in membrane penetration, as evidenced by reduced efficiency of pore formation in proteins mutated at these residues [82]; and $Tryp_{420}$ and His_{428}, which are involved in binding of the proaerolysin to its membrane receptor. In addition, as the proaerolysin cytolytic toxin, the Biomphalysin protein displayed two distinct lobes (Figure 3A). A 3D alignment of the aerolysin domain of Biomphalysin with the proaerolysin template was performed using I-Tasser and TM-align servers. This latter analysis revealed a high degree of similarity between the two structures (TM-score = 0.92; Figure 3B). Despite these structural similarities, neither C-type lectin motifs nor a cleavage site were found using motif prediction software [50,83]. Biomphalysin displays a structural feature that distinguishes it from other β-PFTs. Indeed, Biomphalysin possesses a second lobe which displays no lectin-like domain as it has been reported for aerolysin [50].

A phylogenetic tree was subsequently constructed using 46 sequences of aerolysin-like toxins from different kingdoms (Table I). As expected, the Biomphalysin sequence in this tree appeared to be closely related to a predicted, uncharacterized protein identified in the cnidarian, *N. vectensis* (Figure 4). Curiously, and as also described by another phylogenetic study on β-PFTs [71], this tree comprises several monophyletic groups that contain both eumetazoa and bacteria. This taxonomic distribution suggests that the Biomphalysin gene was probably horizontally transferred several times from bacteria to eumetazoa.

Together, these data strongly suggest that Biomphalysin could be a cytolytic protein related to the β-PFT superfamily.

Biomphalysin hemolytic activity

Most aerolysins characterized to date display potent hemolytic activity. In order to investigate the cytolytic capacity of Biomphalysin, we produced a recombinant protein flanked by an N-terminal hexa-histidine tag. We encountered some difficulties in producing recombinant Biomphalysin (rBiomphalysin) in our bacteria system. We tested different bacterial strains, including *Escherichia coli* BL21 (DE3); BL21 (DE3) pLysE; and BL21(DE3) CodonPlus, Rosetta (with and without classical chaperone expression.). With most of these systems, we obtained a low production level or a cleaved protein (data not shown). Consequently, we decided to produce the rBiomphalysin using an *in vitro* recombinant expression system based on wheat germ extract and cell free transcription and translation system (RTS). Expression of the rBiomphalysin was confirmed by Coomassie blue stained SDS-PAGE (Figure 5A) and by Western blot using an anti-His antibody (Figure 5B) that revealed a tagged protein with the expected size. Wheat germ extract containing rBiomphalysin and wheat germ extract alone used as negative control were tested for haemolytic activity toward sheep red blood cells in presence or absence of snail plasma. Hemolysis was observed for the WGE containing rBiomphalysin in presence or in absence of plasma (Figure 6). The rBiomphalysin concentration necessary for 50% lysis (Ha_{50}) under plasma-free conditions was much higher (50 nM) than that required when rBiomphalysin (1 nM) was incubated with ultra-centrifuged plasma, suggesting that a cofactor present in plasma enhanced the cytolytic effect of Biomphalysin.

rBiomphalysin anti-schistosomal activity

We next investigated Biomphalysin activity on intra molluscan stages of *S. mansoni* (primary sporocysts). To accomplish this, we treated an *in vitro* culture of primary sporocysts with 30 nM rBiomphalysin with or without *B. glabrata* plasma. Motility and beating of flame-cell flagella were assessed every hour during the first 9 h after initiating treatment to distinguish live and dead parasites. Exposure of sporocysts to *B. glabrata* plasma alone or WGE (without rBiomphalysin) or both produced no obvious morphological alterations. After 9 h of treatment with any combination of control conditions, a maximum of 20% of sporocysts died (Figure 7A). No differences were evident between larvae exposed to rBiomphalysin alone and those in various control groups. However, the combination of rBiomphalysin and *B. glabrata* plasma clearly enhanced parasite mortality. We found that parasites died faster: 35% ($p<0.05$, Fisher's exact test) were dead in less than 1 h; at the final time point, 50% of the parasites were dead (Figure 7A). The statistical significance of this result was investigated and confirmed using the Kaplan-Meier test ($p = 0.004$). A microscopic examination of the effects of rBiomphalysin plus *B. glabrata* plasma revealed severe tegumental alterations of *S. mansoni* sporocysts, with evidence of swollen cells sprouting from larvae, darkened and granular bodies and, ultimately, parasite disintegration (Figure 7B).

Because members of the aerolysin family are known to interact with cell membranes of targeted cells, we assessed binding of rBiomphalysin to sporocysts with or without *B. glabrata* plasma using *in vitro* binding assays and analyzed these assays by Western blotting and immunocytochemistry. Immunocytochemistry clearly showed that rBiomphalysin is able to interact with the parasite tegument, an interaction that is not plasma-dependent (Figures 8 and 9). In addition, we observed a heterogeneous staining pattern composed of dots or aggregates in the membrane (Figure 8) similar to that reported in previous studies on hydralysins [45] and proaerolysin [49].

Analysis of Biomphalysin mRNA expression and tissue distribution

The tissue-specific expression of Biomphalysin was investigated by RT-PCR using total RNA extracted from the albumen gland, head-foot, hepato-pancreas, ovotestis organs and hemocytes of *B. glabrata*. β-actin expression was used as a reference. Biomphalysin transcripts were detected only in hemocytes and not in other tissues tested (Figure 10A). Interestingly, Biomphalysin was also detected in cells derived from embryos of *B. glabrata* (Bge cells) maintained in culture. Considering that Bge cells are cultured under aseptic conditions, this latter observation excludes the possibility that Biomphalysin is produced by commensal bacteria present in snail tissues. No size difference was observed between PCR results obtained using genomic DNA or cDNA as a template, indicating that the Biomphalysin gene is intronless. A BLAST search against the Trace Archive Biomphalaria database confirmed the presence of this intronless gene in the snail genome. Considering the suspected anti-schistosomal role of Biomphalysin, we examined whether Biomphalysin expression was modulated by parasite challenge. In these experiments, snails were infected with *S. mansoni* miracidia and Biomphalysin transcripts were quantified by quantitative RT-PCR at different times following exposure (3, 6, 9, 12, 24, 48 and 96 h). Bge cells cultivated in the presence of *in vitro*-transformed sporocysts were also analyzed at the same time points. As shown in Figure 10B, Biomphalysin expression levels did not significantly change after *S. mansoni* challenge compared with uninfected snails or naive Bge cells. These data indicated that Biomphalysin can be considered an immunity-related gene that is constitutively expressed and is not modulated by *S. mansoni* challenge.

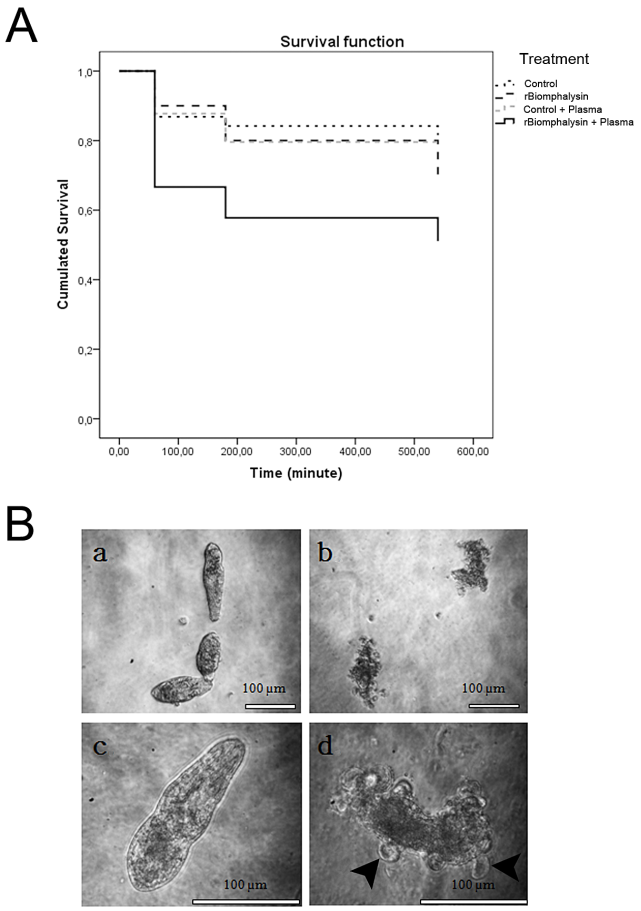

Figure 7. Cytolytic activity and *in vitro* effects of rBiomphalysin on *S. mansoni* sporocysts. A. Kaplan-Meier analysis of sporocyst treated with rBiomphalysin in the presence or absence of *B. glabrata* plasma. B. (a and c) Sporocysts treated with WGE (control). (b and d) Sporocysts treated with rBiomphalysin and plasma. Black arrows indicate swollen cells without cilia.
doi:10.1371/journal.ppat.1003216.g007

Discussion

In order to identify molecular determinants that play a key role in the interaction between *B. glabrata* and *S. mansoni*, we recently developed an interactome approach that allowed us to discover a factor in *B. glabrata* plasma related to the β-PFT superfamily. This molecule was found in the precipitate containing various molecules from *S. mansoni* (SmPoMucs, glycoprotein k, tetraspanin, chaperone stress proteins, anti-oxidant enzymes) and *B. glabrata* (FREPs, lectin like protein AIF…) [30]. In the present publication, we describe the cloning and functional characterization of this β-PFT of *B. glabrata*, which we have named Biomphalysin.

The full-length cDNA of Biomphalysin was 1972 bp encoding a 572-amino-acid protein with a molecular weight of approximately 63 kDa. Biomphalysin displays low similarities toward database β-PFTs at the primary structure level, but contains an aerolysin domain that is a common core of aerolysin-like β-PFTs [40]. Bioinformatic analysis and protein structure prediction revealed that Biomphalysin contains a large number of β-sheets and has a transmembrane β-barrel domain (Figures 1 and 2). A structural

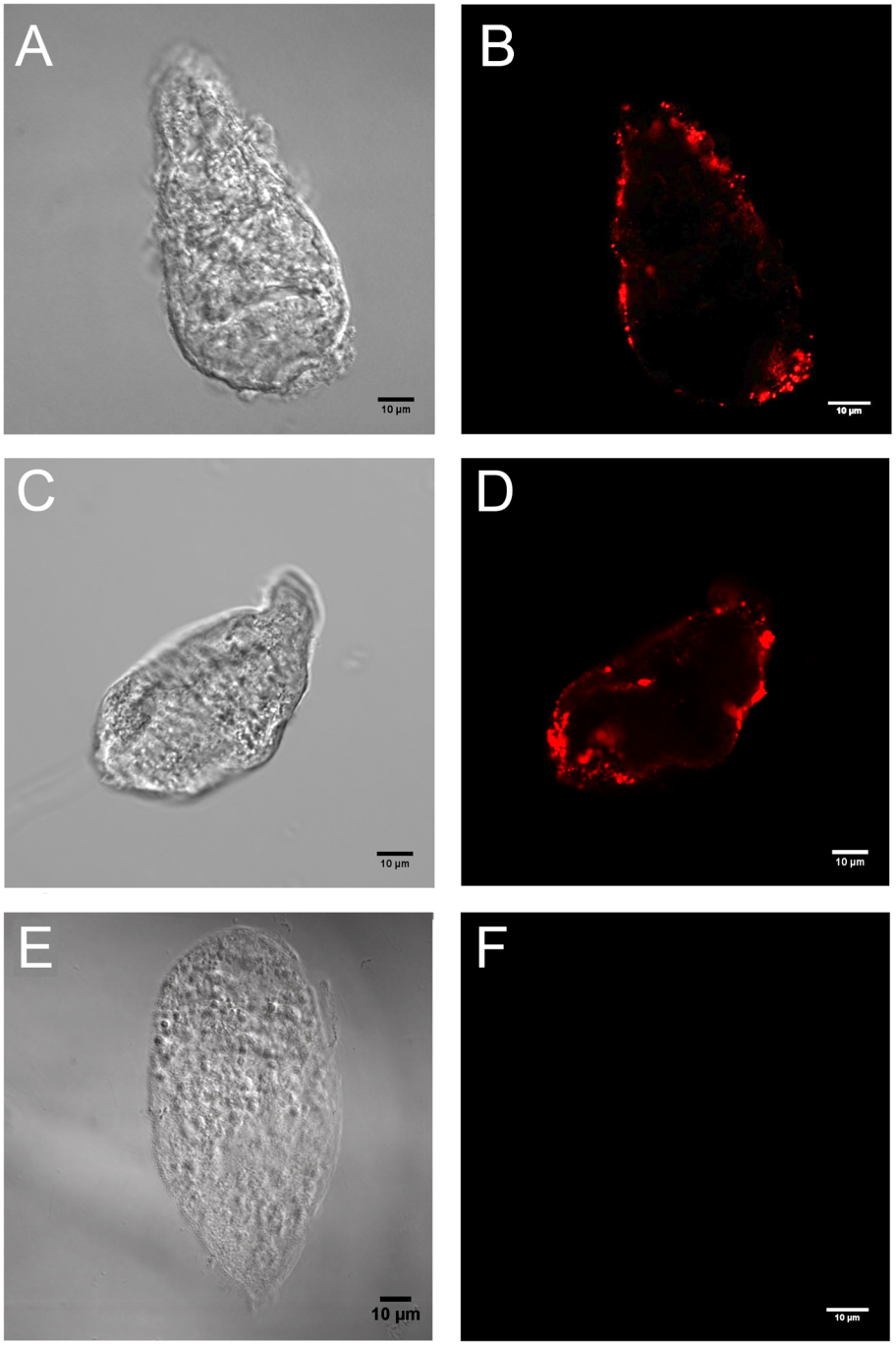

Figure 8. Immunolocalization of rBiomphalysin on *S. mansoni* sporocyst. Sporocysts were treated with rBiomphalysin in presence (A and B) or in absence (C and D) of snail plasma and immunostained using anti-His primary IgG and Alexa Fluor 594-conjugated secondary antibody. Binding of rBiomphalysin to sporocyst membranes was detected by aggregates formation on the parasite tegument in both conditions. Under the same image-acquisition conditions, no signal was detected for the negative control, consisting of incubation of sporocysts with plasma and wheat germ extract alone (E and F). A, C and E represent the image taken under Nomarski light microscopy, whereas B, D and F are the corresponding confocal fluorescent pictures.
doi:10.1371/journal.ppat.1003216.g008

alignment of the aerolysin domain of Biomphalysin with proaerolysin demonstrates structural equivalence, despite the lack of similarity at the amino acid level. Importantly, in addition to these similarities in 3D structure, several key residues involved in β barrel pore formation or receptor binding are conserved. The aerolysins and related toxin family members can be divided into two groups based on their structural shape. A few β-PFTs have two distinct lobes, whereas others, like α toxin, ε toxin and parasporin, have only a single lobe (for a review, see [42]). The common, larger lobe is involved in oligomerization or binding to GPI-anchored receptors, whereas the second, smaller lobe contains a carbohydrate receptor-binding domain. The Biompha-

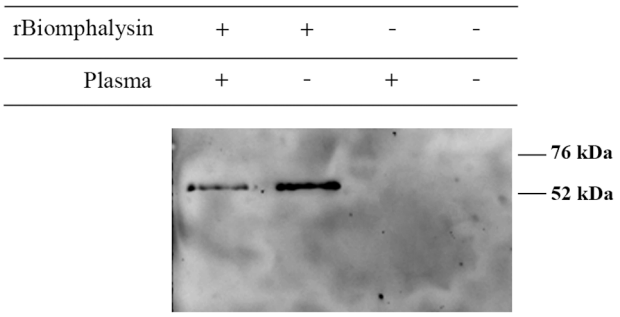

Figure 9. rBiomphalysin binding to the parasite tegument. *In vitro* binding assay was performed on primary sporocysts. rBiomphalysin binding to sporocysts membrane was tested in presence or absence of plasma from snail. After incubation, sporocysts were centrifuged, washed in CBSS, and denatured in Laemmli buffer at 80°C for 10 min. Total lysate of sporocysts were separated by SDS-PAGE and analyzed by Western blot with a monoclonal anti-His_6 antibody.
doi:10.1371/journal.ppat.1003216.g009

lysin smaller lobe, which contains no known domains and displays no identifiable sequence similarities, is an intriguing structure. We postulate that it could be involved in the specificity of Biomphalysin, allowing it to interact with sporocyst antigens or an intermediate molecular partner in *B. glabrata* plasma. Additional studies will be required to address this hypothesis. Interestingly, the phylogenetic tree of aerolysin-like molecules (Figure 4) suggests that Biomphalysin could have been transferred horizontally from bacteria to *B. glabrata*. This hypothesis is strengthened by a recent phylogenetic analysis showing that numerous cross-kingdom horizontal transfers occurred for genes encoding aerolysin-like proteins [71]. We showed that the gene encoding Biomphalysin does not possess intronic regions (Figure 10A), which also argues in favor of a horizontal transfer mechanism. The exclusive expression of Biomphalysin in hemocytes, the immune cells of *B. glabrata*, consolidates the role of Biomphalysin in immunity. Nevertheless, its expression is constitutive and is not modulated by Schistosome

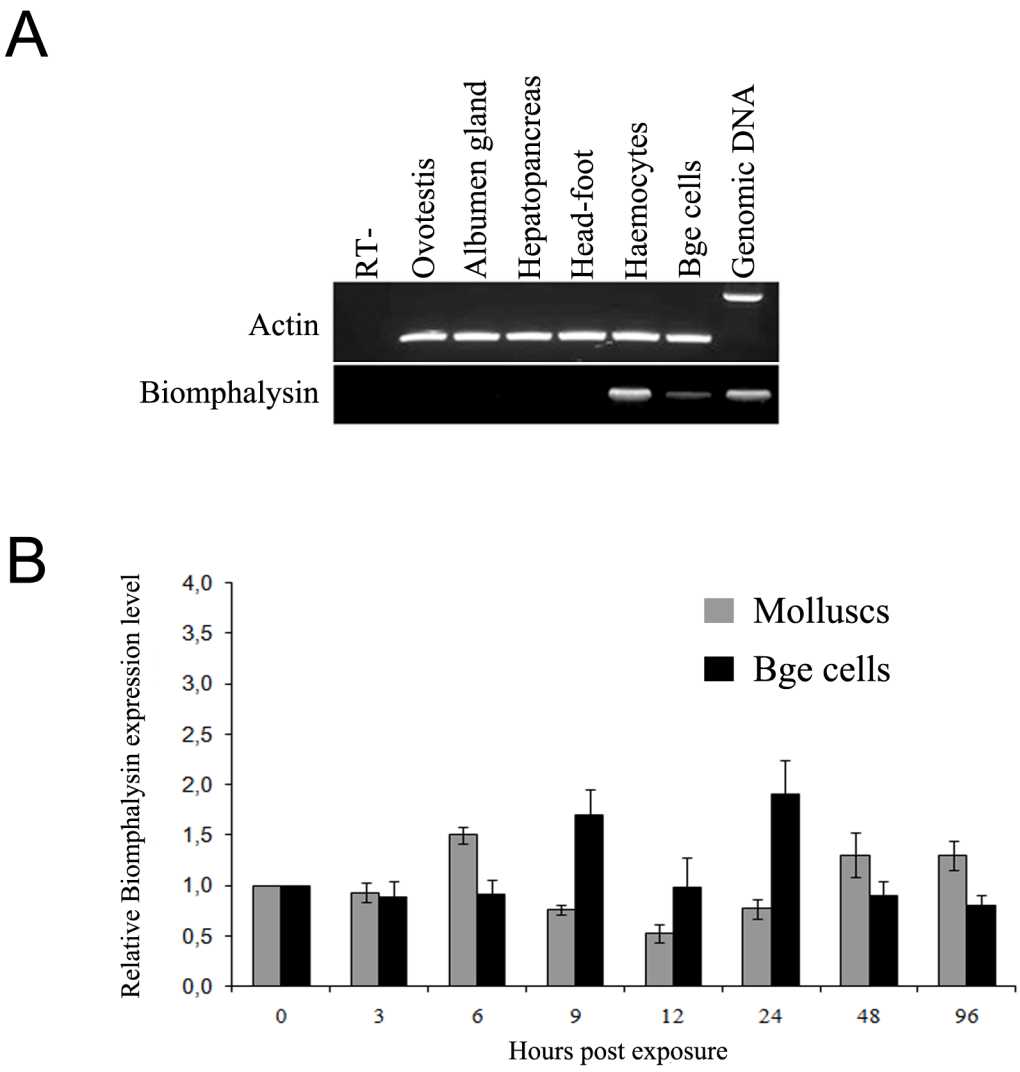

Figure 10. Biomphalysin mRNA tissue distribution and expression in *B. glabrata* in response to *S. mansoni* challenge and in Bge cells in contact with sporocysts. A. Different *B. glabrata* tissues were analyzed by PCR using primers recognizing full-length Biomphalysin; actin was amplified as an endogenous control. Non-reverse transcribed hemocyte RNA was used as a negative control in PCR. B. Biomphalysin transcripts were quantified by Q-PCR in *B. glabrata* challenged with *S. mansoni* for 3, 6, 9, 12, 24, 48 and 96 h and in Bge cells in contact with sporocysts for the same intervals. Biomphalysin mRNA level was normalized to mRNA ribosomal protein S19 transcript abundance using the Roche Applied Science E-method [86]. For graphical representation, the transcription ratio for each challenge was normalized to that obtained for unchallenged snails. Each histogram represents the average value of triplicate experiments ± SD.
doi:10.1371/journal.ppat.1003216.g010

infection. Biomphalysin protein was detected in the plasma of uninfected snails and was shown to interact *in vitro* with parasite proteins, suggesting a sentinel role in preventing pathogen invasion [30].

To further characterize Biomphalysin and validate its biological function, we expressed rBiomphalysin using a cell-free protein expression system, a strategy that seems justifiable in view of the lack of predicted glycosylation events during Biomphalysin processing. As described for most toxins related to the aerolysin family, Biomphalysin possessed hemolytic activity. This activity was detectable at 5 nM Biomphalysin and caused complete erythrocyte lysis at a concentration of 90 nM. Surprisingly, co-incubation with *B. glabrata* plasma greatly enhanced the lytic activity of Biomphalysin, enabling 50-fold less recombinant protein to achieve the same activity level. This intriguing result suggests that one or more plasma factors could act on the maturation of Biomphalysin through proteolytic cleavage or by affecting its capacity to bind the target cell membrane. To understand how such cofactor(s) might mediate or enhance Biomphalysin activity, we performed Biomphalysin–sporocyst binding assays in the presence or absence of *B. glabrata* plasma. Analyses of these assays by Western blotting and immunocytochemistry revealed that Biomphalysin binds to the sporocyst membrane in the absence of plasma; moreover, there was no evidence of any cleavage products (Figures 8 and 9). Consistent with this latter observation, an exhaustive analysis of putative cleavage sites failed to detect such a site in the C-terminal region of Biomphalysin. Although the cytolytic effect of most of aerolysin toxins requires proteolytic activation, a similar lack of a proteolytic processing has been previously reported for hydralysin, a cnidarian hemolytic β-PFT [45]. Our results suggest that a plasma factor induces Biomphalysin activity by mediating the conversion of the oligomeric prepore to a functional pore. Thus, this plasma factor could be a chaperone, a type of functional activation that has been described in other models. For example, it has been shown *in vitro* that the prepore-to-pore transition of anthrax toxin is enhanced by an exogenous chaperone, such as GroEL [84]. We speculate that the small lobe of aerolysin could serve as "bait" to recruit the Biomphalysin activity-inducing factor, which remains to be identified. Further investigation is warranted to elucidate the role of the Biomphalysin small lobe.

In conclusion, this report is the first to characterize a mollusk β-PFT that displays antiparasitic activity. This novel β-PFT, which we have named Biomphalysin to reflect its source, shares structural features and activity with aerolysin-like toxins described in numerous bacteria species. The corresponding gene was probably acquired by horizontal transfer, and the cytolytic activity of Biomphalysin is mediated by a plasma factor that remains to be identified.

Acknowledgments

We thank Anne Rognon and Nathalie Arancibia for technical assistance. We thank all team members for their advice and fruitful discussions. We thank Jérome Boissier for his help with statistical procedures.

Author Contributions

Conceived and designed the experiments: RG JP DD. Performed the experiments: RG JP DD. Analyzed the data: BG DD. Contributed reagents/materials/analysis tools: RG JP YM JFA HH SD. Wrote the paper: GM BG DD.

References

1. Doenhoff MJ, Kusel JR, Coles GC, Cioli D (2002) Resistance of Schistosoma mansoni to praziquantel: is there a problem? Trans R Soc Trop Med Hyg 96: 465–469.
2. Melman SD, Steinauer ML, Cunningham C, Kubatko LS, Mwangi IN, et al. (2009) Reduced susceptibility to praziquantel among naturally occurring Kenyan isolates of Schistosoma mansoni. PLoS Negl Trop Dis 3: e504.
3. Adema CM, Hertel LA, Miller RD, Loker ES (1997) A family of fibrinogen-related proteins that precipitates parasite-derived molecules is produced by an invertebrate after infection. Proc Natl Acad Sci U S A 94: 8691–8696.
4. Loker ES, Adema CM, Zhang SM, Kepler TB (2004) Invertebrate immune systems–not homogeneous, not simple, not well understood. Immunol Rev 198: 10–24.
5. Hanington PC, Forys MA, Dragoo JW, Zhang SM, Adema CM, et al. (2011) Role for a somatically diversified lectin in resistance of an invertebrate to parasite infection. Proc Natl Acad Sci U S A 107: 21087–21092.
6. Baeza Garcia A, Pierce RJ, Gourbal B, Werkmeister E, Colinet D, et al. (2010) Involvement of the cytokine MIF in the snail host immune response to the parasite Schistosoma mansoni. PLoS Pathog 6(9): e1001115. doi:10.1371/journal.ppat.1001115
7. Deleury E, Dubreuil G, Elangovan N, Wajnberg E, Reichhart JM, et al. (2012) Specific versus non-specific immune responses in an invertebrate species evidenced by a comparative de novo sequencing study. PLoS One 7: e32512.
8. Guillou F, Mitta G, Galinier R, Coustau C (2007) Identification and expression of gene transcripts generated during an anti-parasitic response in Biomphalaria glabrata. Dev Comp Immunol 31: 657–671.
9. Ittiprasert W, Miller A, Myers J, Nene V, El-Sayed NM, et al. (2010) Identification of immediate response genes dominantly expressed in juvenile resistant and susceptible Biomphalaria glabrata snails upon exposure to Schistosoma mansoni. Mol Biochem Parasitol 169: 27–39.
10. Raghavan N, Miller AN, Gardner M, FitzGerald PC, Kerlavage AR, et al. (2003) Comparative gene analysis of Biomphalaria glabrata hemocytes pre- and post-exposure to miracidia of Schistosoma mansoni. Mol Biochem Parasitol 126: 181–191.
11. Lockyer AE, Spinks JN, Walker AJ, Kane RA, Noble LR, et al. (2007) Biomphalaria glabrata transcriptome: identification of cell-signalling, transcriptional control and immune-related genes from open reading frame expressed sequence tags (ORESTES). Dev Comp Immunol 31: 763–782.
12. Nowak TS, Woodards AC, Jung Y, Adema CM, Loker ES (2004) Identification of transcripts generated during the response of resistant Biomphalaria glabrata to Schistosoma mansoni infection using suppression subtractive hybridization. J Parasitol 90: 1034–1040.
13. Bouchut A, Coustau C, Gourbal B, Mitta G (2007) Compatibility in the Biomphalaria glabrata/Echinostoma caproni model: new candidate genes evidenced by a suppressive subtractive hybridization approach. Parasitology 134: 575–588.
14. Bouchut A, Roger E, Coustau C, Gourbal B, Mitta G (2006) Compatibility in the Biomphalaria glabrata/Echinostoma caproni model: potential involvement of adhesion genes. Int J Parasitol 36: 175–184.
15. Bouchut A, Sautiere PE, Coustau C, Mitta G (2006) Compatibility in the *Biomphalaria glabrata/Echinostoma caproni* model: Potential involvement of proteins from hemocytes revealed by a proteomic approach. Acta Tropica 98: 234–246.
16. Lockyer AE, Spinks J, Kane RA, Hoffmann KF, Fitzpatrick JM, et al. (2008) Biomphalaria glabrata transcriptome: cDNA microarray profiling identifies resistant- and susceptible-specific gene expression in haemocytes from snail strains exposed to Schistosoma mansoni. BMC Genomics 9: 634.
17. Vergote D, Bouchut A, Sautiere PE, Roger E, Galinier R, et al. (2005) Characterisation of proteins differentially present in the plasma of *Biomphalaria glabrata* susceptible or resistant to *Echinostoma caproni*. Int J Parasitol 35: 215–224.
18. Roger E, Gourbal B, Grunau C, Pierce RJ, Galinier R, et al. (2008) Expression analysis of highly polymorphic mucin proteins (Sm PoMuc) from the parasite Schistosoma mansoni. Mol Biochem Parasitol 157: 217–227.
19. Roger E, Grunau C, Pierce RJ, Hirai H, Gourbal B, et al. (2008) Controlled Chaos of Polymorphic Mucins in a Metazoan Parasite (Schistosoma mansoni) Interacting with Its Invertebrate Host (Biomphalaria glabrata). PLoS Negl Trop Dis 2: e330.
20. Roger E, Mitta G, Mone Y, Bouchut A, Rognon A, et al. (2008) Molecular determinants of compatibility polymorphism in the Biomphalaria glabrata/Schistosoma mansoni model: New candidates identified by a global comparative proteomics approach. Mol Biochem Parasitol 157: 205–216.
21. Mone Y, Gourbal B, Duval D, Du Pasquier L, Kieffer-Jaquinod S, et al. (2010) A large repertoire of parasite epitopes matched by a large repertoire of host immune receptors in an invertebrate host/parasite model. PLoS Negl Trop Dis 4.
22. Mitta G, Adema CM, Gourbal B, Loker ES, Theron A (2012) Compatibility polymorphism in snail/schistosome interactions: From field to theory to molecular mechanisms. Developmental & Comparative Immunology 37: 1–8.
23. Hahn UK, Bender RC, Bayne CJ (2000) Production of reactive oxygen species by hemocytes of Biomphalaria glabrata: carbohydrate-specific stimulation. Dev Comp Immunol 24: 531–541.
24. Hahn UK, Bender RC, Bayne CJ (2001) Killing of Schistosoma mansoni sporocysts by hemocytes from resistant Biomphalaria glabrata: role of reactive oxygen species. J Parasitol 87: 292–299.

25. Bender RC, Broderick EJ, Goodall CP, Bayne CJ (2005) Respiratory burst of *Biomphalaria glabrata* hemocytes: *Schistosoma mansoni*-resistant snails produce more extracellular H2O2 than susceptible snails. J Parasitol 91: 275–279.
26. Bender RC, Goodall CP, Blouin MS, Bayne CJ (2007) Variation in expression of Biomphalaria glabrata SOD1: a potential controlling factor in susceptibility/resistance to Schistosoma mansoni. Dev Comp Immunol 31: 874–878.
27. Goodall CP, Bender RC, Broderick EJ, Bayne CJ (2004) Constitutive differences in Cu/Zn superoxide dismutase mRNA levels and activity in hemocytes of *Biomphalaria glabrata* (Mollusca) that are either susceptible or resistant to *Schistosoma mansoni* (Trematoda). Molecular and Biochemical Parasitology 137: 321–328.
28. Mone Y, Ribou AC, Cosseau C, Duval D, Theron A, et al. (2011) An example of molecular co-evolution: reactive oxygen species (ROS) and ROS scavenger levels in Schistosoma mansoni/Biomphalaria glabrata interactions. Int J Parasitol 41: 721–730.
29. Mitta G, Galinier R, Tisseyre P, Allienne JF, Girerd-Chambaz Y, et al. (2005) Gene discovery and expression analysis of immune-relevant genes from Biomphalaria glabrata hemocytes. Developmental & Comparative Immunology 29: 393–407.
30. Moné Y, Gourbal B, Duval D, Du Pasquier L, Kieffer-Jaquinod S, et al. (2010) A Large Repertoire of Parasite Epitopes Matched by a Large Repertoire of Host Immune Receptors in an Invertebrate Host/Parasite Model. PLoS Negl Trop Dis 4: e813.
31. Bernheimer AW, Avigad LS (1974) Partial Characterization of Aerolysin, a Lytic Exotoxin from Aeromonas hydrophila. pp. 1016–1021.
32. Husslein V, Huhle B, Jarchau T, Lurz R, Goebel W, et al. (1988) Nucleotide sequence and transcriptional analysis of the aerCaerA region of Aeromonas sobria encoding aerolysin and its regulatory region. Molecular Microbiology 2: 507–517.
33. Ballard J, Crabtree J, Roe BA, Tweten RK (1995) The primary structure of Clostridium septicum alpha-toxin exhibits similarity with that of Aeromonas hydrophila aerolysin. Infect Immun 63: 340–344.
34. Hunter SE, Clarke IN, Kelly DC, Titball RW (1992) Cloning and nucleotide sequencing of the Clostridium perfringens epsilon-toxin gene and its expression in Escherichia coli. pp. 102–110.
35. Priest FG, Ebdrup L, Zahner V, Carter PE (1997) Distribution and characterization of mosquitocidal toxin genes in some strains of Bacillus sphaericus. Appl Environ Microbiol 63: 1195–1198.
36. Akiba T, Abe Y, Kitada S, Kusaka Y, Ito A, et al. (2009) Crystal Structure of the Parasporin-2 Bacillus thuringiensis Toxin That Recognizes Cancer Cells. Journal of Molecular Biology 386: 121–133.
37. Okumura S, Saitoh H, Ishikawa T, Mizuki E, Inouye K, et al. (2008) Identification and characterization of a novel cytotoxic protein, parasporin-4, produced by Bacillus thuringiensis A1470 strain. Biotechnology Annual Review: Elsevier. pp. 225–252.
38. Opota O, Vallet-Gély I, Vincentelli R, Kellenberger C, Iacovache I, et al. (2011) Monalysin, a novel ß-pore-forming toxin from the Drosophila pathogen Pseudomonas entomophila, contributes to host intestinal damage and lethality. PLoS Pathog 7: e1002259.
39. Macpherson H, Bergh Ø, TH.. Birkbeck (2012) An aerolysin-like enterotoxin from Vibrio splendidus may be involved in intestinal tract damage and mortalities in turbot, Scophthalmus maximus (L.), and cod, Gadus morhua L., larvae. J Fish Dis 35: 153–167.
40. Szczesny P, Iacovache I, Muszewska A, Ginalski K, van der Goot FG, et al. (2011) Extending the Aerolysin Family: From Bacteria to Vertebrates. PLoS ONE 6: e20349.
41. Rossjohn J, Feil SC, McKinstry WJ, Tsernoglou D, Van Der Goot G, et al. (1998) Aerolysine : A Paradigm for Membrane Insertion of Beta-Sheet Protein Toxins? Journal of Structural Biology 121: 92–100.
42. Knapp O, Stiles B, Popoff MR (2010) The Aerolysin Like Toxin Family of cytolitic, Pore Forming Toxins. The open toxinology Journal 3: 53–68.
43. Jonas D, Schultheis B, Klas C, Krammer PH, Bhakdi S (1993) Cytocidal effects of Escherichia coli hemolysin on human T lymphocytes. pp. 1715–1721.
44. Nelson K, Brodsky R, Buckley J (1999) Channels formed by subnanomolar concentrations of the toxin aerolysin trigger apoptosis of T lymphomas. Cell Microbiol 1: 69–74.
45. Sher DJ, Fishman Y, Zhang M, Lebendiker M, Gaathon A, et al. (2005) Hydralysins: a new category of beta-pore-forming toxins in cnidaria. Characterization and preliminary structure-function analysis. J Biol Chem 280: 22847–22855.
46. Castro-Faria-Neto HC, Martins MA, Bozza PT, Perez SAC, Correa-Da-Silva ACV, et al. (1991) Pro-inflammatory activity of enterolobin: A haemolytic protein purified from seeds of the Brazilian tree Enterolobium contortisiliquum. Toxicon 29: 1143–1150.
47. Sousa MV, Richardson M, Fontes W, Morhy L (1994) Homology between the seed cytolysin enterolobin and bacterial aerolysins. J Protein Chem 13: 659–667.
48. Iacovache I, van der Goot FG, Pernot L (2008) Pore formation: An ancient yet complex form of attack. Biochimica et Biophysica Acta (BBA) - Biomembranes 1778: 1611–1623.
49. Abrami L, Fivaz M, Glauser PE, Parton RG, van der Goot FG (1998) A pore-forming toxin interact with a GPI-anchored protein and causes vacuolation of the endoplasmic reticulum. J Cell Biol 140: 525–540.
50. Rossjohn J, Buckley JT, Hazes B, Murzin AG, Read RJ, et al. (1997) Aerolysin and pertussis toxin share a common receptor-binding domain. EMBO J 16: 3426–3434.
51. Diep DB, Nelson KL, Lawrence TS, Sellman BR, Tweten RK, et al. (1999) Expression and properties of an aerolysin–Clostridium septicum alpha toxin hybrid protein. Molecular Microbiology 31: 785–794.
52. Melton-Witt JA, Bentsen LM, Tweten RK (2006) Identification of Functional Domains of Clostridium septicum Alpha Toxinâ€ Biochemistry 45: 14347–14354.
53. Wilmsen H, Leonard K, Ticheaar W, Buckley J, Pattus F (1992) The aerolysin membrane channel is formed by heptamerization of the monomer. EMBO J 11: 2457–2463.
54. MacKenzie CR, Hirama T, Buckley JT (1999) Analysis of receptor binding by the channel-forming toxin aerolysin using surface plasmon resonance. J Biol Chem 274: 22604–22609.
55. Iacovache I, Paumard P, Scheib H, Lesieur C, Sakai N, et al. (2006) A rivet model for channel formation by aerolysin-like pore-forming toxins. EMBO J 25: 457–466.
56. Howard SP, Buckley JT (1985) Activation of the hole-forming toxin aerolysin by extracellular processing. pp. 336–340.
57. Garland WJ, Buckley JT (1988) The cytolytic toxin aerolysin must aggregate to disrupt erythrocytes, and aggregation is stimulated by human glycophorin. pp. 1249–1253.
58. Song T, Toma C, Nakasone N, Iwanaga M (2004) Aerolysin is activated by metalloprotease in Aeromonas veronii biovar sobria. J Med Microbiol 53(6): 477–482.
59. Bech N, Beltran S, Portela J, Rognon A, Allienne J-Fo, et al. Follow-up of the genetic diversity and snail infectivity of a Schistosoma mansoni strain from field to laboratory. Infection, Genetics and Evolution 10: 1039–1045.
60. Theron A, Pages JR, Rognon A (1997) Schistosoma mansoni: distribution patterns of miracidia among Biomphalaria glabrata snail as related to host susceptibility and sporocyst regulatory processes. Exp Parasitol 85: 1–9.
61. Yoshino T, Laursen J (1995) Production of Schistosoma mansoni daughter sporocysts from mother sporocysts maintained in synxenic culture with Biomphalaria glabrata embryonic (Bge) cells. J Parasitol 81: 714–722.
62. Hansen E (1976) Application of tissue culture of a pulmonate snail to culture of larval of Schistosoma mansoni. New York: Academic Press: 87–97.
63. Sambrook J, Fritsch EF, Maniatis T (1989) Molecular Cloning: a laboratory manual. 2 ed. New York: Cold Spring Harbor Laboratory Press.
64. Galinier R, Roger E, Sautiere P, Aumelas A, Banaigs B, et al. (2009) Halocyntin and papillosin, two new antimicrobial peptides isolated from hemocytes of the solitary tunicate, Halocynthia papillosa. Journal of Peptide Science 15: 48–55.
65. Mattos AC, Kusel JR, Pimenta PF, Coelho PM (2006) Activity of praziquantel on in vitro transformed Schistosoma mansoni sporocysts. Mem Inst Oswaldo Cruz 101 Suppl 1: 283–287.
66. Bagos PG, Liakopoulos TD, Spyropoulos IC, Hamodrakas SJ (2004) PRED-TMBB: a web server for predicting the topology of Î²-barrel outer membrane proteins. pp. W400–W404.
67. Bagos P, Liakopoulos T, Spyropoulos I, Hamodrakas S (2004) A Hidden Markov Model method, capable of predicting and discriminating beta-barrel outer membrane proteins. BMC Bioinformatics (5): 29.
68. Zhang Y, Skolnick J (2005) TM-align: a protein structure alignment algorithm based on the TM-score. pp. 2302–2309.
69. Zhang Y (2008) I-TASSER server for protein 3D structure prediction. BMC Bioinformatics (9): 40.
70. Roy A, Kucukural A, Zhang Y (2010) I-TASSER: a unified platform for automated protein structure and function prediction. Nature Protocols (5): 725–738.
71. Moran Y, Fredman D, Szczesny P, Grynberg M, Technau U (2012) Recurrent Horizontal Transfer of Bacterial Toxin Genes to Eukaryotes. Mol Biol Evol.
72. Capella-Gutierrez S, Silla-Martinez J, T. . TG (2009) trimAl: a tool for automated alignment trimming in large-scale phylogenetic analyses. Bioinformatics 25: 1972–1973
73. Abascal F, Zardoya R, Posada D (2005) ProtTest: Selection of best-fit models of protein evolution. Bioinformatics 21: 2104–2105.
74. Ronquist F, Huelsenbeck JP (2003) MrBayes 3: Bayesian phylogenetic inference under mixed models. . Bioinformatics 19: 1572–1574.
75. Guindon S, Gascuel O (2003) A simple, fast, and accurate algorithm to estimate large phylogenies by maximum likelihood. . Systematic Biology 52: 696–704.
76. Fivaz M, Abrami L, Tsitrin Y, Goot FVd (2001) Aerolysin from Aeromonas hydrophila and related toxins. Curr Top Microbiol Immunol 257: 35–52.
77. Cole AR, Gibert M, Popoff M, Moss DS, Titball RW, et al. (2004) Clostridium perfringens epsilon-toxin shows structural similarity to the pore-forming toxin aerolysin. Nat Struct Mol Biol 11: 797–798.
78. Tsitrin Y, Morton CJ, El Bez C, Paumard P, Velluz M-C, et al. (2002) Conversion of a transmembrane to a water-soluble protein complex by a single point mutation. Nat Struct Mol Biol 9: 729–733.
79. Green M, Buckley J (1990) Site-directed mutagenesis of the hole-forming toxin aerolysin: studies on the roles of histidines in receptor binding and oligomerization of the monomer. Biochemistry 29: 2177–2180.
80. Wilmsen HU, Buckley JT, Pattus F (1991) Site-directed mutagenesis at histidines of aerolysin from Aeromonas hydrophila: a lipid planar bilayer study. Mol Microbiol 5: 2745–2751.

81. Buckley JT, Wilmsen HU, Lesieur C, Schultze A, Pattus F, et al. (1995) Protonation of His-132 promotes oligomerization of the channel-forming toxin Aerolysin. Biochemistry 34: 16450–16455.
82. van der Goot FG PF, Wong KR, Buckley JT. (1993) Oligomerization of the channel-forming toxin aerolysin precedes insertion into lipid bilayers. Biochemistry 32: 2636–2642.
83. Abrami L, Fivaz M, Decroly E, Seidah NG, Jean Fo, et al. (1998) The Pore-forming Toxin Proaerolysin Is Activated by Furin. 273: 32656–32661.
84. Katayama H, Janowiak BE, Brzozowski M, Juryck J, Falke S, et al. (2008) GroEL as a molecular scaffold for structural analysis of the anthrax toxin pore. Nat Struct Mol Biol 15: 754–760.
85. Kyte J, Doolittle RF (1982) A simple method for displaying the hydropathic character of a protein. Journal of Molecular Biology 157: 105–132.
86. Tellmann G, Geulen O (2006) LightCycler 480 Real-Time PCR system: Innovative solutions for relative quantification. Biochemica 16–18.

Discussion

DISCUSSION

Au cours de ce travail de thèse, nous avons cherché à définir le priming immunitaire chez *Biomphalaria glabrata* face à l'un de ses parasites, le tremtatode *Schistosoma mansoni*, et ce tant au niveau des phénotypes qu'au niveau des mécanismes moléculaires sous-jacents. Le priming immunitaire est le nom donné de manière générique au fait que les invertébrés sont parfois capables d'être immunisés et/ou protégés suite à une première rencontre avec un pathogène et d'être alors en mesure de répondre efficacement à toutes rencontres ultérieures avec ce même parasite. En 1998, au laboratoire, il a pu être mis en évidence la mise en place d'un phénomène de résistance acquise rendant le mollusque *Biomphalaria galabrata* résistant à l' infestation par *S. mansoni* (Sire et al. 1998). Cette protection a été interprétée comme la résultante d'une compétition parasitaire entre les stades intramolluscaux du parasite en développement chez le mollusque et les nouveaux stades parasitaires entrants.

Le priming immunitaire chez *Biomphalaria glabrata*

Dans le premier chapitre de cette thèse nous avons pu étudier précisément les processus phénotypiques du priming immunitaire chez *B. galabrata*. Par le biais d'un certain nombre de preuves indirectes nous avons été en mesure de confirmer que la protection à la ré-infestation observée n'était pas la résultante d'une compétition parasitaire mais bien le fait d'une réponse immunitaire du mollusque qui lui permettait de mieux répondre à une seconde infestation. Nous avons par la suite confirmé cette hypothèse en menant des approches de vaccination avec des doses croissantes d'extraits protéiques (voir Chapitre deux). L'augmentation des doses de protéines injectées induit une réponse de plus en plus efficace. Ce résultat bien connu chez les vertébrés (Asano et al. 1982; Frey et al. 2002; Disis et al. 2004; Ni et al. 2013) confirme dans le modèle *B. glabrata* qu'il s'agit bien d'une réponse immunitaire proportionnelle à la stimulation engendrée.

Sire *et al* (1998) ont également démontré que cette résistance se mettait en place progressivement au cours du temps. Afin de mieux comprendre cette dynamique temporelle nous avons dans un premier temps suivi le développement parasitaire chez le mollusque au cours du temps. Nous avons donc pu observer que la protection se mettait en place au cours du développement du sporocyste primaire et devenait totale pendant la migration des premiers sporocystes secondaires (SpII) (Chapitre 1). Nous avons donc mené des approches afin de

savoir si la protection était engendrée par les lésions dues à la migration des SpII. En effet il est connu que des lésions tissulaires sont susceptibles d'engendrer une réponse immunitaire aspécifique visant à prévenir l'infection par des pathogènes opportunistes (Kubo et al. 1984; Franchini and Ottaviani 2000; Paterson et al. 2003). Les expériences de lésions par piqûre ou par l'utilisation d'un canon à particule n'ont entrainé aucune protection. Nous avons donc émis l'hypothèse que le priming immunitaire été engendré par la succession des stimulations immunitaires liées au développement intramolluscal du parasite et plus particulièrement à la présentation successive d'antigènes différents au cours du développement du parasite. En effet le parasite passe successivement, chez le mollusque, de l'état de miracidium, à celui de sporocyste primaire (SpI), puis de sporocyste secondaire (SpII) et enfin de cercaires. Chacun de ces stades larvaires possède une structure épithéliale spécifique qui doit être très certainement associée à des déterminants antigéniques différents. Nous avons donc mené une approche de vaccination avec des extraits protéiques isolés de pool de miracidium, de SpI ou de SpII (Chapitre 2). Nous avons observé que les trois extraits protéiques induisaient une protection. Cette protection est supérieure lors de l'injection d'un extrait protéique de SpI. Le mélange entre des extraits de miracidium et de SpII présente un effet additif et engendre une meilleure protection à la ré-infestation. Il semble clair que la présentation successive de différentes couvertures antigéniques au cours du développement du parasite est responsable de la mise en place progressive d'un priming immunitaire de plus en plus efficace chez *B. glabrata*.

Le fait que différents stades de développement du même parasite puissent générer une protection différente laisse supposer que nous avons un haut niveau de reconnaissance immunitaire chez *B. glabrata*. La question du niveau de spécificité du priming immunitaire se pose donc dans notre modèle. Dans certains cas, le priming immunitaire est aspécifique, c'est notamment le cas de *Tenebrio molitor* et *Anopheles gambiae* (Moret and Siva-Jothy 2003; Rodrigues 2010). Dans des cas extrêmes une simple lésions entraine un priming immunitaire face à des bactéries ou des champignons (Kubo et al. 1984; Franchini and Ottaviani 2000; Paterson et al. 2003). Tous ces exemples présentent une caractéristique en commun, il s'agit d'intéractions entre invertébrés et procaryotes ou champignons. Il semble que cette interaction reposant sur la reconnaissance de motifs tels les LPS de bactéries ou les β-glucanes de champignons soit suffisamment discriminante pour ne pas nécessité un haut niveau de spécificté. Cependant il existe des cas où des interactions entre un invertébré et un pathogène procaryote engendrent un priming immunitaire avec de forts niveaux de spécificité de reconnaissance. Cette spécificité s'exprime au niveau de l'espèce chez la blatte américaine

Periplaneta americana (Faulhaber and Karp 1992), mais peut s'exprimer à des niveaux plus fin chez *Daphnia magna* reconnaissant jusqu'à la souche de *Pasteuria ramosa* (Little et al. 2003). Dans le seul cas que nous connaissons où l'interaction implique deux Eucaryotes métazoaires (le copépode *Macrocyclops albidus* et son parasite *Schistocephalus solidus*), la spécificité est également visible à l'échelle du génotype (Kurtz and Franz 2003). Il est probable que la proximité phylogénétique ces deux espèces en interaction a induit la sélection de processus de reconnaissance complexe et hautement spécifiques permettant de discriminer jusqu'à l'échelle du génotype afin pour le copépode de distinguer les cellules du parasite des ses propres cellules et d'éviter l'auto-immunité. Nous avons donc analysé le niveau de spécificité du priming immunitaire chez *B. glabrata* en interaction avec *S. mansoni* deux Eucaryotes et qui plus est, appartiennent tous deux aux Lophotrochozoaires (Chapitre 1). Pour cela nous avons réalisé une expérience au cours de laquelle nous avons observé le niveau de protection obtenu suite à une infestation par un isolat Brésilien de *Schistosoma mansoni* et des challenges homologues ou hétérologues. Ces challenges ont été réalisés avec différentes souches de *S. mansoni* provenant d'isolats géographiques différents ou d'espèce différente (*Schistosoma rodhaini*). Cette approche nous a permis de mettre en évidence que le niveau de protection engendré était corrélé à la distance génétique entre les parasites de la primo-infestation et ceux du challenge. Une fois encore l'interaction entre deux organismes Eucaryotes présente des taux de spécificité extrêmement élevés. Ces résultats vont dans le sens de l'hypothèse qu'il est essentiel de posséder une grande capacité à reconnaître avec précision un organisme qui serait phylogénétiquement proche afin d'éviter l'auto-immunité.

De ces premières approches s'attachant à l'observation de phénotypes il ressort clairement que le parasite primo-entrant induit chez le mollusque une immunité qui est inefficace contre lui-même mais qui va protéger l'hôte d'une ré-infestation future. Ce phénomène immunitaire a été décrit sous le terme d'immunité concomitante et a pu être mis en évidence dans l'interaction entre *Schistosoma mansoni* et son hôte vertébré (Smithers and Terry 1969). Dans ce cas, les vers adultes vont stimuler le système immunitaire et la réponse adaptative de l'hôte. La réaction engendrée est totalement inefficace contre les adultes déjà présents, en revanche elle va être très efficace et spécifique envers les parasites qui vont pénétrer lors d'un second contact. L'immunité concomitante chez le vertébré est d'autant plus efficace que le parasite de la seconde infestation est génétiquement proche du parasite immunisant (Dumont et al. 2007; Beltran et al. 2010). Evidemment chez le vertébré cette spécificité de reconnaissance est tout à fait classique puisqu'elle est basée sur l'immunité adaptative et donc, la reconnaissance et la production d'anticorps spécifique au pathogène

rencontré. Mais alors comment se fait-il que les parasites présents ne soient pas affectés par cette immunité adaptative ? Et bien les schistosomes sont connus pour adopter une stratégie d'évasion immunitaire de type mimétique (Abu-Shakra et al. 1999; Salzet et al. 2000). Dès lors qu'ils sont dans l'hôte, les parasites vont soit se recouvrir de molécules de l'hôte afin de passer inaperçu, c'est ce que l'on appelle le camouflage moléculaire, soit produire des molécules similaires à celles de l'hôte et les exprimer à leur surface pour échapper au système de reconnaissance, c'est ce que l'on appelle le mimétisme moléculaire. En utilisant cette stratégie rapidement après son entrée dans l'hôte, le parasite s'assure que l'immunité adaptative se mettant en place sera inefficace contre lui puisqu'il sera camouflé de l'activité du système immunitaire.

Chez le mollusque, le parasite induit une immunisation inefficace contre lui mais qui va protéger le mollusque d'une seconde infestation avec des parasites génétiquement proches. C'est exactement le même procédé. De plus il a été démontré que le SpI adoptait également cette stratégie mimétique afin d'échapper au système immunitaire (Daniel et al. 1992). Il est probable que les SpII et les cercaires adoptent également cette stratégie. D'ailleurs l'utilisation d'immun sérum de patients humains infectés dans des approches de western blot a permis de mettre en évidence la présence d'anticorps dirigés contre des protéines de mollusque, ce qui constitue un argument supplémentaire en faveur du mimétisme moléculaire. En effet les cercaires seraient recouvertes de molécules de *B. glabrata* lors de leur pénétration chez l'hôte définitif vertébré générant ainsi des anticorps contre ces molécules antigéniques de mollusque (communication personnelle). On peut donc faire un parallèle intéressant entre ce qui se passe chez le vertébré et chez le mollusque. Il semble que ce phénomène d'immunité concomitante s'exprime chez les deux hôtes de *S. mansoni* toutefois les mécanismes associés doivent forcément être différents, et restent à être mis en évidence chez *B. glabrata*.

Les candidats du priming immunitaire chez *Biomphalaria glabrata*

Si la question du priming immunitaire chez *B. glabrata*, et même chez de nombreux invertébrés, ne fait aucun doute, les mécanismes sous jacents ne sont toujours pas élucidés. De plus en plus d'études posent cette question sans vraiment y apporter de réponses (Moret and Siva-Jothy 2003; Rowley and Powell 2007; Roth and Kurtz 2009; Rodrigues 2010; Wang et al. 2013). Nous avons donc mené une approche de protéomique comparative afin d'identifier des molécules potentiellement impliquées dans cette réponse de priming immunitaire. Suite à des observations histologiques nous avons observé que ce priming immunitaire reposait sur

des facteurs humoraux et que les parasites du challenge dégénéraient spontanément sans encapsulation par les hémocytes. Cette réponse particulière nous a amené à analyser les plasmas des mollusques afin d'en étudier les protéines circulantes et ce, au cours d'une cinétique d'infestation et de ré-infestation homologue.

Dans cette approche nous avons pu constater que la majorité des molécules différentiellement régulées lors de cette cinétique étaient des molécules ayant des activités potentielles immunitaires. Nous avons pu distinguer deux grands types de régulations pour ces molécules. Tout d'abord, des régulations de type mémoire, c'est-à-dire que la quantité de protéine augmentait à 15 jours suite à l'infestation, baissait entre 15 et 25 jours puis augmentait à nouveau lors du challenge parfois plus fortement. Les molécules immunitaires présentant ce profil sont des C-type lectins, la β-chain acetylcholin binding protein et la glutathione peroxidase 3 precursor. Le second type de régulation est une régulation de type réponse maintenue (augmentation lors de la primo-infestation et maintien à un niveau élevé) et concerne des C-type lectins, la mannose C type 2 receptor, la Beta-1,3-glucan binding protein, des Hemagglutinin/amebocyte aggregation factors, la Chitinase, une autre β chain acetylcholine binding protein, la Thymosin et la Glutathione s-transferase mu 3-like. Une molécule semble intéressante également puisqu'il s'agit d'une isoforme d'une Hemagglutinin/amebocyte aggregation factors qui apparait uniquement après le challenge.

La majorité des molécules présentent des profils de type réponse maintenue. Cette régulation implique qu'après une infestation le mollusque investit dans la production de molécules immunitaire afin de se préparer à répondre à une éventuelle ré-infestation. Cette production en continu de molécules doit affecter d'une manière ou d'une autre d'autres traits de vie du mollusque (Hangartner et al. 2013; McNamara et al. 2013). De manière intéressante dans cette étude protéomique nous avons observé une baisse de toutes les fonctions de reproduction du mollusque (gamétogénèse). Cette baisse concomitante à la mise en place et au maintien de l'activité immunitaire pourrait représenter le compromis énergétique attendu. Ainsi en investissant de l'énergie dans l'immunité, l'individu compenserait cette dépense en diminuant ou stoppant ses fonctions de reproduction.

Il est intéressant de noter que toutes les molécules ne présentent pas une régulation de type réponse maintenue mais que certaines sont plutôt régulées de manière ponctuelle suite aux infestations successive à la manière d'une réponse de type mémoire. Cette régulation particulière représente une forme complexe d'immunité avec une mise en mémoire de l'information et une restitution de la réponse suite à un challenge de manière plus rapide et plus intense.

Quoi qu'il en soit, les principales molécules présentant des régulations sont des molécules de reconnaissance et particulièrement les C-type lectins. Ces molécules semblaient déjà jouer un rôle dans le priming immunitaire chez *Chlamys farreri* face à des bactéries (Wang et al. 2013). La spécificité observée lors de la réponse de priming chez *B. glabrata* pourrait être étroitement associée à ces molécules de reconnaissance de type lectines. En effet, Schulenburg (2007) a déjà proposé l'hypothèse que l'association d'un certain nombre de molécules de reconnaissance diversifiées pourrait permettre une reconnaissance très spécifique (Schulenburg et al. 2007), mettant à mal le paradigme établi par Medzhitov et Janeway selon lequel la reconnaissance chez les invertébrés reposerait sur un nombre limité de molécules et serait très peu spécifique (Medzhitov and Janeway 2002). Ainsi, dans notre modèle, on peut observer que des familles de lectines, des molécules très diversifiées, semblent jouer un rôle dans la réponse de priming immunitaire, réponse qui est très spécifique puisque dépendante du génotype du parasite.

Parmi les molécules que l'approche protéomique a mises en lumière, l'une d'entre elle nous a parue très intéressante. Il s'agit de la Biomphalysine. Malgré la régulation observée lors de l'approche protéomique (diminution de la molécule au cours de l'infestation) ce n'est pas la première fois qu'elle est trouvée dans l'interaction avec *S. mansoni*. Cette molécule fait partie de la superfamille des Aérolysines et a été identifiée chez *B. glabrata* lors d'une approche d'interactome visant à caractériser les molécules responsables de la compatibilité dans l'interaction *B. glabrata / S. mansoni* (Mone et al. 2010). La caractérisation de cette molécule a été menée dans le chapitre 4. Nous avons mis en évidence que cette β pore-forming toxin (βPFT) avait été acquise par transfert horizontal depuis des bactéries et qu'elle possédait une forte activité cytotoxique / cytolytique envers les sporocystes de *S. mansoni*. La Biomphalysine est exprimée exclusivement dans les hémocytes et est secrétée dans le plasma. Aucune expression différentielle de la Biomphalysine n'a pu être observée suite à une infestation et/ou ré-infestation par *S. mansoni* que ce soit en terme de transcrits ou en terme de protéine. La Biomphalysine jouerait donc un rôle sentinelle et serait synthétisée constitutivement afin d'être immédiatement disponible pour répondre à toute infection parasitaire. Au cours de la réponse de priming immunitaire, la Biomphalysine est réprimée suite à la primo-infection (voir chapitre 3), il se pourrait donc qu'elle participe à la réponse immunitaire et soit consommée au cours de la réponse pour neutraliser les sporocystes de *S. mansoni* suite à la primo-infestation et au challenge.

Conclusion

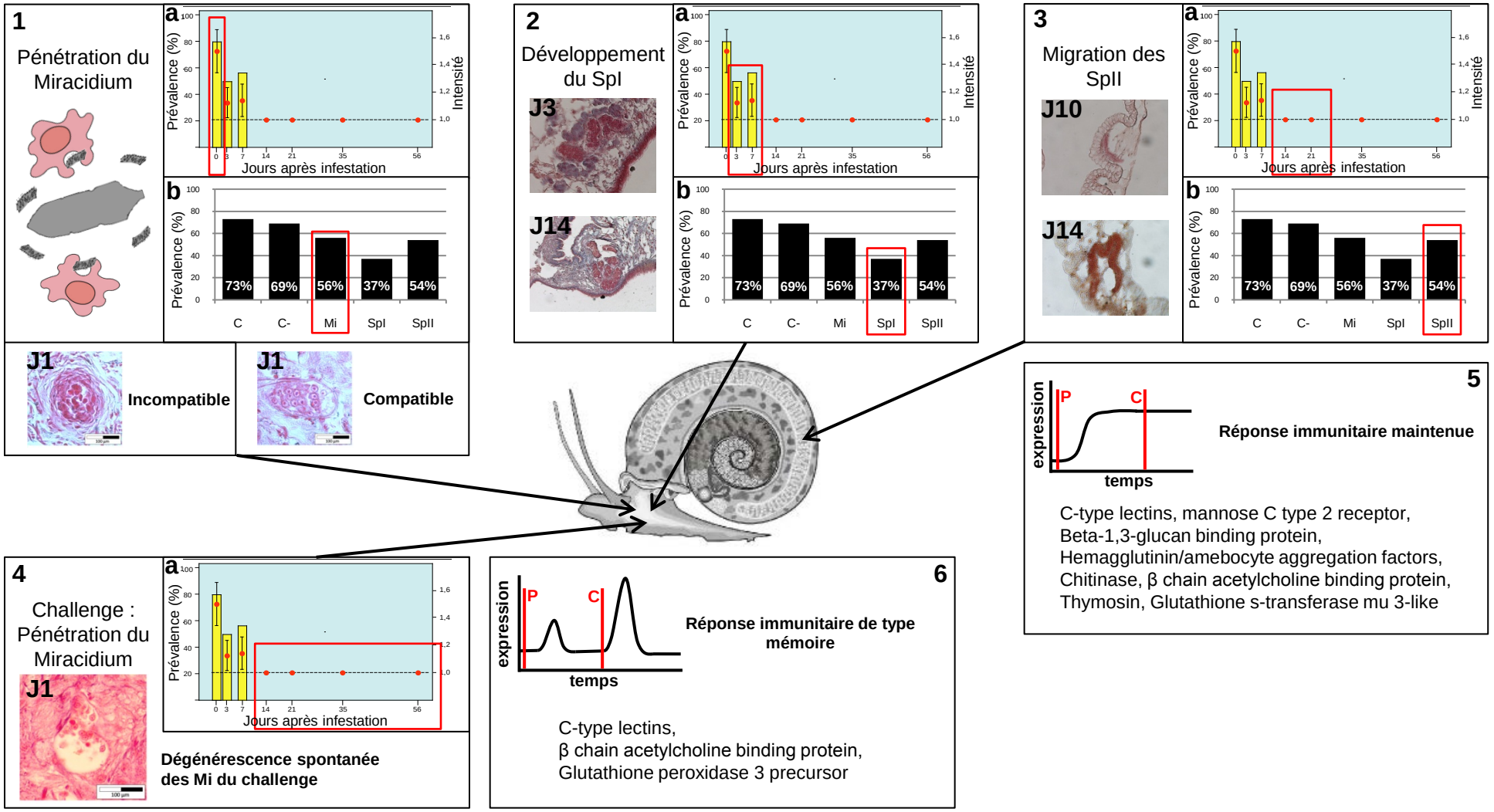

Figure 6 : Mise en place du priming immunitaire.

1), 2) et 3) Etapes du développement larvaire intramolluscal lors de la primo-infestation.. 1) Perte des plaques ciliées, stade post-miracidial, développement en SpI. Sporocyste 1 jour après infestation encapsulé (Incompatible) ou en cours de développement (Compatible). 2) Sporocyste primaire en développement à 3 et 14 jours après infestation. 3) Sporocyste secondaire en migration dans le rein à 10 jours après infestation et dans la gonade à 14 jours après infestation. a) Dynamique temporelle de mise en place du priming immunitaire observée au travers des prévalences et intensités. b) Prévalences observées lors d'une expérience de vaccination par différents extraits de parasite.

C : contrôle d'infestation. C−: protéine exogène. Mi : extrait de miracidium. SpI : extrait de sporocyste primaire. SpII : extrait de sporocyste secondaire.

4) Challenge immunitaire réalisé à partir de 14 jours après la primo-infestation. Sporocyste en dégénérescence dans les tissus du mollusque.

5) et 6) Candidats moléculaire présentant une expression de type réponse maintenue (5) ou une expression de type réponse mémoire (6).

P : Primo-infestation. C : Challenge.

Après ces travaux il apparait aujourd'hui que l'immunité de *B. glabrata* est très complexe. Elle mêle reconnaissance spécifique et mémoire immunitaire. Il est donc possible de décrire un scénario de la mise en place du priming immunitaire pour notre modèle.

Lors de sa rencontre avec un parasite, le système immunitaire du mollusque se met en action. La pénétration du miracidium entraine une première phase de reconnaissance qui se fait au travers de la perte des plaques ciliées (Pan 1996). Le stade post-miracidial résultant de la perte des plaques ciliées est alors confronté au système immunitaire du mollusque. L'interaction précoce du parasite et de son hôte donne lieux à un polymorphisme de compatibilité (Figure 6.1). Si l'interaction est incompatible, le parasite sera reconnu par les hémocytes, encapsulé et détruit. Si l'interaction est compatible le parasite se développera normalement. Il aura alors très peu de temps pour mettre en place son nouveau tégument et sa stratégie mimétique (Daniel et al. 1992; Abu-Shakra et al. 1999; Salzet et al. 2000). Il se recouvre de molécules de l'hôte afin de passer inaperçu (Damian 1987). Durant le court intervalle de temps pendant lequel il capte diverses molécules de l'hôte pour s'en recouvrir il est extrêmement vulnérable et expose ses antigènes à sa surface. D'ailleurs à ce stade il induit déjà une protection chez le mollusque (Figure 6.1.a et 6.1.b). Pour se défendre dans les premiers moments de sa métamorphose, le parasite a mis en place une stratégie immunosuppressive (Duvauxmiret et al. 1992; Guillou et al. 2007). En secrétant des molécules anti-oxydantes notamment il va contrer pour un certain temps la réponse immunitaire avant de passer inaperçu. Il va dès lors continuer à se développer, et grossir dans les tissus du mollusque (Figure 6.2). Le système immunitaire est stimulé et la protection devient plus efficace (Figure 6.2.a). Par ailleurs des extraits de ce stade SpI permettent seuls de vacciner de manière efficace le mollusque (Figure 6.2.b). Par la suite ce SpI va donner des sporocystes secondaires qui migreront jusqu'à la glande digestive du mollusque (Figure 6.3). Lorsqu'ils vont commencer à migrer, on peut supposer que dans un court intervalle de temps après leur sortie, ils vont exposer au mollusque leur surface tégumentaire avant de mettre en place une stratégie mimétique, et donc engendrer une nouvelle stimulation du système immunitaire (Figure 6.3.a et 6.3.b). A ce moment, le parasite pourrait sécréter à nouveau des molécules immunosuppressives. Pour finir ce sont les cercaires qui vont devoir migrer et, comme les SpII, passer inaperçues. Comme je l'ai déjà évoqué précédemment, certains indices laissent penser que les cercaires seraient recouvertes de molécules de *B. glabrata* lors de leur pénétration chez l'hôte définitif vertébré ce qui serait un argument en faveur de leur stratégie mimétique. Ainsi, le premier parasite entrant chez mollusque va stimuler l'immunité par son développement successivement en Mi, SpI, SpII et cercaires. Mais l'immunité qui en

résulte n'est pas efficace contre ce dernier. Cette réponse emmagasinée au travers de mécanismes pour l'instant inconnu mais dont nous connaissons peut être déjà certains acteurs (lectines, facteurs humoraux…) pourra alors être engagée plus rapidement lors d'une seconde rencontre, ne laissant pas le temps au SpI de mettre en place sa stratégie mimétique. Il serait alors immédiatement reconnu et détruit sans l'intervention d'une réponse cellulaire (Figure 6.4). Nous pouvons penser que la reconnaissance rapide lors d'un challenge est portée par ces molécules de reconnaissance produites lors de la primo-infestation et maintenues à un taux élevé (Figure 6.5) ou bien dont l'information est stockée puis restituée rapidement lors d'une seconde rencontre (Figure 6.6).

Perspectives

L'existence du priming immunitaire chez *Biomphalaria glabrata* est une grande avancée dans la compréhension des interactions entre ce mollusque et son parasite naturel *Schistosoma mansoni*. Il reste cependant de nombreuses questions encore sans réponse qu'il serait intéressant d'appréhender.

Les molécules au cœur de la réponse de priming immunitaire

La première étape, celle qui sera la plus importante, sera de pousser plus en avant l'identification des mécanismes moléculaires sous-jacents au priming immunitaire. L'approche protéomique (chapitre 3) nous a apporté une indication sur l'importance de certaines lectines et facteurs humoraux, mais cette approche n'est pas suffisamment puissante pour apporter une vision la plus complète possible des voies métaboliques impliquées dans cette réponse. Pour cela il semble nécessaire de mener des approches plus puissantes de « gene discovery », à l'aide de techniques de séquençage haut débit. Il serait effectivement très intéressant de pouvoir suivre l'expression d'un transcriptome dans sa globalité au cours d'une cinétique d'infestation / ré-infestation par une approche de transcriptomique massive (RNASeq illumina). Cette approche relativement similaire à notre étude protéomique nous permettrait de révéler un grand nombre de transcrits différentiellement exprimés au cours de la réponse de priming immunitaire. De la même façon, la spécificité de cette réponse pourrait être étudiée en réalisant des challenges hétérologues avec différents isolats géographiques ou espèces de Schistosomes (protocole similaire à celui développé dans le Chapitre 1). Par cette approche il serait donc possible d'observer à la fois les molécules clés impliquées dans la

réponse spécifique génotype-dépendante que nous avons pu mettre en évidence (chapitre 1) mais également d'identifier plus précisément les molécules effectrices impliquées dans la réponse humorale de priming immunitaire. Cette approche sera d'autant plus facilitée que le génome de *Biomphalaria glabrata* est en cours d'annotation et sera donc prochainement disponible.

Le support cellulaire de l'information immunitaire

Lors du priming immunitaire dans notre modèle, la réponse engendrée est uniquement humorale et aucune cellule impliquée dans la phagocytose ou l'encapsulation n'a pu être observée au contact des sporocystes. Cependant il semble évident que la production des facteurs humoraux et des molécules de reconnaissance doit reposer sur des types cellulaires particuliers qui doivent maintenant être identifiés. Il est à noter qu'aucune prolifération hémocytaire globale n'ait pu être observée jusqu'à présent lors d'une infestation d'un mollusque par un schistosomes, toutefois il a été démontré récemment des processus de différentiation hémocytaire, les proportions des infrapopulations d'hémocytes changent au cours de l'infestation (Garcia et al. 2010; Cavalcanti et al. 2012). La fonction des ces populations hémocytaires reste mal connue chez *Biomphalaria*, il serait donc intéressant d'étudier chacune de ces populations afin de caractériser plus précisément leurs fonctions. Ces travaux ont déjà été entrepris en parti au laboratoire. Une fois ces populations caractérisées il sera possible de suivre leur comportement et leur proportion par rapport à la population totale par une approche en cytométrie en flux. Il est probable qu'un de ces types cellulaires ait pour fonction d'emmagasiner une information immunitaire afin de produire et secréter des facteurs humoraux en continu (réponse de type maintenue « sustained response »), soit de répondre plus rapidement et/ou plus fortement suite au challenge lors d'un nouveau contact avec le pathogène (réponse de type mémoire). Ce suivit fait partie, au même titre que l'approche de séquençage massif des transcrits, d'un projet à cours terme qui est en cours de développement et dont une partie a débuté au cours de ma thèse puisque j'ai réalisé les échantillonnages des points de cinétique et l'assemblage des transcriptomes, le séquençage des transcrits ayant été réalisé par la plateforme de séquençage Montpellier GenomiX. Des premiers tests de cytométrie en flux ont également été réalisés cette année dans le cadre d'un stage de master 1 que j'ai co-encadré.

L'évolution des systèmes immunitaires invertébrés

Cette étude du système immunitaire de *Biomphalaria glabrata*, un mollusque, s'inscrit également dans une problématique à une échelle nettement plus large qui est d'obtenir une meilleure compréhension de la complexité et de l'évolution des systèmes immunitaires chez les invertébrés. En effet comme je l'ai souvent rappelé au cours de ce manuscrit, l'immunité n'est pas un caractère apparu chez un lointain ancêtre qui se serait complexifiée au cours de l'évolution des espèces pour atteindre un optimum chez les vertébrés gnathostomes avec l'immunité adaptative. Au lieu de cela, il s'agit plutôt d'un moyen de défense qui s'est complexifié de manière indépendante au sein de chaque espèce et ce, en fonction des pressions de sélection imposées par l'environnement biotique et principalement les pathogènes. De ce fait, pour avoir une vision d'ensemble de cette immunité nous n'avons pas d'autre choix que d'étudier chaque espèce indépendamment afin de reconstituer chacune des feuilles constituant cet arbre évolutif des systèmes immunitaires. Ainsi il existe des espèces pour lesquelles nous savons d'ores et déjà qu'il existe un priming immunitaire, dont voici quelques exemples chez les insectes : la blatte américaine *Periplaneta americana* face à *Pseudomonas aeruginosa* (Faulhaber and Karp 1992), le bourdon *Bombus terrestris* face à différentes bactéries du genre *Pseudomonas* et *Paenibacillus* (Sadd and Schmid-Hempel 2006), les fourmis *Camponotus pennsylvanicus* face à des bactéries (Hamilton et al. 2011) et *Lasius neglectus* face à un champignon *Metarhizium anisopliae* (Konrad et al. 2012), le ver de farine *Tenebrio molitor* avec une protection face à *Metarhizium anisopliae* suite à l'injection de LPS (Moret and Siva-Jothy 2003), le moustique *Anopheles gambiae* face à des bactéries du genre *Plasmodium* (Rodrigues 2010) et la drosophile *Drosophila melanogaster* face à *Streptococcus pneumoniae* (Pham et al. 2007), chez les crustacés : la crevette *Litopenaeus vannamei* face à différents virus (Pope et al. 2011; Powell et al. 2011), le copépode *Macrocyclops albidus* face au ver *Schistocephalus solidus* (Kurtz and Franz 2003) et aussi chez les mollusques : la pétoncle *Chlamys farreri* face à des bactéries du genre *Vibrio* (Wang et al. 2013) et le gastéropode *Biomphalaria glabrata* face à *Schistosoma mansoni* (Sire et al. 1998; Portela et al. 2013) et la liste n'est pas exhaustive.

En revanche, certaines espèces ne présentent aucun phénomène de priming immunitaire, c'est le cas de la libellule *Hetaerina americana* (Gonzalez-Tokman et al. 2010), d'une autre espèce de fourmis *Formica selysi* (Reber and Chapuisat 2012) et de la drosophile *Drosophila melanogaster* face au virus Drosophila C virus (Longdon et al. 2013).

On sait également que ce priming se manifeste sous plusieurs formes, augmentation de la capacité de phagocytose (Roth and Kurtz 2009), différentiation des hémocytes (Rodrigues 2010), augmentation de l'activité antimicrobienne (Moret and Siva-Jothy 2003), surexpression de C-type lectines (Wang et al. 2013), et dans notre cas il pourrait s'agir de l'action coordonnée de molécules de reconnaissances (lectines) et de facteur humoraux cytotoxiques / cytolytiques.

En plus de ce priming immunitaire, il a pu être mis en évidence chez certaines espèces un transfert trans-générationnel d'immunité, c'est notamment le cas du ver de farine *Tenebrio molitor* (Moret 2006; Zanchi et al. 2011; Moreau et al. 2012), le crustacé *Daphnia magna* (Little et al. 2003) ou encore le bourdon *Bombus terrestris* (Sadd et al. 2005). Dans le cas de *Biomphalaria glabrata* on sait que certaines molécules antimicrobiennes et antifongiques sont déposées dans les masses d'œufs (Hathaway et al. 2010; Baron et al. 2013), cependant, nous n'avons pas observé de différences de protection suite à l'infestation de jeunes mollusques issus de parents sains ou de parents infestés (cette expérience n'a pas pu être approfondie par manque de temps c'est pourquoi je n'en ai pas présenté les résultats dans ce manuscrit). Il n'y aurait donc pas de priming trans-générationnel chez *Biomphalaria glabrata*, bien que cela reste encore à démontrer clairement.

Il serait très intéressant de compléter, d'une part, la bibliographie qui n'est peut être pas exhaustive, d'autre part les expériences sur d'autres espèces afin d'établir quelles espèces présentent ou non du priming immunitaire dans les grands groupes d'invertébrés (notamment ceux pour lesquels il n'y a aucun représentant comme les céphalopodes, les échinodermes, les spongiaires…), ceci afin de définir pour chacune, les mécanismes régissant ce priming immunitaire et d'explorer sa spécificité mais également sa transmission à la descendance. Tout ceci permettrait de dresser un « état des lieux » de l'immunité innée à travers le règne animal et d'avoir une meilleure vision de l'évolution des systèmes immunitaires innés des ecdysozoaires aux deutérostomiens.

Des études sur le terrain

Etudier le priming immunitaire chez différentes espèces est un challenge très intéressant. Pourtant il est évident qu'une des premières étapes à réaliser dans notre modèle serait de vérifier l'existence de ce priming immunitaire dans les populations naturelles. Dans un premier temps cela permettrait de mieux cerner la spécificité de reconnaissance en milieu naturel avec des populations de parasites extrêmement diversifiées. En effet nous savons que

la diversité génétique des parasites, basée sur l'étude de marqueurs neutres, s'érode très rapidement au laboratoire (Bech et al. 2010). Par conséquent, même si nous avons choisi des isolats géographiques récemment introduits au laboratoire et les plus polymorphes (SmBRE-LE et SmVEN) pour notre étude sur la spécificité génotype dépendante du priming immunitaire, les quelques cycles que ces souches avaient déjà expérimenté au laboratoire ont très certainement réduit leur diversité génétique. Pourtant il nous est apparu lorsque nous avons primé les mollusques avec SmBRE-LE puis ré-infesté avec ce même parasite que la protection engendrée n'était pas complète (chapitre 1). Cette protection incomplète pourrait être liée au fait que le parasite SmBRE-LE qui est le parasite le plus diversifié car le plus récemment introduit au laboratoire présenterait des génotypes suffisamment diversifiés pour ne pas être reconnu lors du challenge par les facteurs humoraux de la réponse de priming induite lors de la primo-réponse.

Etudier le priming immunitaires sur le terrain avec des parasites fraîchement récoltés qui devrait avoir une diversité génétique très élevée permettrait de répondre à cette question et d'observer la spécificité du priming immunitaire en milieu naturel.

Une autre question pourrait être alors étudiée au sein des différents mollusques en interaction avec les schistosomes pour en inférer des indications quant à l'évolution du priming immunitaire au sein de ce groupe. Rien qu'au niveau des espèces du genre *Schistosoma* on peut trouver *S. mansoni* en interaction avec différentes espèces de gastéropodes du genre *Biomphalaria*, *S. haematobium* en interaction avec des espèces du genre *Bulinus*, ou *S. japonicum* en interaction avec des espèces du genre *Oncomelania* (Rollinson and Simpson 1987). Est-ce que dans toutes ces interactions les mécanismes immunitaires sélectionnés sont les mêmes ? Est-ce que le priming immunitaire est présent chez toutes ces espèces et s'exprime de la même façon ? L'étude pourrait même être étendue à d'autres genres au sein des Schistosomatidés et leurs hôtes. De la même façon la question pourrait se poser de savoir si le priming immunitaire chez *B. glabrata* existe face à ses autres parasites qu'ils soient Trématodes (Echinostomatidés, Psilostomatidés, Plagiorchiidés) ou autres (Angiostrongylidés) (Loker and Adema 1995; Hanelt et al. 2008; Redmond et al. 2011; Daoust et al. 2012; Deleury et al. 2012; Pinto and Melo 2013; Tunholi-Alves et al. 2013).

D'un point de vue populationnel

Une autre question qui me semble importante et très intéressante est l'étude populationnelle de l'impact du priming immunitaire tant au niveau de la dynamique des populations d'hôte que de celles du parasite.

Au niveau du mollusque il est évident que l'investissement dans un mécanisme aussi coûteux que le maintien d'une réponse immunitaire ou la mémorisation d'une information immunitaire, doit avoir des répercutions au niveau individuel et populationnel. Comme nous l'avons remarqué en étudiant les mécanismes du priming immunitaire il existe un compromis entre l'investissement du mollusque dans la réponse immunitaire et l'investissement dans les fonctions de reproduction (Chapitre 3). En effet une castration parasitaire chez les mollusques infectés a pu être mise en évidence chez *Biomphalaria glabrata* (Théron and Gérard 1994).
De manière générale l'implication du priming immunitaire sur les populations d'hôtes et de parasites a été abordée par des approches de modélisation mathématique et ce à ma connaissance dans seulement deux articles (Best et al. 2012; Tidbury et al. 2012). Il ressort de ces études que le priming immunitaire tend à déséquilibrer les interactions hôtes / pathogènes sous certaines conditions. Tout d'abord, le nombre d'hôtes susceptibles primés doit être suffisamment élevé pour influencer la dynamique de populations en augmentant de manière conséquente le nombre d'hôte rendus résistant à l'infestation. Il est donc nécessaire que le taux de rencontre et la compatibilité soient suffisamment élevés pour primé de manière efficace une grande proportion de la population d'hôte. Le second facteur important est le taux de protection engendré suite au priming. En effet plus ce taux est élevé (c'est-à-dire plus la protection conférée à l'hôte suite à la primo infestation est importante) et plus le priming aura un impact sur les populations de parasites puisqu'il rendra toute seconde infestation difficile voire impossible. Enfin, le dernier facteur important est le coût engendré par la parasitose sur l'hôte est également important dans la régulation des populations d'hôte cette fois ci. Deux paramètres entrent ici en jeu, la durée de vie suite à la parasitose (un parasite trop virulent va tuer rapidement son hôte et avoir un impact sur les populations) et la baisse de la fécondité souvent associée à la parasitose (si la quantité d'hôtes infectés est importante et qu'ils ne se reproduisent plus, la population déclinera en quelques générations). Enfin le priming immunitaire, par la protection qu'il génère dans la population, pourrait conduire à la disparition du parasite (Tidbury et al. 2012).

Dans notre modèle que pourrions-nous attendre de l'impact du priming sur l'interaction entre *Biomphalaria glabrata* et *Schistosoma mansoni* ?

Il est important de noter que le niveau de protection observé dans la réponse de priming immunitaire est dépendant du niveau de diversité génétique des pathogènes utilisés lors de la primo-infection et du challenge. Au laboratoire la diversité génétique des pathogènes et relativement faible comparativement au milieu naturel et nous observons globalement une réponse de priming immunitaire très efficace lors de challenges homologues (Chapitre 1). Ainsi, il serait important de tester le priming immunitaire en populations naturelles pour voir quel serait le taux de protection en fonction de la diversité des parasites rencontrés sur le terrain.

- Dans le cas ou une forte diversité génétique des parasites serait rencontrée, le priming immunitaire devrait être peu efficace. Un mollusque infesté développerait donc une réponse de priming immunitaire efficace contre les génotypes les plus proches de ceux de la primo-infection mais inefficace contre des parasites génétiquement distants. De ce fait, de manière indirecte le système immunitaire sélectionnerait des génotypes différents ce qui devrait tendre à augmenter la diversité génétique des parasites intra-molluscaux et par voie de conséquence la diversité génétique populationnelle des parasites. Dans l'interaction entre *S. mansoni* et son hôte vertébré le même phénomène a pu être démontré sous l'influence de l'immunité concomitante (Dumont et al. 2007; Beltran et al. 2010). La diversité parasitaire intra-hôte est alors plus élevée dans le cas d'infestations multiples répétées (ce qui se rapproche du scénario rencontré dans le milieu naturel) que dans le cas d'une infestation massive lors d'un seul contact (Theron et al. 2004). D'ailleurs il a pu être démontré que chez les parasites adultes, des changements de partenaires avaient lieu et que les femelles choisissent leur mâle en fonction de la distance génétique du couple (Beltran et al. 2008). Ainsi une femelle va changer de partenaire lorsque la distance génétique la séparant du prétendant est plus importante que celle de son mâle actuel, elle choisit le plus dissimilaire pour s'accoupler (Beltran et al. 2008). Il semblerait donc que le système immunitaire sélectionnant de manière indirecte des nouveaux parasites de génotypes différents favoriserait le changement de partenaire (Beltran et al. 2010). Dans l'interaction de *S. mansoni* avec son mollusque hôte intermédiaire, une méta-analyse des données concernant le sexe des parasites présents dans des mollusques infestés prélevés sur le terrain a révélé que la fréquence des infestations bisexuées était significativement supérieure à celle attendue (Boissier 2001). Si le système immunitaire du mollusque est capable de reconnaître différents génotypes et même différents stades de développement d'un même isolat géographique parasitaire (Chapitres 1 et 2), il est envisageable qu'il soit en mesure de distinguer et de répondre différentiellement à une infestation par un miracidium femelle ou par un mâle. En effet, quoi de plus différent

Nombre de parasites par hôte	1	2	3	4	5	6	7	8	9	total	intensité	% moll infestés par 1 parasite
Dionisio (1)	33	22	9	5	0	0	0	0	0	69	1,79	46%
Dionisio (2)	6	7	2	0	0	0	0	0	0	15		
Cabana	2	1	1	0	0	1	1	0	0	6	3,29	43%
Barreiro	4	1	0	0	1	1	0	0	1	8		
Mali	26	8	0	0	1	0	0	0	0	35	1,34	74%
Guadeloupe	38	4	1	0	0	0	0	0	0	43	1,14	88%

Table 1 : Données de terrain concernant le nombre de génotypes de parasites par mollusques infestés. Tableau basé sur la revue de Eppert *et al.* (2002).

génétiquement qu'un mâle et une femelle ? Le biais de dispersion des infestations bisexuées chez *Biomphalaria glabrata* pourrait donc être la résultante du priming immunitaire et de cette sélection par le système immunitaire du mollusque. Ces infestations bisexuées apporterait un grand avantage pour le parasite puisque la reproduction sexuée ayant lieu au sein de l'hôte vertébré, si des cercaires des deux sexes sortent du mollusque au même moment, elles ont plus de chance de trouver un hôte en même temps et donc de former des couples au sein de ce dernier. De la même façon cette sélection de génotypes différents pourrait augmenter la diversité génétique de la population de parasites (à la manière de ce qui se passe chez le vertébré) et ainsi améliorer le potentiel adaptatif des parasites à leur environnement (Minchella et al. 1995).

- Dans le cas ou une faible diversité génétique des parasites serait rencontrée, le priming immunitaire devrait être très efficace, le premier parasite entrant entraînerait alors une protection qui rendrait le mollusque totalement résistant à la ré-infestation après 7 à 10 jours. Si les rencontres sont peu fréquentes ou les taux de compatibilités très faibles chaque mollusque infesté ne devrait l'être alors que par un nombre limité de sporocystes, le plus souvent un seul génotype devrait être retrouvé chez le mollusque. Certaines données d'études sur le terrain présentent des valeurs qui vont dans le sens de cette hypothèse. D'autres données présentent des résultats différents avec un nombre plus important de parasites par mollusques (voir pour revue (Eppert et al. 2002) et Table 1). Ainsi les données de terrain concernant Dionisio (Eppert et al. 2002), le Mali (Dabo et al. 1997), et la Guadeloupe (Sire et al. 1999) présentent des intensités moyennes de 1,79 ; 1,34 ; et 1,14 respectivement, soit un plus grand nombre de mollusques infestés par un seul génotype (46%, 74% et 88% respectivement. En revanche les données de Cabana et Barreiro (Minchella et al. 1995) présentent une plus faible proportion de mollusques infestés par un seul génotype (43%) mais surtout une intensité très élevée (3.29) (Table 1). Quoi qu'il en soit il est difficile de conclure car de nombreux facteurs peuvent être responsables de ces résultats. D'une part les taux de compatibilité qui en milieu naturel et selon la localité pourrait être très faibles, les parasites n'auraient donc que peu de chance de se développer dans un hôte, mais également le taux de rencontre pouvant être très faible. La durée de vie des mollusques infestés n'est que de quelques mois cela limite donc la possibilité de rencontrer plusieurs parasites (Theron et al. 2004). Tous ces paramètres sont à prendre en compte pour comprendre la dynamique des populations d'hôtes et de parasites. Il faudrait donc pouvoir intégrer tout ceci dans un modèle afin de pouvoir faire varier chaque paramètre indépendamment en fonction des données récupérées sur le terrain.

Les deux hypothèses développées ci-dessus ne sont en fait pas exclusives, et on peut les considérer toutes les deux comme deux instants indépendants dans la lutte que se livrent les hôtes et les parasites. Dans la première, le parasite à pris un avantage sur l'hôte par sa diversité génétique lui permettant d'augmenter sa capacité d'adaptation et sa transmission. Dans la seconde c'est le mollusque qui a pris le dessus en mettant en place une stratégie immunitaire permettant de limiter la transmission du parasite. Cette course aux armements où s'affrontent les mécanismes de défense de l'hôte et les mécanismes d'infectivité du parasite peut se voir comme une balance oscillant tantôt en faveur de l'hôte, tantôt en faveur du parasite. Du fait de l'histoire co-évolutive concernant l'interaction entre les schistosomes et leurs hôtes intermédiaires on peut imaginer être à différent moment de cette course aux armements en fonction de la localité géographique et des pressions sélectives environnementales (biotiques et abiotiques) rencontrées aussi bien par le parasite que par l'hôte (Morgan et al. 2001). L'histoire co-évolutive entre *Schistosoma* et *Biomphalaria* sur le continent africain remonte à environ 10 millions d'années si l'on considère l'espèce *Schistosoma mansoni*. En revanche, son arrivée sur le continent Sud Américain est beaucoup plus récente et se trouve être concomitante avec la traite négrière qui débuta au 16^{ième} siècle et se poursuivit jusqu'au 19^{ième} siècle. Ces différents timing et les histoires de vie de chacun des hôtes (*B. alexandrina* et *B. pfeifferi* en Afrique et *B. glabrata* en Amérique du Sud) et de leurs parasites peuvent expliquer ces différences de stratégies et l'orientation de la balance co-évolutive. Il parait donc nécessaire d'étudier de manière indépendante chaque site afin de récolter des données et de les implémenter dans un modèle afin de comprendre de manière plus globale l'impact du priming immunitaire sur la dynamique des populations d'hôtes et de parasites.

En Conclusion

Le but de ce travail de thèse était d'étudier le phénomène observé par Sire *et al.* en 1998 et de conclure sur l'existence d'un priming immunitaire chez *B. glabrata* face à *S. mansoni*. Puis la seconde étape était de caractériser ce priming immunitaire d'un point de vue mécanistique et phénotypique. Et nous avons réussi, en effet au cours de ce travail de thèse nous avons pu démontrer que l'immunité du mollusque *Biomphalaria glabrata* possédait une composante « mémorielle » avec un phénomène de priming immunitaire. Ainsi nous avons pu mettre en évidence que ce priming était spécifique et dépendant du développement du parasite primo-entrant. Nous avons également pu mettre en lumière les premiers facteurs humoraux

responsables de ce priming immunitaire. Il s'agit pour la plus part de molécules de reconnaissance (lectines) pouvant jouer un rôle dans la reconnaissance spécifique en formant des complexes immuns responsables du haut niveau de spécificité observé. La résolution de ces questions concernant le priming immunitaire chez *B. glabrata* est une avancée cruciale dans la compréhension des processus immunitaire chez les invertébrés tant au niveau de leur diversité qu'au niveau de leur évolution. Ce travail constitue un pavé supplémentaire à l'édifice de l'évolution des systèmes immunitaires depuis les Ecdysozoaires jusqu'aux Deutérostomiens.

Bibliographie

BIBLIOGRAPHIE

Abu-Shakra M, Buskila D, Shoenfeld Y (1999) Molecular mimicry between host and pathogen: examples from parasites and implication. Immunol Lett 67(2): 147-152.

Adema CM, Hertel LA, Miller RD, Loker ES (1997) A family of fibrinogen-related proteins that precipitates parasite-derived molecules is produced by an invertebrate after infection. Proc Natl Acad Sci U S A 94(16): 8691-8696.

Adema CM, Hanington PC, Lun CM, Rosenberg GH, Aragon AD et al. (2010) Differential transcriptomic responses of Biomphalaria glabrata (Gastropoda, Mollusca) to bacteria and metazoan parasites, Schistosoma mansoni and Echinostoma paraensei (Digenea, Platyhelminthes). Molecular Immunology 47(4): 849-860.

Allienne JF, Theron A, Gourbal B (2011) Recovery of primary sporocysts in vivo in the Schistosoma mansoni/Biomphalaria glabrata model using a simple fixation method suitable for extraction of genomic DNA and RNA. Exp Parasitol 129(1): 11-16.

Asano Y, Hirose S, Iwayama S, Miyata T, Yazaki T et al. (1982) Protective Effect of Immediate Inoculation of a Live Varicella Vaccine in Household Contacts in Relation to the Viral Dose and Interval between Exposure and Vaccination. Biken Journal 25(1): 43-45.

Baron OL, Reichhart JM, van West P, Industri B, Ponchet M et al. (2013) Parental transfer of potent immune protection in an inverbreate. PLoS Pathog: submitted.

Baruah K, Ranjan J, Sorgeloos P, MacRae TH, Bossier P (2011) Priming the prophenoloxidase system of Artemia franciscana by heat shock proteins protects against Vibrio campbellii challenge. Fish & Shellfish Immunology 31(1): 134-141.

Bech N, Beltran S, Portela J, Rognon A, Allienne J-F et al. (2010) Follow-up of the genetic diversity and snail infectivity of a Schistosoma mansoni strain from field to laboratory. Infection Genetics and Evolution 10(7): 1039-1045.

Beltran S, Cezilly F, Boissier J (2008) Genetic Dissimilarity between Mates, but Not Male Heterozygosity, Influences Divorce in Schistosomes. Plos One 3(10).

Beltran S, Gourbal B, Boissier J, Duval D, Kieffer-Jaquinod S et al. (2010) Vertebrate host protective immunity drives genetic diversity and antigenic polymorphism in Schistosoma mansoni. J Evol Biol 24(3): 554-572.

Beltran S, Gourbal B, Boissier J, Duval D, Kieffer-Jaquinod S et al. (2011) Vertebrate host protective immunity drives genetic diversity and antigenic polymorphism in Schistosoma mansoni. J Evol Biol 24(3): 554-572.

Benacerraf B (1980) The role of MHC gene products in immune regulation and its relevance to alloreactivity. Nobel lecture.

Bender RC, Broderick EJ, Goodall CP, Bayne CJ (2005) Respiratory burst of *Biomphalaria glabrata* hemocytes: *Schistosoma mansoni*-resistant snails produce more extracellular H2O2 than susceptible snails. The Journal of parasitology 91(2): 275-279.

Bernatchez L, Landry C (2003) MHC studies in nonmodel vertebrates: what have we learned about natural selection in 15 years? J Evol Biol 16(3): 363-377.

Best A, Tidbury H, White A, Boots M (2012) The evolutionary dynamics of within-generation immune priming in invertebrate hosts.

Bloom BR (1976) Immunological Functions of T-Cell Subpopulations. Int J Lepr Other Mycobact Dis 44(4): 553-554.

Bodnar AG (2009) Marine invertebrates as models for aging research. Exp Gerontol 44(8): 477-484.

Boissier J (2001) Sexe et schistosome : écologie des interactions hôte-parasite et parasite-parasite: Université de Perpignan. 391 p.

Bouchut A, Coustau C, Gourbal B, Mitta G (2007) Compatibility in the Biomphalaria glabrata/Echinostoma caproni model: new candidate genes evidenced by a suppressive subtractive hybridization approach. Parasitology 134: 575-588.

Brites D, McTaggart S, Morris K, Anderson J, Thomas K et al. (2008) The Dscam homologue of the crustacean *Daphnia* is diversified by alternative splicing like in insects. Molecular biology and evolution 25(7): 1429-1439.

Cannon JP, Haire RN, Litman GW (2002) Identification of diversified genes that contain immunoglobulin-like variable regions in a protochordate. Nature Immunology 3(12): 1200-1207.

Cannon JP, Haire RN, Rast JP, Litman GW (2004) The phylogenetic origins of the antigen-binding receptors and somatic diversification mechanisms. Immunological Reviews 200: 12-22.

Cavalcanti MGS, Filho FC, Mendonca AMB, Duarte GR, Barbosa C et al. (2012) Morphological characterization of hemocytes from Biomphalaria glabrata and Biomphalaria straminea. Micron 43(2-3): 285-291.

Chou PH, Chang HS, Chen IT, Lin HY, Chen YM et al. (2009) The putative invertebrate adaptive immune protein Litopenaeus vannamei Dscam (LvDscam) is the first reported Dscam to lack a transmembrane domain and cytoplasmic tail. Developmental and Comparative Immunology 33(12): 1258-1267.

Chumkhunthod P, Rodtong S, Lambert SJ, Fordham-Skelton AP, Rizkallah PJ et al. (2006) Purification and characterization of an N-acetyl-D-galactosamine-specific lectin from the edible mushroom Schizophyllum commune. Biochim Biophys Acta 1760(3): 326-332.

Cooper EL, Rinkevich B, Uhlenbruck G, Valembois P (1992) Invertebrate immunity: another viewpoint. Scandinavian journal of immunology 35(3): 247-266.

Coustau C, Mitta G, Dissous C, Guillou F, Galinier R et al. (2003) Schistosoma mansoni and Echinostoma caproni excretory-secretory products differentially affect gene expression in Biomphalaria glabrata embryonic cells. Parasitology 127: 533-542.

Criscitiello MF, de Figueiredo P (2013) Fifty Shades of Immune Defense. PLoS Pathog 9(2): 5.

Dabo A, Durand P, Morand S, Diakite M, Langand J et al. (1997) Distribution and genetic diversity of Schistosoma haematobium within its bulinid intermediate hosts in Mali. Acta Tropica 66(1): 15-26.

Damian RT (1987) Molecular Mimicry Revisited. Parasitol Today 3(9): 263-266.

Daniel BE, Preston TM, Southgate VR (1992) The Invitro Transformation of the Miracidium to the Mother Sporocyst of Schistosoma-Margrebowiei - Changes in the Parasite Surface and Implications for Interactions with Snail Plasma Factors. Parasitology 104: 41-49.

Daoust SP, Rau ME, McLaughlin JD (2012) Plagiorchis elegans (Trematoda) Induces Immune Response in an Incompatible Snail Host Biomphalaria glabrata (Pulmonata: Planorbidae). Journal of Parasitology 98(5): 1021-1022.

Dausset J, Colombani J, Legrand L, Feingold N, Rapaport FT (1970) Genetic and Biological Aspects of the HL-A System of Human Histocompatibility. pp. 591-612.

Davies SJ, Chapman T (2006) Identification of genes expressed in the accessory glands of male Mediterranean Fruit Flies (Ceratitis capitata). Insect biochemistry and molecular biology 36(11): 846-856.

Deleury E, Dubreuil G, Elangovan N, Wajnberg E, Reichhart JM et al. (2012) Specific versus Non-Specific Immune Responses in an Invertebrate Species Evidenced by a Comparative de novo Sequencing Study. Plos One 7(3).

Depczynski M, Bellwood DR (2005) Shortest recorded vertebrate lifespan found in a coral reef fish. Curr Biol 15(8): R288-R289.

Dishaw LJ, Mueller MG, Gwatney N, Cannon JP, Haire RN et al. (2008) Genomic complexity of the variable region-containing chitin-binding proteins in amphioxus. BMC Genet 9: 16.

Disis ML, Schiffman K, Guthrie K, Salazar LG, Knutson KL et al. (2004) Effect of dose on immune response in patients vaccinated with an HER-2/neu intracellular domain protein-based vaccine. Journal of Clinical Oncology 22(10): 1916-1925.

Dong YM, Taylor HE, Dimopoulos G (2006) AgDscam, a hypervariable immunoglobulin domain-containing receptor of the Anopheles gambiae innate immune system. PLoS Biol 4(7): 1137-1146.

Du Pasquier L (2001) The immune system of invertebrates and vertebrates. Comp Biochem Physiol B-Biochem Mol Biol 129(1): 1-15.

Du Pasquier L (2004) Speculations on the origin of the vertebrate immune system. Immunol Lett 92(1-2): 3-9.

Dumont M, Mone H, Mouahid G, Idris MA, Shaban M et al. (2007) Influence of pattern of exposure, parasite genetic diversity and sex on the degree of protection against reinfection with Schistosoma mansoni. Parasitology Research 101(2): 247-252.

Duvauxmiret O, Stefano GB, Smith EM, Dissous C, Capron A (1992) Immunosuppression in the Definitive and Intermediate Hosts of the Human Parasite Schistosoma-Mansoni by Release of Immunoactive Neuropeptides. Proc Natl Acad Sci U S A 89(2): 778-781.

Edelman GM (1959) Dissociation of γ-globulin. J Am Chem Soc 81: 3155-3156.

Edelman GM, Ovary Z, Benacerraf B, Poulik MD (1961) Structural Differences among Antibodies of Different Specificities. Proc Natl Acad Sci U S A 47(11): 1751-&.

Ehrlich P (1900) Toxines et Antitoxines. Transactions of the International Medical Congress : XIII Congrès International de Mèdecine: 28-33.

Endo Y, Mitsui K, Motizuki M, Tsurugi K (1987) The mechanism of action of ricin and related toxic lectins on eukaryotic ribosomes. The site and the characteristics of the modification in 28 S ribosomal RNA caused by the toxins. J Biol Chem 262(12): 5908-5912.

Eppert A, Lewis FA, Grzywacz C, Coura P, Caldas I et al. (2002) Distribution of schistosome infections in molluscan hosts at different levels of parasite prevalence. Journal of Parasitology 88(2): 232-236.

Faro MJ, Perazzini M, Correa Ldos R, Mello-Silva CC, Pinheiro J et al. (2013) Biological, biochemical and histopathological features related to parasitic castration of Biomphalaria glabrata infected by Schistosoma mansoni. Exp Parasitol 134(2): 228-234.

Faulhaber LM, Karp RD (1992) A Diphasic Immune-Response against Bacteria in the American Cockroach. Immunology 75(2): 378-381.

Finstad J, Good RA (1964) Evolution of Immune Response .3. Immunologic Responses in Lamprey. Journal of Experimental Medicine 120(6): 1151-&.

Franchini A, Ottaviani E (2000) Repair of molluscan tissue injury: role of PDGF and TGF-beta. Tissue & Cell 32(4): 312-321.

Frey SE, Newman FK, Cruz J, Shelton WB, Tennant JM et al. (2002) Dose-related effects of smallpox vaccine. New England Journal of Medicine 346(17): 1275-1280.

Fujii N, Minetti CA, Nakhasi HL, Chen SW, Barbehenn E et al. (1992) Isolation, cDNA cloning, and characterization of an 18-kDa hemagglutinin and amebocyte aggregation factor from Limulus polyphemus. J Biol Chem 267(31): 22452-22459.

Garcia AB, Pierce RJ, Gourbal B, Werkmeister E, Colinet D et al. (2010) Involvement of the Cytokine MIF in the Snail Host Immune Response to the Parasite Schistosoma mansoni. PLoS Pathog 6(9): 16.

Goloboff PA, Catalano SA, Mirande JM, Szumik CA, Arias JS et al. (2009) Phylogenetic analysis of 73 060 taxa corroborates major eukaryotic groups. Cladistics 25(3): 211-230.

Gonzalez-Tokman DM, Gonzalez-Santoyo I, Lanz-Mendoza H, Cordoba Aguilar A (2010) Territorial damselflies do not show immunological priming in the wild. Physiological Entomology 35(4): 364-372.

Gourbal BEF, Gabrion C (2006) Histomorphological study of the preputial and clitoral glands in BALB/c mice with experimental Taenia crassiceps infections. Journal of Parasitology 92(1): 189-192.

Granath WO, Yoshino TP (1984) Schistosoma-Mansoni - Passive Transfer of Resistance by Serum in the Vector Snail, Biomphalaria-Glabrata. Experimental Parasitology 58(2): 188-193.

Guillou F, Mitta G, Dissous C, Pierce R, Coustau C (2004) Use of individual polymorphism to validate potential functional markers: case of a candidate lectin (BgSel) differentially expressed in susceptible and resistant strains of Biomphalaria glabrata. Comparative Biochemistry and Physiology B-Biochemistry & Molecular Biology 138(2): 175-181.

Guillou F, Roger E, Moné Y, Rognon A, Grunau C et al. (2007) Excretory-secretory proteome of larval *Schistosoma mansoni* and *Echinostoma caproni*, two parasites of *Biomphalaria glabrata*. Molecular and Biochemical Parasitology 155: 45-56.

Guo P, Hirano M, Herrin BR, Li JX, Yu CL et al. (2009) Dual nature of the adaptive immune system in lampreys. Nature 459(7248): 796-U791.

Hagen M, Filosa MF, Youson JH (1985) The Immune-Response in Adult Sea Lamprey (Petromyzon-Marinus L) - the Effect of Temperature. Comp Biochem Physiol A-Physiol 82(1): 207-210.

Hahn UK, Bender RC, Bayne CJ (2000) Production of reactive oxygen species by hemocytes of Biomphalaria glabrata: carbohydrate-specific stimulation. Dev Comp Immunol 24(6-7): 531-541.

Hahn UK, Bender RC, Bayne CJ (2001) Killing of Schistosoma mansoni sporocysts by hemocytes from resistant Biomphalaria glabrata: role of reactive oxygen species. The Journal of parasitology 87(2): 292-299.

Hamilton C, Lejeune BT, Rosengaus RB (2011) Trophallaxis and prophylaxis: social immunity in the carpenter ant Camponotus pennsylvanicus. Biology Letters 7(1): 89-92.

Hanelt B, Lun CM, Adema CM (2008) Comparative ORESTES-sampling of transcriptomes of immune-challenged Biomphalaria glabrata snails. Journal of Invertebrate Pathology 99(2): 192-203.

Hangartner S, Sbilordo SH, Michalczyk L, Gage MJ, Martin OY (2013) Are there genetic trade-offs between immune and reproductive investments in Tribolium castaneum? Infect Genet Evol 19C: 45-50.

Hanington PC, Zhang SM (2011) The Primary Role of Fibrinogen-Related Proteins in Invertebrates Is Defense, Not Coagulation. J Innate Immun 3(1): 17-27.

Hanington PC, Lun CM, Adema CM, Loker ES (2010a) Time series analysis of the transcriptional responses of Biomphalaria glabrata throughout the course of intramolluscan development of Schistosoma mansoni and Echinostoma paraensei. International Journal for Parasitology 40(7): 819-831.

Hanington PC, Forys MA, Dragoo JW, Zhang SM, Adema CM et al. (2010b) Role for a somatically diversified lectin in resistance of an invertebrate to parasite infection. Proc Natl Acad Sci U S A 107(49): 21087-21092.

Hathaway JJM, Adema CM, Stout BA, Mobarak CD, Loker ES (2010) Identification of protein components of egg masses indicates parental investment in immunoprotection of offspring by Biomphalaria glabrata (Gastropoda, Mollusca). Developmental and Comparative Immunology 34(4): 425-435.

Hauton C, Smith VJ (2007) Adaptive immunity in invertebrates: a straw house without a mechanistic foundation. Bioessays 29(11): 1138-1146.

Hildemann WH, Raison RL, Cheung G, Hull CJ, Akaka L et al. (1977) Immunological Specificity and Memory in a Scleractinian Coral. Nature 270(5634): 219-223.

Homvises T, Tassanakajon A, Somboonwiwat K (2010) Penaeus monodon SERPIN, PmSERPIN6, is implicated in the shrimp innate immunity. Fish & shellfish immunology 29(5): 890-898.

Howard JC (1991) Disease and evolution. Nature 352(6336): 565-567.

Hui X, Li H, Zhou Z, Lam KS, Xiao Y et al. (2010) Adipocyte fatty acid-binding protein modulates inflammatory responses in macrophages through a positive feedback loop involving c-Jun NH2-terminal kinases and activator protein-1. J Biol Chem 285(14): 10273-10280.

Janeway CA (1989) Approaching the Asymptote - Evolution and Revolution in Immunology. Cold Spring Harbor Symposia on Quantitative Biology 54: 1-13.

Janeway CA, Medzhitov R (1998) Introduction: The role of innate immunity in the adaptive immune response. Seminars in Immunology 10(5): 349-350.

Janeway CA, Medzhitov R (2002) Innate immune recognition. Annual Review of Immunology 20: 197-216.

Johnson KN, van Hulten MCW, Barnes AC (2008) "Vaccination" of shrimp against viral pathogens: Phenomenology and underlying mechanisms. Vaccine 26(38): 4885-4892.

Jourdane J, Théron A (1987) Larval development : eggs to cercariae. The Biology of Schistosomes. pp. 83-113.

Kasthuri SR, Premachandra HK, Umasuthan N, Whang I, Lee J (2013) Structural characterization and expression analysis of a beta-thymosin homologue (Tbeta) in disk abalone, Haliotis discus discus. Gene 527(1): 376-383.

Kinnula K, Linnainmaa K, Raivio KO, Kinnula VL (1998) Endogenous antioxidant enzymes and glutathione S-transferase in protection of mesothelioma cells against hydrogen peroxide and epirubicin toxicity. British journal of cancer 77(7): 1097-1102.

Kiss T (2010) Apoptosis and its functional significance in molluscs. Apoptosis 15(3): 313-321.

Knapp O SB, Popoff M. R (2010) The Aerolysin-Like Toxin Family of Cytolytic, Pore-Forming Toxins. The Open Toxinology Journal 3: 53-68.

Koene JM, Sloot W, Montagne-Wajer K, Cummins SF, Degnan BM et al. (2010) Male accessory gland protein reduces egg laying in a simultaneous hermaphrodite. PloS one 5(4): e10117.

Konrad M, Vyleta ML, Theis FJ, Stock M, Tragust S et al. (2012) Social Transfer of Pathogenic Fungus Promotes Active Immunisation in Ant Colonies. PLoS Biol 10(4): 15.

Kubo T, Komano H, Okada M, Natori S (1984) Identification of Hemagglutinating Protein and Bactericidal Activity in the Hemolymph of Adult Sarcophaga-Peregrina on Injury of the Body Wall. Developmental and Comparative Immunology 8(2): 283-291.

Kurtz J (2004) Memory in the innate and adaptive immune systems. Microbes and Infection 6(15): 1410-1417.

Kurtz J (2005) Specific memory within innate immune systems. Trends in Immunology 26(4): 186-192.

Kurtz J, Franz K (2003) Evidence for memory in invertebrate immunity. Nature 425(6953): 37-38.

Lavine MD, Strand MR (2002) Insect hemocytes and their role in immunity. Insect biochemistry and molecular biology 32(10): 1295-1309.

Litman GW (2006) How Botryllus chooses to fuse. Immunity 25(1): 13-15.

Litman GW, Cannon JP, Dishaw LJ (2005) Reconstructing immune phylogeny: New perspectives. Nat Rev Immunol 5(11): 866-879.

Little TJ, Kraaijeveld AR (2004) Ecological and evolutionary implications of immunological priming in invertebrates. Trends in Ecology & Evolution 19(2): 58-60.

Little TJ, Hultmark D, Read AF (2005) Invertebrate immunity and the limits of mechanistic immunology. Nature Immunology 6(7): 651-654.

Little TJ, O'Connor B, Colegrave N, Watt K, Read AF (2003) Maternal transfer of strain-specific immunity in an invertebrate. Curr Biol 13(6): 489-492.

Lockyer AE, Spinks J, Kane RA, Hoffmann KF, Fitzpatrick JM et al. (2008) Biomphalaria glabrata transcriptome: cDNA microarray profiling identifies resistant- and susceptible-specific gene expression in haemocytes from snail strains exposed to Schistosoma mansoni. Bmc Genomics 9.

Lockyer AE, Emery AM, Kane RA, Walker AJ, Mayer CD et al. (2012) Early Differential Gene Expression in Haemocytes from Resistant and Susceptible Biomphalaria glabrata Strains in Response to Schistosoma mansoni. Plos One 7(12): 16.

Loker ES, Adema CM (1995) Schistosomes, Echinostomes and Snails - Comparative Immunobiology. Parasitol Today 11(3): 120-124.

Loker ES, Adema CM, Zhang SM, Kepler TB (2004) Invertebrate immune systems - not homogeneous, not simple, not well understood. Immunological Reviews 198: 10-24.

Longdon B, Cao C, Martinez J, Jiggins FM (2013) Previous Exposure to an RNA Virus Does Not Protect against Subsequent Infection in <italic>Drosophila melanogaster</italic>. PLoS ONE 8(9): e73833.

Mattos ACA, Kusel JR, Pimenta PFP, Coelho PMZ (2006) Activity of praziquantel on in vitro transformed Schistosoma mansoni sporocysts. Mem Inst Oswaldo Cruz 101: 283-287.

Matzinger P (1994) Tolerance, Danger, and the Extended Family. Annual Review of Immunology 12: 991-1045.

Mauri C, Bosma A (2012) Immune Regulatory Function of B Cells. pp. 221-241.

McNamara KB, Wedell N, Simmons LW (2013) Experimental evolution reveals trade-offs between mating and immunity. Biology letters 9(4): 20130262.

Medzhitov R (2009) Approaching the Asymptote: 20 Years Later. Immunity 30(6): 766-775.

Medzhitov R, Janeway CA (1997) Innate immunity: The virtues of a nonclonal system of recognition. Cell 91(3): 295-298.

Medzhitov R, Janeway CA (2002) Decoding the patterns of self and nonself by the innate immune system. Science 296(5566): 298-300.

Miller J, Sprent J (1971) Cell-to-Cell Interaction in Immune Response .6. Contribution of Thymus-Derived Cells and Antibody-Forming Cell Precursors to Immunological Memory. Journal of Experimental Medicine 134(1): 66-&.

Miller JFA (1963) Role of Thymus in Immunity. British Medical Journal(535): 459-&.

Minchella DJ, Sollenberger KM, Desouza CP (1995) Distribution of Schistosome Genetic Diversity within Molluscan Intermediate Hosts. Parasitology 111: 217-220.

Mone Y, Gourbal B, Duval D, Du Pasquier L, Kieffer-Jaquinod S et al. (2010) A Large Repertoire of Parasite Epitopes Matched by a Large Repertoire of Host Immune Receptors in an Invertebrate Host/Parasite Model. Plos Neglect Trop Dis 4(9): 18.

Moreau J, Martinaud G, Troussard JP, Zanchi C, Moret Y (2012) Trans-generational immune priming is constrained by the maternal immune response in an insect. Oikos 121(11): 1828-1832.

Moret Y (2006) 'Trans-generational immune priming': specific enhancement of the antimicrobial immune response in the mealworm beetle, Tenebrio molitor. Proceedings of the Royal Society B-Biological Sciences 273(1592): 1399-1405.

Moret Y, Siva-Jothy MT (2003) Adaptive innate immunity? Responsive-mode prophylaxis in the mealworm beetle, Tenebrio molitor. Proceedings of the Royal Society of London Series B-Biological Sciences 270(1532): 2475-2480.

Morgan JAT, Dejong RJ, Snyder SD, Mkoji GM, Loker ES (2001) Schistosoma mansoni and Biomphalaria: past history and future trends. Parasitology 123: S211-S228.

Mourao MdM, Dinguirard N, Franco GR, Yoshino TP (2009) Role of the Endogenous Antioxidant System in the Protection of *Schistosoma mansoni* Primary Sporocysts against Exogenous Oxidative Stress. PLoS Negl Trop Dis 3(11): e550.

Mowlds P, Barron A, Kavanagh K (2008) Physical stress primes the immune response of Galleria mellonella larvae to infection by Candida albicans. Microbes and Infection 10(6): 628-634.

Nair SV, Del Valle H, Gross PS, Terwilliger DP, Smith LC (2005) Macroarray analysis of coelomocyte gene expression in response to LPS in the sea urchin. Identification of unexpected immune diversity in an invertebrate. Physiol Genomics 22(1): 33-47.

Netea MG, Quintin J, van der Meer JW (2011) Trained immunity: a memory for innate host defense. Cell host & microbe 9(5): 355-361.

Ni JD, Xiong YZ, Wang XJ, Xiu LC (2013) Does increased hepatitis B vaccination dose lead to a better immune response in HIV-infected patients than standard dose vaccination: a meta-analysis? Int J STD AIDS 24(2): 117-122.

Oda T, Tsuru M, Hatakeyama T, Nagatomo H, Muramatsu T et al. (1997) Temperature- and pH-dependent cytotoxic effect of the hemolytic lectin CEL-III from the marine invertebrate Cucumaria echinata on various cell lines. Journal of biochemistry 121(3): 560-567.

Pan SCT (1996) Schistosoma mansoni: The ultrastructure of larval morphogenesis in Biomphalaria glabrata and of associated host-parasite interactions. Japanese Journal of Medical Science & Biology 49(4): 129-149.

Pancer Z (2000) Dynamic expression of multiple scavenger receptor cysteine-rich genes in coelomocytes of the purple sea urchin. Proc Natl Acad Sci U S A 97(24): 13156-13161.

Pancer Z, Rast JP, Davidson EH (1999) Origins of immunity: transcription factors and homologues of effector genes of the vertebrate immune system expressed in sea urchin coelomocytes. Immunogenetics 49(9): 773-786.

Pancer Z, Amemiya CT, Ehrhardt GRA, Ceitlin J, Gartland GL et al. (2004) Somatic diversification of variable lymphocyte receptors in the agnathan sea lamprey. Nature 430(6996): 174-180.

Park SH, Jiang R, Piao S, Zhang B, Kim EH et al. (2011) Structural and functional characterization of a highly specific serpin in the insect innate immunity. J Biol Chem 286(2): 1567-1575.

Pasteur L (1885) Méthode pour prévenir la rage après morsure. Comptes Rendus C. R. T. 101: 765-772.

Paterson HM, Murphy TJ, Purcell EJ, Shelley O, Kriynovich SJ et al. (2003) Injury primes the innate immune system for enhanced toll-like receptor reactivity. Journal of Immunology 171(3): 1473-1483.

Pereira CA, Martins-Souza RL, Correa A, Jr., Coelho PM, Negrao-Correa D (2008) Participation of cell-free haemolymph of Biomphalaria tenagophila in the defence mechanism against Schistosoma mansoni sporocysts. Parasite immunology 30(11-12): 610-619.

Peter J-P (1979) Les médecins français face au problème de l'inoculation variolique et de sa diffusion (1750-1790). Annales de Bretagne et des pays de l'Ouest: 251-264.

Pham LN, Dionne MS, Shirasu-Hiza M, Schneider DS (2007) A specific primed immune response in Drosophila is dependent on phagocytes. PLoS Pathog 3(3).

Pianka ER (1970) On r and K selection. Am Nat 104: 592-597.

Pinto HA, Melo AL (2013) Biomphalaria straminea and Biomphalaria glabrata (Mollusca: Planorbidae) as New Intermediate Hosts of the Fish Eyefluke Austrodiplostomum compactum (Trematoda: Diplostomidae) in Brazil. Journal of Parasitology 99(4): 729-733.

Pointier JP, Paraense WL, DeJong RJ, Loker ES, Bargues MD et al. (2002) A potential snail host of schistosomiasis in Bolivia: Biomphalaria amazonica Paraense, 1966. Memorias Do Instituto Oswaldo Cruz 97(6): 793-796.

Pope EC, Powell A, Roberts EC, Shields RJ, Wardle R et al. (2011) Enhanced Cellular Immunity in Shrimp (Litopenaeus vannamei) after 'Vaccination'. Plos One 6(6).

Portela J, Duval D, Rognon A, Galinier R, Boissier J et al. (2013) Evidence for Specific Genotype-Dependent Immune Priming in the Lophotrochozoan Biomphalaria glabrata Snail. J Innate Immun 5(3): 261-276.

Porter RR (1973) Structural Studies of Immunoglobulins. pp. 713-716.

Powell A, Pope EC, Eddy FE, Roberts EC, Shields RJ et al. (2011) Enhanced immune defences in Pacific white shrimp (Litopenaeus vannamei) post-exposure to a vibrio vaccine. Journal of Invertebrate Pathology 107(2): 95-99.

Ram KR, Wolfner MF (2009) A network of interactions among seminal proteins underlies the long-term postmating response in Drosophila. Proc Natl Acad Sci U S A 106(36): 15384-15389.

Reber A, Chapuisat M (2012) No Evidence for Immune Priming in Ants Exposed to a Fungal Pathogen. Plos One 7(4): 6.

Redmond MD, Hartson RB, Hoverman JT, De Jesus-Villanuevat CN, Johnson PTJ (2011) Experimental Exposure of Helisoma Trivolvis and Biomphalaria Glabrata (Gastropoda) to Ribeiroia Ondatrae (Trematoda). Journal of Parasitology 97(6): 1055-1061.

Ren Q, Du ZQ, Zhao XF, Wang JX (2009) An acyl-CoA-binding protein (FcACBP) and a fatty acid binding protein (FcFABP) respond to microbial infection in Chinese white shrimp, Fenneropenaeus chinensis. Fish & shellfish immunology 27(6): 739-747.

Rodrigues J (2010) Hemocyte differentiation mediates innate immune memory in Anopheles gambiae mosquitoes (vol 329, pg 1353, 2010). Science 330(6003): 448-448.

Rodrigues J, Brayner FA, Alves LC, Dixit R, Barillas-Mury C (2010) Hemocyte differentiation mediates innate immune memory in Anopheles gambiae mosquitoes. Science 329(5997): 1353-1355.

Roger E, Gourbal B, Grunau C, Pierce RJ, Galinier R et al. (2008a) Expression analysis of highly polymorphic mucin proteins (Sm PoMuc) from the parasite Schistosoma mansoni. Molecular and Biochemical Parasitology 157(2): 217-227.

Roger E, Mitta G, Mone Y, Bouchut A, Rognon A et al. (2008b) Molecular determinants of compatibility polymorphism in the Biomphalaria glabrata/Schistosoma mansoni model: New candidates identified by a global comparative proteomics approach. Molecular and Biochemical Parasitology 157(2): 205-216.

Roger E, Grunau C, Pierce RJ, Hirai H, Gourbal B et al. (2008c) Controlled Chaos of Polymorphic Mucins in a Metazoan Parasite (Schistosoma mansoni) Interacting with Its Invertebrate Host (Biomphalaria glabrata). Plos Neglect Trop Dis 2(11): 20.

Rolff J, Siva-Jothy MT (2003) Invertebrate ecological immunology. Science 301(5632): 472-475.

Rollinson D, Simpson AJG (1987) The biology of Schistosomes : From genes to latrines. 472.

Rossjohn J, Feil SC, McKinstry WJ, Tsernoglou D, Van Der Goot G et al. (1998) Aerolysin - A paradigm for membrane insertion of beta-sheet protein toxins? J Struct Biol 121(2): 92-100.

Roth O, Kurtz J (2009) Phagocytosis mediates specificity in the immune defence of an invertebrate, the woodlouse Porcellio scaber (Crustacea: Isopoda). Developmental and Comparative Immunology 33(11): 1151-1155.

Roth O, Sadd BM, Schmid-Hempel P, Kurtz J (2009) Strain-specific priming of resistance in the red flour beetle, Tribolium castaneum. Proceedings of the Royal Society B-Biological Sciences 276(1654): 145-151.

Roth O, Joop G, Eggert H, Hilbert J, Daniel J et al. (2010) Paternally derived immune priming for offspring in the red flour beetle, Tribolium castaneum. Journal of Animal Ecology 79(2): 403-413.

Rowley AF, Powell A (2007) Invertebrate immune systems-specific, quasi-specific, or nonspecific? Journal of Immunology 179(11): 7209-7214.

Rowley AF, Pope EC (2012) Vaccines and crustacean aquaculture-A mechanistic exploration. Aquaculture 334: 1-11.

Sadd BM, Schmid-Hempel P (2006) Insect immunity shows specificity in protection upon secondary pathogen exposure. Curr Biol 16(12): 1206-1210.

Sadd BM, Schmid-Hempel P (2007) Facultative but persistent transgenerational immunity via the mother's eggs in bumblebees. Curr Biol 17(24): R1046-R1047.

Sadd BM, Kleinlogel Y, Schmid-Hempel R, Schmid-Hempel P (2005) Trans-generational immune priming in a social insect. Biology Letters 1(4): 386-388.

Saelee N, Noonin C, Nupan B, Junkunlo K, Phongdara A et al. (2013) beta-thymosins and hemocyte homeostasis in a crustacean. PloS one 8(4): e60974.

Salzet M, Capron A, Stefano GB (2000) Molecular crosstalk in host-parasite relationships: Schistosome- and leech-host interactions. Parasitol Today 16(12): 536-540.

Schmid-Hempel P (2005) Natural insect host-parasite systems show immune priming and specificity: puzzles to be solved. Bioessays 27(10): 1026-1034.

Schone BR, Fiebig J, Pfeiffer M, Gless R, Hickson J et al. (2005) Climate records from a bivalved Methuselah (Arctica islandica, Mollusca; Iceland). Paleogeogr Paleoclimatol Paleoecol 228(1-2): 130-148.

Schulenburg H, Boehnisch C, Michiels NK (2007) How do invertebrates generate a highly specific innate immune response? Molecular Immunology 44(13): 3338-3344.

Sharma R, Yang Y, Sharma A, Awasthi S, Awasthi YC (2004) Antioxidant role of glutathione S-transferases: protection against oxidant toxicity and regulation of stress-mediated apoptosis. Antioxidants & redox signaling 6(2): 289-300.

Sheehy MRJ, Bannister RCA, Wickins JF, Shelton PMJ (1999) New perspectives on the growth and longevity of the European lobster (Homarus gammarus). Can J Fish Aquat Sci 56(10): 1904-1915.

Sire C, Rognon A, Théron A (1998) Failure of *Schistosoma mansoni* to reinfect *Biomphalaria glabrata* snails : acquired humoral resistance or intra-specific larval antagonism ? Parasitology 117: 117-122.

Sire C, Durand P, Pointier JP, Theron A (1999) Genetic diversity and recruitment pattern of Schistosoma mansoni in a Biomphalaria glabrata snail population: A field study using random-amplified polymorphic DNA markers. Journal of Parasitology 85(3): 436-441.

Smithers SR, Terry RJ (1969) Immunity in Schistosomiasis. AnnNY AcadSci 160(A2): 826-&.

Snell GD (1980) Studies on histocompatibility. Nobel lecture.

Stern AM, Markel H (2005) The history of vaccines and immunization: Familiar patterns, new challenges. Health Aff 24(3): 611-621.

Terwilliger DP, Buckley KM, Mehta D, Moorjani PG, Smith LC (2006) Unexpected diversity displayed in cDNAs expressed by the immune cells of the purple sea urchin, Strongylocentrotus purpuratus. Physiol Genomics 26(2): 134-144.

Theron A, Gerard C, Mone H (1992a) Early enhanced growth of the digestive gland of Biomphalaria glabrata infected with Schistosoma mansoni: side effect or parasite manipulation? Parasitol Res 78(5): 445-450.

Theron A, Mone H, Gerard C (1992b) Spatial and energy compromise between host and parasite: the Biomphalaria glabrata-Schistosoma mansoni system. International journal for parasitology 22(1): 91-94.

Theron A, Sire C, Rognon A, Prugnolle F, Durand P (2004) Molecular ecology of Schistosoma mansoni transmission inferred from the genetic composition of larval and adult infrapopulations within intermediate and definitive hosts. Parasitology 129: 571-585.

Théron A, Gérard C (1994) Development of accessory sexual organs in *Biomphalaria glabrata* (Planorbidae) in relation to timing of infection by *Schistosoma mansoni* : consequences for energy utilization patterns by the parasite. Journal of Molluscan Studies 60: 25-31.

Théron A, Pagès JR, Rognon A (1997) *Schistosoma mansoni* : distribution patterns of Miracidia among *Biomphalaria glabrata* snail as related to host susceptibility and sporocyst regulatory processes. Experimental Parasitology 85(1): 1-9.

Théron A, Rognon A, Pagès JR (1998) Host choice by free larval parasites : a study of *Biomphalaria glabrata* snails and *Schistosoma mansoni* miracidia related to host size. Parasitology Research 84: 727-732.

Thornqvist PO, Johansson MW, Soderhall K (1994) Opsonic activity of cell adhesion proteins and beta-1,3-glucan binding proteins from two crustaceans. Dev Comp Immunol 18(1): 3-12.

Thucydide (-400) Histoire de la guerre du Péloponnèse. Livre 2.

Tidbury HJ, Pedersen AB, Boots M (2011) Within and transgenerational immune priming in an insect to a DNA virus. Proceedings of the Royal Society B-Biological Sciences 278(1707): 871-876.

Tidbury HJ, Best A, Boots M (2012) The epidemiological consequences of immune priming. Proceedings of the Royal Society B-Biological Sciences 279(1746): 4505-4512.

Traniello JFA, Rosengaus RB, Savoie K (2002) The development of immunity in a social insect: Evidence for the group facilitation of disease resistance. Proc Natl Acad Sci U S A 99(10): 6838-6842.

Tunholi-Alves VM, Tunholi VM, Golo P, Lima M, Garcia J et al. (2013) Effects of infection by larvae of Angiostrongylus cantonensis (Nematoda, Metastrongylidae) on the lipid metabolism of the experimental intermediate host Biomphalaria glabrata (Mollusca: Gastropoda). Parasitology Research 112(5): 2111-2116.

Vazquez L, Alpuche J, Maldonado G, Agundis C, Pereyra-Morales A et al. (2009) Immunity mechanisms in crustaceans. Innate Immunity 15(3): 179-188.

Vinkler M, Albrecht T (2011) Phylogeny, longevity and evolution of adaptive immunity. Folia Zool 60(3): 277-282.

Wang JJ, Wang LL, Yang CY, Jiang QF, Zhang H et al. (2013) The response of mRNA expression upon secondary challenge with Vibrio anguillarum suggests the involvement of C-lectins in the immune priming of scallop Chlamys farreri. Developmental and Comparative Immunology 40(2): 142-147.

Wang XW, Wang JX (2013) Pattern recognition receptors acting in innate immune system of shrimp against pathogen infections. Fish & shellfish immunology 34(4): 981-989.

Watson FL, Puttmann-Holgado R, Thomas F, Lamar DL, Hughes M et al. (2005) Extensive diversity of Ig-superfamily proteins in the immune system of insects. Science 309(5742): 1874-1878.

Whitfield AE, Rotenberg D, Aritua V, Hogenhout SA (2011) Analysis of expressed sequence tags from Maize mosaic rhabdovirus-infected gut tissues of Peregrinus maidis reveals the presence of key components of insect innate immunity. Insect molecular biology 20(2): 225-242.

Witteveldt J, Cifuentes CC, Vlak JM, van Hulten MlCW (2004) Protection of Penaeus monodon against White Spot Syndrome Virus by Oral Vaccination. pp. 2057-2061.

Wu LT, Chu KH (2010) Characterization of an ovary-specific glutathione peroxidase from the shrimp Metapenaeus ensis and its role in crustacean reproduction. Comp Biochem Physiol B Biochem Mol Biol 155(1): 26-33.

Zanchi C, Troussard JP, Martinaud G, Moreau J, Moret Y (2011) Differential expression and costs between maternally and paternally derived immune priming for offspring in an insect. Journal of Animal Ecology 80(6): 1174-1183.

Zanker KS (2010) Immunology of Invertebrates: Humoral. Encyclopedia of Life Sciences John Wiley & Sons, Ltd: Chichester(DOI: 10.1002/9780470015902.a0000522.pub2).

Zhang SM, Leonard PM, Adema CM, Loker ES (2001) Parasite-responsive IgSF members in the snail Biomphalaria glabrata: characterization of novel genes with tandemly arranged IgSF domains and a fibrinogen domain. Immunogenetics 53(8): 684-694.

Zhang SM, Adema CM, Kepler TB, Loker ES (2004) Diversification of Ig superfamily genes in an invertebrate. Science 305(5681): 251-254.

Zhang SM, Nian H, Wang B, Loker ES, Adema CM (2009) Schistosomin from the snail Biomphalaria glabrata: expression studies suggest no involvement in trematode-mediated castration. Mol Biochem Parasitol 165(1): 79-86.

Zheng X, Xia Y (2012) beta-1,3-Glucan recognition protein (betaGRP) is essential for resistance against fungal pathogen and opportunistic pathogenic gut bacteria in Locusta migratoria manilensis. Dev Comp Immunol 36(3): 602-609.

Annexes

ANNEXES

Production hors thèse :

Annexe 1 : Mating systems and evolution of morpho-anatomical features in Schistosomatidae.

Beltran S, Desdevises Y, Portela J and Boissier J. BMC Evolutionary Biology. 2010

Annexe 2 : Follow-up of the genetic diversity and a parasite life history trait of a *Schistosoma mansoni* strain from field to laboratory.

Bech N, Beltran S, Portela J, Allienne JF, Rognon A, Boissier J and Theron A. Infection, Genetic and Evolution. 2010

Annexe 3 : Whole-genome *in-silico* substractive hybridization (WISH) – using massive sequencing for the identification of unique and repetitive sex-specific sequences: the exemple of *Schistosoma mansoni.*

Portela J, Grunau C, Cosseau C, Beltran S, Dantec C, Parrinello H, and Boissier J. BMC Genomic. 2010

Annexe 4 : Trioxaquine PA1259 alkylates heme in the blood-feeding parasite *Schistosoma mansoni.*

Pradines V, Portela J, Boissier J, Coslédan F, Meunier B and Robert A. Antimicrobial Agents and Chemotherapy. 2011

Annexe 5 : Activity of trioxaquine PA1259 in mice infected by *Schistosoma mansoni.*

Boissier J, Portela J, Pradines V, Coslédan F, Robert A, Meunier B. Comptes Rendus Chimie. 2012

Annexe 6 : Antischistosomal activity of trioxaquines : *in vivo* efficacy and mechanism of action on *Schistosoma mansoni.*

Portela J, Boissier J, Gourbal B, Pradines V, Collière V, Coslédan F, Meunier B, Robert A. PLoS Neglected Tropical Diseases. 2012

Annexe 7 : Chromatin structure changes around satellite repeats on the *Schistosoma mansoni* female sex chromosome suggest a possible mechanism for sex chromosome emergence

Lepesant JM, Cosseau C, Boissier J, Freitag M, Portela J, Climent D, Perrin C, Zerlotini A, Grunau C. Genome Biology. 2012

BMC Evolutionary Biology

RESEARCH ARTICLE Open Access

Mating system drives negative associations between morphological features in *Schistosomatidae*

Sophie Beltran[1*], Yves Desdevises[2], Julien Portela[1], Jérôme Boissier[1*]

Abstract

Background: Sexual morphological features are known to be associated with the mating systems of several animal groups. However, it has been suggested that morphological features other than sexual characteristics could also be constrained by the mating system as a consequence of negative associations. *Schistosomatidae* are parasitic organisms that vary in mating system and can thus be used to explore links between the mating system and negative associations with morphological features.

Results: A comparative analysis of *Schistosomatidae* morphological features revealed an association between the mating system (monogamous *versus* polygynandrous) and morphological characteristics of reproduction, nutrition, and locomotion.

Conclusions: The mating system drives negative associations between somatic and sexual morphological features. In monogamous species, males display a lower investment in sexual tissues and a higher commitment of resources to tissues involved in female transport, protection, and feeding assistance. In contrast, males of polygynandrous species invest to a greater extent in sexual tissues at the cost of reduced commitment to female care.

Background

A mating system reflects the manner in which members of an animal society are structured with respect to sexual behaviour. Three mating systems are generally recognised: monogamy, polygamy, and polygynandry (or promiscuity). In monogamous species, males and females have only one sexual partner at any given time. In polygamous species, one male has a mating relationship with several females (*i.e.*, polygyny) or one female has a mating relationship with several males (*i.e.*, polyandry). Finally, polygynandry is a mating system in which any male mates with any female. Specific morphological features are known to be associated with the mating systems of several animal groups, including primates [1,2], bats [3], birds [4-6], rodents [7], teleost fishes [8], amphibians [9], and insects [10,11]. Logically, as a consequence of sexual selection, such morphological features mainly involve primary or secondary sexual characteristics. However, it has been suggested that morphological features other than such characteristics could also be constrained by the mating system, reflecting evolutionary trade-offs between effective mating and bodily phenotype [3]. Previous authors indicated that males of bat species with mating systems based on female promiscuity had smaller brains and larger testes, whereas species with mating systems involving female fidelity were endowed with larger brains and smaller testes. This pattern was interpreted as an investment trade-off between two metabolically expensive organs [3]. Such an "expensive sexual tissue" hypothesis proposes that more intense sexual selection will affect the evolution of energy-demanding tissue and associated functions as a result of negative association with costly sexual organs, ornaments or armaments [3]. Although this hypothesis has been proven in bats [3], no such link has been demonstrated in mammals [12].

Schistosomes (Trematoda: Schistosomatidae) are endoparasites of birds and mammals [13]. The ~100 species of schistosomes are unusual among the ~18,000

* Correspondence: beltran.sophie@hotmail.fr; boissier@univ-perp.fr
[1]Laboratoire de Parasitologie Fonctionnelle et Evolutive, Centre de Biologie et d'Écologie Tropicale et Méditerranéenne, UMR 5244 CNRS-UPVD, 52 Avenue Paul Alduy, 66860 Perpignan Cedex, France
Full list of author information is available at the end of the article

species of the subclass Digenea because, unlike other digeneans (which are usually hermaphroditic), schistosomes are of two separate sexes. More importantly, schistosomes are the only parasitic organisms that show variability in mating systems. Three such systems have been identified in these worms [14]: (1) Monogamy occurs in ~30 species and, in these species, worm pairs consisting of only one female and only one male can be observed either *in vivo* or after experimental recovery. Moreover, the monogamous female needs the continuous presence of a male to maintain sexual activity, making monogamy compulsory. However, monogamy does not imply faithfulness. Mate changes can occur, as have been shown in the genus *Schistosoma* [15,16]; this means that schistosomes are socially but not genetically monogamous [17]. (ii) Polygyny occurs in ~4 species and, in these species, one male monopolizes more than one female, with other males having no access to these females. (iii) Polygynandry occurs in ~66 species; males and females are never seen *in copula in vivo* (*i.e.*, males and females mate with several partners of the opposite sex over a given period of time). In contrast to monogamous female schistosomes, polygynandrous females are able to attain sexual maturity and to lay eggs even if a male is not continuously present [18]. Schistosomes are therefore the only parasitic organisms that can be used to explore possible links between a chosen mating system and a negative association with a morphological feature. The goals of the present work are (i) to determine if, as a consequence of mate competition, male polygynandrous schistosomes invest more energy (as measured by testis size) in their reproductive organs than do monogamous males; and (ii) to establish whether any negative association between investment in sexual and somatic tissues can be identified. Our prediction was that the larger the investment in sexual tissue, the smaller would be the investment in locomotor and nutritive functions, as measured by relative sucker size and oesophagus length, respectively.

Methods

Data collection

A total of 28 species were included in this study, a number that is limited by DNA sequence information required for the phylogenetic reconstruction used in the comparative analyses. Nineteen species from six genera are monogamous, and nine species from six genera are polygynandrous. DNA sequence information is available for only two polygynous species, which were therefore not included in the analysis. Data on morphological features were collected from published parasite descriptions; these measurements are summarized in Additional file 1, Table S1. The surface area of each organ was calculated from the length (l) and the width (w) of the organ using the ellipsis surface area formula ($l \times w \times \pi/4$). The relative organ length is the length of the organ divided by the body length, and the relative organ surface area is the surface area of the organ divided by the body surface area. We identified three groups of morphological features according to their functions (Figure 1):

1. The "reproduction group" constitutes sexual morphological features of female and male schistosomes. For females, we recorded the relative seminal receptacle surface area (seminal receptacle surface area divided by the total surface area of the body) and the relative ovary length (ovary length divided by the overall length of the body). For males, we determined the number of testes,

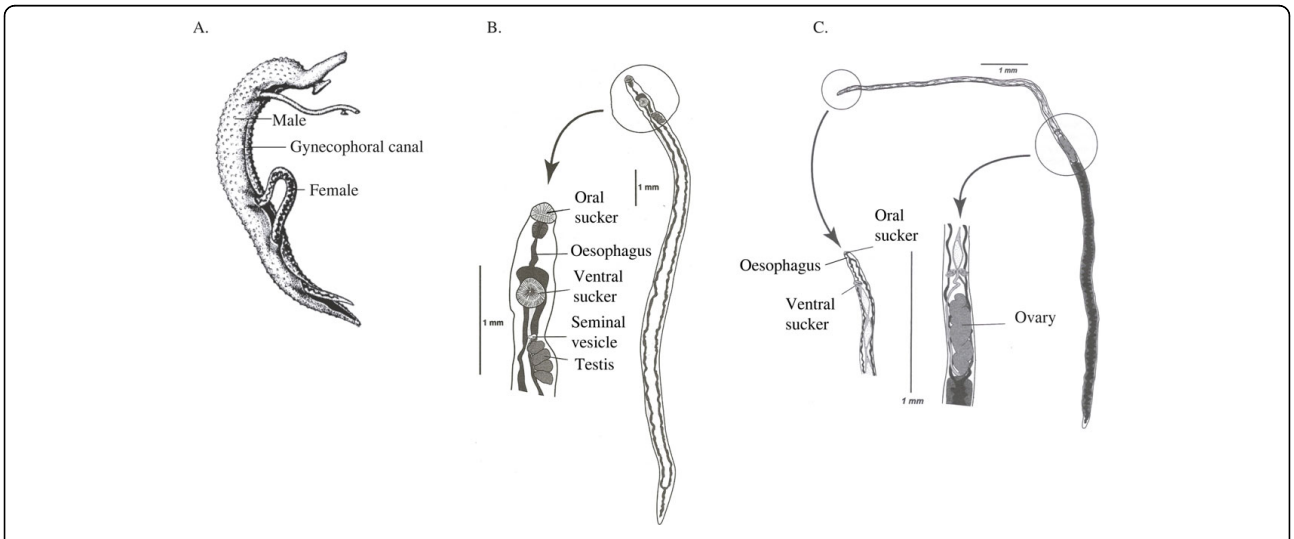

Figure 1 Morphological features recorded. A. Schistosome pair. B. Male schistosome C. Female schistosome

and measured the relative seminal vesicle surface area (seminal vesicle surface area divided by the total surface area of the body) and relative testes surface area (total testes surface area divided by body surface area). We also recorded the relative male gynecophoral canal length (length of the gynecophoral canal divided by the overall length of the body). The gynecophoral canal is a groove on the ventral surface of the male in which the female is held during copulation.

2. The "nutrition group" constitutes somatic morphological features of female and male schistosomes involved in nutrition. For males and females, we recorded the relative oesophagus length (oesophagus length divided by the overall length of the body), which has implications for the transport of food toward gut caecae.

3. The "locomotion group" contains somatic morphological features of female and male schistosomes involved in locomotion. Schistosomes, like all digeneans, possess an oral sucker and a ventral sucker, or acetabulum. Locomotion is achieved by alternate attachment of the suckers on internal host surfaces [19]. For males and females, we measured relative oral and ventral sucker surface areas (sucker surface area divided by the total surface area of the body). We also computed male/female relative sucker-surface-area ratios.

Note that, in addition to its inclusion in the reproduction group, the male gynecophoral canal could appear in all three morphological groups because of its potential involvement in female nutrition (through transtegumental transfer of substances) [20], female sexual maturation [21], female locomotion [22] and possibly mate guarding and female protection against the host immune system [14,23].

Comparative analyses

To control for phylogeny, we performed a phylogenetic reconstruction among the *Schistosomatidae* species using published DNA sequences of complete 18S and 28S rDNA genes, and a partial sequence of the cytochrome oxidase 1 (CO1) mtDNA gene (see Additional file 2, Table S1). Sequences were aligned using MAFFT, version 5 [24,25], and were improved by eye using Se-Al v2.0a11 [26]. After deleting ambiguous regions from the alignments, the final lengths of DNA sequences were 1653 bp (18S), 3741 bp (28S) and 1095 bp (CO1). Because not all species investigated were sequenced for all genes used, we constructed trees from the various datasets and combined these source trees via a supertree with the aid of Rainbow [27], using matrix representation with parsimony and the Baum [28] and Ragan [29] coding scheme [30,31]. The combined matrix was subjected to a parsimony analysis with the heuristic algorithm implemented in PAUP*, using 10 random addition replicates and the tree bisection-reconnection branch-swapping algorithm [32]. Source trees were built via Bayesian analysis with MrBayes 3.1.2 [33] by running four chains of 10^6 generations. The best evolutionary models were chosen by applying a hierarchical likelihood-ratio test using MrModelTest 2.2 [34] for the rDNA sequences, and applying a mixed model to translated mtDNA sequences. The burn-in value was set to 20% of the sampled trees (1% of the number of generations). Following Loker and Brant [13], *Griphobilharzia amoena* was used as the outgroup.

Comparisons of morphological features in relation to monogamous versus polygynandrous mating system were analyzed statistically using non-parametric Mann-Whitney U-tests. We also performed variation partitioning [35,36] of these morphological features between historical (phylogeny) and potentially adaptive (mating system) components. The objective of this analysis is to estimate the fraction of the variation linked to the mating system (the potentially adaptive component), the fraction linked to phylogeny (the historical component), and the fraction linked to both phylogeny and the mating system (the overlap between the two components) for each morphological trait examined. This partitioning technique allows the user to compute the fraction of the variation of the response variable due to each explanatory trait under study (here, mating system and phylogenetic effects) while controlling other(s). This leads to "pure" fractions (here, fractions explained only by the mating system or only by the phylogeny), as well as a common fraction of the variation due simultaneously to both independent traits. We stress that this common fraction (here, the joint variation explained by mating system and phylogeny) is not equivalent to an interaction term in an analysis of variance. This overlap is usually considered to be phylogenetic niche conservatism (sensu Grafen [37]), reflecting the fact that the putative effect of the mating system on morphological features is intermingled with phylogenetic effects if species with the same mating system are closely related. Such variation in decomposition requires the quantification of trait variation due to phylogeny alone. This precludes the use of classical comparative methods, such as independent contrasts [38,39], because such methods cannot quantify phylogenetic inertia per se (see [40]). Here, the expression of the phylogenetic variance is carried out via a principal coordinate analysis on the distance matrix computed from the phylogenetic tree of the species considered. A few principal coordinates were chosen using a broken-stick model [41] to account for phylogeny. Details of the partitioning method used, which is based on the combination of R^2 values resulting from different regressions, can be found in Desdevises et al. [35] and Cubo et al. [42]. Adjusted R^2 values,

which have been shown to be better in a variation-partitioning context, were used here [43]. Principal coordinate analyses were performed using DistPCoA [44]. Variation partitioning and tests of significance of the fractions were computed using the functions "varpart" and "anova.cca" from the "vegan" library [45] of the R statistical language (R Development Core Team 2008; *R: a language and environment for statistical computing*. R Foundation for Statistical Computing, Vienna, Austria. URL http://www.R-project.org). All tests were performed using permutational procedures (9999 permutations/test). The mating system was coded as a binary variable (0/1). In the phylogeny obtained (see below), species were split into two clades–one containing the monogamous species, and the other containing the polygynandrous species. This design does not allow a proper test of whether a transition toward a given mating system is associated with a change in a morphological feature, because the most parsimonious explanation suggests that only one transition in mating system occurred (see [46]). We then computed the principal coordinates within each monophyletic group to test if having a certain mating system is related to modifications in given morphological features, while taking phylogeny into account.

Results

Phylogeny

The supertree analysis led to 14 equally parsimonious trees that were combined by consensus into a majority rule. The consensus was congruent with the tree obtained from phylogenetic analysis of 28s rDNA sequences. Because branch lengths were desirable for the subsequent statistical analysis, based on this phylogenetic tree, we then kept this 28S rDNA tree, where we collapsed some clades as polytomies as obtained in the supertree consensus, and added the taxa from which 28S rDNA sequences were missing (*Schistosoma guineensis*, *S. edwardiense*, *S. hippopotami*) (Figure 2). Branch lengths for these three species were estimated from the phylogenetic analysis based on CO1 mtDNA gene, and resized to be coherent with the lengths computed from the 28S rDNA analysis. This tree was used for the variation partitioning analyses.

Comparative analyses

In the "reproduction group" of features (Figure 3A), males in monogamous species possessed fewer testes, showed lower relative surface areas of both testes and seminal vesicles, but had higher relative gynecophoral canal lengths than did males of polygynandrous species. Both the variation-partitioning mating system and phylogenic analyses showed that all of relative testis surface area, testis number, and relative gynecophoral canal length, were significantly linked to the mating system, with R^2 values greater than 0.4 (*i.e.*, explaining more than 40% of the variance). Females of monogamous species displayed relatively lower seminal receptacle surface areas than did polygynandrous females. However, no significant association was found between this variable and the chosen mating system. Similarly, no difference in relative ovary length among females differing in mating system was observed.

Turning to the "nutrition group" of features (Figure 3B), both males and females of polygynandrous species displayed longer relative oesophagus lengths than did monogamous species. Variation-partitioning analysis suggested that this morphological feature was significantly linked to the mating system, in both sexes.

In the "locomotion group" of features (Figure 3C), males of monogamous species displayed a higher relative sucker surface area than did males of polygynandrous species. There was no difference in sucker surface area between females of monogamous and polygynandrous species. Comparative analyses suggested a significant effect of mating system only on the male/female relative sucker surface area ratio. Thus, sexual dimorphism in sucker surface area was greater in monogamous than in polygynandrous species.

Discussion

It is now well established that, as a consequence of sperm competition, males displaying promiscuous sexual behaviour need to invest more energy in the reproductive organs than do monogamous males [47]. Such a link has been shown in primate, bird, rodent, amphibian, and insect species, and also between different populations of the same species [47]. In parasitic organisms, an impact of sexual selection on morphological features has been demonstrated in polygamous acanthocephalans [48]. In the cited study, it was shown that investment in testicular volume was related to the intensity of male-male competition. Our present work provides the first evidence from a parasitic organism showing that the development of sexual tissue is dependent on the mating system, with polygynandrous male schistosomes investing more energy in reproductive organs (measured by testis size) than do monogamous males. Literature reports on the link between accessory gland size and sperm competition level are few. Recently, it was shown in rodents that the masses of both the seminal vesicle and the anterior lobe of the prostate vary positively with testis weight [7]. Without controlling for phylogeny, we found a similar link between the relative testis and vesicle surface areas in males and the associated relative seminal receptacle surface area in females. Unfortunately, variation-partitioning tests did not show any effect of mating system on the sizes of these accessory

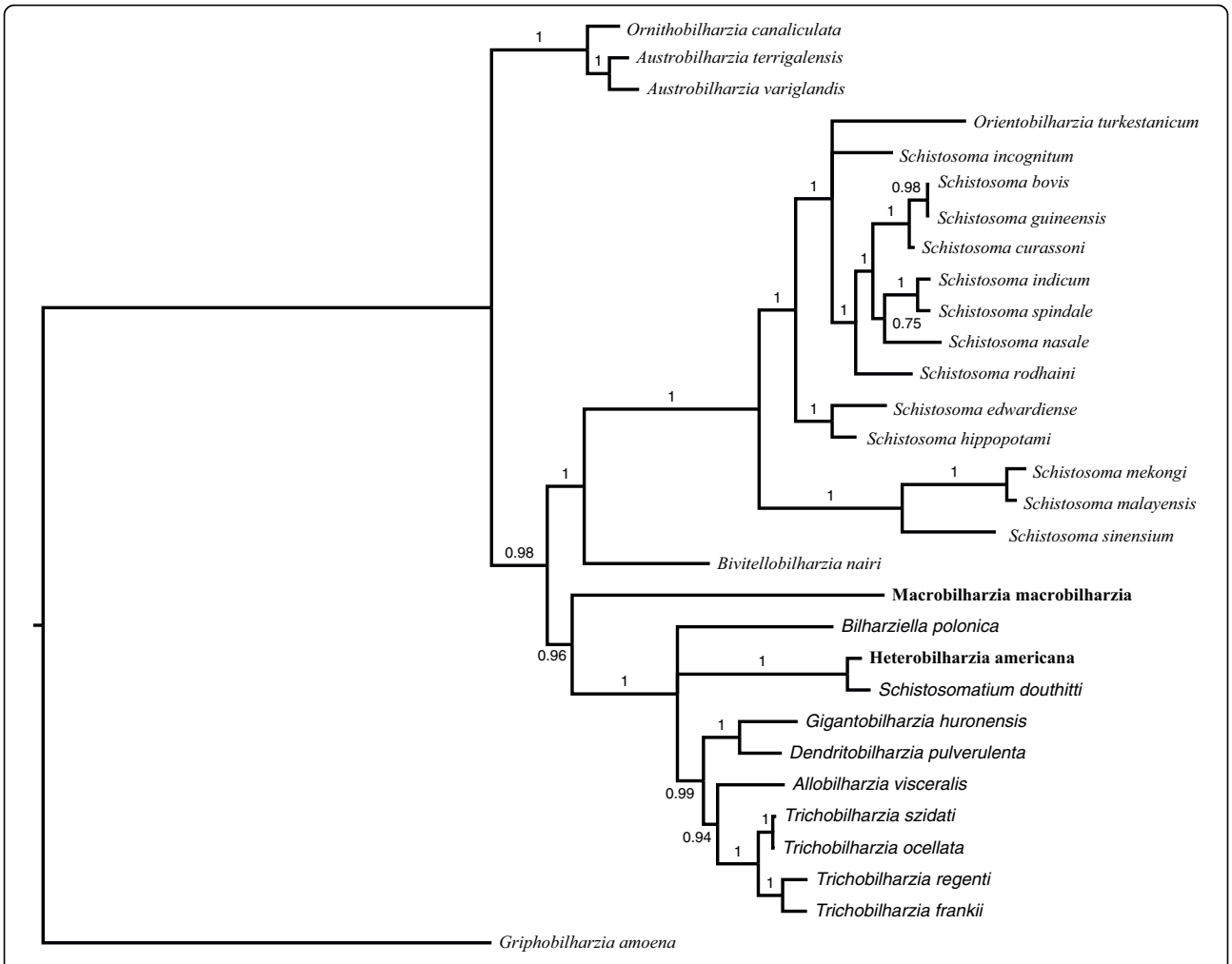

Figure 2 Phylogenetic supertree of several species from the family *Schistosomatidae*, obtained from phylogenetic analyses based on partial 18S and 28S rDNA, and CO1 mtDNA. Numbers near branches are posterior probabilities indicating clade support. These numbers and branch lengths were computed using Bayesian inference based on 28S rDNA sequences (see text for details). Species in regular, bold and italic characters are polygynandrous, polygynous and monogamous, respectively.

sex organs, suggesting that more species need to be included in future analysis.

The gynecophoral canal, a ventral groove in which the female resides, is a male secondary sexual characteristic specific to *Schistosomatidae*. We found that monogamous male schistosomes had gynecophoral canals 7-fold longer than those of polygynandrous males (90% *vs.* 12% of total body length), a difference that can be fully explained by variation in mating systems. When such systems were not considered in previous studies, a negative association was observed between the size of the gynecophoral canal and the number of testes [49]. The level of paternal investment is known to be associated with the mating system [50], and it is generally accepted that the male makes a lower investment in the system when successful paternity is less likely [51]. Thus, if the gynecophoral canal represents a paternal investment, as has indeed been proposed [49], it seems logical that monogamous male schistosomes, which make a greater investment than do polygynandrous males, should possess longer canals.

In *Schistosomatidae*, the gonado-somatic index (*i.e.*, the relative testis surface area) ranges from 3-24% depending on whether the mating system is monogamous or polygynandrous. By comparison, testis mass as a percentage of body weight ranges from 0.12-8.4% in bats and from 0.02-0.75% in primates [3]. It might be expected that more energy is invested in testicular tissue, which is energetically demanding [52], less energy is available for other tissues and functions. The present study shows that if monogamous male *Schistosomatidae* have a lower relative testis surface area than do polygynandrous males, the relative sucker surface area is larger and the relative oesophagus length smaller.

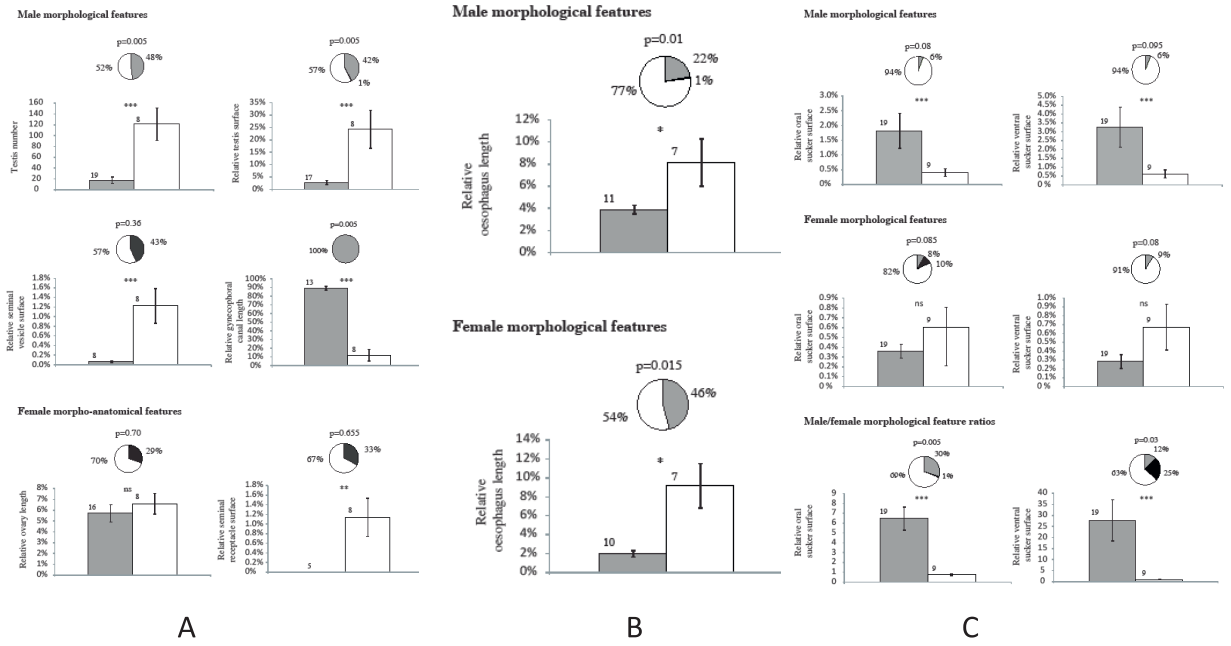

Figure 3 The influence of monogamous (grey histogram) versus polygynandrous (white histogram) mating systems on *Schistosomatidae* morphological features with implications for reproduction (A), nutrition (B) or locomotion (C). *Statistically significant difference using Mann-Whitney U-tests. Pie charts display the variation partitioning between phylogeny in white, mating system in grey, and the overlap between these two components in black. The P-value of the shares evaluation appears above the pie chart. The number above each histogram corresponds to the sample size.

Suckers are very important organs in digeneans because the suckers allow migration and fixation of the worm in the definitive host. In addition, because *Schistosomatidae* are endoparasites that live in the veins of birds or mammals, the organisms must be capable of resisting blood flow. Our present work showed that relative sucker dimorphism was greater in monogamous than in polygynandrous species. This difference is a consequence of a higher relative sucker surface area in monogamous males compared to polygynandrous males, rather than a variation in relative female sucker surface area. More precisely, no difference was apparent in relative sucker surface area between monogamous females and polygynandrous male or female parasites (0.41-0.58% of body surface area when both suckers were considered). Only monogamous males displayed expanded relative sucker surface areas (1.83% and 3.28% of body surface area for the oral and ventral suckers, respectively). This can be explained by the fact that, in monogamous species, the male parasite must maintain and transport its female to egg-laying sites. In contrast, females of polygynandrous species must travel and resist blood flow alone.

Schistosomes ingest red blood cells (the principal diet) using negative pressure created by contraction of the oral sucker muscle and the esophagus [53]. We found that the oesophagus of both male and female polygynandrous parasites was longer than that of monogamous males and females. With polygynandrous males, it may be assumed that the need to produce numerous spermatozoids requires high-level nutrient intake. In addition, because such males need not hold and transport a female, the males can invest more energy in obtaining nutrition. In polygynandrous females, the longer length of the oesophagus compared to that of monogamous females may be a consequence of the absence of continuous pairing. In monogamous schistosomes (at least in the *Schistosoma* genus, for which most information is available), it is well established that the male assists the female to pump blood and to reach sexual maturity [54]. A lone female is stunted and unable to produce eggs [18]. Therefore, as a consequence of the mating system, monogamous females, aided by their males, would be expected to possess a shorter oesophagus than that of polygynandrous females, which live separately from males.

Conclusions

The present study shows that the mating system drives negative associations between somatic and sexual morphological features. Monogamous males invest less in sexual tissues (the testes and associated organs) and more in tissues required for female transport, protection,

and feeding assistance. On the other hand, polygynandrous males make a greater investment in sexual tissues and a lower investment in female care compared to monogamous males. Therefore, sexual selection acts not only on primary and secondary sex organs, but also on somatic organs, the functions of which are beneficial in a given mating system.

Additional material

Additional file 1: Table S1: Morphological features noted for each *Schistosomatidae* species. M, monogamous; P, polygynandrous; NA, no available data.The surface area of each organ was calculated based on the length (l) and the width (w) of the organ using the ellipsis surface area formula ($l \times w \ \pi/4$). The relative organ length is the length of the organ divided by the body length, and the relative organ surface area is the surface area of the organ divided by the body surface area.

Additional file 2: Table S1: Accession numbers of the sequences used for phylogenetic reconstruction.

Acknowledgements
We thank Serge Morand for valuable and constructive comments on the manuscript and Joan Straub for editing the English of the manuscript. This work was supported by the French Ministère de l'Enseignement Supérieur et de la Recherche, the CNRS, and the Agence Nationale de la Recherche (Program Monogamix ANR-08-BLAN-0214-02).

Author details
[1]Laboratoire de Parasitologie Fonctionnelle et Evolutive, Centre de Biologie et d'Écologie Tropicale et Méditerranéenne, UMR 5244 CNRS-UPVD, 52 Avenue Paul Alduy, 66860 Perpignan Cedex, France. [2]*FRE 3355* CNRS-UPMC, Biologie Intégrative des Organismes Marins, Université Paris 06, Observatoire Océanologique, 66650 Banyuls-sur-Mer, France.

Authors' contributions
JB and JP compiled the database. YD performed the phylogenetic and the comparative analyses. SB, YD and JB drafted the manuscript. All authors read and approved the final manuscript.

Received: 15 January 2010 Accepted: 10 August 2010
Published: 10 August 2010

References
1. Harcourt AH, Harvey PH, Larson SG, Short RV: **Testis weight, body weight and breeding system in primates.** *Nature* 1981, **293(5827)**:55-57.
2. Schillaci MA: **Sexual selection and the evolution of brain size in primates.** *PLoS ONE* 2006, **1**:e62.
3. Pitnick S, Jones KE, Wilkinson GS: **Mating system and brain size in bats.** *Proc R Soc B* 2006, **273(1587)**:719-724.
4. Dunn PO: **Forced copulation results in few extrapair fertilizations in Ross's and lesser snow geese.** *Anim Behav* 1999, **57(5)**:1071-1081.
5. Moller AP, Briskie JV: **Extra-paternity, sperm competition and the evolution of testis size in birds.** *Beh Ecol Sociobiol* 1995, **36**:357-365.
6. Pitcher TE, Dunn PO, Whittingham LA: **Sperm competition and the evolution of testes size in birds.** *J Evol Biol* 2005, **18(3)**:557-567.
7. Ramm SA, Parker GA, Stockley P: **Sperm competition and the evolution of male reproductive anatomy in rodents.** *Proc R Soc B* 2005, **272(1566)**:949-955.
8. Stockley P, Gage MJ, Parker GA, Moller AP: **Sperm competition in fishes: the evolution of testis size and ejaculate characteristics.** *Am Nat* 1997, **149(5)**:933-954.
9. Jennions MD, Passmore NI: **Sperm competition in frogs: testis size and a 'sterile male' experiment on *Chiromantis xerampelina* (Rhacophoridae).** *Biol J linn Soc* 1993, **50**:211-220.
10. Gage MJG: **Association between body size, mating pattern, testis size and sperm lenght accross butterflies.** *Proc R Soc B* 1994, **258**:247-254.
11. Simmons LW, Emlen DJ: **Evolutionary trade-off between weapons and testes.** *Proc Natl Acad Sci USA* 2006, **103(44)**:16346-16351.
12. Lemaître J, Ramm S, Barton R, Stockley P: **Sperm competition and brain size evolution in mammals.** *J Evol Biol* 2009, **22**:2215-2221.
13. Loker ES, Brant SV: **Diversification, dioecy and dimorphism in schistosomes.** *Trends in Parasitology* 2006, **22(11)**:521-528.
14. Beltran S, Boissier J: **Schistosome monogamy: who, how, and why?** *Trends Parasitol* 2008, **24**:386-391.
15. Pica-Mattoccia L, Moroni R, Tchuem Tchuente LA, Southgate VR, Cioli D: **Changes of mate occur in *Schistosoma mansoni*.** *Parasitology* 2000, **120**:495-500.
16. Beltran S, Cézilly F, Boissier J: **Genetic dissimilarity between mates, but not male heterozygosity, influences divorce in schistosomes.** *PLoS ONE* 2008, **3(10)**:e3328.
17. Beltran S, Boissier J: **Are schistosomes socially and genetically monogamous?** *P Res* 2009, **104**:481-483.
18. Armstrong JC: **Mating behavior and development of schistosomes in the mouse.** *J Parasitol* 1965, **51**:605-616.
19. Basch PF: **Development and behavior of cultured Schistosoma mansoni fed on human erythrocyte ghosts.** *Am J Trop Med Hyg* 1984, **33(5)**:911-917.
20. Silveira AM, Friche AA, Rumjanek FD: **Transfer of [14C] cholesterol and its metabolites between adult male and female worms of *Schistosoma mansoni*.** *Comp Biochem Physiol* 1986, **85(4)**:851-857.
21. Popiel I: **Male-stimulated female maturation in *Schistosoma*: a review.** *J Chem Ecol* 1986, **12**:1745-1753.
22. Basch PF: **Why do schistosomes have separate sexes?** *Parasitol Today* 1990, **6**:160-163.
23. Boissier J, Mone H: **Male-female larval interactions in *Schistosoma mansoni* infected *Biomphalaria glabrata*.** *Int J Parasit* 2001, **31**:352-358.
24. Katoh K, Misawa K, Kuma K, Miyata T: **MAFFT: a novel method for rapid multiple sequence alignment based on fast Fourier transform.** *Nucleic Acid Res* 2002, **30**:3059-3066.
25. Katoh K, Kuma K, Toh H, Miyata T: **MAFFT version 5: improvement in accuracy of multiple sequence alignment.** *Nucleic Acid Res* 2005, **33**:511-518.
26. Rambaut A: **Se-Al: Sequence Alignment Editor.** 1996 [http://tree.bio.ed.ac.uk/software/seal/].
27. Chen D, Eulesnstein O, Fernandez-Baca D: **Rainbow: a toolbox for phylogenetic supertree construction and analysis.** *Bioinformatics* 2004, **16**:2872-2873.
28. Baum B: **Combining trees as a way of combining data sets for phylogenetic inference, and the desirability of combining gene trees.** *Taxon* 1992, **41**:3-10.
29. Ragan M: **Phylogenetic inference based on matrix representation of trees.** *Mol Phyl Evol* 1992, **1**:53-58.
30. Wiens J, Reeder T: **Combining data sets with different numbers of taxa for phylogenetic analysis.** *Syst Biol* 1995, **44**:548-549.
31. Sanderson M, Purvis A, Henze C: **Phylogenetic supertrees: assembling the trees of life.** *TREE* 1998, **13**:105-109.
32. Swofford D: **PAUP*. Phylogenetic Analysis Using Parsimony (*and Other Methods). Version 4d10. Sinauer Associates, Sunderland, Massachusetts.** 2003.
33. Ronquist F, Huelsenbeck J: **MRBAYES 3: Bayesian phylogenetic inference under mixed models.** *Bioinformatics* 2003, **19**:1572-1574.
34. Nylander JAA: **MrModeltest 2.2. Program distributed by the author.** Evolutionary Biology Centre, Uppsala University 2004.
35. Desdevises Y, Legendre P, Azouzi L, Morand S: **Quantifying phylogenetically structured environmental variation.** *Evolution* 2003, **57(11)**:2647-2652.
36. Borcard D, Legendre P, Drapeau P: **Partialling out the spatial component of ecological variation.** *Ecology* 1992, **73**:1045-1055.
37. Grafen A: **The phylogenetic regression.** *Phil Trans R Soc B* 1989, **326**:119-157.
38. Felsenstein J: **Phylogenies and the comparative method.** *Am Nat* 1985, **125**:1-15.
39. Felsenstein J: **Comparative methods with sampling error and within-species variation: contrasts revisited and revised.** *Am Nat* 2008, **171**:713-725.

40. Westoby M, Leishman M, Lord J: **On misinterpreting the 'phylogenetic correction'.** *J Ecol* 1995, **83(3)**:531-534.
41. Diniz-Filho J, de Sant' Ana C, Bini L: **An eigenvector method for estimating phylogenetic inertia.** *Evolution* 1998, **52**:1247-1262.
42. Cubo J, Legendre P, de Ricqles A, Montes L, de Margerie E, Castanet J, Y D: **Phylogenetic, functional, and structural components of variation in bone growth rate of amniotes.** *Evol Dev* 2008, **10(2)**:217-227.
43. Peres-Neto P, Legendre P, Dray S, Borcard D: **Variation partitioning of species data matrices: estimation and comparison of fractions.** *Ecology* 2006, **87**:2614-2625.
44. Legendre P, Anderson M: **Program DistPCoA. Département de sciences biologiques, Université de Montréal.** 1998.
45. Oksanen J, Kindt R, Legendre P, O'Hara R: **vegan: Community Ecology Package version 1 8-5.** 2007 [http://cran.r-project.org/].
46. Garland T Jr, Bennett AF, Rezende EL: **Phylogenetic approaches in comparative physiology.** *J Exp Biol* 2005, **208(Pt 16)**:3015-3035.
47. Parker GA: **Sperm competition and the evolution of ejaculates: towards a theory base.** Sperm competition and sexual selection, Academic Press; LondonBirkhead TR, Møller AP 1998, 3-54.
48. Sasal P, Jobet E, Faliex E, Morand S: **Sexual competition in an acanthocephalan parasite of fish.** *Parasitology* 2000, **120(Pt 1)**:65-69.
49. Morand S, Muller-Graf CD: **Muscles or testes? Comparative evidence for sexual competition among dioecious blood parasites (Schistosomatidae) of vertebrates.** *Parasitology* 2000, **120(Pt 1)**:45-56.
50. Moller PA, Cuervo JJ: **The evolution of paternity and paternal care in birds.** *Behav Ecol* 2000, **11**:472-485.
51. Neff BD: **Decisions about parental care in response to perceived paternity.** *Nature* 2003, **422(6933)**:716-719.
52. Kenagy GJ, Trombulak SC: **Size and function of mammalian testes in relation to body size.** *J Mammal* 1986, **67**:1-22.
53. Maule AG, Marks NJ: **in Parasitic Flatworms: Molecular Biology, Biochemistry, Immunology and Physiology.** Queen's University, Belfast, Northern Ireland 2006.
54. Basch PF: **Schistosomes. Development, reproduction, and host relations.** New-York: Oxford University Press 1991.

doi:10.1186/1471-2148-10-245
Cite this article as: Beltran *et al.*: Mating system drives negative associations between morphological features in *Schistosomatidae*. *BMC Evolutionary Biology* 2010 **10**:245.

Infection, Genetics and Evolution 10 (2010) 1039–1045

Contents lists available at ScienceDirect

Infection, Genetics and Evolution

journal homepage: www.elsevier.com/locate/meegid

Follow-up of the genetic diversity and snail infectivity of a *Schistosoma mansoni* strain from field to laboratory

Nicolas Bech [1,*], Sophie Beltran [1,*], Julien Portela, Anne Rognon, Jean-François Allienne, Jérôme Boissier, André Théron

Laboratoire de Biologie et d'Écologie Tropicale et Méditerranéenne, UMR 5244 CNRS-UPVD, Université de Perpignan, 52 Avenue Paul Alduy, 66860 Perpignan Cedex, France

ARTICLE INFO

Article history:
Received 20 January 2010
Received in revised form 27 May 2010
Accepted 23 June 2010
Available online 1 July 2010

Keywords:
Schistosoma mansoni strain
Microsatellite markers
Genetic diversity
Snail infectivity
Matching-alleles model

ABSTRACT

Schistosoma mansoni is an endoparasite causing a serious human disease called schistosomiasis. The quantification of parasite genetic diversity is an essential component to understand schistosomiasis epidemiology and disease transmission patterns but some studies on parasite genetic diversity are performed using parasite laboratory strains. However, a potential discrepancy in level of genetic variation between field populations and laboratory strains may have various implications in our deductions. In this study, 246 adult worms were analysed on 15 microsatellite markers to investigate variation of genetic diversity between a founder field isolate and the nine successive laboratory generations during three years of laboratory maintenance. In parallel, we measured a parasite life trait (snail infectivity) at each generation in order to test a potential link between inbreeding and snail infectivity. Our genetic analyses demonstrate a significant genetic differentiation between all parasite generations and a significant isolation by time associated with a decrease in neutral genetic diversity that is likely to be the result of successive bottleneck events. However, while snail infectivity decreases sharply between field isolate and the first laboratory generation, this parasite life trait does not evolve between other laboratory generations and appeared disconnected from this continuous neutral genetic diversity loss. We hypothesize that a sufficient level of compatibility polymorphism at a genomic level is maintained independently of an increase of inbreeding, ensuring the stability in the parasite life trait.

1. Introduction

Schistosomes (Plathyhelminth, Digenea) are endoparasites causing a serious human disease called schistosomiasis. Schistosomiasis ranks second only to malaria in terms of parasite-induced human morbidity and mortality, with more than 200 million people infected (Chitsulo et al., 2000; Crompton, 1999). The quantification of parasite genetic diversity is an essential component to understand schistosomiasis epidemiology and disease transmission patterns (Curtis et al., 2002; Jarne and Théron, 2001). Several studies based on DNA analyses performed directly on parasites from field populations demonstrated a high genetic diversity level (Agola et al., 2009; Curtis et al., 2002; Rodrigues et al., 2002a; Rollinson et al., 2009; Shrivastava et al., 2005; Sire et al., 1999, 2001; Steinauer et al., 2009; Théron et al., 2004). In contrast, analyses on laboratory strains showed a significant loss of diversity (Loverde et al., 1985; Pinto et al., 1997; Shrivastava et al., 2005; Sorensen et al., 2006; Stohler et al., 2004). As an example, it was shown that only 10% and 14% of alleles are found in the two analysed laboratory strains compared to a field population (Stohler et al., 2004). Such discrepancy in level of genetic variation between field populations and laboratory strains may have various implications as for instance when testing drug or vaccine efficiency (Bergquist et al., 2005; McManus and Loukas, 2008; Pearce, 2003).

Comparisons of genetic diversity between field populations and laboratory strains have often concerned disconnected isolates and strains from different origins and we do not know how the reduction of genetic diversity occurs at the passage from field to laboratory and later, during the successive generations of parasites. Only one recent study has genotyped parents and offspring from field isolates kept in the laboratory for only three generations (Steinauer et al., 2008). Moreover, no parasite fitness trait was followed concomitantly to the reduction of neutral genetic diversity during laboratory maintenance. In this study, we use 15 microsatellites markers to analyse the evolution of genetic diversity from a field isolate of wild *Schistosoma mansoni* adult worms, directly collected from naturally infected murine hosts, and at the origin of the laboratory strain, to the ninth laboratory

* Corresponding authors. Tel.: +33 4 68 66 20 50.
E-mail addresses: nicolas.bech@univ-perp.fr (N. Bech), beltran.sophie@hotmail.fr (S. Beltran).
[1] Co-first-authors, have contributed equally.

1567-1348/$ – see front matter © 2010 Elsevier B.V. All rights reserved.
doi:10.1016/j.meegid.2010.06.012

generation obtained after three years of maintenance. In parallel, we measure the evolution of parasite infectivity toward *Biomphalaria glabrata*, intermediate snail host from the same geographic origin.

2. Materials and methods

2.1. Schistosome strain founder and laboratory maintenance

Six naturally *S. mansoni* infected rats (*Rattus rattus*) were trapped in May 2005 at Dans Fond, one of numerous transmission sites located along the marshy forest focus of Grande Terre island in Guadeloupe, West Indies (Théron and Pointier, 1995). Adult schistosomes were collected from each rat using a standard perfusion method (Duvall and DeWitt, 1967). They were carefully washed in physiological saline solution and stored in 70% ethanol. A total of 20 males and 21 females were used for genetic analysis. Worms of this field isolate constituted the "G0" generation.

Miracidia hatched from eggs collected from the livers of the six naturally infected rats were used to infect 50 *B. glabrata* snails individually exposed to 10 larvae. Forty-three of the 46 surviving exposed snails were infected and shed cercariae (i.e. 95.55% of infection). In the laboratory, five mice (Swiss OF1) were infected with cercariae from these snails (see Boissier and Moné, 2000 for snail and mouse infection protocol) to establish the first laboratory generation of adult worms, called "G1". Each laboratory generation of the schistosome strain represented one cycle rotation. The next generations (G2 to G9) passed through five mice (160 cercariae at exposure) and approximately 24 infected snails. The snail strain was founded using 100 uninfected founders from the field, and collected at the same time (May 2005) as the rat trapping and at the same transmission site. The snail population was maintained at a census size of several hundreds of individuals. Snails were allowed to breed freely. The laboratory population was not exposed to any deliberate selection; snails preferentially outcrossed and showed Hardy–Weinberg equilibrium at molecular markers (unpublished data).

2.2. Laboratory sampling and measure of the parasite life trait

Adult worms from G1, G2, G4, G5 and G9 were collected (see Table 1 for details) for the genetic study and their corresponding offsprings (miracidia) were used to expose individually 50 *B. glabrata* snails (7–9 mm in shell diameter) with 10 larvae at each generation. Snail infectivity was measured as the number of snails positively infected divided by the total number of surviving snails.

2.3. Genotyping

'DNA was extracted using a recently published protocol (Beltran et al., 2008). All samples were genotyped on 15 microsatellite markers, SmC1, SmDO11, SmDA28 (Curtis et al., 2001), R95529, SmD57, SmD28, SmD25, SCMSMOXII, L46951 (Durand et al., 2000), SmBR16, SmBR10, SmBR13 (Rodrigues et al., 2007), SmS7-1 (Blair et al., 2001), SmBR1, SmBR6 (Rodrigues et al., 2002b). The relevant DNA fragments were amplified using Polymerase Chain Reaction (PCR). To maximise efficiency and minimize costs, these PCRs were performed in three multiplexes using the QIAGEN multiplex kit. The PCR amplifications of loci: R95529, SmC1, SmDO11, SmBR16 and SmD57 were grouped in the multiplex 1; loci: SmDA28, SmBR1, SmS7-1, SmD28 and SCMSMOXII were grouped in the multiplex 2; and loci: SmD25, L46951, SmBR6, SmBR10 and SmBR13 were grouped in the multiplex 3. These multiplexes were carried out according to the manufacturer's standard microsatellite amplification protocol in the final volume of 10 μL and with 57 °C for annealing temperature. PCR products were diluted in Sample Loading Solution (Beckman Coulter) with red-labeled size standard (CEQ™ DNA size standard kit, 400, Beckman Coulter, Fullerton, CA, USA) and electrophoresed on an automatic sequencer (CEQ™ 8000, Beckman Coulter). Genotypes were determined using the fragment analyzer package from Beckman Coulter.

2.4. Identical multilocus genotypes (MLGs) and rate of clones calculation

We inspected the data to identify identical MLGs which could be the result of the asexual multiplication occurring in the invertebrate host. Detection was performed with Gencount software (available at http://www.ccmar.ualg.pt/maree/index.php?t=falberto). The rate of clones was calculated as the number of identical multilocus genotypes (identical MLGs) on the number of total individuals within generations (Table 1).

2.5. Genetic analyses

We used the software MICRO-CHECKER (Oosterhout et al., 2004) to identify the presence of null alleles or scoring errors due to stuttering. Deviation from Hardy–Weinberg expectancies and linkage disequilibria were analysed using the global tests in FSTAT v.2.9.3.2 (Goudet, 2001). The level of significance was adjusted for multiple testing using a Bonferroni correction. Furthermore, polymorphism was estimated over all loci and for each generation using the number of alleles (A), allelic richness (AR), expected heterozygosity (He), allelic frequencies (see Supplementary Table) and Fis computed with FSTAT v.2.9.3.2. Finally, observed heterozygosity (Ho) was calculated with GENETIX software v.4.05.2 (Belkhir et al., 1996).

2.6. Genetic structuring

Significance of genotypic differentiation between generations was tested using global tests implemented in FSTAT v.2.9.3.2. Correction for multiple tests was adjusted with standard Bonferroni corrections. Pairwise $Fst^{\{ENA\}}$ values were obtained using the ENA (excluding null alleles) correction method to efficiently correct for the positive bias induced by the presence of null alleles on Fst estimation (Chapuis and Estoup, 2007). We described the distribution of microsatellites variability using Principal Component Analysis (PCA) on individuals' genotypes. PCA was conducted using GENETIX software v.4.05.2. We also used the Mantel test implemented in FSTAT to test for 'isolation by time' by regressing pairwise estimated $Fst^{\{ENA\}}$ against time (in days). Finally, we investigated whether recent bottleneck events appear during the generations. These tests compare the observed heterozygosity (Ho) with the expected heterozygosity according to Infinite Allele Model (IAM) (Kimura and Crow, 1964), and Two Phase Model (TPM) (Di Rienzo et al., 1994) given the number of alleles in the given generation. We performed the Wilcoxon signed ranks test implemented in BOTTLENECK software (Cornuet and Luikart, 1996) with 1000 iterations. We did not consider the Stepwise Mutation Model (SMM) (Kimura and Ohta, 1978) because this mutation model is not really appropriate for microsatellite markers (Ellegren, 2000; Estoup et al., 2002).

2.7. Estimated effective population size (Ne)

We estimated effective population size between each generation. We used MCLEEPS software which provides the maximum-likelihood estimator of Ne using Monte Carlo simulations (Anderson et al., 2000). We used this program to compute the likelihoods for Ne values between 10 and 250, in steps of 1, and used 250,000 Monte Carlo replicates for each value of Ne.

Table 1
Summary informations for the 15 microsatellite markers for the generations of *Schistosoma mansoni*. Name and GenBank accession numbers, identical MLGs: identical multilocus genotype on the total N of collected individuals, He: expected heterozygosity, Ho: observed heterozygosity, A: number of alleles, AR: allelic richness and Fis.

Markers (Accession number)		Generations Identical MLGs/N						
		G0	G1	G2	G4	G5	G9	All
		4/41	2/12	12/59	4/16	20/64	25/54	67/246
R95529 (R95529)	He	0.636	0.811	0.549	0.245	0.398	0.188	0.471
	Ho	0.487	0.900	0.600	0.267	0.439	0.208	0.483
	A	9.000	8.000	7.000	3.000	4.000	2.000	9.000
	AR	5.581	8.000	4.969	2.637	3.323	1.915	4.386
	Fis	0.234	−0.110	−0.092	−0.087	−0.101	−0.106	−0.044
SmC1 (AF325694)	He	0.681	0.656	0.540	0.665	0.618	0.608	0.628
	Ho	0.700	0.600	0.500	0.750	0.683	0.574	0.635
	A	5.000	3.000	4.000	3.000	3.000	3.000	5.000
	AR	3.686	3.000	3.206	3.000	2.982	2.995	3.716
	Fis	−0.028	0.085	0.074	−0.129	−0.105	0.055	−0.008
SmD57 (AF202967)	He	0.826	0.850	0.814	0.842	0.832	0.803	0.828
	Ho	0.590	0.700	0.655	0.938	0.887	0.944	0.786
	A	11.000	7.000	9.000	8.000	8.000	6.000	12.000
	AR	7.174	7.000	6.449	7.055	6.366	5.128	7.614
	Fis	0.286	0.176	0.196	−0.114	−0.067	−0.176	0.050
SmBR16 (LO4480)	He	0.689	0.767	0.670	0.658	0.670	0.580	0.672
	Ho	0.700	0.900	0.630	0.813	0.780	0.688	0.752
	A	5.000	5.000	4.000	3.000	3.000	3.000	5.000
	AR	4.127	5.000	3.789	3.000	3.000	2.935	3.632
	Fis	−0.016	−0.174	0.059	−0.234	−0.164	−0.185	−0.119
SmDO11 (AF325698)	He	0.845	0.828	0.823	0.823	0.838	0.496	0.776
	Ho	0.775	0.600	0.818	1.000	0.871	0.574	0.773
	A	10.000	7.000	12.000	7.000	8.000	5.000	13.000
	AR	7.346	7.000	7.269	6.200	6.442	3.186	6.954
	Fis	0.082	0.275	0.006	−0.215	−0.040	−0.158	−0.008
SmDA28 (AF325695)	He	0.547	0.424	0.544	0.500	0.503	0.467	0.498
	Ho	0.659	0.583	0.446	0.933	0.571	0.151	0.557
	A	5.000	2.000	4.000	2.000	2.000	2.000	6.000
	AR	2.918	2.000	2.983	2.000	2.000	2.000	2.495
	Fis	−0.203	−0.375	0.180	−0.867	−0.135	0.677	−0.121
SmBR1 (L81235)	He	0.178	0.341	0.164	0.186	0.220	0.174	0.211
	Ho	0.190	0.417	0.179	0.200	0.250	0.189	0.237
	A	2.000	2.000	2.000	2.000	2.000	2.000	2.000
	AR	1.905	2.000	1.873	1.970	1.945	2.049	1.940
	Fis	−0.096	−0.222	−0.089	−0.077	−0.135	−0.084	−0.117
SmS7-1 (AF330105)	He	0.420	0.159	0.320	0.290	0.444	0.020	0.276
	Ho	0.341	0.167	0.196	0.200	0.270	0.020	0.199
	A	2.000	2.000	2.000	2.000	2.000	2.000	2.000
	AR	2.000	1.978	1.993	1.998	2.000	1.204	1.990
	Fis	0.187	−0.048	0.387	0.311	0.392	0.000	0.205
SmD28 (AF202966)	He	0.484	0.527	0.315	0.129	0.031	0.000	0.248
	Ho	0.537	0.364	0.364	0.133	0.031	0.000	0.238
	A	3.000	2.000	3.000	2.000	2.000	1.000	3.000
	AR	2.823	2.000	2.170	1.897	1.289	1.000	2.178
	Fis	−0.108	0.310	−0.156	−0.037	−0.008	NA	0.000
SCMSMOXII (M85305)	He	0.581	0.714	0.498	0.617	0.615	0.638	0.611
	Ho	0.611	0.636	0.522	0.533	0.623	0.636	0.594
	A	4.000	4.000	4.000	4.000	4.000	4.000	4.000
	AR	3.738	3.996	3.409	3.867	3.516	3.902	3.775
	Fis	−0.051	0.108	−0.049	0.135	−0.012	0.002	0.022
SmBR10 (DQ448293)	He	0.547	0.409	0.534	0.500	0.502	0.463	0.493
	Ho	0.659	0.545	0.434	0.923	0.547	0.185	0.549
	A	5.000	2.000	4.000	2.000	2.000	2.000	6.000
	AR	2.918	2.000	2.968	2.000	2.000	2.000	2.471
	Fis	−0.203	−0.333	0.188	−0.846	−0.088	0.600	−0.114
L46951 (L46951)	He	0.557	0.477	0.395	0.477	0.508	0.493	0.485
	Ho	0.634	0.545	0.404	0.750	0.310	0.646	0.548
	A	4.000	3.000	2.000	2.000	3.000	2.000	4.000
	AR	3.254	2.909	1.999	2.000	2.791	2.000	2.595
	Fis	−0.138	−0.143	−0.025	−0.571	0.390	−0.310	−0.133
SmBR13 (DQ137790)	He	0.840	0.882	0.817	0.737	0.840	0.506	0.770
	Ho	0.854	0.909	0.811	1.000	0.875	0.630	0.846
	A	10.000	8.000	8.000	5.000	7.000	4.000	10.000

Table 1 (*Continued*)

Markers (Accession number)		Generations Identical MLGs/N						
		G0	G1	G2	G4	G5	G9	All
		4/41	2/12	12/59	4/16	20/64	25/54	67/246
	AR	7.270	7.810	6.510	4.761	6.498	2.800	6.451
	Fis	−0.016	−0.031	0.007	−0.357	−0.042	−0.243	−0.114
SmBR6 (AF009659)	He	0.571	0.477	0.392	0.462	0.498	0.498	0.483
	Ho	0.634	0.545	0.396	0.692	0.297	0.722	0.548
	A	4.000	3.000	3.000	2.000	3.000	2.000	4.000
	AR	3.444	2.909	2.341	2.000	2.753	2.000	2.678
	Fis	−0.111	−0.143	−0.010	−0.500	0.403	−0.450	−0.135
SmD25 (AF202965)	He	0.365	0.255	0.438	0.564	0.571	0.398	0.432
	Ho	0.366	0.273	0.510	0.923	0.383	0.431	0.481
	A	3.000	3.000	3.000	3.000	3.000	3.000	3.000
	AR	2.804	2.905	2.896	2.954	2.977	2.195	2.959
	Fis	−0.003	−0.071	−0.164	−0.636	0.350	−0.084	−0.101
All	He	0.584	0.572	0.521	0.513	0.539	0.422	0.525
	Ho	0.582	0.579	0.498	0.670	0.521	0.440	0.548
	A	5.500	4.067	4.733	3.333	3.733	2.929	5.867
	AR	4.066	4.034	3.655	3.156	3.325	2.487	3.722
	Fis	0.003	−0.013	0.044	−0.307	0.035	−0.042	−0.047

2.8. Statistical analyses to follow-up the diversity indices, the parasite life trait, the rate of clones and the estimated effective population size in the course of generations

We observed the evolution of genetic diversity indices (expected heterozygosity: He and allelic richness: AR), of snail infectivity (parasite life trait), of rate of identical MLGs (i.e. rate of clones), and of estimated effective population size (i.e. Ne) in the course of generations. We used linear regression test, implemented in the GRAPH PAD software for Windows, in order to test the link between the genetic diversity indices (AR and He) and time (in days) and between the rate of clones and time (in days). We used logarithmic regression test, implemented in the SPSS 13.0 software for Windows, in order to test the link between the estimated effective population size (Ne) and time (in days). We used Fisher's exact tests, also implemented in the GRAPH PAD software for Windows, in order to test a variation in snail infectivity between field and laboratory generations.

3. Results

3.1. Data analysis

3.1.1. Marker validation and distribution of the genetic diversity

After Bonferroni correction and according to the method implemented in the Micro-Checker software, 8 on 90 tests exhibited null alleles but all were randomly distributed across loci and generations and did not become significant at a global level. Moreover, these null alleles did not affect Hardy–Weinberg expectancies. Departure from Hardy–Weinberg on all markers and all generations was not detected; no Fis value was significantly different from 0 (*P*-value threshold after Bonferroni correction, $P = 0.0006$). No evidence for linkage disequilibria was detected either (*P*-value threshold after Bonferroni correction, $P = 0.0005$). All microsatellite loci were polymorphic with an AR ranging from 1.940 to 7.614 and an He ranging from 0.211 to 0.828 by locus and over all generations (Table 1).

3.1.2. Identical multilocus genotypes and rate of clones

Gencount software detected some identical multilocus genotypes which corresponded to the number of clones in the different generations (Table 1). We obtained 10% of clones for the field generation G0 and 17%, 20%, 25%, 31% and 46% of clones after 1, 2, 4, 5 and 9 passages through laboratory mice, respectively (Table 1).

3.1.3. Estimated effective population size (Ne)

We obtained a Ne of 67 (IC− = 25, IC+ = 250) for the passage from field generation G0 to laboratory generation G1, a Ne of 36 (IC− = 23, IC+ = 58) for the passage from G1 to G2, a Ne of 36 (IC− = 25, IC+ = 49) for the passage from G2 to G4, a Ne of 29 (IC− = 15, IC+ = 57) for the passage from G4 to G5, and a Ne of 18 (IC− = 15, IC+ = 24) for the passage from G5 to G9.

3.2. Genetic structuring

The genetic structuring analysis (based on 15 microsatellite markers and conducted during the three years of laboratory maintenance) showed a genetic structuring among the different generations. Pairwise $Fst^{\{ENA\}}$ values (mean $Fst^{\{ENA\}} = 0.062$) detected different genetic substructures within all generations (Table 2). The Principal Component Analysis seemed to reveal three generation groups. G0 and G1 constituted the first group, G2, G4 and G5 the second group and G9 formed, on its own, the third group. In this genetic pattern, G2, G4 and G5 could represent genetic intermediaries between two G0/G1 and G9 clusters. Thus, in the course of time, the distribution of genetic diversity changed until it became different from the initial genetic structuring. G9, which was the last analysed laboratory generation, appeared particularly more different from the other ones. Furthermore, Mantel test identified significant positive correlation ($N = 15$, ddl = 14, $F = 20.00$, r squared = 60.60%; $P = 0.0006$) between $Fst^{\{ENA\}}$ values and time, indicating a strong 'isolation in the course of time' between generations (Fig. 1).

In all generations, from field generation G0 to laboratory generations G1 to G9, tests for heterozygosity excess revealed recent genetic bottleneck signals according to both IAM and TPM mutation models (Table 3).

Table 2
Pairwise $Fst^{\{ENA\}}$ values for each generation comparison (below diagonal), and their significance level (above diagonal). *P*-value threshold is adjusted with the Bonferroni correction, $P = 0.00333$. Stars indicate the level of significance.

	G0	G1	G2	G4	G5	G9
G0		0.1600	0.0033	0.0033	0.0033	0.0033
G1	0.0219		0.0033	0.0033	0.0033	0.0033
G2	0.0149*	0.0436*		0.0033	0.0033	0.0033
G4	0.0457*	0.0979*	0.0423*		0.0267	0.0033
G5	0.0341*	0.0822*	0.0330*	0.0078		0.0033
G9	0.1037*	0.1699*	0.0941*	0.0629*	0.0725*	

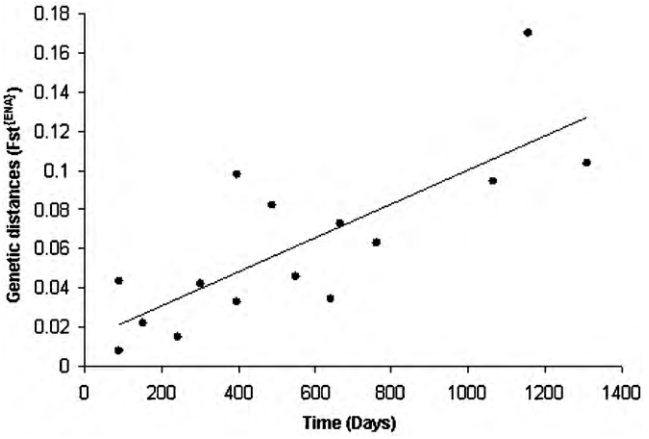

Fig. 1. Pairwise genetic differentiation ($Fst^{[ENA]}$) plotted against time (in days) between generations.

Table 3
Results from BOTTLENECK software for the Wilcoxon signed ranks test which compares observed heterozygosity and expected heterozygosity according to Infinite Allele Model (IAM) and Two Phase Model (TPM). Tests are performed on each generations of *Schistosoma mansoni*.

Generations	Probability (Wilcoxon signed ranks test)		Sign of bottleneck
	IAM	TPM	
G0	0.00066	0.04163	Yes
G1	0.00168	0.02063	Yes
G2	0.00008	0.00107	Yes
G4	0.00011	0.00168	Yes
G5	0.00021	0.00134	Yes
G9	0.00084	0.01279	Yes

3.3. Follow-up of diversity indices, parasite life trait, rate of clones and estimated effective population size (Ne) in the course of time (Figs. 2 and 3)

In the course of generations, the parasite genetic diversity indices, the snail infectivity, the rate of clones and the Ne evolved. Linear regression test showed a significant loss of genetic diversity with time: decrease in expected heterozygosity and allelic richness were correlated to the number of generations or days ($N = 6$, $F = 26.14$, r squared = 86.73%, $P = 0.0069$ for heterozygosity and $N = 6$, $F = 73.14$, r squared = 94.81%, $P = 0.0010$ for allelic richness) (Fig. 2). Concerning the parasite life trait, we obtained 96% of snail infectivity for the field generation G0 and 38%, 30%, 41%, 39% and 38% of snail infectivity after 1, 2, 4, 5 and 9 passages through laboratory mice, respectively. Significant differences in snail infectivity were detected between the field generation G0 and the first laboratory generations G1 (Fisher's exact tests between G0 and all the laboratory generations, P-values < 0.0020). In contrast, no significant variation of infectivity was detected between laboratory generations (Fisher's exact tests between all the laboratory generations, P-values > 0.05) (Fig. 2). In parallel, linear regression test showed a significant increase in rate of clones with time: rate of identical MLGs were correlated to the number of generations or days ($N = 6$, $F = 220.08$, r squared = 98.21%, $P = 0.0001$) (Fig. 3). Logarithmic regression test showed a significant loss of Ne with time ($F = 12.40$, r squared = 89.68%, $P = 0.0390$) (Fig. 3).

4. Discussion

To our knowledge, this is the first study which compares the evolution of genetic diversity on a parasite strain of *S. mansoni* from

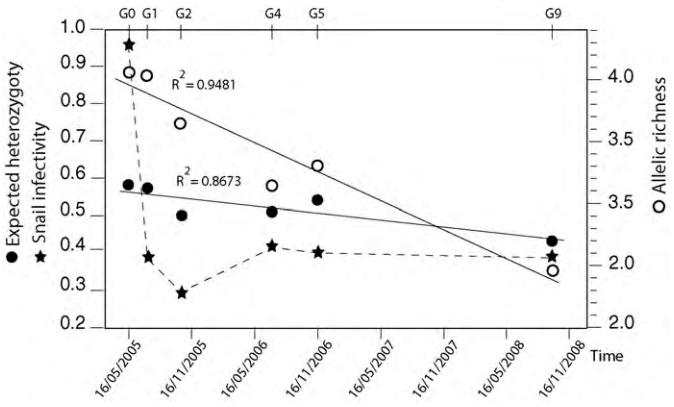

Fig. 2. Loss of genetic diversity indices and snail infectivity with time. The two diversity indices, allelic richness with white circles and expected heterozygosity with black circles, decrease with the time, over the course of the generations. In the course of time, variation in snail infectivity with black stars is detected between the field generation G0 and the laboratory generations G1 to G9.

field founder isolates to nine laboratory generations and concomitantly infectivity to its snail intermediate host *B. glabrata*. Our analyses show a significant increase in identical multilocus genotypes (number of clones) and a significant logarithmic decrease in the estimated effective population size (Ne) in the course of generations. Molecular analyses reveal a significant decrease of genetic diversity indices (AR and He) in the course of generations and finally different genetic substructures among all laboratory generations. Significant differences in allelic frequencies appear between generations (results not shown) with some allelic frequencies decreasing and reaching almost zero (see Supplementary Table). Thus, results seem to reveal three generation groups. G0 and G1 constitute the first group, G2, G4 and G5 the second and intermediary group and G9 forms, on its own, the third group.

What it is interesting is the fact that the loss of genetic diversity occurred gradually from the field isolate to the last laboratory generation analysed. We did not observe a sharp reduction when ongoing from the field to the first lab generation. This should indicate that, in the conditions under which the strain was established (i.e. from 46 infected snails previously exposed to 10 miracidia), the founder effect had limited consequences and both the reduction of genetic diversity and the associated increase of number of parasite clones and decrease of estimated effective size (Ne) should mainly be the results of repeated bottleneck events during laboratory maintenance. Moreover, we may also expect that potential selection pressures exerted by the rodent experi-

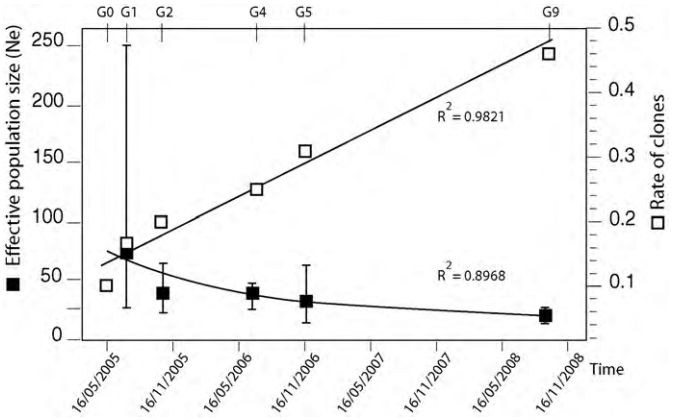

Fig. 3. Loss of estimated effective size (Ne) with black squares and increase in rate of clones (identical MLGs/N) with white squares with time (in day).

mental host (Bremond et al., 1993; Loverde et al., 1985) were limited in our case due to the murine origin of the wild population of schistosomes.

Concerning the evolution of the life history trait, our results show a sharp decrease in compatibility between the field population of snails and parasites, and the laboratory ones. Snail infectivity dropped from 96% in G0 to 38% in G1 and then remained relatively constant between 30% and 41% during the successive laboratory generations.

As regards as the loss of compatibility, these results are similar to those of Théron et al. (2008), showing a massive drop in compatibility during the passage from field to laboratory. To explain such a loss of compatibility, the authors emphasised that the founder effect may cause a random loss of alleles at polymorphic loci that control compatibility through the matched/mismatched status of the host and parasite genotypes as in a matching-alleles model (Agrawal and Lively, 2003; Théron and Coustau, 2005). Under this condition, a proportion of individuals within the snail strain would not be matched by the reduced number of parasite genotypes contained within the genetically depauperate laboratory strain.

Concerning the fact that in the course of laboratory generations, snail infectivity remained stable despite repeated bottlenecks at each maintenance cycle, it is more intriguing. Some hypotheses could be proposed: (1) the measured life trait (snail infectivity) could not be sufficiently sensitive to test the link between genetic diversity loss and fitness decrease; (2) the obtained range of genetic diversity loss was not high enough to observe an evolution in life traits; and/or (3) a substantial level of compatibility polymorphism was maintained independently of the decrease of neutral genetic diversity. This last phenomenon could be linked to recently described genomic mechanisms able to generate high diversification in molecules potentially implicated in the compatibility between *S. mansoni* and *B. glabrata*. Indeed, Roger et al. (2008) have demonstrated that in *S. mansoni*, a complex hierarchical system has evolved, generating high polymorphism in antigenic molecules (SmPoMucs) through somatic recombinatorial processes and differential expression mechanisms (Roger et al., 2008). In this way, each miracidium expressed a unique combination of SmPoMucs derived from a limited set of genes. Similar mechanisms of diversification through somatic recombinations have been previously described for fibrinogen related proteins (FREPS) of *B. glabrata* that participate to the innate immune response of the snail (Zhang et al., 2004).

We showed that neutral DNA and functional markers may have different ways of evolution. Whatever the way of evolution, the parasite neutral genetic diversity and the compatibility (snail infectivity) decrease in the course of laboratory passages. These decreases, associated to an increase in rate of clones and a decrease of estimated effective size (Ne), could be the result of the selection process through the snail host and/or of bottlenecks during laboratory strains' maintenance (resulting from the associated techniques of laboratory maintenance). This element and the number of laboratory passages used have to be taken into account in the future study using laboratory parasite isolates. The population genetic analyses and other studies testing resistance to drugs for example have to use first laboratory passages and not more if they aim to reflect a reality in field parasite populations. In parallel, when it is possible, the bottlenecks resulting from the techniques of laboratory maintenance has to be limited. Finally, integration of population, molecular and functional approaches may be of particular interest to elucidate complex interactions such as in *B. glabrata*/*S. mansoni* compatibility polymorphism.

Acknowledgements

We wish to thank Cécile Perrin, Corentin Barbu and Juliette Langand for their constructive comments and their assistance on analyses, Bernard Dejean for technical assistance and Joan Straub for editing the English of the manuscript. This work was supported by the French Ministère de l'Enseignement Supérieur et de la Recherche, the CNRS, and the Agence Nationale de la Recherche (Program Monogamix ANR-08-BLAN-0214-02 and Biomgenim ANR-07-BLAN-0214-03).

Appendix A. Supplementary data

Supplementary data associated with this article can be found, in the online version, at doi:10.1016/j.meegid.2010.06.012.

References

Agola, L.E., Steinauer, M.L., Mburu, D.N., Mungai, B.N., Mwangi, I.N., Magoma, G.N., Loker, E.S., Mkoji, G.M., 2009. Genetic diversity and population structure of *Schistosoma mansoni* within human infrapopulations in Mwea, central Kenya assessed by microsatellite markers. Acta Trop. 111, 219–225.

Agrawal, A.F., Lively, C.M., 2003. Modelling infection as a two-step process combining gene-for-gene and matching-allele genetics. Proc. R. Soc. B – Biol. Sci. 270, 323–334.

Anderson, E.C., Williamson, E.G., Thompson, E.A., 2000. Monte Carlo evaluation of the likelihood for Ne from temporally spaced samples. Genetics 156, 2109–2118.

Belkhir, K., Borsa, P., Chikhi, L., Raufaste, N., Bonhomme, F., 1996. GENETIX 4.05, logiciel sous Windows TM pour la génétique des populations. Laboratoire Génome, Populations, Interactions, CNRS UMR 5000. Université de Montpellier II, Montpellier (France).

Beltran, S., Galinier, R., Allienne, J.F., Boissier, J., 2008. Cheap, rapid and efficient DNA extraction method to perform multilocus microsatellite genotyping on all *Schistosoma mansoni* stages. Mem. Inst. Oswaldo Cruz 103, 501–503.

Bergquist, N.R., Leonardo, L.R., Mitchell, G.F., 2005. Vaccine-linked chemotherapy: can schistosomiasis control benefit from an integrated approach? Trends Parasitol. 21, 112–117.

Blair, L., Webster, J.P., Barker, G.C., 2001. Isolation and characterization of polymorphic microsatellite markers in *Schistosoma mansoni* from Africa. Mol. Ecol. Notes 1, 93–95.

Boissier, J., Moné, H., 2000. Experimental observations on the sex ratio of adult *Schistosoma mansoni*, with comments on the natural male bias. Parasitology 121, 379–383.

Bremond, P., Pasteur, N., Combes, C., Renaud, F., Théron, A., 1993. Experimental host-induced selection in *Schistosoma mansoni* strains from Guadeloupe and comparison with natural observations. Heredity 70, 33–37.

Chapuis, M.P., Estoup, A., 2007. Microsatellite null alleles and estimation of population differentiation. Mol. Biol. Evol. 24, 621–631.

Chitsulo, L., Engels, D., Montressor, A., Savioli, L., 2000. The global status of schistosomiasis and its control. Acta Trop. 77, 41–51.

Cornuet, J.M., Luikart, G., 1996. Description and power analysis of two tests for detecting recent population bottlenecks from allele frequency data. Genetics 144, 2001–2014.

Crompton, D.W.T., 1999. How much human helminthiasis is there in the world? J. Parasitol. 85, 397–403.

Curtis, J., Sorensen, R.E., Kristen Page, L., Minchella, D.J., 2001. Microsatellite loci in the human blood fluke *Schistosoma mansoni* and their utility for other schistosome species. Mol. Ecol. Notes 1, 143–145.

Curtis, J., Sorensen, R.E., Minchella, D.J., 2002. Schistosome genetic diversity: the implications of population structure as detected with microsatellite markers. Parasitology 125, S51–S59.

Di Rienzo, A., Peterson, A.C., Garza, J.C., Valdes, A.M., Slatkin, M., Freimer, N.B., 1994. Mutational processes of simple-sequence repeat loci in human populations. Proc. Natl. Acad. Sci. U.S.A. 91, 3166–3170.

Durand, P., Sire, C., Théron, A., 2000. Isolation of microsatellite markers in the digenetic trematode *Schistosoma mansoni* from Guadeloupe island. Mol. Ecol. 9, 997–998.

Duvall, R.H., DeWitt, W.B., 1967. An improved perfusion technique for recovering adult Schistosomes from laboratory animals. Am. J. Trop. Med. Hyg. 16, 483–486.

Ellegren, H., 2000. Microsatellite mutations in the germline: implications for evolutionary inference. Trends Genet. 16, 551–558.

Estoup, A., Jarne, P., Cornuet, J.M., 2002. Homoplasy and mutation model at microsatellite loci and their consequences for population genetics analysis. Mol. Ecol. 11, 1591–1604.

Goudet, J., 2001. FSTAT, a program to estimate and test gene diversities and fixation indices (version 2.9.3). Available at http://www2.unil.ch/popgen/softwares/fstat.html.

Jarne, P., Théron, A., 2001. Genetic structure in natural populations of flukes and snails: a practical approach and review. Parasitology 123, S27–S40.

Kimura, M., Crow, J.F., 1964. The number of alleles that can be maintained in a finite population. Genetics 49, 725–738.

Kimura, M., Ohta, T., 1978. Stepwise mutation model and distribution of allelic frequencies in a finite population. Proc. Natl. Acad. Sci. U.S.A. 75, 2868–2872.

Loverde, P.T., De Wald, J., Minchella, D.J., Bosshardt, S.C., Damian, R.T., 1985. Evidence for host-induced selection in *Schistosoma mansoni*. J. Parasitol. 71, 297–301.

McManus, D., Loukas, A., 2008. Current status of vaccines for schistosomiasis. Clin. Microbiol. Rev. 21, 225–242.

Oosterhout, C.V., Hutchinson, W.F., Wills, D.P.M., Shipley, P., 2004. MICRO-CHECKER: software for identifying and correcting genotyping errors in microsatellite data. Mol. Ecol. 4, 535–538.

Pearce, E.J., 2003. Progress towards a vaccine for schistosomiasis. Acta Trop. 86, 309–313.

Pinto, P.M., Brito, C.F., Passos, L.K., Tendler, M., Simpson, A.J., 1997. Contrasting genomic variability between clones from field isolates and laboratory populations of *Schistosoma mansoni*. Mem. Inst. Oswaldo Cruz 92, 409–414.

Rodrigues, N.B., Coura Filho, P., de Souza, C.P., Jannoti Passos, L.K., Dias-Neto, E., Romanha, A.J., 2002a. Populational structure of *Schistosoma mansoni* assessed by DNA microsatellites. Int. J. Parasitol. 32, 843–851.

Rodrigues, N.B., Loverde, P.T., Romanha, A.J., Oliveira, G., 2002b. Characterization of new *Schistosoma mansoni* microsatellite loci in sequences obtained from public DNA databases and microsatellite enriched genomic libraries. Mem. Inst. Oswaldo Cruz 97, 71–75.

Rodrigues, N.B., Silvia, M.R., Pucci, M.M., Minchella, D.J., Sorensen, R., Loverde, P.T., Romanha, A.J., Oliveira, G., 2007. Microsatellite-enriched genomic libraries as a source of polymorphic loci for *Schistosoma mansoni*. Mol. Ecol. Notes 7, 263–265.

Roger, E., Grunau, C., Pierce, R.J., Hirai, H., Gourbal, B., Galinier, R., Emans, R., Cesari, I.M., Cosseau, C., Mitta, G., 2008. Controlled chaos of polymorphic mucins in a metazoan parasite (*Schistosoma mansoni*) interacting with its invertebrate host (*Biomphalaria glabrata*). PLoS Negl. Trop. Dis. 2, e330.

Rollinson, D., Webster, J.P., Webster, B., Nyakaana, S., Jorgensen, A., Stothard, J.R., 2009. Genetic diversity of schistosomes and snails: implications for control. Parasitology 1–11.

Shrivastava, J., Gower, C.M., Balolong, E.J., Wang, T.P., Qian, B.Z., Webster, J.P., 2005. Population genetics of multi-host parasites—the case for molecular epidemiological studies of *Schistosoma japonicum* using larval stages from naturally infected hosts. Parasitology 131, 617–626.

Sire, C., Durand, P., Pointier, J.P., Théron, A., 1999. Genetic diversity and recruitment pattern of *Schistosoma mansoni* in a *Biomphalaria glabrata* snail population: a field study using random-amplified polymorphic DNA markers. J. Parasitol. 85, 436–441.

Sire, C., Durand, P., Pointier, J.P., Théron, A., 2001. Genetic diversity of *Schistosoma mansoni* within and among individual hosts (*Rattus rattus*): infrapopulation differentiation at microspatial scale. Int. J. Parasitol. 31, 1609–1616.

Sorensen, R.E., Rodrigues, N.B., Oliveira, G., Romanha, A.J., Minchella, D.J., 2006. Genetic filtering and optimal sampling of *Schistosoma mansoni* populations. Parasitology 133, 443–451.

Steinauer, M.L., Agola, L.E., Mwangi, I.N., Mkoji, G.M., Loker, E.S., 2008. Molecular epidemiology of *Schistosoma mansoni*: a robust, high-throughput method to assess multiple microsatellite markers from individual miracidia. Infect. Genet. Evol. 8, 68–73.

Steinauer, M.L., Hanelt, B., Agola, L.E., Mkoji, G.M., Loker, E.S., 2009. Genetic structure of *Schistosoma mansoni* in western Kenya: The effects of geography and host sharing. Int. J. Parasitol. 39, 1353–1362.

Stohler, R.A., Curtis, J., Minchella, D.J., 2004. A comparison of microsatellite polymorphism and heterozygosity among field and laboratory populations of *Schistosoma mansoni*. Int. J. Parasitol. 34, 595–601.

Théron, A., Coustau, C., 2005. Are *Biomphalaria* snails resistant to *Schistosoma mansoni*? J. Helminthol. 79, 187–191.

Théron, A., Coustau, C., Rognon, A., Gourbiere, S., Blouin, M.S., 2008. Effects of laboratory culture on compatibility between snails and schistosomes. Parasitology 135, 1179–1188.

Théron, A., Pointier, J.P., 1995. Ecology, dynamics, genetics and divergence of trematode populations in heterogenous environments: the model of *Schistosoma mansoni* in the insular focus of Guadeloupe. Res. Rev. Parasitol. 55, 49–64.

Théron, A., Sire, C., Rognon, A., Prugnolle, F., Durand, P., 2004. Molecular ecology of *Schistosoma mansoni* transmission inferred from the genetic composition of larval and adult infrapopulations within intermediate and definitive hosts. Parasitology 129, 571–585.

Zhang, S.M., Adema, C.M., Kepler, T.B., Loker, E.S., 2004. Diversification of Ig superfamily genes in an invertebrate. Science 305, 251–254.

BMC Genomics

METHODOLOGY ARTICLE Open Access

Whole-genome *in-silico* subtractive hybridization (WISH) - using massive sequencing for the identification of unique and repetitive sex-specific sequences: the example of *Schistosoma mansoni*

Julien Portela[†1], Christoph Grunau[†1], Céline Cosseau[1], Sophie Beltran[1], Christelle Dantec[2], Hugues Parrinello[2] and Jérôme Boissier*[1]

Abstract

Background: Emerging methods of massive sequencing that allow for rapid re-sequencing of entire genomes at comparably low cost are changing the way biological questions are addressed in many domains. Here we propose a novel method to compare two genomes (genome-to-genome comparison). We used this method to identify sex-specific sequences of the human blood fluke *Schistosoma mansoni*.

Results: Genomic DNA was extracted from male and female (heterogametic) *S. mansoni* adults and sequenced with a Genome Analyzer (Illumina). Sequences are available at the NCBI sequence read archive http://www.ncbi.nlm.nih.gov/Traces/sra/ under study accession number SRA012151.6. Sequencing reads were aligned to the genome, and a pseudogenome composed of known repeats. Straightforward comparative bioinformatics analysis was performed to compare male and female schistosome genomes and identify female-specific sequences. We found that the *S. mansoni* female W chromosome contains only few specific unique sequences (950 Kb i.e. about 0.2% of the genome). The majority of W-specific sequences are repeats (10.5 Mb i.e. about 2.5% of the genome). Arbitrarily selected W-specific sequences were confirmed by PCR. Primers designed for unique and repetitive sequences allowed to reliably identify the sex of both larval and adult stages of the parasite.

Conclusion: Our genome-to-genome comparison method that we call "whole-genome *in-silico* subtractive hybridization" (WISH) allows for rapid identification of sequences that are specific for a certain genotype (e.g. the heterogametic sex). It can in principle be used for the detection of any sequence differences between isolates (*e.g.* strains, pathovars) or even closely related species.

Background

Massive sequencing, or next-generation sequencing (NGS), has remarkably reduced the cost, time and amount of biological material required for (re-)sequencing of entire genomes. Recently, for instance, whole-genome wide sequence variation in *Caenorhabditis elegans* was assessed comparing Solexa Sequence Analyser reads to a reference genome (strain-to-reference comparison) [1]. In principle, it is possible with this method to identify differences between genomes without a priori knowledge of their location in the genome. This is a fundamental question in many ecological or medical important species. Here, we describe how to identify differences in the DNA sequence of two genomes obtained by a massive parallel sequencing approach (genome-to-genome comparison). We used the method to identify sex specific sequences in the human blood fluke *Schistosoma mansoni*. *S. mansoni* (Trematoda: Digenea) is a gonochoric endoparasite causing a serious human disease called schistosomiasis. Schistosomiasis ranks second only to malaria in terms of parasite induced human morbidity and mortality, with over 200 million

* Correspondence: boissier@univ-perp.fr
[1] UMR 5244 CNRS-EPHE-UPVD. Parasitologie Fonctionnelle et Evolutive, CBETM. Université de Perpignan, Perpignan, France
[†] Contributed equally
Full list of author information is available at the end of the article

people infected worldwide. In schistosomes, sex is determined by sex chromosomes, with female being the heterogametic sex (ZW) and male the homogametic sex (ZZ) [2]. If male and female adult worms show evident phenotypic dimorphism, the larval stages are morphologically indistinguishable making sex-specific infection, crosses and linkage studies extremely difficult. Traditional methods of identification of W-specific sequences have failed to deliver faithful markers [3]. We reasoned that male (ZZ) *vs*. female (ZW) whole genome comparison would enable to identify female specific sequences that are only present on the W chromosome. We split the bioinformatics analysis into two axes: one for the unique sequences and one for the repetitive sequences which allowed us to identify several new classes of female specific repeats and 105 contigs containing unique sequences.

Results

Biological material

The experimental strategy is outlined in figure 1. In this study we used a *S. mansoni* strain isolated from naturally infected molluscs from Guadeloupe (French West Indies), a Guadeloupean strain of *Biomphalaria glabrata* as intermediate hosts, and the Swiss OF1 mouse strain as final hosts (for the parasite life cycle see figure 2). Methods for mollusc, mouse infections and parasite recovery have been previously described [4]. Briefly, mollusc infection consists in a simple contact in spring water between parasite larvae (miracidia) and molluscs, mouse infection is performed under general anaesthesia and parasite larvae (cercariae) penetrate naturally through the host skin. Finally, parasite recovery is performed by hepatic perfusion of the mouse. Less than 10 μg DNA, in our case from 23 male (5 μg DNA) and 91 female (1.2 μg DNA) adult flukes recovered from mice infected with a single sex and of the same clonal population was extracted using a method adapted to ChIP-Seq but without the immunoprecipitation step [5].

Sequencing

Solexa sequencing was performed on a Genome Analyzer II (Illumina) by single end sequencing according to the manufacturers protocol. Twenty ng of MNase fragmented DNA from each sample was repaired to generate phosphorylated blunt ends. An adenosine was added to the 3' end of the blunt phosphorylated DNA fragments. Illumina's adapters were ligated to the DNA fragments. Size selection was performed using a 2% agarose gel and a slice was excised at 200 bp corresponding to an insert size of 140 bp. The DNA extracted from the gel was then used as a matrix for 18 cycles PCR using Illumina's PCR primers. Each library was purified and quantified using a DNA1000 Chip on a 2100 BioAnalyzer (Agilent Technologies). These libraries were denaturated using NaOH and then diluted to a final concentration of 2 pM. One hundred μl of these diluted libraries were used for clustering on the Cluster Station using Clustering Kit V.2 (Illumina) and sequencing on the Genome Analyzer using a 36 Cycle SBS Kit V.3 (Illumina). A total of 8,600,198 (309,607,128 bp) and 9,355,380 (336,793,680 bp) sequence reads were produced with GAPipeline 1.3 for the male and female, respectively. This translates to roughly one-fold coverage of the genome, which is sufficient for the described approach.

Analysis of unique sequences

ELAND was used to align the reads to the reference genome of *S. mansoni* (Puerto Rico) scaffolds, draft version 3.1 (version: 05/08/2008) [6]ftp://ftp.sanger.ac.uk/pub/pathogens/Schistosoma/mansoni/genome/gene_predictions/GFF/S.mansoni_080508.fasta.gz. The algorithm that is used by the ELAND software aligns only to unique sequences in the genome. Other short-read alignment programs can also be used. ELAND has been developed by Anthony J. Cox (Solexa) to align short read sequence to a reference genome. The first 32 bp of each sequence stretch are used to identify each sequence either as perfect match, 1-mismatch or 2-mismatches. Sequences with mismatches above 2 on the first 32 bp are ignored. The coordinates on the genome of repeat sequences (multiple places in the genome) are not given by the software. A total of 65.2% of the female reads and 70.3% of the male reads were located on the genome by the software. As for many species, the *S. mansoni* genome is sequenced but only partially assembled resulting in a high number (19022) of individual scaffolds. Perl scripts were used to split the alignment results into individual files for each scaffold (SeparateElandReads.pl) and aligned reads ("hits") were counted (AnalyzeElandFiles.pl). Perl scripts can be downloaded from http://methdb.univ-perp.fr/cgrunau/methods/Eland2GBrowse.html. This allowed for identification of scaffolds with a low number of hits in the male and high hit counts in the female, *i.e.* female-specific sequences. For visualization in a genome browser, the ELAND output (s_x_sorted.txt) was converted into the classical ELAND format (s_x_eland_result.txt) with a perl script (available on request), and used for generation of wiggle and gff files with FindPeaks 3.1 [7] and CASHX2.0 [8]. Annotation files were uploaded to an in-house Gbrowse server, and female-specific sequences were confirmed by visual inspection of candidate scaffolds. Regions on these scaffolds that showed hits only from the female genome were used for primer design in order to confirm the bioinformatics analysis (see below). The rational behind this approach is that relatively large (size of a scaffold) differences exist between the female and male genome. Since it

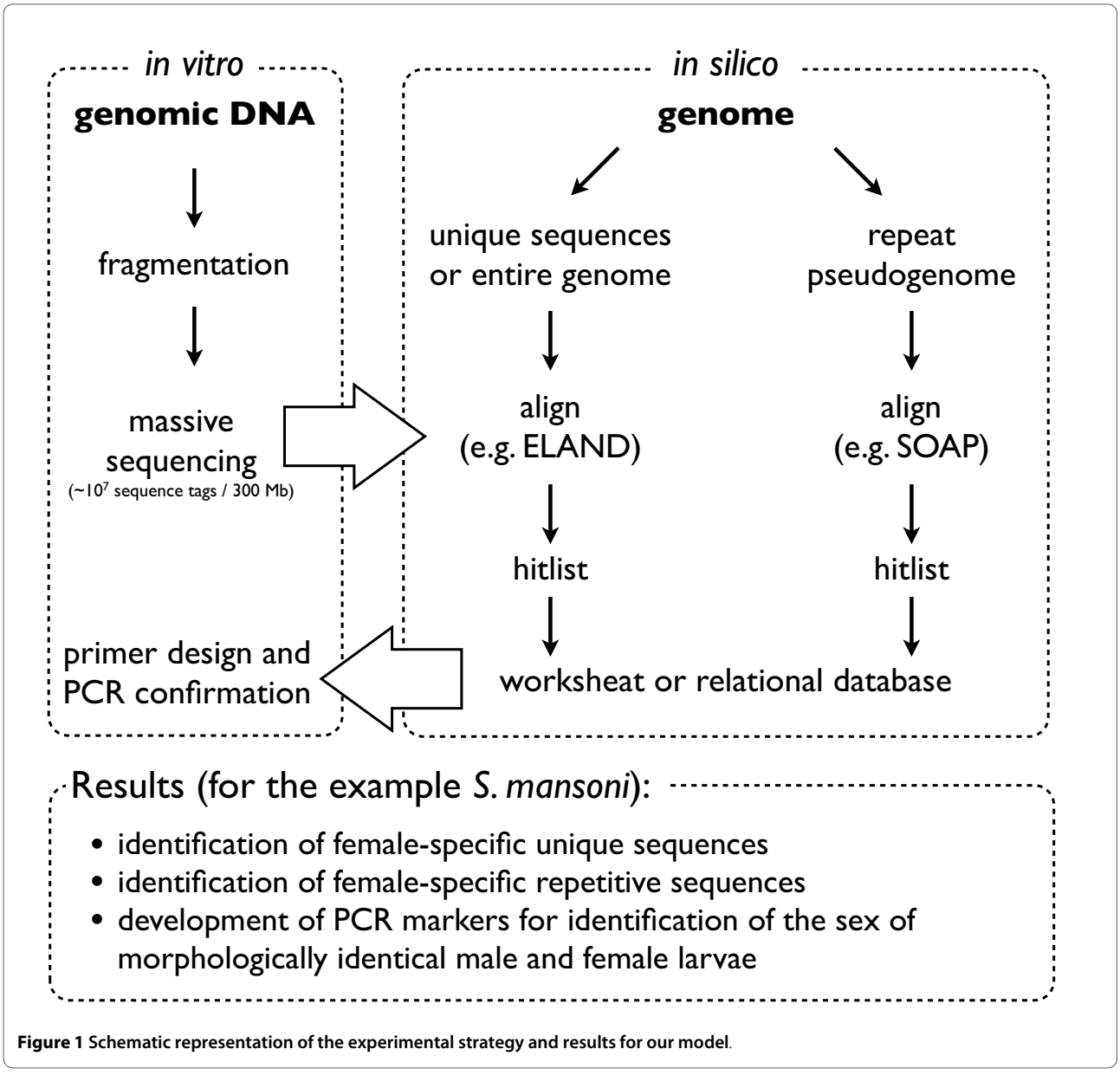

Figure 1 Schematic representation of the experimental strategy and results for our model.

could be possible that there are only small differences between the two genomes, we repeated the analysis by using the CASHX data in a sliding window of 500 bp with a step size of 250 bp and compared the results with a relational database. Further bioinformatics analysis could include repeat finding and gene annotation. In our case, Tandem Repeats finder [9] was used to investigate the presence of tandem repeats in the female specific contigs. ESTs were obtained from public databases (SchistoDB [10], GeneDB http://www.genedb.org/, GenBank http://www.ncbi.nlm.nih.gov/Genbank/, gene prediction algorithms http://compbio.ornl.gov/tools/pipeline/, http://opal.biology.gatech.edu/GeneMark/eukhmm.cgi were used to test for the presence of putative genes, and MotifScan http://hits.isb-sib.ch/cgi-bin/PFSCAN was employed for prediction of function.

Analysis of repetitive sequences

As for many eukaryotes, roughly 40% of the *S. mansoni* genome is composed of repetitive sequences. The conventional alignment algorithms cannot use these sequences, and they are in general not considered for analysis. To make use of these repeats, we exploited the repeatmasker database of *S. mansoni* ftp://ftp.tigr.org/pub/data/Eukaryotic_Projects/s_mansoni/preliminary_annotation/homology_evidence/sma1.repeats.gz, added repeats that were available in the literature [11,12], and a tandem repeat (TR266) that was identified with Tandem Repeat finder (see above). This produced a sequence file

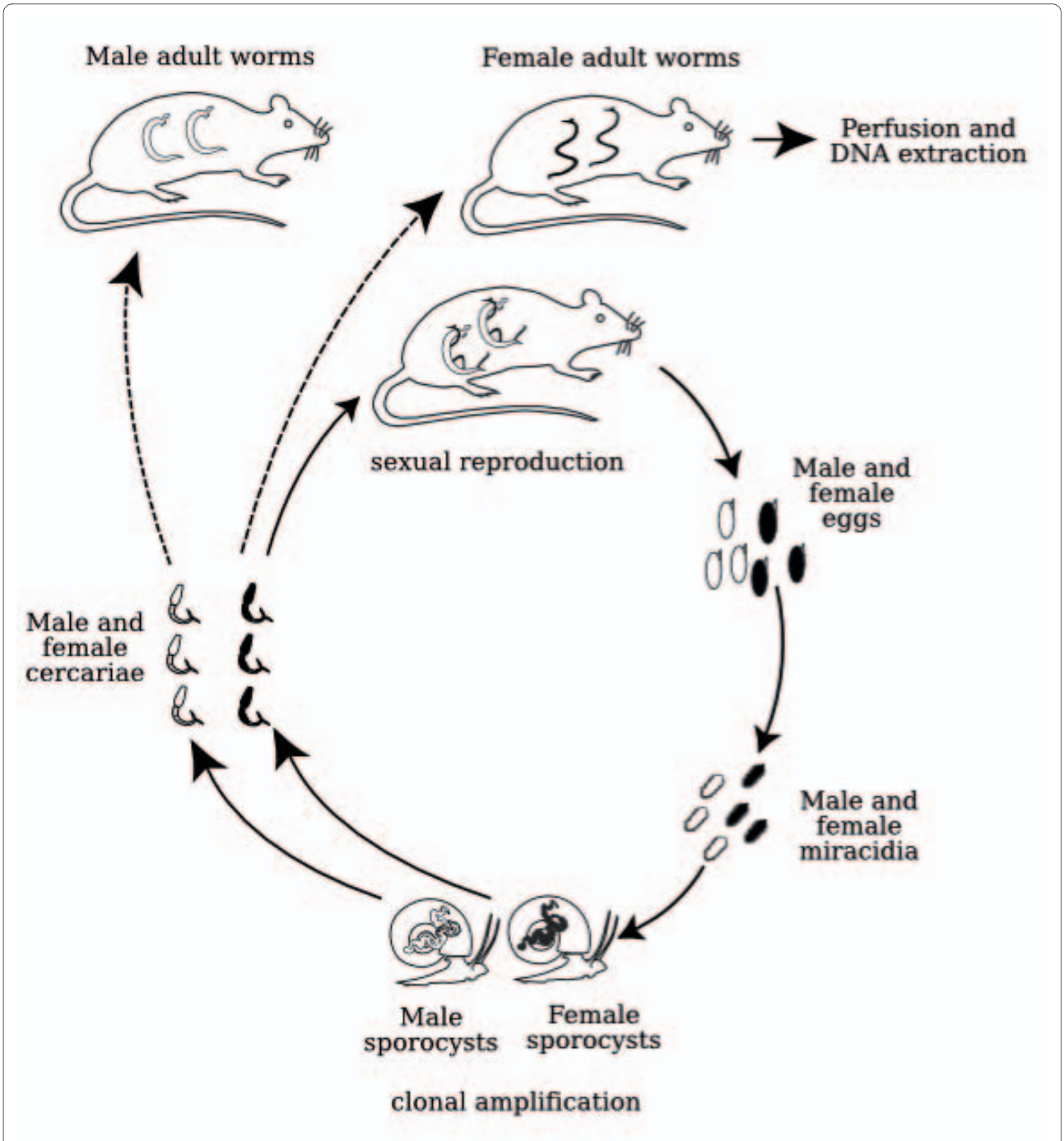

Figure 2 *Schistosoma mansoni* life cycle representing the separated sexes of the parasite. Sexual reproduction occurs between male and female adult worms in the vertebrate definitive host. Sex determination is syngamic, thus one egg produces either a male or a female larva (called miracidium). This larva actively infects a mollusc intermediate host, transforms into intramolluscan larval stages (called sporocysts) and produces, by clonal multiplication, many unisexual larvae (called cercariae) that will actively infect the vertebrate definitive host and transform into adult worms. For our experimental approach, molluscs were infected with a single miracidium, thus produced either male or female cercariae.

that is composed of repeats with each repeat occurring only once (repeat pseudogenome). For other genomes, *de-novo* prediction of repeats would be necessary and the NGS data that do not align to the unique sequences could also be assembled to obtain a repeat pseudogenome. The pseudogenome was indexed with 2bwt-builder of soap2.17 [13], and the Solexa fastq files were used for alignment with SOAP. 16.26% (female) and 15.06% (male)

of the reads mapped to the pseudogenome, *i.e.* were identified as repeats. Taking into account the above-mentioned unique sequences, this leaves 18.54% (female) and 14.64% (male) unidentified. From the soap output, repeats with at least five hits and for which at least 99% of the total hits occurred in the female genome were used for further analysis (Table 1). Soap files were converted into gff format with a tool of the pass utilities [14] and distribution of hits was visualized with Excel (Microsoft Corp.). In the male genome, hits occurred exclusively on the flanks of the repeats corresponding probably to integration and/or excision sites (Additional file 1, figure S1). Sequences are available at the NCBI sequence read archive http://www.ncbi.nlm.nih.gov/Traces/sra/ under study accession number SRA012151.6.

Confirmation of WISH-identified sex-specific sequences

PCR were done to confirm the *in-silico* analysis. *Schistosoma mansoni* W specific primers pairs (SmWSPP, Additional file 2 table S1) were designed in the female-specific regions using Primer 3 http://frodo.wi.mit.edu/ and checked for specificity using Primer-Blast http://www.ncbi.nlm.nih.gov/tools/primer-blast/index.cgi. DNA from male and female adult worms was extracted [15] and PCR amplifications were performed in duplicate. PCR reactions were carried out in a total volume of 10 μl containing 1 μl of 10× buffer (450 mM Tris HCl (pH 8.8), 110 mM ammonium sulfate, 45 mM MgCl, 67 mM beta-mercaptoethanol, 44 μM EDTA (pH 8), 1.13 mg/mL BSA) [16], 2 pmol of each oligonucleotide primer, 1 mM of each dNTP (Promega), 0.5 unit of GoTaq polymerase (Promega, Madison, Wisconsin), 1 μl of extracted DNA and DNase-free water. PCR program consisted in an initial denaturation phase at 95°C for 5 min, followed by a suitable number of cycles at 95°C for 30 s, 60°C for 30 s, 72°C for 60 s or less, and a final extension at 72°C for 10 min. Examples of the results are shown in figure 3.

Ethical note

Our laboratory has received the permit N° A 66040 for experiments on animals from both French Ministry for Agriculture and Fishery (Ministère de l'Agriculture et de la Pêche) and the French Ministry for Higher Education and Research (Ministère de l'Education Nationale de la Recherche et de la Technologie). Housing, breeding and animal care of the mice followed the ethical requirements of our country. The experimenter possesses the official certificate for animal experimentation delivered by both ministries (Décret n° 87-848 du 19 octobre 1987; number of the authorization 007083)

Discussion

WISH is a fast and comparably inexpensive alternative for the identification of differences between genomes

The method we describe here is fast: DNA extraction, sequencing and base calling can be done in a week, alignment and sequence analysis depending on the available computing power in another week, and PCR confirmation in a couple of days. The cost of this procedure is comparable to traditional methods such as subtractive hybridization and was in our case less than 3000 Euros. As a result of massive parallel sequencing and straightforward bioinformatics analysis, we identified 180 female-specific contigs and seven repeats.

WISH identifies unique and repetitive sex-specific sequences

The total genome length of *S. mansoni* is 381,097,121 bp spanning 19,022 contigs [6]. In 1,635 contigs (3,058,411 bp) ELAND found at least one hit in the female genome and no hits in male, and in 1,070 contigs (1,827,612 bp) at least one hit in male but no hits in female. Since about 9,000,000 sequence tags were produced for each genome we expected about 2 hits per 100 bp along the genome, except for the repetitive sequences that are excluded by ELAND. We searched therefore for contigs with at least 1

Table 1: Name and number of female and male hits and length of the selected repeats.

repeat	% of total hits on female	Length (bp)	GenBank acc.nr.
W1	100.00	482	[J04665.1]
R = 407.2	100.00	711	[GU562605]
W2	100.00	715	[U10109.1]
TR266	99.97	267	[GU562608]
R = 879	99.91	654	[GU562606]
Sm_alphafem1	99.86	338	[U12442.1]
R = 564	99.27	1129	[GU562607]

Repeats were considered as female (W) specific if at least five hits occurred and if at least 99% of the total hits occurred in the female genome. %female = (number of hits obtained with SOAP for the female genome * 100/number of hits obtained with SOAP for the female genome + number of hits obtained with SOAP for the male genome)

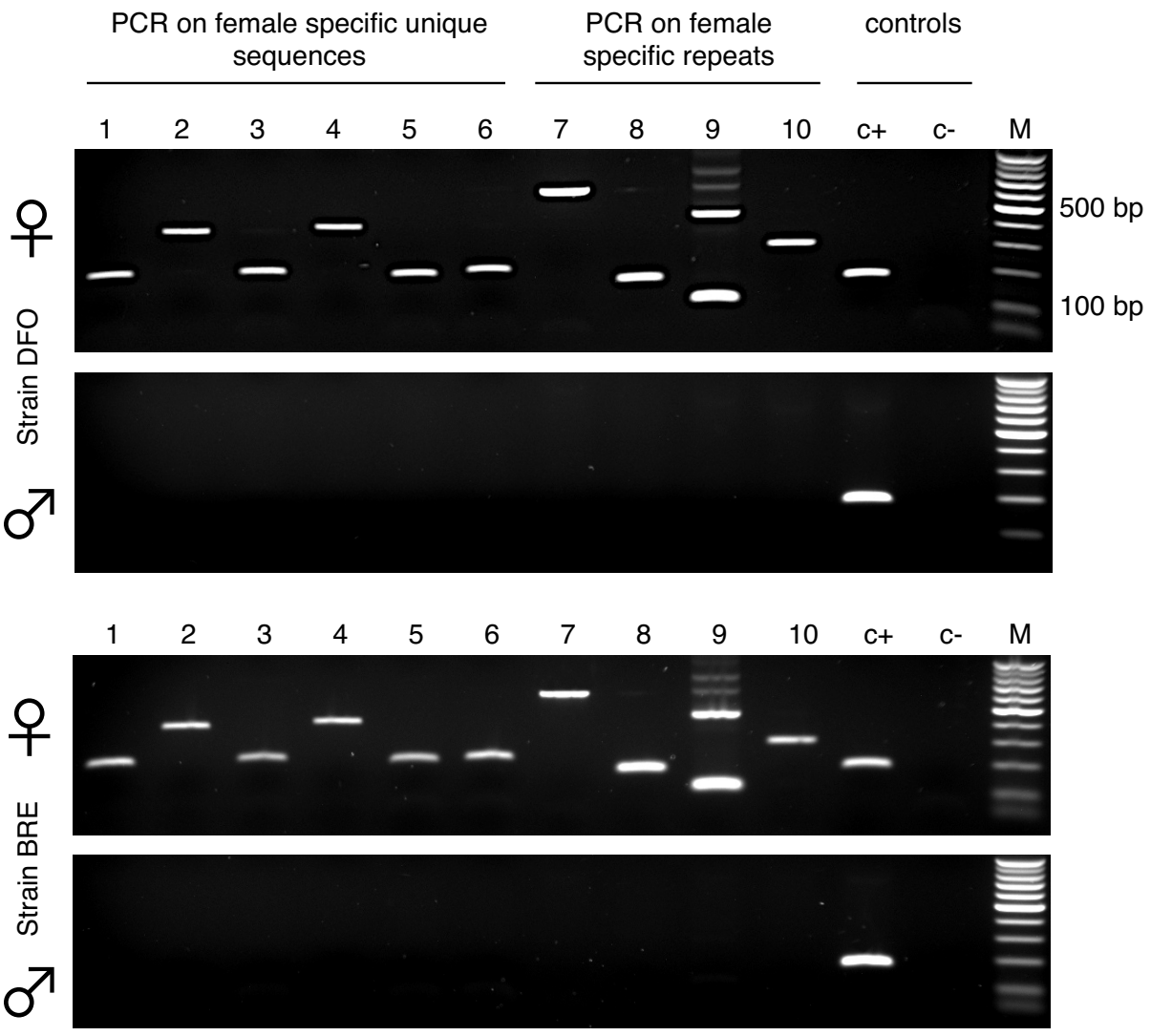

Figure 3 Ethidiumbromid stained agarose gels (1.5%) with PCR products for typical examples of W-specific primer pairs (SmWSPP1-10). Primers and PCR conditions are listed in additional file 2, table S1. Positive control (c+) is a primer pair in the autosomal rhodopsine gene, negative control (c-) is water. M is size marker (100 bp, Promega). Two strains of *S. mansoni* were analysed (DFO (top) and BRE (bottom panel)). On upper part of each panel, PCR products for DNA of female adults, on the bottom part, PCR on DNA of male adults.

hit in the female genome and no hit in males. 888 contigs (1,816,279 bp) fulfilled this criteria, but most were small and only 269 were longer than 2 kb (total length 950,812 bp) (Additional file 3, table S2). All 269 contigs were analyzed by visual inspection. The criterion for regarding a contig here as female-specific was the absence or strong under-representation of CASHX hits in the male genome, and presence in the female genome. 105 contigs (436,269 bp) were retained. We then processed the genome in 500 bp windows with a step size of 250 bp searching for fragments with more than 3 hits/500 bp in the female genome and less than one for the male genome. 304 fragments fulfilled this criterion and they were inspected manually. All fragments were dispersed on the genome and no W-specific regions or pseudo-autosomal regions could be identified. Consequently, the W-specific unique regions span at most 950 kb i.e. about 0.2% of the genome. A preliminary sequence analysis did not reveal any sex determination gene.

Seven repeats (R = 407, R = 879, Sm_alphafem1, R = 564, TR266, W1, W2) were identified as female specific. Three of the sequences had been identified before: Sm_alphafem1 [GenBank:U12442.1] was isolated in 1995 by a subtractive hybridization process as female-specific sequence of the alpha retrotransposon family [12]. The copy-number of the Sm_alphafem family of repeats

(Smα) was estimated to be 20,000-200,000 [17]. W1 [GenBank:J04665.1] was found by Webster and colleagues and its estimated copy number is 500 [11]. The female-specific repetitive DNA W2 [GenBank:U10109.1] was identified by a PCR-based approach (Representational difference analysis) [12]. One of the newly identified repeats (R = 407) has 95% identity to W2, all other pairwise similarities are around 50%. Characteristics are listed in table 1. Assuming that around 1000 copies exist for each repeat other than Sm_alphafem, then this would correspond to around 10.5 Mb (~2.5% of the genome). Blast against the *S. mansoni* genome (assembly 3.1) allowed for identification of contigs that contain these repeat sequences. All contigs were inspected for presence or absence of male and female NGS hits, and used to complete the list of female-specific contigs resulting in a total of 180 contigs (603,758 bp) (Additional file 3, table S2). WISH is a method to identify sequence differences. These sequences can now be analyzed by other methods.

WISH-identified W-specific sequences can be used for sex identification

A possible use (and our primary interest) of the genome comparison is the identification of markers that can be amplified by PCR. We designed primers for some contigs and repetitive sequences (Additional file 2, table S1). All tested primer pairs showed the PCR product at the expected size on the adult female but not on the adult male parasite (Figure 3). For SmWSPP 9 (Sm_alphafem1), W-specific PCR products of different size were amplified probably due to the repetitive nature of the target sequence. The same results were obtained on individual parasite larval stages (data not shown). In addition to male-to-female comparison, WISH can be used to identify genetic differences between strains, pathovars or even closely related species opening up a wide range of possible applications. One possible candidate would be *S. japonicum* for which there is a situation similar to our model (draft genome available, female-specific part of the genome unknown). It might be argued that the method requires the genome to be sequenced. This is obviously true, but currently 1001 genomes are completed, for 1279 the draft assembly is available and 1206 genomes are in progress http://www.ncbi.nlm.nih.gov/genomes/static/gpstat.html. These numbers will continue to increase and for most species of medical and ecological importance the genomes will become available. To determine the mode of sex determination is a challenging question for many species [18]. In the case of *S. mansoni*, female-specific markers have been hunted for the last 30 years and 3 female-specific repeat had been identified by classical methods. These repeats were also identified by our approach and served as a positive control. The reason for their earlier discovery is probably that they are the most abundant female-specific sequences in the *S. mansoni* genome (data not shown). The W1 repeat was used for the identification of female larvae, however, experiments in our laboratory and evidence from other labs indicates that the marker could be used for a certain number of generations but sporadically the PCR would amplify also from the male genome [3,19,20]. We do not exclude that the repeat-based PCR markers we present here do not behave similar. Routinely, we use two unique sequences for sex determination, a strategy that works well in our hands. A detailed description is available as additional files and on our webpage http://methdb.univ-perp.fr/cgrunau/methods/sexing_schisto.html

Conclusions

We show here that using massive sequencing and PCR to detect sex-specific sequences is a reliable and straightforward method to clarify the sex determination issue. The identified markers can be used to identify the sex of individuals in early developmental stages or for adults in species without apparent sexual dimorphism. Sex identification method could also be of clear interest to control the sex in domestic animal reproduction in livestock industry [21,22]. Other applications lie in molecular ecology to identify sex-specific patterns like biased sex-ratio or bias in the dispersal of each sex [23,24]. Naturally, as mentioned above, the method can also be used to detect sequence differences in other scenarios.

Additional material

Additional file 1 Figure S1. Distribution of SOAP hits along the consensus sequence of female-specific repeats. X-axis: repeat sequence in bp, y-axis: number of hits.

Additional file 2 Table S1. Characteristics of *Schistosoma mansoni* W chromosome (female) specific primer pairs.

Additional file 3 Table S2. Female specific contigs (scaffolds of Schistosoma mansoni draft version 3.1.) and available evidence for their identification. All contigs verified by visualization of CASHX hits.

Competing interests

The authors declare that they have no competing interests.

Authors' contributions

CG, CC, and JB conceived and designed the experiments. CG and CC performed *in silico* analyses. JP and SB experimentally verified *in silico* analyses. HP and CD performed sequencing runs. CG, JB and CC wrote the manuscript. All authors read and approved the final manuscript.

Acknowledgements

This work was supported by the ANR (Program Monogamix ANR-08-BLAN-0214-02, Program Schistophepigen ANR-07-BLAN-0119-02 and Program Schisto-Med ANR-08-MIEN-026-01). The authors wish to thank Bernard Dejean for technical assistance.

Author Details

[1]UMR 5244 CNRS-EPHE-UPVD. Parasitologie Fonctionnelle et Evolutive, CBETM. Université de Perpignan, Perpignan, France and [2]Plateforme MGX, Institut de Génomique Fonctionnelle 141, rue de la Cardonille, Montpellier, France

Received: 22 February 2010 Accepted: 21 June 2010
Published: 21 June 2010

References

1. Hillier LW, Marth GT, Quinlan AR, Dooling D, Fewell G, Barnett D, Fox P, Glasscock JI, Hickenbotham M, Huang W, *et al.*: **Whole-genome sequencing and variant discovery in *C. elegans*.** *Nature Methods* 2008, **5(2):**183-188.
2. Short RB: **Presidential address: Sex and the single schistosome.** *Journal of parasitology* 1983, **69(1):**3-22.
3. Grevelding CG: **Genomic instability in *Schistosoma mansoni*.** *Molecular and Biochemical Parasitology* 1999, **101(1-2):**207-216.
4. Boissier J, Mone H: **Experimental observations on the sex ratio of adult *Schistosoma mansoni*, with comments on the natural male bias.** *Parasitology* 2000, **121(Pt 4):**379-383.
5. Cosseau C, Azzi A, Smith K, Freitag M, Mitta G, Grunau C: **Native chromatin immunoprecipitation (N-ChIP) and ChIP-Seq of *Schistosoma mansoni*: Critical experimental parameters.** *Molecular and Biochemical Parasitology* 2009, **166(1):**70-76.
6. Berriman M, Haas BJ, LoVerde PT, Wilson RA, Dillon GP, Cerqueira GC, Mashiyama ST, Al-Lazikani B, Andrade LF, Ashton PD, *et al.*: **The genome of the blood fluke *Schistosoma mansoni*.** *Nature* 2009, **460(7253):**352-358.
7. Fejes AP, Robertson G, Bilenky M, Varhol R, Bainbridge M, Jones SJ: **FindPeaks 3.1: a tool for identifying areas of enrichment from massively parallel short-read sequencing technology.** *Bioinformatics* 2008, **24(15):**1729-1730.
8. Fahlgren N, Sullivan CM, Kasschau KD, Chapman EJ, Cumbie JS, Montgomery TA, Gilbert SD, Dasenko M, Backman TW, Givan SA, *et al.*: **Computational and analytical framework for small RNA profiling by high-throughput sequencing.** *RNA* 2009, **15(5):**992-1002.
9. Benson G: **Tandem repeats finder: a program to analyze DNA sequences.** *Nucleic Acids Research* 1999, **27(2):**573-580.
10. Zerlotini A, Heiges M, Wang H, Moraes RL, Dominitini AJ, Ruiz JC, Kissinger JC, Oliveira G: **SchistoDB: a *Schistosoma mansoni* genome resource.** *Nucleic Acids Research* 2009:D579-582.
11. Webster P, Mansour TE, Bieber D: **Isolation of a female-specific, highly repeated *Schistosoma mansoni* DNA probe and its use in an assay of cercarial sex.** *Molecular and Biochemical Parasitology* 1989, **36(3):**217-222.
12. Drew AC, Brindley PJ: **Female-specific sequences isolated from *Schistosoma mansoni* by representational difference analysis.** *Molecular and Biochemical Parasitology* 1995, **71(2):**173-181.
13. Li R, Li Y, Kristiansen K, Wang J: **SOAP: short oligonucleotide alignment program.** *Bioinformatics* 2008, **24(5):**713-714.
14. Campagna D, Albiero A, Bilardi A, Caniato E, Forcato C, Manavski S, Vitulo N, Valle G: **PASS: a program to align short sequences.** *Bioinformatics* 2009, **25(7):**967-968.
15. Beltran S, Galinier R, Allienne JF, Boissier J: **Cheap, rapid and efficient DNA extraction method to perform multilocus microsatellite genotyping on all *Schistosoma mansoni* stages.** *Memorias do Instituto Oswaldo Cruz* 2008, **103(5):**501-503.
16. Jeffreys AJ, Neumann R, Wilson V: **Repeat unit sequence variation in minisatellites: a novel source of DNA polymorphism for studying variation and mutation by single molecule analysis.** *Cell* 1990, **60(3):**473-485.
17. DeMarco R, Kowaltowski AT, Machado AA, Soares MB, Gargioni C, Kawano T, Rodrigues V, Madeira AM, Wilson RA, Menck CF, *et al.*: **Saci-1, -2, and -3 and Perere, four novel retrotransposons with high transcriptional activities from the human parasite *Schistosoma mansoni*.** *Journal of Virology* 2004, **78(6):**2967-2978.
18. Staelens J, Rombaut D, Vercauteren I, Argue B, Benzie J, Vuylsteke M: **High-density linkage maps and sex-linked markers for the black tiger shrimp (*Penaeus monodon*).** *Genetics* 2008, **179(2):**917-925.
19. Grevelding CG: **The female-specific W1 sequence of the Puerto Rican strain of Schistosoma mansoni occurs in both genders of a Liberian strain.** *Molecular and Biochemical Parasitology* 1995, **71(2):**269-272.
20. Quack T, Doenhoff M, Kunz W, Grevelding CG: ***Schistosoma mansoni:* the varying occurrence of repetitive elements in different strains shows sex-specific polymorphisms.** *Experimental Parasitology* 1998, **89(2):**222-227.
21. Chen J, Wang Y, Yue Y, Xia X, Du Q, Chang Z: **A novel male-specific DNA sequence in the common carp, *Cyprinus carpio*.** *Molecular and cellular probes* 2009, **23(5):**235-239.
22. Horng YM, Huang MC: **Male-specific DNA sequences in pigs.** *Theriogenology* 2003, **59(3-4):**841-848.
23. Scribner KT, Petersen MR, Fields RL, Talbot SL, Pearce JM, Chesser RK: **Sex-biased gene flow in spectacled eiders (Anatidae): inferences from molecular markers with contrasting modes of inheritance.** *Evolution; international journal of organic evolution* 2001, **55(10):**2105-2115.
24. Yannic G, Basset P, Hausser J: **Phylogeography and recolonization of the Swiss Alps by the Valais shrew (*Sorex antinorii*), inferred with autosomal and sex-specific markers.** *Molecular ecology* 2008, **17(18):**4118-33.

doi: 10.1186/1471-2164-11-387
Cite this article as: Portela *et al.*, Whole-genome in-silico subtractive hybridization (WISH) - using massive sequencing for the identification of unique and repetitive sex-specific sequences: the example of Schistosoma mansoni *BMC Genomics* 2010, **11**:387

ANTIMICROBIAL AGENTS AND CHEMOTHERAPY, May 2011, p. 2403–2405 Vol. 55, No. 5
0066-4804/11/$12.00 doi:10.1128/AAC.00082-11

Trioxaquine PA1259 Alkylates Heme in the Blood-Feeding Parasite *Schistosoma mansoni*[▽]

Vincent Pradines,[1] Julien Portela,[2] Jérôme Boissier,[2] Frédéric Coslédan,[3] Bernard Meunier,[3] and Anne Robert[1]*

Laboratoire de Chimie de Coordination du CNRS, 205 route de Narbonne, 31077 Toulouse Cedex 4, France[1]; UMR 5244 CNRS-UPVD, Laboratoire Écologie et Évolution des Interactions, Université de Perpignan, 52 Avenue Paul Alduy, 66860 Perpignan, France[2]; and Palumed, 3 rue de l'Industrie, 31320 Castanet-Tolosan, France[3]

Received 19 January 2011/Returned for modification 25 January 2011/Accepted 31 January 2011

Trioxaquine PA1259 is an efficient drug on larval- and adult-stage schistosomes, able to alkylate heme inside worms treated with it, leading to the formation of covalent heme-drug adducts. Such a mechanism, similar to one reported for other trioxaquines in *Plasmodium*, indicates that heme may be a common target of these trioxane-based drugs in different blood-feeding parasites.

Schistosoma mansoni is a flatworm responsible for a chronic parasitic disease called schistosomiasis (or bilharziasis) (7). Vaccines are not yet available (10), and chemotherapy is the only way to control schistosomiasis. Chemotherapy consists of a single drug, praziquantel (PZQ). Praziquantel has been effectively used for about 40 years, and resistance to it is currently emerging (6, 11). Consequently, the development of new drugs is an urgent need for a highly neglected disease (8, 15, 18, 19).

Hemoglobin metabolism is a common feature of *Schistosoma* and *Plasmodium*. Host hemoglobin is ingested by schistosomes and degraded to amino acids in the ceca of the parasites. The free heme released by this metabolism is polymerized as hemozoin and regurgitated. Hemozoin is a disposal product generated by both *Plasmodium* and *Schistosoma* (14). Targeting the free heme of hematophagous parasites via an alkylation mechanism has been the rationale for the design of hybrid molecules named trioxaquines, containing a 1,2,4-trioxane linked to an aminoquinoline (2, 13, 17).

Since the activities of praziquantel and artemether have already been reported to be complementary on *Schistosoma* (20), our first attempt with hybrid antischistosomal molecules was based on a 1,2,4-trioxane linked to praziquantel. These compounds did not reach the expected level of activity (9). We then decided to evaluate a series of trioxaquines, molecules active against chloroquine-resistant *Plasmodium falciparum* strains, on *Schistosoma mansoni* (1, 5, 12, 13, 16, 17), and several of these molecules were highly active on both larval and mature stages of *S. mansoni* (2). On *Plasmodium*, trioxaquines exhibit a dual mode of action: (i) alkylation of heme via the trioxane entity, and (ii) stacking with heme via the aminoquinoline moiety, leading to the inhibition of hemozoin formation (1, 5, 12). As reported for artemisinin derivatives (16), trioxaquines are efficiently activated by heme, leading to the formation of covalent heme-drug adducts detected in mice infected with *Plasmodium* (malaria) (4).

For a better understanding of the molecular bases of the antischistosomal activity of trioxaquines, we investigated their reactivity toward heme and hemozoin in *S. mansoni*. Mature *S. mansoni* worms were treated with trioxaquine PA1259 (Fig. 1), and we report the characterization of heme-drug adducts generated inside the worms.

The host-parasite system used was an albino variety of *Biomphalaria glabrata* and a strain of *Schistosoma mansoni*, both from Brazil, maintained in Swiss OF1 mice (Charles River, France). Methods for mollusc and mouse infections and for parasite recovery were previously described (3). Mice were percutaneously infected using 120 cercariae and sacrificed 49 days after infection. Groups of 25 adult schistosomes, freshly recovered, were washed, placed in a 6-well Falcon plate containing 3 ml of RPMI 1640 medium (supplemented with L-glutamine and 25 mM HEPES), and stored at 37°C. Trioxaquine PA1259 (B. Meunier, F. Coslédan, and A. Pellet, 21 December 2007, patent application WO/2007/144487) was dissolved in dimethyl sulfoxide (DMSO) (100 mg/ml), diluted in RPMI 1640 medium complemented with 2.17% Tween 80, and added to the worm cultures (final PA1259 concentration, 50 μg/ml; final solvent ratio of 1,000/0.95/3.8 [vol/vol/vol] for RPMI–Tween 80–DMSO). After 3 h, all parasites were dead (no body contractions and no movement during 30 s), whereas control worms (treated with RPMI–Tween 80–DMSO [1,000/0.95/3.8, vol/vol/vol] but without drug) exhibited normal movements. The worms were washed with water, lyophilized, and crushed with sand. The powder obtained was extracted with pyridine (500 μl). The mixture was vigorously stirred for 5 min, submitted to ultrasound for 30 min, and magnetically stirred at 37°C overnight. The pyridine supernatant was withdrawn, filtered, and evaporated to dryness. The residue was dissolved in DMSO (60 μl) and diluted 5 times in a mixture of water-methanol-formic acid (10/90/1, vol/vol/vol).

The liquid chromatography-mass spectrometry (LC-MS) analyses were performed using an Agilent 6140 machine. The following equipment and conditions were used for LC-MS analyses: high-performance liquid chromatographic (HPLC)

* Corresponding author. Mailing address: Laboratoire de Chimie de Coordination du CNRS, 205 route de Narbonne, 31077 Toulouse Cedex 4, France. Phone: 33 5 61 33 31 26. Fax: 33 5 61 55 30 03. E-mail: anne.robert@lcc-toulouse.fr.

▽ Published ahead of print on 7 February 2011.

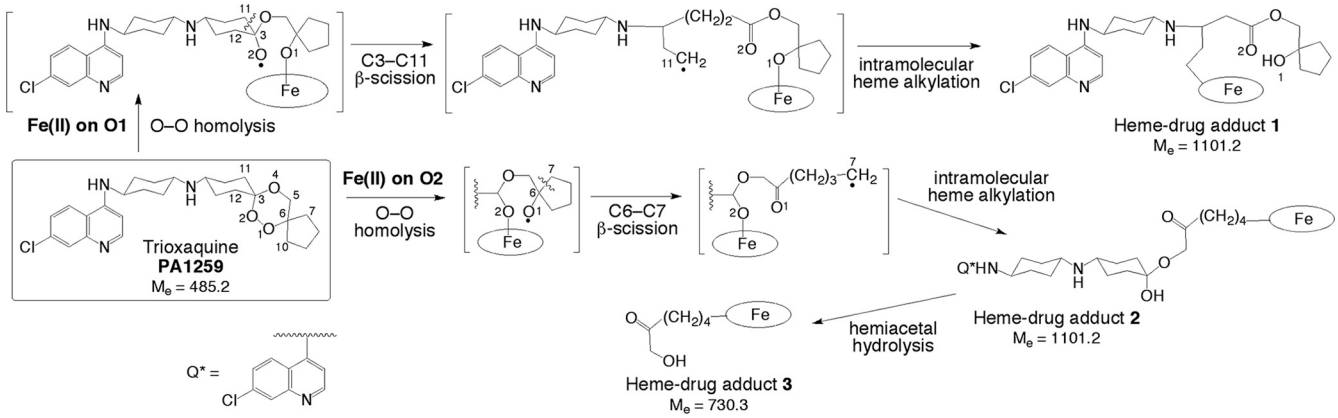

FIG. 1. Reductive activation of trioxaquine PA1259 by iron(II)-heme, leading to the covalent heme-drug adducts 1, 2, and 3.

column, 5-μm C_{18} X-Bridge column (150 by 4.6 mm) (Waters); linear elution gradient from water-formic acid (100/1, vol/vol) to methanol-formic acid (100/1, vol/vol) in 30 min; flow rate, 1 ml min^{-1}; injection volume of 100 μl; UV-visible light at 398 nm; and electrospray ionization (ESI^+)-MS detection with scan range of 300 to 1,200 atomic mass units (amu). The analytic conditions were previously optimized by using chemically prepared heme-PA1259 adducts. Specifically, 3.2 mg of Fe^{III}(PPIX)Cl, 10 mole equivalents of sodium dithionite, and 1.5 mole equivalents of trioxaquine PA1259 were dissolved in 500 μl DMSO. The reaction was carried out at 37°C, under an argon atmosphere, for 2 h.

The LC-MS analyses of extracts of *S. mansoni* worms treated with PA1259 are reported in Fig. 2a to c. Along with the ionic current of heme [retention time (R_t) = 26.1 min; m/z = 616.2; z = 1; M^+ for Fe^{III}(PPIX); Fig. 2a], several chromatographic peaks were detected at R_ts of 24.7, 25.3, 26.3, and 26.5 min, with m/z = 551.3 and z = 2, having an exact mass value of 1,101.2 amu (Fig. 2b). This mass, corresponding to the mass of heme (616.2) plus the mass of PA1259 (485.2), can be assigned to covalent adducts between heme and PA1259. The structures and mechanisms of the formation of these adducts are depicted in Fig. 1. As for artemisinin, alkylation of heme by the drug can indeed occur on the four *meso* positions of the porphyrin macrocycle, giving rise to regioisomeric adducts. In addition, the inner-sphere reductive activation of the peroxide bond of PA1259 can occur with coordination of iron(II)-heme either on O-1 or O-2, giving rise to the formation of alkoxy radicals either on O-2 or O-1, respectively. Subsequent β-scission of the adjacent C-3—C-11 or C-6—C-7 bond, respectively, generated C-centered radicals able to alkylate heme and provide the covalent heme-drug adducts 1 and 2. The covalent adduct 3, resulting from the hydrolysis of the hemiacetal function of adduct 2, was also detected (R_t = 25.1 and 25.7 min; m/z = 730.3; z = 1; Fig. 2c). In addition, the isotopic patterns of signals at m/z 551.3 and 730.3 clearly showed that the corresponding adducts contained one iron atom (M-1 at 550.3 and M-2 at 728.2, respectively, due to ^{54}Fe). In contrast, one chlorine atom was detected in adducts at m/z 551.3 (M + 1 at 552.3 due to ^{37}Cl), whereas adduct 3 contained no chlorine after release of the 7′-chloro-4′-aminoquinoline moiety (Fig. 1). The heme-trioxaquine adducts 1, 2, and 3 were undetectable in all extracts of untreated *S. mansoni* worms. Because the worms treated with PA1259 were carefully washed before lyophilization, the detected adducts 1 to 3 were clearly contained inside the worms and cannot be considered external contamination.

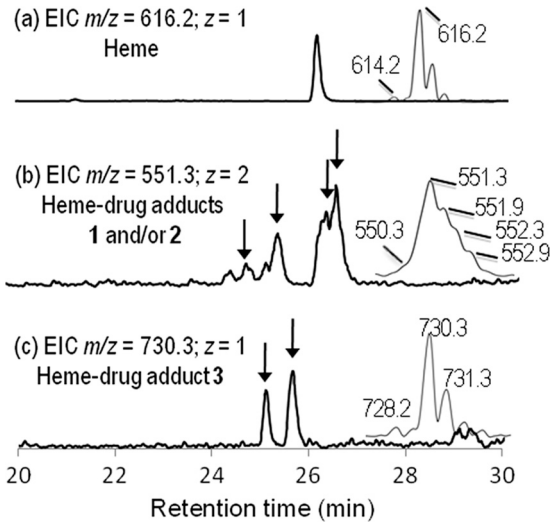

FIG. 2. (a to c) LC-MS analysis of the extract of *Schistosoma mansoni* treated with trioxaquine PA1259 (50 μg/ml). Extracted ionic current (EIC) traces for heme (heme, M^+) (a), "complete" heme-PA1259 adducts 1 and/or 2 (MH^+/2) (b), and heme-PA1259 adduct 3 (MH^+) (c). (The insets at the right show the mass spectra of chromatographic peaks with arrows.)

These results confirm that trioxaquine PA1259 is able to alkylate heme inside *Schistosoma* and also strongly suggest that heme is a relevant target for antischistosomal trioxaquines.

This work was supported by Palumed, CNRS, and Agence Nationale pour la Recherche (grant ANR-08-MIEN-026-02). V.P. and J.P. are indebted to ANR for fellowships.

We thank Sonia Kitoune and Christine Salle (both from Palumed) and Bernard Dejean (from the UMR 5244) for technical assistance.

REFERENCES

1. **Benoit-Vical, F., et al.** 2007. Trioxaquines are new antimalarial agents active on all erythrocytic forms, including gametocytes. Antimicrob. Agents Chemother. **51:**1463–1472.

2. **Boissier, J., F. Coslédan, A. Robert, and B. Meunier.** 2009. Evaluation of the in vitro activity of trioxaquines against *Schistosoma mansoni*. Antimicrob. Agents Chemother. **53:**4903–4906.
3. **Boissier, J., and H. Mone.** 2000. Experimental observations on the sex ratio of adult Schistosoma mansoni, with comments on the natural male bias. Parasitology **121:**379–383.
4. **Bousejra-El Garah, F., C. Claparols, F. Benoit-Vical, B. Meunier, and A. Robert.** 2008. The antimalarial trioxaquine DU1301 alkylates heme in malaria-infected mice. Antimicrob. Agents Chemother. **52:**2966–2969.
5. **Coslédan, F., et al.** 2008. Selection of a trioxaquine as a drug-candidate. Proc. Natl. Acad. Sci. U. S. A. **105:**17579–17584.
6. **Doenhoff, M. J., J. R. Kusel, G. C. Coles, and D. Cioli.** 2002. Resistance of Schistosoma mansoni to praziquantel: is there a problem? Trans. R. Soc. Trop. Med. Hyg. **96:**465–469.
7. **Gryseels, B., K. Polman, J. Clerinx, and L. Kestens.** 2006. Human schistosomiasis. Lancet **368:**1106–1118.
8. **Keiser, J., et al.** 2009. Mefloquine – an amino alcohol with promising antischistosomal properties in mice. PLoS Negl. Trop. Dis. **3:**e350.
9. **Laurent, S. A.-L., et al.** 2008. Synthesis of trioxaquantel derivatives as potential new antischistosomal drugs. Eur. J. Org. Chem. **2008:**895–913.
10. **McManus, D. P., and A. Loukas.** 2008. Current status of vaccines for schistosomiasis. Clin. Microbiol. Rev. **21:**225–242.
11. **Melman, S. D., et al.** 2009. Reduced susceptibility to praziquantel among naturally occurring Kenyan isolates of *Schistosoma mansoni*. PLoS Negl. Trop. Dis. **3:**e504.
12. **Meunier, B.** 2008. Hybrid molecules with a dual mode of action: dream or reality? Acc. Chem. Res. **41:**69–77.
13. **Meunier, B., and A. Robert.** 2010. Heme as trigger and target for trioxane-containing antimalarial drugs. Acc. Chem. Res. **43:**1441–1451.
14. **Oliveira, M. F., et al.** 2005. Structural and morphological characterization of hemozoin produced by *Schistosoma mansoni* and *Rhodnius prolixus*. FEBS Lett. **579:**6010–6016.
15. **Ribeiro-dos-Santos, G., S. Verjovski-Almeida, and L. C. C. Leite.** 2006. Schistosomiasis–a century searching for chemotherapeutic drugs. Parasitol. Res. **99:**505–521.
16. **Robert, A., F. Benoit-Vical, C. Claparols, and B. Meunier.** 2005. The antimalarial drug artemisinin alkylates heme in infected mice. Proc. Natl. Acad. Sci. U. S. A. **102:**13676–13680. (Erratum, **103:**3943, 2006.)
17. **Robert, A., O. Dechy-Cabaret, J. Cazelles, and B. Meunier.** 2002. From mechanistic studies on artemisinin derivatives to new modular antimalarial drugs. Acc. Chem. Res. **35:**167–174.
18. **Sayed, A. A., et al.** 2008. Identification of oxadiazoles as new drug leads for the control of schistosomiasis. Nat. Med. **14:**407–412.
19. **Xiao, S.-H., et al.** 2007. In vitro and in vivo activities of synthetic trioxolanes against major human schistosome species. Antimicrob. Agents Chemother. **51:**1440–1445.
20. **Xiao, S.-H., et al.** 2002. Recent investigations of artemether, a novel agent for the prevention of schistosomiasis japonica, mansoni and haematobia. Acta Trop. **82:**175–181.

C. R. Chimie 15 (2012) 75–78

Contents lists available at SciVerse ScienceDirect

Comptes Rendus Chimie

www.sciencedirect.com

Preliminary communication/Communication

Activity of trioxaquine PA1259 in mice infected by *Schistosoma mansoni*

Jérôme Boissier [a,b], Julien Portela [a,b], Vincent Pradines [c], Frédéric Coslédan [d], Anne Robert [c,*], Bernard Meunier [c,d]

[a] *Université de Perpignan Via Domitia, 66860 Perpignan, France*
[b] *CNRS, UMR 5244, écologie et évolution des interactions (2EI), 66860 Perpignan, France*
[c] *Laboratoire de chimie de coordination du CNRS, 205, route de Narbonne, 31077 Toulouse cedex 4, France*
[d] *Palumed, 3, rue de l'industrie, 31320 Castanet-Tolosan, France*

ARTICLE INFO

Article history:
Received 5 October 2011
Accepted after revision 15 November 2011
Available online 16 December 2011

Keywords:
Drug design
Heme proteins
Iron
Medicinal chemistry
Redox chemistry
Schistosomiasis
Trioxanes

ABSTRACT

Schistosomiasis is a chronic life-threatening parasitic disease concerning more than 200 million people in the World. Little attention has been paid to schistosomiasis over the last 30 years, and praziquantel is the only drug in use to control this disease. In the absence of a vaccine, there is a real need for new drugs in order both to improve the efficacy of the treatment and to delay the development of praziquantel resistant schistosomes. The present note reports the significant reduction of the worm burden after oral administration of trioxaquine PA1259 to mice infected by *Schistosoma mansoni*.

RÉSUMÉ

La schistosomiase (ou bilharziose) est une parasitose tropicale qui atteint plus de 200 millions de personnes, dans le monde. Peu de recherches ont été faites dans ce domaine depuis une trentaine d'années et le praziquantel est le seul médicament actuellement utilisé en clinique humaine. En l'absence de vaccin, il est indispensable de trouver de nouvelles molécules actives, à la fois pour augmenter l'efficacité du traitement et pour retarder l'émergence de souches de schistosomes résistants. Après traitement par voie orale de souris infectées par *Schistosoma mansoni*, la trioxaquine PA1259 conduit à une réduction significative de la charge parasitaire.

1. Introduction

Little attention has been paid to schistosomiasis (also known as bilharzia, bilharziosis or snail fever) over the last 30 years, for many different reasons including the fact that tourists traveling in endemic zones can easily escape from this parasitic disease by avoiding contact with infected waters. This neglected disease is a major parasitic disease with more than 200 million infected people in more than 74 countries in the tropical and subtropical zones, and continues to spread [1,2], even in areas where it was previously under control [3].

Schistosomiasis is caused by the trematode worms *Schistosoma* spp. (five species infect humans) which reside mainly in the abdominal veins of the infected vertebrates [4]. Infection occurs by penetration, through the skin of humans, of cercariae, the larval schistosome stages freely swimming in contaminated water. Then, parasite larvae invade capillaries and lymphatic vessels and accumulate in the liver for a rapid growth with portal vein blood. Four to 6 weeks after the infection, young adult worms migrate to the mesenteric veins (*S. mansoni* and *S. japonicum*) or the vesical plexus (*S. haematobium*) for a sexual maturation

* Corresponding author.
E-mail addresses: boissier@univ-perp.fr (J. Boissier), anne.robert@lcc-toulouse.fr (A. Robert), bmeunier@lcc-toulouse.fr (B. Meunier).

1631-0748/$ – see front matter © 2011 Académie des sciences. Published by Elsevier Masson SAS. All rights reserved.
doi:10.1016/j.crci.2011.11.008

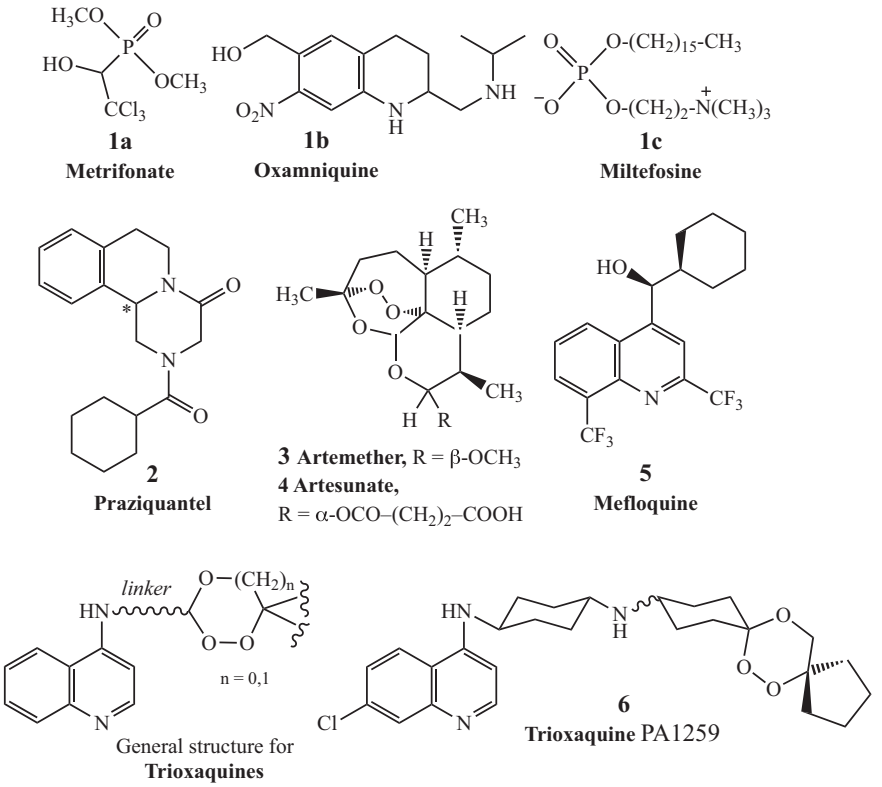

Fig. 1. Structures of metrifonate, oxamniquine, miltefosine, mefloquine, praziquantel, and artemisinin and trioxaquine derivatives.

and mating period. For *S. mansoni*, egg production (200 to 2000 eggs/female per day) begins 6 weeks after the initial infection and continues for the all life of the worms. The lifespan of an adult schistosome averages 3 to 5 years, but can be as long as 30 years. So, the theoretical reproduction potential of one schistosome pair can reach 600 billion eggs [4]. The immune response of the host to schistosome eggs induces chronic inflammation, fibrosis and ulceration of the tissues at the sites of egg accumulation: intestine and liver for *S. mansoni* and *S. japonicum* or the genito-urinary tract for *S. haematobium*. So, the late and life-threatening consequences of chronic schistosomiasis include bladder cancer or serious kidney dysfunction and severe damage of the liver and spleen.

It should be noted that despite the high level of prevalence of this tropical disease, few therapies are accessible. Several vaccine strategies have been explored without success over the last 30 years including IgE antibodies [5] or genomic approaches [6,7]. Few drugs have been developed for the treatment of schistosomiasis over the last century. *In vivo* trematode models for chemotherapy have been recently reviewed [8]. Among the few drugs that have been used, one can mention antimony derivatives, metrifonate (**1a**) and oxamniquine (**1b**) (see Fig. 1 for structures) [9]. Most of these molecules have been withdrawn from the market because of toxicity and/or lack of efficacy. Oxamniquine is only efficient on *S. mansoni*, but not on *S. japonicum* which is endemic in Asia. In addition, it is too expensive, and its commercial availability is uncertain [10]. Consequently, praziquantel **2** (PZQ), a pyrazinoisoquinoline marketed as a racemate, is the only current drug of choice for the treatment of all schistosome species infecting humans. Since only one enantiomer is active, the (–)-(*R*) one [11], it is reasonable to consider that the drug target is chiral (possibly a calcium carrier protein) [12–14]. Few years after its discovery by researchers of two German companies, E. Merck (Darmstadt) and Bayer (Leverkusen), in the mid-1970s [15], PZQ has been widely used due to its qualities: efficacy by oral administration, safety and affordability (5 to 7 USD cents for a 600 mg-tablet). This drug is orally administered at a single dose of 40 mg/kg of body weight, curing 60 to 90% of the patients, or substantially decreasing the worm burden and egg production when complete curing is not achieved.

During the last 30 years, PZQ has been widely used as the only drug in order to reduce the morbidity of schistosomiasis. The main risk in monotherapies to treat pathogen-induced diseases is the risk of development of drug-resistant strains, as observed in malaria with chloroquine-resistant strains of *Plasmodium falciparum* [16]. Possible resistance of schistosomes to PZQ has been reported during the recent years [17–21]. Up to now, the level of PZQ resistance in schistosome species isolated from treated but uncured patients is relatively low, with ED_{50} values that do not exceed five to six times those of drug-susceptible isolates (ED stand for "effective dose", and ED_{50} is the amount of drug that produces a therapeutic response in 50% of the subjects taking it). However, a decrease of the observed drug-susceptibility creates a real

concern in having a single drug to control a disease affecting millions of people in endemic countries.

To our knowledge, there is currently no new anti-schistosomal drug in clinical development: the only proposal is to produce the active enantiomer of PZQ for less than the cost of the racemic drug [9]. Antiandrogens (Ro 13-3978) have been investigated in the early 1980s [22,23]. Oxadiazoles have recently been identified as new drug leads [24]. A recent report suggested that thioredoxin gluthatione reductase, a parasitic enzyme with several functions, might be a target for antischistosomal therapy [25]. Miltefosine, an alkylphosphocholine analogue registered in India to treat visceral leishmaniasis [26], has recently been considered for antischistosomal activity [27]. However, it is associated with severe gastrointestinal side-effects and a high level of teratogenicity and fetotoxicity until several months after the end of treatment [28]. New PZQ analogs have also been recently considered [29].

Schistosomes are hematophagous parasites which ingest and lyze in their oesophagus the red blood cells of their vertebrate hosts [30]. The proteolytic digestion of hemoglobin occurs in the schistosome intestine, generating amino acids that are directly used by the parasite, and free heme, which is an out-of-control redox active entity when not inserted within its apoproteins (hemoglobin or heme-enzymes). To avoid the toxicity of iron(II)-heme, the parasite is able to aggregate it as a dark pigment very similar to hemozoin, the pigment produced by *Plasmodium* in malaria [31,32]. Due to this similitude in hemoglobin catabolism between *Schistosoma* spp. and *Plasmodium* spp., several antimalarial drugs targeting heme metabolism have been evaluated as potential antischistosomals: artemisinin and its semi-synthetic derivatives (artemether **3** and artesunate **4**) [33–36], synthetic peroxides containing a trioxolane entity (instead of a 1,2,4-trioxane as in artemisinin) [37], or mefloquine **5** [38]. With the different peroxidic molecules, the dose to reduce by 50% the worm number in infected mice (ED_{50}) can be as high as 200 to 400 mg/kg, whereas the ED_{50} value of PZQ is usually between 50 and 110 mg/kg for susceptible parasite strains [39]. So, the curative dose of peroxide drugs should be far above the dose that will be acceptable for an efficient monotherapy. However, it should be noticed that artemisinin derivatives are active on the schistosomules during the first 21 days of the infection [35], while PZQ has a limited activity on this parasite stage, but has a more potent activity on adult worms (6 to 7 weeks post-infection for *S. mansoni*). This stage-dependent activity creates desirable complementary effects between these two types of drugs [40,41]. So, we have evaluated *in vitro* several trioxaquines (see Fig. 1 for the general structure) initially designed as antimalarials [42–47]. In a first study carried out on cultured *S. mansoni*, the activity of the trioxaquine PA1259 (**6**) (Fig. 1) was significantly higher than that of ARTM or MFQ, and close to that of PZQ, both on larval- and adult-parasite stages [48].

2. Results and discussion

In the present study, we report the antischistosomal activity of PA1259 in mice infected with *S. mansoni*. The host-parasite system used was an albino variety of *Biomphalaria glabrata* from Brazil and a strain of *S. mansoni*, also from Brazil, maintained in Swiss CD1 mice (Depré, Bourges, France). Detailed methods for mollusc and mouse infections and for parasite recovery were previously described [49]. Groups of 5 mice were percutaneously infected with 120 *S. mansoni* cercariae. The parasite-mouse contact lasted 45 minutes, allowing the penetration and development of 36 ± 4 cercariae. After 21 days or 49 days for evaluation on larval and adult stages, respectively, mice were orally treated by PA1259 diluted in 200 μL of excipient (an aqueous solution of methylcellulose 0.6% wt/v, containing 0.5 vol% of Tween 80). Fourteen days after treatment, mice were sacrificed and perfused by the method of Duvall et al. [50]. The blood was filtered, liver and mesenteric veins were dilacerated in order to count the worms. The worm burden reduction was calculated with respect to infected mice treated with the excipient alone. The treatment schedule consisted of four consecutive doses of 50 mg/kg each, given over a total period of 9 hours (interval between two doses was 3 hours). In mice treated by PA1259 49 days post-infection, 20 ± 5 worms were collected, corresponding to a worm burden reduction of 40% (control mice: 33 ± 5 worms). Similar treatment carried out with PZQ instead of PA1259 resulted in 86% of worm burden reduction. In mice treated 21 days post-infection, 17 ± 7 or 21 ± 6 parasites were collected after treatment by PA1259 or PZQ, respectively (control mice: 39 ± 5 parasites). These values correspond to a reduction of the worm burden of 53% and 41% with PA1259 and PZQ, respectively. So, the level of protection provided by PA1259 is slightly higher than that of PZQ for larval stage-, but lower for adult stage worms, indicating that PZQ remains the most potent on adult schistosomes up to now.

The significant activity of PA1259 on larval stage of *S. mansoni* prompted us to evaluate the efficacy of this drug on 21-day-old schistosomulae, when given in association with PZQ. The current objective of the WHO is indeed to associate a new drug to PZQ in order to improve efficiency of praziquantel, to clear if possible all the parasite stages at the time of treatment, and to delay the emergence of drug resistance.

For this reason, we evaluated the efficacy of PA1647, which is the diphosphate salt of PA1259, when given to mice in association with PZQ (salts of PA1259 are indeed more soluble than the base form in pharmacological excipients such as the tween/methylcellulose mixture). The overall drug dose and treatment schedule were the same as reported above for monotherapies: four equal doses of each drug (a 50/50 mixture: 25 mg/kg of PA1647/25 mg/kg of PZQ) administrated by oral route every 3 hours. This treatment resulted in a reduction of 73% of the schistosomula burden, with respect to mice treated with the excipient alone. By comparison, the worm burden reduction was 24% after 4×50 mg/kg of PZQ, and 18% after 4×50 mg/kg of PA1647. In a rough estimate, an additive effect between PZQ and PA1647 would have provided at best $(24 + 18)/2 = 21\%$ worm burden reduction. So, a reduction of 73% reveals a probable synergistic effect of PZQ and the PA1647 on 21-day-old schistosomulae.

It should be noted that, in all cases, the treatment induced no detectable toxicity in mice: all mice survived without change in behavior, and when they were perfused, 14 days post-treatment, their weight was not significantly different than that of control mice (± 5%), and there was no visible damage to organs (except usual damages due to schistosomiasis).

3. Conclusion

The trioxaquine PA1259, and its diphosphate salt PA1647, are efficacious drug candidates against *S. mansoni* after oral administration to infected mice. Moreover, when the association PA1647–PZQ was given orally to infected mice, it was more efficient to reduce parasitemia than PZQ alone. This synergy opens the way to a bitherapy approach that might target all the parasite human stages.

Acknowledgements

This work was supported by Palumed, CNRS, and Agence nationale pour la recherche (ANR grant No. ANR-08-MIEN-026-02). Vincent Pradines and Julien Portela are indebted to ANR for fellowships. The authors thank Sonia Kitoune and Christine Salle (both from Palumed), and Bernard Dejean (from UMR 5244) for technical assistance.

References

[1] D.G. Colley, P.T. LoVerde, L. Savioli, Science 293 (2001) 1437.
[2] C.H. King, K. Dickman, D.J. Tisch, Lancet 365 (2005) 1561.
[3] S. Liang, C.H. Yang, B. Zhong, D.C. Qiu, Bull. World Health Organ. 84 (2006) 139.
[4] B. Gryseels, K. Polman, J. Clerinx, L. Kestens, Lancet 368 (2006) 1106.
[5] A. Capron, M. Capron, D. Dombrowicz, G. Riveau, Int. Arch. Allergy Immunol. 124 (2001) 9.
[6] P.J. Hotez, J.M. Bethony, D.J. Diemert, M. Pearson, A. Loukas, Nat. Rev. Microbiol. 8 (2010) 814.
[7] G.N. Gobert, Infect. Disord. Drug Targets 10 (2010) 251.
[8] J. Keiser, Parasitology 137 (2010) 589.
[9] S. Everts, Chem. Eng. News 84 (2006) 34.
[10] F.F. Stelma, S. Sall, B. Daff, S. Snow, M. Niang, B. Gryseels, J. Infect. Dis. 176 (1997) 304.
[11] M.H. Wu, C.C. Wei, Z.Y. Xu, H.C. Yuan, W.N. Lian, Q.J. Yang, M. Chen, Q.W. Jiang, C.Z. Wang, S.J. Zhang, Z.D. Liu, R.M. Wei, S.J. Yuan, L.S. Hu, Z.S. Wu, Am. J. Trop. Med. Hyg. 45 (1991) 345.
[12] P. Andrews, H. Thomas, R. Pohlke, J. Seubert, Med. Res. Rev. 3 (1983) 147.
[13] G. Ribeiro-dos-Santos, S. Verjovski-Almeida, L.C. Leite, Parasitol. Res. 99 (2006) 505.
[14] M.J. Doenhoff, D. Cioli, J. Utzinger, Curr. Opin. Infect. Dis. 21 (2008) 659.
[15] G. Leopold, W. Ungethüm, E. Groll, H.W. Diekmann, H. Nowak, D.H. Wegner, Eur. J. Clin. Pharmacol. 14 (1978) 281.
[16] N.K. Shah, G.P. Dhillon, A.P. Dash, U. Arora, S.R. Meshnick, N. Valecha, Lancet Infect. Dis. 11 (2011) 57.
[17] P.G. Fallon, M.J. Doenhoff, Am. J. Trop. Med. Hyg. 51 (1994) 83.
[18] M.J. Doenhoff, J.R. Kusel, G.C. Coles, D. Cioli, Trans. R. Soc. Trop. Med. Hyg. 96 (2002) 465.
[19] D. Alonso, J. Munoz, J. Gascon, M.E. Valls, M. Corachan, Am. J. Trop. Med. Hyg. 74 (2006) 342.
[20] M. Ismail, S. Botros, A. Metwally, S. William, A. Farghally, L.F. Tao, T.A. Day, J.L. Bennett, Am. J. Trop. Med. Hyg. 60 (1999) 932.
[21] S.D. Melman, M.L. Steinauer, C. Cunningham, L.S. Kubatko, I.N. Mwangi, N.B. Wynn, M.W. Mutuku, D.M.S. Karanja, D.G. Colley, C.L. Black, W.E. Secor, G.M. Mkoji, E.S. Loker, PLoS Negl. Trop. Dis. 3 (2009) e504.
[22] H. Link, H.R. Stohler, Eur. J. Med. Chem. 19 (1984) 261.
[23] J. Keiser, M. Vargas, J.L. Vennerstrom, J. Antimicrob. Chemother. 65 (2010) 1991.
[24] A.A. Sayed, A. Simeonov, C.J. Thomas, J. Inglese, C.P. Austin, D.L. Williams, Nat. Med. 14 (2008) 407.
[25] A.N. Kuntz, E. Davioud-Charvet, A.A. Sayed, L.L. Califf, J. Dessolin, E.S.J. Arner, D.L. Williams, PLoS Med. 4 (2007) 1071.
[26] S. Sundar, T.K. Jha, C.P. Thakur, J. Engel, H. Sindermann, C. Fischer, K. Junge, A. Bryceson, J. Berman, N. Engl. J. Med. 347 (2002) 1739.
[27] M.M. Eissa, M.Z. El-Azzouni, E.I. Amer, N.M. Baddour, Int. J. Parasitol. 41 (2011) 235.
[28] T.P.C. Dorlo, P.P.A.M. van Thiel, A.D.R. Huitema, R.J. Keizer, H.J.C. de Vries, J.H. Beijnen, P.J. de Vries, Antimicrob. Agents Chemother. 52 (2008) 2855.
[29] Y.X. Dong, J. Chollet, M. Vargas, N.R. Mansour, Q. Bickle, Y. Alnouti, J.G. Huang, J. Keiser, J.L. Vennerstrom, Bioorg. Med. Chem. Lett. 20 (2010) 2481.
[30] P.J. Brindley, B.H. Kalinna, J.P. Dalton, S.R. Day, J.Y.M. Wong, M.L. Smythe, D.P. McManus, Mol. Biochem. Parasitol. 89 (1997) 1.
[31] K. Kloetzel, R.M. Levert, Am. J. Trop. Med. Hyg. 15 (1966) 28.
[32] M.F. Oliveira, J.C.P. D'Avita, C.R. Torres, P.L. Oliveira, A.J. Tempone, F.D. Rumjanek, C.M.S. Braga, J.R. Silva, M. Danso-Petretski, M.A. Oliveira, W. de Souza, S.T. Ferreira, Mol. Biochem. Parasitol. 111 (2000) 217.
[33] S.H. Xiao, J. Utzinger, J. Chollet, Y. Endriss, E.K. N'Goran, M. Tanner, Int. J. Parasitol. 30 (2000) 1001.
[34] J. Utzinger, J. Chollet, Z.W. Tu, S.H. Xiao, M. Tanner, Trans R. Soc. Trop. Med. Hyg. 96 (2002) 318.
[35] S.H. Xiao, M. Tanner, E.K. N'Goran, J. Utzinger, J. Chollet, R. Bergquist, M.G. Chen, J. Zheng, Acta Trop. 82 (2002) 175.
[36] S.H. Lu, T. Kumagani, Q.H. Ai, X.L. Yan, H. Ohmae, Y. Yabu, S.W. Li, L.Y. Wen, H. Maruyama, N. Ohta, Parasitol. Int. 55 (2006) 63.
[37] S.H. Xiao, J. Keiser, J. Chollet, J. Utzinger, Y.X. Dong, Y. Endriss, J.L. Vennerstrom, M. Tanner, Antimicrob. Agents Chemother. 51 (2007) 1440.
[38] J. Keiser, J. Chollet, S.H. Xiao, J.Y. Mei, P.Y. Jiao, J. Utzinger, M. Tanner, PLoS Negl. Trop. Dis. 3 (2009) e350.
[39] D. Cioli, S.S. Botros, K. Wheatcroft-Francklow, A. Mbaye, V. Southgate, L.A.T. Tchuente, L. Pica-Mattoccia, A.R. Troiani, S.H.S. El-Din, A.N.A. Sabra, J. Albin, D. Engels, M.J. Doenhoff, Int. J. Parasitol. 34 (2004) 979.
[40] S.H. Xiao, J.Q. You, J.Y. Mei, H.F. Guo, P.Y. Jiao, M. Tanner, Parasitol. Int. 49 (2000) 25.
[41] J. Utzinger, J. Chollet, J.Q. You, J.Y. Mei, M. Tanner, S.H. Xiao, Acta Trop. 80 (2001) 9.
[42] O. Dechy-Cabaret, F. Benoit-Vical, A. Robert, B. Meunier, Chem. Biochem. (2000) 281.
[43] O. Dechy-Cabaret, F. Benoit-Vical, C. Loup, A. Robert, H. Gornitzka, A. Bonhoure, H. Vial, J.F. Magaval, J.P. Séguéla, B. Meunier, Chem. Eur. J. 10 (2004) 1625.
[44] F. Benoit-Vical, J. Lelièvre, A. Berry, C. Deymier, O. Dechy-Cabaret, J. Cazelles, C. Loup, A. Robert, J.F. Magnaval, B. Meunier, Antimicrob. Agents Chemother. 51 (2007) 1463.
[45] F. Bousejra-El Garah, C. Claparols, F. Benoit-Vical, B. Meunier, A. Robert, Antimicrob. Agents Chemother. 52 (2008) 2966.
[46] A. Robert, O. Dechy-Cabaret, J. Cazelles, B. Meunier, B. Acc. Chem. Res. 35 (2002) 167.
[47] B. Meunier, A. Robert, Acc. Chem. Res. 43 (2010) 1444.
[48] J. Boissier, F. Coslédan, A. Robert, B. Meunier, Antimicrob. Agents Chemother. 53 (2009) 4903.
[49] J. Boissier, H. Moné, Int. J. Parasitol. 31 (2001) 352.
[50] R.H. Duvall, W.B. DeWitt, Am. J. Trop. Med. Hyg. 16 (1967) 483.

OPEN ACCESS Freely available online

PLoS NEGLECTED TROPICAL DISEASES

Antischistosomal Activity of Trioxaquines: *In Vivo* Efficacy and Mechanism of Action on *Schistosoma mansoni*

Julien Portela[1,2], Jérôme Boissier[1,2]*, Benjamin Gourbal[1,2], Vincent Pradines[3], Vincent Collière[3], Frédéric Coslédan[4], Bernard Meunier[3,4], Anne Robert[3]*

1 Université de Perpignan Via Domitia, Perpignan, France, **2** CNRS, UMR 5244, Écologie et Évolution des Interactions, Perpignan, France, **3** Laboratoire de Chimie de Coordination du CNRS, Toulouse, France, **4** Palumed, Castanet-Tolosan, France

Abstract

Schistosomiasis is among the most neglected tropical diseases, since its mode of spreading tends to limit the contamination to people who are in contact with contaminated waters in endemic countries. Here we report the *in vitro* and *in vivo* anti-schistosomal activities of trioxaquines. These hybrid molecules are highly active on the larval forms of the worms and exhibit different modes of action, not only the alkylation of heme. The synergy observed with praziquantel on infected mice is in favor of the development of these trioxaquines as potential anti-schistosomal agents.

Citation: Portela J, Boissier J, Gourbal B, Pradines V, Collière V, et al. (2012) Antischistosomal Activity of Trioxaquines: *In Vivo* Efficacy and Mechanism of Action on *Schistosoma mansoni*. PLoS Negl Trop Dis 6(2): e1474. doi:10.1371/journal.pntd.0001474

Editor: Timothy G. Geary, McGill University, Canada

Received August 22, 2011; **Accepted** November 25, 2011; **Published** February 14, 2012

Funding: This work was supported by Palumed, CNRS, and Agence Nationale pour la Recherche ANR grant no. ANR-08-MIEN-026-02. The funders had no role in study design, data collection and analysis, decision to publish, or preparation of the manuscript.

Competing Interests: The authors have declared that no competing interests exist.

* E-mail: boissier@univ-perp.fr (JB); anne.Robert@lcc-toulouse.fr (AR)

Introduction

Malaria and schistosomiasis are the two most important parasitic diseases in tropical and sub-tropical areas. The parasite species responsible of these diseases are quite different: *Plasmodium* is an intracellular protozoa while *Schistosoma* is a metazoan worm. However these parasites share a common feature, they are both hematophagous. During their development in human blood stream, they digest a large quantity of host hemoglobin. As a consequence of the proteolytic digestion of this heme-containing protein, free heme is released and constitutes a major threat for both parasites due to its easy reduction by endogenous electron sources. The iron chelated by the protoporphyrin-IX ligand of heme is particularly efficient in oxygen reduction by monoelectronic transfer. This catalytic dioxygen reduction is at the origin of highly toxic reactive oxygen species (ROS). Despite their high phylogenetic divergence, convergent evolution has conducted these two parasite species to use a similar heme detoxification pathway. The hemozoin pigment, known as malaria pigment in *Plasmodium*, is an aggregation of heme dimers turning the iron inactive. Hemozoin is a dark-black inert crystalline pigment, which is structurally identical in *Plasmodium* and *Schistosoma* [1,2].

The treatment and control of schistosomiasis currently rely on the use of a single drug, the praziquantel (PZQ, Figure 1). Praziquantel, a safe and effective drug, has been used for the last fourty years. However, several schistosome strains with lower sensitivity to praziquantel with possibility of resistance have been identified in African countries [3,4]. Having a single drug to treat a disease that affects hundred millions of people is a real concern, due to the possible resistance of the parasite to this drug. As a consequence, in the last ten years important efforts have been made in either developing new drug series [5–7a,b], or testing existing drugs originally used on non-related diseases [8–13]. Among the existing medications, the antimalarial drugs targeting heme (i.e. before the hemozoin formation) are particularly interesting since free heme is not present in non-infected persons. In this field, two major series of molecules can be considered according their mechanism of action: trioxane-based molecules, that are heme-alkylating agents [14–17], and aminoquinoline-based molecules, that are heme-stacking agents [18,19]. Trioxane-based molecules, whether naturally extracted or chemically synthesized, have shown moderate anti-schistosomal activities [10–11]. Similarly, aminoquinoline derivatives have been shown to be efficient against schistosomes experimentally infected animals, e.g. the treatment with mefloquine (MFQ) significantly reduced the number of eggs [20]. Because schistosomiasis and malaria are co-endemic in several countries, using an anti-malarial molecule against schistosomiasis might select drug-resistance in malaria parasites [8,9]. However, many malaria patients treated with artemisinin-based combination therapy (ACT) are indeed co-infected with schistosomes. In fact, a study carried out in Côte-d'Ivoire evidenced that children infected with *S. haematobium*, treated with mefloquine-artesunate administered in accordance with the currently recommended malaria treatment schedule, showed significantly higher egg reduction rates compared to children treated with artesunate (ARTS) or mefloquine alone [21].

The future challenge in the treatment of schistosomiasis may be not to use native anti-malarial drugs but to develop new drugs considering the mechanism of action of the anti-malarial molecules targeting free heme. In these conditions, it might be useful to develop an anti-schistosomal peroxide-based drug that will be also active against malaria parasites, with the requirement

Author Summary

Schistosomiasis is a tropical disease affecting more than 200 million people throughout the sub-tropical and tropical world. The treatment and control of schistosomiasis rely on the use of a single drug, the praziquantel and no vaccine is available. However, schistosome species with low sensitivity or resistance to praziquantel have been identified in several countries. It is an urgent need to develop new drugs against this parasite. In this context, our study reports the activity the trioxaquine PA1259. PA1259 is an hybrid drug containing two pharmacophores within a single molecule: a trioxane and an aminoquinoline. Initially developed against malaria, the trioxaquines target the heme a disposal product resulting from the digestion of the hemoglobin. The first action of the trioxaquine is an alkylation of the heme with the trioxane entity, and the second action is stacking with the heme due to the aminoquinoline moiety. In this study we show that this new drug is active *in vitro* against all schistosome stages (cercariae, schistosomule and adult). The PA1259 is also active *in vivo* and shows synergistic action in association with praziquantel. This opens the route to an efficient bitherapy of a highly neglected disease.

that the drug should not easily induce the selection of drug-resistant strains of *Plasmodium*. This strategy should provide new molecules active on both parasites with limited side effects.

Trioxaquines (TXQ) are hybrid drugs containing two pharmacophores within a single molecule: a 1,2,4-trioxane and a 4-aminoquinoline [22]. Initially developed against malaria, they exhibit a dual mode of action: alkylation of heme with the trioxane entity, and stacking with heme due to the aminoquinoline moiety, leading to inhibition of hemozoin formation *in vitro* [23–25]. As reported for artemisinin derivatives [14,15], owing to their trioxane entity, trioxaquines are indeed efficiently activated by iron(II)-heme, leading to the formation of covalent heme-drug adducts detected in the spleen of malaria infected mice [16,24]. Because of the relationship of 1,2,4-trioxane-containing drugs with heme metabolism, we have decided to evaluate the *in vitro* activity of trioxaquines on *Schistosoma mansoni*. Several of these molecules were found highly active on both larval and mature stages of *S. mansoni* [12]. A better understanding of the molecular bases of the antischistosomal activity of trioxaquines is requested to design new active drugs, and to optimize the existing drug candidates. As a confirmation that heme is a general target of drugs active against blood-feeding parasites, we recently reported that trioxaquine PA1259 alkylates heme in female adult *S. mansoni*, and heme-drug adducts were identified from treated worms [26] (for the structure of PA1259, see Figure 1). Although important, this feature is probably not the only mode of action of trioxaquines in schistosomes. So, we decided to further evaluate their reactivity toward hemozoin, and also to attempt to have a general picture of damages induced by trioxaquines in *S. mansoni*. For this purpose, the action of a trioxaquine "prototype", PA1259, was compared to that of three other drugs: the reference drug praziquantel (PZQ), artemether (ARTM) and mefloquine (MFQ) (Figure 1).

Materials and Methods

1. Ethics Statement

The laboratory has received the permit N° A 66040 for experiments on animals from both French "Ministère de l'Agriculture et de la Pêche" and French "Ministère de l'Enseignement supérieur et de la Recherche". Housing, breeding and animal care of the mice followed the ethical requirements of our country. The experimenter possesses the official certificate for animal experimentation delivered by both ministeries (décret n° 87–848 of October 19th 1987; authorization no 007083). Animal experimentation follows the guidelines of the French CNRS. The different protocols used in this study have been validated by the French veterinary agency. Before parasite infection, mice were anaesthetized by injection of 0.1 mL/10 g of body weight of a mixture of Rompun (0.5 mL, 20 mg/mL; Bayer) and Imalgène (1.0 mL, 100 mg/mL; Rhône Mérieux) in 8.5 mL of autoclaved NaCl 8.5 ($^{o}/_{oo}$).

2. Parasite and host strains for antischistosomal assays

The host-parasite system used was an albino variety of *Biomphalaria glabrata* from Brazil and a strain of *Schistosoma mansoni*, also from Brazil, maintained in Swiss CD1 mice (Depré, Bourges, France). Detailed methods for mollusc and mouse infections and for parasite recovery were previously described [27].

3. *In vitro* antischistosomal activity

In vitro tests were performed on both free larval (cercariae) and parasitic stages (schistosomules and adult worms). Cercariae were recovered in spring water under binocular microscope. Parasitic stages were recovered after percutaneous infection of mice using either 120 or 400 parasite cercariae. Mice exposed to 400 cercariae were sacrificed at 21 days after infection for schistosomule recovery, while mice exposed to 120 cercariae were sacrificed at 49 days after infection for adult recovery. Schistosomules or adult worms, freshly recovered, were washed and placed in RPMI 1640 medium (supplemented with L-glutamine and Hepes 25 mM) and store in incubator chamber at 37°C.

Ten to 20 freshly recovered 21day-schistosomules or 49day-adults were placed in 24-well or in 6-well Falcon plate containing 1 mL or 3 mL of RPMI 1640 medium (supplemented with L-glutamine and Hepes 25 mM), respectively. Fifty cercariae were placed in 24-well Falcon plate containing 1 mL of spring water. The drugs PA1259, PZQ, ART or MFQ were first dissolved in DMSO to give mother solutions at 100 mg/mL. All further dilutions were done in DMSO except the last one that was realized in RPMI 1640 or spring water, for parasitic stage or free larval stage, respectively. The dilution was complemented with Tween 80 in order to obtain this final ratio dilution: culture medium/Tween80/DMSO, 1000/0.95/3.8, v/v/v. These drug solutions were added to Falcon plate that contained worms. The *S. mansoni* cultures were then incubated with each drug at final concentration of 5 or 50 µg/mL for larval stages (cercariae or schistosomules) or adult stage, respectively (a concentration of 5 µg/mL corresponds to 10, 16, 17, and 13 µM for PA1259, PZQ, ARTM, and MFQ, respectively). Control worms were treated with the same culture medium/Tween 80/DMSO, but without drug. Each test was performed in duplicate. Every 30 minutes, moving worms were counted, in order to define the percentage of survivors. Observation was extended to 8 h. Kaplan-Meier survival analyses followed by pairwise log-rank tests were used to compare survival data. Parasites showing no body contractions during a 30-s observation may be considered dead.

4. *In vivo* antischistosomal activity

Mice were infected percutaneously with 120 cercariae each. Twenty-one days (schistosomule stage) or 49 days (adult worm stage) post-infection, groups of five mice were treated orally. In monotherapy, PZQ or PA1259 oral treatment was performed at 100 mg/kg/d for five consecutive days, or at four doses of

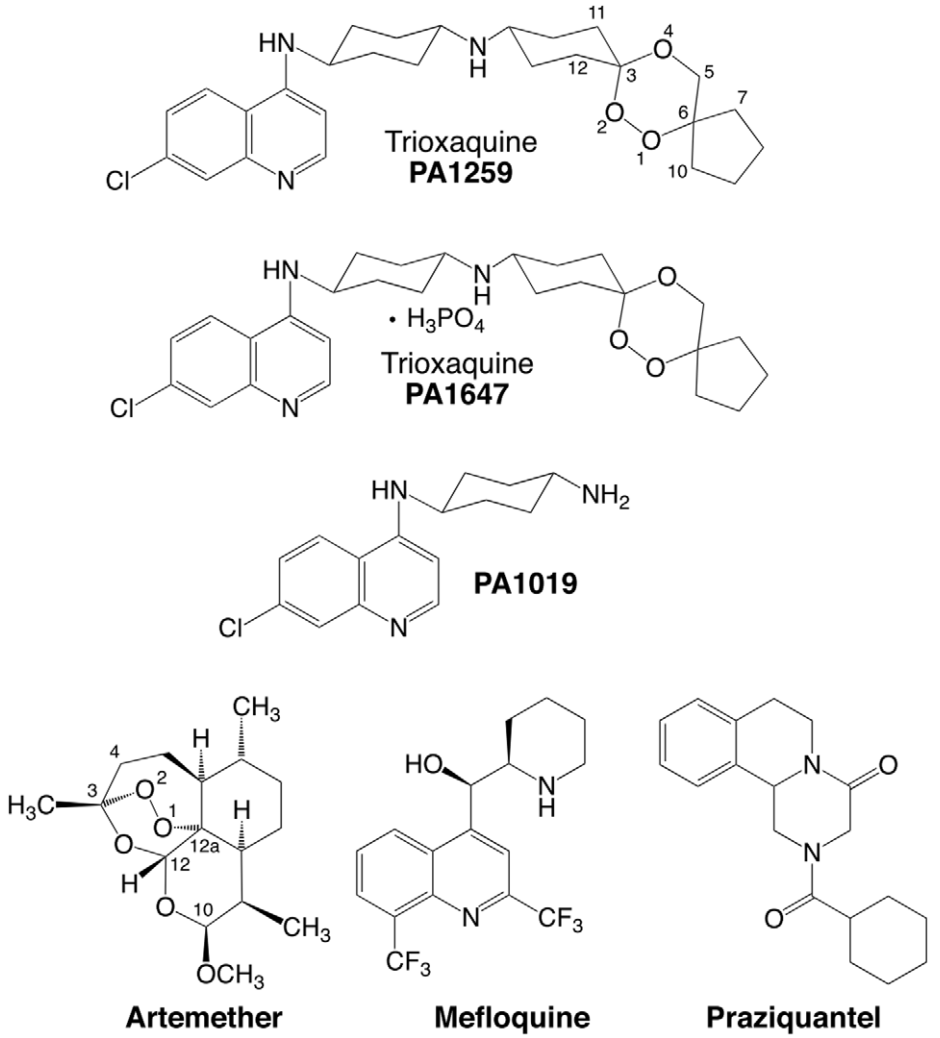

Figure 1. Structures of drugs. Praziquantel (PZQ), mefloquine (MFQ), artemether (ARTM), and trioxaquines PA1259 and PA1647.
doi:10.1371/journal.pntd.0001474.g001

50 mg/kg each, given every three hours (overall treatment period: 9 h). For bitherapy evaluation, treatments were made at the following PZQ/PA1647 wt/wt ratio: 100/0, 75/25, 50/50, 25/75, and 0/100. Administration consisted in 4 oral doses of 50 mg/kg each, given every three hours (total drug dose: 200 mg/kg). In all cases, control mice were treated with solvent but without drug. Fifteen days after treatment, mice were killed and worms were recovered by retrograde perfusion. The viscera were observed to count the worms in each mouse.

5. ROS production by *S. mansoni* adult worms following praziquantel or PA1259 treatment

As a preliminary, the *in vitro* concentration of PZQ or PA1259 that kills half of the parasites after one hour of incubation (LC_{50}) was determined (30-secondes immobilized worms were considered as killed, since no worms recovered an activity after that 30-sec period of immobilization). For this purpose, the following ranges of concentrations were tested: 0, 0.01, 0.1, 0.5, 1, 2.5, 5 μg/mL for PZQ, and 0, 5, 10, 20, 30, 40, 50 μg/mL for PA1259. The incubation medium and drug solvents were as described above for *in vitro* treatment of schistosomes. LC_{50} values found were 50 μg/mL and 0.075 μg/mL for PA1259 and PZQ respectively. No difference was observed between male and female worms.

a. Hydrogen peroxide (H_2O_2) and superoxide anion ($O_2^{\bullet -}$) quantification. Four males and two females of *S. mansoni* adult worms were disposed in a 24-well plate with 1 mL of RPMI. Worms were incubated during one hour with 0.075 μg/mL of PZQ and 50 μg/mL of PA1259 that correspond to the LC_{50} values of the drugs. Untreated worms were processed in a same manner and treated with the excipient. For each drug treatment and control experiments, ten replicate samples were analyzed. Drug treated- and untreated worms were washed 3 times with Krebs-Ringer phosphate buffer (KRPG), sonicated and the total protein amount were quantified. Fifty μL of supernatant were disposed in a 96-well plate. Hydrogen peroxide was quantified with Amplex® Red (50 μL per well, prepared according to the manufacturer's instructions). Optic density was measured with a microplate reader at 570 nm. Superoxide $O_2^{\cdot -}$ was quantified with NBT (50 μl of 0.2% NBT (Sigma) dissolved in KRPG per well). The variation of OD resulting from the formation of formazan was measured with a microplate reader at 620 nm. Results were monitored at 0, 10, 20, 30, 45, 60, 90 and 120 minutes and were presented as OD values corrected by sample protein amount.

b. Nitric oxide (NO) quantification. Five *S. mansoni* adult females were disposed in a 24 well plate with 1 mL of RPMI and treated for 1 h with 0.075 μg/mL of PZQ and 50 μg/mL of PA1259, respectively. Worms were then washed with RPMI solution, and NO production was quantified by incubating for one hour the treated and untreated females with DAF-2DA substrate (2 μM per well). Then females were disposed on slides and observed under UV illumination using a Leica® DMLB® microscope. Pictures were taken and analyzed by using the imageJ software [28]. Briefly DAF-2 fluorescence intensity was quantified over the entire worm surface and results were expressed as mean DAF-2 fluorescent intensity/pixel. For each female picture, mean DAF-2 fluorescent intensity was calculated by separating the Red image from the Green, and Blue ones (RGB). Indeed Red-image was more appropriated to calculate fluorescence since DAF-2 fluorescent background was more attenuated.

6. Chemicals

PA1259 and PA1019, synthetized as reported in the patent application WO/2007/144487, and PA1647 were provided by Palumed. PA1647 is the diphosphate salt of PA1259 (stoichiometry checked by CHN-elemental analysis). Artemether (ARTM) was a gift from Rhône-Poulenc Rohrer Doma (Antony, France). Praziquantel (PZQ) and mefloquine (MFQ) were purchased from Sigma-Aldrich, as well as sodium dithionite ($Na_2S_2O_4$), dimethylsulfoxyde (DMSO, ACS spectrophotometric grade ≥99.9%), pyridine (≥99%), and methanol (Chromasolv ≥99.9%). Formic acid (99+%) was from ACROS. Hemin (ferriprotoporphyrin IX chloride, 98.0%) from bovine blood was purchased from Fluka (Switzerland). All chemicals and solvents were used as purchased without further purification. Milli-Q water (resistivity ≥18.2 MΩ) was used for LC-MS eluent preparation.

7. Extraction of heme and heme-drug adducts from *S. mansoni* worms

Adult *S. mansoni* females were recovered in mice seven weeks after infection, and maintained in culture in RPMI 1640 medium, supplemented with L-glutamine and Hepes 25 mM, at 37°C. Groups of twenty-five schistosomes, freshly recovered, were carefully washed with RPMI 1640 medium, then treated with PA1259 or ARTM at 50 μg/mL for 3 hours. Then, worms were crushed with sand, and the obtained powder was extracted with pyridine (500 μL). The mixture was vigorously stirred (vortex), placed in an ultrasonic bath for 30 min and, finally, magnetically stirred at 37°C overnight. After centrifugation at 4000 rpm for 30 min, the supernatant was withdrawn and filtered through ptfe 0.45 μm syringe filters before analysis by HPLC or LC-MS.

8. LC-MS analysis

a. HPLC conditions for heme-drug adducts. The LC-MS analyses were performed using a Agilent 6140 equipment (HPLC column: 5 μm C18 X-Bridge, 150×4.6 mm, Waters; linear elution gradient from water/formic acid, 100/1, v/v to methanol/formic acid, 100/1, v/v in 30 min; flow rate = 1 mL×min^{-1}; injection volume: 100 μL; UV-vis. detection at 398 nm (λ_{max} of heme), and ESI$^+$-MS detection). The analytic conditions were previously optimized by using chemically prepared heme-PA1259 adducts [3.2 mg of Fe^{III}(PPIX)Cl, 10 molar equivalent of sodium dithionite and 1.5 molar equivalent of trioxaquine PA1259 were dissolved in 500 μL DMSO. The reaction was carried out at 37°C, under an argon atmosphere, for 2 h].

b. Mass spectrometry conditions. The ionization was performed in electrospray mode, using an Agilent 6410 triple quadrupole setup (source temperature = 350°C, gas flow nebulizer = 13 L.min^{-1}). The detection and quantification were performed in scanning mode (total ionic current) with a step size of 0.1 atomic mass units (amu) and scan range of 300–1200 amu.

9. Electronic Microscopy

a. Scanning electron microscopy (SEM). Schistosomes were fixed with 2% glutaraldehyde in Sorensen buffer (0.1 M, pH = 7.4) for 1 hour, washed with cacodylate buffer (0.1 M sodium cacodylate) for 12 hours. After dehydration and critical point drying, they were mounted on microscope stubs, followed by platinum sputtering during 160 seconds. We used a SEM-FEG microscope (JEOL JSM 6700F) with an accelerating voltage of 30 kV. The head of schistosomes was first located, and photographs were then recorded, with magnification ×1000, ×2000, or ×5000 (50 photographs per worm; two worms for each treatment).

b. Transmission electron microscopy (TEM). Schistosomes were fixed with 2% glutaraldehyde in Sorensen buffer (0.1 M, pH = 7.4) for 1 hour, washed with the same buffer for 12 hours. They were postfixed with 1% OsO_4 in Sorensen buffer 0.05 M and saccharose 0.25 M for 1 hour. Schistosomes were dehydrated by incubation in successive aqueous ethanol solutions containing an increasing proportion of ethanol up to 100 vol%, and then embedded in LR Whyte resin (medium grade acrylic resin, Electron Microscopy Sciences). After 48 h of polymerization at −20°C under UV irradiation, ultrathin sections (50 nm) were mounted on 150 mesh collodion-coated copper grids and poststained with 3% uranyl acetate in 50% ethanol, and with 8.5% lead citrate, before being examined on a HU12A Hitachi electron microscope, at an accelerating voltage of 75 kV.

c. X-ray analysis. The presence of iron in hemozoin pellets was assessed by using a TEM-FEG (JEOL JEM 2100F) electronic microscope, with an accelerating voltage of 200 kV, equipped with an element analyzer (PGT, resolution 136 eV). This analysis has been performed on the ultrathin sections of schistosomes previously analyzed by TEM.

Results

1. *In vitro* activity of trioxaquine PA1259 on free and parasitic stages of *S. mansoni*

The *in vitro* activities of PA1259 (■), praziquantel (★), artemether (◆), and mefloquine (●) on cercaria-, 21 day-old schistosomules, and 49 day-old adult worms are reported in Figure 2A, 2B, and 2C, respectively, as Kaplan-Meier plots. When treated with PZQ at 5 μg/mL, after 4 h of contact with the drug, all cercaria were immobilized for a 30 s-observation time. To obtain such immobility after treatment with PA1259 or MFQ required only 60 or 90 min, respectively. In the presence of ARTM, 8 h after treatment, more than 80% of cercariae were still moving (Figure 2A). The treatment of 21-day schistosomules with PZQ at 5 μg/mL resulted in a complete immobilization of all larvae after 3 h of contact. With PA1259 or MFQ, the same effect was obtained after 5 h and 8 h, respectively. When ARTM was used in the same conditions, no significant effect was observed after 8 h (Figure 2B). The treatment of 49-day adult schistosomes with drugs at 50 μg/mL resulted in complete immobilization of all worms in 2 h in the presence of PZQ, and 3 h in the presence of MFQ or PA1259. With ARTM at the same concentration, more than 60% of worms were still moving after 8 h (Figure 2C).

In addition, the activity of PA1019, which is the 4-aminoquinoline residue contained in PA1259, was evaluated on schistosomules and adult worms. Seven hours of contact of PA1019 was required

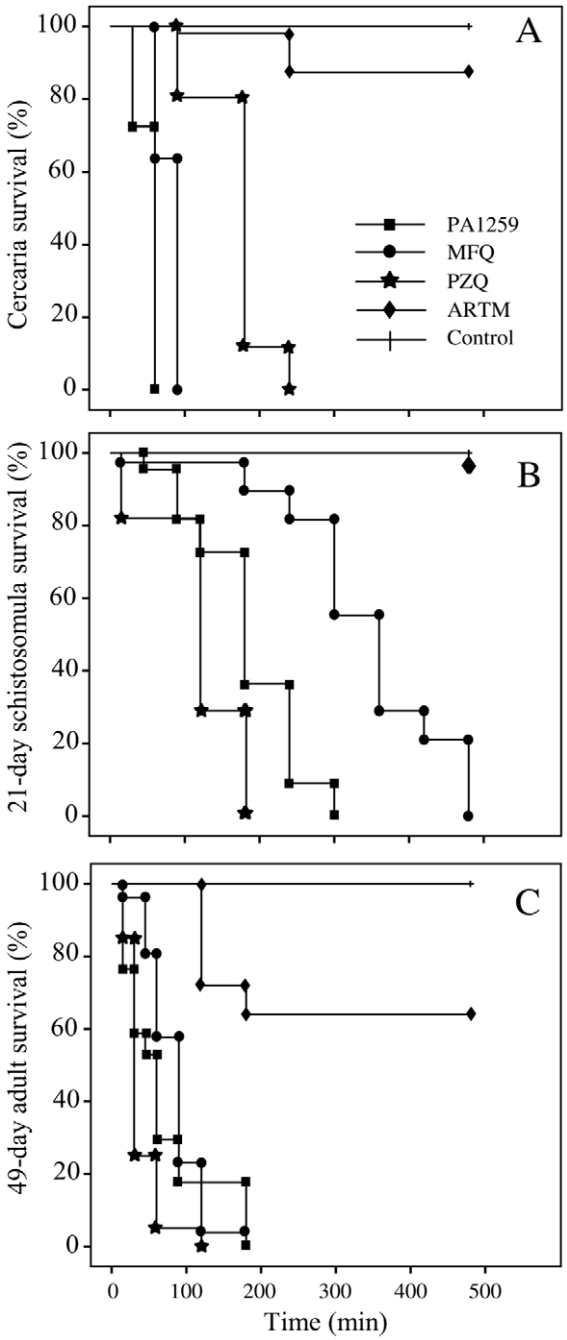

Figure 2. Comparative *In vitro* activities. PA1259 (■), praziquantel (★), artemether (◆), and mefloquine (●) on cercariae (A), on 21-days old schistosomules (B) and on 49-days old adult (C) *S. mansoni*. Cultured larvae (cercariae or schistosomules) or adults were treated with compounds at 5 µg/ml or 50 µg/ml, respectively.
doi:10.1371/journal.pntd.0001474.g002

to immobilize only 27% of schistosomules and 79% of adult worms.

2. Activity of trioxaquine PA1259 on mice infected by *S. mansoni*

In mice infected by *S. mansoni*, the reduction of worm burden upon oral treatment by PA1259 or PZQ is reported in Table 1. In mice treated with PA1259 at five daily doses of 100 mg/kg starting from day 21 post-infection, 26.6±5.4 worms were collected 15 days later. When treatment was done at day 49 post-infection, 21.0±7.0 worms were collected. These values correspond to a reduction of 31% and 42% on larval and adult stage, respectively, with respect to mice treated by excipient alone (control mice). With the same treatment schedule, PZQ induced a worm burden reduction of 20% and 79% on schistosomules and adult worms, respectively. With four doses of 50 mg/kg of PA1259 given every three hours, the reduction of the worm burden was 53% (16.8±7.2 worms) or 40% (20.0±5.1 worms) on larval stage or adult stages, respectively. The same treatment schedule but with PZQ induced a worm burden reduction of 41% and 86% on schistosomules and adult worms, respectively. These treatments did not induce any visible adverse effect in mice.

3. Trioxaquine - praziquantel association on mice infected by *S. mansoni* schistosomules

The effect of a combination of PZQ and trioxaquine PA1647 on the reduction of the worm burden in *S. mansoni* infected mice is reported in Table 2. The first course consisted of 4 oral treatments with 50 mg/kg of drug given every three hours. The drug combinations were 100% of PZQ (line 2), 75 wt% PZQ/25 wt% PA1647 (line 3), 50 wt% PZQ/50 wt% PA1647 (line 4), 25 wt% PZQ/75 wt% PA1647 (line 5), and 100% of PA1647 (line 6), respectively. In these conditions, the reduction of the schistosomules burden with respect to control mice was 24% with 100% PZQ (line 2), 73% with 75 wt% PZQ/25 wt% PA1647, (line 4), and 18% with 100% of PA1647 (lines 2, 4, and 6, respectively). These treatments did not induce any visible adverse effect in mice.

4. Microscopy

Adult *S. mansoni* females were treated in *vitro* with PA1259, PZQ, ARTM or MFQ at 50 µg/mL for three hours, and compared with untreated worms (excipient only).

a. Photon microscopy. Upon treatment with trioxaquine PA1259 at 50 µg/mL, a brown cloud of small dark crystals readily appeared in the culture medium (right part of the Figure 3A). Few minutes after treatment, the black color inside the gut of worms (Figure 3D and 3E, untreated worms) turned to light brown (Figure 3B). After one hour, the gut walls of treated worms were no more visible, and the brown pigment invaded the whole worm body (Figure 3C). Such a modification was observed with none of the reference drugs, namely PZQ, ARTM, or MFQ.

b. Scanning electron microscopy (SEM). First of all, the general morphology of worms was rather affected, especially after treatment with mefloquine or trioxaquine PA1259 (Figure S1). Worms treated with PA1259 were convoluted (Figures 3C and S1c). The schistosomes treated by mefloquine seemed stiff, contracted (with a mean diameter significantly reduced with respect to untreated, Figure S1d). Worms treated with PZQ exhibited local drastic swelling (encircled zone in Figure S1b). In some cases, the breaking of the worm occurred during the preparation for microscopy. These events, not related to the drug treatment, are indicated as white crosses in Figure S1.

Second, chistosomes exhibit spines along all the length of body, but with a higher density in the hindbody and forebody parts with respect to midbody part, and on the dorsal side with respect to the ventral one (Figure S7). The ciliated sensory papillae were also well visible. The treatment with trioxaquine PA1259 induced a drastic disorganization of spines, which became rough and bushy (Figure S2c). In some places, the disappearance of spines, along with dilated spine sockets, was observed, suggesting that spines have been drawn back (Figure S3c). The spines were nearly unchanged upon treatment with PZQ or ARTM (Figure S2, panels b and e,

Table 1. *In vivo* effect of PA1259 and praziquantel.

Treatment	Administration	Schistosomula		Adult	
		Mean number of worms ± SD	Worm reduction	Mean number of worms ± SD	Worm reduction
Control		38.6±5.4	_	33.4±5.0	_
PA1259	5×100 mg/kg[a]	26.6±5.3	31%*	21.0±7.0	42%*
PZQ	5×100 mg/kg[a]	30.7±2.4	20%	7.4±7.8	79%*
Control		35.4±5.0	_	33.4±5.0	_
PA1259	4×50 mg/kg[b]	16.8±7.2	53%*	20.0±5.1	40%*
PZQ	4×50 mg/kg[b]	21.0±6.0	41%*	4.8±6.5	86%*

Effect on worm recovery of two administration protocols of PA1259 and praziquantel (PZQ) administered to mice harbouring either a 21-day-old schistosomula or 49-day-old adult *S. mansoni* infection.
[a]The five doses of 100 mg/kg were administered daily during five consecutive days.
[b]The four doses of 50 mg/kg were administered every three hours (overall treatment period: 9 h).
*Significant difference compared to the control group at 5% level (Mann-Whitney U test). SD stands for standard deviation.
doi:10.1371/journal.pntd.0001474.t001

respectively). However, PZQ induced damages to sensory papillae that became subsided, losing their domed shape and their sensory cilium (arrows in Figure S2b and Figure S3b). Extensive blistering occurred with ARTM (arrows in Figure S3e). Treatment with MFQ induced a cavernous aspect of the worm, with disappearance of spines, and complete destruction of the external structures (Figure S2d).

Third, the tegument of control schistosomes exhibited normal circular ridges with regular clefts (Figure 4a). After treatment with PZQ or trioxaquine PA1259, the transverse tegumental ridges encircling the body worm were not observable any longer. Swelling induced loosing of the clefts, and fusions of ridges were always observed (Figure 4, panels b and c, respectively, and S4). Ridges were damaged, but still visible after treatment by artemether (Figure 4e and S4e), in contrast to females treated with praziquantel or PA1259, which showed a complete fusion of the ridges. PZQ mainly induced swelling and formation of holes, probably corresponding to damaged sensory papillae (arrow in Figure S3b). In the case of PA1259, the fusion of ridges was accompanied by formation of long irregular and disorganized splits (arrows in Figure S4c). Worms treated with PA1259 were also characterized by swelling, and dilated and/or empty spine sockets were visible (Figure S3c). After treatment with artemether, there were both rather undamaged regions, with well-conserved ridges and regions showing extensive vesiculations, burst of blebs, erosion of the tegument and sloughing (Figures 4e and S3e). The extensive blistering observed upon treatment with artemether was not present with the other drugs. Blebs were so large that they fused together, inducing a detachment of large parts of the tegument layer, and splits parallel to the ridges. Magnification of this peeling phenomenon is depicted in Figure S5b, and compared with erosion and peeling subsequent to PA1259 treatment (Figure S5a). In the latter case, focal sloughing was also present, but no rest of the tegumental layer could be observed. After ARTM treatment, round holes, about 1 µm large, were also visible in the underlying layer (Figure S5b). MFQ treatment induced the most destructive damages with a cavernous aspect of worm surfaces (Figures 4d and S4d). In addition, whether the treatment, the oral and ventral suckers were affected in most of the worms examined, showing serious deformations and extensive swelling (data not shown).

c. Transmission electron microscopy of S. mansoni (TEM). By ultramicrotomy, ultrathin (50 nm) transverse sections of *S. mansoni* adult females were prepared. For each drug treatment, three worms were analyzed by TEM (four sections prepared for each worm).

First, the hemozoin pellets appeared as 200–300 nm large contrasted dark grey disks. Early crystallization of hemozoin was visualized at the surface of lipid droplets giving dark grey circles with light grey inside [29]. The presence of iron was assessed by energy dispersive (X-ray) microscopy in mature- or in formation-hemozoin pellets (noted 3 and 2, respectively, in Figure 5a). By

Table 2. *In vivo* effect of PA1647 combined with praziquantel on 21-day-old schistosomula.

		21-day Schistosomula	
	Treatment	Mean number of worms ± SD	Worm reduction
1	Control (excipient alone)	43.4±4.9	_
2	4× (PZQ 50 mg/kg)	33.0±1.6	24%
3	4× (PZQ 37.5 mg/kg + PA1647 12.5 mg/kg)	31.0±2.7	29%
4	4× (PZQ 25 mg/kg + PA1647 25 mg/kg)	11.6±3.9	73%*
5	4× (PZQ 12.5 mg/kg + PA1647 37.5 mg/kg)	31.5±3.1	27%
6	4× (PA1647 50 mg/kg)	35.8±4.4	18%

The treatment schedule consisted in four doses of 50 mg/kg (sum of the two drugs) every three hours.
*Significant difference compared to the control group at 5% level (Mann-Whitney U test). SD stands for standard deviation.
doi:10.1371/journal.pntd.0001474.t002

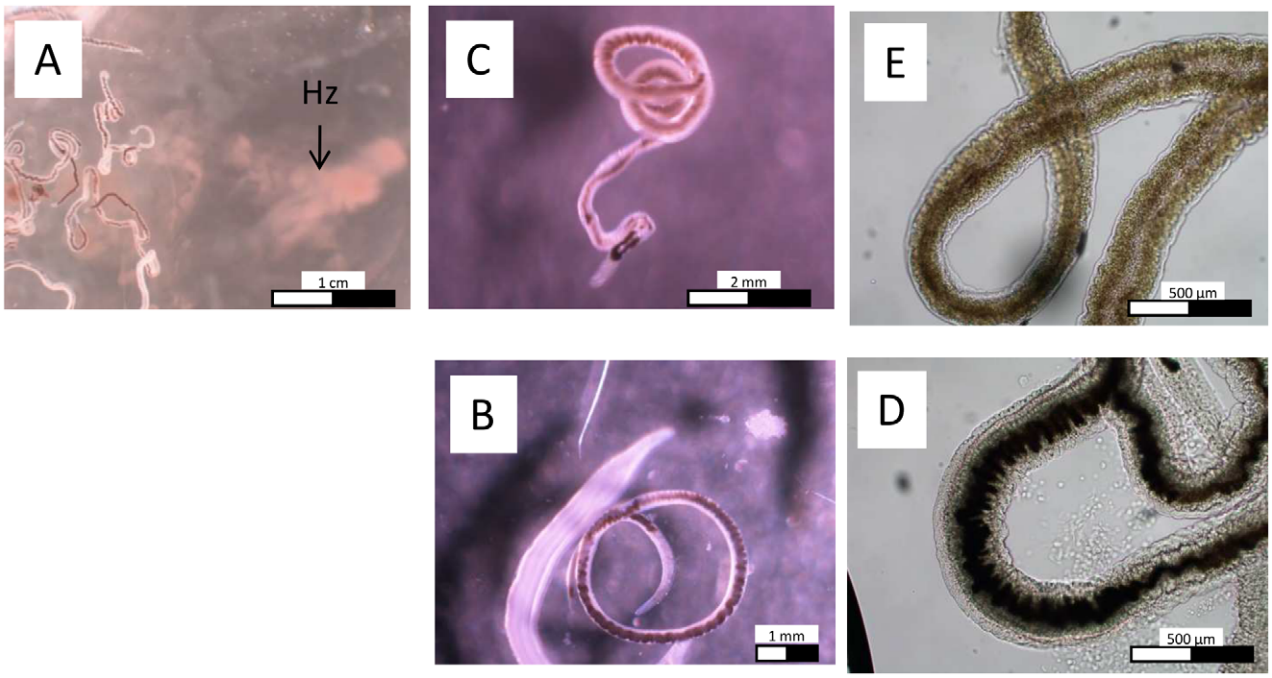

Figure 3. Optic microscopy of treated worms. *S. mansoni* females treated with PA1259 at 50 µg/mL (A, C, and E), compared to control worms (B and D). Hz stands for hemozoin. In B and D: black Hz in a well defined gut; in C: Few minutes after treatment, Hz turns to brown inside the gut; in E) one hour after treatment the brown pigment was transfered outside of the gut.
doi:10.1371/journal.pntd.0001474.g003

contrast, no iron was detected in many uncontrasted locations (noted 1 in Figure 5a).

Images obtained for control worms, compared with those obtained after treatment with mefloquine (MFQ), praziquantel (PZQ), and trioxaquine PA1259 are depicted in Figure 6. The gut of *S. mansoni* adult females treated with PA1259 (panel d) exhibited a drastically lower hemozoin content with respect to control worms (panel a). Upon treatment with MFQ or PZQ, the hemozoin content was significantly reduced with respect to control worms (panels b and c, respectively), but in much lower proportion than upon treatment with PA1259. In addition, upon treatment by PA1259, a part of remaining hemozoin pellets migrated across the epithelium and was found lining its external membrane (Figure 6, panels e and f).

Second, the vitelline cells of control female worms were well characterized (Figure S6a). Ultrastructure of vitelline cells of worms treated with PZQ and ARTM exhibited focal fusion of vitelline balls in vitelline droplets (vd on Figure S6, panels b and e, respectively). However, the most part of vitelline cells remained intact. By contrast, extensive alterations appeared in schistosomes treated with PA1259 and, in a greater extent with MFQ (panels c and d, respectively). Fusion in the process of vitelline balls (arrows on Figure S6, panel c1), and formation of lipid droplets were seen (ld in panel d2).

Third, the tegumental matrix (t), spine and spine sockets (s), and muscle bundles (m) were clearly visible on many transmission electron micrographs of control worms (Figure 7, panels a). After treatment with PZQ, the extent of tegumental damages was significantly different depending on the parasite sections. However, in the most part of cases, the tegumental matrix was slightly modified, but significant swelling of the underlying muscle bundles occurred (Figure 7, panels b). Treatment with PA1259 (Figure 7, panels c) caused complete disappearance of the tegument matrix and severe swelling and disorganization of the sub-tegumental muscle layer (m). Some spines were still visible (s). The severity of tegumental damages induced by treatment with MFQ are visible in Figure 7d. All the worm sections exhibited complete lysis of tegument, extensive disappearance of spines, and collapse of internal structures. ARTM induced deep clefts in the tegument, but the damages were drastically less important than those caused by PA1259 or MFQ (Figure 7, panels e).

5. Molecular mechanism of damages induced by antischistosomal drugs

a. Reduced or radical oxygen species: NO•, $O_2^{\bullet -}$, H_2O_2. Dosage of reduced oxygen species $O_2^{\bullet -}$, H_2O_2, and NO•, is reported in pannels A, B, and C of Figure 8, respectively. In worms treated with PZQ, the production of $O_2^{\bullet -}$ was roughly twice higher than that of control worms (Figure 8A: PZQ (■): OD = 0.0075, Control (◆): 0.0041). By contrast, treatment with PA1259 (▲, OD = 0.0031) did not improve the production of $O_2^{\bullet -}$ with respect to control. The production of H_2O_2 whether control, PZQ, or PA1259 treated worm, was not significantly different (optic density values being 0.0017, 0.0019, and 0.0016 for control (◆), PZQ (■), and PA1259 (▲)-treated worms, respectively; Figure 8B). The production of NO• was very low in control worms (Figure 8, panel C1, intensity 44±14, pannel C4). Females treated with PZQ exhibited a slightly enhanced fluorescence due to NO• located near the tegument (Figure 8, panel C2, intensity 67±16, pannel C4), whereas, in females treated with PA1259, the fluorescence due to NO• was very high, and mainly detected inside the gut and near the vitelline cells (Figure 8, panel C4 and C3, respectively, intensity 190±43, panel C5).

b. Characterization of covalent heme-drug adducts. The LC-MS profile of the extract of worms treated by ARTM is depicted in Figure 9. Chromatographic peaks with retention times 28.8, 29.4, and 29.9 min exhibited an intense ionic current with

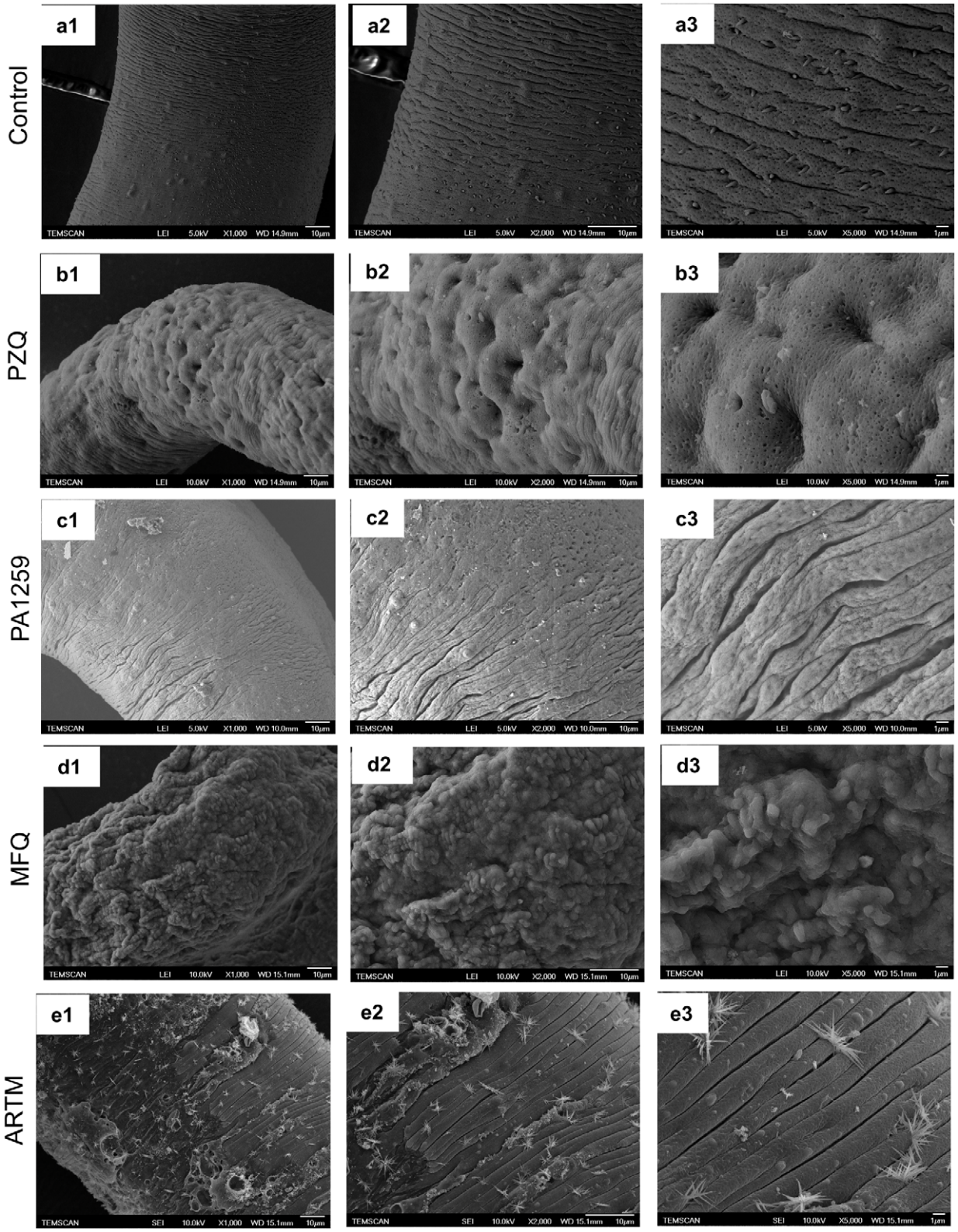

Figure 4. SEM images of the mid-body region of *S. mansoni* adult females. Control worms (a), compared to worms treated with b) praziquantel (PZQ), c) trioxaquine PA1259, d) mefloquine (MFQ), or e) artemether (ARTM). Magnification ×1000 (a1-e1), ×2000 (a2-e2), ×5000 (a3-e3); the bars stand for 10 μm.
doi:10.1371/journal.pntd.0001474.g004

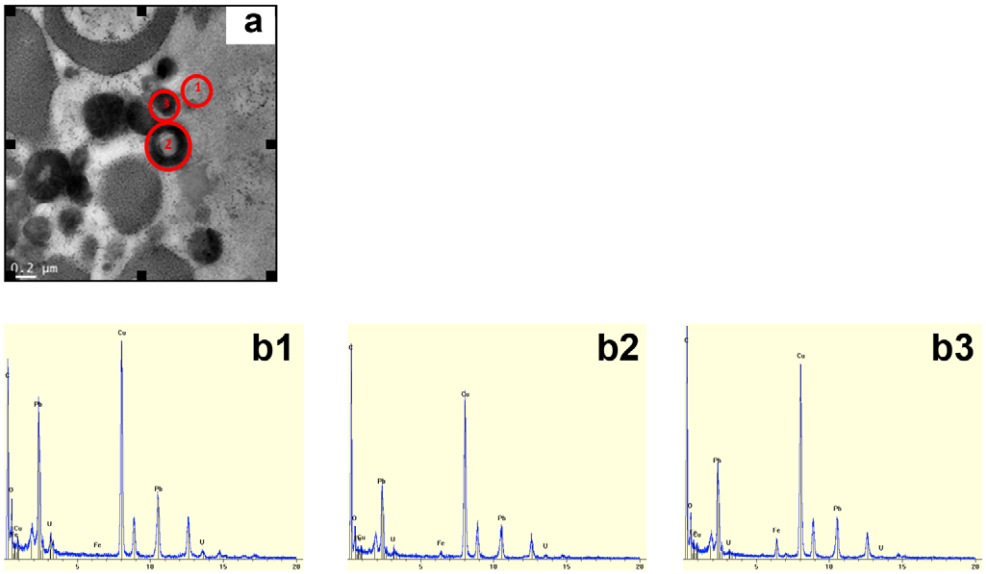

Figure 5. Hemozoin detection. (a) TEM image of hemozoin pellets of untreated *S. mansoni* female. (b) Element analysis of 3 differents part of the picture (a): b1. Background: low contrasted zone, b2. Hemozoin pellets in early stage formation, b3. Hemozoin pellets at final stage.
doi:10.1371/journal.pntd.0001474.g005

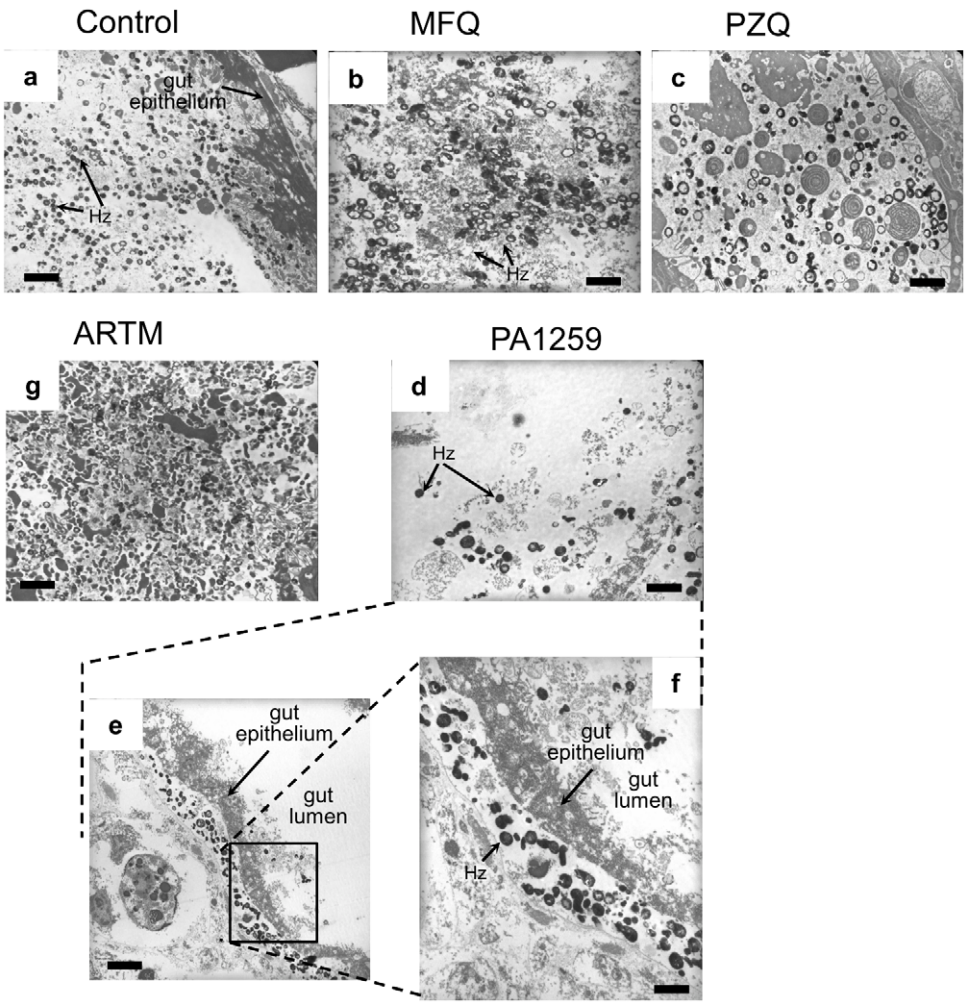

Figure 6. TEM images of hemozoin (Hz) inside the gut. Control worms (a), compared to worms treated with b) mefloquine (MFQ), c) praziquantel (PZQ) or d, e, f) trioxaquine PA1259, and g) artemether. The scale bars stand for 2 μm in panels a, b, c, d, f, and g, and for 5 μm in panel e.
doi:10.1371/journal.pntd.0001474.g006

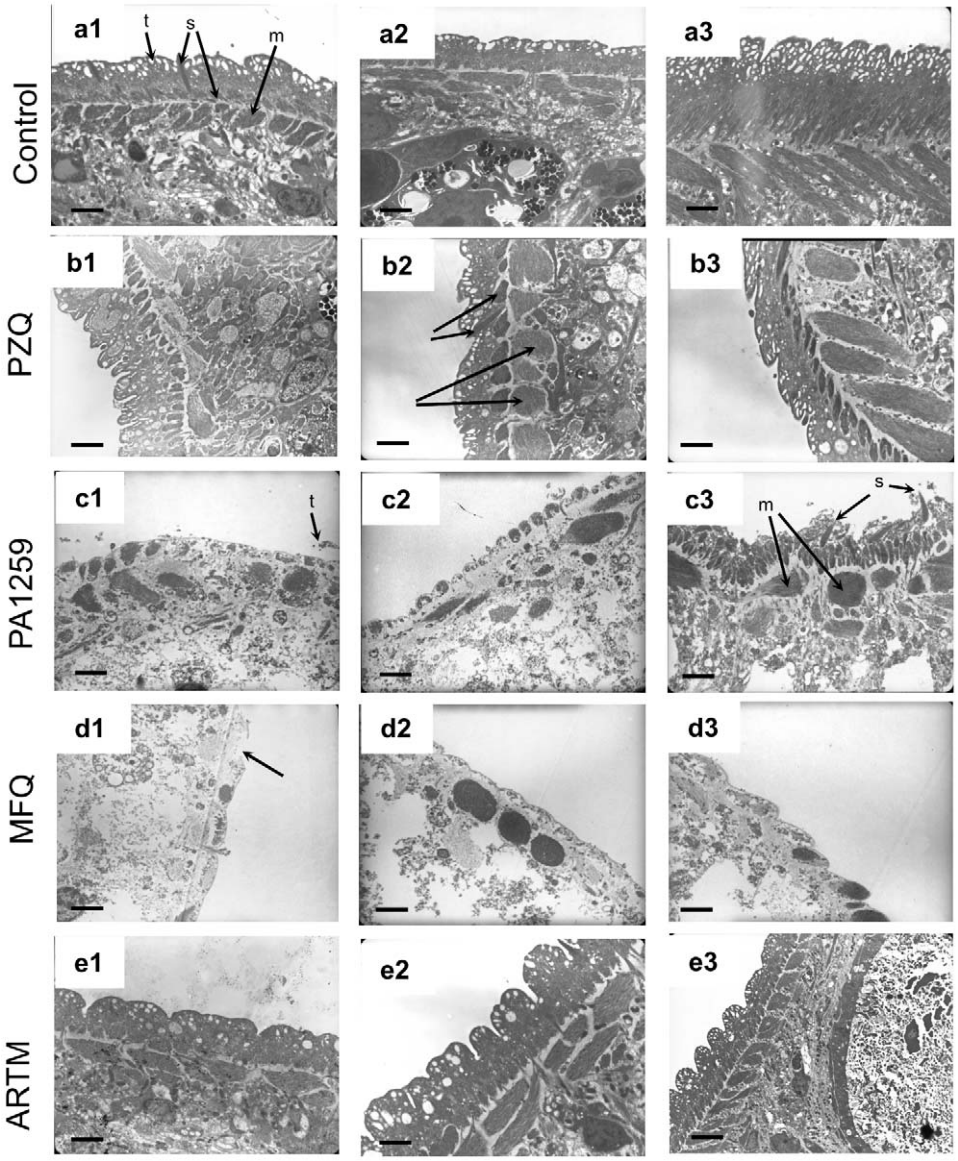

Figure 7. TEM images of tegument. Control worms (a), compared to worms treated with b) praziquantel (PZQ), c) trioxaquine PA1259, d) mefloquine (MFQ), or e) artemether (ARTM). The scale bars stand for 2 μm in panels a1-e1, and for 1 μm in panels a2-e2.
doi:10.1371/journal.pntd.0001474.g007

$m/z = 854.4$ amu ($z = 1$) (compound **2**, Figure 9c). Trace amounts of a compound having $m/z = 936.4$ amu was also detected (compound **1**, Figure 9b).

The LC-MS analyses of extracts of *S. mansoni* worms treated with PA1259 are reported in Figure 10a-c. Along with the ionic current of heme [$R_t = 26.1$ min, $m/z = 616.2$, $z = 1$, M^+ for Fe^{III}(PPIX), Figure 10a], several chromatographic peaks were detected at $R_t = 24.7$, 25.3, 26.3, and 26.5 min, with $m/z = 551.3$ and $z = 2$, having an exact mass value of 1101.2 amu (Compounds **3**, **4**, Figure 10b). Another product **5** was also detected ($R_t = 25.1$ and 25.7 min, $m/z = 730.3$, $z = 1$, Figure 10c).

c. Heme oxidative cleavage in S. mansoni. Twenty five freshly recovered *S. mansoni* adults were maintained in RPMI for 3 h, but without drug treatment, and then extracted with pyridine as described above. The LC-MS analysis of the extract exhibited the presence of two chromatographic peaks with the same m/z value of 347.1 amu ($R_t = 13.8$ and 14.1 min). We failed to detect a significant amount of these compounds in schistosomes treated with ARTM or MFQ under similar conditions.

Discussion

1. *In vitro* activity of trioxaquine PA1259 on free and parasitic stages of *S. mansoni*

The *in vitro* activities of PA1259 (■) on cercariae, schistosomules, and adult worms *S. mansoni* are reported in Figure 2A, 2B, and 2C, respectively, along with activities of praziquantel (★), artemether (◆), and mefloquine (●) given as comparison. Results depicted in Figure 2 show that PA1259 exhibits a significant antischistosomal activity on all parasite stages. Concerning the free cercarial stages, PA1259 and MFQ have similar efficacy (all cercariae were dead within 60–90 min, Figure 2A). These two drugs are significantly more efficacious than PZQ (after 90 min of treatment with PZQ, 80% of cercariae were still moving, and

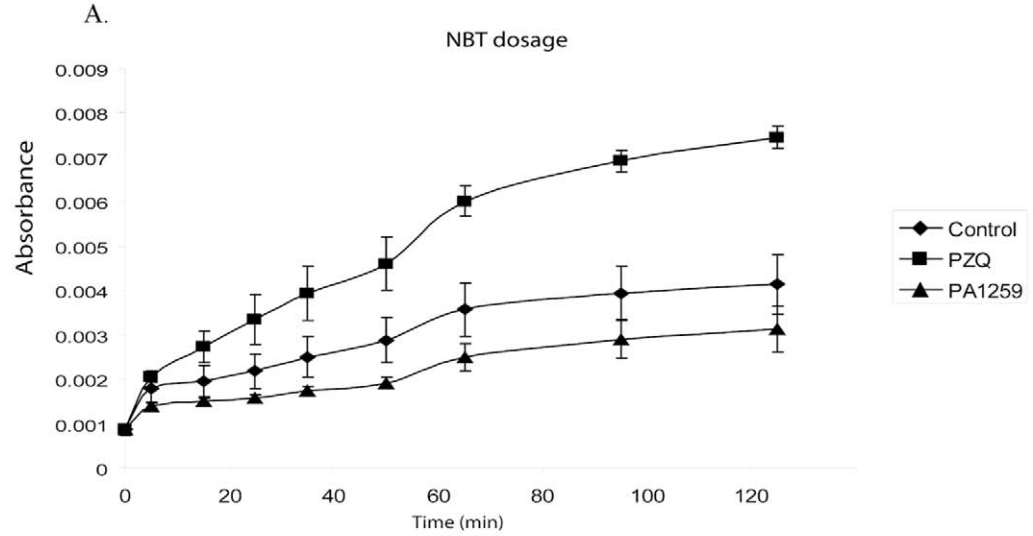
A.
NBT dosage
Absorbance
0.009
0.008
0.007
0.006
0.005
0.004
0.003
0.002
0.001
0
0
20
40
60
80
100
120
Time (min)
Control
PZQ
PA1259

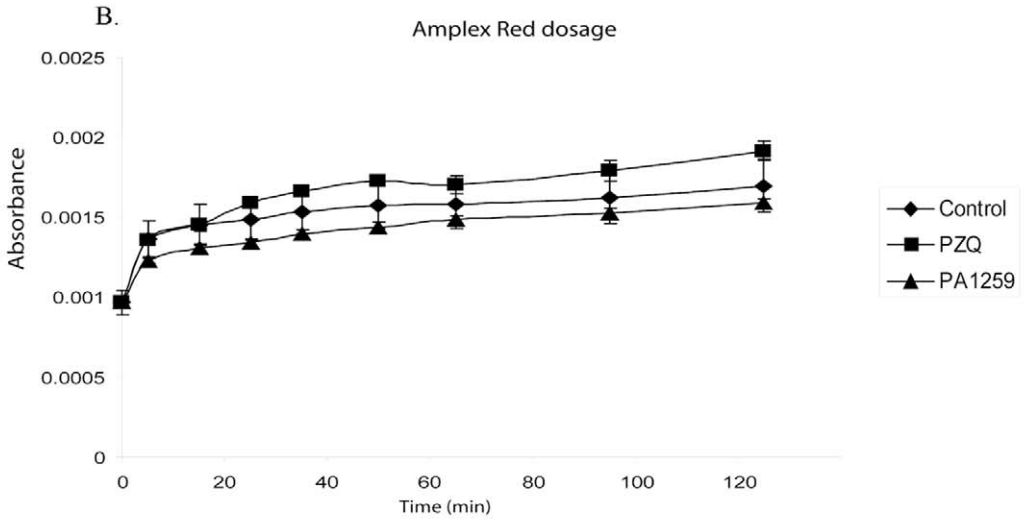
B.
Amplex Red dosage
Absorbance
0.0025
0.002
0.0015
0.001
0.0005
0
0
20
40
60
80
100
120
Time (min)
Control
PZQ
PA1259

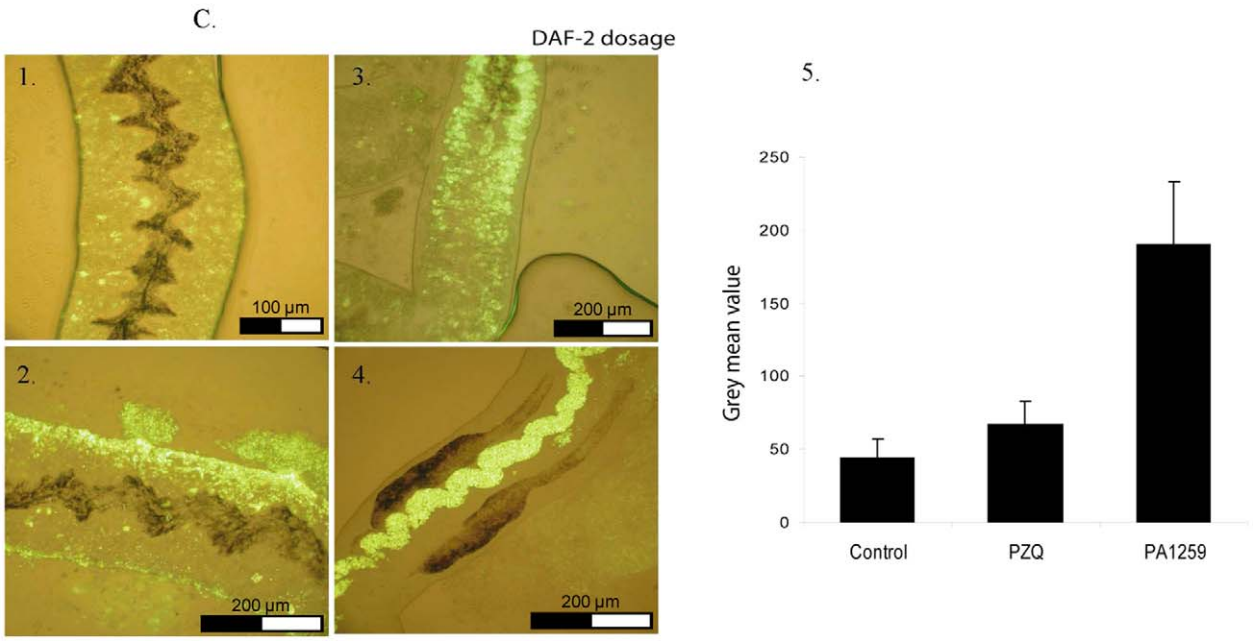
C.
DAF-2 dosage
1.
100 µm
3.
200 µm
2.
200 µm
4.
200 µm
5.
Grey mean value
250
200
150
100
50
0
Control
PZQ
PA1259

Figure 8. Reduced or radicals oxygen species dosage. A. Superoxide anion ($O_2^{\bullet -}$) was dosed using Nitro Blue Tetrazolium method B. Hydrogen peroxide (H_2O_2) was dosed using Amplex Red method. B. Nitric Oxide (NO•) was dosed using DAF-2 method.
doi:10.1371/journal.pntd.0001474.g008

4 hours was needed to immobilize all cercariae). On the schistosomules stage, the time required to kill all schistosomules was 3 h, 5 h, or 8 h, with PZQ, PA1259, or MFQ, respectively (Figure 2B). So, PZQ and PA1259 are more active than MFQ. On adult parasites, the activities of these three last molecules are not significantly different ($p>0.05$), with all worms killed at 2–3 h (Figure 2C). The *in vitro* activities obtained for both MFQ and PZQ are consistent with previous reports [30,31]. Compared to MFQ, PA1259 is more potent on schistosomule stage, and has the same activity on adult stage. It is noteworthy that MFQ, based on a quinoline moiety, is active on the cercarial stage, whereas ARTM, containing a trioxane, is not. This feature suggests that the quinoline part of PA1259 may play a role in its activity against schistosomes (especially the cercarial stage), and that the parasite heme is not the only target of this drug (cercariae do not contain heme). In fact, a non-heme target has recently been proposed for MFQ [30]. ARTM is inactive on cercariae and schistosomules, and only poorly active on adult worms. In fact, this latter drug was reported to be active only when hemin was added in the culture medium [32].

In addition, the activity of PA1259 on schistosomules and adult worms was compared with that of PA1019 which is the 4-aminoquinoline residue contained in PA1259 (see Figure 1 for the structure of PA1019). PA1019 was only poorly active, and 7 h were required to immobilize only 27% of schistosomules and 79% of adult worms. By contrast, treatment with PA1259 immobilized 100% of schistosomules and adult worms after 5 h or 3 h, respectively. This result support an additive or synergistic effect of the quinoline and trioxane moieties of PA1259.

2. Activity of trioxaquine PA1259 on mice infected by *S. mansoni*

In *S. mansoni* mice, the reduction of worm burden upon oral treatment by PA1259 or PZQ is reported in Table 1. The administration of trioxaquine PA1259 at five daily doses of 100 mg/kg resulted in a reduction of 31% and 42% on larval and adult stage, respectively. With four doses of 50 mg/kg every three hours, the reduction of worm burden was 53% or 40% on larval or adult stages, respectively. Whatever the used protocol, the activity of PA1259 on larval stage was very close (slightly higher) to that of PZQ. On adult stage, PA1259 exhibited a significant activity, with a reduction of the worm burden being half of that obtained with PZQ. It is noteworthy that the efficacy of PA1259 was very close on schistosomules and adult worms, whereas PZQ exhibited a significantly higher efficacy on adult schistosomes compared to schistosomules. This feature suggests a different mode of action for these two drugs. For comparison purpose, quinoline- or artemisinin-based molecules present variable efficacy. For instance, among quinoline-based molecules, MFQ exhibits a significant efficacy against schistosome infections, but chloroquine is inactive against schistosome infections [8]. For comparison, artemisinin derivatives or synthethic trioxolanes mainly possess activity against schistosomules [33,34]. In a mouse model, ARTM was reported to be inactive at 800 mg/kg on adult *S. mansoni* infection [33].

In addition, on *S. mansoni* schistosomules, 4 doses of 50 mg/kg of PA1259 every three hours (total dose of 200 mg/kg given over a period 9 hours) was found to be a more efficacious protocol than a total dose of 500 mg/kg given over a period of 5 days (100 mg/kg administered daily).

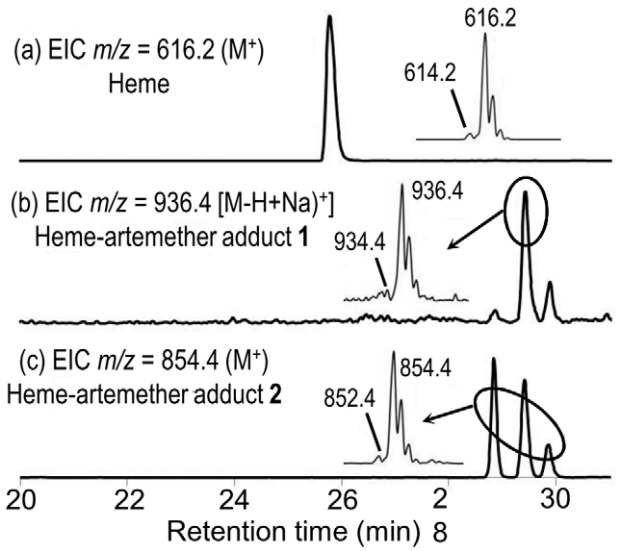

Figure 9. LC-MS analysis of the extract of *Schistosoma mansoni* treated with artemether (50 μg/mL). Extracted ionic current (EIC) traces for: (a) $m/z = 616.2$ (Heme, M^+); (b) $m/z = 936.4$ ("Complete" heme-artemether adduct **1**, $(M\text{-}H+Na)^+$; (c) $m/z = 854.4$ (heme-artemether adduct **2**, MH^+). (Inserts correspond to the mass spectra of circled chromatographic peaks).
doi:10.1371/journal.pntd.0001474.g009

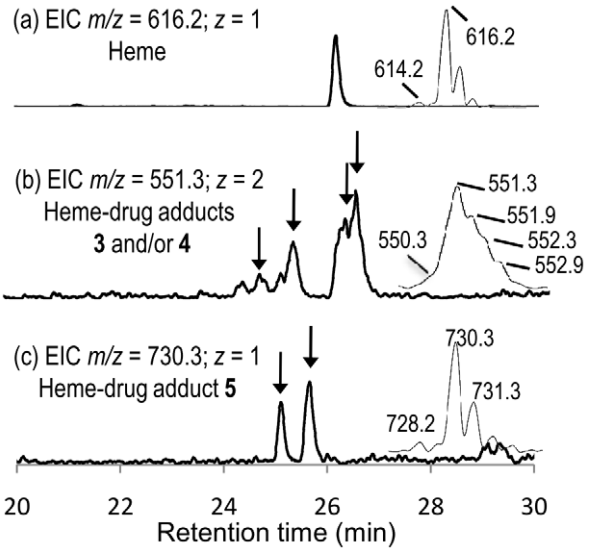

Figure 10. LC-MS analysis of the extract of *Schistosoma mansoni* treated with trioxaquine PA1259 (50 μg/mL). Extracted ionic current (EIC) traces for: (a) $m/z = 616.2$ (Heme, M^+); (b) $m/z = 551.3$ ("Complete" heme-PA1259 adducts **3** and/or **4**, $MH^+/2$); (c) $m/z = 730.3$ (heme-PA1259 adduct **5**, MH^+). (Inserts correspond to the mass spectra of chromatographic peaks with arrows).
doi:10.1371/journal.pntd.0001474.g010

3. Trioxaquine - praziquantel association on mice infected by *S. mansoni* schistosomules

Owing to the complementarity of PZQ and trioxane based drugs against schistosomes, we investigated the reduction of the worm burden in mice infected by 21-day *S. mansoni* schistosomules when orally treated with an association of PZQ and trioxaquine PA1647, the diphosphate salt of PA1259 (Figure 1). Five courses were done with different proportions of PZQ and PA1647. Each course consisted of four oral doses of (PZQ + PA1647), at a total amount of 50 mg/kg for each dose (Table 2). The reduction of the schistosomule burden with respect to control mice was 73% with 50 wt% PZQ/50 wt% PA1647, (corresponding to 32 mol% of PA1647, line 4). For comparison, it was only 24% or 18% when PZQ or PA1647, respectively, were used as monotherapy (lines 2 and 6, respectively). A simple additive effect between PZQ (24% worm burden reduction at 50 mg/kg), and PA1647 (18% worm burden reduction at 50 mg/kg) would have provided at best a (24+18)/2 = 21% worm reduction with the combination PZQ 25 mg/kg + PA1647 25 mg/kg. In fact, such a combination resulted in a significantly higher reduction of 73% (line 4). So, the results are consistent with an additive or synergistic effect against schistosomules.

Then, due to this promising effect of PZQ and PA1647 on schistosomules, the PZQ/PA1647 association should be considered as a drug-association candidate for future clinical tests, after additional optimization on the association drug ratio, in order to target all parasite stages.

4. Microscopy

Adult *S. mansoni* females were treated in *vitro* with PA1259, praziquantel, artemether or mefloquine were examined by photon- and electron microscopy (SEM and TEM), with special focus on hemozoin, vitelline cells, musculature and tegument. In all cases, morphological alterations were apparent, but in highly variable extent and nature. The main observations reported in the Result Section were summarized in Table 3 where the most specific results have been indicated in bold. The following points are worth being emphasized.

a. Photon microscopy. Upon treatment by trioxaquine PA1259, adult females schistosomes readily regurgitated hemozoin, which is visible as a brown ''cloud'' in the right part of the Figure 3A. Few minutes after treatment, the remaining Hz, which was black in control worms (Figure 3D and 3E), turned to light brown color inside the gut of the treated worms (Figure 3B). Some time later, the gut walls of treated worms were no more visible, and the brown pigment invaded the whole worm body (Figure 3C). Such a modification was observed with none of the reference drugs, namely PZQ, ARTM, or MFQ. It strongly suggests that hemozoin is one of the targets of PA1259.

b. Scanning electron microscopy (SEM). The tegument of trematodes is usually considered for its key role in nutrient absorption [33], secretory functions [34], and parasite protection against the host immune system [35]. Tegument is considered as the target (or one of the targets) of PZQ because it was shown by SEM that the biologically active levo-PZQ enantiomer was more prone to induce tegumental damages in *S. mansoni* than dextro-PZQ [36].

Table 3. Relative intensity of damages on cultured *S. mansoni*, observed by electron microscopy.

	Treatment	PZQ	PA1259	MFQ	ARTM
Target	Hemozoin	++	**++++**	++	+
	Vitelline cells	+	++	**+++**	+
	Tegument	+	+++	+++	**++**
	Musculature	**+++**	+++	+++	-

doi:10.1371/journal.pntd.0001474.t003

Worms treated with PA1259 were convoluted (Figures 3C and S1c). In fact, during the antischistosomal evaluation of trioxaquines, we have tested 90 trioxaquines (partial results have been reported in reference 12). With all active drugs of this series, the female *S. mansoni* worms adopted the shape of a loosen knot. It was so general, that it was possible to use this fact to detect trioxaquine-treated worms in blind assays [Boissier and Portela, unpublished work].

The disorganization of spines and the dilated spine sockets induced by PA1259 (Figure S2c and S3c, respectively) might be due to damages of the subjacent musculature of these retractile structures.

It should be noted that tegumental erosion and peeling upon *in vitro* treatment of *S. mekongi* [37] or *in vivo* treatment of other trematode parasite, such as *Clonorchis sinensis* [38], or *Fasciola hepatica* [39] by ARTM have been reported in the recent years.

Severe deformations of the tegument surface were seen in many worms, resulting in significant changes of the overall morphology of the worms. These facts suggest a drastic effect of drugs not only on the external tegument matrix, but also on the subjacent structures such as worm musculature. The observation of damages on a given part of the worms, namely hemozoin, tegument or suckers does not indicate that such a part of the worm is the location of the main target of the drug, even less the only drug target. Indirect widespread damages are indeed expected upon treatment in lethal conditions. However, we observed a significant number of differences between the damages induced by PZQ, ARTM, MFQ and PA1259, which are probably related to different mechanisms of action for these different drugs.

c. Transmission electron microscopy (TEM). Beyond the general morphology and aspect of *S. mansoni* external structures, we examined the effect of the different drugs under a transmission electron microscope of ultrathin transverse sections of schistosomes. If the SEM study of trematode parasites has been well documented in literature, transmission-electron microscopy (TEM) studies are less common [40,41].

Upon treatment with PA1259, MFQ or PZQ, the hemozoin content was significantly reduced with respect to control worms (Figure 6). A semi-quantitative estimation was carried out by counting the number of hemozoin pellets on a total surface of 200–300 μm^2 in the mid-body region. The mean number of hemozoin pellets per μm^2 was 1.6 for control schistosomes, 1.2 after treatment with ARTM, 0.8 and 0.6 after treatment with MFQ and PZQ, respectively, and close to 0.1 after treatment with PA1259. Then the gut hemozoin content of schistosomes treated by PA1259 was about 10% of that of untreated schistosomes. In addition, upon treatment by PA1259, a part of remaining hemozoin pellets was found lining the external epithelium membrane (Figure 6, panels e and f), suggesting perforation of the gut epithelium. However, the total hemozoin content in the gut lumen and epithelium was 0.2 pellet per μm^2 after treatment with PA1259.

After treatment with PZQ, the tegumental matrix was slightly modified, but significant swelling of the underlying muscle bundles occurred (Figure 7, panels b). This feature argues that a main PZQ target should be musculature, instead of tegument, as previously reported [42]. TEM micrographs of worms treated by PA1259 exhibited complete disappearance of the tegument and severe swelling and disorganization of the sub-tegumental muscle (Figure 7, panels c). These images should be linked to SEM

images, where worms became swollen, with retraction of spines into spine sockets, and extensive erosion of the tegument (Figure S3c and S5, respectively).

MFQ and PA1259 were the two drugs inducing the most severe damages to the tegument. These modifications may lead to exposure of worm surface antigen, resulting in attack of the parasite by host immune system. This fact had to be confirmed by investigation of the molecular processes responsible for the morphologic damages.

In previous reports, decrease of hemozoin gut content, as well as gut epithelium alteration, was observed in *S. mansoni* worms treated with quinine [43]. However, the authors did not observed alteration of tegument after quinine treatment. Extensive tegumental damage has been observed in both male and female worms treated with MFQ [29,44]. Similar observations were obtained with *S. japonicum* parasite treated with MFQ [45]. Almost the same observations, (i) damage of tegumental and subtegumental structures, (ii) alteration of gut epithelial cells and (iii) fusion of vitelline balls were obtained in *S. mansoni* worms treated with artemether [46], but in a lower extent. Despite some common effects of drugs targeting heme, whatever their structural origins, trioxane-based, aminoquinoline-based or hybrid molecules (PA1259), on schistosomes, it is clear that the intensity of the effect and the morphological aspect after treatment vary according to the drug itself.

Upon treatment with PZQ, the most important damages were observed on the musculature of schistosomes, whereas tegument and vitelline cells were much less affected. MFQ was the most destructive drug, especially on vitelline cells. Upon treatment with PA1259, the more specific effect was a drastic decrease in hemozoin content, along with damages on the tegument and vitelline cells. The damages induced by artemether were much less severe and focalized on the tegument surface. This suggests certain specificity in the mode of action of each compound. The hybrid structure of trioxaquine PA1259 should explain interaction with heme polymerization, due to the 1,2,4-trioxane ring, and a severe effect on the musculature and tegument, as shown with the quinolone-based MFQ.

5. Molecular mechanism of damages induced by antischistosomal drugs

a. Reduced or radical oxygen species: NO•, $O_2^{\bullet -}$, H_2O_2. Quantification of ROS was performed on adult worms at a drug concentration giving the same proportion of immobilized worms, for PZQ and PA1259 [28a]. Results are reported in Figure 8. In worms treated with PZQ, the production of $O_2^{\bullet -}$ was twice higher than that of control worms. By contrast, treatment with PA1259 did not improve the production of $O_2^{\bullet -}$ with respect to control (Figure 8A). The production of H_2O_2 production whether control, PZQ, or PA1259 was similar (Figure 8B). The most significant feature was NO• production, which was very low in control worms. Females treated with PZQ exhibited a slightly enhanced production of NO• (×1.5) near the tegument, whereas, in females treated with PA1259, the fluorescence due to NO• was very high (×4.3 with respect to control worms) and mainly detected inside the gut and near the vitelline cells (Figure 8C). Then, the reactive oxygen species produced are different, in nature, in localization, and in quantities, when worms are treated with either PZQ or PA1259. These results strongly suggest that these drugs have different targets and mechanisms of action on schistosomes. Oxadiazoles may also act as nitric oxide donors [6b]. Quantification of gene transcripts showed that anti-oxidant metabolism is increased when worms are exposed to a sub-lethal dose of PZQ. Our results are consistent with reference 47.

b. Characterization of covalent heme-drug adducts. The alkylation ability of the drug toward heme was investigated in *S. mansoni* treated with ARTM or PA1259. In both cases, heme-drug adducts were detected by LC-MS analysis of the worm extracts.

In the extract of worms treated by ARTM (Figure 9), the product having ionic current $m/z = 854.4$ amu is consistent with the formation of heme-artemether covalent adducts **2** depicted in Figure 11. The reductive activation of the O–O bond of artemether by iron(II)-heme, followed by homolytic cleavage of the C3–C4 bond, resulted in the formation of a primary alkyl radical centered at C4. As previously reported with the heme model manganese(II)-tetraphenylporphyrin, this radical was able to alkylate the porphyrin macrocycle, leading to covalent heme-drug adducts [48]. As for artemisinin, alkylation of heme by the drug can indeed occur on the four *meso* positions of the porphyrin macrocycle, giving rise to regioisomeric adducts **1**. The "South" cycle of the artemether moiety was subsequently rearranged by nucleophilic attack of the hydroxyl function at C12a onto the acetal C10, to generate the heme-artemether adduct **2**, bearing a 5-membered lactone. Such a mechanism is very similar to the rearrangement reported for artemisinin derivatives having an amine function at C10 [49]. Trace amounts of "complete" covalent heme-artemether adducts **1** ($M_e = 914.4$ amu), were also detected, with $m/z = 936.4$ amu, corresponding to the substitution of a proton of a propionic side chain of heme by sodium [(M-H+Na)$^+$].

The LC-MS analyses of extracts of *S. mansoni* worms treated with PA1259 are reported in Figure 10a–c. The exact mass value of 1101.2 amu (Figure 10b) corresponds to the mass of heme (616.2) plus the mass of PA1259 (485.2), and can be assigned to

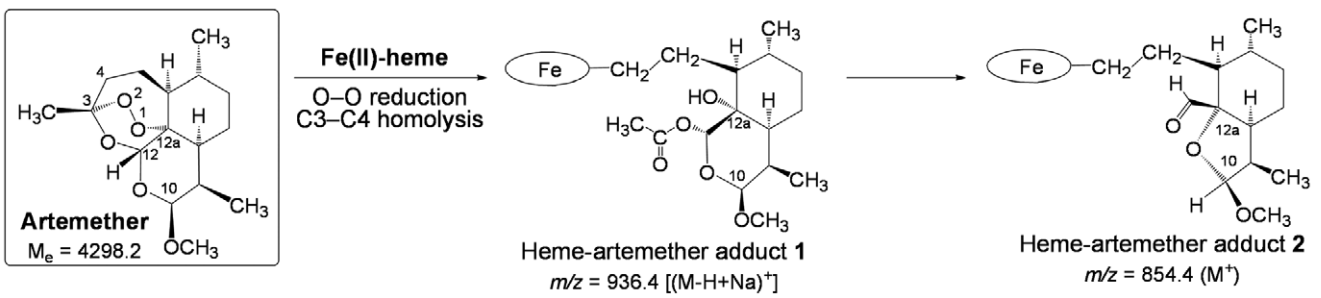

Figure 11. Mechanism of alkylation of heme by artemether (the oval stands for the protoporphyrin-IX ligand).
doi:10.1371/journal.pntd.0001474.g011

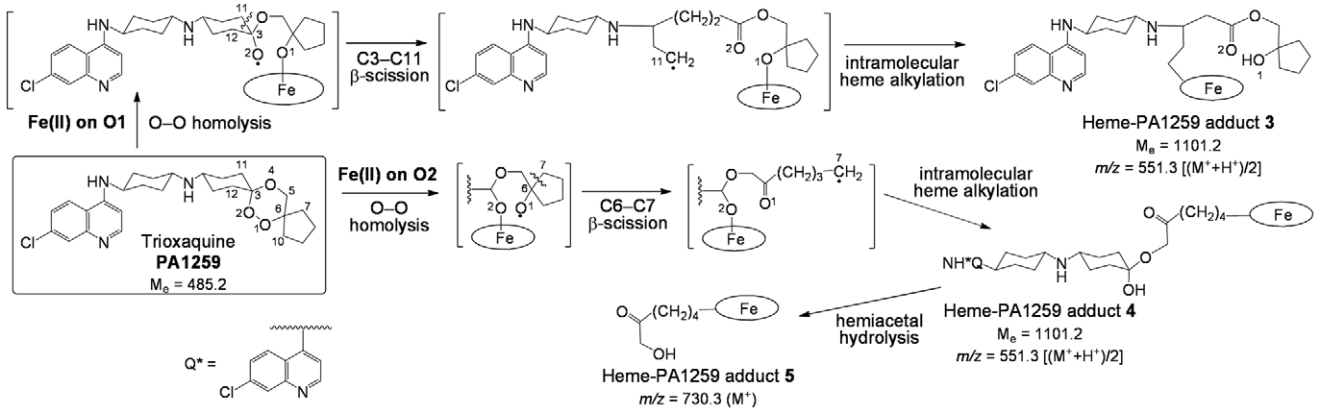

Figure 12. Mechanism of alkylation of heme by trioxaquine PA1259 (the oval stands for the protoporphyrin-IX ligand).
doi:10.1371/journal.pntd.0001474.g012

covalent adducts between heme and PA1259. The structures and mechanisms of formation of these adducts are depicted in Figure 12. It should be noted that the inner-sphere reductive activation of the peroxide bond of PA1259 can occur with coordination of iron(II)-heme either on O1 or O2, giving rise to the formation of alkoxy radicals either on O2 or O1, respectively. Subsequent β-scission of the adjacent C3–C11 or C6–C7 bond, respectively, generated C-centered radicals able to alkylate heme and provide the covalent heme-drug adducts **3** and **4**. The covalent adduct **5**, resulting from the hydrolysis of the hemiacetal function of adduct **4**, was also detected (Figure 10c). In addition, the isotopic patterns of signals at m/z 551.3 and 730.3 clearly showed that the corresponding adducts contained one iron atom (M-1 at 550.3 and M-2 at 728.2, respectively, due to ^{54}Fe). By contrast, one chlorine atom was detected in adducts at m/z 551.3 (M+1 at 552.3 due to ^{37}Cl), whereas adduct **5** contained no chlorine after release of the 7′-chloro-4′-aminoquinoline moiety (Figure 12). The heme-drug adducts **2–5** were undetectable in all extracts of untreated *S. mansoni* worms. Because the worms treated with ARTM or PA1259 were carefully washed before lyophilization, the detected adducts were clearly contained inside the worms, and cannot be considered as an external contamination.

c. Heme oxidative cleavage in *S. mansoni*. A heme oxidase activity has been previously reported in *S. japonicum* [50], which may account to supply iron to schistosomes by catabolism of the heme of the host. Then, we were interested to detect heme fragments that might result from the possible oxidative cleavage of the heme macrocycle by the parasites. The LC-MS analysis of untreated worms showed the presence of two chromatographic peaks with the same m/z value of 347.1 amu. These peaks were also produced (with same mass spectrum and retention time values) by reaction of hemin or β-hematin, the synthetic analogue of hemozoin, in the presence of hydrogen peroxide [El Rez, Pradines and Robert, unpublished data]. The mass and UV absorption ($\lambda_m = 280$ nm) of these heme fragments suggest a common dipyrrolic structure. Possible structures are depicted in Figure 13, which result from oxidative cleavage of C5–C6, C7–C8, and C15–C16 (**6a**), C5–C6, C15–C16, and C17–C18 (**6b**), or C10–C11 and C19–C20 (**6c**) of heme ligand, in a similar way as the cleavage protoporphyrin-IX to biliverdin-IX by mammalian heme oxygenases. Obviously, the cleavage of the heme ring results in a drastic loss of visible absorbance, and discoloration of the pigment. Interestingly, treatment with ARTM or MFQ did not produce a significant amount of that heme fragment.

Conclusion

A multidisciplinary approach allowed us to propose the following mode of action of the antischistosomal trioxaquine PA1259. First, the easy absorption due to the quinoline moiety of PA1259 should allow the drug to interact with the schistosome process of polymerization of heme to hemozoin. The reaction of the peroxide function of trioxaquine with free heme resulting from the degradation of hemoglobin was assessed by the production of heme-drug adducts characterized in worm extracts. As heme-drug adducts are probably able to inhibit the heme polymerization, and are themselves unable to polymerize (this feature has been demonstrated for heme-artemisinin adducts [51]), this reaction

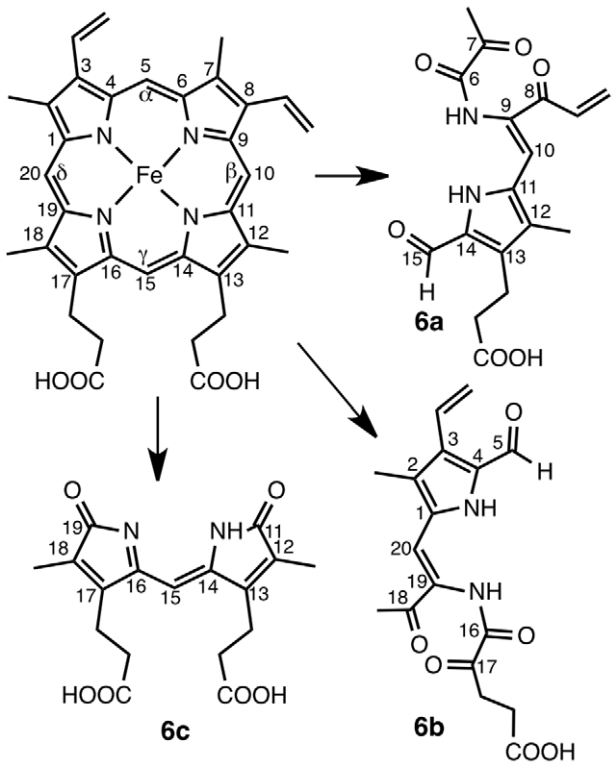

Figure 13. Oxidative cleavage of heme to fragment with *m/z*= 347.2 (M^+).
doi:10.1371/journal.pntd.0001474.g013

led to accumulation in the worm of soluble redox-active heme derivatives. Then, the iron chelated by the protoporphyrin-IX ligand of heme or heme-drug adducts induced the production of reactive oxygen species, which should readily destroy hemozoin by radical chain reactions, resulting in (i) drastic discoloration of worms from black to brown, and (ii) much lower density of hemozoin in worms treated with PA1259 than in control worms, as observed in microscopy (Figures 3 and 6).

The high quantity of nitric oxide detected in the parasite gut is certainly an important element of this oxidative stress (Figure 8). Third, this oxidative stress would cause gastrodermis perforation and the passage of the gut content through the gastrodermis, as observed by electronic microscopy (Figure 6). The oxidative cleavage of heme also releases free iron that should increase the production of radical oxygen species. Finally, the substructure of the tegument was altered by the invasion of oxygen reactive species (Figures 4 and 7).

However, several questions remain to be adressed. Indeed, the fact that cercariae are heavily affected by treatment, the external tegumental alteration, and the effect on vitelline cells observed with PA1259 are not directly explained by reaction of the drug with heme. But the sequence hemoglobin/heme/hemozoin is not the single source of iron in schistosomes and several other iron proteins may play a role. Schistosomes have high demand for iron and are dependent on host iron for early development within the mammalian host [52]. In each stage, from miracidia to adult, schistosomes express tegumental divalent metal transporters involved in iron uptake [53]. Moreover, schistosomes are known to bind host transferrin at their surface [52]. The parasite also possesses two ferritin isoforms involved in storage and release of iron [54,55]. One isoform, called yolk-ferritin or ferritin 1, is predominantly found in mature egg laying female, where it has been localized in the vitelline cells and in the ovary [56]. Vitelline stores of iron are implicated in eggshell formation [57]. Interestingly, the two isoforms of ferritin are also expressed in the parasite egg suggesting these molecules are also synthesized by embryo [57]. These observations emphasize the importance of iron in schistosome metabolism and egg formation, even on worm stages that do not ingest hemoglobin yet. Ferritin has not yet been characterized in cercariae, however the expressed sequence tags of ferritin 2 are available in sequence database suggesting that cercariae express this enzyme. Several recent articles suggest that iron metabolism should be a valuable target for either chemotherapy or vaccine development against schistosomes [58,59].

Using an anti-schistosomal drug that is also active on malaria parasites is a real matter of discussion [PA1259 is curative on *P. vinckei petteri* infected mice orally treated at 25 mg/kg/day during four days (5/5 mice cured without recrudescence at Day-30, unpublished data from Palumed)]. Such dual activity might be considered as an advantage since patients are suffering from both diseases in many endemic areas. One the other side, one can argue about the possibility to generate trioxane-resistant strains of *P. falciparum*. But we should keep in mind that no trioxaquine-resistant strain has been selected after two years of drug pressure (unpublished results).

In conclusion, trioxaquine PA1259 is the most active against schistosomes among the trioxane-containing drugs that have been tested up to now. Its phosphate salt, PA1647 acts in synergy with praziquantel, specially against schistosomules, when infected mice are treated by oral administration. This opens the route to an efficient bitherapy of a highly neglected disease.

Supporting Information

Figure S1 SEM images of *S. mansoni* adult females. Control worms (a), compared to worms treated with b) praziquantel (PZQ), c) trioxaquine PA1259, d) mefloquine (MFQ), or e) artemether (ARTM). White crosses are breaks related to the preparation for microscopy.
(TIF)

Figure S2 SEM images of the dorsal face of the head region of *S. mansoni* adult females. Control worms (a), compared to worms treated with b) praziquantel (PZQ), c) trioxaquine PA1259, d) mefloquine (MFQ), or e) artemether (ARTM). Magnification ×5000; the bars stand for 1 μm. Sensory papillae are noted sp. Crystals caused by buffer are noted buf.
(TIF)

Figure S3 SEM images of the mid-body region of *S. mansoni* adult females. Control worms (a), compared to worms treated with b) praziquantel (PZQ), c) trioxaquine PA1259, d) mefloquine (MFQ), or e) artemether (ARTM). Magnification ×5000; the scale bars stand for 1 μm.
(TIF)

Figure S4 SEM images of the mid-body region of *S. mansoni* adult females. Control worms (a), compared to worms treated with b) praziquantel (PZQ), c) trioxaquine PA1259, d) mefloquine (MFQ), or e) artemether (ARTM). Magnification ×1000; the scale bars stand for 10 μm.
(TIF)

Figure S5 SEM images of tegumental damages in *S. mansoni* adult females. Worms treated with a) trioxaquine PA1259, or b) artemether (ARTM) (tail region). Magnification ×2000 (a1,b1) or ×5000 (a2,b2); the scale bars stand for 10 μm (a1-b1), or for 1 μm (a2-b2).
(TIF)

Figure S6 TEM images of vitelline cells (vc) containing vitelline balls (vb). Control worms (a), compared to worms treated with b) praziquantel (PZQ), c) trioxaquine PA1259, d) mefloquine (MFQ), or e) artemether (ARTM). The scale bars stand for 1 μm in panels a1-e1, and 2 μm in panels a2-e2. Fusion of vitelline balls (vb) in vitelline droplets (vd); ld stands for lipid droplets.
(TIF)

Figure S7 SEM images of the tail region of *S. mansoni* adult females. Control worms (a), compared to worms treated with b) trioxaquine PA1259. Magnification ×2000 (a1, b1) or ×5000 (a2, b2). The scale bars stand for 10 μm (a1, b1) or 1 μm (a2, b2).
(TIF)

Acknowledgments

The authors thank Sonia Kitoune and Christine Salle (both from Palumed), and Bernard Dejean (from UMR 5244) for technical assistance. The authors also thank Gabriel Mouahid for helpful comments on electronic microscopy.

Author Contributions

Conceived and designed the experiments: JB FC BM AR. Performed the experiments: JP JB BG VP VC FC AR. Analyzed the data: AR JB BM. Contributed reagents/materials/analysis tools: JP BG VP VC FC AR. Wrote the paper: JB BG BM AR FC.

References

1. Oliveira MF, d'Avila JC, Torres CR, Oliveira PL, Tempone AJ, et al. (2000) Haemozoin in *Schistosoma mansoni*. Mol Biochem Parasitol 111: 217–221.
2. Oliveira MF, Kycia SW, Gomez A, Kozar AJ, Bohle DS, et al. (2005) Structural and morphological characterization of hemozoin produced by *Schistosoma mansoni* and *Rhodnius prolixus*. FEBS Lett 579: 6010–6016.
3. Ismail M, Botros S, Metwally A, William S, Farghally A, et al. (1999) Resistance to praziquantel: direct evidence from *Schistosoma mansoni* isolated from Egyptian villagers. Am J Trop Med Hyg 60: 932–935.
4. Gryseels B, Mbaye A, de Vlas SJ, Stelma FF, Guisse F, et al. (2001) Are poor responses to praziquantel for the treatment of *Schistosoma mansoni* infections in Senegal due to resistance? An overview of the evidence. Trop Med Int Health 6: 864–873.
5. Laurent SAL, Boissier J, Coslédan F, Gornitzka H, Robert A, et al. (2008) Synthesis of trioxaquantel derivatives as potential new antischistosomal drugs. Eur J Org Chem. pp 895–913.
6. a) Sayed AA, Simeonov A, Thomas CJ, Inglese J, Austin CP, et al. (2008) Identification of oxadiazoles as new drug leads for the control of schistosomiasis, Nature Med 14: 407–412. b) Rai G, Sayed AA, Lea WA, Luecke HF, Chakrapani H, et al. (2009) Structure mechanism insights and the role of nitric oxide donation guide the development of oxadiazole-2-oxides as therapeutic agents against schistosomiasis, J Med Chem 52: 6474–6483.
7. a) Abdulla MH, Ruellas DS, Wolff B, Snedecor J, Lim KC, et al. (2009) Drug discovery for schistosomiasis: hit and lead compounds identified in a library of known drugs by medium-throughput phenotypic screening. PLoS Negl Trop Dis 3: e478. b) Dong YX, Chollet J, Vargas M, Mansour NR, Bickle Q, et al. (2019) Praziquantel analogs with activity against juvenile Schistosoma mansoni, Bioorg Med Chem Lett 20: 2481–2484.
8. Keiser J, Chollet J, Xiao SH, Mei JY, Jiao PY, et al. (2009) Mefloquine – an aminoalcohol with promising antischistosomal properties in mice. PLoS Negl Trop Dis 3: e350.
9. World Health Organization (WHO) 2004 Artemether Protects Against Schistosome Infection. TDR News No 62.
10. Utzinger J, Tanner M, Keiser J (2010) ACTs for schistosomiasis: do they act? Lancet Infect Dis 10: 579–580.
11. Xiao SH, Keiser J, Chollet J, Utzinger J, Dong YX, et al. (2007) In vitro and in vivo activities of synthetic trioxolanes against major human schistosome species. Antimicrob Agents Chemother 51: 1440–1445.
12. Boissier J, Coslédan F, Robert A, Meunier B (2009) Evaluation of the in vitro activity of trioxaquines against *Schistosoma mansoni*. Antimicrob Agents Chemother 53: 4903–4906.
13. Eissa MH, El-Azzouni MZ, Amer EI, Baddour NM (2011) Miltefosine, a promising novel agent for schistosomiasis mansoni. Int J Parasitol 41: 235–242.
14. a) Robert A, Dechy-Cabaret O, Cazelles J, Meunier B (2002) From mechanistic Studies on artemisinin derivatives to new modular antimalarial drugs. Acc Chem Res 35: 167–174. b) Meunier B, Robert A (2010) Heme as trigger and target for trioxane-containing antimalarial drugs. Acc Chem Res 43: 1441–1451.
15. Robert A, Benoit-Vical F, Claparols C, Meunier B (2005) The antimalarial drug artemisinin alkylates heme in infected mice. Proc Natl Acad Sci USA 102: 13676–13680.
16. Bousejra-El Garah F, Claparols C, Benoit-Vical F, Meunier B, et al. (2008) The antimalarial trioxaquine DU1301 alkylates heme in malaria-infected mice. Antimicrob Agents Chemother 52: 2966–2969.
17. Pradines V, Portela J, Boissier J, Coslédan F, Meunier B, et al. (2011) Trioxaquine DU1259 alkylates heme in the blood-feeding parasite *Schistosoma mansoni*. Antimicrob Agents Chemother 55: 2403–2405.
18. Wellems TE (2002) Plasmodium chloroquine resistance and the search for a replacement antimalarial drug. Science 298: 124–126.
19. Vippagunta SR, Dorn A, Matile H, Bhattacharjee AK, Karle JM, et al. (1999) Structural specificity of chloroquine-hematin binding related to inhibition of hematin polymerization and parasite growth. J Med Chem 42: 4630–4639.
20. Van Nassauw L, Toovey S, Van Op den Bosch J, Timmermans JP, Vercruysse J (2008) Schistosomicidal activity of the antimalarial drug, mefloquine, in *Schistosoma mansoni*-infected mice. Travel Med Infect Dis 6: 253–258.
21. Keiser J, N'Guessan NA, Adoubryn KD, Silué KD, Vounatsou P, et al. (2010) Efficacy and safety of mefloquine, artesunate, mefloquine-artesunate, and praziquantel against *Schistosoma haematobium*: randomized, exploratory open-label trial. Clin Infect Dis 50: 1205–1213.
22. Dechy-Cabaret O, Benoit-Vical F, Robert A, Meunier B (2000) Preparation and antimalarial activities of "trioxaquines", new modular molecules with a trioxane skeleton linked to a 4-aminoquinoline. ChemBioChem 1: 281–283.
23. Benoit-Vical F, Lelièvre J, Berry A, Deymier C, Dechy-Cabaret O, et al. (2007) Trioxaquines are new antimalarial agents active on all erythrocytic forms, including gametocytes. Antimicrob Agents Chemother 51: 1463–1472.
24. Coslédan F, Fraisse L, Pellet A, Guillou F, Mordmüller B, et al. (2008) Selection of a trioxaquine as a drug-candidate. Proc Natl Acad Sci USA 105: 17579–17584.
25. Meunier B (2008) Hybrid molecules with a dual mode of action: dream or reality? Acc Chem Res 41: 69–77.
26. Pradines V, Portela J, Boissier J, Coslédan F, Meunier B, et al. (2011) Trioxaquine PA1259 alkylates heme in the blood-feeding parasite *Schistosoma mansoni*. Antimicrob Agents Chemother 55: 2403–2405.
27. Boissier J, Moné H (2001) Male-female larval interactions in *Schistosoma mansoni*-infected *Biomphalaria glabrata*. Int J Parasitol 31: 352–358.
28. a) Moné Y, Ribou AC, Cosseau C, Duval D, Théron A, et al. (2011) An example of molecular co-evolution: reactive oxygen species (ROS) and ROS scavenger levels in Schistosoma mansoni/Biomphalaria glabrata interactions. Int J Parasitol 41: 721–30. b) Collins TJ (2007) ImageJ for microscopy. BioTechniques 43: S25–S30.
29. Pisciotta JM, Sullivan D (2008) Hemozoin: oil versus water. Parasitol Internat 57: 89–96.
30. a) Manneck T, Haggenmuller Y, Keiser J (2010) Morphological effects and tegumental alterations induced by mefloquine on schistosomules and adult flukes of *Schistosoma mansoni*. Parasitology 137: 85–98. b) Holfreter MC, Loebermann M, Klammt S, Sombetzki M, Bodammer P, et al. (2011) *Schistosoma mansoni*: schistosomicidal effect of mefloquine and primaquine in vitro. Exp Parasitol 127:270–276.
31. Pica-Mattoccia L, Cioli D (2004) Sex- and stage-related sensitivity of *Schistosoma mansoni* to in vivo and in vitro praziquantel treatment. Int J Parasitol 34: 527–33.
32. Xiao S, Chollet J, Utzinger J, Matile H, Mei J, et al. (2001) Artemether administered together with haemin damages schistosomes in vitro. Trans R Soc Trop Med Hyg 95: 67–71.
33. Pappas PW (1975) Membrane transport in helminth parasites: a review. Exp Parasitol 37: 469–530.
34. Wilson RA, Barnes PE (1979) Synthesis of macromolecules by the epithelial surfaces of *Schistosoma mansoni*: an autoradiographic study. Parasitology 78: 295–310.
35. Cox FEG (1979) Death of a schistosome. Nature 278: 401–402.
36. Xiao S, Shen B, Chollet J, Tanner M (2000) Tegumental changes in adult *Schistosoma mansoni* harboured in mice treated with praziquantel enantiomers. Acta Trop 76: 107–117.
37. Jiraungkoorskul W, Sahaphong S, Sobhon P, Riengrojpitak S, Kangwanrangsan N (2006) *Schistosoma mekongi*: the in vitro effect of praziquantel and artesunate on the adult fluke. Exp Parasitol 113: 16–23.
38. Xiao SH, Keise J, Xue J, Tanner M, Morson G, et al. (2009) Effect of single-dose oral artemether and tribendimidine on the tegument of adult *Clonorchis sinensis* in rats. Parasitol Res 104: 533–541.
39. Keiser J, Morson G (2008) Fasciola hepatica: tegumental alterations in adult flukes following in vitro and in vivo administration of artesunate and artemether. Exp Parasitol 118: 228–237.
40. Gobert GN, Stenzel DJ, McManus DP, Jones MK (2003) The ultrastructural architecture of the adult *Schistosoma japonicum* tegument. Int J Parasitol 33: 1561–1575.
41. Xiao SH, Xue J, Shen B (2010) Transmission electron microscopic observation on ultrastructural alterations in *Schistosoma japonicum* caused by mefloquine. Parasitol Res.
42. Redman CA, Robertson A, Fallon PG, Modha J, Kusel JR, et al. (1996) Praziquantel: an urgent and exciting challenge. Parasitol Today 12: 14–20.
43. Corrêa Soares JBR, Menezes D, Vannier-Santos MA, Ferreira-Pereira A, Almeida GT, et al. (2009) Interference with hemozoin formation represents an important mechanism of schistosomicidal action of antimalarial quinoline methanols. Plos Negl Trop Dis 3: e477.
44. Manneck T, Braissant O, Ellis W, Keiser J (2011) *Schistosoma mansoni*: antischistosomal activity of the four optical isomers and the two racemates of mefloquine on schistosomula and adult worms in vitro and in vivo. Exp Parasitol 127: 260–269.
45. Xiao SH, Zhang CW (2010) Further observation on histopathological alterations of adult *Schistosoma japonicum* harbored in mice following treatment with mefloquine at a smaller single dose. Parasitol Res 107: 773–781.
46. Xiao S, Shen B, Utzinger J, Chollet J, Tanner M (2002) Ultrastructural alterations in adult *Schistosoma mansoni* caused by artemether. Mem Inst Oswaldo Cruz 97: 717–724.
47. Aragon AD, Imani RA, Blackburn VR, Cupit PM, Melman SD, et al. (2009) Towards an understanding of the mechanism of action of praziquantel. Mol Biochem Parasitol 164: 57–65.
48. Robert A, Meunier B (1998) Alkylating properties of antimalarial artemisinin derivatives and synthetic trioxanes when activated by a reduced heme model. Chem Eur J 4: 1287–1296.
49. Laurent SAL, Robert A, Meunier B (2005) C10-Modified Artemisinin derivatives: efficient heme-alkylating agents. Angew Chem Int Ed 44: 2060–2063.
50. Liu WQ, Li YL, Ruppel A (2001) Studies on the activity and immunohistochemistry of heme oxygenase in *Schistosoma japonicum*. Zhongguo Ji Sheng Chong Xue Yu Ji Sheng Chong Bing Za Zhi 19: 84–86. article in Chinese, abstract available in English. To our knowledge, there is no report available in English on heme oxygenase activity in schistosomes.
51. Loup C, Lelièvre J, Benoit-Vical F, Meunier B (2007) Trioxaquines and heme-artemisinin adducts inhibit the *in vitro* formation of hemozoin better than chloroquine. Antimicrob Agents Chemother 51: 3768–3770.
52. Clemens LE, Basch PF (1989) *Schistosoma mansoni*: effect of transferrin and growth factors on development of schistosomula in vitro. J Parasitol 75: 417–421.
53. Smyth DJ, Glanfield A, McManus DP, Hacker E, Blair D, et al. (2006) Two isoforms of a Divalent Metal Transporter (DMT1) in *Schistosoma mansoni* suggest a

surface-associated pathway for iron absorption in schistosomes. J Biol Chem 281: 2242–2248.
54. Hirzmann DJ, Preis D, Symmons P, Kunz W (1992) Ferritins of *Schistosoma mansoni*: sequence comparison and expression in female and male worms. Mol Biochem Parasitol 50: 245–254.
55. Delcroix M, Medzihradski K, Caffrey CR, Fetter RD, McKerrow JH (2007) Proteomic analysis of adult *S. mansoni* gut contents. Mol Biochem Parasitol 154: 95–97.
56. Schüssler P, Pötters E, Winnen R, Bottke W, Kunz W (1995) An isoform of ferritin as a component of protein yolk platelets in *Schistosoma mansoni*. Mol Reprod Dev 41: 325–330.
57. Jones MK, McManus DP, Sivadorai P, Glanfield A, Moertel L, et al. (2007) Tracking the fate of iron in early development of human blood flukes. Int J Biochem Cell Biol 39: 1646–1658.
58. Glanfield A, McManus DP, Anderson GJ, Jones MK (2007) Pumping iron: a potential target for novel therapeutics against schistosomes. Trends Parasitol 23: 583–588.
59. Tang LF, Yi XY, Zeng XF, Wang LQ, Zhang SK (2004) *Schistosoma japonicum*: isolation and identification of peptide mimicking ferritin epitopes from phage display library. Acta Biochim Biophys Sinica 36: 206–210.

Genome Biology

RESEARCH Open Access

Chromatin structural changes around satellite repeats on the female sex chromosome in *Schistosoma mansoni* and their possible role in sex chromosome emergence

Julie MJ Lepesant[1*], Céline Cosseau[1], Jérome Boissier[1], Michael Freitag[2], Julien Portela[1], Déborah Climent[1], Cécile Perrin[1], Adhemar Zerlotini[3] and Christoph Grunau[1]

Abstract

Background: In the leuphotrochozoan parasitic platyhelminth *Schistosoma mansoni*, male individuals are homogametic (ZZ) whereas females are heterogametic (ZW). To elucidate the mechanisms that led to the emergence of sex chromosomes, we compared the genomic sequence and the chromatin structure of male and female individuals. As for many eukaryotes, the lower estimate for the repeat content is 40%, with an unknown proportion of domesticated repeats. We used massive sequencing to *de novo* assemble all repeats, and identify unambiguously Z-specific, W-specific and pseudoautosomal regions of the *S. mansoni* sex chromosomes.

Results: We show that 70 to 90% of *S. mansoni* W and Z are pseudoautosomal. No female-specific gene could be identified. Instead, the W-specific region is composed almost entirely of 36 satellite repeat families, of which 33 were previously unknown. Transcription and chromatin status of female-specific repeats are stage-specific: for those repeats that are transcribed, transcription is restricted to the larval stages lacking sexual dimorphism. In contrast, in the sexually dimorphic adult stage of the life cycle, no transcription occurs. In addition, the euchromatic character of histone modifications around the W-specific repeats decreases during the life cycle. Recombination repression occurs in this region even if homologous sequences are present on both the Z and W chromosomes.

Conclusion: Our study provides for the first time evidence for the hypothesis that, at least in organisms with a ZW type of sex chromosomes, repeat-induced chromatin structure changes could indeed be the initial event in sex chromosome emergence.

Background

The origin and evolution of sexuality is one of the most fascinating topics in evolutionary biology. Sex can be determined by several mechanisms, such as environmental stimuli (environmental sex determination) or genetic differences between males and females (genetic sex determination). Genetic sex determination is mainly based on the acquisition of sex chromosomes, a more stable strategy than environmental determinism, especially when the environment becomes variable. The principle steps leading to the emergence and evolution of sex chromosomes have been proposed by Charlesworth *et al.* [1] and Rice [2]. In this model, the emergence of a locus with female fertility and male sterility and another locus with male fertility and female sterility led to the establishment of a small sex-determining region on ordinary autosomes in hermaphrodite ancestors. These so-called proto-sex chromosomes are hardly distinguishable. To prevent the production of infertile individuals, recombination of these loci becomes restricted [3,4]. This crucial step is intensively debated and two mechanisms of action have been proposed: (i) structural changes by translocation or inversion (reviewed in [5]); or (ii) chromatin status changes involving heterochromatization of the heterosexual chromosome [4,6-9]. Heterochromatization of the sex-determining region has been shown in species with

[1]Université de Perpignan Via Domitia, CNRS, UMR 5244 Ecologie et Evolution des Interactions (2EI), 52 Avenue Paul Alduy, 66860 Perpignan Cedex, France
Full list of author information is available at the end of the article

primitive or nascent sex chromosomes, such as in papaya or tilapia (reviewed in [10]). The suppression of recombination between the heterochromosome and its homologue would trigger gradual degradation of the heterochromosome (Y in XY systems, or W in WZ systems) because genes that are not essential for males (in XY systems) or females (in WZ systems) show accelerated rates of mutation and deletion. Consequently, the heterochromosome becomes progressively gene-poor (for example, [11]) and in the extreme case the degradation process can lead to the complete loss of the heterochromosome (for example, [12]).

We decided to investigate the role of chromatin structural changes in sex chromosome emergence by using a basal metazoan species harboring a ZW system, the acoelomate *Schistosoma mansoni*. Schistosomes are parasitic plathyhelminthes that are responsible for schistosomiasis (bilharziosis), an important parasitic human disease ranking second only to malaria in terms of parasite-induced human morbidity and mortality [13]. *S. mansoni*'s life cycle is characterized by passage through two obligatory hosts: the fresh-water snail *Biomphalaria glabrata* (or other *Biomphalaria* species, dependent on the geographical location), for the asexual stage; and human or rodents for the sexual adult stage. The sex of the parasite is determined in the eggs (syngamic determination). Eggs are excreted with the host feces and free-swimming larvae (miracidia) are released when the eggs come into contact with water. These miracidiae infect the freshwater mollusk host and transform into primary and secondary sporocysts. Finally, a third larval stage, the cercariae, capable of infecting the vertebrate host, is released into the water. Once in the human or rodent host, morphological differences between female and male adults develop, and these then mate and produce eggs. In the larval stages, schistosome males and females are genetically different but morphologically identical; the sexual dimorphism (that is, the phenotypic expression of sex differentiation) is restricted to the adult stage. All stages are experimentally accessible, which allows the study of chromatin structural modifications for all stages of the life cycle.

Analysis of metaphase spreads indicates that sex is determined in schistosomes by sex chromosomes, with female being the heterogametic sex (ZW) and male the homogametic sex (ZZ) [14]. In some schistosoma species, there is a clear size difference between W and Z, while in other species, such as *S. mansoni*, discrimination is solely based on chromatin structure [15]. This makes *S. mansoni* a model of choice to study the involvement of chromatin structural changes in sex determination of a model harboring a ZW system. In addition, and in contrast with most other plathyhelminth species, schistosomes are gonochoric [16]. This suggests that, in general, being hermaphrodite is an advantage in this phylum, probably through minimizing the risk that is associated with finding a mate inside the host [17]. In Schistosomatidae, the acquisition of separated sexes was concomitant with the invasion of warm-blooded animals [16]. This could be explained by the benefit that genetic diversity provides against the sophisticated immune system of warm-blooded vertebrate hosts and/or by the specialization of each gender for a limited set of 'domestic tasks' [16,18,19]. This particular feature of schistosomes in the plathyhelminth phylum provides the opportunity to study sex chromosome emergence.

The genome of *S. mansoni* was sequenced and initially only partially assembled (version 3.1 with 19,022 scaffolds) [20]. During the preparation of this manuscript, an improved version with assembly at the chromosome level became available (version 5.2 with 882 scaffolds) [21], and Criscione *et al.* [22] constructed a linkage map for 210 version 3.1 scaffolds using microsatellite markers. They identified eight linkage groups corresponding to the seven autosomes and one sex chromosome [22], indicating that the sex chromosomes recombine. Nevertheless, Criscione *et al.* discovered a small region of roughly 18 Mb on the sex chromosome that shows recombination repression. Several open questions remain to be answered. First, it is not clear what are the genetic differences between W and Z chromosomes of *S. mansoni*, or in other words, what are the W- and what are the Z-specific sequences. Second, the mechanism of recombination repression between *S. mansoni* sex chromosomes is not clear. As outlined above, either inversion events or heterochromatization [7,9,23] have been proposed for other species. The specific objectives of the present study were to determine what the sex-specific DNA sequences of *S. mansoni* are, and how heterochromatization of the W chromosome might be initiated. We present here evidence that *S. mansoni* sex chromosomes contain large pseudoautosomal regions. Outside these regions, Z-specific sequences are composed of unique sequences and interspersed repeats. W-specific sequences are almost entirely composed of satellite-type repeats located in the heterochromatic region of the W chromosome. While no female-specific gene could be identified, many of the female repeats are transcribed in the larval stages of the parasite but never in the adults. This loss of transcriptional activity and the development into adults is accompanied by chromatin structural changes around the W-specific repeats. We develop a model in which female-specific repeats are expressed to induce a change in chromatin structure of the W chromosome specifically in the sexual part of the life cycle, leading to functional heterogametism.

Results

The *S. mansoni* sex chromosomes Z and W share large pseudoautosomal regions

We had previously sequenced genomic DNA of female and male *S. mansoni* individuals of the DFO strain using Illumina sequencing (National Center for Biotechnology Information Sequence Read Archive (NCBI SRA) submission number SRA012151). We aligned the 8,600,198 sequences from the male samples and the 9,355,380 sequences from the female samples to the 19,022 known scaffolds of the *S. mansoni* genome assembly using SOAP. We then calculated for each scaffold the ratio between sequences that match with the scaffold in question ('hit') for the male and the female DNA. The rationale behind this approach was that, in males (ZZ), Z-specific scaffolds should show two times higher hit counts than in females (WZ). We searched for scaffolds with at least 10 hits per 1 kb in the female and the male genome, at least 10 kb in length, and a male/female hit-count ratio ≥1.68. Using these parameters we identified 15 scaffolds spanning 6,436,718 bp (roughly 10% of the estimated size of the sex chromosomes [22]). We consider these scaffolds (Smp_scaff000398, Smp_scaff018906, Smp_scaff000301, Smp_scaff001995, Smp_scaff000218, Smp_scaff000465, Smp_scaff000514, Smp_scaff000425, Smp_scaff001883, Smp_scaff001948, Smp_scaff000059, Smp_scaff000044, Smp_scaff000576, Smp_scaff000019, Smp_scaff018900) to be specific for the Z chromosome. We confirmed these *in silico* results for representative regions in a subset of 13 arbitrarily chosen scaffolds (5 Z-specific and 8 pseudoautosomal) by quantitative PCR (qPCR; Table 1). With the exception of one scaffold (Smp_scaff000120), qPCR confirmed next generation sequencing hit-count ratios. When the working draft of the fully assembled sequence W/Z chromosome became available [21], we repeated the SOAP alignment. In this new assembly, Smp_scaff000019 was placed on chromosome 2. We showed before [24] that at least 105 scaffolds (436,269 bp) were specific for the W chromosome in females (male DNA did not align to these scaffolds). In conclusion, in genome assembly version 3.1 more than 90% of the non-repetitive part of the Z chromosome and the W chromosome are identical (pseudoautosomal). In version 5.2, the pseudoautosomal region spans 70% of the assembled W/Z chromosome.

Table 1 Comparison of the ratio of relative amounts of genomic DNA in male and female adults of *S. mansoni*

	Male (ZZ)/female (WZ)	
Scaffold	NGS hit-count ratio	qPCR ratio
Smp_scaff000059	1.76	2.00 ± 0.15
Smp_scaff000425	1.82	1.76 ± 0.11 (region 1)
Smp_scaff000425	1.82	1.83 ± 0.11 (region 2)
Smp_scaff000012	1.3	1.61 ± 0.03
Smp_scaff000047	1.06	0.87 ± 0.04 (region 1)
Smp_scaff000047	1.06	0.87 ± 0.12 (region 2)
Smp_scaff000074	1.02	0.87 ± 0.06 (region 1)
Smp_scaff000074	1.02	0.99 ± 0.13 (region 2)
Smp_scaff000019	1.69	1.76 ± 0.07
Smp_scaff000120	1.61	1.10 ± 0.08
Smp_scaff000054	0.95	1.04 ± 0.09
Smp_scaff000034	0.94	1.07 ± 0.13
Smp_scaff000050	0.93	0.99 ± 0.21
Smp_scaff000024	0.93	0.95 ± 0.09
Smp_scaff000252	0.95	0.93 ± 0.03
Smp_scaff000264	0.96	0.93 ± 0.02

Relative amounts of genomic DNA in male and female adults of *S. mansoni* were measured by next generation sequencing (NGS) hit counts or qPCR in 13 scaffolds (3 scaffolds were sampled in the 2 different regions, 'region 1' and 'region 2').

The Z-specific region of the Z chromosome is composed of unique sequences and interspersed repeats

The region that is covered by the 15 Z-specific scaffolds contains 205 putative genes (according to the gene predictions in SchistoDB). For 118 genes, a function could be predicted based on sequence similarities (Additional file 1). Among those there are at least four genes that code for proteins that are predicted to be involved in spermatogenesis or for which paralogous genes show testis-specific expression. Nevertheless, for the moment it cannot be concluded that these genes are involved in sex differentiation and further analysis is necessary to clarify the role of these genes. Interspersed repeats were also observed in this genomic region but none of them are Z-specific. The Z-specific region in assembly 3.1 is 6.5 Mb in size. In assembly version 5.2 it spans about 18 Mb and, according to [21], contains 782 genes.

A region on the sex chromosomes with repressed recombination contains Z-specific sequences but also pseudoautosomal sequences

Having identified pseudoautosomal scaffolds and Z- and W-specific sequences, we searched for the location of these sequences on the chromosomes. For the Z-specific scaffolds we explored an existing linkage map for the sex chromosomes [22]. The results are represented in Figure 1. All mapped Z-specific scaffolds are located in a region of the Z-chromosome for which repression of recombination was described. However, this region also contains pseudoautosomal scaffolds with a hit-count ratio of around 1. Consequently, recombination repression in this region is not due only to absence of sister chromatid sequences. This result was confirmed with assembly version 5.2. In this assembly, a block of sequences originally identified as linkage group 8 [22] was inserted at position 20 to 25 Mb. Consequently, this region recombines, but two smaller regions at 12 to 15

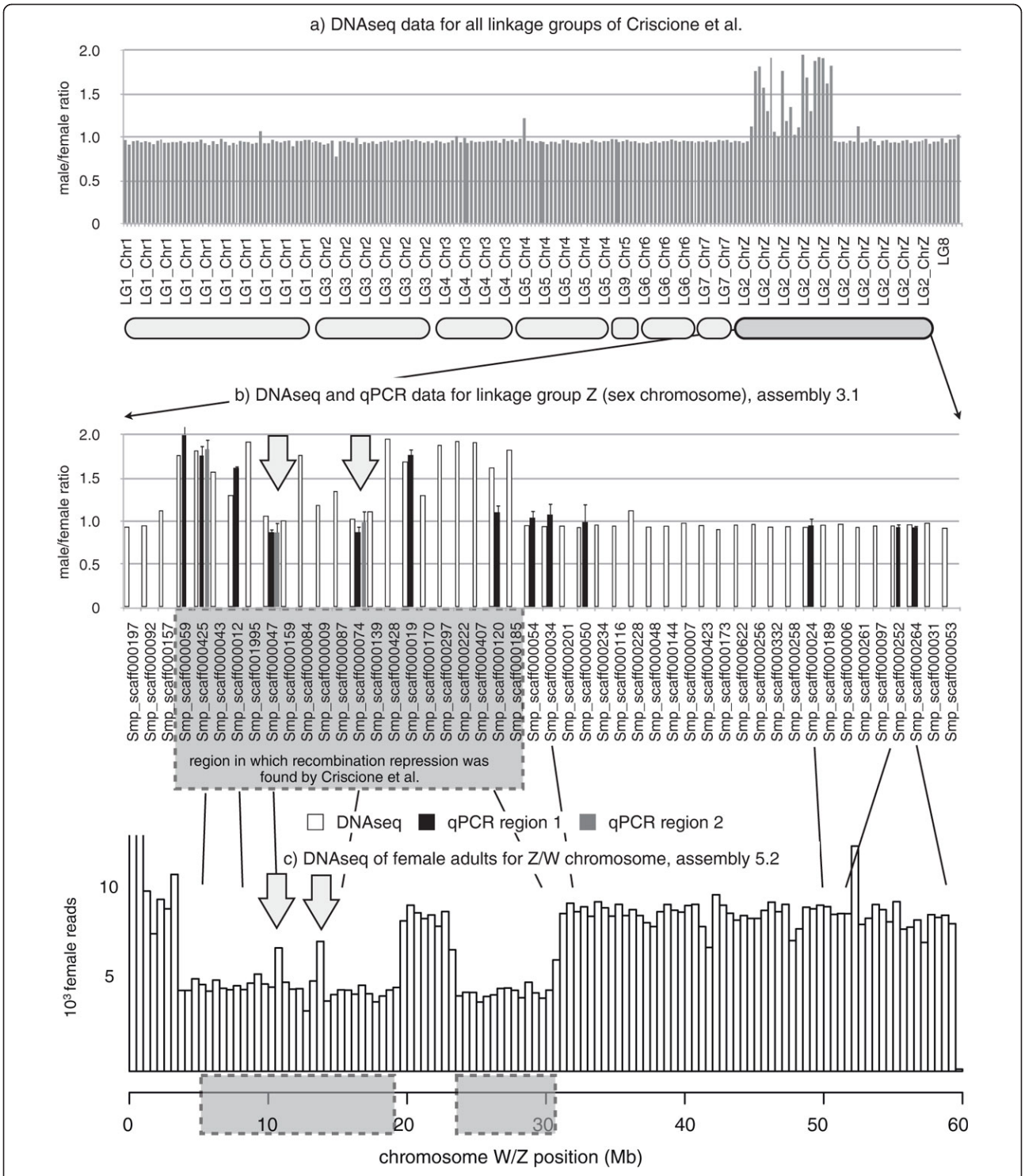

Figure 1 Next generation sequencing hit-count ratios between male and female genomes. **(a)** All scaffolds arranged by Criscione *et al*. [22] in linkage groups. For autosomes, the expected ratio would be 1; for Z-specific scaffolds, the expected ratio would be 2 . Scaffolds are in the order defined by Criscione *et al*. **(b)** Male/female hit-count ratios and qPCR ratios for the Criscione *et al*. linkage group 2 (sex chromosomes). **(c)** Profile of hit counts along the latest version of the sex chromosome [21] for DNA extracted from females. One bar corresponds to 0.5 Mb. Arrows indicate the two pseudoautosomal blocks within the region where recombination is repressed.

Mb are homologous on the Z and W chromosome but recombination repression occurs (Figure 1).

The female-specific region of the W chromosome is composed of repetitive sequences

As mentioned above, in an earlier publication we had shown that at least 105 scaffolds (436,269 bp) are specific for the W chromosome in females. We had also indications that a large part of female-specific sequences are composed of repetitive sequences because they matched to known repeats in a repeat database. Nevertheless, 15 to 19% of the massive sequencing data did not correspond to any of the known scaffolds and repeats [24]. These results suggested that they might relate, at least in part, to unknown repetitive sequences. We therefore *de novo* assembled all massive sequencing reads that did not match with unique sequences in the *S. mansoni* genome. SOAP was used to remove *in silico* all female and male reads that correspond to unique sequences, and velvet in combination with a commercial long read assembler was used to assemble the remaining sequences into 8,594 individual repeat contigs (minimum length 80 bp; maximum length 2,169 bp; average length 168 bp). The minimum length corresponds to the used velvet parameter. We then applied our earlier described whole-genome *in silico* subtractive hybridization (WISH) approach [24] to identify female-specific repeats. Thirty-three new repeat sequences were identified to be specific for the female W chromosome, giving a total of 36 W-specific repeats (combined literature data and our data). Several *in silico* methods were used to classify the repeats and their specificity was confirmed by PCR on male and female individuals (abundant in females, very weak signal or absence of amplification in males). The results are summarized in Table 2. Three repeats were already known, 33 repeats are new. The size of the consensus sequence for each assembled repeat was confirmed by PCR on female and male individuals (Additional files 2 and 3). EST data and RT-PCR show that at least eight repeats are transcribed. For a subset, copy number was estimated by qPCR and is moderate (100 to 400 copies), with the exception of SMAlphafem-1 (several thousand copies, confirming earlier estimations [25]). The copy number was estimated using quantitative DNA with a unique W-specific region on scaffold Smp_scaff018821 as reference (positions 2,194 to 2,312).

We used SchistoDB to identify genes that could be located within the region that is spanned by the repeats. Eight putative genes were identified in the vicinity of the repeats (not more than 5 kb away). Manual inspection of all loci showed that female next generation sequencing hits can be found for four putative genes, and male hits are absent (Smp_186230, Smp_190410, Smp_117150, Smp_117160). However, three genes (Smp_190410, Smp_117150, and Smp_117160) are identical and the predicted coding regions are small (243 bp for Smp_190410, 327 bp for Smp_186230). No significant similarity to known proteins could be found with blastx. Blast against the genome shows that these putative genes are not unique and it remains to be answered whether these sequences are actually transcribed and code proteins.

Female-specific repeats are arranged as large satellite type blocks in the heterochromatic region of chromosome W

To identify the localization of the most abundant female-specific repeats, W1, W3-8 and W13, we used fluorescent *in situ* hybridization (FISH) on late secondary sporocyst metaphases (Figure 2). All studied repeats are (i) arranged as large satellite blocks and (ii) localized in the heterochromatic region of the W chromosome (darker propidium iodide staining), either in the pericentromeric region or on the euchromatin/heterochromatin boundary of the long arm. None of the tested repeats was found on the short arm of chromosome W. Repeats W6 and W7 are specific for the pericentromeric region of the q-arm, and W1 and W4 are located on the frontier of the heterochromatic region. W1 was already known [26] and we confirm the earlier FISH results that localized it to the distal part of the heterochromatic region of Wq [27]. Hirai *et al.* [27] described a euchromatic gap region (eg3) in the vicinity of the W1 chromosome. We did not see this gap, which might be due to the lower resolution of our equipment or differences between the used *S. mansoni* strains. W1 shows genetic instability and in some cases was also found in males [28]. The reason for this could be the close proximity to euchromatin and one might expect such a behavior also for W4. W3, W5 and W8 can be found in both the pericentromeric and the frontier region. W13 is localized roughly in the middle of the heterochromatic part of the q-arm. Results are summarized in Table 2. Copy number estimates (Table 2) correspond to what was found in the literature: 500 to 1,000 copies per genome for W1 [26] and 20,000 to 200,000 for SMAlphafem-1 [25].

Several of the female-specific repeats are transcribed in larvae but not in adults

EST data suggested that some of the repeats could be transcribed and transcription of W1 and SMAlphafem-1 was described for cercaria [29]. We extracted RNA from different life cycle stages and quantified the transcription level for repeats W3, W4, W5 and SMAlphafem-1. For repeats W3 we did not find significant transcription above background; however, repeats W4, W5 and SMAlphafem-1 are transcribed in the larval stages. No transcripts could be detected in adult couples or

Table 2 W-chromosome-specific repeats of *S. mansoni*

GenBank accession number	Name	Length (bp)	Percentage female hits	Repeat family[a]	Transcription evidence	FISH localization	Copy number estimate[b]	Reference
U12442	SMAlphafem-1	338	99.86	SMAlpha retroposon	RT-PCR	p-arm	60,000 - 70,000	[61,62]
J04665	W1	482	100	Retro		Middle of q-arm at frontier between heterochromatin and euchromatin as satellite, middle of q-arm	500	[26,27]
U10109	W2	715	100				400	[62]
HQ880214	W3	786	100	LTR, highly similar to W2, highly similar to R = 407	No transcription (RT-PCR)	As satellite in the middle of q-arm at frontier between heterochromatin and euchromatin or also in the pericentromeric region	200	
HQ880209	W4	1132	99.52	Highly similar to R = 879	RT-PCR	Same location as W1	800	
HQ880217	W5	1129	99.27	LTR, similar to Perere-2, identical to R = 564	EST and RT-PCR	Either at the frontier of heterochromatin and euchromatin of the q-arm or in the pericentromeric region, or at both locations		
HQ880215	W6	310	99.88	Retro	EST	In the pericentromeric region		
HQ880210	W7	1000	100	DNA transposon, 97% identical to GenBank accession number XP_002570219 (hypothetical protein Smp_186230)		In the pericentromeric region		
HQ880218	W8	266	99.97	Tandem repeat (previously described as TR266), DNA transposon		Either at the frontier of heterochromatin and euchromatin of the q-arm or in the pericentromeric region		
HQ880211	W9	803	100	LINE2, similar to SjR2 retrotransposon	EST			
HQ880212	W10	682	100	LTR				
HQ880213	W11	376	100	LINE, similar to R = 170				
HQ880216	W12	264	100	Retro, 97 to 100% identical to several hypothetical S.m. proteins				
HQ880219	W13	258	100	Retro		In the middle of the heterochromatic part of the q-arm as satellite		
HQ880220	W14	209	100	DNA transposon, similar to R = 170				
HQ880221	W15	185	96.62	DNA transposon				
HQ880222	W16	164	100	Similar to R = 116				
HQ880223	W17	160	100	LTR				
HQ880224	W18	160	100	LTR	EST			
HQ880225	W19	139	100	Retro, 100% identical to GenBank accession number XP_002569391 (hypothetical protein Smp_181820)	EST			
HQ880226	W20	138	100					
HQ880227	W21	138	99.84	DNA transposon, similar to R = 116				
HQ880228	W22	132	100	DNA transposon				
HQ880229	W23	125	100	DNA transposon				

Table 2 W-chromosome-specific repeats of *S. mansoni* (Continued)

HQ880230	W24	115	99.56	Retro, similar to Sh122 repeat and R = 31	
HQ880231	W25	112	99.65	LTR	
HQ880232	W26	111	100	DNA transposon	
HQ880233	W27	110	100	DNA transposon, similar to R = 133 and Sh microsatellite C2	
HQ880234	W28	108	100	Similar to Sh microsatellite C140	
HQ880235	W29	97	100	Similar to Sb Sbov20 repeat	
HQ880236	W30	96	99.05	LTR	
HQ880237	W31	92	100	LTR	
HQ880238	W32	89	96.88	DNA transposon	
HQ880239	W33	86	99.86	LTR	
HQ880240	W34	82	100	DNA transposon	
HQ880241	W35	80	100	Retro	EST

Because of the WZ-type chromosome set of females, these repeats are female-specific. [a]Combined Censor, Blast, Teclass results. [b]qPCR based. LINE, long interspersed element; LTR, long terminal repeat.

immature females (Figure 3). At the genomic DNA level, we observed ≤20% differences in repeat copy numbers (measured by qPCR) between different biological samples, but we did not observe a decrease in copy number, that is, shrinking of repeats, during the life cycle. Absence of transcription in adults is not, therefore, due to absence of repeats in the genome.

The chromatin structure around the female-specific repeats changes during the life cycle

Repeat transcription has been linked to chromatin structural changes [30]. We therefore analyzed histone isoforms that could potentially be associated with the female-specific repeats. Chromatin immunoprecipitation followed by massive sequencing (ChIP-Seq) was used to analyze the

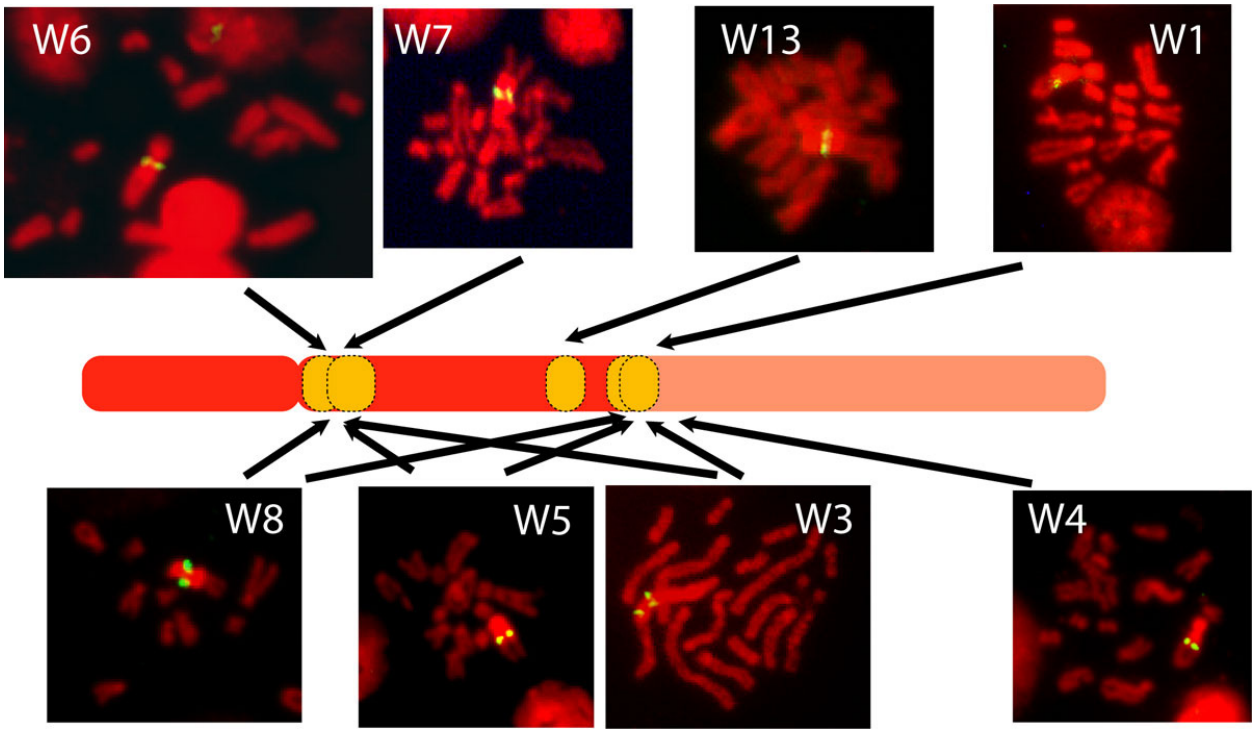

Figure 2 FISH results with representative pictures of metaphase spreads (chromosomes stained with propidium iodide, probes labeled with fluorescein isothiocyanate, pictures taken separately, colorized and overlaid). The positions are indicated on a schematic representation of the W chromosome. The heterochromatic region of the chromosome is in dark red.

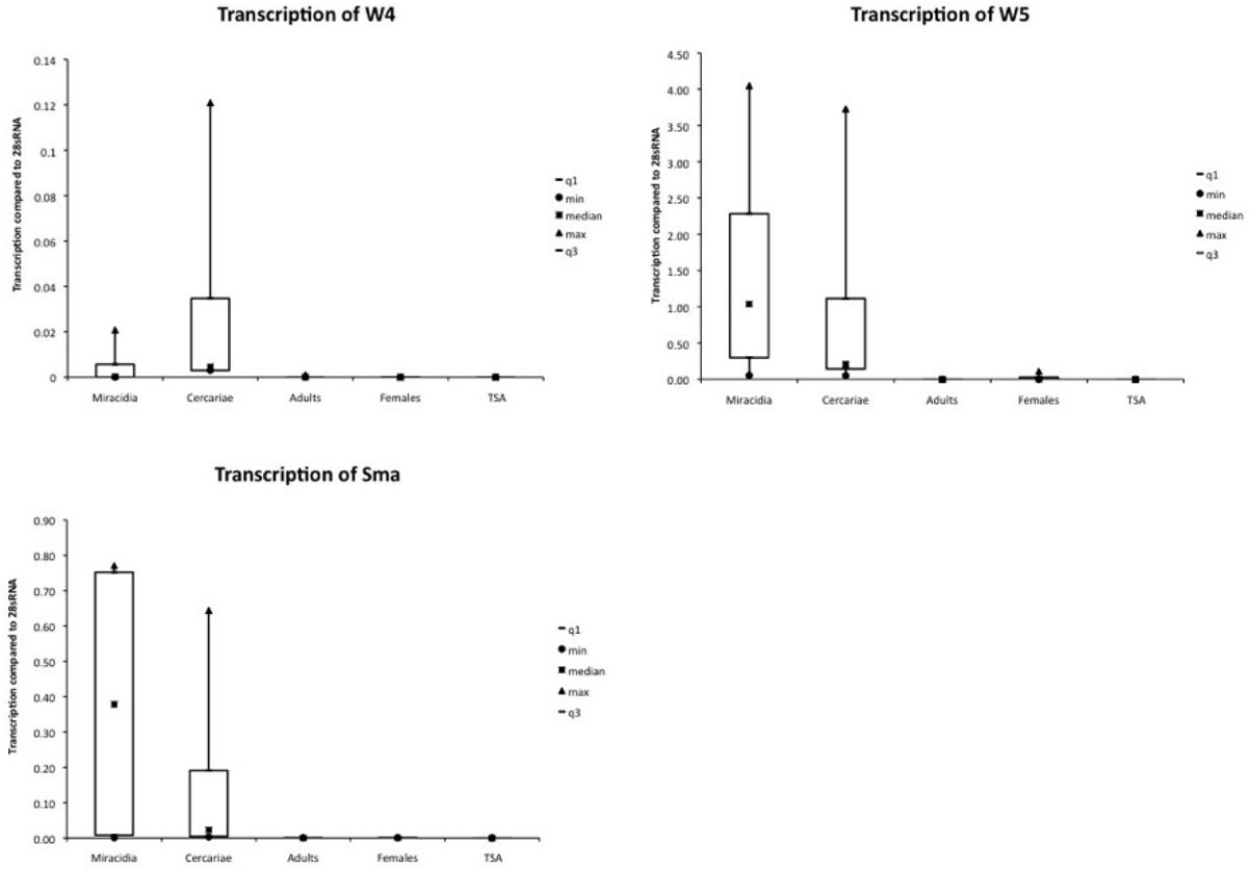

Figure 3 Transcription levels for repetitive sequences SMAlphafem-1 (Sma), W4 and W5. Transcription was calculated as a ratio to 28S RNA. Experiments were repeated three to five times for each sample. Maximum, triangle; minimum, circle; quantil 2 to 4, large rectangle.

abundance of acetylated histone H3K9 (H3K9Ac) around the repeats in miracidia, cercariae and adult couples. All 36 female-specific repeats show a characteristic gradual decrease in H3K9 acetylation level from the larval stages to the adult stages. Among the total of 8,594 repeats in the genome, only 1,113 repeats show such a gradual decrease in H3K9 acetylation. The probability that such a pattern could be observed by chance for all 36 W-specific repeats is negligible (the individual term binomial distribution probability is 1.1^{-32}). To verify the ChIP-Seq data by ChIP combined with qPCR, we focused on two transcribed repeats (W4 and W5) and one non-transcribed repeat (W3). We used antibodies against H3K9Ac, tri-methylated H3K4 (H3K4Me3) that are characteristic for actively transcribed euchromatin, and the heterochromatin markers tri-methylated H3K9 (H3K9Me3), and tri-methylated H3K27 (H3K27Me3). A region in the body of the alpha-tubulin gene was used as reference for calculating the relative amount of immunoprecipitated DNA. The results are shown in Figure 4. Both euchromatic markers (H3K9Ac and H3K4Me3) are enriched at the repeats in the miracidia stages where transcription was observed. In contrast, there are much fewer euchromatic markers around the repeats in adults. In the qPCR-based experiments, cercariae occupy an intermediate position. Based on the combined ChIP-seq and ChIP-qPCR data, we conclude a clear decrease in H3K9 acetylation from miracidia to cercaria and adults. Also, the abundance of the second euchromatic marker, methylation of H3K4, decreases from miracidia to cercaria and remains constant during the development into adults. The heterochromatic markers H3K9Me3 and H3K27Me3 are abundant in cercaria but low in miracidia and adults. In summary, around the female-specific repeats we observed three distinct types of chromatin structure in the three different life-cycle stages: in miracidia the repeats are clearly euchromatic, in cercaria a large proportion is heterochromatic, and in adults we can find a peculiar chromatin structure without classical euchromatic or heterochromatic markers, but associated with transcriptional silence.

Histone deacetylase inhibition does not induce transcription of W-specific repeats in adults

We tested whether the observed changes in chromatin structure are a result or the cause of the changes in

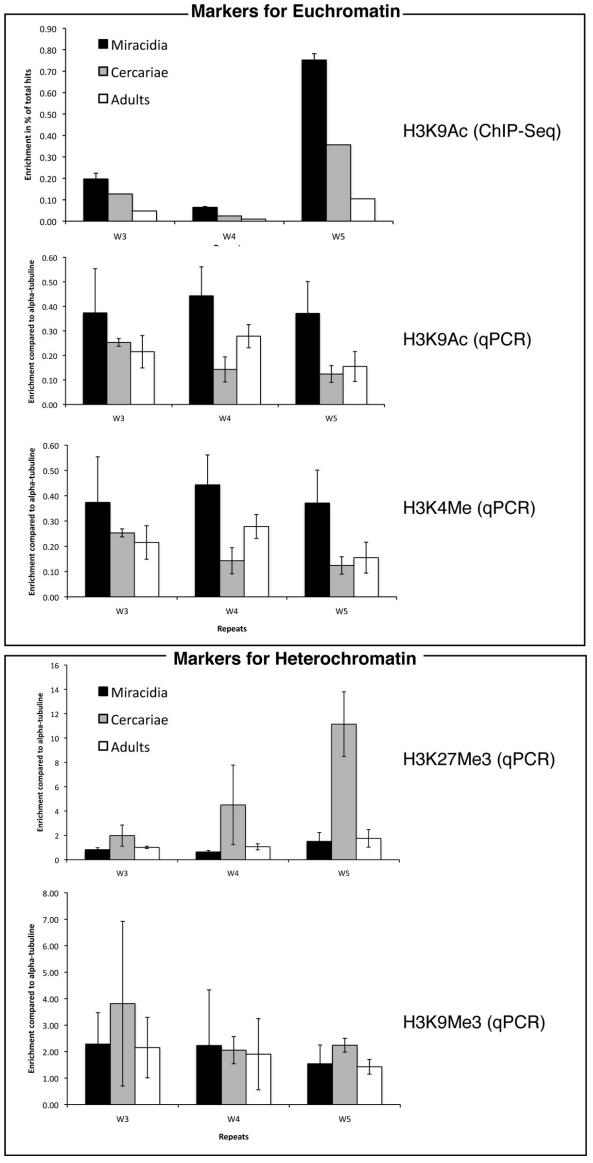

Figure 4 Chromatin structural changes around female-specific repeats W3, W4 and W5 during the life cycle of *S. mansoni* from miracidia (black) to cercariae (grey) and adult couples (white). Measured by ChIP-Seq (upper panel) and ChIP-qPCR (all other panels). Average of three independent ChIP-qPCR experiments, two ChIP-Seq experiments for miracidia and a single ChIP-Seq experiment for cercariae and adults.

transcription. If hypoacetylation of histones were the cause of transcriptional inactivation, then inactivation of histone deacetylase would relieve repression. On the other hand, if transcription of repeats is the origin of chromatin structural changes, inhibition treatment should not lead to detectable changes in transcription because each transcriptional increase would reinforce deacetylation and counteract the inhibition. We treated adult parasites with trichostatin A (TSA), an inhibitor of histone deacetylases at increasing concentrations *in vitro*. After 2 hours of treatment with ≥20 μM TSA, mobility changes were observed (worms first straightened up and ceased moving, and convulsive movements were observed at higher concentrations and longer incubation times (Additional file 4)). We then measured the transcription levels for repeats W4, W5 and Sm-alpha-female at 20 μM TSA and for 4 hours. In none of the cases was transcription activated. In contrast, an increase of transcription of retrotransposons Perere3 and Saci7, used as control, was observed (by 45 and 23%, respectively). The lactate dehydrogenase test shows no difference in cytotoxicity between TSA-treated and mock-treated worms.

Discussion

Despite tremendous advancements in the past, the elements that are responsible for the establishment of sex chromosomes remain still enigmatic. According to Müller's ratchet model, sexual reproduction evolved because deleterious mutations could be eliminated by recombination between the parental autosomes [31]. To maintain isolation of two different sexes, recombination must, however, be repressed (at least partially) between the sex chromosomes. Zones in which recombination is repressed between sex chromosomes were meanwhile identified in many species. Accumulation of repeats on the heterogametic sex chromosome was also found in many examples, although their role is unknown and many authors still consider them as junk DNA. The view that repetitive DNA is non-functional was challenged by the discovery of transcription from repeats on autosomes and the production of small RNA that could be related to heterochromatization events [32]. The presence of large heterochromatic blocks is also a common feature of sex chromosomes. So far, these observations were made in isolation from each other, and generally in different species, which makes the construction of a hypothetical model difficult. Here we present for the first time a comprehensive analysis of sequence composition, gene and repeat content, chromatin structure and repeat transcription of the sex-specific chromosome regions of the Z and W chromosomes of our biological model *S. mansoni*. Recombination repression has been described before in this region of interest [22]. Our data, in relation to previous reports, allows the current models for the suite of events that led to sex chromosome differentiation in *S. mansoni* to be refined and could represent a general model for this process in species with genetic sex determination of the Z/W type.

Z- and W-specific sequences

Criscione *et al.* [22] identified a region of 20 scaffolds in which recombination repression was observed and

suggested that these are Z-specific sequences. We indeed found a male/female sequence reads hit and/or qPCR ratio of ≥1.5 for 13 of these scaffolds, indicating an overrepresentation in the male genome. However, seven scaffolds in this region showed no disequilibrium of hit counts and/or qPCR between males and females (male/female hit ratio ≤1.4), that is, the sequences are not specific to the Z chromosome (Figure 1). In other words, recombination is repressed but the homologous sequences on the sister chromosomes are still present. We find at least two blocks of sequences that are shared between the Z and W chromosome located in the large region with recombination repression. This result was confirmed with the most recent version of the genome assembly. We see three possible conclusions that can be drawn from our results. Either the Z/W sequence blocks are inverted, and additionally or alternatively the sequences are heterochromatic, thus preventing recombination. It is also possible that the scaffolds in the original assembly of the *S. mansoni* genome were chimeric. Indeed, of the 48 scaffolds originally found in linkage group Z/W [22], 4 are on other chromosomes in the 5.2 assembly. It will be difficult to formally exclude the possibility that our results are due to misassembly.

We did not find any paralogues to sex determination genes among the predicted genes on the Z-specific scaffolds. The specific region of the W chromosome is largely composed of large satellite blocks of at least 36 different W-specific repeats. These repeats are abundant on the W chromosome but our PCR analysis on different male individuals indicates that these sequences can also sometimes be found on other chromosomes. The strength of the PCR signal suggests, however, that they are present in very low copy number there. Analysis of the genomic sequence shows that they can occur intermingled with other repeats on autosomal scaffolds as individual sequences or as small blocks of up to five repeats in tandem. Our understanding of these results is that these repeats exist as large satellite blocks on the W chromosome but can occasionally be transferred to autosomes by a so far unknown mechanism. Such a behavior was described for W1 [28] and could depend on the chromatin structure around the repeats and/or flanking regions. Several of these W-specific repeats are transcribed in the miracidia and cercariae stages but never in the adults.

Role of W-specific repeats

In most species that possess sex chromosomes of the Y or W type it was found that (i) repetitive sequences accumulate on these chromosomes, (ii) large regions are heterochromatic and (iii) these chromosomes deteriorate or are completely absent in the extreme case. We show that the W chromosome in *S. mansoni* is no exception to this rule. What is unknown, however, is the suite of events in the evolution of sex chromosomes and the role of the different elements in sex determination. We believe our present study sheds some light on this matter. Heterochromatization of the W chromosome in schistosomes has been known for a long time and has been even used as a marker for sex identification in morphologically indistinguishable cercariae [14,15,33]. Based on cytogenetic analysis, some authors argued that heterochromatization of the W starts in miracidia [14]. Since it is impossible to determine chromosome banding in miracidia and then reuse the larvae for infection and production of adults, these results are difficult to verify. Our results clearly show that the repeats that are located in the W heterochromatic region carry a euchromatic signature in miracidia and lose their euchromatic character progressively during the development into adults. This process is accompanied by a decrease of transcription until complete silencing of the repeats in the sexually mature adult stage. During the miracidia to cercaria transition - that is, precisely when sexual dimorphism starts to develop - the repeats heterochromatize. Sex-specific repeats are found in many species [34-36]. In some cases transcription has been described and it was suspected that these repeats play a role in the sex determination process [37,38]. The transcription of repetitive elements of the satellite type in *S. mansoni* is particularly interesting in the light of the recent discovery of stage-dependent expression of the elements that constitute the RNA interference (RNAi) pathway in schistosomes [39,40]. In many organisms RNAi and chromatin structural changes are linked [32,41-43] and it is tempting to speculate that transcription of W-specific repeats is actually the origin of chromatin compaction on the W chromosome during the life cycle. A hypothetical scheme is shown in *Figure* 5. In our model, reset of the repeat chromatin structure occurs during early embryogenesis (formation of miracidia). In the miracidia, repeats are euchromatic and several of them are transcribed. Transcripts are processed through a pathway that has similarity to RNAi and a hypothetical repeat-induced silencing complex is formed that induces the formation of heterochromatin around the repeats. At this stage, miracidia have infected the mollusk host and develop via sporocyst stages into cercaria. In cercaria, most of the repeats are heterochromatic and not transcribed. We hypothesize that the heterochromatization extends beyond the repeat frontiers and that nearby loci are silenced. If a sex determination locus is found among these loci, the heterochromatization would lead to a dose effect that could be the origin of the formation of the female adult phenotype. Once the task of silencing this locus in *cis* (or *trans*) is accomplished, repeats are not anymore transcribed and the chromatin

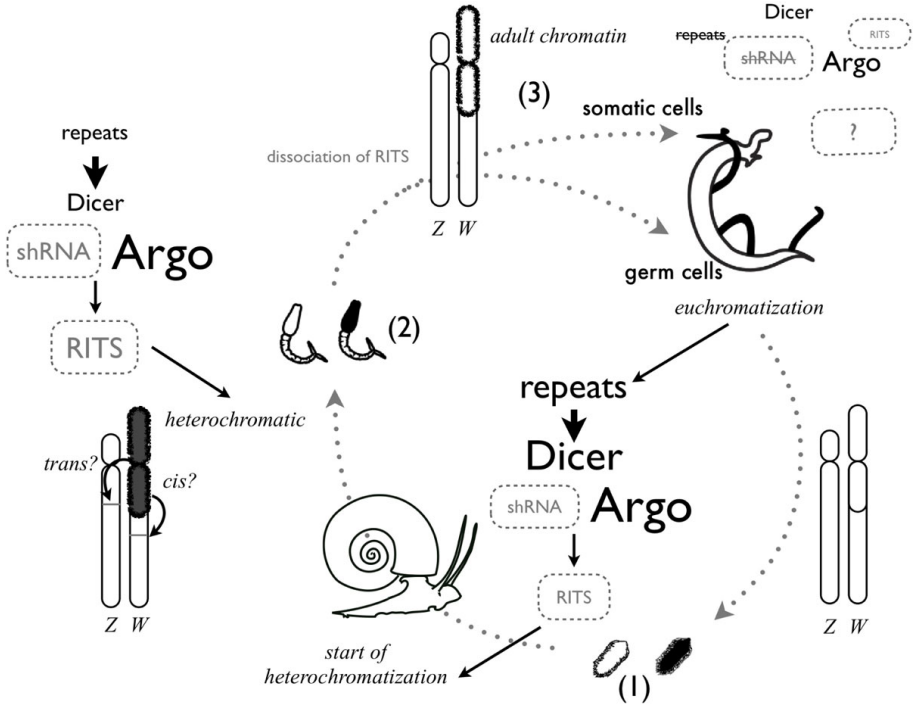

Figure 5 Hypothetical model of the relationship between W-specific repeat transcription and heterochromatin formation. In black, experimentally confirmed situation; in grey, hypothetical elements. Letter size corresponds to relative strength of the phenomenon. (1) Miracidia do not show sex dimorphism. The W chromosome is euchromatic and repeats are transcribed. Large amounts of Dicer and Argonaute proteins are present [39,40,58]. Dicer could produce small heterochromatic RNA (shRNA) that could bind to Argonauts and could build a RITS (RNA-induced initiation of transcriptional gene silencing) complex similar to those in yeast [42] that initiates heterochromatization around the repeat region of the W chromosome. (2) After infection of the snail host, cercariae are produced. Also, these larvae do not show sex dimorphism. Repeats are still transcribed but transcription of Dicer has decreased [39]. Accumulation of RITS complex around the repeat region progressively leads the loss of its euchromatic character. Finally (3), in dimorphic adults, the repeat region becomes transcriptionally inactive, and heterochromatin is maybe locked by HP1 or related chromatin proteins such as KDM2A [59], or a second histone modification mark is missing [60]. Dicer and Argonaut are less abundant. RITS is no longer necessary. Sexual reproduction occurs during this stage. Recombination is repressed by non-permissive chromatin. Late in germ cell production or during embryogenesis, erasure of chromatin marks occurs (epigenetic reset). The cycle restarts with a euchromatic W chromosome.

structure of the pericentromeric W chromosome is fixed into an unknown but transcriptionally silent configuration. We can only speculate about the proteins that are involved since our data indicate that neither the euchromatic markers H3K9Ac and H3K4Me3 nor the heterochromatic markers H3K9Me3 and H3K27Me3 are abundant. This model is supported by our finding that *in vitro* treatment of adults does not lead to detectable transcription from the W-specific repeats while autosomal retrotransposons can be activated.

One could argue that the function of repeat-induced silencing is purely defensive and down-regulates retrotransposon expression in general. Such a mechanism was described as the repeat-associated small interfering RNA (rasiRNA)-mediated pathway [44] in *Drosophila* ovary cells and is believed to protect the (female) germ line from transposable elements. If this were the case for *S. mansoni*, transcription should be observed in the ovary. Our data do not support this view.

Conclusions

Most authors agree that suppression of recombination is an initial event in sex chromosome emergence, although it is not clear by what mechanism it is caused. Chromosome rearrangements (for example, inversions) or the action of modifier genes have been proposed (reviewed, for example, in [45]). Other authors see conformation differences (chromatin structural changes, differences in replication timing) as the origin for recombination inhibition [3,5]. Accumulation of repeats is a general feature of Y/W-type chromosomes. Some consider it an important feature with unknown function [36], while others see repeat accumulation as the result of recombination suppression [1] or solely as a genome defense mechanism [7], placing it late in the suite of events that characterize evolution of sex chromosomes.

With the present work we contribute two new elements that allow us to exclude some of the current hypotheses and to refine others. First, we show that the

presence of satellite repeats on the W chromosome does not lead in all life cycle stages to heterochromatization. Consequently, it is not their presence itself that induces the heterochromatin formation. We show that all W-specific repeats are euchromatic in the miracida stage. Our ChIP-Seq data tell us that this is not a general feature of autosomal and pseudoautosomal repeats, but specific for the W-specific satellites. Second, we demonstrate that the euchromatization occurs concomitantly with transcription and that transcription always precedes heterochromatization.

Based on these findings, we propose two not necessarily exclusive scenarios for the emergence of sex chromosomes. In the first model, transcription of non-coding RNA from repetitive DNA elements was the initial event in sex chromosome evolution of schistosomes. Non-coding RNA would have induced heterochromatization and suppression of recombination. Both favored expansion of repeats and organization in large blocks (satellites). Satellite expansion would have reinforced the system and led finally to the beginning of genetic changes in the W chromosome. The very basal phylogenetic position of leuphotrochozoans such as *S. mansoni* permits a general model for the main stages of sex chromosome evolution to be proposed: the establishment of a sex-determining region, recruitment of repeats for production of non-coding RNA, RNA-directed heterochromatization and repeat expansion, local suppression of recombination, and shrinkage of the chromosome by deletion.

In the second model, a small mutation and/or local heterochromatization could have been the initial event, leading to recombination repression in the first place. Repetitive DNA accumulated subsequently. During germ cell formation or during early embryogenesis euchromatization occurs. Cytogenetic evidence in other species in which the female is the heterogametic sex shows that the W chromosome is often condensed in somatic cells, and becomes euchromatic in early oocytes (reviewed in [46]). This releases transcription repression and repeats are transcribed, leading subsequently to heterochromatization. Our preliminary data suggest that chromatin structural changes do not occur in *trans* - that is, not on the Z chromosome but on the adjacent regions of the W chromosome (not shown).

We cannot formally exclude that sex determination is based on a specific protein-coding gene that is absent or present on the W chromosome. But we show that the most pronounced difference in transcription between ZZ and ZW individuals is at the level of 'non-coding' RNA. We therefore favor the hypothesis that sex differentiation in *S. mansoni* is based on developmental stage-dependent tagging of the W chromosome by non-coding RNA and a chromatin marking system. Our model predicts that chromatin structural changes influence transcription of one or several genes in the close vicinity of the core heterochromatic region and that transcriptional activation or inactivation of these leads to morphological and/or physiological changes that are the bases for development of the male and female phenotypes in the adult stage.

Materials and methods

Parasite culture and drug treatment

Eggs were axenically recovered from 60-day infected hamster livers and miracidia were hatched from eggs in 5 ml of spring water over 2 to 3 hours under light. Miracidia were concentrated by sedimentation on ice for 15 minutes. Cercariae were recovered from infected snails (4 weeks post-infection) and collected by pipetting. They were then concentrated by cold centrifugation (4° C) at 1,200 rpm for 5 minutes and the supernatant was removed. Eight-week-old adult worms were recovered by portal perfusion of hamsters with 0.8% (w/v) NaCl and 0.8% (w/v) trisodium citrate [47]. If necessary, miracidia, cercariae and adults were kept at -80°C.

For infection with a single sex, *B. glabrata* snails 4 to 5 mm in diameter were individually exposed to a single miracidium in 5 ml of springwater. The snails were then each isolated and maintained in round, clear plastic containers for 24 hours and kept all together for 5 weeks. Snails were fed fresh lettuce *ad libitum* and the water was maintained at 25°C and changed weekly. The photoperiod during the entire experiment was equilibrated to 12 hours light:12 hours dark [48].

Adults were recovered by portal perfusion of hamsters. Ten individuals were kept in 250 μl RPMI medium (Invitrogen-Gibco, Carlsbad, USA) and treated with an ethanol solution of the histone deacetylase inhibitor TSA (Invitrogen) at different final concentrations (2 μM, 20 μM, 50 μM, 100 μM and 200 μM). To the untreated control, a corresponding volume of ethanol was added. The cytotoxic effect of the drug was measured using the Roche Cytotoxicity Detection Kit (Roche no. 04744926001), which is based on the measurement of lactate dehydrogenase activity released from dead and lysed cells into the supernatant [49]. Behavior was observed every hour until 6.5 hours and after 21 hours of treatment. Individuals were filmed with a conventional numerical camera adapted to a stereomicroscope after 5, 6.5 and 21 hours of treatment.

Sequencing of genomic DNA, alignment, and assembly of repeats

Solexa sequencing was performed at the sequencing facilities of GenomiX Montpellier (France) on a Genome Analyzer II (Illumina) by single end sequencing (36 bp) according to the manufacturer's protocol. The software

SOAP is usually employed to map unique sequences and reject repetitive sequences. We took advantage of this algorithm and used SOAP 2.17 [50], evoking the -u and -r 0 options to split the sequence reads into those corresponding to unique or repetitive sequences. The resulting fasta files of unmapped reads (-u) was assembled with velvet using a coverage cutoff of 4 and a minimum contig length of 80 bp. For a second assembly round Sequencher v4.5 was used with minimum match 93%, minimum overlap 60 bp.

In silico analysis

Velvet-assembled repeats were then used for the whole-genome *in silico* subtractive hybridization (WISH) procedure [24]. This method compares different massive sequencing datasets with a reference genome and identifies sequences that are under-represented in one data set. Censor [51], Teclass [52] and blast [53] were used for repeat annotation.

For identification of genes in the vicinity of W-specific repeats, all repeat sequences were compared to the genome using blast searches of the SchistoDB database [54] and genes 5 kb upstream and downstream of regions containing these repeats were manually analyzed.

Confirmation of sex-specific sequences by PCR

PCRs were carried out in a final volume of 25 μl containing 0.2 μmol of each oligonucleotide primer (Additional file 5), 0.2 mmol of each dNTP (Promega), 0.625 U of GoTaq polymerase (Promega) used with the recommended buffer and completed to the final volume with DNase-free water. The PCR program consisted of an initial denaturation phase at 95°C for 5 minutes followed by 20 cycles at 95°C for 30 s, 60°C for 90 s, 72°C for 30 s and a final extension at 72°C for 5 minutes. The PCR products were separated by electrophoresis through a 2% TBE agarose gel.

FISH on *S. mansoni* metaphases

Metaphase spreads were prepared essentially as described by Hirai and LoVerde [55]. Sporocysts were obtained by dissection of two to three snails, each infected with five miracidia, at 28 to 29 days post-infection. Probes for repetitive DNA were prepared by cloning PCR products (for primers see Additional file 5) on genomic DNA as template into pCR2.1-TOPO (Invitrogen #K4510-20). Clones were sequenced to confirm the repeat assembly, labeled with the BioPrime DNA labeling system (Invitrogen #18094-011) and hybridized as described before [55]. Chromosomes were counterstained with propidium iodide and observed under an epifluorescence microscope (AKIOSKOP 2, Zeiss) equipped with a Leica DC 300 FX digital camera. Between 7 and 34 female metaphases were studied for each repeat.

RNA extraction, cDNA synthesis and qPCR

Total RNA was purified from three independent preparations of larvae and adults. For the larval stages, RNA was extracted from 10,000 miracidia and 10,000 cercariae using 500 μl Trizol (Invitrogen). Fifty adult couples were solubilized in 500 μl Trizol with a MagNA Lyser and Green beads (Roche). RNA was treated with DNase I (Invitrogen) for 15 minutes at 37°C, followed by inhibition of the enzyme for 10 minutes at 65°C. PCR of 28s rDNA was used to test for genomic DNA contaminations. The DNase I treatment was repeated as many times as necessary to eliminate contaminations with genomic DNA. RNA was purified with the QIAGEN RNeasy kit. First strand cDNA was synthesized using 10 μl of the total RNA preparation, in a final volume of 20 μl (10 mM dNTPs, 0.1 M DTT, 40 U RNase out, 0.15 μM random primers) with 200 U of SuperScript II RT (Invitrogen). After reverse transcription, the cDNAs were purified with the PCR clean-up system (Promega) and eluted into 40 μl 10 mM Tris/Cl (ph 7.5). Real-time PCR analyses were performed using the LightCycler 2.0 system (Roche Applied Science) and LightCycler Fast-start DNA Master SYBR Green I kit (Roche Applied Science).

qPCR amplification was done with 2.5 μl of cDNA in a final volume of 10 μl (3 mM $MgCl_2$, 0.5 μM of each primer, 1 μl of master mix). Primers were designed with the LightCycler Probe design software or the primer3plus web based interface [56]. The following protocol was used: denaturation, 95°C 10 minutes; amplification and quantification (40 cycles), 95°C for 10 s, 60°C for 5 s, 72°C for 16 s; melting curve, 60 to 95°C with a heating rate of 0.1 C/s and continuous fluorescence measurement, and a cooling step to 40°C. For each reaction, the crossing point (Ct) was determined using the 'fit point method' of the LightCycler Software 3.3. PCR reactions were done in duplicates and the mean value of Ct was calculated. 28s rRNA was used as an internal control and the amplification of a unique band was verified by electrophoresis through 2% TBE agarose gels for each qPCR product. Primer sequences and expected PCR product size are listed in Additional file 5. For all qPCR, efficiency was at least 1.89.

Chromatin status analysis by ChIP and qPCR

Native ChIP and ChIP-Seq were performed as described before [57]. In brief, antibodies against histone isoforms (Table 3) were used to precipitate chromatin in sporocysts, cercaria and adults. The resulting DNA was analyzed either by ChIP-Seq or qPCR. ChIP-Seq data are available at the NCBI SRA under accessions SRX088545, SRX088544, SRX088543 and SRX087825. For ChIP-Seq

Table 3 Antibodies used for native ChIP (N-ChIP)

Antibody	Host	Product	Lot	Saturating quantity used for N-ChIP[a]
H3K9ac	Rabbit	Upstate, 07-352	DAM16924924	8 μl
H3K4me3	Rabbit	Upstate, 04-745	NG1680351	4 μl
H3K9me3	Rabbit	Abcam, Ab8898	733951	4 μl
H3K27me3	Rabbit	Diagenode, pAb-069-050	A29900242	8 μl

[a]Saturating quantities for H3K9ac and H3K9me3 antibodies were previously determined [56]. Saturating quantities for H3K4me3 and H3K27me3 were determined in this study by a titration experiment (data not shown).

analysis, a repeat pseudogenome was constructed in which each identified repeat sequence occurred only once. Then SOAP2 [50] was used to align roughly 100,000 36-bp reads for miracidia of two strains (GH2 and BRE), cercaria and adult couples (both GH2) to this pseudogenome. Hit counts for each repeat were normalized by the total number of aligned reads and compared for the different stages.

Additional material

Additional file 1: List of male-specific scaffolds with putative genes.

Additional file 2: Video of adult schistosomes treated with TSA at 100 μM. Individuals were filmed with a conventional numerical camera adapted to a stereomicroscope after 5 hours of treatment.

Additional file 3: Video of adult mock-treated schistosomes. Individuals were filmed with a conventional numerical camera adapted to a stereomicroscope after 5 hours of treatment.

Additional file 4: Photographs of ethidium bromide stained PCR products after migration through 2% agarose gels. PCR amplification was used to confirm size and sex-specificity of assembled W-specific repeats. Genomic DNA of two female (F1, F2) and two male individuals (M1, M2) was used as template.

Additional file 5: Primers used in this study.

Abbreviations

bp: base pair; ChIP: chromatin immunoprecipitation; ChIP-qPCR: chromatin immunoprecipitation followed by quantitative PCR; ChIP-Seq: chromatin immunoprecipitation followed by massively parallel sequencing; EST: expressed sequence tag; FISH: fluorescence *in situ* hybridization; H3K27Me3: histone H3 tri-methylated on lysine 27; H3K4Me3: histone H3 tri-methylated on lysine 4; H3K9: histone H3 lysine 9; H3K9Ac: histone H3 acetylated on lysine 9; H3K9Me3: histone H3 tri-methylated on lysine 9; NCBI SRA: Sequence Read Archive at the National Center for Biotechnology Information; PCR: polymerase chain reaction; qPCR: quantitative PCR; RNAi: RNA interference; TSA: trichostatin A.

Acknowledgements

The authors are grateful to the Plant Genome and Development Laboratory (UMR5096) of the University of Perpignan for access to their fluorescence microscope. Anne Rognon, Bernard Dejean and Kristina Smith provided important support. The work received financial support from the CNRS (PostDoc fellowship to CC) and the programs 'Schistophepigen' and 'Monogamix' from the French National Agency for Research (ANR).

Author details

[1]Université de Perpignan Via Domitia, CNRS, UMR 5244 Ecologie et Evolution des Interactions (2EI), 52 Avenue Paul Alduy, 66860 Perpignan Cedex, France. [2]Department of Biochemistry and Biophysics, ALS 2011, Oregon State University, Corvallis, OR 97331-7305, USA. [3]CEBio - Centro de Excelência em Bioinformática, Rua Araguari, 741/301 - Barro Preto - BH/MG - CEP 30190-110, Brazil.

Authors' contributions

JMJL did most of the experimental work and wrote the manuscript, CC conducted ChIP experiments, JB performed TSA treatment and edited the manuscript, MF performed ChIP-Seq, JP and DC did PCR and qPCR confirmation of W- and Z-specific sequences, CP contributed to data analysis, AZN did part of the bioinformatics work, and CG designed the experiment, performed FISH experiments, edited the manuscript and analyzed the massive sequencing data.

Competing interests

The authors declare that they have no competing interests.

Received: 23 November 2011 Revised: 13 February 2012
Accepted: 29 February 2012 Published: 29 February 2012

References

1. Charlesworth D, Charlesworth B, Marais G: **Steps in the evolution of heteromorphic sex chromosomes.** *Heredity* 2005, **95**:118-128.
2. Rice WR: **Sexually antagonistic male adaptation triggered by experimental arrest of female evolution.** *Nature* 1996, **381**:232-234.
3. Jablonka E: **The evolution of the peculiarities of mammalian sex chromosomes: an epigenetic view.** *BioEssays* 2004, **26**:1327-1332.
4. Nicolas M, Marais G, Hykelova V, Janousek B, Laporte V, Vyskot B, Mouchiroud D, Negrutiu I, Charlesworth D, Moneger F: **A gradual process of recombination restriction in the evolutionary history of the sex chromosomes in dioecious plants.** *PLoS Biol* 2005, **3**:e4.
5. Jablonka E, Lamb MJ: **The evolution of heteromorphic sex chromosomes.** *Biol Rev Camb Philos Soc* 1990, **65**:249-276.
6. Zhang YE, Vibranovski MD, Landback P, Marais GA, Long M: **Chromosomal redistribution of male-biased genes in mammalian evolution with two bursts of gene gain on the × chromosome.** *PLoS Biol* 2010, **8**:e1000494.
7. Steinemann S, Steinemann M: **Y chromosomes: born to be destroyed.** *BioEssays* 2005, **27**:1076-1083.
8. Gorelick R: **Evolution of dioecy and sex chromosomes via methylation driving Muller's ratchet.** *Biol J Linn Soc* 2003, **80**:353-368.
9. Griffin DK, Harvey SC, Campos-Ramos R, Ayling LJ, Bromage NR, Masabanda JS, Penman DJ: **Early origins of the × and Y chromosomes: lessons from tilapia.** *Cytogenet Genome Res* 2002, **99**:157-163.
10. Fraser JA, Heitman J: **Chromosomal sex-determining regions in animals, plants and fungi.** *Curr Opin Genet Dev* 2005, **15**:645-651.
11. Handley LJ, Ceplitis H, Ellegren H: **Evolutionary strata on the chicken Z chromosome: implications for sex chromosome evolution.** *Genetics* 2004, **167**:367-376.
12. Just W, Baumstark A, Suss A, Graphodatsky A, Rens W, Schafer N, Bakloushinskaya I, Hameister H, Vogel W: **Ellobius lutescens: sex determination and sex chromosome.** *Sex Dev* 2007, **1**:211-221.
13. King CH: **Parasites and poverty: the case of schistosomiasis.** *Acta Trop* 2010, **113**:95-104.
14. Liberatos JD, Short RB: **Identification of sex of schistosome larval stages.** *J Parasitol* 1983, **69**:1084-1089.
15. Grossman AI, Short RB, Cain GD: **Karyotype evolution and sex chromosome differentiation in Schistosomes (Trematoda, Schistosomatidae).** *Chromosoma* 1981, **84**:413-430.
16. Loker ES, Brant SV: **Diversification, dioecy and dimorphism in schistosomes.** *Trends Parasitol* 2006, **22**:521-528.
17. Despres L, Maurice S: **The evolution of dimorphism and separate sexes in schistosomes.** *Proc R Soc Lond B* 1995, **262**:175-180.
18. Basch PF: **Why do schistosomes have separate sexes?.** *Parasitol Today* 1990, **6**:160-163.

19. Read AF, Nee S: **Male schistosomes: more than just muscle?.** *Parasitol Today* 1990, **6**:297, author reply 297.
20. Berriman M, Haas BJ, LoVerde PT, Wilson RA, Dillon GP, Cerqueira GC, Mashiyama ST, Al-Lazikani B, Andrade LF, Ashton PD, Aslett MA, Bartholomeu DC, Blandin G, Caffrey CR, Coghlan A, Coulson R, Day TA, Delcher A, DeMarco R, Djikeng A, Eyre T, Gamble JA, Ghedin E, Gu Y, Hertz-Fowler C, Hirai H, Hirai Y, Houston R, Ivens A, Johnston DA, *et al*: **The genome of the blood fluke *Schistosoma mansoni*.** *Nature* 2009, **460**:352-358.
21. Protasio AV, Tsai IJ, Babbage A, Nichol S, Hunt M, Aslett MA, De Silva N, Velarde GS, Anderson TJ, Clark RC, Davidson C, Dillon GP, Holroyd NE, Loverde PT, Lloyd C, McQuillan J, Oliveira G, Otto TD, Parker-Manuel SJ, Quail MA, Wilson RA, Zerlotini A, Dunne DW, Berriman M: **A systematically improved high quality genome and transcriptome of the human blood fluke *Schistosoma mansoni*.** *PLoS Negl Trop Dis* 2012, **6**:e1455.
22. Criscione CD, Valentim CL, Hirai H, LoVerde PT, Anderson TJ: **Genomic linkage map of the human blood fluke *Schistosoma mansoni*.** *Genome Biol* 2009, **10**:R71.
23. Zhang W, Wang X, Yu Q, Ming R, Jiang J: **DNA methylation and heterochromatinization in the male-specific region of the primitive Y chromosome of papaya.** *Genome Res* 2008, **18**:1938-1943.
24. Portela J, Grunau C, Cosseau C, Beltran S, Dantec C, Parrinello H, Boissier J: **Whole-genome in-silico subtractive hybridization (WISH) - using massive sequencing for the identification of unique and repetitive sex-specific sequences: the example of *Schistosoma mansoni*.** *BMC Genomics* 2010, **11**:387.
25. DeMarco R, Kowaltowski AT, Machado AA, Soares MB, Gargioni C, Kawano T, Rodrigues V, Madeira AM, Wilson RA, Menck CF, Setubal JC, Dias-Neto E, Leite LC, Verjovski-Almeida S: **Saci-1, -2, and -3 and Perere, four novel retrotransposons with high transcriptional activities from the human parasite *Schistosoma mansoni*.** *J Virol* 2004, **78**:2967-2978.
26. Webster P, Mansour TE, Bieber D: **Isolation of a female-specific, highly repeated *Schistosoma mansoni* DNA probe and its use in an assay of cercarial sex.** *Mol Biochem Parasitol* 1989, **36**:217-222.
27. Hirai H, Tanaka M, LoVerde PT: ***Schistosoma mansoni*: chromosomal localization of female-specific genes and a female-specific DNA element.** *Exp Parasitol* 1993, **76**:175-181.
28. Grevelding CG: **Genomic instability in *Schistosoma mansoni*.** *Mol Biochem Parasitol* 1999, **101**:207-216.
29. Fitzpatrick JM, Protasio AV, McArdle AJ, Williams GA, Johnston DA, Hoffmann KF: **Use of genomic DNA as an indirect reference for identifying gender-associated transcripts in morphologically identical, but chromosomally distinct, *Schistosoma mansoni* cercariae.** *PLoS Negl Trop Dis* 2008, **2**:e323.
30. Reinhart BJ, Bartel DP: **Small RNAs correspond to centromere heterochromatic repeats.** *Science* 2002, **297**:1831.
31. Felsenstein J: **The evolutionary advantage of recombination.** *Genetics* 1974, **78**:737-756.
32. Fukagawa T, Nogami M, Yoshikawa M, Ikeno M, Okazaki T, Takami Y, Nakayama T, Oshimura M: **Dicer is essential for formation of the heterochromatin structure in vertebrate cells.** *Nat Cell Biol* 2004, **6**:784-791.
33. Grossman AI, McKenzie R, Cain GD: **Sex heterochromatin in *Schistosoma mansoni*.** *J Parasitol* 1980, **66**:368-370.
34. Tone M, Nakano N, Takao E, Narisawa S, Mizuno S: **Demonstration of W chromosome-specific repetitive DNA sequences in the domestic fowl, *Gallus g. domesticus*.** *Chromosoma* 1982, **86**:551-569.
35. Griffiths R, Holland PW: **A novel avian W chromosome DNA repeat sequence in the lesser black-backed gull (Larus fuscus).** *Chromosoma* 1990, **99**:243-250.
36. Kejnovsky E, Hobza R, Cermak T, Kubat Z, Vyskot B: **The role of repetitive DNA in structure and evolution of sex chromosomes in plants.** *Heredity* 2009, **102**:533-541.
37. Shapiro JA, von Sternberg R: **Why repetitive DNA is essential to genome function.** *Biol Rev Camb Philos Soc* 2005, **80**:227-250.
38. Ugarkovic D: **Functional elements residing within satellite DNAs.** *EMBO Rep* 2005, **6**:1035-1039.
39. Krautz-Peterson G, Skelly PJ: ***Schistosoma mansoni*: the dicer gene and its expression.** *Exp Parasitol* 2008, **118**:122-128.
40. Luo R, Xue X, Wang Z, Sun J, Zou Y, Pan W: **Analysis and characterization of the genes encoding the Dicer and Argonaute proteins of *Schistosoma japonicum*.** *Parasit Vectors* 2010, **3**:90.
41. Volpe TA, Kidner C, Hall IM, Teng G, Grewal SI, Martienssen RA: **Regulation of heterochromatic silencing and histone H3 lysine-9 methylation by RNAi.** *Science* 2002, **297**:1833-1837.
42. Verdel A, Jia S, Gerber S, Sugiyama T, Gygi S, Grewal SI, Moazed D: **RNAi-mediated targeting of heterochromatin by the RITS complex.** *Science* 2004, **303**:672-676.
43. Kanellopoulou C, Muljo SA, Kung AL, Ganesan S, Drapkin R, Jenuwein T, Livingston DM, Rajewsky K: **Dicer-deficient mouse embryonic stem cells are defective in differentiation and centromeric silencing.** *Genes Dev* 2005, **19**:489-501.
44. Pelisson A, Sarot E, Payen-Groschene G, Bucheton A: **A novel repeat-associated small interfering RNA-mediated silencing pathway downregulates complementary sense gypsy transcripts in somatic cells of the *Drosophila* ovary.** *J Virol* 2007, **81**:1951-1960.
45. Bergero R, Charlesworth D: **The evolution of restricted recombination in sex chromosomes.** *Trends Ecol Evol* 2009, **24**:94-102.
46. Jablonka E, Lamb MJ: **Meiotic pairing constraints and the activity of sex chromosomes.** *J Theor Biol* 1988, **133**:23-36.
47. Theron A, Pages JR, Rognon A: ***Schistosoma mansoni*: distribution patterns of miracidia among Biomphalaria glabrata snail as related to host susceptibility and sporocyst regulatory processes.** *Exp Parasitol* 1997, **85**:1-9.
48. Boissier J, Rivera ER, Mone H: **Altered behavior of the snail Biomphalaria glabrata as a result of infection with *Schistosoma mansoni*.** *J Parasitol* 2003, **89**:429-433.
49. Cosseau C, Azzi A, Rognon A, Boissier J, Gourbière S, Roger E, Mitta G, Grunau C: **Epigenetic and phenotypic variability in populations of *Schistosoma mansoni*-a possible kick-off for adaptive host/parasite evolution.** *Oikos* 2010, **119**:669-678.
50. Li R, Yu C, Li Y, Lam TW, Yiu SM, Kristiansen K, Wang J: **SOAP2: an improved ultrafast tool for short read alignment.** *Bioinformatics* 2009, **25**:1966-1967.
51. **Censor.** [http://www.girinst.org/censor/].
52. Abrusan G, Grundmann N, DeMester L, Makalowski W: **TEclass - a tool for automated classification of unknown eukaryotic transposable elements.** *Bioinformatics* 2009, **25**:1329-1330.
53. **BLAST..** [http://blast.ncbi.nlm.nih.gov/Blast.cgi?CMD=Web&PAGE_TYPE=BlastHome].
54. Zerlotini A, Heiges M, Wang H, Moraes RL, Dominitini AJ, Ruiz JC, Kissinger JC, Oliveira G: **SchistoDB: a *Schistosoma mansoni* genome resource.** *Nucleic Acids Res* 2009, **37**:D579-582.
55. Hirai H, LoVerde PT: **FISH techniques for constructing physical maps on schistosome chromosomes.** *Parasitol Today* 1995, **11**:310-314.
56. **Primer3..** [http://www.bioinformatics.nl/cgi-bin/primer3plus/primer3plus.cgi].
57. Cosseau C, Azzi A, Smith K, Freitag M, Mitta G, Grunau C: **Native chromatin immunoprecipitation (N-ChIP) and ChIP-Seq of *Schistosoma mansoni*: critical experimental parameters.** *Mol Biochem Parasitol* 2009, **166**:70-76.
58. Chen J, Yang Y, Guo S, Peng J, Liu Z, Li J, Lin J, Cheng G: **Molecular cloning and expression profiles of Argonaute proteins in *Schistosoma japonicum*.** *Parasitol Res* 2010, **107**:889-899.
59. Frescas D, Guardavaccaro D, Kuchay SM, Kato H, Poleshko A, Basrur V, Elenitoba-Johnson KS, Katz RA, Pagano M: **KDM2A represses transcription of centromeric satellite repeats and maintains the heterochromatic state.** *Cell Cycle* 2008, **7**:3539-3547.
60. Brunmeir R, Lagger S, Simboeck E, Sawicka A, Egger G, Hagelkruys A, Zhang Y, Matthias P, Miller WJ, Seiser C: **Epigenetic regulation of a murine retrotransposon by a dual histone modification mark.** *PLoS Genet* 2010, **6**:e1000927.
61. Hirai H, Spotila LD, LoVerde PT: ***Schistosoma mansoni*: chromosomal localization of DNA repeat elements by in situ hybridization using biotinylated DNA probes.** *Exp Parasitol* 1989, **69**:175-188.
62. Drew AC, Brindley PJ: **Female-specific sequences isolated from *Schistosoma mansoni* by representational difference analysis.** *Mol Biochem Parasitol* 1995, **71**:173-181.

doi:10.1186/gb-2012-13-2-r14
Cite this article as: Lepesant *et al.*: Chromatin structural changes around satellite repeats on the female sex chromosome in *Schistosoma mansoni* and their possible role in sex chromosome emergence. *Genome Biology* 2012 **13**:R14.

Résumé : L'immunité des invertébrés a longtemps été définie comme reposant sur une immunité innée simple basée sur une reconnaissance peu spécifique. Cependant depuis 20 ans les preuves que l'immunité des invertébrés présente de la spécificité se multiplient. De la même façon un phénomène de mémoire immunitaire nommé priming immunitaire a également été décrit chez ces derniers. Dans le cadre de ce travail de thèse j'ai pu étudier sous différents aspect le priming immunitaire chez *Biomphalaria glabrata,* un mollusque d'eau douce, face à son parasite naturel *Schistosoma mansoni*. Dans un premier temps nous avons pu démontrer que le priming immunitaire était spécifique du génotype du premier parasite entrant dans le mollusque. De plus, il apparaît que la succession des différents stades de développement du parasite stimule l'immunité séquentiellement afin d'engendrer une protection totale. Enfin nous nous sommes intéressés aux mécanismes sous jacents à ce priming immunitaire en focalisant notre attention sur les facteurs humoraux impliqués dans cette réponse de priming immunitaire. Nous avons observé différentes molécules pouvant être associées à la réponse de priming tant dans la spécificité de reconnaissance que dans la phase effectrice de la réponse immunitaire.

Mots clés : *Biomphalaria glabrata, Schistosoma mansoni,* priming immunitaire.

Abstract : Invertebrate immunity was defined as simple and based on an aspecific recognition. Since twenty years there are some evidence that invertebrate immunity presented high levels of specificity. In the same way, a memory process named "immune priming" was also described in invertebrates. In this work, we studied under different aspects the immune priming in *Biomphalaria glabrata*, a fresh water snail, against its natural parasite *Schistosoma mansoni*. In a first approach we demonstrated that immune priming was genotype dependent. It also appeared that the successive developmental stages of the parasite are responsible of the total protection that occurred. Finally we were interested on the molecular mechanisms responsible of this immune priming and we identified some molecular candidates in the plasma of the snails. These molecules could be implicated in the specific recognition and/or in the parasite killing.

Key words : *Biomphalaria glabrata, Schistosoma mansoni,* immune priming.